

SPONSORED BY THE



Federal Ministry
of Education
and Research

Funded by

DFG Deutsche
Forschungsgemeinschaft

German Research Foundation



STATUS CONFERENCE RESEARCH VESSELS 2024

Conference transcript

SCHRIFTENREIHE PROJEKTRÄGER JÜLICH

„Bibliographic information published by the Deutsche Nationalbibliothek.
Die Deutsche Nationalbibliothek lists this publication in the Deutsche
Nationalbibliografie; detailed bibliographic data are available in the Internet at
<http://dnb.d-nb.de>.“

Für den Inhalt der einzelnen Beiträge tragen die Autoren die Verantwortung.

Published by

Forschungszentrum Jülich GmbH
Zentralbibliothek, Verlag
52425 Jülich, Germany
Phone: 02461 61-5368
Fax: 02461 61-6103
E-mail: zb-publikation@fz-juelich.de
Internet: www.fz-juelich.de/zb

Edited by and layout

Projectmanagement Jülich, Forschungszentrum Jülich GmbH

Photo credits

Titel (left to right): GEOMAR/Karen Hissmann; Manfred Schulz TV&FilmProduktion/
Max-Planck Institut Bremen; Universität Hamburg/LDF/Denecke

Schriftenreihe Projektträger Jülich Volume 18
ISBN 973-3-95806-747-9

The contributions are abstracts of the results of past research cruises. These results were presented at the Status Conference Research Vessels 2024 at MARUM, the Center for Marine Environmental Sciences at the University of Bremen.

The complete volume is freely available on the Internet on the Jülicher Open Access Server (JuSER) at www.fz-juelich.de/zb/openaccess.

This is an Open Access publication distributed under the terms of the Creative Commons Attribution License 4.0, which permits unrestricted use, distribution, and reproduction in any medium, provided the original work is properly cited.

STATUS CONFERENCE RESEARCH VESSELS 2024

Conference transcript

FOREWORD

Dear participants,

The ocean, with its marginal seas, is our planet's largest water reservoir and contains 96% of its water. This water is important for the heat balance of the Earth and the control of the global climate system. The ocean's water masses store a large proportion of human-caused carbon dioxide from the atmosphere and absorb much of the heat generated by solar radiation. At the same time, marine ecosystems are exposed to increasing stress. Oceans and coastal seas are of enormous importance not only as natural areas, but also as living and economic regions, and represent a valuable source of many resources. Climate change and other social challenges, as well as the question of energy security are playing an increasingly important role. Germany, as part of international initiatives for climate change, is politically and internationally committed to protecting the oceans and contributes to the implementation of internationally agreed goals. The scientific findings of marine research are of central importance and the very basic data of the ocean are obtained during expeditions with research vessels.



In Germany, we researchers are able to use a fleet of state-of-the-art research vessels for our research. Every two years, the large pool of marine data collected during these expeditions across all disciplines are presented at the so-called "Status Conference Research Vessels". First launched in 2020 and since affected by the Covid pandemic, this year, the conference can take place in person for the first time. It is therefore my great pleasure to cordially welcome you to the 3rd Status Conference Research Vessels, 2024, at MARUM, the Center for Marine Environmental Sciences at the University of Bremen. Since its foundation, MARUM has developed into an internationally recognized center for marine research. MARUM's position within the University of Bremen was considerably strengthened in 2012 when MARUM became the first and only Research Faculty of the University of Bremen. Through MARUM, the University of Bremen closely collaborates with the Alfred Wegener Institute Helmholtz Centre for Polar and Marine Research in Bremerhaven (AWI), the Max Planck Institute for Marine Microbiology in Bremen (MPI), the Senckenberg Institute by the Sea in Wilhelmshaven (SGN), the Leibniz Centre for Tropical Marine Research (ZMT), the University of Oldenburg, and the private Constructor University in Bremen. MARUM is also the home of the Cluster of Excellence "The Ocean Floor – Earth's Uncharted Interface".

During the two days of the conference, the scientific results of the expeditions will be the focus of the discussions. I look forward to the greatest possible exchange of experiences, as well as inspiration for future research, which will allow us to understand the ocean as a sustainable resource for our planet.

GERHARD BOHRMANN

Professor for General Geology and Marine Geology, MARUM-Center for Marine Environmental Sciences and Faculty of Geosciences, University of Bremen

TABLE OF CONTENTS

FOREWORD	5
-----------------------	----------

ABSTRACTS

AL534	17
--------------------	-----------

Technology Evaluation and Testing for New Underwater Observation Concepts

AL534/2	25
----------------------	-----------

RiverOceanPlastic: Land-ocean transfer of plastic debris in the North Atlantic

AL543	33
--------------------	-----------

Sedimentary fluxes of trace elements and greenhouse gases in the southwestern Baltic Sea – Results from SEDITRACE cruise

AL548	39
--------------------	-----------

Mine Monitoring in the German Baltic Sea – Dumped munition monitoring

AL549 AND AL568B	45
-------------------------------	-----------

First-time evidence for a shift in spawning phenology of Western Baltic cod

AL553 AND AL556	51
------------------------------	-----------

Baltic Sea Integrative Long-term Data Series & Baltic Cod 2021

AL557	57
--------------------	-----------

Carbon Fluxes and their Controls in the North Sea

AL561	61
--------------------	-----------

Reconstructing sediment deposition and provenance in the Skagerrak to characterize human impacts in the North Sea

AL568	69
--------------------	-----------

A test cruise of the LIGHTHOUSE ROV System

EMB214	73
---------------------	-----------

Integrated carboN and TracE Gas monitoRing for the bALTic sea (BONUS INTEGRAL) – Summer verification

EMB217	79
---------------------	-----------

Results of research cruise EMB217

EMB230, EMB237, EMB256, EMB261, EMB264, EMB271 AND EMB280 83

The state of the Baltic Sea in 2020–2021 – ecosystem variability and long-term changes

EMB232, EMB246, EMB247 AND EMB258 89

Mapping of habitats (biotopes) and their biotic communities on the seabed in the coastal waters of Mecklenburg-Vorpommern

EMB238, EMB267 AND EMB268..... 95

Chasing the signals of bottom-trawling in benthic ecosystems of the western Baltic Sea

EMB239 AND EMB269 103

Living along gradients- spatiotemporal variability of macrobenthic communities in the southwestern Baltic Sea

EMB262 107

Baltic Sea sediments as archives of phytoplankton adaptation to climate change

EMB265 111

Acoustic and in-situ observations of mixing processes in the Kattegat and Western Baltic Sea

EMB276 115

Novel insights into the biogeochemistry of the redox zone in the Baltic Sea

HE525 119

Pleistocene Boulder Detection Testing the Manta Ray

HE527 125

In between the Storms on the North Sea

HE528 AND HE572 129

Benthic community changes over 50 years in the German Bight, North Sea

HE529, HE561 AND HE574 135

Development of nature conservation measures: European flat oyster restoration in the German Bight

HE533 141

Spatial diversity of marine protists along the Northern Norway Fjords during the sub-Arctic summer

HE537	145
Project: MESSAGER Methane seepage near abandoned drill sites in the German North Sea Sector	
HE541	151
Importance of exchange processes between water and sediments in the German Bight	
HE544 AND HE548	157
Acoustic Seafloor Classification of the German EEZ- Impact of sediment types, bioturbation, and natural and man-made seabed features on hydroacoustic images	
HE562 AND HE581	163
Dynamics of benthic communities in the German North Sea	
HE569	167
Changing North Sea (ChaNoS)	
HE570	173
Fjord Export – Characterizing the Biological Carbon Pump using imaging approaches	
HE578	179
Fluxes and fate of microplastics in northern European waters: Large Scale Transport – South to North (JPI-O FACTS)	
HE582	187
The fate of organic matter in sandy sediments	
M144	195
Eastern Mediterranean Paleoclimate and Ecosystems during the Rise of Early Civilizations	
M152/2	201
Persistent organic pollutants in air and surface waters of the Equatorial Atlantic – distributions and air-sea exchange	
M157	207
Persistent organic pollutants in air and surface waters of the Equatorial Atlantic – distributions, air-sea exchange and trans-Atlantic transport	
M162	213
Fluid flow along the Gloria Fault, central North Atlantic	

M164	219
AMOC components at 47°N	
M165	223
Marine Particle off Northwest Africa; from source to sink	
M168	229
Magmatic and geodynamic evolution of the King's Trough Complex – the "Grand Canyon" of the North Atlantic	
M169	237
Tracing Origin and Distribution of Geogenic and Anthropogenic Dissolved and Particulate Critical High-technology Metals in the Southern North Sea	
M170 AND M175	243
On the formation of deep valleys at oceanic transform faults – constraints from M170 and M175	
M174	247
Composition, function and environmental controls of the microbiome in the epipelagic Atlantic and Pacific Ocean	
M176	253
Are the opening of the Bay of Biscay and the origin of the Azores-Biscay Rise linked to the Azores mantle plume?	
M176/2	261
Rainbow non-buoyant hydrothermal plume GEOTRACES study	
M177	267
Fluids migrate across Paleozoic rock and the Quaternary sediments and escape from the seafloor in the eastern Gotland Basin/Baltic Sea	
M178	271
Hazards off Etna: Landslide Nucleation under Tremor (HazELNUT)	
MSM81	277
Onset and modifications in intensity and pathways of water mass exchange between the Southeast Pacific and the South Atlantic with focus on the Falkland Plateau	
MSM93	283
Submesoscale Dynamics in Fram Strait	

MSM94	291
Subpolar North Atlantic transport variability	
MSM95	299
Mapping, fauna and trawling impacts of the deep Arctic seafloor	
MSM96	305
Metal geochemistry meets machine learning: Assessing sedimentary and pore-water rare earth element variability from local to basin scale across the NE Atlantic Ocean	
MSM97	311
High Resolution Reflection Seismic Imaging of the Cenozoic Barrier Structures of the West-Schleswig Block and the Fluid Migration System of the blowout structure 'Figge Maar'	
MSM98	315
Project VARIOSEEP – Variability, amount and fate of methane seepage in the German North Sea	
MSM98/2	319
Submarine landslides, tunnel valleys, and pits – results from seismo-acoustic studies	
MSM99	325
Baltic Sea Deep Water Ventilation	
MSM99/2	329
The enigmatic pockmarks of the southeastern North Sea	
MSM100	335
Geophysical Investigations for Barrier Structures and their Integrity in the subsurface of the German North Sea by means of 3D-Seismic data	
MSM101	341
Paleoclimate and Biogeochemistry Nova Scotia Margin	
MSM102	345
Morphology, stratigraphy and sedimentary record of the Northwest Atlantic Mid-Ocean Channel, Labrador Sea	
MSM103	351
Investigation of Potential Offshore Groundwater in the Gulf of St. Lawrence, Canada	
MSM104	357
Sinking particles, their production, transfer and preservation	

MSM106	359
WASCAL students meet science – Educating West-African students by Training-Through-Research	
PS121	363
Supplementary Users IMMIPlanS 2019 „Innovative Molecular Methods in Plankton Studies“ and CARCASS „Carbon Transport via Arctic Pelagic Animals Sinking to the Deep-Sea Seafloor“	
PS124	369
Occurrence of microplastics in the southern Weddell Sea	
PS126	373
Time-Series Studies at the LTER (Long-Term Ecological Research) Observatory HAUSGARTEN	
PS128	383
East Antarctic Ice Sheet Instability (EASI-1): History of the East Antarctic Ice Sheet	
SO272	387
Kerguelen Plateau Drift Deposits: outstanding high-resolution chronicle of Cenozoic climatic and oceanographic changes in the southern Indian Ocean	
SO273	395
ROV-Sampling and Mapping of the Marion Rises at the Southwest Indian Ridge (SWIR)	
SO276	403
Depth transects and connectivity along gradients in the North Atlantic and Nordic Seas in the frame of the IceAGE project (Icelandic marine Animals: Genetics and Ecology) (IceAGE3)	
SO277	415
Seafloor processes in the central Mediterranean region – results from SO277 OMAX	
SO278	423
Mud volcanoes along the Euro-African collision zone in the eastern Mediterranean Sea	
SO279	429
NAPTRAM: North Atlantic plastic transport mechanisms, sinks, and interactions with biota	
SO280	437
Icelandic marine Animals: Genetics and Ecology meets Diversity along latitudinal gradients in the deep sea of the Atlantic Ocean (IceDivA)	

SO283	443
Mooring Rescue in the South Atlantic	
SO284	453
Tropical Atlantic Circulation and Climate	
SO285	459
TRAFFIC: Trophic TRAnSfer eFFICIency in the Benguela Current (SO285/SO283)	
SO286	465
Icelandic marine Animals: Genetics and Ecology meets Diversity along latitudinal gradients in the deep sea of the Atlantic Ocean 2 (IceDivA2)	
SO287	473
Pan-Atlantic connectivity of marine biogeochemical and ecological processes and the impact of anthropogenic pressures	
SO288	483
Measuring Tectonic Strain Build-up On The Seafloor With The GeoSEA Array	

POSTER

M169	491
Platinum input from German Rivers into the North Sea	
M169	495
Geochemical fate of trace metals including high-technology elements during riverine export into the North Sea: results from ultrafiltration and passive sampling	
M176/2	499
Do hydrothermal systems at the Mid-Atlantic Ridge affect the distribution of dissolved Rubidium, Uranium and Vanadium?	
MSM96	505
Rare earth element cycling in oxic pore waters from the Northeast Atlantic: benthic fluxes and implications for the use of Nd isotopes as a past water mass proxy	
MSM96	509
Influence of seafloor topography on benthic nutrient fluxes in deep-sea sediments of the North Atlantic	

MSM98/2	513
Tunnel valleys in the southeastern North Sea: Complex incision patterns dating back to MIS16?	
MSM100	519
Vertical acoustic blanking anomalies in 2D and 3D seismic data from the German North Sea: Imaging artifacts by shallow gas-bearing incised channels	
MSM101	525
Post-glacial palaeoceanographic changes on the Scotian Shelf – first results	
PS123 AND PS127	529
Opportunistic collection of bathymetric transit data during Expeditions PS123 and PS127 with R/V Polarstern	
PS127	535
Autonomous measurement platforms for energy and material exchange between ocean and atmosphere (OCEANET): Atmosphere	
SO264	537
SONNE-EMPEROR: The Plio/Pleistocene to Holocene development of the pelagic North Pacific	
SO264	543
Tephrostratigraphy for late Pleistocene sediments of the Minnetonka Seamount (~47°N 169°E; Emperor Seamount Chain) based on core SO264-55-1	
SO287	549
Planktonic and Micronektonic Scattering Layer distribution along latitudinal section: from North East Atlantic to Eastern Tropical Pacific Oceans	
SO287	557
Metagenomic insights into variability of microbial diversity and functions in the Eastern Tropical Pacific Ocean	
SO288	561
Monitoring strain on the seafloor offshore Northern Chile using acoustic direct-path ranging techniques	
SO288	567
Deep Ocean Heterogeneity Inferred From Offshore Geodetic Experiments	

ABSTRACTS

AL534

Technology Evaluation and Testing for New Underwater Observation Concepts

AUTHORS

Centre for Marine Environmental Sciences (MARUM), University of Bremen |
Bremen, Germany

R. Bachmayer, P. Gutierrez, A. Kausche



Figure 1: Overview of cruise track AL534 from Toulon, France to Malaga, Spain.

MOTIVATION

In order to access, explore, observe and monitor the deep sea typically larger robust uncrewed underwater platforms, tethered or autonomous, are being used. While tethered platforms often suffer limitations in their mobility due to the tether, AUVs are lacking the responsiveness to operator input in order to react quickly to in-situ observations. In order to alleviate this problem, we are developing new operational concepts that exploit recent technological developments in communication, sensing and control, while leveraging existing infrastructure.

Several key developments in recent years such as optical underwater communication, low light optical sensors, compliant actuators and software developments show great promise.

In consequence we have developed several robotic systems that deploy one or more of these emerging techniques and technologies. Part of the roadmap of these developments is frequent testing and evaluation in order to detect early potential shortcomings and adjust the development. As part of the R&D cycle it is necessary to perform besides frequent laboratory and tank testing, test in the real environment to properly assess the viability of the solution in the "real world". To this extend the technology cruise AL534, on board the R/V ALKOR were key for further development.

CRUISE OBJECTIVES

The objectives of the cruise onboard the R/V ALKOR (AL534) were two-fold. First and foremost, to conduct in the Ligurian Sea in the St. Tropez Canyon (Figure 1), performance tests on several robotic systems utilizing new technologies, namely new software and hardware architecture, optical communication and low light underwater imaging system for small autonomous underwater vehicles. On top of the technology tests we tested the feasibility and practicality of a new operational concept, using a fly-out vehicle, see Figure 2.

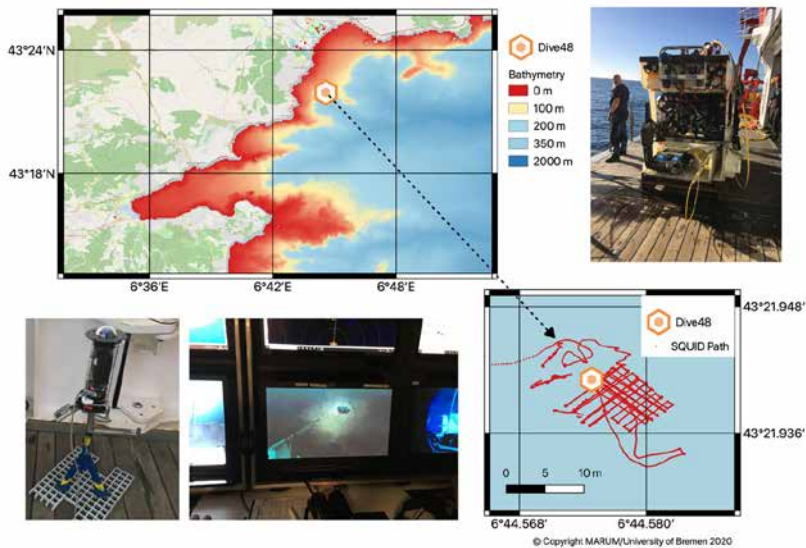


Figure 2: Image panel in the upper left and lower right show location and trajectory of the ROV MARUM SQUID dives for an optical survey of the experimental site. The image on the lower left shows the stationary bottom node on deck. The bottom middle image shows a photo of the ROV control console as the mini ROV was controlled via the optical communication link from the larger ROV as shown on deck in the picture on the upper right.

The objective of the second portion of the cruise in the Alboran Sea was the recovery of three seafloor observational systems (P- and T-Lance) at location POS500-2 (27.02.20 N36°26.270'–W2°45.780') and a MeBo-Cork at N36°23.44'–W002°52.94', see Figure 1 .

CRUISE SUMMARY

To summarize this first portion of the cruise, a total of five consecutive dives (ROV MARUM SQUID dives #47–#51) were conducted between the 22.2–24.2. 2020.

The ROV MARUM SQUID (Figure 2 upper right panel) was used as carrier and deployment platform for all the experiments.

The ROV showed itself as an excellent experimental platform for these kinds of tests, providing physical stability, power and high bandwidth communication subsea. Testimony of the efficacy of the ship and ROV operations was, that despite leaving our station in the Ligurian sea after 2.5 days, due to incoming bad weather, we completed 5 successful dives and achieved all of our expedition objectives in this first stage.

OPTICAL SEAFLOOR NODE

As a first experiment the ROV deployed standalone sea-floor node (Figure 2 lower left panel) with optical modem (256 kbaud data rate) and an autonomous light seeking pan and tilt camera. The setup was used to test the optical communication bandwidth and robustness between the ROV and the stationary seafloor node under different environmental settings (see Figure 3). For that purpose, the node was autonomously orienting the camera towards an object of interest with a light seeking algorithm, taking images and transmitting it to the ROV via the optical link.

The ROV thrusters were used to create sediment clouds likely to be encountered during seafloor operations. Even under difficult lighting conditions (Figure 3) the modem was able to perform the data transfer over a distance 3–5 m.

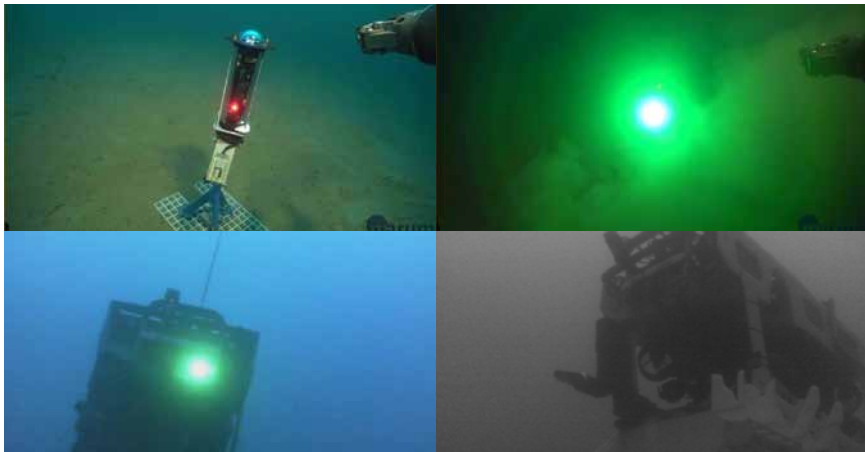


Figure 3: Left upper panel shows the bottom imaging and communication node in clear water right upper panel communicating through suspended sediment. The lower panels show the ROV from the bottom node view on the left with a recorded and stored color image while the ROV is optically communication (green light source) and on the right the black and white image transmitted to the ROV within 0.5 seconds.

LOW-LIGHT LOW-POWER IMAGING SYSTEM

The experiments were dedicated to evaluate the performance of a new low light camera system for a small underwater vehicle. The downward looking camera and lighting system is already integrated electrically and mechanically into the vehicle which was mounted at the front of the ROV as shown in Figure 4 (right).

The dives #48 and #49 were performed, with dive #48 dedicated to perform a coarse optical survey of the area (~100m²) with the survey trajectory shown in the lower right panel of Figure 2. Due to last minute changes of the expedition plans the ROV was not outfitted a calibrated downward looking camera to provide a photomosaic, instead the ROV's standard cameras were used in order to provide a basis for comparison for the dives using a new low light camera. The experiments were conducted during dives # 49 and #51, results from the low light camera are shown in Figure 4.

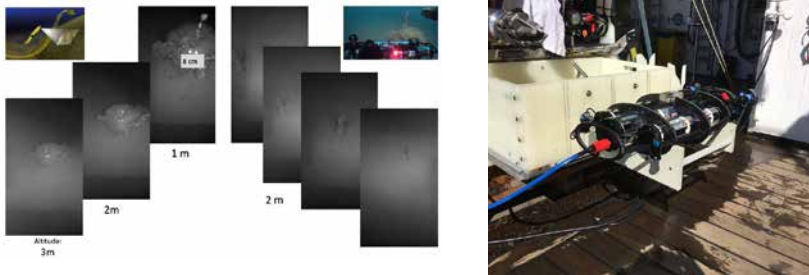


Figure 4: The left figure shows a series of images of two different targets collected at different altitudes with the low light low power camera system. For comparison a color image of the left target as seen by the standard ROV camera with full lighting is shown in the upper right. The right panel shows the skeleton of the small AUV Manatee mounted at the front of the payload compartment of the ROV.

FLY-OUT MINIROV

During dive # 50 a new concept of a flyout mini ROV from the larger ROV MARUM Squid was being tested. A miniROV was carried in the payload bay of the larger ROV (Figure 5) to the seafloor. The miniROV was, mechanically connected to the larger ROV for test-purposes but was completely controlled via an optical modem. During these tests the viability of this operational concept were examined and some close-up images acquired from the fly-out or daughter vehicle, shown in the lower panels of Figure 5.

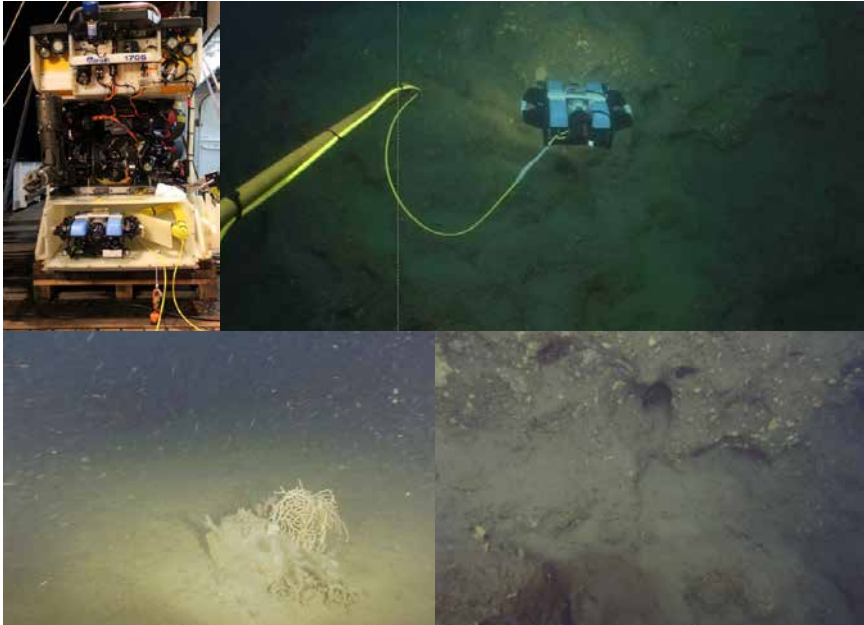


Figure 5: Left upper panel shows the miniROV inside the ROV MARUM SQUID payload bay on deck. The left panel shows the view from the larger ROV as the small, for safety purpose attached min ROV approaches a cliff wall. The lower two pictures show closeup views as captured from the miniROV.

OBSERVATORY RECOVERY

Because of worsening weather conditions, we started transiting to our next site. We sailed from the 24.–27. February to the Alboran Sea ($36^{\circ}26.26' \text{ N}-002^{\circ}44.74' \text{ E}$). There we successfully recovered two long-term seafloor observatories (P- and T-probes) from about 900m depth with the ROV MARUM SQUID, see Figure 2. Unfortunately both probes were compromised and no data could be retrieved. The attempt to recover a MEBO CORK observatory at $36^{\circ}23.44' \text{ N}-002^{\circ}52.94' \text{ W}$ had to be abandoned due to high surface currents and impending bad weather.

CONCLUSION

In summary the expedition AL534 was from the technological standpoint, albeit having to be shortened due to inclement weather a great success. All the experiments provided valuable insights into the technologies their limitations and potential. The reference list gives an idea of the different developments that spawned from these tests with some being already deployed others being in the integrations phase.

ACKNOWLEDGEMENTS

We would like to acknowledge the support of Captain Jan – Peter Lass and the entire crew of the R/V Alkor for their handling of the vessel and gear under the encountered variable conditions. The ROV MARUM SQUID operational team did a fantastic job handling our not so common requests. Furthermore the expedition would not have been

successful without the logistic support of the MARUM logistics team. We are also very grateful to the French and Spanish government to generously granting us access to their waters for this expedition.

The cruise has received funding from MARUM through the DFG supported Cluster of Excellence "The Ocean Floor – Earth's Uncharted Interface". Portions of this project have also received funding from the European Union's Horizon 2020 research and innovation programme under grant agreement No 731103 (EU Marine Robots). Further funding for the research was also provided by the Werner-Siemens Foundation.

Station	Date	Lat/Lon
Ligurian Sea		
(A)#47	22.02.20	N43°21.890'–E6°44.519' (A)
(A)#48	23.02.20	N43°21.936'–E6°44.568' (A)
(A)#49	23.02.20	N43°21.936'–E6°44.568' (A)
(A)#50	24.02.20	N43°21.936'–E6°44.568' (A)
(A)#51	24.02.20	N43°21.936'–E6°44.568' (A)
Alboran Sea		
POS500-2	27.02.20	N36°26.270'–W2°45.780'
MEBO_CORK	28.02.20	N36°23.44'–W002°52.94'

SCIENTIFIC OUTPUT

LIST OF PUBLICATIONS

Gregorek D, Srinivas S, Nasrulla S, Paul S, Bachmayer R, Towards energy-optimized on-board computer vision for autonomous underwater vehicles, OCEANS 2022, Hampton Roads, pp. 1–6, 2022. Doi: 10.1109/OCEANS47191.2022.9977107.

Gutiérrez-Flores P, Bachmayer R, Concept development of a modular system for marine applications using ROS2 and micro-ROS, 2022 IEEE/OES Autonomous Underwater Vehicles Symposium (AUV), pp. 1–6, 2022. Doi: 10.1109/AUV53081.2022.9965867.

Antonelli G, et al., Advancing the EU marine robotics research infrastructure network: the EU marine robots project, OCEANS 2021: San Diego – Porto, pp. 1–10, 2021. Doi: 10.23919/OCEANS44145.2021.9705791.

Bachmayer R, Kausche A, et al., Concept development for a minimally invasive autonomous underwater vehicle, 2020 IEEE/OES Autonomous Underwater Vehicles Symposium (AUV), pp. 1–3, 2020. Doi: 10.1109/AUV50043.2020.9267943.

LIST OF CONFERENCE PRESENTATIONS

2020 | **Concept development for a minimally invasive autonomous underwater vehicle** IEEE/OES Autonomous Underwater Vehicles Symposium (AUV2020), St. John's, Canada.

2021 | **Advancing the EU marine robotics research infrastructure network: the EU marine robots project** IEEE/MTS OCEANS 2021, San Diego – Porto, USA/Portugal.

2022 | **Concept development of a modular system for marine applications using ROS2 and micro-ROS** IEEE/OES Autonomous Underwater Vehicles Symposium (AUV2022), Singapore, Singapore.

2022 | **Towards energy-optimized on-board computer vision for autonomous underwater vehicles** IEEE/MTS OCEANS 2022, Hampton Roads, USA.

DATA

AL534: <https://oceanrep.geomar.de/id/eprint/49100>

AL534/2

RiverOceanPlastic: Land-ocean transfer of plastic debris in the North Atlantic

AUTHORS

GEOMAR Helmholtz Centre for Ocean Research Kiel | Kiel, Germany

A. Beck, E. Achterberg, M. Haeckel, M. Lenz

BACKGROUND

Since 1950, 8300 Mio t of plastics have been produced and 4900 Mio t discarded (Geyer et al. 2017). While the global amounts of produced and discarded plastic are constrained relatively well, reliable estimates on the amount ending up in the environment are lacking. Approximately 50–60% of the plastic that is produced is less dense than seawater (Andrady 2011), and about 60% of the positively buoyant plastic debris that enters the oceans from land is likely transported offshore (Lebreton et al., 2012). Floating plastic debris therefore tends to be transferred from land to sea and accumulate within restricted coastal waters and oceanic gyres (Lebreton et al., 2012). Long distance transport of MP from riverine sources to the open ocean is poorly understood, in part, because little is known regarding transport mechanisms from the rivers to accumulation areas in the centre of subtropical gyres. Off shore transfer is considered to occur through surface currents and winds (Maximenko et al., 2012).

The North Atlantic is estimated to contain approximately 20% of the global amount of floating plastic debris (Cózar et al., 2014). Most of this material is concentrated in an area that Cózar et al. (2014) described as the inner accumulation zone of the North Atlantic subtropical gyre, and which spans from the Azores to Bermuda. For a range of rivers plastic concentrations have been reported (e. g., Lebreton et al., 2017) indicating that Asian rivers are providing the largest concentrations and fluxes, with 67% of global emissions. Limited data are available on European rivers discharging into the Atlantic, but suggest they are much smaller sources than e. g., the Yangtze River (Zhao et al., 2014). The data for the plastic debris discharge from European rivers into coastal waters, and the particle characteristics and behaviour, are thus limited.

The cruise working area is located in the NW European shelf area, including outflows of major European rivers, as source regions or intermediates for transport to the plastic garbage patch of the North Atlantic gyre. The work is complemented by separate sampling activities undertaken by a Portuguese group in coastal zones around and between the Azores archipelago as part of the HOTMIC project as these are extensively contaminated with plastic debris. Due to oceanographic circulation structures, the Azores

act as a retention zone for plastic debris from Europe, and the interface between continental sources and the open ocean accumulation zone.

The distribution of microplastic debris in European coastal waters is heterogeneous (e. g., Maes et al., 2018), but there are clear hotspots at river mouths (Galgani et al., 2000). The putative river source of most plastic debris in this region appears to be increasing over the past several decades (Maes et al., 2018). Reported macroplastic litter densities are especially high in certain regions of the planned study region, including south Portugal and the Bay of Biscay, and the litter abundance is directly proportional to proximity to the coast (Pham et al., 2014). Microplastic abundances on beaches along the planned cruise track are also some of the highest observed throughout Europe (Lots et al., 2017).

Abundant macroplastic debris represents the largest mass of plastic on European beaches, and is the likely source of much of the microplastics in coastal waters (Martins and Sobral, 2011). In the water column, the mass of microplastics can exceed that of macroplastics (Van Cauwenberghe et al., 2013), and microplastics are also more abundant by number on beaches (Martins and Sobral, 2011). Both macro- and microplastics can have deleterious effects on marine ecosystems, and the distribution of these stressors is therefore important to constrain.

The coastal and open oceans represent a major, but yet unconstrained, sink for plastics. It is likely that plastic-biota interactions are a key driver for the fragmentation, aggregation, and vertical transport of plastic litter from surface waters to sedimentary sinks. However, the magnitude of the plastic flux as well as the flux rates from the rivers to coastal waters and the open ocean, and from the surface to deep waters, are very poorly constrained, as is the impact of plastic-biota interactions on transport and ecological health. Cruise AL534/2 integrates riverine source observations and shelf sea sampling to build a mechanistic understanding of MP transport and its biological impact reaching from rivers to the coastal water column and sinks at the seabed.

Cruise AL534/2 serves as a second cruise of a number of connected research cruises to build an understanding of the transport pathways of plastic and microplastic debris in the North Atlantic from the input through rivers and air across coastal seas into the accumulation spots in the North Atlantic gyre and the vertical export to its sink at the seabed. The first cruise (POS536) was conducted during August-September 2019 and visited the inner accumulation zone of the North Atlantic garbage patch (in the North Atlantic gyre) and focused on vertical transport processes. AL534/2 focused on land-ocean transfer of MPs to determine the fate of plastics (including larger size classes (>5 mm, MP, but also sub-MP) during transfer from rivers to coastal waters and towards ocean waters.

SAMPLE COLLECTION METHODS

Cruise AL534/2 took advantage of a planned transit in which R/V Alkor returned from a working area in the Mediterranean Sea to home port in Kiel, Germany. The cruise covered the entire western mainland European coast, from the Strait of Gibraltar to the Elbe River mouth (Figure 1). Stations were chosen along the route to target estuarine outflows from the major river systems, as well as provide good coverage of western Europe shelf seas.

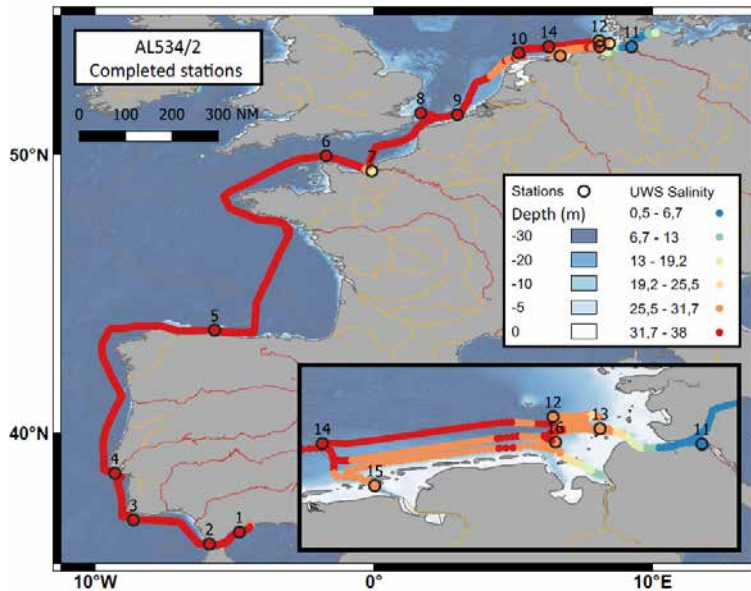


Figure 1: Track chart of R/V ALKOR Cruise AL534/2. Bathymetry from GEBCO (2020). Salinity data from underway thermosalinograph are shown along the cruise track.

The planned work during AL534/2 included a variety of sampling methods that were repeated at every station: 1) a CTD cast to collect water column salinity and temperature profiles, and discrete samples between surface and seafloor, 2) sediment sampling with Van Veen grab and mini-multi corer (mini-MUC), 3) suspended particle and plankton sampling using a towed Bongo net and vertical WP3 net, and 4) surface neuston sampling using a catamaran trawl. At a subset of stations with deep water (>100 m), in situ pumps were planned to collect suspended particles from 500-1000 L water between surface and seafloor, although this was not always possible. Additional sampling was planned throughout the cruise track, including surface water sample collection from the ship's underway seawater supply, and during calm weather, floating litter surveys to count the abundance of floating debris.

SELECTED RESULTS

Maintaining the original sampling station plan was challenging due to poor weather conditions, but many of the major European rivers were sampled as planned. Depth profiles from the last half of stations of salinity and temperature are shown in Figure 2. The shallow stations were generally mixed throughout the water column, but many stations show low salinity surface layers indicative of river outflows, especially Station 9 (Rhine), Station 13 (Elbe), and Station 15 (Ems).

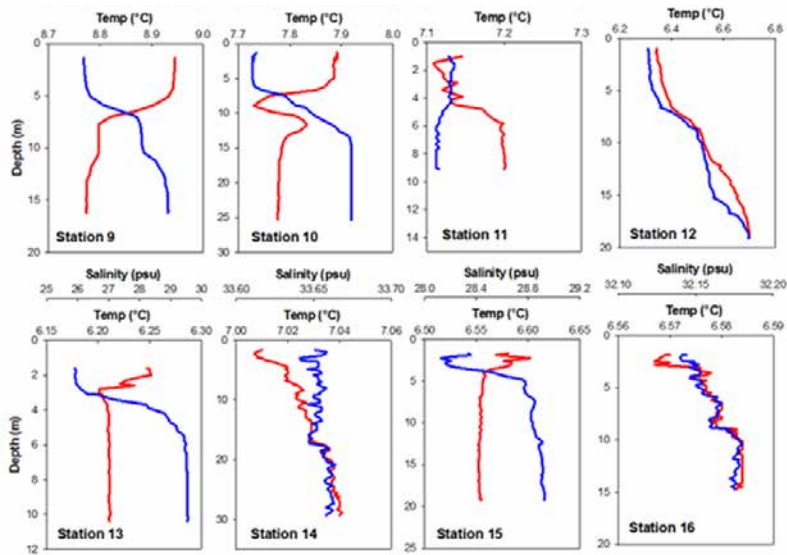


Figure 2: Depth profiles of water column salinity and temperature. Station IDs correspond to those indicated in Figure 1.

Microplastic concentrations in surface water ranged between 0.2 and 4.3 particles per cubic meter (Figure 3). The Seine, Rhine, and Elbe Rivers all showed especially high concentrations of MP. Although river outflow sampling was successful, most of the river stations did not show markedly higher levels of microplastic particles, in comparison to sampling in the North Atlantic gyre during 2019 (cruise POS536). This suggests rapid transport from coastal regions to the ocean gyre accumulation zones, or long-term accumulation, or both.

Plastic fragments collected from the sea surface were predominantly polyethylene, polypropylene, and polystyrene, whereas fibers were predominantly polyacrylate and polyester (Figure 3). The abundance of these polymers is consistent with their low density (for the fragments; i. e., density < seawater) and morphology (fibers). In contrast, the most abundant polymer found in sediments was PVC, which is more dense than seawater. These results indicate retention of specific polymer types in coastal regions, and likely export of others to the open ocean.

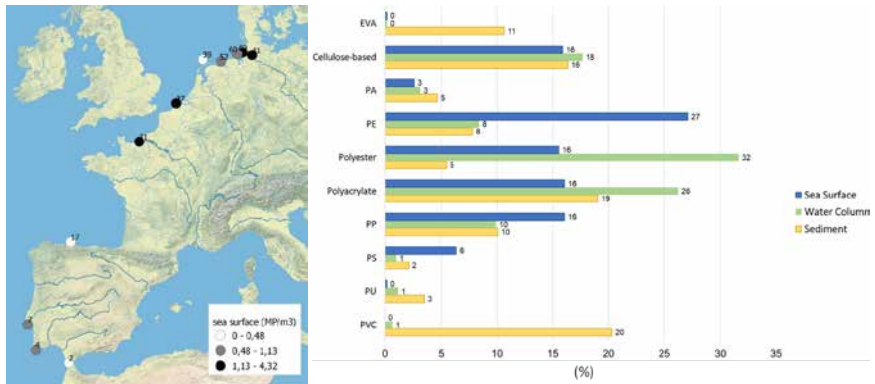


Figure 3: (left) Microplastic abundance in the surface neuston catamaran trawl samples. (right) Polymer types of microplastics at the sea surface (blue), water column (green), and sediment (yellow). (Data from J. Raimundo and C. Lopes, IPMA).

To assess the abundance and composition of microplastics associated with gelatinous zooplankton and to assess the role of gelatinous zooplankton in transporting MP across marine food webs. Gelatinous zooplankton were collected along different sampling locations during cruise AL534-2, and examples of microplastic contaminations on inner and outer morphological structures (e. g. umbrella, tentacles, gastrovascular system) of examined specimens is shown in Figure 4. Artificial fibers and particles were associated with the outer and inner morphological structures of collected gelatinous organisms, i. e., on the subumbrella and in the gastric pouch of medusae or on the combs of ctenophores, respectively.

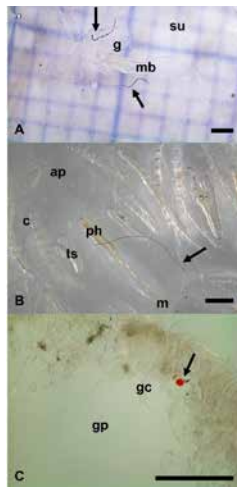


Figure 4: Artificial particles (arrows) associated to outer and inner morphological structures of gelatinous zooplankton. (A) Fibers attached to the subumbrella (su) of the hydromedusa *Liriope* sp. (location #4; mb: manubrium, g: gonad), (B) fibers attached to the outer surface of the ctenophore *Pleurobrachia* sp. (location #3; m: mouth, ph: pharynx, ap: anal pore, c: comb, ts: tentacle sheet with tentacle), (C) red (microplastic?) particle caught in the gastric cirri (gc) of the scyphomedusa *Aurelia* sp. (location #12; gp: gastric pouch).

The results obtained thus far for cruise AL534/2 indicate substantial supply of (micro) plastic debris from European rivers, but also apparent export to coastlines or the open ocean. Oceanographic modelling is underway to clarify the likely fate of this plastic pollution. Results also indicate that polymer types undergo fractionation due to the varying density of different polymer types leading to preferential export (low density polymers) or retention in coastal regions (high density polymers).

REFERENCES

Andrady AL, "Microplastics in the Marine Environment.", *Marine Pollution Bulletin* 2011, 62 (8): 1596–1605. <https://doi.org/10.1016/j.marpolbul.2011.05.030>.

Cózar A, Echevarría F, González-Gordillo JJ, Irigoien X, Úbeda B, Hernández-León S, Palma ÁT, Navarro S, García-de-Lomas J, Ruiz A, Fernández-de-Puelles ML, Duarte CM, Plastic debris in the open ocean, *Proceedings of the National Academy of the Sciences of the USA* 2014, 111, 10239–10244.

Galgani F, Leaute JP, Moguedet P, Souplet A, Verin Y, Carpentier A, Goraguer H, Latrouite D, Andral B, Cadiou Y, Mahe JC, Litter on the sea floor along European coasts, *Marine pollution bulletin* 2000, 40(6), pp.516–527.

Geyer R, Jambeck J, Lavender Law K, Production, use, and fate of all plastics ever made, *Science Advances* 2017, 3(7):e1700782, DOI: 10.1126/sciadv.1700782.

Lebreton LCM, et al., River plastic emissions to the world's oceans, *Nat. Commun.* 2017, 8, 15611 doi: 10.1038/ncomms15611.

Lebreton LCM, Greer SD, Borrero JC, Numerical modelling of floating debris in the world's oceans, *Marine Pollution Bulletin* 2012, 64, 653–661.

Lots FA, Behrens P, Vijver MG, Horton AA, Bosker T, A large-scale investigation of microplastic contamination: abundance and characteristics of microplastics in European beach sediment, *Marine Pollution Bulletin* 2017, 123(1-2), 219–226.

Maes T, Barry J, Leslie HA, Vethaak AD, Nicolaus EEM, Law RJ, Thain JE, Below the surface: Twenty-five years of seafloor litter monitoring in coastal seas of North West Europe (1992–2017), *Science of The Total Environment* 2018, 630, 790–798.

Martins J & Sobral P, Plastic marine debris on the Portuguese coastline: a matter of size?, *Marine pollution bulletin* 2011, 62(12), 2649–2653.

Maximenko M, Hafner J, Niiler P, Pathways of marine debris derived from trajectories of Lagrangian drifters, *Marine Pollution Bulletin* 2012, 65, 51–62.

Van Cauwenberghe L, Devriese L, Galgani F, Robbins J, Janssen CR, Microplastics in sediments: A review of techniques, occurrence and effects, *Marine Environmental Research* 2015, 11, 5–17.

Zhao S, Zhu L, Wang T, Li D, Suspended microplastics in the surface water of the Yangtze estuary system, China: first observations on occurrence, distribution, *Mar. Pollut. Bull.* 2014, 86, 562–568.

SCIENTIFIC OUTPUT

LIST OF CONFERENCE PRESENTATIONS

2021 | **Microplastic sample preparation avoiding contamination from sample arrival to measurement** Wasser, Virtual.

2021 | **From micro- to nano-plastics, to molecular pollutants; a matter of size and surface** 35th European Colloid & Interface Society Conference, Athens, Greece.

2023 | **Legacy and Emerging Per- and Polyfluoroalkyl Substances (PFAS) along the Western European Coast – Riverine Outflows, Vertical Profiles and Retrospective Screening** Dioxin 2023, Maastricht, The Netherlands.

DATA

Physical oceanography (CTD):

<https://portal.geomar.de/metadata/leg/show/355040>

Geochemical data, sediment cores (22 datasets total):

<https://pangaea.de/?q=AL534%2F2>

CRUISE REPORT

AL534/2: doi: 10.3289/CR_AL534-2.

AL543

Sedimentary fluxes of trace elements and greenhouse gases in the southwestern Baltic Sea – Results from SEDITRACE cruise

AUTHORS

GEOMAR Helmholtz Centre for Ocean Research Kiel | Kiel, Germany
F. Scholz, H. W. Bange

Christian Albrechts Universität zu Kiel, Department of Geosciences | Kiel, Germany
J. Scholten

Eidgenössisch-Technische Hochschule Zürich, Department of Earth Sciences |
Zürich, Switzerland
S. Fleischmann, D. Vance

GOALS OF THE CRUISE

Coastal sediments represent an important source or sink of carbon, macronutrients, bio-essential metals and greenhouse gases in the ocean. In the coming decades, source and sink fluxes will be altered by global environmental change and the associated trends of ocean deoxygenation and acidification as well as sea-level change and an anticipated increase in coastal erosion. Due to the broad range of sedimentary redox conditions in close vicinity and well-characterized seasonal cycles of temperature, salinity and oxygen, Kiel Bight is an ideal location to investigate those trends under well-defined boundary conditions. The following general research questions were addressed during R/V Alkor cruise 543:

1. What is the impact of variable redox conditions and organic carbon fluxes on the sedimentary release or burial and isotope fractionation of bioactive trace elements (e. g., nickel, barium)?
2. What is the impact of diffusive sedimentary fluxes versus submarine ground water discharge (SGD) on the distribution of radium, radon and greenhouse gases (methane and nitrous oxide) in the water column?
3. How does coastal erosion at the cliffs surrounding Kiel Bight affect biogeochemical processes in the water column and sediments?

To address these questions, 12 target sites were identified (Figure 1) where an extensive program of water, suspended particulate matter (SPM), pore water and sediment sampling was realized. These sites cover different water depths, sediment types (mud,

sandy mud, muddy sand) and bottom water redox conditions (fully oxic to anoxic and sulfidic). The sampling sites are equally distributed across the western Kiel Bight to gain an overview about the distribution of organic carbon burial and benthic fluxes across the entire study area.

Originally, it was planned to realize AL543 as a multiday cruise where relatively shallow sampling stations in Kiel Bight are combined with deeper stations within the Baltic Proper. Due to the Covid-19 pandemic and the related restriction of the number of overnight participants aboard R/V Alkor during multi-day cruises (6 instead of 12), the principal investigators were forced to modify this plan. According to the hygiene concept for research cruises aboard R/V Alkor, up to 12 scientists could participate in one-day cruises. Therefore, the distant stations within the Baltic Proper were cancelled so that all sampling stations could be reached within the framework of 6 consecutive one-day-cruises (23.08.–28.08.2020) departing and arriving at the home dock of R/V Alkor in Kiel.

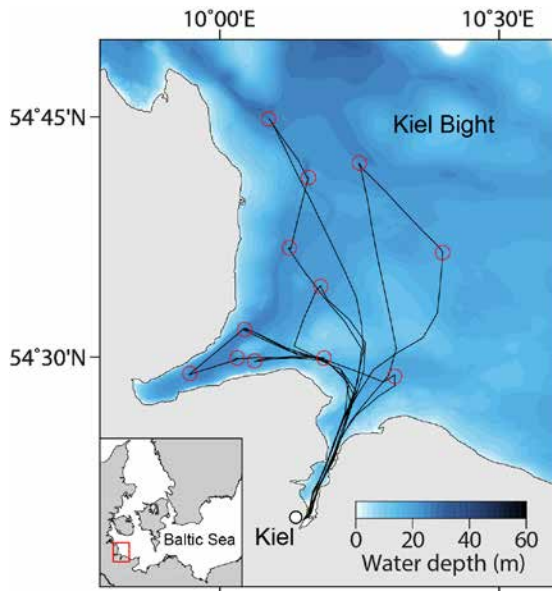


Figure 1: Bathymetric map showing the cruise track and sampling stations of AL543.

REDOX AND NUTRIENT CYCLING ACROSS KIEL BIGHT

Overall, the biogeochemical water column setting during AL543 in August 2020 reflected a typical summer period (e. g., Lennartz et al., 2014) with strong stratification, depleted nutrient concentrations in the mixed layer and depleted O_2 concentrations (i. e., hypoxic/anoxic conditions) in the bottom layer (i. e. below the pycnocline) which, in turn, were associated with enhanced nutrient concentrations in the bottom layer. Prior work on sediment biogeochemical processes and benthic fluxes in Kiel Bight has mostly focused

on the long-term monitoring station in Boknis Eck (e. g., Dale et al., 2013). Our detailed survey revealed a complex pattern of organic carbon turnover rates and sedimentary redox conditions in Kiel Bight. Shallow areas above 15 m water depth and distal stations within the open Kiel Bight were characterized by oxic bottom water and oxic to iron-reducing (ferruginous) surface sediments. By contrast, near-shore stations within the deeper areas (25–30 m) of Eckernförde Bay were characterized by oxygen-deficient bottom waters and highly sulfidic surface sediments. The Stollergrund-Rinne, a narrow channel at the transition from outer Kiel Fjord to Eckernförde Bay, was found to be anoxic and sulfidic below 16 m water depth. This complex pattern of bottom water redox conditions in Kiel Bight may not only be explained by differing rates of organic carbon deposition but also by variable rates of bottom water ventilation leading to a variable drawdown of oxygen and other electron acceptors (i. e., nitrate and nitrite) below the pycnocline. Differing rates of bottom water ventilation are likely related to the complex seafloor topography that was left behind by the Scandinavian ice sheet during the last deglaciation.

BENTHIC-PELAGIC COUPLING OF BIOACTIVE TRACE ELEMENTS

The concentrations and isotope compositions of nickel (Ni) and barium (Ba) were determined in water column, pore water and sediment samples at selected sites within Kiel Bight. The following paragraphs represent excerpts of conference abstracts and publications that arose from the post-cruise work.

Ni is an important bio-essential trace metal in the ocean, and an important component of several enzymes central to the global carbon, nitrogen, and oxygen cycles. Like other similar bio-essential trace metals, Ni appears to show a major imbalance in its modern oceanic metal concentration and isotope budgets. This apparent imbalance suggests that some sources and sinks in the ocean as well as processes fractionating Ni isotopes are currently not well understood. The data obtained for pore water samples from AL543 show an increase in dissolved Ni concentration with sediment depth coincident with increasing ammonia concentrations. This observation is consistent with the release of Ni to pore waters from respired organic matter. Pore water Ni isotopes (expressed as $\delta^{60}\text{Ni}$) increase from around +0.5 ‰ at the top to up to +2.3 ‰ in the bottom of the cores, suggesting an isotopically heavy benthic Ni flux from organic carbon-rich reducing sediments.

Ba isotopes are a promising new tracer for riverine freshwater input to the ocean and marine biogeochemical cycling. However, Ba fluxes from marine sediments have not yet been characterized with respect to Ba isotope fractionation, which could explain an imbalance in the ocean's Ba budget. The surface water Ba concentration and Ba isotope inventory of the brackish water column of Kiel Bight can generally be explained by mixing of riverine freshwater and Atlantic seawater. However, the deep-water below the pycnocline is characterized by a pronounced positive Ba concentration anomaly (up to 915 nM) that is accompanied by a $\delta^{138}\text{Ba}$ of $\sim +0.25$ ‰, which is lighter than expected

from the seawater-freshwater mixing line. Pore water profiles indicate a Ba flux across the sediment-water interface, which contributes to the enrichment in isotopically light Ba in the deep-water. Water column Ba concentrations closely correlate with those of the nutrients phosphate and silica, which are removed from surface waters by biological processes and recycled from the sediment by diffusion across the sediment-water interface. As nutrient-to-Ba ratios differ among sites and from those observed in open-marine systems, we hypothesize that Ba is removed from surface waters by adsorption onto biogenic particles (rather than assimilation) and regenerated within surface sediments upon organic matter degradation.

SGD AND GREENHOUSE GAS FLUXES

Dissolved methane (CH_4) concentrations were generally enhanced in the bottom layer compared to the mixed layer, whereas in the majority of the profiles dissolved nitrous oxide (N_2O) concentrations were depleted in the bottom layer compared to the mixed layer. This indicates that CH_4 had been released from the sediments whereas N_2O seemed to have been consumed either in the sediments or in the bottom waters. It remains unclear, however, whether or not processes associated with SGD modulated the trace gas concentrations in the bottom waters. Compared to the sedimentary diffusive inorganic nitrogen (DIN) and phosphate (PO_4^{3-}) inputs to the Eckernförde Bay, SGD-derived fluxes are lower (DIN) or in the same range (PO_4^{3-}) suggesting that SGD-derived nitrogen inputs have only minor influence on the nutrient balance in the Eckernförde Bay (Kreuzburg et al., 2023).

IMPACT OF COASTAL EROSION ON BIOGEOCHEMICAL CYCLING

Erosion of glacial till at coastal cliffs represents the main source of lithogenic sediments to Kiel Bight. Upon transport through the surf zone and into the deeper basins of Kiel Bight, glacial till interacts with seawater, which may result in the release of fixation of elements. Preliminary work on SPM, pore water and sediment samples collected during AL543 revealed that most of the calcium carbonate contained in glacial till (~30 %) is dissolved during sediment transport or after deposition. This process of calcium carbonate dissolution generates alkalinity and thus represents a net sink for CO_2 in the Baltic Sea (Wallmann et al., 2022). Furthermore, sediments in the deeper basins are depleted in potassium and enriched in magnesium, manganese (Mn) and iron (Fe) relative to the glacial till. These trends maybe explained by iron exchange and redox shuttling. The latter term refers to a mechanism where iron and manganese are remobilized from sediments above the pycnocline and re-deposited and buried as Mn carbonate and Fe sulfide minerals below the pycnocline. This process is known to operate in permanently anoxic and sulfidic basins of the Baltic Sea (e. g., Gotland Deep) (Scholz et al., 2013) but has so far not been reported for seasonally anoxic shallow basins.

REFERENCES

Dale AW, Bertics VJ, Treude T, Sommer S, et al., Modeling benthic-pelagic nutrient exchange processes and porewater distributions in a seasonally hypoxic sediment: evidence for massive phosphate release by Beggiatoa?, *Biogeosciences* 2013, 10, 629–651.

Kreuzburg M, Scholten J, Hsu F-H, Liebetrau V, et al., Submarine Groundwater Discharge-Derived Nutrient Fluxes in Eckernförde Bay (Western Baltic Sea), *Estuaries and Coasts*, 2023 46, 1190–1207.

Lennartz ST, Lehmann A, Herrford J, Malien F, et al, Long-term trends at the Boknis Eck time series station (Baltic Sea), 1957-2013: does climate change counteract the decline in eutrophication?, *Biogeosciences*, 2014, 11, 6323–6339.

Scholz F, McManus J, Sommer S, The manganese and iron shuttle in a modern euxinic basin and implications for molybdenum cycling at euxinic ocean margins, *Chemical Geology* 2013, 355, 56–68.

Wallmann K, Diesing M, Scholz F, Rehder G, et al, Erosion of carbonate-bearing sedimentary rocks may close the alkalinity budget of the Baltic Sea and support atmospheric CO₂ uptake in coastal seas, *Frontiers in Marine Science* 2022, 9, <https://doi.org/10.3389/fmars.2022.968069>.

SCIENTIFIC OUTPUT

LIST OF PUBLICATIONS

Deng K, Rickli J, Suhrhoff TJ, Du J, et al., Dominance of benthic fluxes in the oceanic beryllium budget and implications for paleo-denudation records, *Science Advances* 2023, 9, doi: 10.1126/sciadv.adg3702.

Kreuzburg M, Scholten J, Hsu F-H, Liebetrau V, et al., Submarine Groundwater Discharge-Derived Nutrient Fluxes in Eckernförde Bay (Western Baltic Sea), *Estuaries and Coasts* 2023 46, 1190–1207.

Marks S, Die Rolle des submarine Grundwassereintrags für die Verteilung von Methan (CH₄) und Lachgas (N₂O) in der Beltsee, MSc thesis 2021, University of Kiel, Kiel, 51 pp.

Scholz F, Cheng J, Zhang Z, Vosteen P, et al, Benthic-pelagic coupling and isotopic fractionation of barium in Kiel Bight, SW Baltic Sea, *Frontiers in Marine Science* 2023, 10, doi.org/10.3389/fmars.2023.1101095.

LIST OF CONFERENCE PRESENTATIONS

2022 | **The benthic flux of Ni from reducing environments: the example of the Baltic Sea**
Goldschmidt Conference, Honolulu, USA.

2023 | **Benthic-pelagic coupling and isotopic fractionation of barium in a seasonally hypoxic Fjord** XIAMEN Symposium for Marine Environmental Sciences, XIAMEN, China.

2023 | **Dominance of Benthic fluxes in the Oceanic Beryllium Budget and Implications for Paleo-denudation Records** Goldschmidt Conference, Lyon, France.

DATA

Pore water geochemical data for sediment cores:

<https://doi.org/10.1594/PANGAEA.950065>

Additional pore water geochemical and barium isotope data:

<https://doi.org/10.1594/PANGAEA.954866>

Solid phase geochemical and barium isotope data:

<https://doi.org/10.1594/PANGAEA.954868>

Water column (CTD) chemistry data:

<https://doi.org/10.1594/PANGAEA.950055>

Barium isotope data for water column samples:

<https://doi.org/10.1594/PANGAEA.954860>

Geochemistry of coastal cliffs:

<https://doi.org/10.1594/PANGAEA.954869>

Manganese and barium concentration data:

<https://doi.org/10.1594/PANGAEA.954856>

CRUISE REPORT

AL543: <https://oceanrep.geomar.de/id/eprint/50968/>

AL548

Mine Monitoring in the German Baltic Sea – Dumped munition monitoring

AUTHORS

GEOMAR Helmholtz Center for Ocean Research Kiel | Kiel, Germany
M. Kampmeier, J. Greinert

INTRODUCTION

ALKOR cruise AL548 took place as part of the EMFF (European Maritime and Fisheries Fund)-funded project BASTA (Boost Applied munition detection through Smart data inTegration and AI workflows; <https://www.basta-munition.eu>) and as continuation of the munition monitoring started within the BMBF-funded project UDEMM (Environmental Monitoring for the Delaboration of Munition in the Sea; <https://udemmm.geomar.de/>).

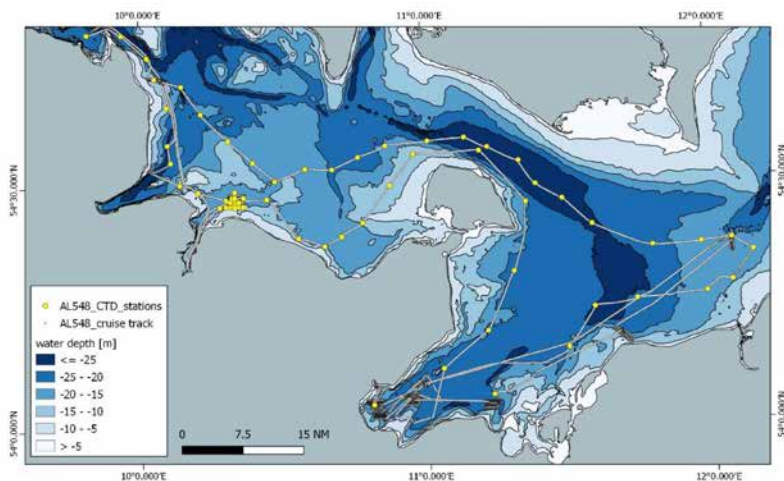


Figure 1: Cruise track of AL548 cruise. Yellow dots indicate Water samples taken via CTD along the German Baltic coastline, following the constraint routes from the WW II.

In October 2018, a first cruise (POS530 MineMoni2018) was conducted, to gather data for a broad baseline study in the German Baltic Sea. Results show a moderate contamination level on regional and coastal scale, but indicate higher levels for specific local areas. Within UDEMM, expertise was developed to detect, exactly locate and monitor munition (e. g. torpedoes, sea mines, ground mines) on the seafloor using optical and hydroacoustic means. In addition, chemical analyses of dissolved contaminants in

the water and sediments was performed. Data acquired during this cruise are used in BASTA, which aims for enhanced munition detection via AUV-based artificial intelligence applied on multi-sensor datasets. At the same time, the project ExPlOTect (Ex-situ, near-real-time exPlosive compound deTectioN in seawater) (also EMFF-funded) addresses the need for an innovative approach to detect explosive compounds in seawater. A prototype system was used and successfully tested for the first time during this cruise (Figure 2).

The main focus was placed onto the two already known dumpsites Kolberger Heide and Lübeck Bight. Additionally, new areas Falshöft (Schleswig-Holstein) and Cadet Channel, Trollegrund and Großklützhöved (Mecklenburg-Vorpommern) were explored. In each area high-resolution multibeam mapping was performed and contact lists, indicating potential munition objects were produced on board. AUV surveys were conducted to ground-truth possible contacts via detailed photograph and magnetometer mapping. This was complemented with towed video (TV)-CTD profiles (Figure 1). The transits to and between those sites were planned along former constraint routes during WWII. These routes were main targets of the British Air Force and mines and bombs can be expected along these ways. During transits water samples were taken with on a CTD- (conductivity, temperature, depth) rosette-mounted Niskin bottles in regular distances, in order to obtain a comprehensive understanding munition compounds (inter alia trinitrotoluene (TNT)) measurements across the German Baltic Sea.

AIMS OF THE CRUISE

1. The first aim of the cruise was to continue mapping of marine munition dumpsites, in order to execute a baseline study of the extent of contamination. Therefore, areas, which had been mapped in 2018 (POS530), were extended and areas of suspicious contacts were ground-truthed via AUV and TV-CTD.
2. The development of an artificial intelligence algorithm, which is able to identify munition based on a multi-sensor dataset is an aim of the BASTA project. During the cruise multi-sensor data were collected from munition sites including multibeam, magnetic and underwater photographs. This data will be used to train a neural network and improve automated contact picking.
3. The cruise was the very first field test of the newly developed 'ex-situ near-online STV analysis device' (a.k.a. Explotector) within the project ExPlOTect.

RESULTS

In the Kolberger Heide region, remapping of hot-spot areas allowed for the comparison of current munition positions to older data sets, revealing potential rearrangements. High-resolution AUV-basedbphotomosaics aided in the distinction of munition items from rocks on the seafloor. Initial results from water samples in this area showed substantial peaks

in TNT, RDX, and ADNT, but issues related to natural dissolved organic matter in water were identified. Future work will focus on eliminating these interferences and integrating the chemical data into the BASTA database for munition search and identification. While multibeam mapping of the Falshöft area revealed patterns of en-route dumping, but small-scale munition like grenades and cartridges could not be confirmed via multibeam.

In the central dumpsite of Haffkrug, munition was found east of the official site boundaries, with more than 200 possible contacts detected. The seafloor in the northern area is highly disturbed by anchor marks. The central area of Pelzerhaken contains over 1,000 contacts, with clusters of different munition types frequently found. AUV photos and TV-CTD footage revealed diverse munition components, including munition boxes, bombs, rockets, grenades, and grenade cartridges (Figure 2). The munition dumpsite was also used as dumpsite for heavy metal rich blast furnace ash, which created red and yellow-colored sediments and slag blocks, possibly affecting magnetic measurements.

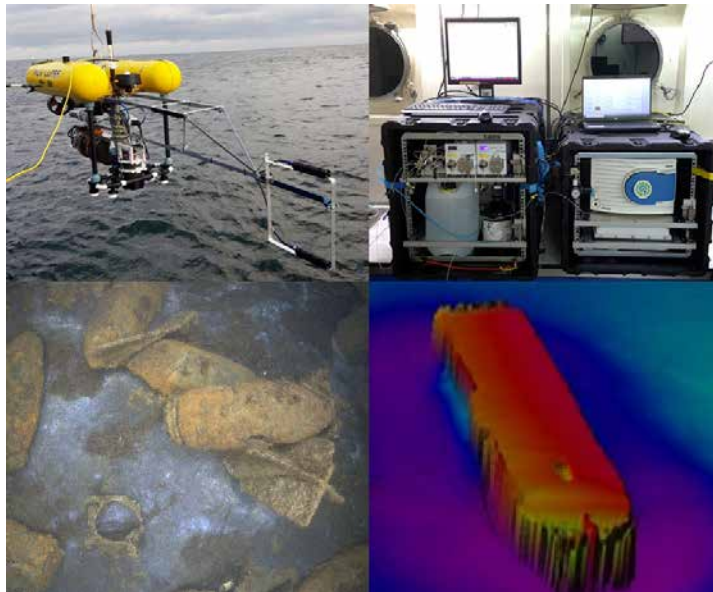


Figure 2: top left: Girona500 AUV with gradiometer array. Top right: Explodector for on board TNT Analysis. Bottom left: Grenades and bombs in the munition dumpsite Haffkrug. Bottom right: Capsized barge in Großklützhöved, which lost its munition load during sinking.

In Trollegrund, calibration of AUV-based magnetic sensors was performed since no distinct contacts were identified. During calibration, four single magnetic anomalies were detected accidentally. In Großklützhöved, mapping identified two sunken barges with munition and a large sediment mount, possibly created by sediment dumping from a nearby harbor.

Overall, the research involved mapping, identification, and analysis of munition and sediment in various underwater areas, with a focus on enhancing detection methods and understanding the seafloor's composition and potential interference factors.

REFERENCES

Kampmeier M, Greinert J, Strehse, J, Beck AJ, Wichert U, Diller N, Kurbjuhn T, Wenzlaff E, & Schröder J, RV Poseidon POS526 Cruise Report (Issue September) 2019, <http://oceanrep.geomar.de/id/eprint/47567>.

Kampmeier M, van der Lee EM, Wichert U, & Greinert J, Exploration of the munition dumpsite Kolberger Heide in Kiel Bay, Germany: Example for a standardised hydroacoustic and optic monitoring approach, *Continental Shelf Research* 2020, 198, 1–39. <https://doi.org/https://doi.org/10.1016/j.csr.2020.104108>.

Kampmeier M, RV LITTORINA L13-20 Cruise Report 04.–11.07.2020 BASTA, GEOMAR Helmholtz Centre for Ocean Research Kiel, Kiel, Germany, 15 pp.

Leipe T, Naumann M, Tauber F, Radtke H, Friedland R, Hiller A, Arz HW, Regional distribution patterns of chemical parameters in surface sediments of the south-western Baltic Sea and their possible causes, *Geo-Marine Letters* 2017, 37(6), 593–606. <https://doi.org/10.1007/s00367-017-0514-6>.

Leipe T, Kersten M, Heise S, Pohl C, Witt G, Liehr G, Zettler M, Tauber F, Ecotoxicity assessment of natural attenuation effects at a historical dumping site in the western Baltic Sea, *Marine Pollution Bulletin* 2005, 50(4), 446–459. <https://doi.org/10.1016/j.marpolbul.2004.11.049>.

SCIENTIFIC OUTPUT

LIST OF PUBLICATIONS

Frey T, Kampmeier M, Seidel M, Uncovering the secrets of German marine munitions dumpsites – High-performance UXO detection and visualization, *Hydro International* 2020, <https://www.hydro-international.com/content/article/uncovering-the-secrets-of-german-marine-munition-dumpsites>.

Kampmeier M, Michaelis P, Wehner D, et al., Workflow towards autonomous and semi-automated UXO Survey and Detection, *Proceedings of Meetings on Acoustics* 2021, doi: 10.1121/2.0001492.

Beck A J, Gledhill M, Kampmeier M, et al., Explosives compounds from sea-dumped relic munitions accumulate in marine biota, *Science of The Total Environment*, Volume 806, Part 4, 2022, 151266, ISSN 0048-9697, doi: 10.1016/j.scitotenv.2021.151266.

Frey T, Kampmeier M, Michaelis P, et al., Tackling Cost Drivers of Maritime UXO Surveys, NATO EOD Demonstrations and Trials 2021, conference paper, https://www.eodcoe.org/files/en/events/nato-eod-demonstrations-trials-2021/book-papers-demo-2021/book2021_16feb2022_corr.pdf.

LIST OF CONFERENCE PRESENTATIONS

2021 | **Towards automation and automatization of UXO detection in German Baltic Sea dump sites** Underwater Acoustic Conference and exhibition, Online.

2021 | **Workflow towards autonomous and semi-automized UXO Survey and Detection** Proceedings of Meetings on Acoustics 2021, Online.

2021 | **Tackling Cost Drivers of Maritime UXO Surveys** NATO EOD Demonstrations and Trials 2021, Bratislava, Slovakia.

DATA

As data on munitions is classified as sensitive data, the data could not be published publicly.

CRUISE REPORT

AL548: doi:10.3289/CR_AL548.

AL549 AND AL568B

First-time evidence for a shift in spawning phenology of Western Baltic cod

AUTHORS

University of Hamburg, Institute of Marine Ecosystem and Fishery Science |
Hamburg, Germany
S. Funk, C. Möllmann

MOTIVATIONAL BACKGROUND OF THE WINTER COD CRUISES

The Western Baltic cod (WBC) stock and the fisheries depending on it collapsed recently. Stock size is presently below the reference point $MSY B_{lim}$ (management biomass limit; ICES, 2023) and annual fishing opportunities for the fishery (i. e., total allowable catches) have been severely limited. Hence, since 2022 total allowable catch of WBC was set to a bycatch-quota only, posing a significant socio-economic threat to the German and Danish Western Baltic coastal fisheries.

A major obstacle to halting the stock decline and implementing a sustainable management of WBC is the poor knowledge of its ecology and population dynamics. Especially, the reasons for the mostly low recruitment (i. e., year-class strength) since the 2010s (ICES, 2023) are largely unknown. Recent studies have demonstrated that the population is already and will likely continue to suffer from the effects of climate change, i. e., ocean warming and ocean acidification (Voss et al. 2019, Funk 2020, Möllmann et al. 2021, Receveur et al. 2022). However, the complex mixture of processes leading variable reproductive success remained unclear so far (Hüssy, 2011; Hinrichsen et al., 2012; Hüssy et al., 2012).

A common process in Atlantic cod and other fish species affecting recruitment is a temporal shift in phenology, i. e., earlier spawning activity due to accelerated gonad maturation in response to changing thermal conditions (e. g., McQueen and Marshall, 2017) (Figure 1). Such phenological changes can include the entire or only parts of a population and can subsequently affect egg and larval survival.

The spawning season of cod in the Western Baltic Sea is known to extend from January to May but is assumed to peak in March (Kändler, 1944, 1961; Bleil and Oeberst, 1997, Bleil et al., 2009; Hüssy 2011). Spawning of cod in January has been already reported in studies from the 1940s and 1960s (Kändler, 1944, 1961). However, observed cod egg abundances have been very low compared to those observed later during February/March and have been only attributed to spawning activity in the Kiel Bight.

However, since temperatures have increased in the Western Baltic Sea during recent decades, both in winter (i. e., mild winters) as well as in summer (i. e., extended heatwaves) effects on cod phenology, such as observed in other ecoregions, seem likely (e. g., for North Sea & Irish Sea see McQueen and Marshall, 2017). First indications for a shift in spawning activity towards an earlier time in the year were provided by local gill net fishers and charter vessel captains located in the harbours of Burgstaaken and Heiligenhafen (Schleswig-Holstein, Germany) reporting the occurrence of increasing numbers of spawning cod individuals on their traditional spawning grounds within the channels of the Kiel Bight, Mecklenburg Bight and Fehmarn Belt already in January (pers. comm. local fishers).

This indication of a possible shift in the spawning phenology of WBCs prompted the University of Hamburg to propose the cruise programme for the "Winter Cod 2021–2025" cruises, which aims to (i) investigate whether a shift in the spawning activity of WBCs towards an earlier date can indeed be observed, and (ii) determine the extent of such an early winter spawning activity compared to the extent in the traditional main spawning season in March.

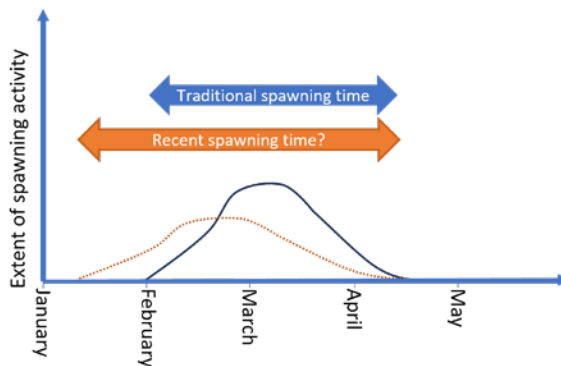


Figure 1: Schematic representation of a potential shift in spawning phenology of Western Baltic cod including both a shift towards earlier beginning of spawning activity and a change in the extent of spawning activity over the spawning period.

WINTER COD SAMPLING PROGRAM

Here we present the results from the first two out of five winter cod cruises of the University of Hamburg AL549 (January 2021) and AL568b (January 2022).

Originally, the cruise program of the winter cod cruises consisted of a station grid of a total of 35 ichthyoplankton stations in the Kiel Bight, Fehmarn and Mecklenburg Bight sampled via Bongo nets (150 μm , 300 μm , and 500 μm) to collect ichthyoplankton samples (fish eggs and larvae) as well as potential food organism (i. e. zooplankton with particular focus on Calanoid Copepods, known main prey organism of cod early life

stages). Ichthyoplankton sampling is supplemented by bottom trawling on spawning sites within the area to collect gonad samples to determine gonadal ripening stages of adult cod individuals. In 2021 the sampling program has been revisited and extended. From 2022 on, the sampling area comprised a grid of a total of 43 ichthyoplankton stations, with the additional 8 stations located in the little Belt and entrance of the Great Belt to cover a larger part of the Belt Sea area.

FIRST EVIDENCE FOR A SHIFT IN WBC SPAWNING

The first winter cod cruise in 2021 (AL549) already brought first evidence of early winter spawning activity of WBC in January in the Belt Sea. While WBC spawning activity in January has already been described for the Bay of Kiel, our observations of adult males and females in spawning stages in the Mecklenburg Bight represent, to our knowledge, the first scientific record of spawning activity in January in the eastern part of the Belt Sea. Overall, however, the trawl activities undertaken resulted in extremely low cod catches, which can be significantly linked to the extreme stock decline in 2020 (see ICES, 2023). Particularly noteworthy among the catches are the observations of large spawning individuals >70 cm in the Vejsnæs channel area, which may indicate that the early winter spawning activity of the WBC might be mainly attributed to larger and older individuals, so-called "super-spawners". In addition, first analyses of ichthyoplankton samples confirmed the presence of WBC larvae in the study area. While in the literature the observations of WBC larvae in the Kiel Bight were only based on a single occasion, we were able to observe a total number of 13 cod larvae in the Bongo 500 µm net samples over a total number of 35 ichthyoplankton stations in our study area. This included the observation of a cod larva in Mecklenburg Bight, which to our knowledge is also the first observation of a cod larva in this area so early in the year.

On the second winter cod cruise in 2022 (AL568b), significantly fewer larvae were observed, with a total of 3 larvae in the Bongo 500 µm net samples at 43 ichthyoplankton stations. In contrast to AL549, the sampling area in 2022 had been furthermore extended to stations in the Little Belt and entrance of the Great Belt area. At this stage, it can only be speculated whether and to what extent differences in hydrography and related differences in gonadal ripening have led to the observed differences in larval numbers between January 2021 and 2022. Unfortunately, a malfunction of the trawl winch prevented all planned trawl activities of the trip. In order to still be able to take maturity stage samples of adult WBC, the cruise participants developed an angling-based sampling design of shipwrecks in the study area. Surprisingly, the cod catches on the wrecks resulted in significantly higher numbers than the trawl catches during the previous cruise albeit the WBC stock in 2022 was even lower than in 2021. It was hypothesized that the higher catches on the wrecks could be attributed to a preference of WBC for hard structures such as wrecks even during the spawning season. Most of the cod on the wrecks showed maturity stages in the spawning stages. Running individuals were observed over the entire sampling area and thus also supported the results from 2021 for a shift of the spawning season of cod in the Mecklenburg Bight. Furthermore, we

observed surprisingly high proportion of juvenile females in the length classes 31–40 cm and 41–50 cm on the wreck sites, which have often only been observed in very small proportions in trawl surveys. This observation could possibly indicate a bias in classical trawl sampling due to the limited consideration of hard-structured areas (Funk et al. 2020, ICES 2021). The observation of spawning cod on wrecks at shallow 20 m depths showed that spawning and pre-spawning aggregations can also be found in shallower areas contrary to what has been assumed in the literature so far. Classically, the 20 m depth line is often associated with the limit for spawning activity of cod (Bleil and Oeberst 2002, Hüsey 2011, Eero et al. 2019). Management measures such as territorial restrictions on the activities of small gillnet vessels during the cod spawning season in the Western Baltic Sea are also based on this 20 m depth line. Our results, however, show that for a comprehensive protection of spawning and pre-spawning aggregations of WBC a fisheries closure in areas shallower than 20 m should be also considered.

REFERENCES

Bleil M, Oeberst R, The timing of the reproduction of cod (*Gadus morhua morhua*) in the western Baltic and adjacent areas, ICES CM 1997, CC: 02.

Bleil M, Oeberst R, Spawning areas of the cod stock in the western Baltic Sea and minimum length at maturity, *Archive of Fishery and Marine Research* 2002, 49: 243-258.

Bleil M, Oeberst R, Urrutia P, Seasonal maturity development of Baltic cod in different spawning areas: importance of the Arkona Sea for the summer spawning stock, *Journal of Applied Ichthyology* 2009, 25: 10–17.

Eero M, Hinrichsen, H-H, Hjelm J, et al., Designing spawning closures can be complicated: Experience from cod in the Baltic Sea, *Ocean & Coastal Management* 2019, 169: 129–136, doi: 10.1016/j.oceoaman.2018.12.018.

Funk S., Krumme U, Temming A, et al., Gillnet fishers' knowledge reveals seasonality in depth and habitat use of cod (*Gadus morhua*) in the Western Baltic Sea, *ICES Journal of Marine Science* 2020, 77(5): 1816–1829, doi: 10.1093/icesjms/fsaa071.

Funk S, Spatio-temporal distribution, food intake and growth of cod (*Gadus morhua* L.) in the Western Baltic Sea, *Doctoral Dissertation* 2020, University of Hamburg, Hamburg, Germany.

Kändler R, Untersuchungen über den Ostseedorsch während der Forschungsfahrten mit dem R.F.D. "Poseidon" in den Jahren 1925-1938, *Berichte der Deutschen Wissenschaftlichen Kommission für Meeresforschung* 1944, 11(2): 137–245.

Kändler R, Über das Vorkommen von Fischbrut, Decapodenlarven und Medusen in der Kieler Förde, *Kieler Meeresforschung* 1961, 17: 48–64.

Hinrichsen H-H, Hüsey K, Huwer B, Spatio-temporal variability in western Baltic cod early life stage survival mediated by egg buoyancy, hydrography and hydrodynamics, *ICES Journal of Marine Science* 2012, 69(10): 1744–1752, doi: 10.1093/icesjms/fss137.

Hüsey K, Review of western Baltic cod (*Gadus morhua*) recruitment dynamics, *ICES Journal of Marine Science* 2011, 68(7): 1459–1471, doi: 10.1093/icesjms/fsr088.

Hüsey K, Hinrichsen, H-H, Huwer B, Hydrographic influence on the spawning habitat suitability of western Baltic cod (*Gadus morhua*), *ICES Journal of Marine Science* 2012, 69(10): 1736–1743, doi: 10.1093/icesjms/fss136.

ICES, Cod (*Gadus morhua*) in subdivisions 22–24, western Baltic stock (western Baltic Sea), In Report of the ICES Advisory Committee 2023, *ICES Advice* 2023, cod.27.22–24, doi: 10.17895/ices.advice.21820494.

ICES, Inter-benchmark process on western Baltic cod (IBPWEB), *ICES Scientific Reports* 2021, 3:87, doi: 10.17895/ices.pub.5257.

McQueen K., Marshall CT, Shifts in spawning phenology of cod linked to rising sea temperatures, *ICES Journal of Marine Science* 2017, 74(6): 1561–1573, doi: 10.1093/icesjms/fsx025.

Möllmann C, Cormon X, Funk S, et al., Tipping point realized in cod fishery, *Scientific reports* 2021, 11: 14259, doi: 10.1038/s41598-021-93843-z.

Receveur A, Bleil M, Funk S, et al., Western Baltic cod in distress: decline in energy reserves since 1977, *ICES Journal of Marine Science* 2022, 79(4): 1187–1201, doi:10.1093/icesjms/fsac042.

Voss R, Quaas MF, Stiasny MH, et al., Ecological-economic sustainability of the Baltic cod fisheries under ocean warming and acidification, *Journal of Environmental Management* 2019, 238: 110–118, doi:10.1016/j.jenvman.2019.02.105.

DATA

AL549

Station data:

(currently under review at PANGAEA)

Physical oceanography:

(currently under review at PANGAEA)

Gadus morhua stomach content data:

(currently under review at PANGAEA)

Gadus morhua body and gonad measurements:

(currently under review at PANGAEA)

AL568b

Station data:

<https://doi.org/10.1594/PANGAEA.955079>

Physical oceanography (CTD):

<https://doi.org/10.1594/PANGAEA.956042>

Gadus morhua stomach content data:

<https://doi.org/10.1594/PANGAEA>

Gadus morhua body and gonad measurements:

<https://doi.org/10.1594/PANGAEA.955064>

CRUISE REPORT

AL549: doi: 10.3289/cr_al549

AL568b: doi: 10.3289/CR_AL568b

AL553 AND AL556

Baltic Sea Integrative Long-term Data Series & Baltic Cod 2021

AUTHORS

GEOMAR Helmholtz Centre for Ocean Research Kiel | Kiel, Germany
T. Reusch, J. Dierking

STUDY SYSTEM AND QUESTIONS

The Baltic Sea is a macro-regional sea under particularly pronounced anthropogenic pressures, including eutrophication, contaminant accumulation, fishing and non-indigenous species, as well as rapid vectors of change, most notably warming and the spread of oxygen minimum zones. It has therefore been identified as a “time machine” reflecting possible multiple-pressure futures of other coastal areas worldwide, and can serve as a test bed for marine environmental management under these conditions (Reusch et al 2018). The Baltic is also characterized by a horizontal salinity gradient from the connection to the North Sea in the west to the freshwater-dominated systems in the north-east. This leads to compositional changes in species pools and food webs along the salinity gradient as marine species “drop out” and freshwater species appear in the communities. Moreover, marine species such as cod are occurring at the very border of their distribution and environmental tolerance. The general question of the integrated long-term cruise program is thus as to how the interaction of hydrographic change and anthropogenic pressures affects the condition, reproduction, population size and population structure of individual species, as well as the structure and functioning of biological communities over time. More specific questions include whether change in the Baltic has revealed tipping points or regime shifts. Increasingly we also focus on the evolutionary perspective and ask how local adaptations and adaptation potential determine the fate of species in this system. Documented long-term overfishing exacerbates the precarious abiotic situation for many fish stocks, and may have contributed to distorted size and age distributions via fisheries-induced evolution. We will present recent results on signatures of selection and genomic changes in eastern Baltic cod based on analyses of our tissue and otolith collection at the conference.

CONCEPT OF THE BALTIC SEA INTEGRATIVE LONG-TERM DATA SERIES

Long-term data series have been highlighted as one of the best available tools to separate short-term fluctuations from long-term directional change (Lotze et al 2012), and thus to understand consequences of global change and anthropogenic pressures for biological systems. To address questions regarding the changing Baltic, the GEOMAR Helmholtz Centre for Ocean Research Kiel and its precursors have assembled one of the best available long-term data and sample series of the pelagic systems of the Baltic Sea,

spanning the time period 1986 to the present. The concept has been integrative, i. e., combining hydrographic assessments, surveys and sampling of the planktonic system (including jellyfish), and measurements and sampling of key fish species including cod, herring and sprat. The spatial focus has been on the deep, productive Bornholm Basin, home of the largest commercial fisheries in the Baltic, where the same station grid has been covered annually (Figure 1), but starting in 2021 has also included sampling on a station grid in Kiel and Mecklenburg Bight (western Baltic Sea) to contribute to the West Cod cruise program led by IMF-Hamburg University, as well measurements and sampling along the salinity gradient. The cruises AL553 in April and AL556 in May 2021 contribute to the long-term data series and West Cod program, but have also included additional, project-based work, including food web sampling for dietary tracer analysis and high-quality tissue sampling for genomic work. At the status conference, we will provide an overview of the outcomes and observations of the 2021 cruises, put these new observations in the context of the Baltic Sea Integrative Long-term Data Series, and then present examples of project applications and insights achieved with this data and sample treasure.

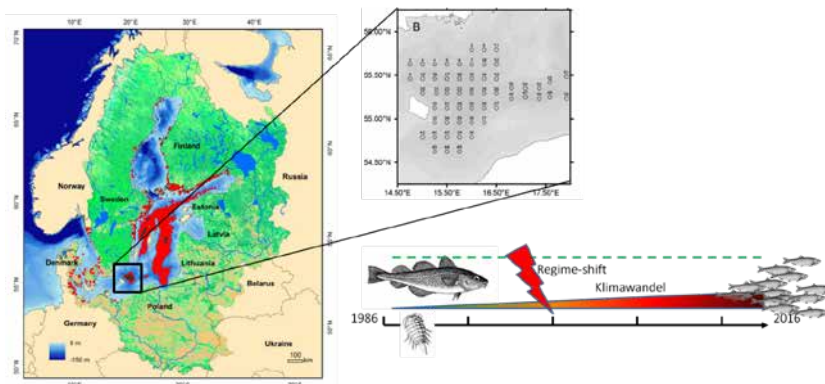


Figure 1: Study system Baltic Sea (left panel) with a close-up of the station grid in Bornholm Basin (cut-out) covered by the cruises AL553 and AL556 in 2021, and consistently throughout the Baltic Sea Integrative Long-term Data Series since the year 1986. During the time period 1986 to the present, a regime shift with spreading anoxia in deep water (red areas left panel), a corresponding decline of benthic fauna including the crustacean *Saduria entomon* and a shift from a cod-dominated to a planktivorous fish dominated system took place in the study area (depicted in the bottom right). Both cruises also covered additional stations in the Kiel and Mecklenburg Bight (western Baltic Sea) to contribute to the West cod cruise program by IMF-Hamburg University, and additional stations in the Arkona Basin and Gdansk Deep to cover part of the salinity gradient of the Baltic Sea.

PROJECT APPLICATIONS AND INSIGHTS ACHIEVED

We here focus on two core lines of work and output, changes in Eastern Baltic cod (EBC) size structure and individual growth rates in association with full genome data to identify a genomic basis of such change (Figure 2), and the characterization of the to date little described trophic interactions and food web positions of common Baltic Sea jellyfish species based on stable isotope analysis (Figure 3). In order to identify the "smoking

gun" of fisheries induced evolution as causal driver for the observed size structure declines, the EBC system is ideal as strong overfishing over long time has been well documented (ICES data), the population is no longer in exchange with the Western Baltic cod (Hemmer-Hansen et al. 2018), and there is a dramatic decline in phenotypic traits such as length at maturity (Reusch et al. 2018). At the conference, we will also give a brief overview of additional examples of time series output, including the use of data in cod stock assessments and the input to the Western Baltic cod cruise program on the spawning activity and larval occurrence of western Baltic cod. We close with a short perspective on the tremendous value of integrative long-term data series, including new questions that have arisen in the context of the current discussion regarding the possible establishment of a western Baltic Sea National Park, and on the application of new technology to increase the impact of cruise data for monitoring efforts.

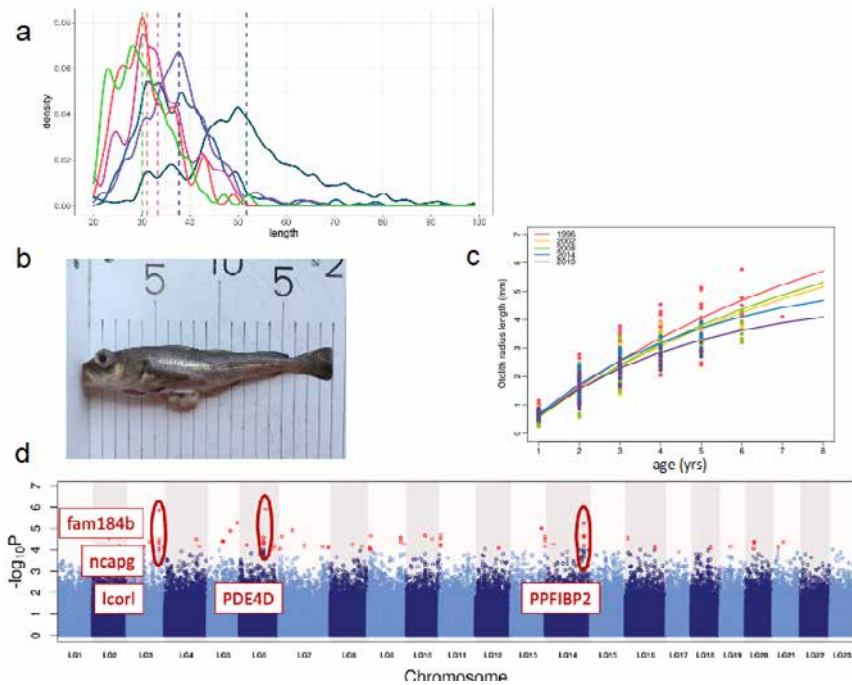


Figure 2: a, Size distribution density plot of the eastern Baltic cod catches 1996-2021, data basis GEOMAR cruises, compilation Kwi Young Han, GEOMAR. b, Mature female of Eastern Baltic cod with 20cm SL. c, Decline in individual growth rates in Eastern Baltic cod from 1996–2019, modelled according to the von Bertalanffy growth model. Age readings were based on otolith microchemistry and followed the novel method developed by Hussy et al. (2021). Unpublished data dissertation Kwi Young Han (GEOMAR) and Karin Hussy, DTU Aqua (Lyngby, DK). d, Full genome analysis of cod DNA attached to historical otoliths, and subsequent genome-wide association study (GWAS) based on >600,000 SNPs (single nucleotide polymorphisms) and regions associated with growth rate in samples of 152 cod individuals from 1996–2019. Marked outlier regions contain genes relevant for maturity, growth and life-history traits. Unpublished data dissertation Kwi Young Han & Thorsten Reusch (GEOMAR).

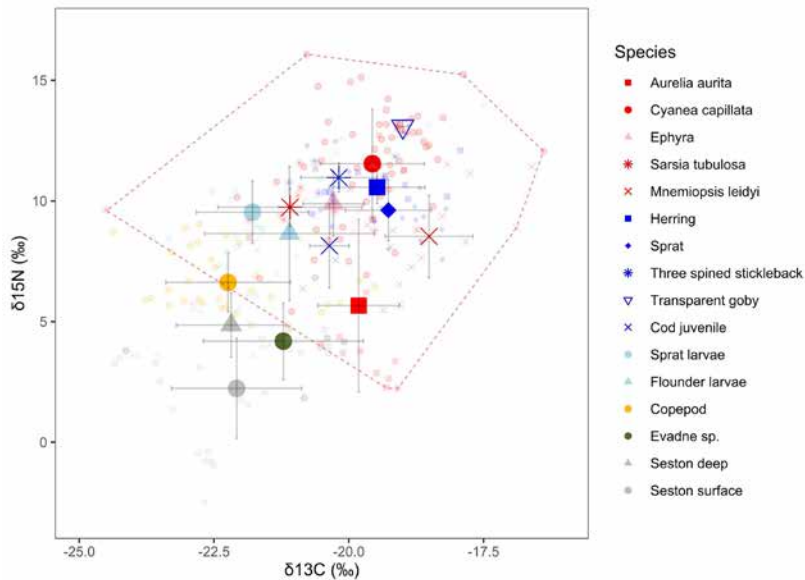


Figure 3: Characterization of the trophic positions and isotopic niches of common Baltic jellyfish species (red coloration) compared to larvae and adults of different Baltic fish species (blue coloration), based on N nitrogen (N) and carbon (C) stable isotope analysis of samples obtained during cruises AL553 and 556 as well as expeditions in previous years. $\delta^{15}\text{N}$ is a measure of the trophic position (higher values = higher trophic position), and $\delta^{13}\text{C}$ of organic matter sources at the base of the food web and of benthic versus pelagic feeding. Isotope values of organic material and primary consumers at the base of the food web (seston, *Evadne* sp.) and of copepods as common food source of jellyfish, fish larvae and planktivorous fish larvae) are given for reference. Large symbols represent mean values with error bars based on standard deviations. Smaller transparent symbols represent the single data points. The dashed red line represents the convex-hull area spanning the jelly-web (i. e., the isotopic niche covered by all jellyfish species combined), demonstrating the wide dietary niche covered by this group. At the status conference, we will provide a more in-depth discussion of the trophic role of jellyfish in the Baltic Sea by focusing on datasets with higher spatial and temporal resolution. The figure is part of the manuscript Stoltenberg et al. trophic interactions and food web position of Baltic Sea jellyfish species assessed with stable isotope and fatty acid analysis (in prep.)

REFERENCES

Hemmer-Hansen J, Hüsey K, Baktoft H, Huwer B, Bekkevold D, Haslob H, Herrmann J-P, Hinrichsen H-H, Krumme U, Mosegaard H, Nielsen EE, Reusch TBH, Storr-Paulsen M, Velasco A, von Dewitz B, Dierking J, Eero M, Genetic analyses reveal complex dynamics within a marine fish management area, *Evolutionary Applications* 2019, 12:830–844.

Hüsey K, Krüger-Johnsen M, Thomsen TB, Heredia BD, Næraa T, Limburg KE, Heimbrand Y, McQueen K, Haase S, Krumme U, Casini M, Mion M, Radtke K, It's elemental, my dear Watson: validating seasonal patterns in otolith chemical chronologies, *Canadian Journal of Fisheries and Aquatic Sciences* 2021, 78:551–566.

Köster FW, Huwer B, Kraus G, Diekmann R, Eero M, Makarchouk A, Örey S, Dierking J, Margonski P, Herrmann JP, Tomkiewicz J, Oesterwind D, Kotterba P, Haslob H, Voss R, Reusch TBH, Egg production methods applied to Eastern Baltic cod provide indices of spawning stock dynamics, *Fisheries Research* 2020, 227:105553.

Lotze HK, Sea of Plenty? Historical trends, current issues, and future perspectives on our use of seafood, in Food For Thought: A Multidisciplinary Discussion, R.S. Stewart and K. S.A., Editors. 2012, Cape Breton University Press.

Reusch TBH, Dierking J, Andersson HC, Bonsdorff E, Carstensen J, Casini M, Czajkowski M, Hasler B, Hinsby K, Hyytiäinen K, Johannesson K, Jomaa S, Jormalainen V, Kuosa H, Kurland S, Laikre L, MacKenzie BR, Margonski P, Melzner F, Oesterwind D, Ojaveer H, Refsgaard JC, Sandström A, Schwarz G, Tonderski K, Winder M, Zandersen M, The Baltic Sea as a time machine for the future coastal ocean, Science Advances 2018, 4: eaar8195.

SCIENTIFIC OUTPUT

LIST OF PUBLICATIONS

Jaspers C, Ehrlich M, Pujolar JM, Künzel S, Bayer T, Limborg MT, Lombard F, Browne WE, Stefanova K, Reusch TBH, Invasion genomics uncover contrasting scenarios of genetic diversity in a widespread marine invader, Proceedings of the National Academy of Sciences 2021, 118:e2116211118.

Stoltenberg I, Dierking J, Müller-Navarra DC, Javidpour J., Review of jellyfish trophic interactions in the Baltic Sea, Marine Biology Research 2021, 17:311-326, doi: 10.1080/17451000.2021.1964532.

LIST OF CONFERENCE PRESENTATIONS

2023 | **Trophic interactions in the rapidly changing western and central Baltic Sea** Jan Dierking: Invited presentation at the Stockholm University DEEP seminar series, Stockholm, Sweden

2023 | **Nationalpark Ostsee, mögliche Schutzkonzepte, Potenziale und Herausforderungen** Thorsten Reusch: Invited presentation for the CDU members of parliament Schleswig-Holstein, GEOMAR Kiel, Germany

2023 | **Gezielte Maßnahmen oder Blindflug – was wissen wir über die westliche Ostsee, und welche Rolle spielt dies für den geplanten Nationalpark Ostsee?** Jan Dierking: Invited presentation at the Runder Tisch Meerforschung Schleswig-Holstein, Umweltministerium Schleswig-Holstein, Kiel, Germany

2023 | **Meeresschutz und die Ostsee-Zeitmaschine – welche Lehren wir aus dem Randmeer vor unserer Haustür ziehen können** Jan Dierking and Thorsten Reusch: Visit of the "Meeresschutzbeauftragte" of the German federal government, Sebastian Unger, Kiel, Germany

DATA

AL553 Cruise data in the GEOMAR OSIS repository:

<https://portal.geomar.de/de/>

[kdmi;jsessionId=0B7AC6FDAB86F192C93DCE9DD2D09688#_48_INSTANCE_5P8d_=metadata%2Fleg%2Fshow%2F358406](https://portal.geomar.de/de/kdmi;jsessionId=0B7AC6FDAB86F192C93DCE9DD2D09688#_48_INSTANCE_5P8d_=metadata%2Fleg%2Fshow%2F358406)

AL553 Cruise data in the GEOMAR OSIS repository:

https://portal.geomar.de/de/kdmi;jsessionId=0B7AC6FDAB86F192C93DCE9DD2D09688#_48_INSTANCE_5P8d_=metadata%2Fleg%2Fshow%2F358411

CRUISE REPORT

AL553: [doi:10.3289/CR_AL553](https://doi.org/10.3289/CR_AL553).

AL556: [doi:10.48433/cr_al556](https://doi.org/10.48433/cr_al556).

AL557

Carbon Fluxes and their Controls in the North Sea

AUTHORS

Helmholtz Centre hereon GmbH | Geesthacht, Germany

H. Thomas*

* also at: *Institute for Chemistry and Biology of the Oceans, University of Oldenburg | Oldenburg, Germany*

We investigated the alkalinity formation in the Wadden Sea and the southern North Sea, as well as respective exchange processes with and impacts on the open North Sea. The new observations of this expedition constitute the pivotal point of the DAAD project “The ocean’s alkalinity: Connecting geological and metabolic processes and time-scales”, which has been funded by the BMBF as part of the German-French initiative “Make Our Planet Great Again” (MOPGA) in support of the Paris Agreement (COP21). The project addresses the role of oceans as regulators of atmospheric carbon dioxide (CO₂), thus making a crucial contribution to maintaining climate on Earth in a habitable range. This regulatory function is biogeochemically performed by the ocean’s CO₂ and pH buffer capacity: alkalinity. Alkalinity is generated by rock weathering, and by natural and human-induced anaerobic processes in sediments of coastal seas. The processes in coastal seas are related to eutrophication such that enhanced nutrient runoff increases alkalinity generation and the risk of deoxygenation and acidification. Climate change and its mitigation both have the potential to perturb the long-term stability of the ocean’s alkalinity: ice retraction will expose rock surface, hitherto covered, to weathering and erosion. Attempts to mitigate and lower atmospheric CO₂ levels will necessarily involve the use of bioenergy to a large extent, which in turn comes with the need to massively employ fertilizers and consequently, eutrophication of coastal seas. Our research will investigate in which measure and to which extent human activities and climate change affect the ocean’s alkalinity, particularly the impact of nitrogen fertilizers on coastal seas including the subsequent risk of acidification and deoxygenation. The project will be carried out collaboratively with the Universities of Oldenburg, Hamburg and Exeter (UK), and the Alfred Wegener Institute for Polar and Sea Research.

AL557: NUTRIENTS, TRACE ELEMENTS

Approximately 500 samples have been taken for dissolved inorganic carbon (DIC) and alkalinity (A_T), paralleled by approximately 100 samples for the two long-lived Radium isotopes ²²⁶Ra and ²²⁸Ra. These data are being used (Mears et al, 2024) to establish DIC and AT sources and transports into and out of the North Sea. A total of 265 water samples were analyzed for nutrient concentrations (ammonium, nitrate, nitrite, phosphate,

silicate) and 27 trace elements (e. g., copper, cobalt, iron, gadolinium, lanthanum, molybdenum, nickel). A principal component analysis of these results indicated riverine input for nutrients and anthropogenic trace elements (e. g., copper, cobalt, gadolinium), conservative mixing for molybdenum and uranium as well as primary production and remineralization of nutrients in the deeper waters of the northern North Sea (Przibilla et al., in prep).

The depth profiles for sediments and pore waters from the sampled muddy stations indicated distinct differences between Helgoland mud area and the Skagerrak which is a long-term depot-center for the North Sea. The Skagerrak sediments contained more organic carbon and overall fresher organic matter (indicated by nitrogen isotope analysis) than the Helgoland mud area sediments. The trace element concentrations (arsenic, copper, iron, lead, manganese, molybdenum) were also higher in the Skagerrak sediments, indicating higher accumulation of anthropogenic contamination here. Further, the pore water silicate data was used for a silica model (Spiegel et al, 2023).

Additional sediment samples from Multicorer and Van Veen Grab Sampler were subject to incubation experiments. Undisturbed sediment cores were used for the measurement of benthic fluxes of oxygen, nutrients, DIC and TA. Samples from the surface sediment were incubated in Flow-Through-Reactors (FTR) to measure reaction rates for oxygen consumption and nitrogen turnover. The employment of ¹⁵N-labeled stable isotope tracer enabled to disentangle ammonification, nitrification, and denitrification (Minutolo et al., in review). Additional sediment cores were sampled for vertical chlorophyll-a concentration profiles to estimate benthic fluxes of plankton-derived POC to the benthic particle diffusion rates. These results contributed to joint publication with the APOC project (Zhang et al., in review).

EMPIRICAL TREND

The inorganic carbon data from the AL557 cruise facilitate a long-term comparison with recent data set collected between 2001 and 2011. The basic intent is to compare these empirical trends (including AL557 data) with model output to better understand the change in inorganic carbon inventory over decadal time scales. The outcome of this comparison would then be useful for outcome of the project CARBOSTORE (e. g. climate focus paper), and the broader aim of quantifying carbon stocks and their change over time.

REFERENCES

Minutolo, F., Dähnke, K., Metzke, M., Holtappels, M., Neumann, A. (2023), Benthic oxygen and nitrogen process rates in the southern North Sea: Sedimentary mud and phaeophytin-a are reliable predictors of oxygen consumption and nitrogen turnover. Submitted to Continental Shelf Research, in review.

Przibilla, A., Zimmermann, T., Sanders, T., Pröfrock, D. (in preparation). Dissolved trace elements and nutrients in the North Sea – a current baseline.

Spiegel, T., A.W. Dale, N. Lenz, M. Schmidt, S. Sommer, H.T. Kalapurakkal, A. Przibilla, S. Lindhorst, Wallmann, K. (2023). Biogenic silica cycling in the Skagerrak. *Frontiers in Marine Science* 10: 1141448.

Zhang, W., Porz, L., Yilmaz R., Kuhlmann, J., Neumann, A., Liu, B., Müller, D., Spiegel, T., Holtappels, M., Ziebarth, N., Taylor, B., Wallmann, K., Kasten, S., Daewel, U., Schrum, C., Impact of bottom trawling on long-term carbon sequestration in shelf sea sediments. *ESS Open Archive*. February 07, 2023. DOI: 10.22541/essoar.167578408.84551876/v1.

Mears et al., (2024), The Skagerrak: the North Sea's as export gate for DIC and Alkalinity, in preparation (also MSc thesis, C. Mears).

SCIENTIFIC OUTPUT

LIST OF THESIS

Rohrweber, A.-C., PhD, Univ. Hamburg (2025)

Przibilla, A., PhD, Univ. Hamburg (2025)

Meyer, J., PhD, Univ. Oldenburg (2025)

Freund, W., PhD, Univ. Oldenburg (2025).

Minutolo, F., PhD, Univ. Hamburg (2024)

Mears, C., MSc, Univ. Hamburg, completed (2022)

Schröder, L., BSc, Univ. Hamburg, completed (2022)

CRUISE REPORT

AL557: doi:10.3289/CR_AL557

AL561

Reconstructing sediment deposition and provenance in the Skagerrak to characterize human impacts in the North Sea

AUTHORS

GEOMAR Helmholtz Centre for Ocean Research Kiel | Kiel, Germany

T. Spiegel, N. Lenz, S. Sommer, A. Dale, M. Schmidt

Aarhus University, Institute for Geoscience | Aarhus, Denmark

C. Böttner

INTRODUCTION AND OBJECTIVES

The AL561 research cruise was carried out in the framework of the project APOC ("Anthropogenic impacts on particulate organic carbon cycling in the North Sea"). It is a collaborative project between the research institutes GEOMAR, AWI, HEREON, UHH, and BUND to understand how particulate organic carbon (POC) cycling contributes to carbon sequestration in the North Sea. Since industrial times, the North Sea is affected by natural and human impacts including fisheries (pelagic fishers, bottom trawling), resource extraction (sand mining), offshore wind park constructions, sediment management (dredging) and eutrophication. Thereby it is crucial to comprehend how the marine carbon system is interlinked with these processes.

The Skagerrak represents the major sink area for fine-grained sediments from the North Sea region facilitated by low bottom current velocities that promote the settling of particles (Rodhe 1996; de Haas et al., 2002; Diesing et al., 2021). Furthermore, the Skagerrak serves as the primary depocenter for POC in the North Sea (Diesing et al., 2021), as the influx of fine-grained sediments carries significant amounts of POC into the area (van Weering et al., 1987). If any of the natural and human processes changed the sediment and POC budget in the North Sea, the effect can likely be seen in the sedimentary record of the Skagerrak.

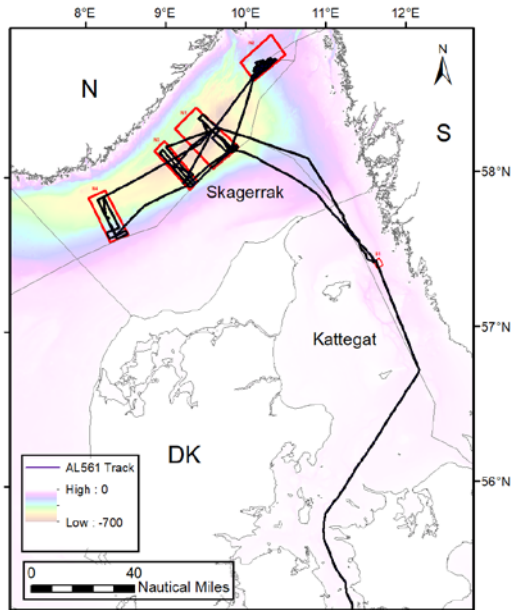


Figure 1: AL561 cruise track and main working areas in the Skagerrak and Kattegat (red boxes).

A major object of APOC targets the reconstruction of POC accumulation and sedimentation rates in the Skagerrak and whether it changed over time. The terrigenous mud and autochthonous marine particles are transported and redistributed by the tidally and wind driven current regime across the North Sea shelf which enter the Skagerrak by a cyclonic current pattern. To quantify the lateral influx of sediments and POC into the Skagerrak, a high-resolution age-depth model is established covering the last 120 years. The model utilizes the natural radionuclide ^{210}Pb in combination with the anthropogenic time markers ^{137}Cs , ^{14}C and mercury to identify the temporal variability in sedimentation rates. The solid phase and pore water geochemistry and benthic lander data are coupled to the precise age dating in a numerical reaction transport model to reconstruct historical POC variations at the seafloor and constrain the lateral POC transport under changing environmental conditions in the North Sea.

Another primary goal is to reconstruct the provenance of the sediments which are deposited in the Skagerrak. The origin and transport pathways of the sediments are reflected by its composition of radiogenic isotope ratios and mineralogy of fine-grained sediment fraction. Detrital sediment originating from the weathering of Precambrian Scandinavian rocks exhibit low $^{176}\text{Hf}/^{177}\text{Hf}$ and $^{143}\text{Nd}/^{144}\text{Nd}$ ratios but high $^{87}\text{Sr}/^{86}\text{Sr}$ ratios, whereas the sediment originating from central European rivers are characterized by the opposite trend. The clay mineral composition of the North Sea is dominated by illite and chlorite, which differs from smectite-dominated clay compositions originating from European rivers (Irion and Zöllmer, 1999). Surface sediment samples from

different parts of the North Sea are used to trace and characterize the most important sediment sources. By analysing the radiogenic isotopes and clay mineral compositions in Skagerrak sediments, it is feasible to identify and quantify the contributions of the principal source regions for the detrital sediment transported to the Skagerrak. This finding is applied to down-core sediments of the Skagerrak to assess temporal and spatial changes of sedimentary transport processes in the North Sea, which will help to evaluate influences of human activities and climate forcing factors in the last century.

FIRST RESULTS AND INTERPRETATION

During AL561 cruise 5 gravity cores and 9x7 multi-cores were recovered from high accumulation sites in the Skagerrak and Kattegat, where sampling licences had been approved by Norwegian and Swedish authorities (red boxes in Figure 1) to investigate sedimentation transport processes over the last 120 years. The coring sites were selected based on high-resolution subbottom profiling data, which was recorded during night-shifts. Subsampling of recovered sediment cores, i. e. porewater and sediment sampling, was conducted at high resolution in order to examine the origin of sediment and POC, sediment transport processes, and mineralization processes over time. Moreover, the processes of sedimentation and respiration in the water column and the benthic layer were considered by sampling of suspended matter and surface sediment with 4 CTD-Rosette and 3 Benthic Lander deployments.

Onboard processing of porewater samples was performed for dissolved ammonium, phosphate and silicate using standard methods (Grasshoff et al., 1997) on a Hitachi U-2001 spectrophotometer. Total alkalinity was measured onboard by titration with hydrochloric acid (Ivanenkov and Lyakhin, 1978).

Land-based analyses involved the measurement of nitrate and nitrite by spectrophotometry (Grasshoff et al., 2002). The composition of major elements in the pore waters was determined by ICP-OES. Sediment samples were analysed for organic and inorganic carbon using a EuroEA 3000 element analyser. Biogenic silica was measured by a wet-leaching procedure based on the method of Müller and Schneider (1993). Activities of ^{210}Pb and ^{137}Cs were measured by gamma spectrometry on n-type planar or coaxial Canberra Ge-detectors. Grain size distributions were measured with a laser-diffraction particle-sizer and evaluated based on graphical methods. Porosity was determined from the loss of water after freeze-drying the sediment samples.

The ^{210}Pb and ^{137}Cs data were integrated into age-depth models to determine the temporal variability of sedimentation rates. The sedimentation rates were combined with sediment, pore water and benthic lander data to set up transport reaction models to identify POC accumulation and turnover rates. Furthermore, machine learning models were applied to spatially upscale ^{210}Pb and porosity data to calculate mass accumulation rates and provide a sediment budget across the Skagerrak region.

Sediment samples were analysed for radiogenic Sr, Nd, and Hf isotope compositions of the detrital clay-size fraction as well as for semiquantitative clay mineral analyses. For separation and purification of Sr, Nd, and Hf, standard ion chromatographic procedure was applied (Cohen et al., 1988; Galer & O'Nions, 1989; Pin & Zalduegui, 1997). The radiogenic isotope measurements were performed on a Nu Plasma high-resolution multi-collector inductively coupled plasma mass spectrometer (MC-ICP-MS). For clay mineral analyses, the clay fraction was measured at the University of Kiel (CAU) by x-ray diffractometry (XRD) using a D8 Discover (Bruker AXS) with a Cu-cube as well as θ - θ geometry.

Skagerrak – Recent change of sedimentation rate

First results of the age-depth model reveal a consistent net decrease in sedimentation rates across six stations in the Skagerrak (Figure 2). The model adequately reproduces the measured radionuclide and mercury data by setting a single sedimentation rate decline at 1963. On average, sedimentation rates decreased from 0.36 to 0.15 cm yr⁻¹ during this period. We hypothesize that the observed decline in sedimentation rates is the result of a weakening of the Central North Sea Current between 1960–1990. Since this period, less material was likely carried to the Skagerrak on a direct pathway through the central North Sea. Instead, the sediment was transported through the southern North Sea, where the large sediment catchment areas of the Wadden Sea likely reduced the sediment load before it reached the Skagerrak. However, we stress that the available data does not allow for a quantitative analysis of the reasons behind the sedimentation rate decline in the Skagerrak. Hence, our findings demonstrate the need for a more comprehensive understanding of the controls on sedimentation rate decline, particularly in the dynamic North Sea environment where human and natural processes interact. We recommend to constrain our results by examining additional sediment cores in the Skagerrak and integrating this data into larger-scale physical models that consider non-steady state particle transport in the North Sea. Furthermore, it is essential to investigate and quantify the temporal evolution of natural and anthropogenic impacts in the North Sea, i. e. by identifying the temporal variability of the provenance of sediments transported into the Skagerrak.

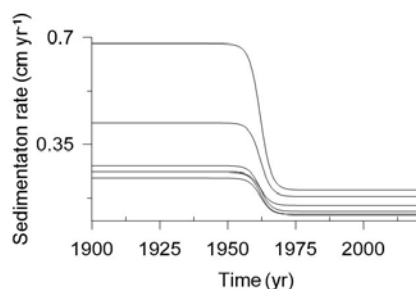


Figure 2: Change in sedimentation rates in the Skagerrak since 1900. The presented single change at 1963 is the model configuration designed to achieve the best fit to the radionuclide and time marker data. The change in sedimentation rates is modelled using a Boltzmann equation for a smoothed transition.

Main provenance of trapped sediment

The provenance dataset reveals geographical areas of distinct isotopic compositions and concentrations of clay mineral phases of illite, kaolinite, chlorite and smectite. Surface sediment samples in the southern North Sea transported from European rivers and the Baltic Sea area are characterized by high $^{143}\text{Nd}/^{144}\text{Nd}$ -ratios and low $^{87}\text{Sr}/^{86}\text{Sr}$ -ratios. In contrast, surface sediments collected from Scandinavian fjords and Baltic Sea flowing into the Skagerrak exhibit low $^{143}\text{Nd}/^{144}\text{Nd}$ -ratios but high $^{87}\text{Sr}/^{86}\text{Sr}$ -ratios (Figure 3). Moreover, the distribution pattern of the clay minerals shows high smectite contents in the Southern North Sea, especially in the German Bight. High concentrations of illite and chlorite were detected in the northern and central part of the North Sea as well as in the Scandinavian fjords. Radiogenic isotope signatures and clay mineral contents in sediments from the central part of the Skagerrak suggest a mixture of sediments originating from old crustal rocks from Scandinavia and younger volcanic rocks from central Europe. Thereby the material derived from the Atlantic, Scandinavia and European rivers representing the main sediment sources. The combination of radiogenic isotopes and clay mineral data suggests that the Atlantic is a predominant source for the Skagerrak sediments. In contrast, Scandinavian fjords and central European rivers appear to be minor contributors to the main depocenter of the North Sea.

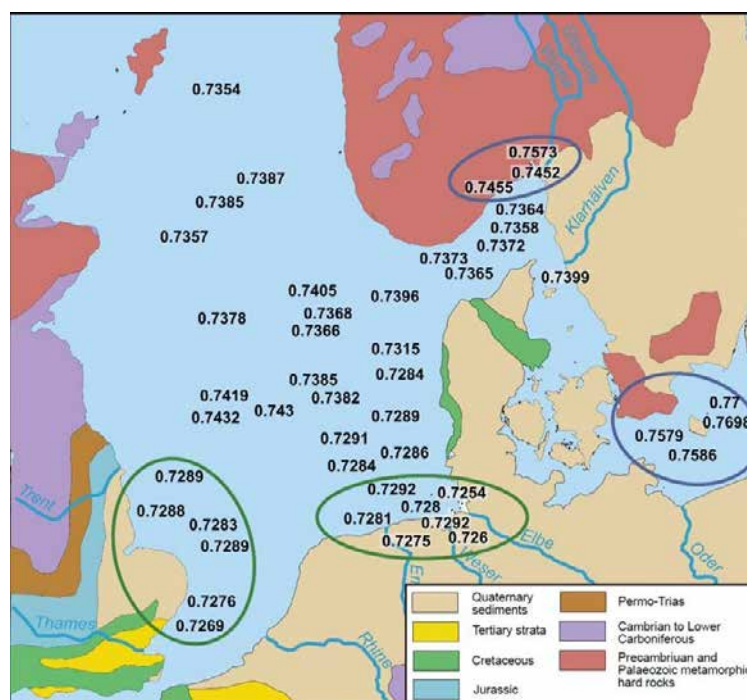


Figure 3: Change in sedimentation rates in the Skagerrak since 1900. The presented single change at 1963 is the model configuration designed to achieve the best fit to the radionuclide and time marker data. The change in sedimentation rates is modelled using a Boltzmann equation for a smoothed transition.

CONCLUSION AND OUTLOOK

In order to test our hypothesis for the decline in sedimentation rates in the Skagerrak, we aim to extend the provenance study from surface sediments to the entire down-core lengths. Identifying potential alterations in the relative contributions from various sediment source regions over time might give insight into the reasoning for the sedimentation rate decrease in 1963 in the Skagerrak. A second step forward is to integrate the transient sedimentation rates into numerical transport reaction models to quantify POC turnover rates in the Skagerrak and the lateral POC input from the North Sea over time.

ACKNOWLEDGEMENTS

This research cruise was approved by the “Gutachterpanel Forschungsschiffe” of the German Research Foundation under license no. GPF 21-2_028.

We highly acknowledge the financial support from BMBF, which was granted to GEOMAR under ID 03F0874B to conduct this research cruise and the subsequent experiments and analyses.

REFERENCES

Cohen AS, O'Nions RK, Siegenthaler R, Griffin WL, Chronology of the pressure-temperature history recorded by a granulite terrain, *Contributions to Mineralogy and Petrology* 1988, 98, 303–311.

de Haas H, van Weering TCE, Recent sediment accumulation, organic carbon burial and transport in the northeastern North Sea, *Marine Geology* 1997, 136, 173–187.

de Haas H, van Weering TCE, de Stigter H, Organic carbon in shelf seas: sinks or sources, processes and products, *Continental Shelf Research* 2022, 22, 691–717.

Diesing M, Thorsnes T, and Bjarnodottir LR, Organic carbon densities and accumulation rates in surface sediments of the North Sea and Skagerrak, *Biogeosciences* 2021, 18, 2139–2160.

Galer SJG, O'Nions RK, Chemical and Isotopic Studies of Ultramafic Inclusions from the San Carlos Volcanic Field, Arizona: A Bearing on their Petrogenesis, *Journal of Petrology* 1989, 30, 1033–1064.

Grasshoff K, Erhardt M, Kremling K, *Methods of Seawater Analysis*, Wiley-VCH, Weinheim.

Irion, G., Zöllmer, V., 1999, Clay mineral associations in fine-grained surface sediments of the North Sea, *J. Sea Research* 2002, 41, 119–128.

Ivanenkov VN, Lyakhin YI, Determination of the alkalinity of seawater. *Methods Hydrochem. Stud. Ocean* 110–115. Rodhe J., 1996. On the dynamics of the large-scale circulation of the Skagerrak, *Journal of Sea Research* 1978, 35 (1–3), 9–21.

Müller PJ, Schneider R, An automated leaching method for the determination of opal in sediments and particulate matter, *Deep Sea Research Part I: Oceanographic Research Papers* 1993, 40 (3), 425–444.

Pin C, Zalduegui JFS, Sequential separation of light rare-earth elements, thorium and uranium by miniaturized extraction chromatography: Application to isotopic analyses of silicate rocks, *Analytica Chimica Acta* 1997, 339, 79–89.

van Weering TCE, Berger GW, Kalf J, Recent sediment accumulation in the Skagerrak, Northeastern North Sea, *Neth. J. Sea Res.* 1987, 21, 177–189.

Wells AK, Kirkaldy JF, *Outline of historical geology* 1966, (6th ed.). Th. Murby, London.

SCIENTIFIC OUTPUT

LIST OF PUBLICATIONS

Spiegel T, Dale AW, Lenz N, Schmidt M, Sommer S, Kalapurakkal HT, Przibilla A, Lindhorst S, Wallmann K, Biogenic silica cycling in the Skagerrak. *Front. Mar. Sci.* 2023, 10, 1141448. <https://doi.org/10.3389/fmars.2023.1141448>.

Zhang W, Porz L, Yilmaz R, Kuhlmann J, Neumann A, Liu B, Müller D, Spiegel T, Holtappels M, Ziebarth N, Taylor B, Wallmann K, Kasten S, Daewel U, Schrum C, (Submitted), Impact of bottom trawling on long-term carbon sequestration in shelf sea sediments. Open Access ESS Open Archive. DOI 10.22541/essoar.167578408.84551876/v1.

LIST OF CONFERENCE PRESENTATIONS

2023 | Lenz, N., Spiegel, T., Hathorne, E., Wallmann, K., Frank, M., **Reconstruction of the provenance of detrital sediments in the Skagerrak region by using radiogenic Nd-Sr-Hf isotopes and clay mineral.** Goldschmidt Conference, Lyon, France.

DATA

All data currently stored at OSIS data repository (Ocean Science Information System, GEOMAR, Kiel):

https://portal.geomar.de/kdmi#_48_INSTANCE_5P8d_=metadata%2Fleg%2Fshow%2F359126

Atmospheric CH₄/CO₂/H₂O data:

Schmidt, M., Weiß, T. (2022), Continuous atmospheric gas monitoring using PICARRO CRDS; CH₄/CO₂/H₂O data, georeferenced with dship data.

Depth/Conductivity/Temperature/Oxygen/Sound-velocity/Salinity/Density/

Fluorescence/ Turbidity data:

Schmidt, M. (2023), Georeferenced sensor data of a Video-CTD device (4 hydrocasts).

Alkalinity/Major elements/Trace elements/Cl/SO₄/Nutrients/Porosity/TOC/TIC/TN data:

Spiegel, T., Lenz, N., Dale, A., Sommer, S. (2023), Porewater and sediment geochemistry of gravity core-, MUC-, and BIGO Lander samples.

SES2000/EK60 data:

Böttner, C. (2023), Single beam hydroacoustic water column data and sediment echosounder raw data and SEG Y data.

CRUISE REPORT

AL561: <https://oceanrep.geomar.de/id/eprint/54458/>

AL568

A test cruise of the LIGHTHOUSE ROV System

AUTHORS

GEOMAR Helmholtz Centre for Ocean Research Kiel | Kiel, Germany
T. Kwasnitschka, H. Hauss, V. Stenvers, M. Rohleder, O. Jahns

The operation of remotely operated vehicles (ROV) in the deep sea is severely impaired by the lack of omnidirectional vision, a short range of visibility and lack of standardized imaging workflow. This leads to diminished situational awareness of pilots and mission specialists, inefficient maneuvers and a low amount of gathered intelligence that falls far behind operational or scientific requirements.



Figure 1: ROV PHOCA with the LIGHTHOUSE modifications during the deployment.

The goal of the Helmholtz Validation Fund Project 68 LIGHTHOUSE was to construct an integrated omnidirectional imaging framework that will allow both overview and close-up scans of the environment around a dynamically moving ROV. The project has the following components:

1. Core element is the SeaVision camera and structured light system developed by Kraken. Functionality of this system was expanded to meet the requirements of this project. 3 of these units were placed around an ROV, delivering a real-time 3D point cloud of the environment.

2. The GEOMAR LED lighting technology was integrated with SeaVision to form a lighting array that can be flexibly controlled to minimize light scattering.
3. A line of point of interest cameras was developed, resulting in both a wide-field navigation camera and a high resolution camera for scientific purposes, using custom metric optics developed by Zeiss. These cameras were interfaced with the overall system and timed to the global lighting system.
4. A topside visualization environment was based on a contemporary gaming engine including support for VR devices.

The objective of this cruise was to conduct the final and complete field test of the LIGHTHOUSE situational awareness system for remotely operated vehicles, developed in the HVF 0068 Project LIGHTHOUSE. This included three dives of the ROV PHOCA in the Norwegian Sognefjord, during which the optical and acoustic sensors were validated. Moreover, as part of the EU H2020 project iAtlantic (grant agreement 818123), we investigated the response of pelagic deep-sea fauna to warming and suspended sediment (which will be introduced to pelagic ecosystems by deep-sea mining activities). To this end, we captured the jellyfish *Periphylla periphylla* and conducted shipboard experiments.

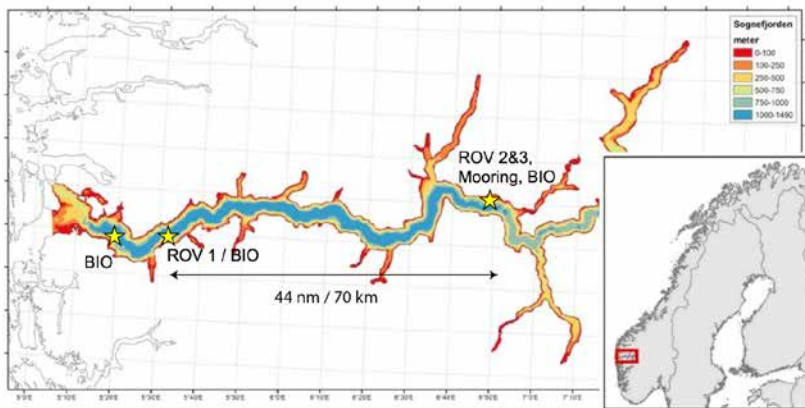


Figure 2: Positions (asterisks) of R/V ALKOR Cruise AL568 stations within the Sognefjord. Compare the station list for details on biological sampling. Modified from Buhl-Mortensen et al, 2020.

REFERENCES

Buhl-Mortensen L, Buhl-Mortensen P, Glenner H, Bamstedt U, Bakkeplass K, The inland deep sea-benthic biotopes in the Sognefjord. in: Seafloor geomorphology as benthic habitat, Elsevier 2020, S. 355-372. doi: 10.1016/B978-0-12-814960-7.00019-1.

SCIENTIFIC OUTPUT

Please note that the main objective of the cruise were technical field trials that did not produce scientific products.

LIST OF PUBLICATIONS

Stenvers VI, Hauss H, Bayer T, Havermans C, Hentschel U, Schmittmann L, Sweetman A, Hoving HJT, Experimental mining plumes and ocean warming trigger stress in a deep pelagic jellyfish. *Nature Communications* 2023.
<https://doi.org/10.1038/s41467-023-43023-6>.

LIST OF CONFERENCE PRESENTATIONS

2023 | **Impacts of global warming and deep-sea mining induced sediment plumes on midwater animals** iAtlantic Final General Assembly, Online.

2022 | **Impacts of global warming and deep-sea mining induced sediment plumes on midwater animals** iAtlantic Final General Assembly, Online.

2022 | **Impacts of global warming and mining induced sediment plumes on the midwater medusae *Periphylla periphylla*** Smithsonian NMNH No Bones Lunch Seminar, Washington D.C., USA.

2022 | **Impacts of global warming and mining induced sediment plumes on the midwater medusae *Periphylla periphylla*** Ocean Science Meeting, All virtual conference.

2021 | **Impacts of global warming and mining induced sediment plumes on the midwater medusae *Periphylla periphylla*** 16th Deep-Sea Biology Symposium, Brest, France.

DATA

Biological data: Stenvers, Vanessa; Hauss, Helena; Schmittmann, Lara; Bayer, Till; Havermans, Charlotte; Hentschel, Ute; Sweetman, Andrew K; Hoving, Henk-Jan T (2023), Physiological and behavioural responses of the deep pelagic jellyfish *Periphylla periphylla* exposed to sediment plumes and increasing temperatures. PANGAEA, <https://doi.org/10.1594/PANGAEA.957367>

CRUISE REPORT

AL568: DOI 10.3289/cr_al568.

EMB214

Integrated carbon and Trace Gas monitoring for the Baltic sea (BONUS INTEGRAL) – Summer verification

AUTHORS

Leibniz-Institute for Baltic Sea Research Warnemünde | Rostock, Germany

G. Rehder, H. Bittig, E. Jacobs, M. Kolbe, L. Kreuzer, S. Otto

University of Rostock | Rostock, Germany

S. Velasco-Sobeck

Uppsala University | Uppsala, Sweden

L. Gutierrez Loza

Institute of Oceanology of the Polish Academy of Sciences | Sopot, Poland

K. Koziorowska, P. Makuch

Tallinn University of Technology, Department of Marine Systems | Tallinn, Estonia

S. Lainela

Finnish Meteorological Institute | Helsinki, Finland

M. Honkanen

SCOPE AND FIELD CAMPAIGN OVERVIEW

The cruise INTEGRAL SUMMER, which took place in the Baltic Sea from May 21st to June 3rd 2019, was one of two cruises which served the overall scope of the BONUS Blue Baltic Project BONUS INTEGRAL. Cruise EMB 214 was the “early summer” counterpart of cruise INTEGRAL WINTER, which had taken place on R/V Aranda in February 2019. The project aimed to provide seasonal basin-wide maps for pCO₂, pCH₄, and, if possible, pN₂O for the Baltic Sea, to improve the carbon system understanding, and to demonstrate the value and representativeness of systems continuously monitoring carbon system and trace gas parameters for the ecosystem monitoring of the Baltic Sea.

During INTEGRAL SUMMER, the ship traversed all major Baltic Sea basins, continuously surveying surface trace gas distribution, pH, parameters with the potential to be used for smart extrapolation algorithms, and standard hydrographical parameters. The cruise track has been designed for best assessment of the areas for which the continuously operating instrumentation on the SOOP (Ship Of Opportunity) lines and fixed stations in the BONUS INTEGRAL network are representative, and for detailed studies in coastal gradient systems. The work program was complemented by several vertical CTD/rosette

deployments for the investigation of the vertical structure of the carbon system and trace gases, with special emphasis on the Gulf of Bothnia, where a special focus addressed the C/N/P dynamics. To foster our understanding of drivers for coastal gradients, a series of hydrographical sections using the ScanFish was recorded.

The work program was designed to close gaps in existing data series in space and time and the interpretation and work up of the results has to be seen in that context.

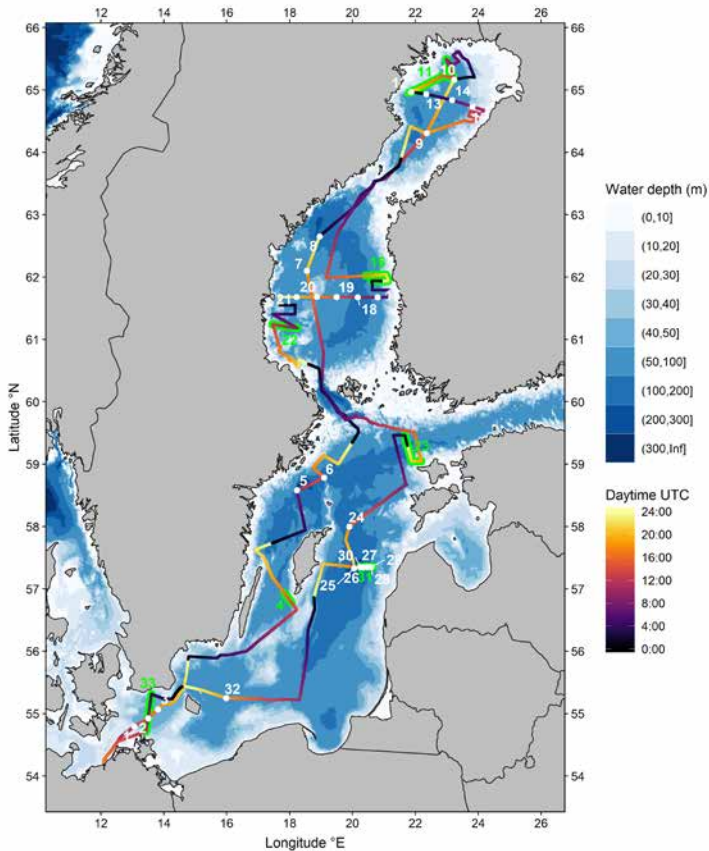


Figure 1: Cruise Track for the BONUS INTEGRAL summer cruise, May 21st to June 5th 2019, with underlying bathymetry. The color code of the track indicates the time of day (UTC). CTD sampling stations are indicated as white dots, ScanFish Transects as green lines.

SURFACE PCO₂ AND GHG DATA

One of the core actions of the cruise was a continuous surface survey of pCO₂, pCH₄, pN₂O, pO₂, pH, and various auxiliary data. The cruise track was designed to a.) retrieve data from areas rarely sampled for GHGs and b.) to provide information on cross-slope gradients of the observed parameters. The latter task served as an evaluation of the

representativeness of data from several autonomous platforms within the research consortium, including stationary (moorings) and commuting (SOOP lines), in some cases related to the European ICOS Research Infrastructure (ICOS RI). For the dissolved gases, a bubble-type air-sea equilibration system linked to a series of cavity enhanced absorption spectrometers (CEAS) was used, as described in Sabbaghzadeh et al., (2021) and (Gülzow et al., 2011). An overview of the data for the mole fractions of carbon dioxide and nitrous oxide is given in Figure 2.

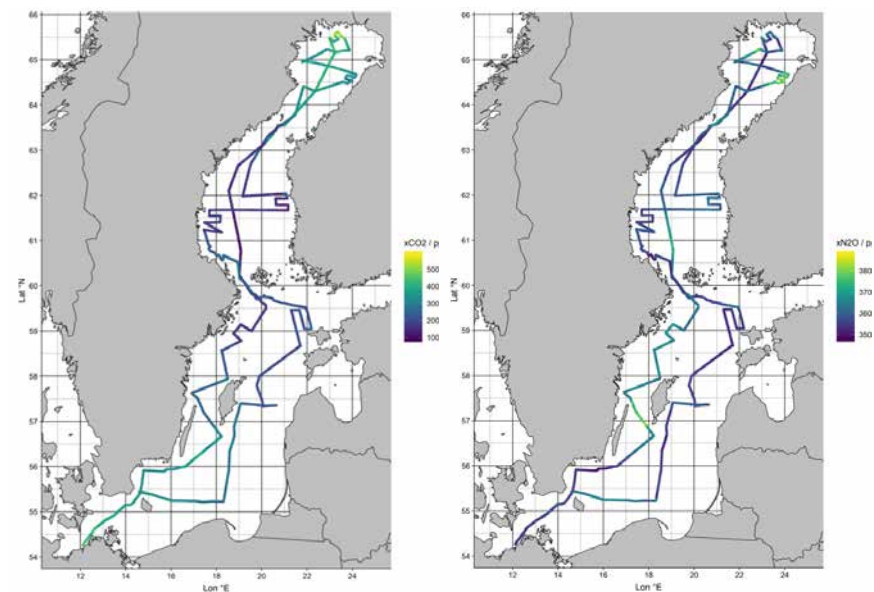


Figure 2: Representation of $x\text{CO}_2$ (left) and $x\text{N}_2\text{O}$ (right) along the entire cruise track.

Recently, the data of the BONUS INTEGRAL SUMMER (EMB 214) and WINTER cruise were used, together with data from SOOP Finnmaid and SOOP Tavastland operated by partners of the consortium, to derive a $p\text{CO}_2$ climatology for the Baltic Sea (Bittig et al., 2024 in press). To do so, the data served as backbone for a smart interpolation based on the main patterns of variability derived from a 3D-ecosystem model (Neumann et al., 2022).

CARBON SYSTEM PARAMETERS IN THE NORTHERN BASINS

The joined interpretation of carbon system and $p\text{CO}_2$ data from the BONUS INTEGRAL winter and summer cruises, for the first time, allowed for a data-constrained estimate of the net carbon production for the Bothnian Sea. Here, the timing of cruise 214 of R/V Elisabeth Mann Borgese was perfect in that the vessel traversed the Bothnian Sea directly after the spring bloom, with maximum imprint of spring production on surface $p\text{CO}_2$ and surface total carbon, while the winter cruise on R/V Aranda had taken place prior to the

onset of spring primary production. As a consequence, the related change in the surface layer total carbon content gives a good approximation of the net carbon removal during the spring bloom. Minimum $p\text{CO}_2$ in the Bothnian Sea was below $100 \mu\text{atm}$, and values mostly between 100 and $200 \mu\text{atm}$. This is far below the minimum values for $p\text{CO}_2$ of 200 – $250 \mu\text{atm}$ in the model by (Fransner et al., 2019), suggesting an underestimation of the carbon uptake during the spring bloom in our current understanding of the biogeochemistry of the Bothnian Sea.

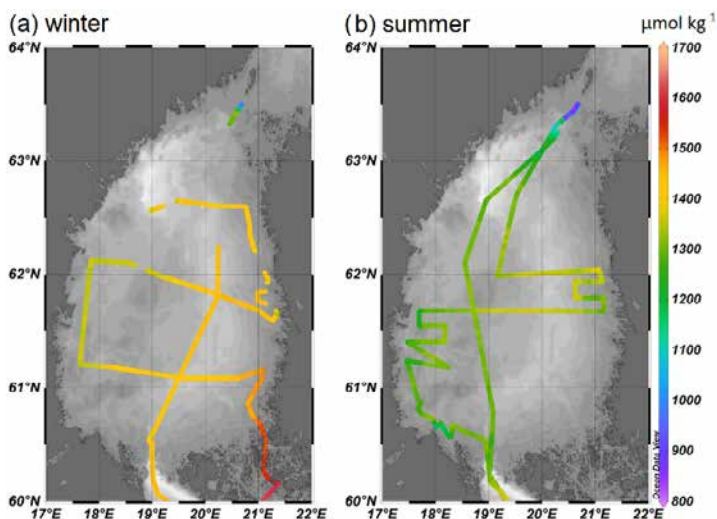


Figure 3: Surface dissolved inorganic carbon calculated from partial pressure of carbon dioxide and parameterized alkalinity.

This is confirmed by a calculated loss of DIC in the central Bothnian Bay based on direct DIC measurement comparison as well as comparison of the DIC derived from the $p\text{CO}_2$ survey (Figure 3). This work has been presented at the Baltic Earth Science conference in 2022 and is currently in preparation for publication (Honkanen et al., 2022).

N₂O DYNAMICS IN A CROSS-SLOPE TRANSECT

During the cruise, a transect of eight stations was sampled from the central Gotland Deep across the Latvian slope, extending to waters shallower than the depth of the halocline and redoxcline, which separated oxygenated water above from the euxinic deep waters. The scope of this sampling campaign was to investigate the nitrous oxide cycling by using N_2O concentration fields and isotopic fingerprinting including stable ^{15}N and ^{18}O , as well as site preference of N-isotopes in N_2O . The results suggest simultaneous production by denitrification and consumption of nitrous oxide in the euxinic waters, and enhanced production of nitrous oxide in the sediments in the suite of temporary re-oxidation events (Bardhan et al., in prep).

THE SOCIAL AND NETWORKING COMPONENT

Cruise EMB 214 was also a strategic component of the networking and education component of the BONUS Blue Baltic project BONUS INTEGRAL. While basically all equipment was provided by IOW, six pH students from 5 different host institutes in five pan-Baltic nations took part in the cruise, all involved in the lab work and deepening their understanding in the analytical procedures of carbon system and trace gas measurements. The cruise also hosted a master thesis and provided data for a Humboldt Post Doc fellowship (P. Bardhan). Moreover, on May 26th, EMB reached its northernmost position at 65°37,15N; 23° 22,44E, after a night without real darkness, about as far North as you can travel in the Baltic, farther North than the Elisabeth Mann Borgese ever reached, which motivated a memorable group photo with crew and scientific party in “the very North”.



Figure 4: Group Photo with insert map on the northernmost position RV Elisabeth Mann Borgese ever reached.

REFERENCES

Fransner F, Gustafsson E, Tedesco L, Vichi M, Hordoir R, Roquet F, Nycander J, Non-Redfieldian Dynamics Explain Seasonal pCO₂ Drawdown in the Gulf of Bothnia, *Journal of Geophysical Research: Oceans* 2018, 123(1), 166–188, doi:10.1002/2017jc013019.

Gülzow W, Rehder G, Schneider v. Deimling J, Seifert T, Tóth Z, One year of continuous measurements constraining methane emissions from the Baltic Sea to the atmosphere using a ship of opportunity, *Biogeosciences* 2011, 10, 81–99, doi:10.5194/bg-10-81-2013.

Sabbaghzadeh B, Arévalo-Martínez D L, Glockzin M, Otto S, Rehder G, Meridional and Cross-Shelf Variability of N₂O and CH₄ in the Eastern-South Atlantic, *Journal of Geophysical Research: Oceans* 2021, 126(11), doi:10.1029/2020jc016878.

Neumann T, Radtke H, Cahill B, Schmidt M, Rehder G, Non-Redfieldian carbon model for the Baltic Sea (ERGOM version 1.2) – implementation and budget estimates, *Geoscientific Model Development* 2022, 15(22), 8473–8540, doi:10.5194/gmd-15-8473-2022.

SCIENTIFIC OUTPUT

LIST OF PUBLICATIONS

Bittig HC, Jacobs E, Neumann T, Rehder G, A regional pCO₂ climatology of the Baltic Sea from insitu pCO₂ observations and a model-based extrapolation approach, *Earth System Science Data* (in press).

Bardhan P, Frey C, Rehder G, Bange HW, The distribution and isotopomeric characterization of nitrous oxide in the Eastern Gotland Basin (central Baltic Sea), in prep.

Velasco Sobeck S, Methan und Distickstoffmonoxid in den nördlichen Becken der Ostsee, Scientific thesis as part of the first state examination for the teaching profession Gymnasium , 66 pages (in German), 2020.

LIST OF CONFERENCE PRESENTATIONS

2022 | **An estimate of the net carbon production in the Bothnian Sea during the spring bloom using carbon system data** Baltic Earth Conference, Hel Peninsula, Poland.

DATA

Continuous trace gas and pCO₂ measurements:
<https://doi.pangaea.de/10.1594/PANGAEA.931313>

Discrete nutrient, trace gas and CO₂-system measurements:
<https://doi.pangaea.de/10.1594/PANGAEA.931325>

CRUISE REPORT

EMB214: Submitted to GPF head office

EMB217

Results of research cruise EMB217

AUTHORS

Leibniz-Institute for Baltic Sea Research | Warnemünde, Germany
P. Holtermann

CRUISE SUMMARY

The EMB217 cruise was dedicated to the DFG-Funded project ROBOTRACE (The role of bottom boundary layer turbulence for the exchange of tracer) and was the third in the project. The purpose was to sample the ROBOTRACE stations during a calm summer season. This allows to understand the seasonality of the oxygen transport in the central Baltic Sea. The sampled stations and main transect were on the eastern part of the Gotland Basin (TS1, Figure 1). For the background condition during the cruise, two moorings chains, including ADCP, T, S and oxygen sensors, were deployed along the transect. Short term deployments of oxygen microprofilers, oxygen eddy-covariance and chamber landers were performed along the transect.

The transect was sampled several times with a shear microstructure probe (MSS-90L) including a fast response oxygen optode and accompanied by nutrient samples taken with watersamplers mounted on a standard CTD rosette. Besides these main tasks, maintenance of the IOW longterm mooring NE and GODESS were performed and a lagrangian drifter (Jetsam, Univ. Florida) was tested for its use in the Baltic Sea.

AIM OF THE CRUISE

The cruise is the third and last of the ROBOTRACE project. It aims to fill the seasonal pictures of bottom boundary mixing processes in a stratified basin and the accompanying oxygen fluxes due to turbulence. Prior cruises were EMB169 (autumn 2017) and EMB177 (winter 2018). The major scientific question was the investigation of the relevant processes transporting oxygen (or limiting the transport) from the oxygenized surface water to the sediment and into the hypoxic transition zone. Investigated by prior research, it was found that boundary mixing processes are the most relevant mixing processes (Holtermann et al. 2012; Holtermann and Umlauf 2012) in the central Baltic Sea. This leads to the scientific need to understand the transport and consumption processes of oxygen at the basin boundary, this includes the oxygen transport from the open water into the BBL and from the BBL into the sediment, as the sedimentary oxygen demand is a major oxygen sink. The previous cruises had a similar aim and scientific location, making it possible to directly compare the results.

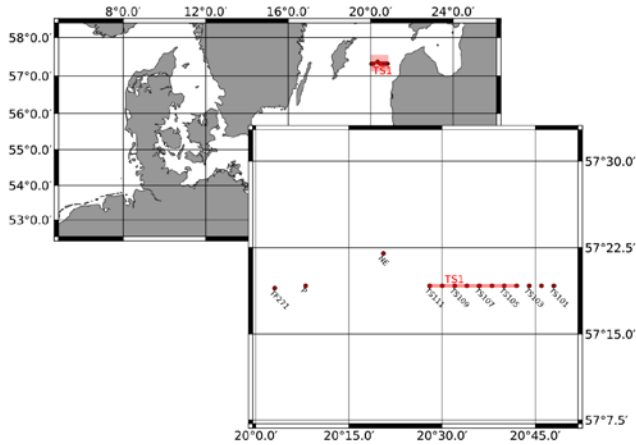


Figure 1: Track chart of R/V Elisabeth Mann Borgese Cruise EMB217 (A). Working stations as blackpoints and transect TS1 in red (B).

RESULTS

The cruise provided, especially in combination with the preceding cruises EMB169 and EB177, a valuable dataset of the mixing processes in the central Baltic Sea during a summer situation. By the mounting of a fast oxygen optode onto the microstructure probe in combination with the shear data this dataset can be used to infer the vertical oxygen fluxes through the halocline. The amount of vertical mixing was, not unexpected, almost by an order of magnitude reduced, compared to an autumn situation. The total amount of mixing, as well as the processes contributing to the vertical oxygen fluxes are analysed in (Holtermann et al. 2022). Figure 2 shows the differences between the seasons with the data of EMB217 displayed in panel e.

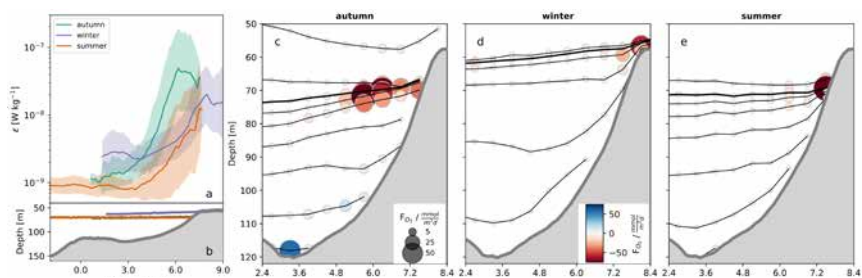


Figure 2: (see also, Holtermann et al. 2022). Cross-slope variability of (a) cruise-averaged halocline dissipation rates, (b) bathymetry (in gray) and average halocline depths for the three cruises, respectively, and (c–e) cruise-averaged downward oxygen fluxes for fall, winter, and summer, respectively. Shaded areas in (a) mark one standard deviation of the natural variability encountered on the individual transect surveys. Circle markers in (c–e) indicate diapycnal oxygen fluxes across selected isopycnals (black) spaced at 0.5 kg m⁻³ intervals in the vicinity of the halocline. The size of the symbols indicates the magnitude of the fluxes, the color (red = downward, blue = upward) their direction as shown in the legends. Thick black isopycnals mark the halocline. Gray-shaded areas indicate the bathymetry.

By an extrapolation of the transect data an overall oxygen budget of the central Baltic Sea was derived. The most striking result of the EMB217 dataset was the strong focus of the oxygen transport processes to the basin rim. A fraction of less than 25% of the area, which is directly at the basin boundaries is responsible for more than 80% of the oxygen transport through the halocline, Figure 3.

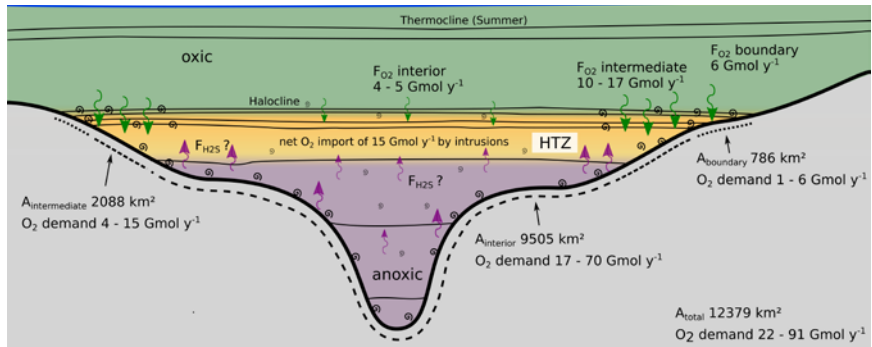


Figure 3: (see also, Holtermann et al. 2022). Oxygen transport and transformation pathways in the central Baltic Sea. Black lines indicate isopycnals. Whirls mark turbulent regions and arrows show oxygen and H₂S transport pathways.

REFERENCES

Holtermann P, and Umlauf L, „The Baltic Sea Tracer Release Experiment. 2. Mixing processes“, J. Geophys. Res. 2012, 117:C01022. doi:10.1029/2011JC007445.

Holtermann P, Umlauf L, Tanhua T, Schmale O, Rehder G, and Waniek J, The Baltic Sea Tracer Release Experiment. 1. Mixing rates, J. Geophys. Res. 2012, 117:C01021. doi: 10.1029/2011JC007439.

SCIENTIFIC OUTPUT

LIST OF PUBLICATIONS

Holtermann P, Pinner O, Schwefel R, and Umlauf L, The Role of Boundary Mixing for Diapycnal Oxygen Fluxes in a Stratified Marine System, Geophysical Research Letters 2020, 49, e2022GL098917. 10.1029/2022GL098917.

LIST OF CONFERENCE PRESENTATIONS

2019 | **Lateral transport, not vertical mixing, is the most important oxygen transport process for the hypoxic transition zone in the Baltic Sea** WTD, Vilm, Germany

2021 | **The role of boundary mixing for diapycnal oxygen fluxes in the Baltic Sea** VEPOSSS, Online

2022 | **The role of advection for the ventilation of the hypoxic deep water of the Baltic Sea** GONE, Liege, Belgium.

2023 | **Disentangling the role of different physical transport processes for the evolution of Anoxia in the central Baltic Sea** MISU Seminar, Stockholm, Sweden.

2023 | **The role of physical transport processes for the evolution of anoxia in a semi-enclosed marine system** IUGG, Berlin, Germany.

DATA

Physical oceanography (CTD, MSS data used for the article Holtermann et al. 2022):
<http://doi.io-warnemuende.de/10.12754/data-2022-0002>

Description of the cruise with contact information for full data access:
<https://iowmeta.io-warnemuende.de/geonetwork/srv/eng/catalog.search#/metadata/IOW-IOWMETA-EMB217-2019>

CRUISE REPORT

EMB217: https://doi.pangaea.de/10.2312/cr_emb217

EMB230, EMB237, EMB256, EMB261, EMB264, EMB271 AND EMB280

The state of the Baltic Sea in 2020–2021 – ecosystem variability and long-term changes

AUTHORS

Leibniz-Institute for Baltic Sea Research Warnemünde | Rostock, Germany
M. Naumann, A. Kremp, J. Kuss

THE BALTIC SEA ECOSYSTEM

As an intra-continental sea with a densely populated catchment area, the Baltic Sea is of high economic and social importance for the riparian states. It is the mission of the Leibniz-Institute for Baltic Sea Research Warnemünde (IOW) to provide knowledge for keeping the Baltic in a good ecological state. Warming, eutrophication and oxygen depletion are the most severe environmental threats the Baltic Sea faces today. The stratification of the water column, resulting from a restricted water exchange, neglectable tides and a positive water balance with a freshwater surplus, is one of the main reasons for a slow overturning circulation and the development of so called extended “dead zones” in the central Baltic Sea. To decipher the development of these balance between freshwater outflow and sporadic inflow of salty oxygenated water, the overturning circulation and the consequences for the ecosystem in its full range present and future variability is one of the main aspects of the IOW long term observation programme.

THE ECOSYSTEM STATE OF THE YEAR 2020-2021: METEOROLOGICAL /HYDROGRAPHIC ASSESSMENT

For the southern Baltic Sea area, the Warnemünde weather station recorded in the winter 2019/2020 a record “cold sum” of the air temperature of 0 Kd (Kelvin days) and 2020/2021 a value of 32.7 Kd. Both winter seasons leading to a classification as mild, ranked as first and 17th warmest winter since the beginning of recording in 1948. The summer “heat sum’s” of 234.3 Kd (2020) and 284.7 Kd rank at 14th and 6th position over the past 73 years, but they are far below the record of 394.5 Kd in 2018. The long-term average heat sum is 159.7 +/- 75.1 Kd.

During both years no larger saline inflow events occurred. It lead to continuation of stagnant hydrographic conditions in the deep basins of the Baltic Sea, characterized by slow water exchange and widespread hypoxic to euxinic areas (Figure 1). The observed minor inflows ventilated the deepwater of the Arkona Basin and Bornholm Basin, and the upper halocline of the Eastern Gotland Basin.

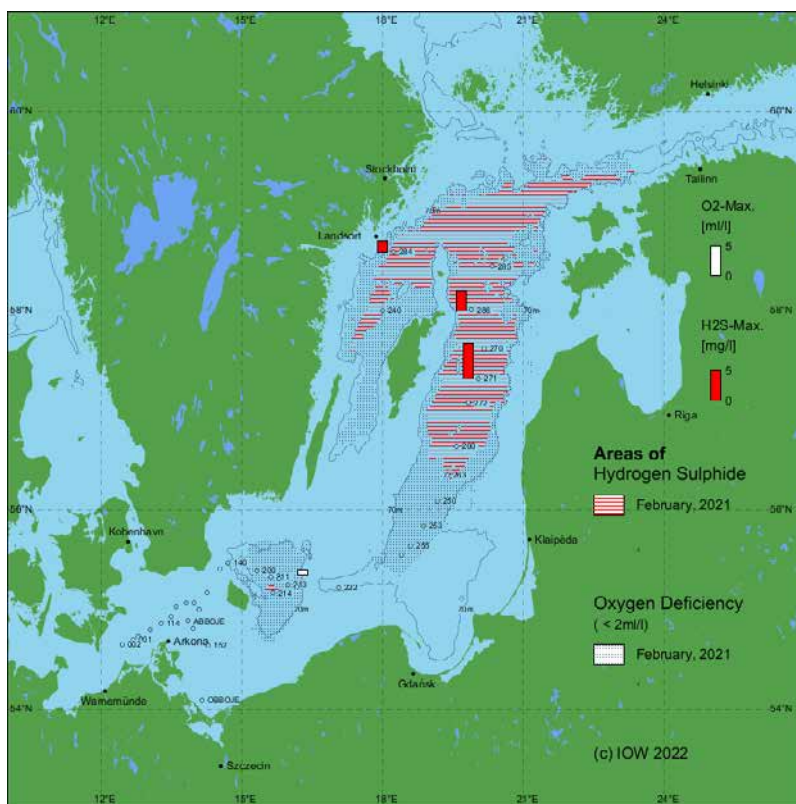


Figure 1: Areas of oxygen deficiency and hydrogen sulphide in the near bottom layer of the Baltic Sea – the situation in February 2021 (EMB256). Bars show the maximum oxygen and hydrogen sulphide concentrations of this layer in 2021; the figure additionally contains the 70 m -depth line.

CHEMICAL PARAMETERS

The oxygen decline since the last Major Baltic Inflow (2014-2016) generally continued in the central Baltic Sea deep basins. However, slight improvements in certain years occurred, but didn't change the general bad situation and the trend. So the situation in the deep water of the Fårö Deep was in 2020 with regard to concentrations of hydrogen sulphide slightly lower compared to 2021 and the western Gotland Sea (Landsort Deep and Karlsö Deep) somehow lower concentrations in 2021. However, in 2021 a pulse of oxygenated water brought some oxygen to the southern part of the eastern Gotland Sea, which propagated further northwards just below the halocline.

The winter nutrient concentrations of phosphate and nitrate in surface water were clearly higher in 2021 as in a couple of previous years and moved further away from HELCOM target values that appeared within reach for nitrate in recent years. For the Gotland Sea the winter nutrient concentrations of surface water in January/February 2021 were within the range of recent years. Only for the Karlsö Deep a clearly higher nitrate concentration in surface water is documented for winter 2021.

In the deep water, a worsening of the situation regarding the major nutrients phosphate and ammonium occurred in the year 2021 due to the ongoing development of oxygen loss (increasing hydrogen sulphide concentrations). Highest values for 2021 were determined for phosphate in the deep water of the Gotland Deep (5.4 $\mu\text{mol/l}$), Fårö Deep (4.4 $\mu\text{mol/l}$), and Karlsö Deep (4.0 $\mu\text{mol/l}$) since 2017. Nitrate was depleted in euxinic condition and ammonium accumulated to maxima in 2021 in the Bornholm Deep (4.0 $\mu\text{mol/l}$), Gotland Deep (22.8 $\mu\text{mol/l}$), Fårö Deep (12.2 $\mu\text{mol/l}$) and Landsort Deep (10.3 $\mu\text{mol/l}$) at least since 2017.

THE BIOLOGICAL STATE

In 2021 a total of 165 phytoplankton species were recorded on 5 annual monitoring cruises. Mean annual biomass of phytoplankton in the study area was, at 928 $\mu\text{g L}^{-1}$, higher than the 20-year mean. In spring 2021, Chl a concentrations reflected phytoplankton biomass poorly, due to high representation of non-diatom and mixotroph taxa including the ichthyotoxic Raphidophyte *Heterosigma akashiwo*, blooming in Kiel Bight in February. By May, Chl a and biomass had declined in the South, but were still increasing towards the North. The summer phytoplankton production was largely shaped by diatoms in the Southern Baltic constituting 80 to >90% of the biomass here in July. Peak phytoplankton biomasses of up to 8000 $\mu\text{g L}^{-1}$ were measured. Cyanobacteria only dominated in the central Baltic. In November, diatoms dominated the phytoplankton community throughout the study area.

The zooplankton species composition reflected the lack of major inflow events during 2020-2021. Generally, species with a broad salinity tolerance and characteristic of the brackish waters dominated from the Kiel Bight to the Baltic Proper. The observed species number of 45–54 taxa was below the number observed during inflow years (up to 70 Taxa). This was attributed to the lack of halophilic organisms like the copepods *Calanus* spp., *Centropages typicus* or the cladoceran *Penilia avirostris* which were observed only as single findings in 2020 and were absent in 2021. For this reason, a usual gradient in the taxa diversity from the Kiel Bight to the Arkona Sea was also not observed. The zooplankton was characterized by an abundance in both years, which continued a series of years of low stock size that started around 2010. The total stock of 4.8×10^4 ind. m^{-3} in 2020 was the lowest value recorded since 20 years and accounts for only 1/6 of the long-term average. Although a small recovery in the abundance was observed in 2021 (8.0×10^4 ind. m^{-3}), the series of negative long-term anomalies was continued. Although cladocerans showed a slight increase in 2021, their abundance was together with that of rotifers, Copepoda, cyclopoid and calanoid copepods, and polychaete larvae considerably below their long-term means. Only bivalve and gastropod larvae achieved their long-term average concentrations.

The 124 species found in the macrozoobenthos in 2021 mark a medium diversity. The species number found at the eight monitoring stations ranged between 20 and 67. In all regions, the oxygen supply in bottom waters in the current year was always higher than

2 ml l⁻¹. Except for the southern Mecklenburg Bay with its decline, the diversity at all stations was similar or slightly increased compared to the recent years. Depending on the region, the abundances ranged from 254 to 7687 ind. m⁻², and the biomass (ash free dry weight) from 0.8 g m⁻² to 32 g m⁻². Altogether fifteen species of the German Red List (Categories 1, 2, 3 and G) were observed at the eight monitoring stations. With six, the number of invasive species in 2021 was low, as expected and only the spionid polychaetes *Marenzelleria viridis* and *M. neglecta* reached noteworthy abundances in the Pomeranian Bay. *Mya arenaria* and *Amphibalanus improvisus* have been common faunal elements in the southern Baltic Sea for more than a hundred years. Finally, the ascidian *Molgula manhattensis* was observed as a cryptic neozoa species in the Bay of Kiel.

THE IOW LONG-TERM OBSERVATION PROGRAM

The IOW long-term observation program serves to collect data on the seasonal and long-term variability of the hydrographic, chemical and biological state of the ecosystem from the Bornholm Sea to the central Baltic Sea. The program is complemented by observations in the western Baltic Sea, conducted for the national monitoring financed by the Federal Maritime Agency (BSH). The density of the station network is determined by the requirements of the physical investigations of the dynamics of the water exchange and the Baltic Sea circulation. Chemical-biological investigations are limited to a few selected stations. In addition, permanent measuring stations are operated at key positions, which complement the spatial image in high temporal resolution. The work comprises 45 sea days per year, divided into five cruises of about 9 days duration. The observation program has continued to build up time series at key stations continuously since 1969. The gathered long-term data form the necessary basis for research on the natural variability of the Baltic Sea ecosystem, anthropogenic influences and the effects of climate change. And thus, they are indispensable for the fulfilment of the IOW's research mission. As an example, long-term data series of dissolved oxygen and hydrogen sulphide concentrations were used to compile distribution maps (see Figure 1) and to analyse trends in the last 50 years. Further, the data serves as standard for calibration and intercomparison of several model results for hypoxic area in the Baltic Sea. The observations of this program support essentially such model studies like KRAPF et al. (2022) analyzing this oxygen depletion issue on longer time scales of the past and future predictions. All data obtained are freely available to researchers and the general public in databases of the Institute (IOWDB), the Federal Environment Agency (MUDAB) and, in an international context, at ICES/HELCOM. They support cooperation in the Baltic Sea region and environmental policy assessments of the ecosystem status of the Baltic Sea.

REFERENCES

Naumann M, Gräwe U, Mohrholz V, Kuss J, et al., Hydrographic-hydrochemical assessment of the Baltic Sea 2020, Marine Science Reports 2021, 119, doi: 10.12754/msr-2021-0119.

Dutz J, Kremp A, Zettler M L, Biological assessment of the Baltic Sea 2020, Marine Science Reports 2022, 120, doi: 10.12754/msr-2022-0120.

Naumann M, Gräwe U, Mohrholz V, Kuss J, et al., Hydrographic-hydrochemical assessment of the Baltic Sea 2021, Marine Science Reports 2023, 123, doi: 10.12754/msr-2023-0123.

Kremp A, Dutz J, Zettler M L, Biological assessment of the Baltic Sea 2021, Marine Science Reports 2024, – in review.

Krapf K, Naumann M, Dutheil C, Meier H E M, Investigating hypoxic and euxinic area changes based on various datasets from the Baltic Sea, Frontiers in Marine Science 2022, doi: 10.3389/fmars.2022.823476.

SCIENTIFIC OUTPUT

PUBLICATIONS

Naumann M, Gräwe U, Mohrholz V, Kuss J, et al., Hydrographic-hydrochemical assessment of the Baltic Sea 2020, Marine Science Reports 2021, 119, doi: 10.12754/msr-2021-0119.

Dutz J, Kremp A, Zettler M L, Biological assessment of the Baltic Sea 2020, Marine Science Reports 2022, 120, doi: 10.12754/msr-2022-0120.

Naumann M, Gräwe U, Mohrholz V, Kuss J, et al., Hydrographic-hydrochemical assessment of the Baltic Sea 2021, Marine Science Reports 2023, 123, doi: 10.12754/msr-2023-0123.

Kremp A, Dutz J, Zettler M L, Biological assessment of the Baltic Sea 2021, Marine Science Reports 2024, – in review.

Krapf K, Naumann M, Dutheil C, Meier H E M, Investigating hypoxic and euxinic area changes based on various datasets from the Baltic Sea, Frontiers in Marine Science 2022, doi: 10.3389/fmars.2022.823476.

DATA

All physical oceanographic and chemical data can be investigated and downloaded from the IOW oceanographic database IOWDB at: institute
<https://odin2.io-warnemuende.de/#/>

The data are imported also into the national and international databases MUDAB and ICES.

CRUISE REPORT

Cruise reports of the IOW long-term observation program are available at <https://www.io-warnemuende.de/fahrtberichte.html> (for cruises since 2001).

EMB232, EMB246, EMB247 AND EMB258

Mapping of habitats (biotopes) and their biotic communities on the seabed in the coastal waters of Mecklenburg-Vorpommern

AUTHORS

Leibniz-Institute for Baltic Sea Research Warnemünde | Rostock, Germany

P. Feldens, D. Marx, A. Feldens, A. Herbst, A. Darr, M.L. Zettler

A good environmental status of our oceans is more important than ever. The Baltic Sea is particularly vulnerable to anthropogenic pressures due to its unique and fragile ecosystem (marine and limnic influence, shallow depth, limited water exchange through the shallow Danish Strait system). The aim of the ATLAS project commissioned by the State Office for the Environment, Nature Conservation and Geology M-V (LUNG) was to create an up-to-date database for the coastal waters off Mecklenburg-Western Pomerania within the 12 nautical mile zone and to document the distribution and extent of the habitats and the benthic communities found in them, forming a baseline for future monitoring and environmental assessment. Broad benthic habitat types (BHT) were mapped according to the MSFD as well as other benthic habitat types (OHT) protected according to §30 of the German Federal Nature Conservation Act (BNatSchG), the EU Habitats Directive and the HELCOM Red List (HELCOM 2013a). The latter include reefs, sublittoral sandbanks, species-rich areas of gravel, coarse-sand and shell-gravel areas as well as seagrass meadows and other marine macrophyte populations. In addition, HELCOM HUB biotope types (HELCOM 2013b) were modelled and mapped. For this purpose, both own and external data were used, which were necessary for the analysis and creation of the maps. The project duration was 2.5 years (18.06.2019–31.12.2021), during which EMB was both chartered for several research cruises for the project work, with additional working days granted for scientific purposes.

Schiele et al. (2015) have already presented an area-wide mapping of the biotope types in the German territory and the EEZ of the Baltic Sea. However, this is available at a spatial resolution of 1 x 1 km. The mapping presented here was realized in three focus areas on 50 x 50 m resolution and therefore reflects a level of detail that does not yet exist for the coastal waters of Mecklenburg-Western Pomerania. This enables a precise recording of protected and other biotopes, on the basis of which protected area designations can be made.

The coastal waters off Mecklenburg-Western Pomerania within the 12 nautical mile zone (focus areas Plantagenet Ground (PG), Darss Sill (DS) and outer Wismar Bay (WB) are

shown in Figure 1) were mapped, with about 50 stations each in the focus areas and 93 stations outside the focus areas being sampled biologically and geologically. In addition, there were 5 (in DS and PG) to 7 (in WB) video transects and 1 (in PG) to 4 (in WB and DS) diver stations. Further 2 transects (in DS) and 6 dive stations (in WB) were located outside the focus area boundaries. The areas were fully surveyed with side-scan sonar (100 to 900 kHz) and partially mapped with multibeam echosounder and sediment echosounder (the latter only outside national parks).

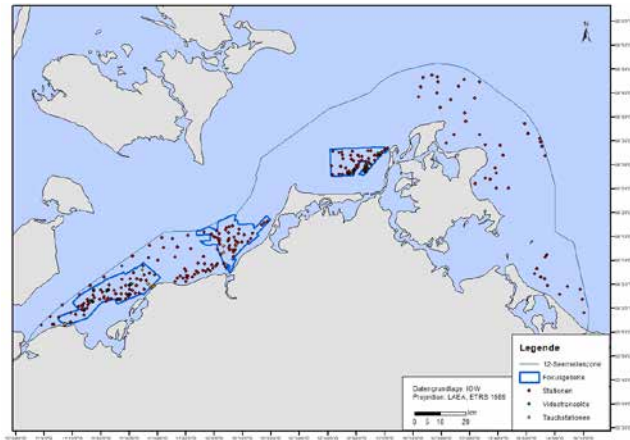


Figure 1: Areas surveyed in full coverage with hydroacoustic methods during EMB258, EMB247, EMB246, EMB232 are marked in blue, with sediment samples (stations), video transects and diving stations marked in addition.

Geological mapping was carried out for all areas based on the acoustic data and sediment samples (example for PG in Figure 2). In addition, block distribution maps were calculated semi-automatically on a 50 m x 50 m grid using neural networks (Feldens et al. 2019, Feldens 2020, Feldens et al. 2023) and used to calculate reef distribution (Figure 3). The results again clearly show the high heterogeneity of the geological composition of the shallow areas of the Baltic Sea, which is also characteristic for the distribution of biotope types. These data, together with the benthological investigation of grab samples, camera transects and dives, served as the basis for modelling the HUB biotope distribution using a random forest model (results for PG are shown in Figure 4). Detailed results and descriptions of the geological, geophysical and biological sampling were reported to the authorities (Marx et al. 2021) and are uploaded to the GeoSeaPortal (geoseaportal.de, geological information) operated by BSH and currently prepared for submission to emodnet (habitat maps).

Figures 2, 3 and 4 show example results obtained for the Plantagenet Ground. The total area of PG is 172 km², of which about 17 % is reef area. Reefs were mapped according to Heinicke et al. (2021) into core, marginal and developing areas. Mussels cover the

reef throughout the area, often with filamentous algae. In the central and eastern parts of the PG, there are mussel communities on mixed substrate (AA.M1E1) and coarse sediments (AA.I1E1). A peat area with a thin sand layer colonised by mussels (AA.G+AA.J1E1) was verified by underwater video. Seagrass occurrences were recorded from hydroacoustic data and verified by video footage and are located in the east of the focus area on fine sand, down to approx. 9 m water depth and thinning to the north (not shown in this abstract). A sandbank of fine to mixed sand is located in the northeast of the focus area. Typical species such as *Bathyporeia pilosa*, *Cerastoderma glaucum*, *Pygospio elegans*, *Macoma balthica*, *Mya arenaria* and *Mytilus edulis* are found on this sandbank, but in low abundance.

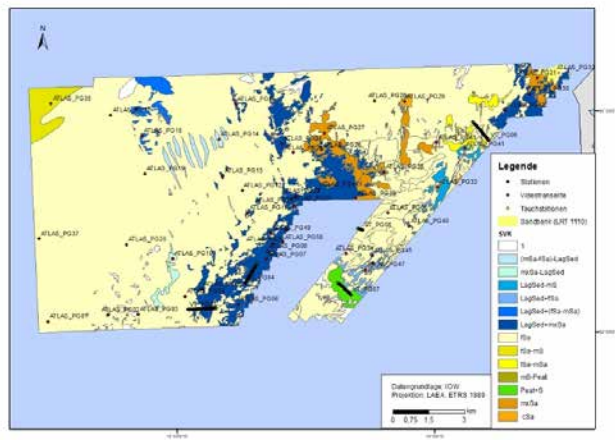


Figure 2: Sediment distribution on the Plantagenet Ground.

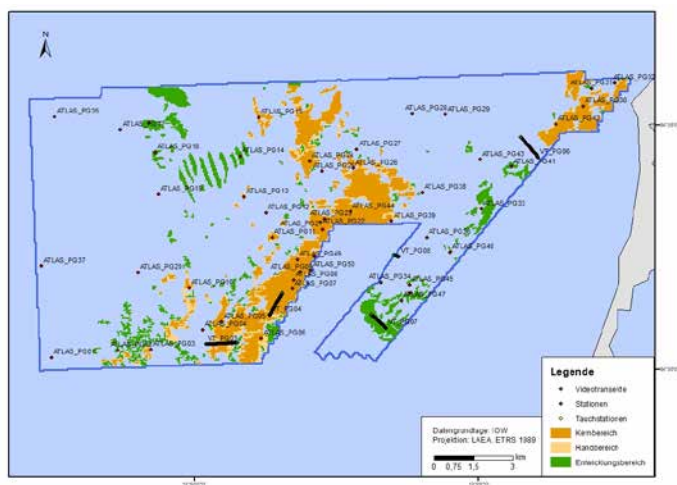


Figure 3: Reef distribution on the Plantagenet Ground, separated into core, marginal and development reefs.

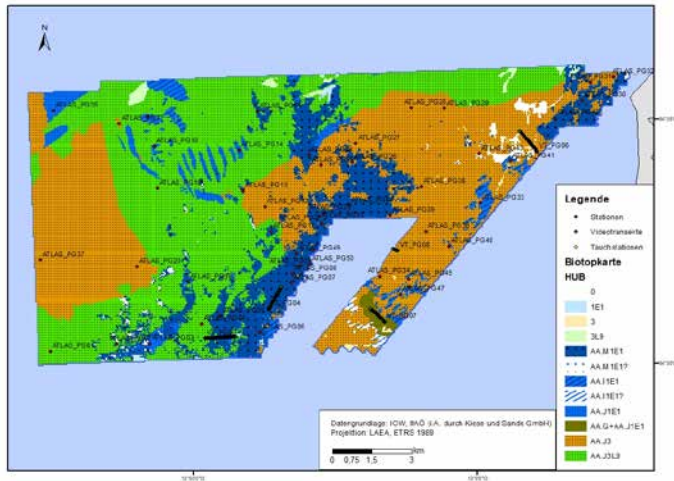


Figure 4: Biotope map according to HELCOM HUB (2013b). AA.G+AA.J1E1: Peat + mussel community on sandy sediment. AA.11E: mussel community on coarse sediment. AA.11E1?: not classifiable, but likely mussel community on coarse sediment. AA.J1E1: mussel community on sandy sediment. AA.J3: Mixed endobenthic community on sandy sediment. AA.J3L3: Brackish water mussel community on sandy sediment. AA.M1E1: Mussel community on mixed substrate. AA.M1E1?: unclassifiable, but likely mussel community on mixed substrate.

As a follow-up to this project, biotope maps have been produced for the entire German Baltic Sea (Marx et al. under review), based on the results of the ATLAS and LEGRA projects. These maps provide a more accurate picture of the state of the seabed in the German Baltic Sea. However, the spatial extent of habitats and protected biotopes at high resolution is still unknown for large parts of the Baltic Sea. Further mapping is therefore needed to establish baselines for detecting not only spatial but also temporal changes due to natural and anthropogenic causes and stressors (e. g. due to increasing heat waves, construction work, fishing impacts, but also protection and restoration measures). The interplay between applied and basic research, and thus between research institutes and authorities, can contribute to the direct implementation of conservation measures.

REFERENCES

Feldens P, Darr A, Feldens A, and Tauber F, Detection of Boulders in Side Scan Sonar Mosaics by a Neural Network, *Geosciences* 2019, 9(4) 159.

Feldens P, Super Resolution by Deep Learning Improves Boulder Detection in Side Scan Sonar Backscatter Mosaics, *Remote Sensing* 2020, 12(14): 2284.

Feldens A, Marx D, Herbst A, Darr, A, Papenmeier S, Hinz M, Zettler M L, Feldens P, Distribution of Boulders in Coastal Waters of Western Pomerania, German Baltic Sea, *Front. Earth Sci.* 2023, 11, doi:10.3389/feart.2023.1155765.

Heinicke K, Bildstein T, Reimers H-C, Boedeker D, Leitfaden zur großflächigen Abgrenzung und Kartierung des Lebensraumtyps „Riffe“ in der deutschen Ostsee (EU-Code 1170; Untertyp: geogene Riffe), BfN-Skripten 2021, 612.

<https://www.bfn.de/sites/default/files/2021-11/Skript612.pdf> (Zugriff am 11.11.2021)

HELCOM Red List of Baltic Sea Underwater Biotopes, Habitats and Biotope Complexes. Baltic Sea Environment Proceedings No. 138; 2013a.

HELCOM HUB. Technical Report on the HELCOM Underwater Biotope and Habitat Classification. Baltic Sea 862 Environment Proceedings No. 139; 2013b.

CRUISE REPORTS

EMB232: doi:10.48433/cr_emb232

EMB246: doi:10.48433/cr_emb246

EMB247: doi:10.48433/cr_emb247

EMB258: doi:10.48433/cr_emb258

SCIENTIFIC OUTPUT

LIST OF PUBLICATIONS

Feldens A, Marx D, Herbst A, Darr A, Papenmeier S, Hinz M, Zettler M L, Feldens P, Distribution of Boulders in Coastal Waters of Western Pomerania, German Baltic Sea, Front. Earth Sci. 2023, 11, doi:10.3389/feart.2023.1155765.

Feldens P, Super Resolution by Deep Learning Improves Boulder Detection in Side Scan Sonar Backscatter Mosaics, Remote Sensing 2020, 12(14): 2284.

Marx D, Feldens A, Papenmeier S, Feldens P, Darr A, Zettler M L, Heinicke K, Habitats and Biotopes in the German Baltic Sea, Biology (under review).

Marx D, Feldens P, Feldens A, Herbst A, Darr A, Zettler M L, Kartierung der Lebensräume (Biotope) und deren Lebensgemeinschaften am Meeresboden in den Küstengewässern Mecklenburg-Vorpommerns, Report to LUNG 2021.

LIST OF CONFERENCE PRESENTATIONS

2021 | **Methodological steps for mapping reefs using the Plantagenet Ground as an example** BfN workshop "Recording, modelling, monitoring – innovative approaches to the characterisation and ecological assessment of reef biocoenoses in the North Sea and Baltic Sea"

DATA

Sediment distribution maps:

Feldens, A. & Feldens, P.: Map of sediment distribution in the 12 nautical miles zone of Mecklenburg-Vorpommern (Plantagenet Grund, Darss Sill, Outer Wismar Bay), www.geoseaportal.de, 2022.

Boulder distribution maps:

submitted to [geoseaportal.de](http://www.geoseaportal.de), pending publication.

EMB238, EMB267 AND EMB268

Chasing the signals of bottom-trawling in benthic ecosystems of the western Baltic Sea

AUTHORS

Leibniz-Institute for Baltic Sea Research Warnemünde (IOW) | Rostock, Germany

M. Gogina, P. Feldens, M. Schönke, P. Rooze, J. Piontek, M.A. Zeller, M.E. Böttcher, F. Pohl, C. Meeske, P. Roeser, C. Schmidt, K. Jürgens

Institute of Zoology, University of Cologne | Cologne, Germany

M. Sachs, H. Arndt, M. Hohlfield

Institute for Biosciences, University of Rostock | Rostock, Germany

S. Forster, M. Powilleit

GEOMAR Helmholtz Centre for Ocean Research | Kiel, Germany

D. Clemens, S. Sommer

Senckenberg am Meer, German Centre for Marine Biodiversity Research (DZMB) | Wilhelmshaven, Germany

K.H. George, A. Ostmann, P. Martinez Arbizu

Thunen Institute of Baltic Sea Fisheries | Rostock, Germany

D. Oesterwind

GFZ German Research Centre for Geosciences | Potsdam, Germany

J. Kallmeyer

Mobile bottom-contacting fishing (MGF) can disrupt sediment structures and negatively affect benthic habitats and their communities. In the North and Baltic Sea, MGF has also been conducted with high frequency in most marine protected areas (MPAs). However, only a few studies have investigated the impacts of this pressure in the German EEZ of the Baltic Sea until now. The joint project MGF-Baltic Sea (MGF-Ostsee) aims to investigate potential effects of the planned exclusion of MGF on benthic ecosystems in MPAs as part of the DAM sustainMare mission – “Protection and sustainable use of marine spaces.” During the EMB238 (June 2020) and EMB267 (June 2021) expeditions, the first baseline investigations of the state before under high MGF pressure and before closure for trawling with mobile bottom-contacting gears were carried out in sandy silt and sand habitats of the Natura 2000 areas “Fehmarn Belt” and “Odra Bank,” respectively. Sediments and

benthic communities were surveyed where MGF was known to be still present to be able to track the ecosystem’s development to a presumably more undisturbed state after the fishing exclusion. To evaluate the influence of MGF independently of other drivers, comparable study areas were identified inside and outside each MPA, whereby trawling in the reference areas outside was expected to continue after the closure.

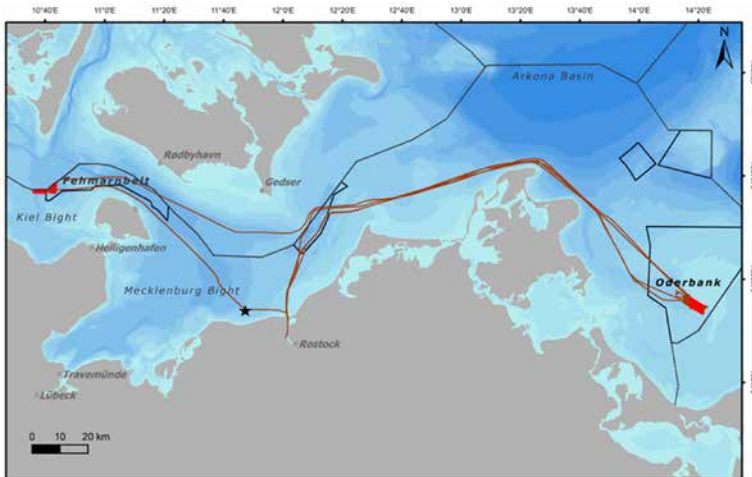


Figure 1: Track chart of the cruise EMB267 from the cruise report, showing in bright red the focus areas Fehmarn Belt (left, first sampled during cruise EMB238) and Odra Bank (right, sampled during most of the EMB267 program). The black star indicates the location of the trawling experiment during the cruise EMB268.

The “Fehmarn Belt” and “Odra Bank” MPAs represent contrasting benthic Baltic Sea ecosystems in terms of sediment type, salinity, water depth, and their biocenoses; thus, different developments in benthic communities and sediment functions after the MGF exclusion can be expected. Observations targeted all biological components, from prokaryotes to macrofauna, using various methods. Furthermore, the seafloor was characterized with regard to sedimentology, surface morphology, biogeochemistry, sediment-water-interface exchange fluxes, and visible trawl marks. The sampling design accounted for small-scale variability. Other research vessels surveyed demersal fish concurrently (Oesterwind et al., 2023).

Hydroacoustic seafloor mapping that was used to detect the MGF impact by the analysis of trawl marks was particularly successful in the muddy sediments of the Fehmarn Belt, where marks cover 3–5% of the seafloor. Data obtained during EMB238 contributed to the development of an acoustic-based trawling intensity index, which allows comparison of past and future MGF activities in this area and represents an important addition to the often limited (like VMS and logbook data) or unavailable (for smaller vessels) fishing effort data (Schönke et al., 2022). Hydroacoustic mapping showed that fishing intensity was similar in the selected areas inside and outside MPA.

Detailed sedimentological and biogeochemical analysis of dissolved and solid phases from the surface sediment layers (upper 20–30 cm) revealed significant differences between the Fehmarn Belt (sampled during EMB238) and the more permeable, sandy Odra Bank sediments (EMB267). Respective study areas within and outside of each MPA were mostly comparable in terms of e. g. grain size, porosity and organic matter. For some parameters, small-scale differences were observed between the areas inside and outside the MPA Fehmarn Belt. Geochemical data from EMB238 cruise were used to calibrate an early diagenetic biogeochemical model simulating physical disturbance events in the sediment (Rooze et al., 2024). Trawling effects on early diagenesis of studied sandy silt sediments were unveiled. Mercury distributions measured in the sediment allowed constraining mixing depths and sedimentation rates. Integration of modeling results with seafloor mapping and fauna data suggested that bioturbation rather than bottom-trawling dominated sediment mixing. EMB238 data showed that bottom fishing can generate chlorophyll a distributions in vertical sediment profiles that can easily be confused with bioturbation (Forster et al., 2023, submitted). Here it could be relevant to point out that mercury profiles refer to mixing on decadal time-scales, whereas chlorophyll a is indicative on shorter time-scales due to decomposition.

In situ flux measurements were conducted using landers to assess benthic carbon turnover and oxygen demand, nitrogen cycle transformations, and phosphate retention in the sediment. A mass balance for sediment and associated processes was established for the Fehmarn Belt. Particularly, oxygen consumption showed considerable variation, indicating physical disturbances of sediment structure, potentially due to small-scale differences in trawling. Close before completing our scientific program of the EMB238 cruise, we had the misfortune to witness trawling impact directly on our equipment deployed within the MPA, where it was still legal at that time.



Figure 2: Exemplary still images illustrating the visible effects of trawling on bottom sediment habitats impacted by trawl door and ground gear (or foot rope) in (a, b, c) the Fehmarn Belt (EMB238) and (d and e) in the Bay of Mecklenburg (EMB268), and no detected trawling marks in (c) Odra Bank sand (EMB267).

Biological surveys of individual organism groups highlighted strong differences between Fehmarn Belt (during the EMB238 cruise) and Odra Bank (during the EMB267 cruise), with very distinct communities and diversities. Particularly for the higher trophic levels, such as macrozoobenthos and fish, a decrease in salinity was associated with the expected reduction in species numbers (87 macrozoobenthic taxa identified in Fehmarn Belt samples, only 31 in Odra Bank). Differences in distribution were also reflected by key species in ecosystem functioning and community functional indexes such as bioturbation and bioirrigation potentials (Gogina et al., 2022). Also for most groups at the lower trophic levels, such as prokaryotes, protists, microphytobenthos, and meiofauna, the taxonomic community composition in Fehmarn Belt and Odra Bank were markedly different but at similar diversity. Complete diversity analyses for microbes in Baltic Sea sediments were conducted for the first time, describing several previously unknown taxa of prokaryotes, microbial eukaryotes and meiofauna. An essential prerequisite for future studies using eDNA is the extensive expansion of the databases, which were very incomplete for the Baltic Sea. For heterotrophic protists and meiofauna, this was achieved by linking morphological analyses and cultures with the molecular characterization of taxa (Sachs et al., 2023; Schoenle et al., 2022). For prokaryotes (bacteria, archaea), the functional potential (metagenomes) and active metabolism (metatranscriptomes) were analyzed. With the help of marker genes, microbial processes can be localized and related to environmental factors including MGF. For example, sulfate reduction rates were found to be similar in different MPAs, but the dominant sulfate-reducing taxa varied significantly between the areas (suggesting their functional redundancy). Vertical distribution patterns were used to derive potential prokaryotic indicators for disturbance of sediment structure for each MPA.

Differences in biodiversity and sediment functions among the two MPAs underscore the need for a site-specific assessment of MGF influence. Minimal differences or absence thereof between project study areas inside and outside of each MPA before MGF exclusion suggest that a comparison of these areas in time-series studies is suitable to monitor changes after MGF exclusion. Time-series results will provide a foundation for the development of long-term adapted fisheries management strategies.

In this context, a trawling experiment was conducted at a coastal site in the Bay of Mecklenburg during EMB268 to investigate direct short-term effects of MGF (Figures 1 and 2). The area is heavily fished and inhabited by a macroinvertebrate community dominated by long-lived clam *Arctica islandica* (similar to the Fehmarn Belt MPA focus area). The muddy-silty seafloor was trawled by a commercial fishing vessel and ecosystem components were sampled before, immediately after, over the next few hours and on the next day to capture induced changes. First results showed the resuspension and sedimentation of the disturbed sediment, changes in the sediment structure (Forster et al., 2023, submitted), in macrozoobenthos and microorganisms, as well as in the distribution of redox-sensitive elements and redox boundary.

REFERENCES

Forster S, Runkel C, Lemke J, Pülm L, Powilleit M, Bottom fishery impact generates tracer peaks easily confused with bioturbation traces, *Biogeosciences Discuss.* [submitted] 2023, doi:10.5194/bg-2023-145.

Sachs M, Dünn M, Arndt H, Benthic heterotrophic protist communities of the Southern Baltic analyzed with the help of curated metabarcoding studies, *Biology* 2023, 12, 1010, doi:10.3390/biology12071010.

Schoenle A, Hohlfeld M, Rybarski A, Sachs M, Freches E, Wiechmann K, Nitsche F, Arndt H, Cafeteria in extreme environments: Investigations on *C. burkhardae* and three new species from the Atacama Desert and the deep ocean. *European Journal of Protistology* 2022, 85, 125905, doi:10.1016/j.ejop.2022.125905.

SCIENTIFIC OUTPUT

LIST OF PUBLICATIONS

Forster S, Runkel C, Lemke J, Pülm L, Powilleit M, Bottom fishery impact generates tracer peaks easily confused with bioturbation traces, *Biogeosciences Discuss.* [submitted] 2023, doi:10.5194/bg-2023-145.

Gogina M, Renz JR, Forster S, Zettler ML, Benthic macrofauna community bioirrigation potential (BIPc): Regional map and utility validation for the South-Western Baltic Sea, *Biology* 2022, 11(7), 108, doi:10.3390/biology11071085.

Oesterwind D, Köhler L, Paar M, Henseler C, Kriegl M, Gogina M, Schubert H, Martínez Arbizu P, Trophic ecology and seasonal occurrence of two Red List fish species in the Western Baltic Sea – Two of a kind?, *Marine Biodiversity* 2023, 53, 60, doi:10.1007/s12526-023-01368-7.

Rooze J, Zeller MA, Gogina M, Roeser P, Kallmeyer J, Schönke M, Radtke H, Böttcher ME, Bottom-trawling signals lost in sediment: A combined biogeochemical and modeling approach to early diagenesis in a perturbed coastal area of the southern Baltic Sea, *Science of the Total Environment* 2024, 906, 167551, doi:10.1016/j.scitotenv.2023.167551.

Sachs M, Dünn M, Arndt H, Benthic heterotrophic protist communities of the Southern Baltic analyzed with the help of curated metabarcoding studies, *Biology* 2023, 12, 1010, doi:10.3390/biology12071010.

Schoenle A, Hohlfeld M, Rybarski A, Sachs M, Freches E, Wiechmann K, Nitsche F, Arndt H, Cafeteria in extreme environments: Investigations on *C. burkhardae* and three new species from the Atacama Desert and the deep ocean. *European Journal of Protistology* 2022, 85, 125905, doi:10.1016/j.ejop.2022.125905.

Schönke M, Clemens D, Feldens P, Quantifying the physical impact of bottom trawling based on high-resolution bathymetric data, *Remote Sensing* 2022, 14, 2782, doi:0.3390/rs14122782.

LIST OF CONFERENCE PRESENTATIONS

2021 | **Predicting distribution of macrofauna over space and time in response to habitat, climate change, eutrophication and fishing** IMBIZO 6: Buoyant Solutions for Ocean Sustainability, online.

2021 | **Food web organisation of the fish community reflects prey availability in two protected areas of the western Baltic Sea** Baltic Sea Science Congress, Aarhus, Denmark.

2021 | **Impact of bottom contact trawling on benthic biogeochemical cycling in the Southern Baltic Sea** Goldschmidt Conference, online.

2022 | **How fast do Trawlmarks degenerate? A field study in muddy sediments near Fehmarn Island, Germany** EGU General Assembly, Vienna, Austria.

2022 | **Short-term anthropogenic impact of mobile bottom-contact fishing on the biogeochemistry of coastal sediments and its long-term effects on mineral distribution** EGU General Assembly, Vienna, Austria.

2022 | **Effects of Bottom-Trawling on Early Diagenesis: A Combined Field and Model-Based Approach** Ocean Biogeochemistry Gordon Research Conference, Barcelona, Spain.

2022 | **Anthropogenic impact of mobile ground-contact fishing on the biogeochemistry of Baltic Sea surface sediments Part I: Short term effects from a monitored trawling experiment** 4th Baltic Earth Conference, Jastarnia, Poland.

2022 | **Mineral distribution and biogeochemistry of coastal sediments affected by anthropogenic impact of mobile bottom-contact fishing** International Sedimentology Congress, Beijing, China.

2022 | **MGF-Ostsee – Ausschluss mobiler grundberührender Fischerei in Schutzgebieten der Ostsee** 3rd Küstensymposium, Küste im Wandel, Hamburg, Germany.

2022 | **Trawl tracks or bioturbation traces: Confusing chlorophyll tracer peaks in the sediment** 6th Nereis Park conference on Bioturbation in the past and present: from terrestrial to marine ecosystems, Logonna-Daoulas, Brest, France.

2023 | **Does salinity matter? - Ciliates in the southern Baltic** ECOP-ISOP joint meeting, Vienna, Austria.

2023 | **The effects of bottom-trawling on early diagenesis in the Baltic Sea** Baltic Sea Science Congress, Helsinki, Finland.

2023 | **Der mögliche Einfluss der mobilen grundberührenden Fischerei (MGF) auf die Meiofauna in der Ostsee** Langen Nacht der Wissenschaft, Wilhelmshaven, Germany.

DATA

MBES raw data:

<https://doi.org/10.5281/zenodo.6597161>

Amplicon sequence variant table of benthic heterotrophic protists:

<https://doi.org/10.1594/PANGAEA.961784>

Environmental data related to amplicon sequencing:

<https://doi.org/10.1594/PANGAEA.961796>

Benthic macrofauna data:

IOW Macrozoobenthos database (available on request), will be submitted to PANGAEA

CRUISE REPORT

EMB238: [doi:10.2312/cr_emb238](https://doi.org/10.2312/cr_emb238)

EMB267: [doi:10.48433/cr_emb267](https://doi.org/10.48433/cr_emb267)

EMB268: [doi:10.48433/cr_emb268](https://doi.org/10.48433/cr_emb268)

EMB239 AND EMB269

Living along gradients- spatiotemporal variability of macrobenthic communities in the southwestern Baltic Sea

AUTHORS

Leibniz-Institute for Baltic Sea Research Warnemuende (IOW) | Rostock, Germany
K. Romoth, A. Darr, A. Herbst, D. Marx, P. Feldens, M.L. Zettler

The living conditions of benthic species and communities in the southwestern Baltic Sea are characterized by a high variability of natural environmental conditions. This variability affects the development cycles of single individuals through its temporal component, as well as the distribution of species and thus the composition of benthic communities through its spatial component. The importance of individual environmental parameters for macrozoobenthos and phytobenthos depends mainly on the spatial scale considered. Local effects are mainly influenced by substrate characteristics, as well as biological effects (competition, predation) and flow exposure, while at the regional and supra-regional level, as well as in temporal aspects, the characteristics of the water body have the greatest significance. The most important parameters known to be salinity, temperature, and oxygen content. While local-scale variability leads to the formation of different communities and thus to high local diversity through species specialization, species richness decreases along the salinity gradient. In particular, specialists are absent at low salinities or occupy different ecological niches in areas with lower salinity than in fully marine areas.

In addition to this natural stress, stressors resulting from human activities are increasingly affecting benthic communities. Large-scale effects are caused, for example, by direct and indirect consequences of eutrophication (deterioration of light climate, increase in the frequency, duration and intensity of oxygen deficiency) and by mechanical pressure from bottom-contacting fishing gear. Construction activities, sediment extraction and disposal (legacy sites), as well as additional biological interactions (competition, predation) by introduced species (neobiota) can locally lead to intensive temporary or even permanent changes in benthic habitats. Due to the rapidly increasing pressure, the EU's marine environmental policy has created a framework for achieving a good environmental status or favorable conservation status of marine organisms and habitats with the Marine Strategy Framework Directive (MSFD) and the Habitats Directive (HD). The implementation of these directives includes a regular assessment of the state of marine ecosystems.

The cruises EMB239 and EMB269 proceeded in the southwestern Baltic Sea between Kiel Bay and Pomeranian Bay and were a sequel of cruises started in 2009 within the framework of subsequent projects funded by the German Federal Agency for Nature

Conservation (BfN). One aim has been the implementation of the Habitats Directive and the further development of HD monitoring. Therefore, a long-term data series has been established, assessing the temporal variability and environmental state in special offshore habitats (reefs, sandbanks) in the German Exclusive Economic Zone (EEZ). Another aim has been the investigating of the temporal and spatial variability of endo- and epibenthic communities along different natural and anthropogenic gradients as a basis for the development of monitoring strategies under the frame of the MSFD and for the development of high-resolution maps of benthic biotopes. Sampling of benthic communities was carried out by using a combination of different devices (van Veen grab, dredge, and video). On EMB239, the cruise was also shared with the ATLAS project to create synergies in biotope mapping. This project was funded by the State Office for Environment, Nature Conservation and Geology Mecklenburg-Western Pomerania and aimed to map the distribution and extent of habitats and the benthic communities occurring in them in the German coastal waters.

The mapping data resulting from EMB239 and EMB269 (and additional data since 2010) were used to create maps (according to MSFD, HELCOM HUB) for the entire German Baltic Sea at a high spatial resolution of 1 km. In two nature conservation areas of the EEZ and selected focus areas in the coastal waters, resolution even reaches 50 m x 50 m. Spatial delineation of benthic biotopes and communities was achieved by utilizing predictive habitat modeling. The resulting maps provide a new level of spatial detail and are the essential basis for future monitoring, status assessment as well as for protection and management measures.

The benthic data collected were also included in the MSFD assessment 2023, which covers a reporting period of 6 years and aims to achieve and maintain good environmental status through the identification of pressures and impacts and the implementation of appropriate management measures. For the assessment of the environmental status of the Baltic Sea, the Benthic Quality Index (BQI) was used as an indicator of soft-bottom macrofauna. Based on this indicator, only a few areas in the German Baltic Sea achieved good ecological status. Furthermore, the processing of the data for the upcoming HD assessment 2024 already indicates, that the pressure of use remains high in the Baltic Sea due to numerous stressors. The conservation status of many habitats such as submerged sandbanks and reefs was classified unfavorable in the last HD assessment. Regarding the evaluation criteria of habitat structure and species inventory considered in the monitoring, no trends could be observed so far that could lead to a change in the evaluation.

SCIENTIFIC OUTPUT

LIST OF PUBLICATIONS

(for the projects LEGRA (Jan. 2019–Dec. 2024) and ATLAS (Jun. 2019–Dec. 2021))

Feldens A, Marx D, Herbst A, Darr A, Papenmeier S, Hinz M, Zettler ML, Feldens P, Distribution of boulders in coastal waters of Western Pomerania, German Baltic Sea, *Frontiers in Earth Science* 2023, 11, 1155765, doi: 10.3389/feart.2023.1155765.

Greathead C, Magni P, Vanaverbeke J, Buhl-Mortensen L, Janas U, Blomqvist M, Craeymeersch JA, Dannheim J, Darr A, Degraer S, Desroy N, Donnay A, Griffiths Y, Guala I, Guerin L, Hinchin H, Labrune C, Reiss H, Van Hoey G, Birchenough SNR, A generic framework to assess the representation and protection of benthic ecosystems in European marine protected areas, *Aquatic Conservation: Marine and Freshwater Ecosystems* 2020, 30, 1253–1275, doi: 10.1002/aqc.3401.

Marx D, Feldens A, Papenmeier S, Feldens P, Darr A, Zettler ML, Heinicke K, Habitats and Biotopes in the German Baltic Sea, *Biology* [accepted] 2023, 12.

Nygård H, Lindegarth M, Darr A, Dinesen GE, Eigaard OR, Lips I, Developing benthic monitoring programmes to support precise and representative status assessments: a case study from the Baltic Sea, *Environmental Monitoring and Assessment* 2020, 192, 795, doi: 10.1007/s10661-020-08764-7.

Romoth K, Darr A, Papenmeier S, Zettler ML, Gogina M, Substrate heterogeneity as a trigger for species diversity in marine benthic assemblages, *Biology* 2023, 12, 825, doi: 103390/biology12060825.

Romoth K, Gogina M, Beisiegel K, Darr A, Zettler ML, First record of the common sun star *Crossaster papposus* (L., 1767) in the Baltic Sea in over 100 years, *Oceanological and Hydrobiological Studies* 2022, 51, 143-148, doi: 10.26881/oandhs-2022.2.02.

Schaub I, Friedland R, Zettler ML, Good-Moderate boundary setting for the environmental status assessment of the macrozoobenthic communities with the Benthic Quality Index (BQI) in the south-western Baltic Sea, *Marine Pollution Bulletin* [submitted] 2023.

Schöne BR, Huang X, Jantschke A, Mertz-Kraus R, Zettler ML, High-resolution reconstruction of dissolved oxygen levels in the Baltic Sea with bivalves – a multi-species comparison (*Arctica islandica*, *Astarte borealis*, *Astarte elliptica*), *Frontiers in Marine Sciences* 2022, 9, 820731, doi: 103389/fmars2022820731.

LIST OF CONFERENCE PRESENTATIONS

2021 | **Biotopkarte Fehmarnbelt** [Biotope map Fehmarnbelt] BfN-Kolloquium Meeresnaturschutz, Vilm, Germany

2022 | **Biotopkarten des NSG Kadetrinne** [Biotope maps of the nature conservation area Kadet Trench] BfN-Kolloquium Meeresnaturschutz, Vilm, Germany

2023 | **Biotopkarten der Ostsee** [Biotope maps of the Baltic Sea] BfN-Kolloquium Meeresnaturschutz, Vilm, Germany

DATA

SSS raw data:

available on request through the State Office for Environment, Nature Conservation and Geology Mecklenburg-Western Pomerania (LUNG MV) or the IOW geo database

Benthic macrofauna data:

available on request through the Federal agency for Nature conservation (BfN) or the IOW Macrozoobenthos database

CRUISE REPORTS

EMB239: doi:1048433/cr_emb239

EMB269: doi:1048433/cr_emb269

EMB262

Baltic Sea sediments as archives of phytoplankton adaptation to climate change

AUTHORS

Department of Biological Oceanography, Leibniz-Institute for Baltic Sea Research
Warnemuende | Rostock, Germany

A. Kremp

Department of Marine Geology, Leibniz-Institute for Baltic Sea Research
Warnemuende | Rostock, Germany

H.W. Arz, O. Dellwig, M. Czymzik

Limnological Institute, University of Konstanz | Konstanz, Germany

L. Epp

Institute for Chemistry and Biology of the Marine Environment, University of Oldenburg | Oldenburg, Germany

P. Böning

Current climate change is a major threat to marine biodiversity with severe effects on ecosystem function and stability. Therefore, robust approaches for ecosystem assessments under global change are needed. In the Baltic Sea, phytoplankton are already starting to show shifts in species composition and abundance, putatively linked to specific traits of the different groups. Yet it is unclear whether the ecosystem was affected similarly by past changes and how its composition will change in the future. PHYTOARK, a Collaborative Excellence project funded by the Leibniz Competition in 2020, investigates the hypothesis that phytoplankton communities can recover from biodiversity loss and restore their function after climate driven regime shifts of the past and the future. This can be done using "sediment archives" represented by permanently anoxic sediments that have preserved living and dead phytoplankton remains throughout the Holocene history of the Baltic Sea.

Cruise EMB 262 PHYTOARCHIVE was conducted to collect long (covering the past 8000 years) and short (covering up to 200 years back in time) sediment cores in April 2021 from permanently anoxic sediments of the deep basins of the Baltic Sea (Figure 1).

Cores were dated based on trace metal and radionuclide analyses and correlation to previously dated cores from the same site. Thus, the temporal frame and respective environmental dynamics of the past approximately 8000 years are now well established.

Ancient DNA has been extracted from >300 sediment horizons through the different cores. Due to extensive fragmentation of ancient Phytoplankton DNA, new, specific suitable primers for the ancient matrix were developed. In parallel with the primer design, bioinformatic and analytic pipelines were established. Community DNA analyses so far revealed several major shifts in phytoplankton community composition throughout the Holocene history of the Baltic Sea. Harmful algal blooms caused by species of the toxic genus *Alexandrium*, for example, were apparently common and much more extensive than today thousands of years ago.

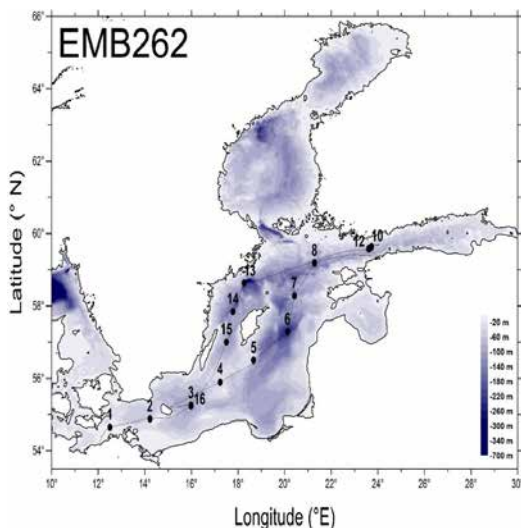


Figure 1: Cruise track of EMB 262 in April 2021. Sediment cores were taken at Stations 3.

Resurrection experiments were carried out as planned on processed sediment layers from short and long cores. Multiple strains of the diatom *Skeletonema marinoi* were successfully revived from both, short and long cores: Sediment slurries from long cores yielded 40 revived strains of *S. marinoi* from 10 time points through the past approx. 8000 years. To our knowledge this is the first example of millennial survival of phytoplankton resting stages, with an interesting potential for further studies on the genetic base and physiological mechanism of long-term dormancy and survival. Characterization of temperature dependent traits revealed synchrony of temperature adaptations with the dynamics of warm and cold phases.

Millennial population genomics, i. e. whole genome analyses and comparison of *S. marinoi* and the dinoflagellate *Apocalathium malmogiense* underway. A quantitative PCR assay (ddPCR) was established for both target species, and the hybridisation capture methodology enabled the isolation of species specific DNA from the sediment matrix. Results show a correlation of key species population dynamics with climate conditions.

As indicated by decadal monitoring data – dinoflagellate dominance (*A. malmogiense*) is correlated with warmer climate compared to diatom dominance (*S. marinoi*), seen during cold phases. Interestingly, these patterns do not necessarily reflect reaction norms and physiological capacities, pointing to complex ecological niches and equally complex genomic acclimation/adaptation strategies. Analyses are underway to investigate the genomic basis of adaptation patterns. Model development (WP3) and setup has been completed and simulations for community changes are ow running.

SCIENTIFIC OUTPUT

DATA

All physical oceanographic and chemical data can be investigated and downloaded at:

IOWDB – the oceanographic database of the institute

<https://odin2.io-warnemuende.de/#/>

The data is imported into the national and international databases MUDAB and ICES.

CRUISE REPORT

EMB262: doi:10.48433/cr_emb262

EMB265

Acoustic and in-situ observations of mixing processes in the Kattegat and Western Baltic Sea

AUTHORS

Leibniz-Institute for Baltic Sea Research Warnemünde | Rostock, Germany

L. Umlauf, P. Holtermann

BACKGROUND

During this short cruise (seven days at sea, including transit) with R/V Elisabeth Mann Borgese, we explored the potential of acoustic echo sounding techniques (wideband single-beam and multibeam systems) for the quantitative investigation of turbulence and other small-scale processes in the water column. These activities were embedded in the research project „Four dimensional Research applying Modeling and Observations for the Sea and Atmosphere“ (FORMOSA), funded by the German Leibniz-Association (WGL) in the framework of the national funding line “Cooperative Excellence”. The cruise took place in May 2021 in the Kattegat region and the western Baltic Sea (Arkona Basin) under severe Corona restrictions. These included a mandatory single occupancy of the cabins, such that only seven of the regular twelve board places were available for the scientific staff. Corona regulations also did not permit measurements too far away from the next German harbor, effectively allowing us to conduct measurements only in the southern part of the planned study area in the Kattegat (south of approximately 57°30'N). Despite these severe restrictions and the short duration of the cruise, we were able to obtain a rather unique data set, as discussed in more detail in the following.

INSTRUMENTATION

The key instruments for the investigation of turbulence and stratification parameters were two MSS90-L turbulence microstructure profilers from Sea & Sun Technology (Germany), equipped with two airfoil shear probes for turbulence measurements, a fast FP07 thermistor, a turbidity meter, a fast-response optode, and precision CTD sensors. Turbulence measurements were performed in a “two-yo” mode from the stern of the ship, while slowly (speed: 1–2 kn) cruising against wind and waves along pre-defined transects. The hydrographic structure of the water column was observed with a SBE 911plus CTD system (Seabird Electronics, USA), embedded in a rosette system with a set of 13 free-flow bottles from Hydrobios (Germany).

Near-surface velocity data were obtained with a 300-kHz Workhorse ADCP (Teledyne, USA), mounted in the moon pool of the ship jointly with other acoustic devices. These included an EK80 broad-band echo sounding system (Kongsberg, Norway) with two split-beam transducers (Simrad ES70-7C with 45–90 kHz and Simrad ES7120-7C with

90–150 kHz). A multibeam echo sounder of type R2Sonic2024 from R2Sonic (USA) was mounted in the hull of the ship. Both types of echo sounding systems were used to obtain high-resolution backscatter signals from the water-column for the acoustic analysis of turbulence and other small-scale physical processes (Muchowski et al., 2022).

Finally, first technical tests with the Unmanned Surface Vehicle (USV) MESSIN (developed by the Institute of Automation of the University of Rostock) were conducted to evaluate its potential for the autonomous collection of near-surface data. For cruise EMB265, MESSIN, was equipped with a 300-kHz downward looking ADCP (Workhorse Monitor from RDI, USA) and a small CTD system (CTD48M from Sea & Sun Technology, Germany) for near-surface velocity and stratification measurements.

CRUISE ACTIVITIES AND FIRST RESULTS

Most of our activities focused on the mixing of salty North Sea waters and brackish outflow waters from the Baltic Sea in the Kattegat region with the help of turbulence microstructure and acoustic observations. This region is a well-known hotspot of mixing and water mass transformation, affecting the properties of water masses entering into the Baltic Sea, and those outflowing through the Danish straits and propagating north towards the Skagerrak (Burchard et al., 2018). These water mass transformation processes can be detected and quantified only with in-situ turbulence observations that were, to our knowledge, lacking for this region at the time of the cruise.

Figure 1 shows turbulence microstructure data across a narrow submarine channel located on the western side of the Kattegat (between stations SK21 and SK22, as shown in more detail in the cruise report). In this region, the outflowing warm and fresh waters from the Baltic Sea, overlaying the colder and salty North Sea waters, generate a shallow density interface between approximately 5 m and 20 m depth (upper panel). The mixing of these two water masses is essential for the water mass properties of the outflowing current that propagates further along the Swedish west coast as well as for the effective exchange of water masses between the North Sea and Baltic Sea. Figure 1 shows that the pycnocline separating these water masses is strongly turbulent, suggesting active water mass transformation. Strong turbulence is also observed in the deeper parts inside the channel, pointing at the importance of these narrow channel, which are not well resolved in many numerical models, for energy dissipation. As energy dissipation is directly related to bottom friction in this case, these findings may have consequences for the exchange across the Danish straits. Similar measurements have been conducted across other submarine channels and, to investigate the impact of topographically induced mixing, across the topographic slopes at the side basins. In virtually all cases, we were able to identify strong mixing in regions with strong vertical temperature and salinity gradients, again pointing at importance of the Kattegat for water mass transformation.

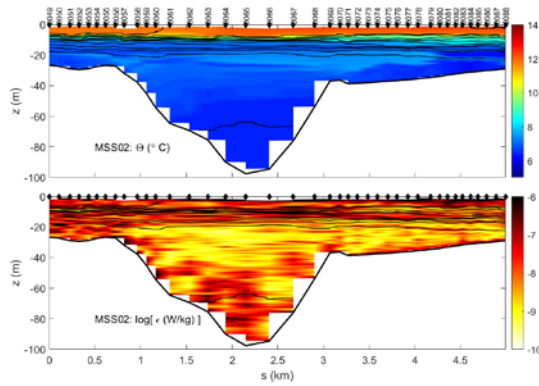


Figure 1: Conservative temperature (top) and logarithm of turbulence dissipation rate from densely-spaced microstructure profiles across a submarine channel in the Kattegat region (x-axis is along-track distance from West to East). Black lines indicate isopycnals. Black markers at the top each panel show the position of individual microstructure casts.

Figure 2 shows raw backscatter data from a short cross-slope transect near station SK04 in the Kattegat (see cruise report for station locations), close to the Swedish coast. These data illustrate the potential broadband acoustics for high-resolution imaging of small-scale physical processes like internal waves and boundary-layer turbulence, both clearly visible in the backscatter data.

The encouraging results from cruise EMB265 partly motivated a follow-up project for which research institutes and universities from Germany, Sweden, and Norway are at the moment developing plans to collaborate to investigate turbulent mixing and water mass transformation in the Northern Kattegat and Skagerrak. These activities will combine high-resolution numerical modeling and targeted field experiments based on methods similar to those used during EMB265.

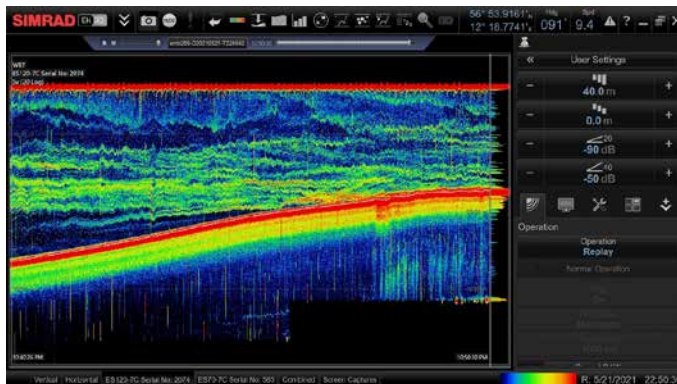


Figure 2: Screenshot of EK80 raw backscatter data from a transect starting near the coast. The strongest backscatter peak (red colors) indicates the sloping bottom topography. Clearly visible are indications of small-scale internal-wave motions and elevated near-bottom turbulence.

REFERENCES

Burchard H, Bolding K, Feistel R, Gräwe U, Klingbeil K, MacCready P, van der Lee, EM, The Knudsen theorem and the Total Exchange Flow analysis framework applied to the Baltic Sea, Progress in Oceanography 2018, 165, 268-286.

Muchowski J, Umlauf L, Arneborg L, Holtermann P, Weidner E, Humborg C, & Stranne C, Potential and Limitations of a Commercial Broadband Echo Sounder for Remote Observations of Turbulent Mixing, Journal of Atmospheric and Oceanic Technologies 2022, 39. 12.

SCIENTIFIC OUTPUT

LIST OF PUBLICATIONS

Holtermann H, Muchowski J, & Umlauf L, Water mass transformation and mixing in the Kattegat region, In preparation.

DATA

All data:

<https://iowmeta.io-warnemuende.de/geonetwork/srv/eng/catalog.search#/metadata/IOW-IOWDATA-EMB265-unvalidated>

CRUISE REPORT

EMB265: Submitted to GPF, under review

EMB276

Novel insights into the biogeochemistry of the redox zone in the Baltic Sea

AUTHORS

Leibniz-Institute for Baltic Sea Research | Warnemünde, Germany

M. Voss, H. Schulz Vogt, K. Gentsch, O. Dellwig, M. Kolbe

Woods Hole Oceanographic Institution | Woods Hole, MA, USA

C. Hansel, D. Hardisty, C. Ostrander, L. Taenzer, W. Pardis

AIMS OF THE CRUISE

During EMB276 cruise the biogeochemistry of the water column with special focus on the redox zone was investigated at a total of seven stations in the eastern Gotland Sea and the Faroe Deep. For this purpose, profiles were made with the CTD and the pump CTD and samples were taken for redox-sensitive trace metals including manganese (Mn), iodine, oxygen and nitrogen. A novel instrument (SOLARIS) to measure reactive oxygen species (ROS) was integrated into the CTD on board and tested for the first time in the water column spanning the oxic to anoxic zone with an emphasis on the suboxic region. Successful high-resolution nutrient and sensor profiles were recorded with the pump CTD. These data allow for the first time new insights into the co-distribution of Mn with other elemental cycles such as nitrogen, ROS, and trace metals.

RESULTS

Nutrient profiles reveal typical and expected gradients across all the stations sampled. Nicely reflected are the differences with respect to the stratification in the Gotland Sea and Fårö Deep (Dellwig et al., 2012). The first shows multiple small intrusions with slightly elevated oxygen concentrations, while the other Deep is more stable in its conditions. Nitrification rates were highest below the redoxcline and may be impacted by oxygen and substrate availability.

The distribution of dissolved and particulate Mn was conducted via discrete sampling along the water column. The colorimetric assay leucoberbelin blue was used to directly quantify Mn oxides along the depth profile. These data illustrate that Mn oxide concentrations are negligible at the surface but increase within the mixed layer and peak at the upper part of the redoxcline where oxygen levels are low. In contrast to expectations, this Mn oxide peak does not overlap with peak superoxide concentrations. In fact, the highest superoxide concentrations occurred at ~25–35 m in depth, rather than at the surface (see for example Figure 1). In the near-surface waters superoxide varied between 1.6 and 7.6 nM across stations, while the subsurface peaks spanned between 2.0 and

15.1 nM. A subsurface maximum in superoxide was consistently seen in every profile, regardless of time of day. At stations where multiple superoxide profiles were made, we observed that the concentrations of superoxide and the depth of the peak varied slightly throughout the day. A comparison with other data that was collected indicates that the superoxide maxima lay below the euphotic zone, and often coincided with a dip in fluorescence and oxygen values. The lack of light at this depth eliminates light-driven reactions as the source of superoxide, suggesting that heterotrophic activity is the likely source. These data are exciting as they point to microbial activity as the predominant source of ROS within this region, rather than the typically assumed pathway of photoexcitation of organic matter.

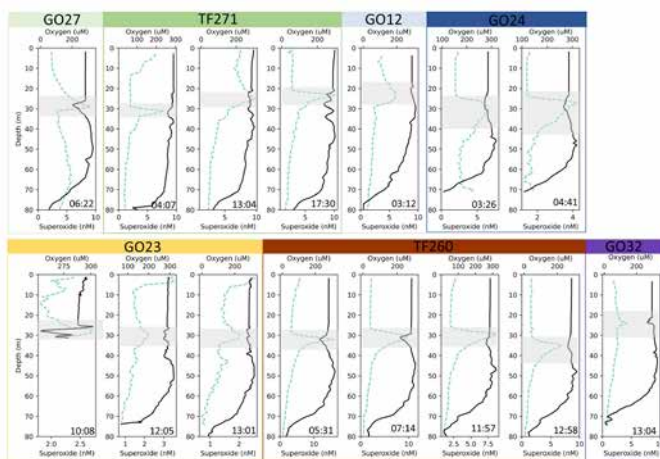


Figure 1: Representative plots of the ROS superoxide (green) versus oxygen (black) at several stations.

Thallium (Tl) preferentially (ad)sorbs to Mn oxides and thus its distribution is controlled in part by Mn cycling. Tl isotope ratio data were also generated to waters and particles to better understand how Tl and its isotopes are cycled in the Baltic Sea relative to Mn. At two East Gotland stations Tl isotope ratio data were also generated for a short sediment core. Dissolved Tl concentrations rapidly decrease below the oxycline at all stations. Dissolved Tl isotope compositions ($\epsilon^{205}\text{Tl}$) are conservative across all stations and, near the bottom of the Gotland Basin at station TF271, this seawater $\epsilon^{205}\text{Tl}$ value is transferred to sediments. To summarize, Tl behaves non-conservatively in Baltic seawater, but Tl isotopes are conservatively distributed in Baltic seawater and sediments and suggest that no measurable isotopic fractionation is imparted during any Tl removal processes. Notably, the Baltic seawater $\epsilon^{205}\text{Tl}$ value today is slightly higher than expected based on conservative mixing. Follow up analyses of a short sediment core collected during an earlier EMB cruise (EMB201) indicate that this higher-than-expected seawater $\epsilon^{205}\text{Tl}$ value originated ~1950 – at the same time independent datasets track an increased influx of

coal and fossil fuel combustion products to the Baltic Sea (Kaiser et al., 2022). Coal and cement combustion and its byproducts are known to have high TI contents, and so it seems very likely that these anthropogenic activities have shifted the seawater $\delta^{205}\text{Tl}$ value in the Baltic Sea.

We also collected and measured iodine speciation in samples from the Baltic Sea in order to understand the iodine cycle and its co-distribution with Mn and ROS. Dissolved I speciation—including iodate (IO_3^-), iodide (I^-), dissolved organic iodine (DOI)—were measured from seven stations using chromatography and mass spectrometry. Our data demonstrate two significant features not previously observed in the Baltic Sea or any other global anoxic basins: 1) Unusually depleted IO_3^- above the chemocline of the central Baltic Sea, where the O_2 is abundant (see Figure 2); 2) Unlike the majority of the global ocean, the total iodine in the Baltic Sea water column is not constant, even considering the dilution factor of freshwater introduced into the Baltic Sea Basin. The imbalance between rapid reduction expected in anoxic waters and sluggish re-oxidation may be responsible for the depleted IO_3^- in the surface Baltic Sea. Additionally, the non-conservative nature of iodine might be the result of sorption by particles in the water column, such as Mn-oxides or organics. Validation of these hypotheses is currently on-going.

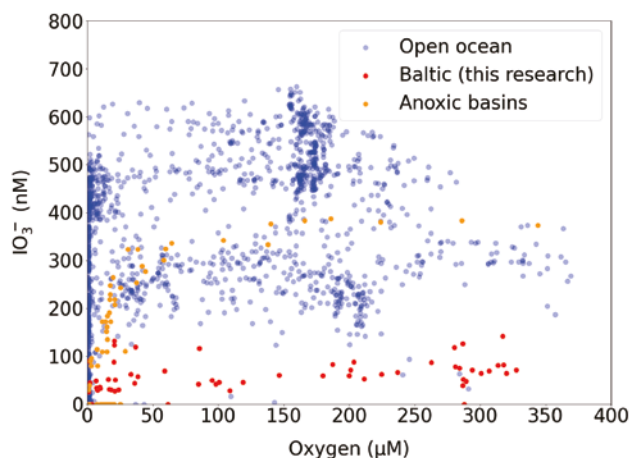


Figure 2: Comparison of iodate (IO_3^-)-oxygen (O_2) relationship between the Baltic Sea and other low- O_2 marine settings. The IO_3^- in the Baltic Sea is overall lower than other locations, even when O_2 is abundant.

CONCLUSION

Overall, these data indicate that light-independent processes, likely microbial respiration, are responsible for peak superoxide formation within the Baltic Sea water column. Follow up experiments will link microbial respiration rates and ROS formation and decay. Our data also suggest that ROS cycling may not be directly responsible for Mn redox profiles and instead low oxygen heterotrophic activity may drive Mn oxide formation. The redox

(re)cycling of Mn overlaps with thallium and iodine redox processes, which will be directly targeted in shipboard incubations next year.

REFERENCES

Kaiser J, Abel S, Arz HW, Cundy AB, et al., The East Gotland Basin (Baltic Sea) as a candidate global boundary stratotype section and point for the Anthropocene series, *The Anthropocene Review* 2022, 10, doi:10.1177/20530196221132709.

Dellwig O, Schnetger B, Brumsack H.-J, Grossart H.-P and Umlauf L, Dissolved reactive manganese at pelagic redoxclines (part II): Hydrodynamic conditions for accumulation, *Journal of Marine Systems* 2012, 90, 31-41. doi.org/10.1016/j.jmarsys.2011.08.007.

SCIENTIFIC OUTPUT

LIST OF PUBLICATIONS

Papers in prep. only

LIST OF CONFERENCE PRESENTATIONS

2022 | **Complexity of Synergistic and Competing Reactions Involved in Setting Manganese Oxide Distributions within Surface Waters** Goldschmidt Conference, Honolulu, HI, USA.

2022 | **Superoxide Dynamics in an Ocean Hypoxic Zone** AGU Ocean Sciences Meeting Virtual, Hawaii, USA.

2022 | **Towards a Better Understanding of Thallium Isotope Cycling in Modern Redox-stratified Settings** American Geophysical Union Fall Meeting, Chicago, IL, USA.

2022 | **Iodine Speciation in the Redox-stratified Baltic Sea and Implications for I/Ca Paleoredox Interpretations** American Geophysical Union Fall Meeting, Chicago, IL, USA.

2023 | **The Geomicrobiology of Superoxide in the Marine Water Column: A Case Study from the Baltic Sea** Geological Society of America Meeting, Pittsburgh, PA, USA.

DATA

Physical oceanography (CTD) and Metadata:

<https://iowmeta.io-warnemuende.de/geonetwork/srv/eng/catalog.search#/metadata/IOW-IOWMETA-EMB276-2021>

CRUISE REPORT

EMB276: doi:10.48433/cr_emb276

HE525

Pleistocene Boulder Detection Testing the Manta Ray

AUTHORS

University of Bremen | Bremen, Germany

H. Keil, N. Römer-Stange, V. Spieß

Fraunhofer Institute for Wind Energy Systems | Bremerhaven, Germany

S. Wenau, V. Bihler, C. Ramos Cordova

INTRODUCTION

The shallow geology of the North and Baltic Sea in the last 400.000 years was mainly influenced by several glacial ice advances in the Elsterian, Saalian and Weichselian and the corresponding interglacial phases causing regression and transgression phases and partially exposed large areas to pro-glacial and terrigenous sedimentation. While the Weichselian glaciation was restricted to the northern regions the Elsterian and Saalian glaciers transported large amounts of eroded material from Scandinavia southwards. This material shows a broad range of grain sizes including coarse grains and stones up to boulders of several meters in diameter. While certain typical subglacial features like moraines and eskers or the highly erosive subglacial tunnel valleys are locations of concentration for glacial till, glacial boulders, often transported as 'payload' frozen in the glacier, are found widespread in northern Europe and not always linked to certain geologic structures (e. g. Ehlers, 1990, 1994, Streif, 2002).



Figure 1: Famous granite boulder "Alter Schwede" found 1999 within river Elbe during dredging activities and displaced towards river shore. Diameter 4.5 – 6m, weight 217t.

In the German North Sea especially the region east of the Elbe Palaeovalley (EPv) is known for abundant stones on the seafloor which is also reflected in naming convention in charts ("Steingrund", "Sylter Außenriff"). In the Baltic Sea up to the 70s of the last century the so called Boulder Fishery was common down to water depths of 20 m because these boulders were used in constructions on land. These historic and present evidences relate only to boulders on the seafloor deposited mainly during the Weichselian which can be well detected and located with modern multibeam systems or deep towed sidescan sonars. However, based on the observations and also based on findings in terrestrial sand pits, it is clear that boulders have been also transported in the earlier glacial periods and were subsequently buried by successive deposition processes.

From a geotechnical perspective glacial boulders with a diameter larger than one meter pose a significant hazard to the installation of offshore constructions (e. g. Holeyman et al., 2015). Windmill foundations, which have to be rammed up to 80 m into the seafloor can be damaged or even blocked completely causing high follow-up costs because additional piles are needed and damaged piles need to be treated properly. Therefore, methods to locate buried boulders or at least to mitigate risks are an important factor for the development of offshore windfarms, increasing cost efficiency and supporting a renewable energy transition.

THE SEISMIC BEAMFORMER FRAME 'MANTA RAY'

While geologic interfaces characterized by changes in density and/or seismic velocity cause reflections of seismic waves which then can be processed to structural images of the subsurface, isolated objects like boulders or faults cause scattering of acoustic waves which shows up on seismic section in the form of diffraction hyperbolas (e. g. Landa et al., 1987, Landa & Keydar, 1998). Depending on object size and signal wavelength the amplitude of these diffracted waves is weaker by several orders of magnitudes compared to reflected energy, however, it still contains valuable information on the corresponding sources and methods have been established to separate reflected energy from diffracted energy in seismic data (diffraction imaging), driven mostly in the field of exploration geophysics to better image for instance small faults (e. g. Khaidukov et al., 2004, Fomel et al., 2007, Moser et al., 2008, Bauer et al., 2017, Schwarz, 2019).

A disadvantage of diffraction imaging with 2D-seismic data is, however, that the lateral position of diffraction events is ambiguous and that the separation of the two energy types is quite challenging at complex heterogeneous interfaces. To overcome these issues the BMWi project BoulderDetection aimed on the application of beamforming technology for seismic data.



Figure 2: Aluminum Tow Frame used on cruise HE525 (without equipped hydrophones).

For this purpose a tow frame construction of appropriate size was designed (Figure 2) which was equipped with conventional hydrophones in a rectangular pattern and combined with a conventional high resolution seismic source. The operation can therefore be described as a kind of 'subseafloor multibeam' system. This approach has several advantages: 1. a precise lateral location of subsurface targets is possible; 2. the acoustic source can be chosen to fit to the intended target depth and size; 3. reflection/diffraction separation is facilitated because apart from the center beams reflected energy is relatively weak; 4. compared to a 3D-seismic survey not a full coverage of the area is needed.

The frame design was based on extensive modelling efforts and some balancing between the needs for resolution and handling capabilities on research vessels. The prototype tested on cruise HE525 therefore was 8x2.5m in size and equipped with loops of a conventional 24 channel streamer section (Figure 2). For motion correction, necessary for all multibeam systems, a MRU was mounted directly on the frame.

RESULTS

The tow frame was tested successfully on cruise HE569 in an area north of Helgoland known for abundant stones and boulders on the sea floor (Michaelis et al., 2019). This test had two parts, first the whole handling procedure needed testing and second the detection of boulders on the seafloor should be possible. Consequently the study area was first investigated with the shipboard multibeam EM710, which allowed a first assessment of potential boulder locations which were then investigated with the tow frame. The processed data can be displayed as a 3d cube of diffraction energy and careful choice of threshold values can then provide locations potential constructional hazards (Figure 3).

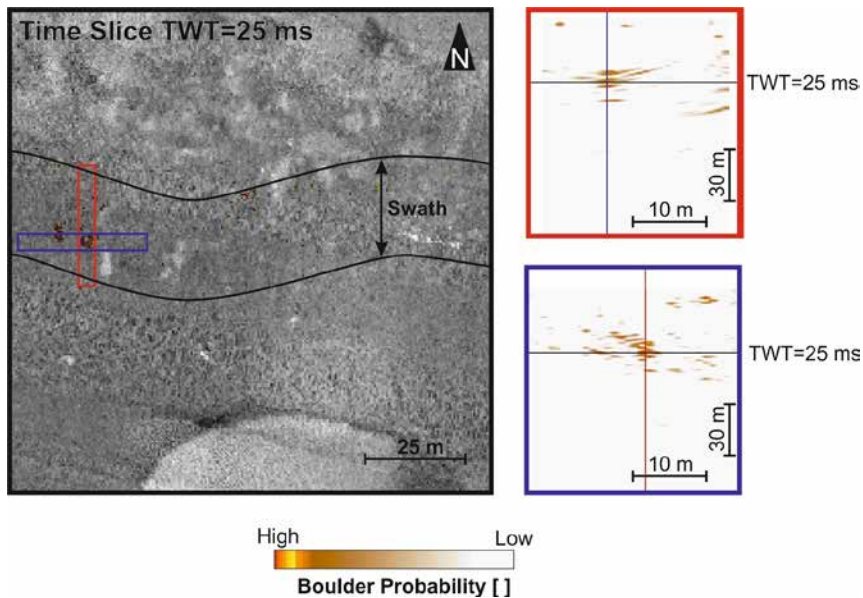


Figure 3: Example of calculated probability of a boulder diffraction. Left: gray scaled Multibeam backscatter image showing a boulder on the seafloor at the intersection of the red and blue rectangle. Right: calculated diffraction amplitude at the red and the blue survey crossing of this target with the tow frame. Maximum amplitude can be picked at the location of the surficial boulder.

The associated project was finished in 2019 and since then the patented methodology was successfully applied in several smaller and larger commercial site surveys in the Baltic Sea area to mitigate risks during offshore wind farm construction phases.

REFERENCES

Bauer A, Schwarz B, Gajewski D, Utilizing Diffractions in Wavefront Tomography, *Geophysics* 2017, 82(2), doi: 10.1190/geo2016-0396.1.

Ehlers J, *Allgemeine und Historische Quartärgeologie* 1994, Stuttgart: Enke.

Fomel S, Landa E, Taner T, Poststack Velocity Analysis by Separation and Imaging of Seismic Diffractions, *Geophysics* 2007, 72(6), doi: 10.1190/1.2781533.

Holeyman A, P Peralta P, Charue N, Boulder-Soil-Pile Dynamic Interaction, *Frontiers in Offshore Geotechnics III* 2015, edited by Vaughan Meyer, Leiden, Netherlands: CRC Press/Balkema.

Khaidukov V, Landa E, Moser TJ, Diffraction Imaging by Focusing-Defocusing: An Outlook on Seismic Superresolution, *Geophysics* 2004, 69(6), doi: 10.1190/1.1836821.

Landa E, Shtivelman V, Gelchinsky B, A Method for Detection of Diffracted Waves on Common-Offset Sections, *Geophysical Prospecting* 1987, 35(4), doi: 10.1111/j.1365-2478.1987.tb00823.x.

Landa E, Keydar S, Seismic Monitoring of Diffraction Images for Detection of Local Heterogeneities, *Geophysics* 1998, 63(3), doi: 10.1190/1.1444387.

Michaelis R, Hass HC, Mielck F, et al., Hard-substrate habitats in the German Bight (South-Eastern North Sea) observed using drift videos, *Journal of Sea Research* 2019, 144, 78–84, doi: 10.1016/j.seares.2018.11.009.

Moser T J, Howard CB, Diffraction Imaging in Depth, *Geophysical Prospecting* 2008, 56(5), doi: 10.1111/j.1365-2478.2007.00718.x.

Schwarz B, Coherent Wavefield Subtraction for Diffraction Separation, *Geophysics* 2019, 84(3), doi: 10.1190/geo2018-0368.1.

Streif H, The Pleistocene and Holocene Development of the Southeastern North Sea Basin and Adjacent Coastal Areas, In *Climate Development and History of the North Atlantic Realm* 2002, Berlin, Heidelberg: Springer, doi: 10.1007/978-3-662-04965-5_25.

SCIENTIFIC OUTPUT

LIST OF PUBLICATIONS

Römer-Stange N, Wenau S, Bihler V, et al., Boulder Detection in the Shallow Sub-Sea-floor by Diffraction Imaging With Beamforming on Ultra-High Resolution Seismic Data – A Feasibility Study, *Earth and Planetary Science* 2022, 9(6), doi: 10.1029/2021EA002156.

Wenau S, Schwarz B, Bihler V, et al., Derisking Offshore Windfarm Installation by Sub-Sea-floor Boulder Detection Based on Dedicated Seismic Diffraction Imaging, *First Break* 2022, 40(11), doi: 10.3997/1365-2397.fb2022092.

LIST OF CONFERENCE PRESENTATIONS

2018 | **A Seismic Beamforming Approach for the Detection Of Boulders in the Shallow Sub-Sea-floor** Near Surface Geophysics 2018 3rd Applied Shallow Marine Geophysics Conference, Porto, Portugal.

2020 | **Sub-Sea-floor Object Detection through Dedicated Diffraction Imaging** Near Surface Geophysics 2020 4th Applied Shallow Marine Geophysics Conference, Online conference EAGE.

2021 | **Dedicated Diffraction Imaging for Sub-Sea-floor Object Detection** 2nd
Geoscience & Engineering in Energy Transition Conference, Strasbourg, France.

2022 | **Dedicated Diffraction Imaging for Sub-Sea-floor Object Detection** Seismic2022
Conference, Aberdeen, United Kingdom.

2023 | **Diffraction Imaging for Sub-sea-floor Object Detection: A case study from the German Baltic Sea** 83. Annual Meeting of the Deutsche Geophysikalische Gesellschaft, Bremen, Germany

DATA

Raw Seismic Data:

Data-Server of working group of Marine Technology and Environmental Sciences,
University of Bremen, Contact authors for details on data access.

Continuous Thermosalinograph measurements:

<https://doi.pangaea.de/10.1594/PANGAEA.909013>

Processed Seismic Data:

<https://doi.pangaea.de/10.1594/PANGAEA.939091>

Multibeam Raw Data:

<https://doi.pangaea.de/10.1594/PANGAEA.939091>

Processed Multibeam Data:

<https://doi.pangaea.de/10.1594/PANGAEA.939376>

CRUISE REPORT

HE525: doi: 10.1594/PANGAEA.900253

HE527

In between the Storms on the North Sea

AUTHORS

Institute for Chemistry and Biology of the Marine Environment, Carl von Ossietzky
Universität Oldenburg | Oldenburg, Germany

T. H. Badewien

The research cruise with the vessel Heincke leg HE527, was carried out as part of projects funded by the MWK Lower Saxony, was a comprehensive expedition aimed at understanding various environmental issues in the North Sea. The projects 'Makroplastics', 'COD (Coastal Ocean Darkening)' and 'BIME (Barrier Island Mass Effect)' formed the basis of this expedition, focusing on macroplastic pollution, light distribution in marine waters and the influence of barrier islands on organic matter in the North Sea.

MACROPLASTIC POLLUTION AND DISTRIBUTION

A primary objective of HE527 was to complement the macroplastic pollution data collected during the HE503 cruise. The team deployed advanced tracking and measurement techniques, deploying 9 small box GPS drifters, 11 eddy GPS drifters and several wooden drifters (see Figure 1). This equipment played a crucial role in mapping the distribution and beaching patterns of macroplastics. The GPS technology of the drifters allowed precise tracking of macroplastic movements, providing valuable insights into the pathways and accumulation zones of these pollutants (Meyerjürgens et al. 2019, Meyerjürgens et al. 2023). These data are essential for the development of effective mitigation strategies. An exploratory analysis of seafloor litter dynamics in the SE German Bight was conducted (Meyerjürgens et al. 2022).

SPECTRAL LIGHT FIELD AND OPTICALLY ACTIVE SUBSTANCES IN THE NORTH SEA

Another important aspect of the cruise was the study of the spectral light field and optically active substances in various North Sea water bodies. Understanding the light distribution in marine waters is crucial for assessing the photosynthetic activity of marine organisms and the overall health of aquatic ecosystems. The study also involved testing new measurement methods and sensors specifically designed for use in coastal waters. The data were also used to develop a new light field parameterisation for coastal waters (Wollschläger et al. 2020). These innovative tools are expected to improve the accuracy and efficiency of future oceanographic research (Zielinski et al. 2022).

MOLECULAR COMPOSITION OF DISSOLVED ORGANIC MATTER

Research extended to analysing the molecular composition of dissolved organic matter in the North Sea. Particular attention was paid to the influence of freshwater discharge, groundwater discharge from barrier islands and the Wadden Sea, and primary production in the water column. This comprehensive approach aimed to uncover the complex relationships between different organic and inorganic components of the sea and how these interactions affect the marine environment (Speidel et al. 2024).

STUDY AREA AND TRANSECTS

The study covered a wide geographical area, including the rivers Ems, Weser and Elbe, the German coastal areas of the North Sea and the German Bight. Investigations were carried out along transects extending from the coast to the open sea. This extensive coverage ensured a thorough understanding of the diverse marine environments and the varying impacts of human and natural activities on these areas.

SUCCESS AND FUTURE IMPLICATIONS

The cruise with the research vessel *Heincke*, leg HE527, went as planned and was considered a great success by all participants. The results of this cruise are expected to make a significant contribution to the current understanding of marine pollution, in particular to the third party funded projects on macroplastic distribution and the factors influencing ocean light penetration and organic matter composition. The data sets have been published in the PANGAEA database and the methodologies developed during this expedition will undoubtedly help to shape future environmental policy and research directions, particularly in the field of marine conservation and sustainable ocean management.



Figure 1: Deployment of drifter during the research cruise HE527.

REFERENCES

Meyerjürgens J, Badewien TH, Garaba SP, Wolff JO, & Zielinski O, A state-of-the-art compact surface drifter reveals pathways of floating marine litter in the German bight, *Frontiers in Marine Science* 2019, 6, 58, Volume 6 – 2019 | <https://doi.org/10.3389/fmars.2019.00058>.

Meyerjürgens J, Schöneich-Argent RI, & Badewien TH, An exploratory analysis of seabed litter dynamics in the SE German Bight, *Marine pollution bulletin* 2022, 177, 113515, <https://doi.org/10.1016/j.marpolbul.2022.113515>.

Meyerjürgens J, Ricker M, Aden C, Albinus M, Barrelet J, Freund H, ... & Badewien T H, Sources, pathways, and abatement strategies of macroplastic pollution: an interdisciplinary approach for the southern North Sea, *Frontiers in Marine Science* 2023, 10, 1148714, <https://doi.org/10.3389/fmars.2023.1148714>.

Speidel LG, Silva da RC, Beck M, Dellwig O, Wollschläger J, Dittmar T, Seidel M, Rivers and tidal flats as sources of dissolved organic matter and trace metals in the German Bight (North Sea), *Biogeochemistry* 2024 (Springer), accepted).

Wollschläger J, Tietjen B, Voß D, & Zielinski O, An empirically derived trimodal parameterization of underwater light in complex coastal waters – A case study in the North Sea, *Frontiers in Marine Science* 2020, 7, 512, <https://doi.org/10.3389/fmars.2020.00512>.

Zielinski O, Pieck D, Schulz J, Thölen C, Wollschläger J, Albinus M, Badewien TH, ... & Winkler H, The Spiekeroog coastal observatory: A scientific infrastructure at the land-sea transition zone (southern North Sea), *Frontiers in Marine Science* 2022, 8, 754905, <https://doi.org/10.3389/fmars.2021.754905>.

SCIENTIFIC OUTPUT

LIST OF PUBLICATIONS

Meyerjürgens J, Schöneich-Argent RI, & Badewien TH, An exploratory analysis of seabed litter dynamics in the SE German Bight, *Marine pollution bulletin* 2022, 177, 113515, <https://doi.org/10.1016/j.marpolbul.2022.113515>.

Meyerjürgens J, Ricker M, Aden C, Albinus M, Barrelet J, Freund H, ... & Badewien T H, Sources, pathways, and abatement strategies of macroplastic pollution: an interdisciplinary approach for the southern North Sea, *Frontiers in Marine Science* 2023, 10, 1148714, <https://doi.org/10.3389/fmars.2023.1148714>.

Speidel LG, Silva da RC, Beck M, Dellwig O, Wollschläger J, Dittmar T, Seidel M, Rivers and tidal flats as sources of dissolved organic matter and trace metals in the German Bight (North Sea), *Biogeochemistry* 2024 (Springer), accepted).

Wollschläger J, Tietjen B, Voß D, & Zielinski O, An empirically derived trimodal parameterization of underwater light in complex coastal waters—A case study in the North Sea, *Frontiers in Marine Science* 2020, 7, 512, <https://doi.org/10.3389/fmars.2020.00512>.

DATA

Badewien, TH; Rohardt, G (2019): Continuous thermosalinograph oceanography along Heincke cruise track HE527: <https://doi.org/10.1594/PANGAEA.903015>

Badewien, TH (2019): Links to master tracks in different resolutions of HEINCKE cruise HE527, Bremerhaven – Bremerhaven, 2019-03-19 - 2019-03-31: <https://doi.org/10.1594/PANGAEA.900953>

Badewien, TH; Wisotzki, A (2019): Physical oceanography during HEINCKE cruise HE527: <https://doi.org/10.1594/PANGAEA.902153>

Wollschläger, J; Henkel, R; Voß, D et al. (2020): Hyperspectral underwater light field measured during the cruise HE527 with RV HEINCKE: <https://doi.org/10.1594/PANGAEA.912054>

Wollschläger, J; Henkel, R; Voß, D et al. (2020): Upwelling radiance L_u measured during the cruise HE527 with RV HEINCKE: <https://doi.org/10.1594/PANGAEA.912052>

Wollschläger, J; Henkel, R; Voß, D et al. (2020): Above water irradiance E_s measured during the cruise HE527 with RV HEINCKE: <https://doi.org/10.1594/PANGAEA.912046>

Wollschläger, J; Henkel, R; Voß, D et al. (2020): Downwelling irradiance E_d measured during the cruise HE527 with RV HEINCKE: <https://doi.org/10.1594/PANGAEA.912044>

Wollschläger, J; Tietjen, B; Voß, D et al. (2021): Hyperspectral absorption coefficient measurements during the cruise HE527 with RV HEINCKE: <https://doi.org/10.1594/PANGAEA.928543>

HE528 AND HE572

Benthic community changes over 50 years in the German Bight, North Sea

AUTHORS

Alfred Wegener Institute Helmholtz Centre for Polar and Marine Research |
Bremerhaven, Germany
J. Dannheim

The benthic ecosystem of the German Bight (North Sea) is subject to continuous change as a consequence of natural environmental variations and human activities. Examples for natural environmental variation are seasonal temperature fluctuations and medium- to long-term climatic oscillations such as the North Atlantic Oscillation (NAO) (Kröncke et al. 2001). Human activities such as sediment extraction and dumping (Witt et al. 2004), bottom trawling (Kaiser et al. 2006), and offshore constructions (e. g., wind farms) cause direct physical disturbance of the seafloor (Dannheim et al. 2020). Other activities such as eutrophication, pollution, climate change and also bottom trawling (e. g., Kaiser et al. 2006, Clark and Frid 2001) act on larger scales and affect ecosystems through their influence on community metabolism and food web interactions (Kröncke 2011). Structural changes in benthic communities are reliable indicators for substantial long-term environmental variations because of the relatively stable habitat conditions in the subtidal as well as the stationary life style and the longevity of many benthic organisms.

Continuous observations (monitoring) of benthic populations and communities on an appropriate spatial and temporal resolution are a valuable tool for observing and analyzing ongoing changes in marine ecosystems (Perry et al. 2004), and the scientific merit of an environmental monitoring program increases with the duration of the program (Southward et al. 1995). For example, the long-term monitoring program on the macrozoobenthos of the German Bight, which has been initiated by E. Rachor in 1969, could clearly show long-term structural changes of benthic communities in that region in response to climatic variations (Schröder 2003, Shojaei et al. 2016). Similar results have been generated from other continuous long-term observations (e. g. Kröncke et al. 2001, Kröncke 2011).

Latest publications on our monitoring program provided evidence for (a) high functional redundancy among species and (b) turnover of species over time (Rishworth et al. 2020). Communities displayed a rapid functional recovery which confirms the self-organizing ability of the ecosystem in response to stressors, which may be attributed to the high functional redundancy in the temperate shelf sea system of the North Sea (Shojaei et al. 2021).

The aim of the R/V Heincke cruises HE528 and HE572 were to proceed the 50th and 52nd annual sampling of the long-term benthic research program. The program of the cruise comprised sampling of soft-bottom infauna with van Veen grab and benthic bioturbation investigated with the sediment profile imaging camera at the four long-term station FSd, Slt, SSd and WB (Figure 1).

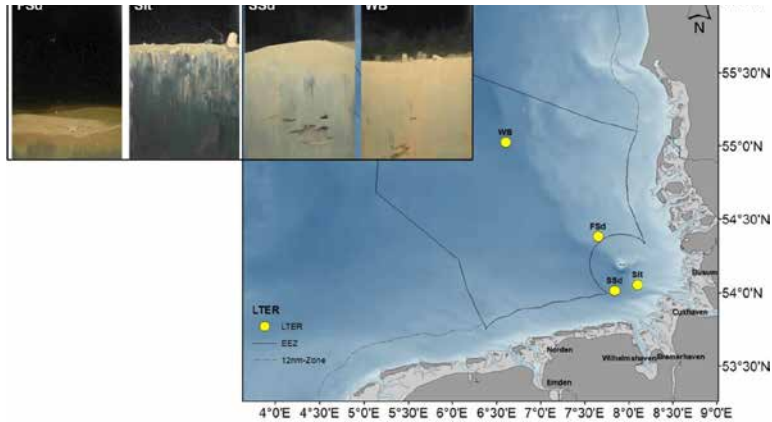


Figure 1: Map of sampling stations of the benthic long-term series FSd, Slt, SSd and WB and sediment profile images of all four stations taken during HE528.

The results of the last 50 years of sampling allow for the quantification of long-term dynamics in macrozoobenthic communities under the influence of e. g., climate change. For the analysis we applied the species exchange ratio (SER) following the concept of Hillebrand et al. (2018). SER measured the proportional exchange of species between an earlier and later sample in a time series and is based on the Jaccard's similarity index. SER was compared between each year (a) and the following consecutive year (a + 1). In order to analyse how biodiversity changes over the whole 50 years, i. e., long-term changes in turnover independent of interannual short-term variability, we assessed SER for all combinations of years, i. e., turnover between year (a) and the following years (a+1, a+2, ...a+50).

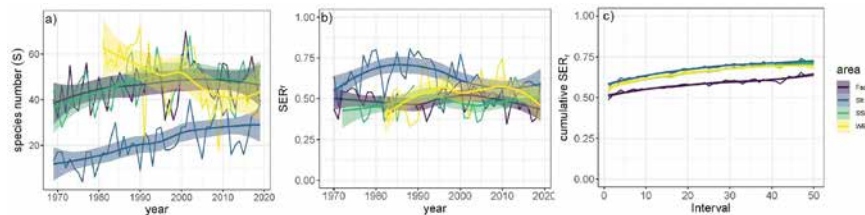


Figure 2: Species dynamics of (a) species richness (S), (b) species exchange rates (SER) between years over study time and (c) species exchange rate (SER) cumulative over 50 years at all four long-term stations.

We found no significant trends in species number (Figure 2a) except for station SlT ($R^2=0.41$, $p<0.01$). We tested whether species turnover rates changed significantly over half a century for all four stations, but were unable to detect a significant change (Figure 2b). At all stations, exchange rates accumulated significantly ($p<0.01$) in species turnover, reflected by an increase with increasing temporal distance between sampling points (Figure 2c). Significant increase of SERr was in the same range for all stations reflected by similar slopes.

Our current analysis suggests that classical diversity measures are able to detect strong impacts, i. e., the increase of species number at the SlT station is the recovery after sewage sludge dumping disturbance. The dumping site was 8 km north of the long-term station and dumping took place until 1980. Thereafter, more species were able to settle over the last years after cessation of dumping. However, classical diversity measures are unable to detect the variability and dynamics of species populations. Our results provide evidence that on average 53% of the species are exchanged from year to year. The high species turnover between years demonstrate that macrobenthos of the North Sea has a variable species pool as response to natural and anthropogenic stressors. The cumulative species exchange rate increased by 0.3% per year which adds up to 13% species exchange increase over 50 years. Thus, benthic communities shifted significantly over the last five decades and got more variable over time (i. e., increased exchange rates).

With the R/V Heincke cruise HE528 in 2019 we were able to finalise half of a century of sampling, enabling us to analyse macrozoobenthic changes in the North Sea. Such time series over 50 years are rare but simultaneously valuable to detect long-term changes. Thus, we were pleased to proceed our monitoring in 2021 with the cruise HE572 as the continuous sampling was interrupted for the first time after 50 years by Corona. However, HE572 samples are currently analysed, as are the pictures from the sediment profile imaging camera taken during both cruises at the long-term stations.

REFERENCES

Clark RA, Frid CLJ, Long-term changes in the North Sea ecosystem, *Environmental Reviews* 2001, 9, 131–187, doi: 10.1139/a01-005.

Dannheim J, Bergström L, Birchenough SNR, Brzana R, et al., Benthic effects of offshore renewables: identification of knowledge gaps and urgently needed research, *ICES Journal of Marine Science* 2020, 77, 1092–1108, doi: 10.1093/icesjms/fsz018.

Hillebrand H, Blasius B, Borer ET, Chase JM, et al., Biodiversity change is uncoupled from species richness trends: Consequences for conservation and monitoring, *Journal of Applied Ecology* 2018, 55, 169–184, doi:10.1111/1365-2664.12959.

Kaiser MJ, Clarke KR, Hinz H, Austen MCV, et al., Global analysis of response and recovery of benthic biota to fishing, *Marine Ecology Progress Series* 2006, 311, 1–14, doi: 10.3354/meps311001.

Kröncke I, Zeiss B, Rensing C, Long-term variability in macrofauna species composition off the island of Norderney (East Frisia, Germany) in relation to changes in climatic and environmental conditions, *Senckenbergiana maritima* 2001, 31, 65–82, doi: 10.1007/BF03042837.

Kröncke I, Changes in Dogger Bank macrofauna communities in the 20th century caused by fishing and climate, *Estuarine Coastal and Shelf Science* 2011, 94, 234–245, doi: 10.1016/j.ecss.2011.06.015.

Perry RI, Batchelder HP, David LM, Chiba S, et al., Identifying global synchronies in marine zooplankton populations: issues and opportunities, *ICES Journal of Marine Science* 2004, 61, 445–456, doi: 10.1016/j.icesjms.2004.03.022.

Rishworth GM, Adams JB, Bird MS, Carrasco NK, et al., Cross-continental analysis of coastal biodiversity change, *Philosophical Transactions Royal Society B* 2020, 375, 20190452, doi: 10.1098/rstb.2019.0452.

Schröder A, Long term trends and dynamics of macrozoobenthos in the German Bight (North Sea), Dissertation, University of Bremen 2003, 265 pp, urn:nbn:de:gbv:46-diss000008525.

Shojaei MG, Gutow L, Dannheim J, Rachor E, et al., Common trends in German Bight benthic macrofaunal communities: Assessing temporal variability and the relative importance of environmental variables, *Journal of Sea Research* 2016, 107, 25–33, doi: 10.1016/j.seares.2015.11.002.

Shojaei MG, Gutow L, Dannheim J, Schröder A, et al., Long-term changes in ecological functioning of temperate shelf sea benthic communities, *Estuarine, Coastal and Shelf Science* 2021, 249, 107097, doi: 10.1016/j.ecss.2020.107097.

Southward AJ, Hawkins SJ, Burrows MT, Seventy years' observations of changes in distribution and abundance of zooplankton and intertidal organisms in the western English Channel in relation to rising sea temperature, *Journal of Thermal Biology* 1995, 20, 127–155, doi: 10.1016/0306-4565(94)00043-l.

Witt J, Schröder A, Knust R and Arntz WE, The impact of harbour sludge disposal on benthic macrofauna communities in the Weser estuary, *Helgoland Marine Research* 2004, 58, 117–128, doi: 10.1007/s10152-004-0177-3.

SCIENTIFIC OUTPUT

LIST OF PUBLICATIONS

Rishworth GM, Adams JB, Bird MS, Carrasco NK, et al. Cross-continental analysis of coastal biodiversity change, *Philosophical Transactions Royal Society B* 2020, 375, 20190452, doi: 10.1098/rstb.2019.0452.

LIST OF CONFERENCE PRESENTATIONS

2022 | **Biodiversity changes of benthic communities over 50 years in the German Bight, North Sea** North Sea Days, Wageningen, the Netherlands.

DATA

Thermosalinograph oceanography:
<https://doi.org/10.1594/PANGAEA.903016>

Thermosalinograph oceanography:
<https://doi.org/10.1594/PANGAEA.944725>

CRUISE REPORT

HE528: doi:10.2312/cr_he528

HE572: doi:10.48433/cr_he572

HE529, HE561 AND HE574

Development of nature conservation measures: European flat oyster restoration in the German Bight

AUTHORS

Alfred Wegener Institute Helmholtz Centre for Polar and Marine Research |
Bremerhaven, Germany

B. Pogoda, T. Hausen, S.E.A. Pineda-Metz

The Natura 2000 site Borkum Reef Ground (BRG) in the German Bight is a marine protected area (MPA) extending over 625 km² and water depths from 18 m to 33 m. The MPA was also defined as a national conservation area (NSG) in 2017 and includes the habitat type 1110 "sandbanks", the habitat type 1170 "reefs" as well species-rich gravel, coarse sand and shell gravel areas (KGS).

In this area, the European flat oyster (*Ostrea edulis*; Figure 1; Olsen 1883, Pogoda 2019a) once formed historically and ecologically relevant reef habitat for the North Sea. The species is an ecosystem engineer, building three-dimensional biogenic reef structures which are recognized as biodiversity hotspots (e. g., Möbius 1893, Pogoda et al. 2019, Pogoda et al. 2020a). Today, no intact oyster habitats remain in the German Bight. *O. edulis* populations are classified as functionally extinct in the German North Sea and under severe threat throughout Europe (Pogoda 2019a). Due to their ecological value, *O. edulis* reefs are now a focus of European conservation measures aiming at protection, preservation and restoration of biogenic reef structures.

In Germany, the restoration of biogenic reefs, namely the European oyster is an obligatory management measure of high priority for the MPA BRG (BfN 2020). Against this background, a 4x4 nm research area in the BRG MPA was implemented by the German Federal Water and Shipping Authority (WSV, WSA) for the implementation of the first European flat oyster restoration measures (Figure 1). Within the frame of project RESTORE, two pilot reef units (á 100 sqm) were built using a limestone base and both adult and juvenile oysters in July 2020 by (Pineda-Metz et al. 2023).

The work conducted during the expeditions HE529, HE561 and HE574 contributed to the site selection process, the baseline monitoring post-reef construction, as well as the test application and optimization of monitoring tools for non-invasive oyster habitat and biodiversity monitoring.

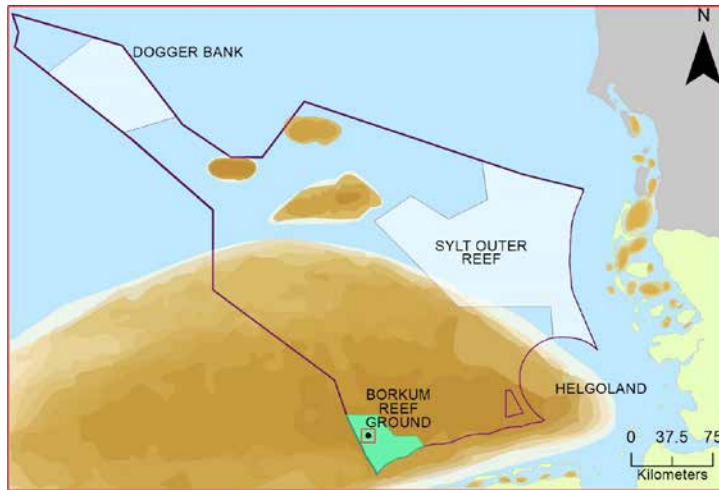


Figure 1: Map of the German Bight, the German Exclusive Economic Zone (EEZ) in the North Sea: Natura2000 sites (MPAs) Dogger Bank, Sylt Outer Reef and Borkum Reef Ground (BRG; green), oyster reef restoration research area and pilot oyster reef (red polygon/black dot). Brown areas represent the historical distribution of *Ostrea edulis* in the North Sea. Modified after Pineda-Metz et al. (2023).

Work during HE529 consisted of bathymetric surveys, which contributed data used to define optimal sites for deployment of the reefs as well as suitability maps for oyster restoration within the German Bight (Pogoda et al. 2020c, 2023). Both HE561 and HE574 surveyed the deployed reef units, conducted imagery surveys with tethered, remote and autonomous devices (e. g., OFOS, ROV, AUV), as well as water sampling for the collection of environmental DNA (eDNA). These efforts contributed to the first records on benthic fauna present at the pilot oyster reef (Pineda-Metz et al. 2023). All work conducted within the frame of these three cruises contributed to the work of the three phases of the RESTORE project and its involvement in the international network Native Oyster Restoration Alliance (NORA) (Pogoda et al. 2019, 2020).

HE529 created depth profiles and investigated seabed qualities by under water (UW) video recordings at selected locations to support and to inform site selection for the designated pilot oyster reefs in NSG BRG. For the selection of an optimal site within the NSG BRG, precise depth gradients as well as the seabed composition were of great importance. Grab samples were collected at several selected stations for ground truthing and for sediment samples for experimental work on oyster larval settlement (Colsoul et al. 2020). Benthos surveys showed a low abundances, dominated by mobile macrofauna such as asteroids (e. g. *Asterias rubens*) and decapods (e. g. *Cancer pagurus*). The multibeam surveys showed a depth gradient of ~3m within the area of interest (Pogoda & Hausen 2019).

HE561 was limited by corona restrictions and bad weather conditions. The offshore diving mission in BRG was cancelled and the cruise focused on ROV method development for applications in offshore conditions in BRG: high current velocities.

HE574 assessed the first phase of reef succession and associated benthos organisms of the pilot oyster reef. A number of sessile invertebrates (e. g. *Metridium senile*) were identified as early colonizers of the reef. The presence of mobile macrofauna such as asteroids (e. g. *Asterias rubens*) and decapods (e. g. *Cancer pagurus*) was confirmed. Both groups being potential *O. edulis* predators. In terms of method development of non-invasive biodiversity monitoring tools, the feasibility of using a CTD-Rosette to collect eDNA and the capacity of the eDNA methodology for describing local biodiversity was tested and successfully implemented.

From a cruise perspective, a total of 13 days were spent at sea, across 3 years: 3 days for HE529 in 2019, 5 days for HE561 in 2020, and 5 days for HE 574 in 2021. HE529 involved 7 scientists of 3 sections of the Alfred Wegener Institute (AWI), three of them being early career scientists. The results of this expedition resulted in 2 data sets stored in the PANGAEA data repository (Pogoda 2019b, Pogoda & Rohardt 2019), a scientific publication (Pogoda et al. 2020c) and a script of the BfN (Pogoda et al. 2020b). The scientific crew of HE561 consisted of a mix of scientists, professional divers, and media personnel. Photographic material collected by the latter, is still being used for national and international conferences (e. g. international conferences NORA 3 and NORA 4), as well as for the Restoration Ecology WG's webpage (<https://heimische-auster.de>) and other outreach events; whereas the scientific production contributed 3 data sets stored in the PANGAEA data repository (Pogoda 2021a, Pogoda 2021b, Pogoda & Rohardt 2021a) and 1 scientific publication (Pineda-Metz et al. 2023). The expedition HE574 grouped together 6 scientists of two German institutions, 1 from BfN and 5 of the AWI (of three 3 sections). The cruise resulted in 3 data sets which are stored in the PANGAEA data repository (Pogoda 2021c, Pogoda 2021d, Pogoda & Rohardt 2021b), as well as 1 scientific publication (Pineda-Metz et al. 2023).

REFERENCES (WITHOUT HEINCKE RELATED PUBLICATIONS, SEE BELOW)

BfN, Managementplan für das Naturschutzgebiet „Borkum Riffgrund“ (MPBRg), Bundesamt für Naturschutz 2020, Report (BAnz AT): Az. MAR-34324-04.

Merk V, Colsoul B, Pogoda B, Return of the native: Survival, growth and condition of European oysters reintroduced to German offshore waters, *Aquatic Conservation: Marine and Freshwater Ecosystems* 2020, 30(11), 2180-2190, doi:10.1002/aqc.3426.

Möbius K, Über die Thiere der schleswig-holsteinischen Austernbänke, ihre physikalischen und biologischen Lebensverhältnisse, Berlin: Deutsche Akademie der Wissenschaften, 1893.

Olsen TO, The piscatorial atlas of the North Sea, English Channel, and St. George's Channels: Illustrating the fishing ports, boats, gear, species of fish (how, where, and when caught), and other information concerning fish and fisheries, London: Taylor and Francis 1883.

Pogoda B, Current status of European oyster decline and restoration in Germany, *Humanities* 2019a, 8(1), 1–12, doi:10.3390/h8010009.

Pogoda B, Brown J, Hancock B, Preston J, Pouvreau S, Kamernas P, Sanderson W, von Nordheim H, The Native Oyster Restoration Alliance (NORA) and the Berlin Oyster Recommendation: bringing back a key ecosystem engineer by developing and supporting best practice in Europe, *Aquatic Living Resources* 2019, 32, 13, <https://doi.org/10.1051/alr/2019012>.

Pogoda B, Boudry P, Bromley C, Cameron TC, Colsoul B, Donnan D, Colsoul B, Donnan D, Hancock B, Hugh-Jones T, Preston J, Sanderson WG, Sas H, Brown J, Bonacic K, von Nordheim H, zu Ermgassen PSE, NORA moving forward: developing an oyster restoration network in Europe to support the Berlin Oyster Recommendation, *Aquatic Conservation: Marine and Freshwater Ecosystems* 2020a, 30(11), 2031–2037, doi:10.1002/aqc.3447.

Pogoda B, Colsoul B, Hausen T, Merk V, Peter C, Wiederstellung der Bestände der Europäischen Auster (*Ostrea edulis*) in der deutschen Nordsee (RESTORE Voruntersuchung). Bundesamt für Naturschutz 2020b, doi:10.19217/skr582.

SCIENTIFIC OUTPUT

LIST OF PUBLICATIONS (SELECTED)

Pogoda B, Hausen T, Wiederherstellung der Bestände der Europäische Auster (*Ostrea edulis*) in der deutschen Nordsee (Voruntersuchung): Entwicklung und praktische Erprobung von Methoden und Verfahren zum nachhaltigen Bestandsaufbau, Cruise No. HE529, 10.04.2019-12.04.2019, Port of Sailing: Bremerhaven (Germany) – Port of Arrival: Bremerhaven (Germany), Gutachterpanel Forschungsschiffe 2019, doi:10.2312/cr_he529.

Pogoda B, Rohardt G, Continuous thermosalinograph oceanography along Heincke cruise track HE529, PANGAEA 2019, doi:10.1594/PANGAEA.903017.

Pogoda B, Link to master tracks in different resolutions of HEINCKE cruise HE529, Bremerhaven – Bremerhaven, 2019-04-10 – 2019-04-12, PANGAEA 2019, doi:10.1594/PANGAEA.902278.

Pogoda B, Merk V, Colsoul B, Hausen T, Peter C, Pesch R, Kramer M, Jaklin S, Holler P, Bartholomä A, Michaelis R, Prinz K, Site selection for biogenic reef restoration in offshore environments: The Natura 2000 area Borkum Reef Ground as a case study for native oyster restoration. *Aquatic Conservation: Marine and Freshwater Ecosystems* 2020, 30(11), 2163–2179, doi:10.1002/aqc.3405.

Colsoul B, Pouvreau S, Di Poi C, Pouil S, Merk V, Peter C, Pogoda B, Addressing critical limitations of oyster (*Ostrea edulis*) restoration: identification of nature-based substrates for hatchery production and recruitment in the field. *Aquatic Conservation: Marine and Freshwater Ecosystems* 2020, 30(11), 2101–2115. <https://doi.org/10.1002/aqc.3454>

Pogoda B, Master tracks in different resolutions of HEINCKE cruise HE561, 2020-09-13 – 2020-09-17, PANGAEA 2021a, doi:10.1594/PANGAEA.926918.

Pogoda B, Rohardt G, Continuous thermosalinograph oceanography along Heincke cruise HE561, PANGAEA 2021a, doi:10.1594/PANGAEA.932289.

Pogoda B, Master track of HEINCKE cruise HE561 in 1 sec resolutions (zipped, 1.5 MB), PANGAEA 2021b, doi:10.1594/PANGAEA.926919.

Pogoda B, Master track of HEINCKE cruise HE574 in 1 sec resolutions (zipped, 1.9 MB), PANGAEA 2021c, doi:10.1594/PANGAEA.933517.

Pogoda B, Master tracks in different resolutions of HEINCKE cruise HE574, 2021-04-12 – 2021-04-17, PANGAEA 2021d, doi:10.1594/PANGAEA.933521.

Pogoda B, Rohardt G, Physical oceanography during HEINCKE cruise HE574, PANGAEA 2021b, doi:10.1594/PANGAEA.934148.

Pogoda B, Hausen T, Rothe M, Bakker F, Hauser S, Colsoul B, Dureuil M, Krause J, Heinicke K, Pusch C, Eisenbarth S, Kreutle A, Peter C, Pesch R, Come, tell me how you live: Habitat suitability analysis for restoration, *Aquatic Conservation: Marine and Freshwater Ecosystems* 2023, 33(7), 678–695, doi:10.1002/aqc.3928.

Pineda-Metz SEA, Colsoul B, Niewöhner M, Hausen T, Peter C, Pogoda B, Setting the stones to restore and monitor European flat oyster reefs in the German North Sea, *Aquatic Conservation: Marine and Freshwater Ecosystems* 2023, 33(7), 661–677, doi:10.1002/aqc.3945.

Pogoda B, Hausen T, Restoration of European flat oysters (*Ostrea edulis*) in the German North Sea, Cruise No. HE561, 13.09.2020-17.09.2020, Port of Sailing: Bremerhaven (Germany) – Port of Arrival: Bremerhaven (Germany), Gutachterpanel Forschungsschiffe 2020, doi:10.48433/cr_he561.

Pogoda B, Hausen T, Restoration of European flat oysters (*Ostrea edulis*) in the German North Sea, Cruise No. HE685, 13.04.2021-17.04.2021, Port of Sailing: Bremerhaven (Germany) – Port of Arrival: Bremerhaven (Germany), Gutachterpanel Forschungsschiffe 2021, doi:10.48433/cr_he574.

LIST OF CONFERENCE PRESENTATIONS (SELECTED)

2019 | Merk, Pogoda et al. **Performance of first reintroduced native oyster to European offshore grounds** NORA2 Conference, Edinburgh, UK.

2019 | Pogoda et al. **Site selection for biogenic reef restoration in offshore environments: The Natura 2000 area Borkum Reef Ground as a case study for native oyster restoration** NORA2 Conference, Edinburgh, UK.

2020 | Merk, Pogoda et al. **Ostrea edulis Pilot Reef in Natura 2000 Site Borkum Reefground** NORA3 Online Conference

2021 | Pogoda et al. **The late holocene demise of a sublittoral oyster bed in the North Sea** NORA4 Online Conference

2022 | Pogoda, Pineda-Metz, Krause et al. **Angewandter Meeresnaturschutz: Wiederansiedlung der Europäischen Auster im Rahmen des Schutzgebietsmanagements** Meeresumweltsymposium, Hamburg, Germany

2023 | Pogoda et al. **European oyster restoration in Germany: Projects RESTORE & PROCEED** Progress in Marine Conservation, Stralsund, Germany

DATA

Physical oceanography HE529 (Thermosalinograph):
<https://doi.pangaea.de/10.1594/PANGAEA.903017>

Physical oceanography HE561 (Thermosalinograph):
<https://doi.pangaea.de/10.1594/PANGAEA.932289>

Physical oceanography HE574 (CTD):
<https://doi.pangaea.de/10.1594/PANGAEA.934148>

CRUISE REPORT

HE529: doi:10.2312/cr_he529.

HE561: doi:10.48433/cr_he561.

HE574: doi:10.48433/cr_he574.

HE533

Spatial diversity of marine protists along the Northern Norway Fjords during the sub-Arctic summer

AUTHORS

Ecological Chemistry, Department of Biosciences, Alfred Wegener Institute (AWI),
Helmholtz Centre for Polar and Marine Research | Bremerhaven, Germany

U. John, K. Anestis, P. Egbers, C. Hörstmann, N. Kühne, S. N. Wilms, K. Klemm,
S. Neuhaus, S. Wohlrab

Helmholtz Institute for Functional Marine Biodiversity at the University of Oldenburg
(HIFMB) | Oldenburg, Germany

U. John, C. Bunse, K. Klemm, S. Wohlrab

Norwegian Institute for water research | Oslo, Norway

S. Gran-Stadniczeňko, B. Edvardsen, L. Šupřaha, J. Tebben

Section for Aquatic Biology and Toxicology, Department of Biosciences, University
of Oslo | Oslo, Norway

S. Gran-Stadniczeňko

Department of Marine Sciences, University of Gothenburg | Göteborg, Sweden

C. Bunse

Analytical BioGeoChemistry, Helmholtz Zentrum München, German Research
Center for Environmental Health | Neuherberg, Germany

R. Henkel, D. Voss

Mediterranean Institute of Oceanography MIO, Bât. Méditerranée, Campus de
Luminy-Océanomed | Marseille, France

C. Hörstmann

ICBM: Institute for Chemistry and Biology of the Marine Environment, University of
Oldenburg | Oldenburg, Germany

F. Moritz

CRUISE OVERVIEW

Climate change has a substantial effect on polar regions, stronger than on temperate ones. This results in polar, coastal waters experiencing higher average water temperatures,

with shallower and stronger stratifications in summer and higher glacier melting rates. These environmental changes are major stressors for aquatic organisms in polar fjords and the adjacent coastal systems, strongly influencing the microbial community structure in the land-sea environment. In this study, the protists' diversity, distribution, and functional ecology were examined along the northern Norwegian coast from Vesterålen to Tanafjorden as part of a research cruise (R/V Heincke HE533) using an 18S rRNA gene sequencing approach. In addition, physicochemical samples and measurements were collected, allowing analyses to identify the main drivers for differences in the studied protist communities. Significant differences in protist diversity were found among the different fjords and between the western (Vesterålen, Balsfjorden, and Lyngenfjord) and north areas (Porsangerfjord, Laksefjord, and Tanafjord). Temperature, salinity, and phosphate seem to be the main drivers for differences in the protist community composition in these regions, positively correlating with the western fjords and negatively with the northern ones. Metabarcoding analyses revealed dinoflagellates, cryptophytes, and ochrophytes as the most abundant groups on the northern Norwegian coast. It also allowed for identifying some toxic species, especially detecting a bloom of the ichthyotoxic haptophyte *Chrysochromulina leadbeateri* in Balsfjorden. This is the first comprehensive spatial study on protist communities along different fjords in sub-Arctic and temperate by a metabarcoding in Scandinavia, allowing for better identification and functional understanding of key contributors. This helps for better monitoring and understanding these unique and productive ecosystems subject to rapid environmental changes.

CHRYSOCHROMULINA LEADBEATERI BLOOM

2019 was the most harmful algal event ever recorded in the region (even in Northern Europe), causing massive mortalities of farmed salmon. During HE533 the oceanographic and biodiversity aspects of the bloom were studied in unprecedented detail, based on metabarcoding and physico-chemical and biotic factors related with the dynamics and distribution of the bloom. Light- and electron-microscopical observations of nanoplankton samples from diverse locations confirmed that *C. leadbeateri* was dominant in the bloom and the primary cause of associated fish mortalities. Cell counts by light microscopy and flow cytometry were obtained throughout the regional bloom within and adjacent to five fjord systems. Metabarcoding sequences of the V4 region of the 18S rRNA gene from field material collected during the bloom and a cultured isolate from offshore of Tromsøy island confirmed the species identification. Sequences from three genetic markers (18S, 28S rRNA gene and ITS region) verified the close if not identical genetic similarity to *C. leadbeateri* from a previous massive fish-killing bloom in 1991 in northern Norway. The distribution and cell abundance of *C. leadbeateri* and related *Chrysochromulina* species in the recent incident were tracked by integrating observations from metabarcoding sequences of the V4 region of the 18S rRNA gene. Metabarcoding revealed at least 14 distinct *Chrysochromulina* variants, including putative cryptic species. *C. leadbeateri* was by far the most abundant of these species, but with high intraspecific genetic variability. Highest cell abundance of up to 2.7×10^7 cells L^{-1} of *C. leadbeateri* was found in Balsfjorden; the high cell densities were associated with stratification near the

pycnocline (at ca. 12 m depth) within the fjord. The cell abundance of *C. leadbeateri* showed positive correlations with temperature, negative correlation with salinity, and a slightly positive correlation with ambient phosphate and nitrate concentrations. The spatio-temporal succession of the *C. leadbeateri* bloom suggests independent initiation from existing pre-bloom populations in local zones, perhaps sustained and supplemented over time by northeastward advection of the bloom from the fjords.

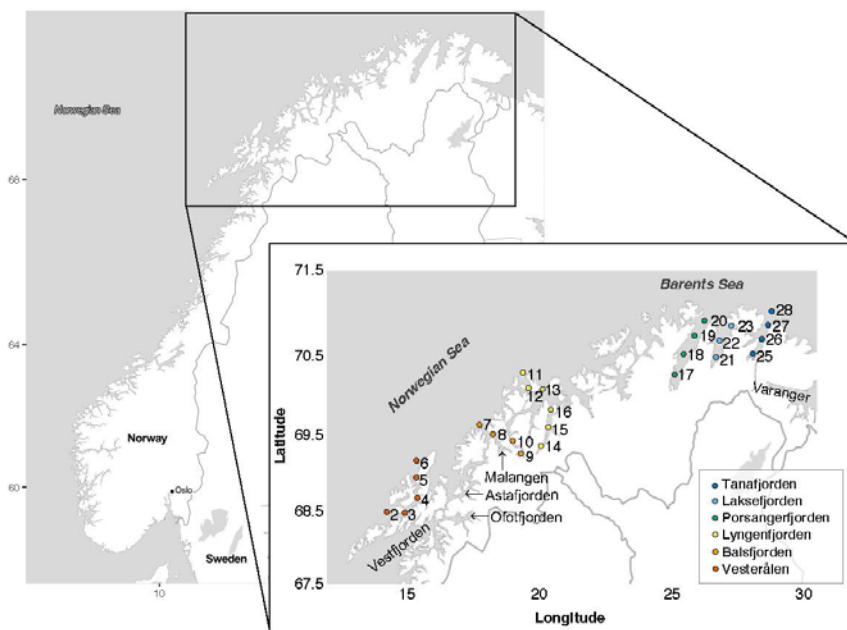


Figure 1: Sampling area and stations investigated aboard RV Heincke cruise HE533. Transects along the northern Norwegian coast included Vesterålen (St 2–6), Balsfjorden (St 7–10), Lyngenfjorden (St 11–16), Porsangerfjorden (St 17–20), Laksefjorden (St 21–23), and Tanafjorden (St 25–28).

REFERENCES

Dzurisin D, A comprehensive approach to monitoring volcano deformation as a window on the eruption cycle, *Reviews of Geophysics* 2003, 41(1), 1.1–1.29, doi:10.1029/2001RG000107.

Schurr B, Asch G, Hainzl S, Bedford J, et al., Gradual unlocking of plate boundary controlled initiation of the 2014 Iquique earthquake, *Nature* 2014, 512, doi: 10.1038/nature13681.

SCIENTIFIC OUTPUT

LIST OF PUBLICATIONS

John U, Wisotzki A, Physical oceanography during HEINCKE cruise HE533. 2019, <https://doi.org/10.1594/PANGAEA.903511>.

John U, Šupraha L, Gran-Stadniczeňko S, Bunse C, Cembella A, Eikrem W, Janouškovec J, Klemm K, Kühne K, Naustvoll L, Voss D, Wohlrab S, Edvardsen B, Spatial and biological oceanographic insights into the massive fish-killing bloom of the haptophyte *Chrysochromulina leadbeateri* in northern Norway, Harmful Algae: Special issue on HABs and climate change 2022, Article number 102287, doi.: 10.1016/j.hal.2022.102287.

Otte A, Insights into a harmful algal bloom of the haptophyte *Chrysochromulina leadbeateri* via metatranscriptomics, Master Thesis 2021, University of Bremen.

LIST OF CONFERENCE PRESENTATIONS

2023 | **High-resolution multi-omics analyses provide insights into a toxic algal bloom and cellular processes of the ichthyotoxic and mixotroph *Chrysochromulina leadbeateri***
ICHA20 Conference, Hiroshima, Japan.

DATA

John, Uwe, Wisotzki, Andreas, 2019, Physical oceanography:
<https://doi.org/10.1594/PANGAEA.903511>.

CRUISE REPORT

HE533: submitted, not yet published

HE537

Project: MESSAGER Methane seepage near abandoned drill sites in the German North Sea Sector

AUTHORS

BGR-Federal Institute for Geosciences and Natural Resources | Hannover, Germany

K. Schwalenberg, U. Barckhausen, M. Blumenberg, H. Müller, S. Müller, S. Schlömer

GFZ – Helmholtz Centre Potsdam, German Research Centre of Geosciences | Potsdam, Germany

K. Heeschen

MARUM – Center for Marine Environmental Sciences, University of Bremen | Bremen, Germany

C. Hilgenfeldt, M. Römer

GEOMAR – Helmholtz Centre for Ocean Research | Kiel, Germany

K. Reeck

SUMMARY

The two-week scientific cruise HE 537 with R/V Heincke took place from 13.–26. July 2019 and was dedicated to investigate possible gas leakage from former drill sites in the German North Sea Sector. Previous studies have addressed methane seepage escaping near abandoned drill sites in the Central North Sea. These “shallow gas” releases with a possible anthropogenic component may be a relevant and so far unconsidered methane source and may contribute to ocean acidification and climate warming (Vielstädte et al., 2015, 2017). Methane seepage has also been observed near former drill sites or at natural seep sites in the British and Dutch North Sea sectors (Leifer, 2015, Römer et al., 2017). So far, it was still highly vague how relevant abandoned boreholes in the Central North Sea are in terms of gas seepage, and how much methane is naturally escaping from the seafloor.

Based on seismic data available to the *Geopotenzial Deutsche Nordsee Project* (www.gpdn.de), and work by Müller et al. (2018) and Römer et al. (2017), we selected nine former drill sites in the German North Sea Sector, i. e. Entenschnabel: i) an area, which partly showed strong amplitude anomalies possibly pointing at shallow gas in the sediments, ii) an area, with no gas indications, iii) a reference site without drilling, and iv) an area in the adjacent Dutch Dogger Bank with known natural gas seepage.

To detect gas seepage and shallow gas in sediments we conducted a multidisciplinary study including high-resolution shipboard hydro-acoustic methods, oceanography and water sampling, sediment sampling, geochemical analysis for hydrocarbons, video profiling, methane profiling, and electromagnetic measurements of the shallow seafloor (Schwalenberg et al., 2019).

We detected a minimum of 166 flares, which point at free gas releases from the seafloor. The flares show a relation to subsurface salt diapirs, particularly at "Berta" where 60% of the observed flares were found. The flares were in many cases related to acoustic blanking and high amplitude reflections in sediment profiler echograms. Dissolved methane concentrations in bottom waters near Berta ($\text{CH}_4 \sim 100\text{nM}$) were ten times the background value in the Entenschnabel ($\text{CH}_4 < 10\text{nM}$). We found no indications of induced gas seepage at the visited former drill sites (Römer et al., 2021a).

Electromagnetic seabed mapping revealed local resistivity anomalies within the first meter of sediments, indicating the presence of small amounts of free gas below a flare cluster at Berta.

Further south, at salt diapir "Britta", an area with several depressions, but without any gas release, was detected in hydro-acoustic and backscatter data. The depressions have dimensions of some meters to 25 m across and up to 0.50 m depth. Electromagnetic mapping revealed shallow conductivity anomalies over the pockmark-like structures, which point at sediment heterogeneities and higher porosity, as the presence of free gas would cause higher resistivity anomalies.

The results of cruise HE537 and Project Messenger were published in Römer et al., (2021a).

Open questions that arose from the project comprise the temporal and spatial variability of the gas submissions, the source and fate of the released methane, the extension of knowledge on potential leakage from abandoned wells in the German North Sea, the origin and nature of the pockmark structures near Britta, and the electromagnetic signature of shallow subsurface gas. These questions have been the scientific motivation for project VARIOSEEP, cruise MSM98, conducted in January 2021 (see Römer et al., 2021b).

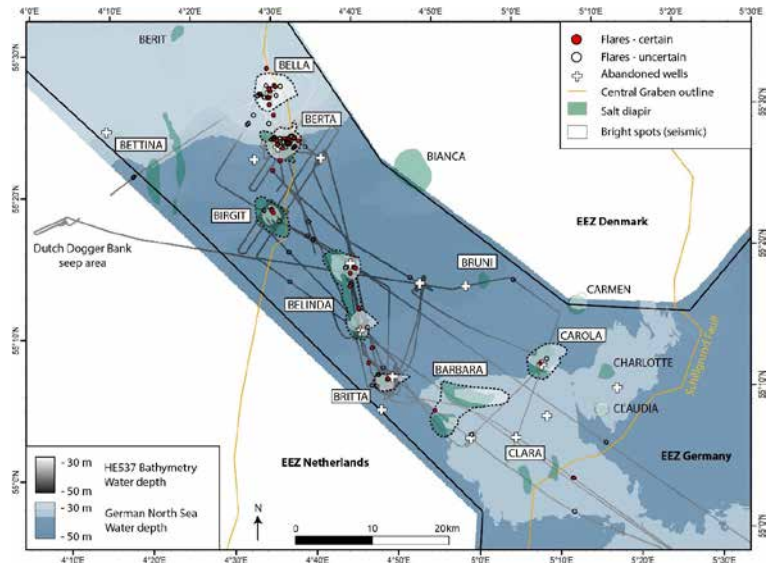


Figure 1: Map compiling flare detections in the Entenschnabel in relation to subsurface salt diapirs and bright spots as well as abandoned wells. Almost 90% of all detected flares were found in the vicinity of subsurface salt diapir structures (Römer et al., 2021a).

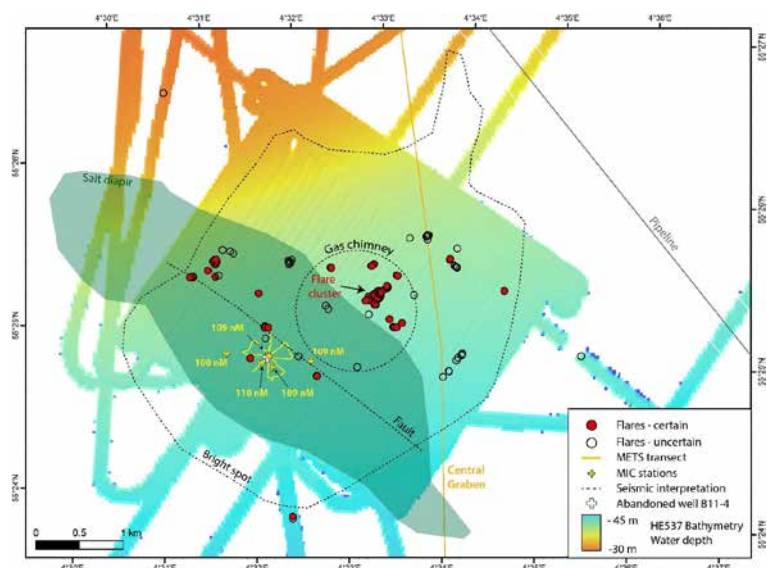


Figure 2: Map compiling data acquired at salt diapir Berta, where most of the flare findings were concentrated (Römer et al., 2021a). Seismic interpretation (bright spot extent, subsurface fault indication, and gas chimney) was depicted from Müller et al. (2018). Insert map shows sediment electric conductivity data, which are lower over the flare cluster possibly due to the presence of shallow free gas.

REFERENCES

- Leifer I, Seabed bubble flux estimation by calibrated video survey for a large blowout seep in the North Sea, *Mar. Pet. Geol.* 2015, 68, 743–752. doi: 10.1016/j.marpetgeo.2015.08.032.
- Müller S, Reinhardt L, Franke, et al., Shallow gas accumulations in the German North Sea, *Mar. Pet. Geol.* 2018, 91, 139–151. doi: 10.1016/j.marpetgeo.2017.12.016.
- Römer M, Wenau S, Bohrmann G, et al., Assessing marine gas emission activity and contribution to the atmospheric methane inventory: a multidisciplinary approach from the Dutch Dogger Bank seep area (North Sea), *Geochem. Geophys. Geosyst.*, 2017, 18, 2617–2633. doi: 10.1002/2017gc006995.
- Römer M, Blumenberg M, Heeschen K, et al., Seafloor Methane Seepage Related to Salt Diapirism in the Northwestern Part of the German North Sea, *Front. Earth Sci.* 2021a, 9:556329. doi: 10.3389/feart.2021.556329.
- Römer M, Schwalenberg K, Barckhausen U, et al., Variability, amount and fate of methane seepage in the German North Sea, Cruise No. MSM98, 08.01.2021–23.01.2021, Emden (Germany) – Emden (Germany), Bonn: MARIA S. MERIAN-Berichte. Gutachterpanel Forschungsschiffe, 2021b.
- Schwalenberg K, Barckhausen U, Blumenberg M, et al., Project: MESSENGER Methane seepage near abandoned drill sites in the German North Sea Sector Cruise No. HE 537, 13.–26.07.2019, Bremerhaven – Bremerhaven (Germany), Bonn: Heincke-Berichte. Gutachterpanel Forschungsschiffe., 2019.
- Vielstädte L, Karstens J, Haeckel M, et al., Quantification of methane emissions at abandoned gas wells in the central North Sea, *Mar. Pet. Geol.*, 2015, 68, 848–860. doi: 10.1016/j.marpetgeo.2015.07.030.
- Vielstädte L, Haeckel M., Karstens J, et al., Shallow gas migration along hydrocarbon wells-an unconsidered, anthropogenic source of biogenic methane in the North Sea, *Environ. Sci. Technol.*, 2017, 51, 10262–10268. doi: 10.1021/acs.est.7b02732.

SCIENTIFIC OUTPUT

LIST OF PUBLICATIONS

Römer M, Blumenberg M, Heeschen K, Schloemer S, Müller H, Müller S, Hilgenfeldt C, Barckhausen U and Schwalenberg K, Seafloor Methane Seepage Related to Salt Diapirism in the Northwestern Part of the German North Sea. *Front. Earth Sci.* 2021,9:556329. doi: 10.3389/feart.2021.556329.

LIST OF CONFERENCE PRESENTATIONS

2020 | Barckhausen U, Römer M, Blumenberg M, Heeschen KU, Schlömer S, Müller H, Müller S, Hilgenfeldt C, Schwalenberg K, **Methane emissions from abandoned offshore wells – First data from a 2019 research cruise to the Dogger Bank, German North Sea** EGU, Vienna, Austria.

2021 | Römer M, Blumenberg M, Heeschen K, Schlömer S, Müller H, Müller S, Hilgenfeldt C, Barckhausen U, Schwalenberg K, **Methane seepage in the northwestern part of the German North Sea** GeoKarlsruhe, Germany.

2021 | Blumenberg M, Schlömer S, Römer M, Heeschen K, Müller H, Barckhausen U, Müller S, Schwalenberg K, **Investigating Methane Seepage and Abandoned Wells in the Northwestern Part of the German North Sea** AGU Fall Meeting, New Orleans, USA.

2022 | Müller H, Schwalenberg K, Reeck K, Hilgenfeldt C, **Marine near-surface electromagnetic signatures of methane gas and palaeo rivers in the central North Sea** – In: Börner, J., Yogeshwar, P., Grinat, M. (Eds.), – Protokoll über das 29. Schmucker-Weidelt-Kolloquium für Elektromagnetische Tiefenforschung: virtuell, 29. September – 1. Oktober 2021.

DATA

HE537 Cruise Track:

<https://doi.pangaea.de/10.1594/PANGAEA.905303>

Swath sonar multibeam bathymetry during HE537:

<https://doi.pangaea.de/10.1594/PANGAEA.912849>

Sediment echo sounding with SES-2000 during HE537:

<https://doi.pangaea.de/10.1594/PANGAEA.910739>

Simrad EK80 echo sounding data during HE537:

<https://doi.pangaea.de/10.1594/PANGAEA.911928>

Thermosalinograph oceanography during HE537:
<https://doi.pangaea.de/10.1594/PANGAEA.910958>

Physical Oceanography during HE537:
<https://doi.pangaea.de/10.1594/PANGAEA.907544>

Sediment electric conductivity profiles of benthic EM profiler Neridis during HE537:
<https://doi.pangaea.de/10.1594/PANGAEA.915610>
<https://doi.pangaea.de/10.1594/PANGAEA.915605>
<https://doi.pangaea.de/10.1594/PANGAEA.915602>

Methane sensor (METS) stations during HE537:
<https://doi.pangaea.de/10.1594/PANGAEA.915779>
<https://doi.pangaea.de/10.1594/PANGAEA.915772>
<https://doi.pangaea.de/10.1594/PANGAEA.915776>
<https://doi.pangaea.de/10.1594/PANGAEA.915770>
<https://doi.pangaea.de/10.1594/PANGAEA.915774>
<https://doi.pangaea.de/10.1594/PANGAEA.915777>
<https://doi.pangaea.de/10.1594/PANGAEA.915771>
<https://doi.pangaea.de/10.1594/PANGAEA.915769>
<https://doi.pangaea.de/10.1594/PANGAEA.915775>
<https://doi.pangaea.de/10.1594/PANGAEA.915773>
<https://doi.pangaea.de/10.1594/PANGAEA.915778>

Sediment samples collected during HE537:
on request per email martin.blumenberg@bgr.de

Water samples collected during HE537:
on request per email martin.blumenberg@bgr.de

Golden Eye electromagnetic data collected during HE537:
on request per email hendrik.mueller@bgr.de

CRUISE REPORT

HE537: doi:10.2312/cr_he537

HE541

Importance of exchange processes between water and sediments in the German Bight

AUTHORS

Helmholtz-Zentrum Hereon | Geesthacht, Germany

J.E.E van Beusekom, A. Neumann, B. Van Dam

Max-Planck-Institute for Marine Microbiology | Bremen, Germany

S. Ahmerkamp, F. Jalaluddin, F. Lange

Alfred-Wegener-Institut, Helmholtz-Zentrum für Polar- und Meeresforschung |

Bremerhaven, Germany

M. Holtappels

CRUISE OVERVIEW

From Sep. 14th 2019 (departure Bremerhaven) until Sep. 27th 2019 (arrival Bremerhaven) 12 scientists from AWI, from HZG, from the MPI-Bremen and from the University Kiel investigated biogeochemical exchange processes between water and sediment at the eight stations between 20m and 30m depth along the German North Sea coast (German Bight). Focus was on the benthic turnover processes including bio-irrigation and advective porewater exchange in coastal sands. We hypothesized that accumulation processes (driven by coastward directed bottom currents) of suspended matter and associated organic matter would lead to higher turnover rates at the coastal stations. With two landers (AWI, MPI-Bremen) oxygen fluxes were quantified in relation to topography and permeability. Sediment samples were taken with grabs and a multicorer and further investigated on board including respiration rates and nutrient fluxes. Special attention was given to the relation between alkalinity and denitrification. For that matter, DIC, alkalinity, nutrients were measured both in the porewater and in the water column. ¹⁵N sediment incubations were carried out for quantifying nitrogen turnover. Afterwards, benthic macrobenthos community was determined. To quantify the exchange between water and sediment, Radium was enriched on board from large water volumes and measured on board. A newly developed video sled system was deployed successfully to characterize the benthic communities at the sampling stations. The cruise was scheduled for the second half of September enabling us to describe the transition between the summer situation with high turnover rates and the autumn with low turnover rates. Despite stormy weather conditions (storm during Sep. 17th and 18th), all but one lander deployment could be carried out successfully.

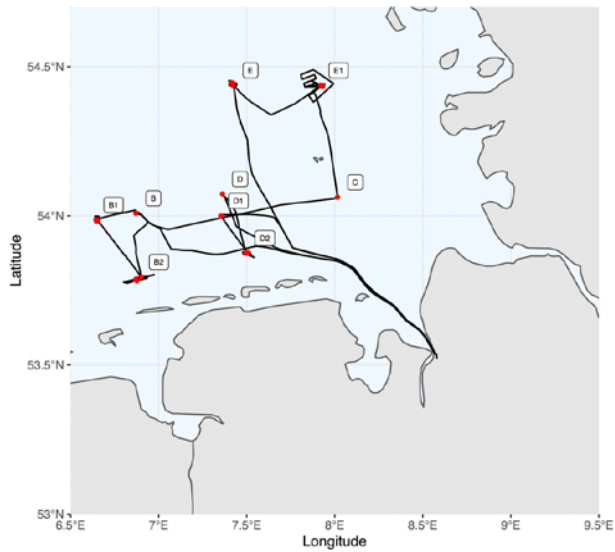


Figure 1: Map with cruise track and stations.

HYDROGRAPHIC CONDITIONS

The water column was generally well mixed, with salinities mostly between 32.4 and 33.3 and temperatures between 16.1°C in the north and 18.2°C in the south. Nutrient concentrations were generally low with nitrate generally around 0.2 μM , ammonium around 0.3 μM , nitrite around 0.02 μM , phosphate around 0.3 μM and silicate around 4 μM . Concentrations were slightly lower near the surface. Highest concentrations were observed in the inner German Bight. Chlorophyll levels were around 2 $\mu\text{g/l}$.

BENTHIC FLUXES

The benthic flux measurements were carried out in the framework of the NOAH-project (North Sea Observations and Assessment of Habitats, 2013–2019) to better describe the benthic habitats in the North Sea. Together with results from other Heincke-cruises, results show a clear seasonality in benthic fluxes with lowest fluxes at the end of the winter period and highest fluxes during the end of the summer period (Neumann et al., 2021, Figure 2). A multivariate, partial least squares analysis identified faunal activity, in specifically bioturbation and bio-irrigation, alongside temperature, as the most important drivers of oxygen and nutrient fluxes. Their combined effect explained 63% of the observed variability in oxygen fluxes, and 36–48% of variability in nutrient fluxes. In sandy sediments, bio-irrigation and advective exchange contribute equally to oxygen consumption in sandy sediments (Neumann et al., 2021).

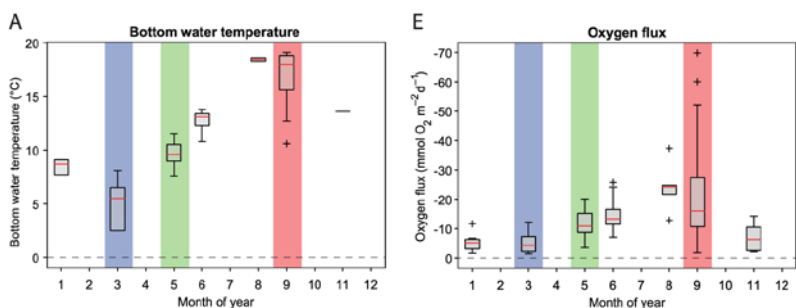


Figure 2: Bottom water temperature and benthic oxygen fluxes observed in core incubations during several Heincke-Cruises including HE541 carried out in the framework of the NOAH-project (2013–2019) (Neumann et al., 2021).

²²⁴RADIUM

Estimating sediment-water exchange of porewater especially in sandy sediments is extremely challenging as both in situ and ex situ observation techniques have to be applied (e. g. Neumann et al. 2021). ²²⁴Ra and alkalinity measurements taken during the He 541 cruise and other cruises were used to estimate sediment water exchange. Results suggest that coastal sediments of the southern North Sea are currently not a major sources of TA to the water column. This is because TA production in deeper anaerobic sediments is counter-balanced by re-oxidation and TA consumption in overlying oxic sediment, causing net TA fluxes to be small and variable (Van Dam et al., 2022). Results further suggest that in the North Sea, sediment-water irrigation is app. two times higher than previously observed in part due to measured porewater ²²⁴Ra activities higher than previously assumed.

SUGAR EXTRACTIONS

Laboratory experiments suggest that biofilm forming microorganism and benthic diatoms influence the flow-regime in sandy sediments via a network of biogenic polymers. To study the effect of biogenic polymers on benthic exchange fluxes in situ, we sequentially extracted, and quantified the water-soluble, colloidal, and water-insoluble sugars from dried sediment and linked these to measurements of bedform migration, permeability, oxygen penetration depths and microbial activity. Preliminary multivariate statistical analyses indicate that the colloidal sugar fraction explains 43% of the variance of all measured physical and biological properties, which makes this glycan fraction a good predictor for benthic-pelagic exchange fluxes. Using immunofluorescence microscopy, we were able to confirm the ubiquitous presence of colloidal sugars on individual sand grains and the pore space.

VIDEO SLED

We tested an upgraded video sled (Hereon) to get a better overview of the sediment surface and of the animals living on or near the sediment. As an example, we show two pictures from station B2 where large sand dunes were observed (Figure 3). Other pictures

document sandeel quickly hiding in the sand. This kind of bio-irrigation could not be assessed in our experiments, but the underestimation of sediment water exchange as indicated by the ^{224}Ra measurements suggests this kind of macrofaunal activity as a potential contribution to sand water exchange.



Figure 3: Two images taken near station B2 by the upgraded video sled document the differences between sandy sediments on top of a sand dune (upper picture with a *Chelidonichthys lucerna*) and in sand dune valley (with a richer epibenthic fauna).

ACKNOWLEDGEMENTS

Despite the weather conditions, the cruise was successful (8 out of 9 stations). This was largely due to the extremely competent support by the Captain and crew of the *Heincke*, for which we are very grateful.

REFERENCES

Van Dam B, Lehmann N, Zeller M, Neumann A, et al., Benthic alkalinity fluxes from coastal sediments of the Baltic and North seas: comparing approaches and identifying knowledge gaps, *Biogeosciences* 2022, 19, 3775–3789, <https://doi.org/10.5194/bg-19-3775-2022>.

Neumann A, van Beusekom JEE, Eisele A, Emeis KC, et al., Macrofauna as a major driver of benthic-pelagic exchange in the southern North Sea, *Limnology and Oceanography* 2021, 66, 2203–2217, <https://doi.org/10.1002/lno.11748>

SCIENTIFIC OUTPUT

LIST OF PUBLICATIONS

Benthic alkalinity fluxes from coastal sediments of the Baltic and North seas: comparing approaches and identifying knowledge gaps. *Biogeosciences* 2022, 19, 3775–3789, <https://doi.org/10.5194/bg-19-3775-2022>.

Neumann A, van Beusekom JEE, Eisele A, Emeis KC, et al., Macrofauna as a major driver of benthic-pelagic exchange in the southern North Sea, *Limnology and Oceanography* 2021, 66, 2203–2217, <https://doi.org/10.1002/lno.11748>.

Norbisrath M, Pätsch J, Dähnke K, Sanders, et al., Metabolic alkalinity release from large port facilities (Hamburg, Germany) and impact on coastal carbon storage, *Biogeosciences Discussions* 2022, 1–22, <https://doi.org/10.5194/bg-19-5151-2022>.

DATA

Physical oceanography during Heincke-Cruise HE541:
<https://doi.pangaea.de/10.1594/PANGAEA.908166>

Station list and links to master tracks in different resolutions of HEINCKE cruise HE541:
<https://doi.org/10.1594/PANGAEA.908147>

CRUISE REPORT

Not available

HE544 AND HE548

Acoustic Seafloor Classification of the German EEZ- Impact of sediment types, bioturbation, and natural and man-made seabed features on hydroacoustic images

AUTHORS

Senckenberg am Meer | Wilhelmshaven, Germany
A. Bartholomä, I. Bruns, P. Holler(t)

INTRODUCTION

The research mission of both cruises HE544 and HE548 was embedded in the joint project "Acoustic seabed classification in the southern North Sea - variability in the acoustic mapping of large-scale sediment type patterns in the German EEZ (ASKAWZ)" started in 2012 and have been carried out until end of 2021 in cooperation with the Federal Maritime and Hydrographic Agency (BSH). Together with the Institute of Geosciences at Kiel University (CAU), the Alfred Wegener Institute Helmholtz Centre for Polar and Marine Research (AWI) on Sylt, Senckenberg am Meer (SaM) and the Leibniz Institute for Baltic Sea Research (IOW) the spatial sediment distribution and the habitat types in the German Exclusive Economic Zone (EEZ) were recorded on a large scale using hydro-acoustic measurement methods, mainly with side-scan sonar systems. The mapping results can be found as digital map service "Seabed Sediments 1 : 10 000" on the BSH geodata portal (GeoSeaPortal) and the website of the MDI-DE (Marine Data Infrastructure Germany). On that high resolution scale, the maps provide information on the composition of the seabed at an unprecedented level of detail. They provide specialized information on the distribution of sediment types, which supports, among others, the Federal Agency for Nature Conservation (BfN) in the national implementation of the European Directive on the Conservation of Fauna, Flora and Habitats (FFH) and the competent authorities in the implementation of measures within the framework of the Marine Strategy Framework Directive. Based on the mapping in the EEZ and several repeated surveys, the research topics were focused on sand dynamics around hard seafloor substrates and the hydrodynamic conditions (Bartholomä et al. 2020, Galvez et al. 2020), new methods of seafloor classification (Galvez 2021, 2022) and the documentation of the temporal occurrence of morphological features like pock marks (Kraemer et al. 2017).

SCIENTIFIC TOPICS OF THE CRUISES HE 544 AND HE548

In the third project phase, in addition to the mapping work in the three MPA's of the German North Sea "Borkum Reefground", "Sylter Outerreef" and "Doggerbank", our research topic focused on the evaluation of drag marks from bottom fishing with regard to their conservation capacity and impact on the various sediment types and the associated biocoenoses.

DETECTION AND CLASSIFICATION OF BOTTOM TRAWL MARKS

Bottom trawl fishing on flatfishes (e.g. plaice or sole) and other species like codfish and herring affects the seafloor in terms of a physical impact on the sediment as well as it endangers benthic organisms – not only target and bycatch species. In order to assess how long the benthic habitat can be considered as disturbed, hydro-acoustic methods have been used to examine the distribution and characteristics of trawl marks as well as the properties of the sediments they are found in. At the two Study sites western margin of the MPA “Doggerbank” and the “wind farm area” northwesterly of Helgoland (Figure 1).

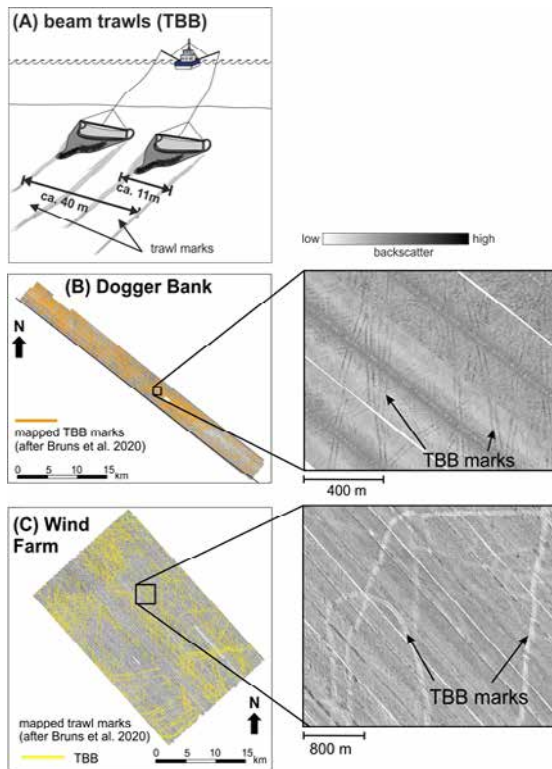


Figure 1: (A) Schematic drawing of typical pair-towed beam trawls (TBB) with the dimensions of the corresponding trawl marks (modified after Bruns et al. 2020). (B) Side scan sonar (SSS) mosaic of the Dogger Bank study site. The orange lines represent the trawl marks that were manually mapped by Bruns et al. (2020). The zoom-in shows examples of TBB marks. (C) In the SSS mosaic of the Wind Farm study site, after Bruns et al. (2020) manually mapped TBB marks (yellow lines).

Trawl marks were classified regarding the sediment-type, their morphology and their appearance in backscatter-data to assess their stability. Different stages of age could be derived from the data due to backscatter intensity. Moreover, the amount of trawled area (swept area, SA), which is calculated from VMS-data, was correlated with the swept area based on mapped trawl marks. SA-maps as well as mapped trawl marks clearly display

annual to monthly changes in fishing activity. It has become clear, that in-situ observations only show a small proportion of the effective trawled area per raster cell in the study area. Here, the main controlling factors are grain-size, water depth and the used trawling gear. The state of preservation of the drag marks depends, among other things, on the sediment type and the hydrodynamic conditions near the bottom. In tough, clayey sediments there is a higher conservation potential than in sandy sediments. In addition to the sediment composition, the preservation of drag marks depends on the general sediment dynamics. The state of preservation of the drag marks makes it possible to estimate the long-term stability of the sediments with regard to erosion, rearrangement and sedimentation.

The research of physical properties of the sediment with and without bottom trawling impact was the main focus of HE 544. Trawl marks have widths of a few decimeters up to several meters and the gear can penetrate <10 cm up to 35 cm into the seabed (e.g., Eigaard et al., 2016; Bruns et al., 2020). The vertical impact should increase with the bottom trawling intensity.

PHYSICAL IMPACT OF BOTTOM TRAWLING ON SEAFLOOR SEDIMENTS

Assuming the relevance of bottom trawling for sediment re-mobilization and changes in the physical properties of the sediment (e.g., grain size) this should be visible in the geotechnical properties such as sediment strength and its resistance to mobilization. Studies that investigated the influence of bottom trawling on geotechnical properties. Apart from various modelling studies, there are only a few in-situ case studies available which were carried by means of dynamic (free fall) penetrometer. We performed geotechnical in-situ measurements of the sediment strength in the southwestern German North Sea using the dynamic free-fall penetrometer "Nimrod", which was developed at MARUM, University of Bremen (Stark et al. 2011, 2012). Stark, Wilkens, et al. (2011) detected sediment mobilization by using the dynamic penetrometer "Nimrod", where mobilization is manifested by a layer with lower sediment strength above a stronger layer in the penetrometer data. Following this, we deployed the free-fall penetrometer "Nimrod" to determine the changes in sediment strength (quasi-static bearing capacity) compared to the reference sites (absent trawl marks). On our survey side-scan sonar mosaics were used to map the spatial trawl mark density (abundance). The "Nimrod"-Measurements took place in trawled and un-trawled sites of the study area.

Our results attest a higher penetration depth of Nimrod and a lower sediment strength in the trawled area compared to the un-trawled reference sites (Bruns et al. 2023). This is likely related to an increase in water content and a decrease in bulk density of the sediment that was re-worked by bottom trawling. In the trawled area, we expected that the penetrometer data may also reflect a change from the re-worked (trawled) surface and subsurface sediment to the pristine subsurface sediment.

Table 1: Maximum penetration depth penmax in mbsf (meters below seafloor) and the maximum quasi-static bearing capacity qsbcmx in kPa (please note an uncertainty of 15 %) measured with the dynamic free-fall penetrometer Nimrod in the un-trawled and the trawled area of the HE544 site. The mean values penmaxM and qsbcmxM refer to the arithmetic mean of penmax and qsbcmx, respectively, across each area (un-trawled and trawled) (Bruns et al. 2023).

	penmax [mbsf]			qsbcmx [kPa]		
	min.	max.	penmaxM	min.	max.	qsbcmxM
un-trawled	0.04	0.39	0.18	58.92	127.3	77.7
trawled	0.02	0.72	0.31	7.89	109.1	58.6

This identification of individual layers (less consolidated above more consolidated sediment) indicating mobilized sediment as observed by Stark et al. (2011), was not possible in this study. This is probably related to a limited overall penetration depth of the dynamic penetrometer and therefore the pristine subsurface (i. e., not influenced by bottom trawling) could not be reached.

REFERENCES

Bartholomä A, Capperucci R, Becker L, Battershill C, Hydrodynamics and hydroacoustic mapping of a benthic seafloor in a coarse grain habitat of the German Bight, *Geo Marine Letters* 2020, 40, 183-195, <https://doi.org/10.1007/s00367-019-00599-7>.

Bruns I, Bartholomä A, Menjua F, Kopf A, Physical impact of bottom trawling on seafloor sediments in the German North Sea, *Front. Earth Sci.* 2023, 11:1233163. doi: 10.3389/feart.2023.1233163.

Bruns I, Holler P, Capperucci RM, Papenmeier S, Bartholomä A, Identifying trawl marks in North Sea sediments, *Geosciences* 2020, 10, 422, doi:10.3390/geosciences10110422.

Eigaard OR, Bastardie F, Breen M, Dinesen GE, Hintzen NT, Laffargue P, Rijnsdorp AD, Estimating seabed pressure from demersal trawls, seines, and dredges based on gear design and dimensions, *ICES Journal of Marine Science* 2016, 73(1), 17. doi: 10.1093/icesjms/fsv099.

Galvez DS, Papenmeier S, Hass HC, Bartholomä A, Fofonova V, Wiltshire KH, Detecting shifts of submarine sediment boundaries using side-scan mosaics and GIS analyses, *Marine Geology* 2020, 430, 106343, ISSN 0025-3227, <https://doi.org/10.1016/j.margeo.2020.106343>.

Galvez SD, Papenmeier S, Sander L, Bartholomä A, Wiltshire KH, Ensemble mapping as an alternative to baseline seafloor sediment mapping and monitoring, *Geo-Marine Letters* 2022, 42, 11, <https://doi.org/10.1007/s00367-022-00734-x>.

Galvez DS, Papenmeier S, Sander L, Hass HC, Fofonova V, Bartholomä A, Wiltshire KH, Ensemble Mapping and Change Analysis of the Seafloor Sediment Distribution in the Sylt Outer Reef, German North Sea from 2016 to 2018, *Water* 2021, 13, 2254. <https://doi.org/10.3390/w13162254>.

Krämer K, Holler P, Herbst G, Bratek A, Ahmerkamp S, Neumann A, Bartholomä A, van Beusekom JEE, Holtappels M, Winter Ch, Abrupt emergence of a large pockmark field in the German Bight, south-eastern North Sea, *Scientific Reports* 2017, 7, 5150. DOI:10.1038/s41598-017-05536-1.

Stark N, Coco G, Bryan KR, Kopf A, In-Situ Geotechnical Characterization of Mixed-Grain-Size Bedforms Using A Dynamic Penetrometer, *Journal of Sedimentary Research* 2012, 82(7), 540–544. doi: 10.2110/jsr.2012.45

Stark N, Wilkens R, Ernstsen VB, Lambers-Huesmann M, Stegmann S, Kopf A, Geotechnical Properties of Sandy Seafloors and the Consequences for Dynamic Penetrometer Interpretations: Quartz Sand Versus Carbonate Sand, *Geotechnical and Geological Engineering* 2011, 30(1), 1–14. doi: 10.1007/s10706-011-9444-7.

SCIENTIFIC OUTPUT

LIST OF PUBLICATIONS

Bruns I, Holler P, Capperucci RM, Papenmeier S, Bartholomä A, Identifying trawl marks in North Sea sediments, *Geosciences* 2020, 10, 422, doi:10.3390/geosciences10110422.

Bruns I, Bartholomä A, Menjua F, and Kopf A, Physical impact of bottom trawling on seafloor sediments in the German North Sea, *Front. Earth Science* 2023, . 11:1233163. doi: 10.3389/feart.2023.1233163.

LIST OF CONFERENCE PRESENTATIONS

2019 | **Spatial and temporal variability of trawl marks in the area of Dogger Bank (German Exclusive Economic Zone, North Sea)** GeoHab, St. Petersburg, Russia.

CRUISE REPORT

HE548: https://doi.org/10.2312/cr_he548

HE544: https://doi.org/10.2312/cr_he544

HE562 AND HE581

Dynamics of benthic communities in the German North Sea

AUTHORS

Alfred Wegener Institute, Helmholtz Centre for Polar and Marine Research |
Bremerhaven, Germany

J. Beermann, L. Gutow, B. Glückselig, M. Guský

Due to their wide structural and functional diversity, benthic organisms and communities have been recognised as sensitive indicators for environmental change (e. g. Shojaei et al. 2016). Extensive research effort is being made to understand the responses of benthic habitats and communities to environmental change and to assess the usefulness of various numerical multivariate indices based on benthic community composition (Borja et al. 2011; van Loon et al. 2018), in order to evaluate the ecological status of marine ecosystems. The increasing understanding of the structure and functioning of benthic communities provides important tools to test the usefulness and efficiency of modern measures of marine management and conservation.

Accordingly, benthic habitats and communities are intensively used as proxies for the assessment of the environmental status according to several European directives and regional marine conventions. Long-term observations on the development of species populations in particular help to understand the implications of ongoing environmental changes and support the development of new indicators of the environmental status of biotopes and ecosystems. The Federal Republic of Germany is obliged to regularly assess and evaluate the status of the benthic communities in its territorial waters. Within a series of past, ongoing and future research projects in cooperation with the German Federal Agency for Nature Conservation (BfN), the Alfred Wegener Institute Helmholtz Centre for Polar and Marine Research (AWI) conducts long-term monitoring programs as well as specific targeted investigations on benthic habitats, species assemblages and populations to (1) fulfil the requirements of relevant legislative directives and conventions for the German Exclusive Economic Zone (EEZ) and (2) to evaluate the efficiency of specific conservation and management measures. In particular, the European Habitats Directive, the Marine Strategy Framework Directive (MSFD, directive 2008/56/EG), and the Oslo-Paris Convention (OSPAR) provide the framework for the investigations conducted in these projects.

During the cruises HE562 and HE581 of R/V HEINCKE, benthic communities were investigated in the German Exclusive Economic Zone (EEZ) of the North Sea. The samplings of the in- and epifauna were conducted in the central and southern EEZ as well as at the Borkum Reef Ground, the Dogger Bank and the Sylt Outer Reef, which are protected areas according to the European Habitats Directive. A newly initiated long-term

monitoring program targeted broad habitat types in the German Bight. As part of another, established long-term monitoring program, 25 stations were sampled at Borkum Reef Ground and the Sylt Outer Reef. Further, samples were taken at Dogger Bank and the Sylt Outer Reef to investigate the recovery of the benthic ecosystem after cessation of chronic bottom trawling. The in- and epifauna were sampled using a van Veen grab, an epibenthos dredge and a towed underwater video system.

Building on established monitoring programs, the collected data allow for the elucidation of spatiotemporal dynamics of benthic communities and the delimitation of protected habitat types, supporting the fulfillment of national sovereign duties of the Federal Republic of Germany to implement the EU MSFD as well as the EU Habitats Directive.

REFERENCES

Borja A, Barbone E, Basset A, et al., Response of single benthic metrics and multi-metric methods to anthropogenic pressure gradients, in five distinct European coastal and transitional ecosystems, *Marine Pollution Bulletin* 2011, 62, 499–513, <https://doi.org/10.1016/j.marpolbul.2010.12.009>.

van Loon WMGM, Walvoort DJJ, Hoey G, et al., A regional benthic fauna assessment method for the Southern North Sea using Margalef diversity and reference value modelling, *Ecological Indicators* 2018, 89, 667–679, <https://doi.org/10.1016/j.ecolind.2017.09.029>.

Ghodrati Shojaei M, Gutow L, Dannheim J, Rachor E, et al., Common trends in German Bight benthic macrofaunal communities: assessing temporal variability and the relative importance of environmental variables, *Journal of Sea Research* 2016, 107, 25–33, <https://doi.org/10.1016/j.seares.2015.11.002>.

SCIENTIFIC OUTPUT

LIST OF PUBLICATIONS

Beermann J, Gutow L, Wührdemann L, Heinicke K, et al., Characterization and differentiation of sublittoral sandbanks in the southeastern North Sea, *Biodiversity and Conservation* 2023, 32, 2747–2768, <https://doi.org/10.1007/s10531-023-02629-4>.

Gutow L, Guský M, Beermann J, Gimenez L, et al., Spotlight on coarse sediments: comparative characterization of a poorly investigated seafloor biotope in the German Bight (SE North Sea), *Estuarine, Coastal and Shelf Science* 2022, 275(107996), <https://doi.org/10.1016/j.ecss.2022.107996>.

Teschke K, Kraan C, Kloss P, Andresen H, et al., CRITTERBASE, a science-driven data warehouse for marine biota, Scientific Data 2022, 9(483), <https://doi.org/10.1038/s41597-022-01590-1>.

LIST OF CONFERENCE PRESENTATIONS

2023 | **Spatial distribution of amphipod assemblages in Marine Protected Areas of the German Bight (North Sea)** 10th International Crustacean Congress, Wellington, New Zealand.

2022 | **Charakterisierung und Differenzierung sublitoraler Sandbänke in der südöstlichen Nordsee** 31. Meeresumwelt-Symposium, Hamburg, Germany.

DATA

Continuous thermosalinograph:

<https://doi.org/10.1594/PANGAEA.932290>

<https://doi.pangaea.de/10.1594/PANGAEA.944731>

CRUISE REPORT

HE562: https://doi.org/10.48433/cr_he562

HE581: https://doi.org/10.48433/cr_he581

HE569

Changing North Sea (ChaNoS)

AUTHORS

University of Bremen | Bremen, Germany

H. Keil, A. K. Baltz

Lower Saxony Institute for Historical Coastal Research | Wilhelmshaven, Germany

D. A. Hepp

Aarhus University | Aarhus, Denmark

K. J. Andresen

The recent glacial history of the North Sea resulted in complex structural patterns in the uppermost depositional regimes, entailing incisions of variable sizes with variable infills, units with prograding sequences, erosional interfaces, highly discontinuous reflectors and partially also highly continuous reflectors. A common property of most of these observed structures is that they are confined to small and often intercalated structures, therefore imposing challenges to acoustic structural imaging and interpretation, especially if only two-dimensional line information is available.

Therefore, although the general Quaternary history of the North Sea is well investigated (e. g. Lamb et al., 2017, Ehlers et al., 2011, Philipps et al., 2017, and several others) there is still a considerable lack of understanding these small scaled sedimentary units, their stratigraphic relation and regional distribution. Major units and depositional regimes like tunnel valleys or the Elbe Palaeovalley (EPV) may thereby serve as main marker systems to confine the interpretation of small scaled units (e. g. Özmaral et al., 2022, Coughlan et al., 2018, Abegunrin et al., 2023).

Cruise HE569 was carried out in the German and Danish North Sea as a joined expedition of University of Bremen and Aarhus University to foster the principal understanding of shallow subsurface structures in the North Sea, to provide a basis for a large scale regional assessment of the distribution of terrigenous and pro- to subglacial deposits and to address questions related to the interaction between the EPV and an assumed Weichselian proglacial lake and between the EPV and the eastern Dogger Bank drainage system.

For this purpose mainly the existing network of seismoacoustic datasets in the North Sea was extended by a set of elongated high resolution and ultra-high resolution multichannel seismic datasets (HR-MCS), supported by several selected sampling sites. Two high

resolution 3D seismic surveys were planned to allow a more appropriate imaging of small scaled depositional features, however, due to weather and time constraints unfortunately could only partially be carried out.

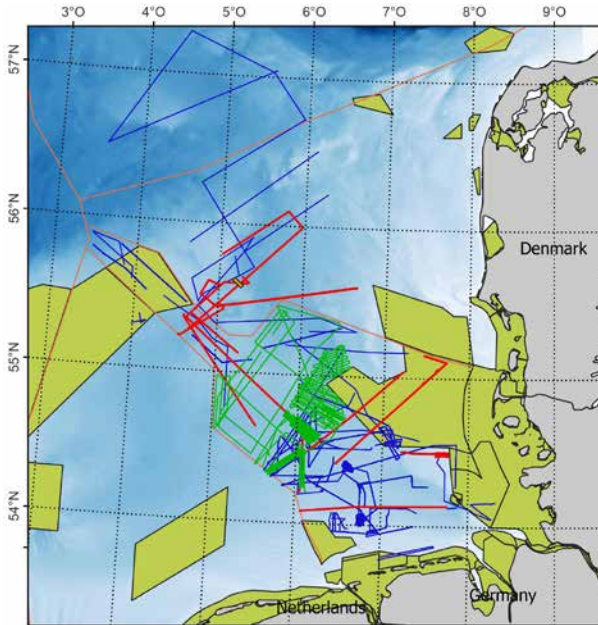


Figure 1: HR-MCS data acquired at University of Bremen in the last 15 years. Blue – existing before HE569, Red –HE569, Green – after HE569.

Comparing the HR-MCS data available in Bremen before and after the cruise (Figure 1), several gaps in the existing data network could be closed, connecting several rather isolated areas which had been target of investigations on earlier cruises. Additionally the seismic data network was extended towards North-East. In the last two years and in the framework of ongoing cooperation with the BSH this dataset could be expanded even further (Figure 1) providing today an unrivaled coverage of high resolution acoustic data information of the German North Sea for the assessment of late Pleistocene sedimentary processes.

To further analyze the Holocene eastern Dogger Bank drainage system a high resolution P-Cable 3D-seismic cube could be acquired in the area of the Danish EPV. 3D-data boosts interpretation possibilities by providing a time-slice view of the area (Figure 2) which allows to image small scaled features like buried river systems properly and provide information on the distribution of infill sediments. The area selected for investigation was described already based on low resolution 3D-seismic data (Prins & Andresen, 2019) and the new 3D-data provides an opportunity for better resolving the river features and

in turn increase the understanding of the drainage systems' properties and its link to the EPV. The 3D-data has been analyzed further in a 60 ECTS MSc thesis project but results are yet to be published.

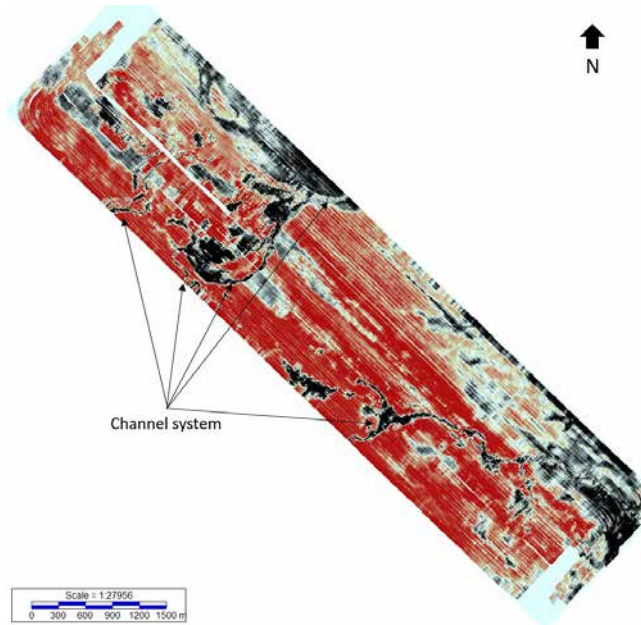


Figure 2: Time slice (82 ms TWT) of P-Cable 3D dataset. Depressions and channels appear as phase reversals in this visualization.

South of the Dogger Bank the uppermost sedimentary units show an exceptional, laterally homogeneous stratified internal structure with a pronounced tabular lower boundary. As a second peculiarity this unit is also representable in subbottom profiler data (Figure 3). In this the unit differs significantly from the typical discontinuous and rather chaotic facies types encountered at most locations of the south-eastern North Sea. The observed properties may potentially be attributed to sediments deposited in a calm lake environment and therefore might hint towards the existence of a supposed proglacial lake south of an Weichselian ice barrier connecting the British with the Scandinavian ice shield over the Dogger Bank area (Carr et al., 2006, Ehlers et al., 2011, Böse et al., 2012, Philipps et al., 2017, Hughes et al., 2016). The additional lines will help to better confine this unit and to better understand its interconnection to the EPV.

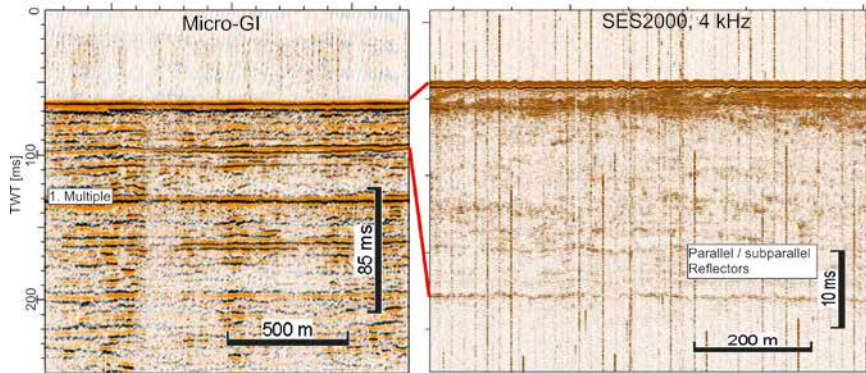


Figure 3: Short section of profile GeoB21-026. Left - HR-MCS data with Micro-GI seismic source shows significant horizontal reflector at 100 ms TWT with several parallel reflectors above. Right - corresponding SES2000 SBP profile with higher resolution.

Last but not least an improved understanding of sedimentary units of the upper 100m of the North Sea is also important for the development of suitable foundations ground models for offshore installations, namely offshore wind developments. Accordingly the investigations carried out in this cruise as well as the future analysis of the data was supported by the German Federal Maritime and Hydrographic Agency (BSH) and results also contributed to other ongoing projects in this applied sector of geophysical research (e. g. SYNCORE).

REFERENCES

- Abegunrin A, Hepp DA, Gugliotta M, et al., The submerged Palaeo-Ems River in the Quaternary stratigraphic context of the German North Sea, *The Holocene* 2023. doi: 10.1177/09596836231197732.
- Böse M, Lüthgens C, Lee JR, et al., Quaternary Glaciations of Northern Europe, *Quaternary Science Reviews* 2012, 44, doi: 10.1016/j.quascirev.2012.04.017.
- Carr SJ, Holmes R, van der Meer JJM., et al., The Last Glacial Maximum in the North Sea Basin: Micromorphological Evidence of Extensive Glaciation, *Journal of Quaternary Science* 2006, 21(2), doi: 10.1002/jqs.950.
- Coughlan M, Fleischer M, Wheeler AJ, et al., A Revised Stratigraphical Framework for the Quaternary Deposits of the German North Sea Sector: A Geological-Geotechnical Approach, *Boreas* 2018, 47(1), doi: 10.1111/bor.12253.
- Ehlers J, Grube A, Stephan H, et al., Pleistocene Glaciations of North Germany—New Results, *Quaternary Glaciations - Extent and Chronology – A Closer Look 2014*, Elsevier, doi: 10.1016/B978-0-444-53447-7.00013-1.

Hughes ALC, Gyllencreutz R, Lohne ØS, et al., The Last Eurasian Ice Sheets - a Chronological Database and Time-Slice Reconstruction, DATED-1, *Boreas* 2016, 45(1), doi: 10.1111/bor.12142.

Lamb RM, Harding R, Huuse M, et al., The early Quaternary North Sea Basin, *Journal of the Geological Society* 2018, 175(2), doi: 10.1144/jgs2017-057.

Özmaral A, Abegunrin A, Keil H, et al., The Elbe Palaeovalley: Evolution from an Ice-Marginal Valley to a Sedimentary Trap (SE North Sea), *Quaternary Science Reviews* 2022, 282: , doi: 10.1016/j.quascirev.2022.107453.

Phillips E, Hodgson DM, Emery AR, The Quaternary Geology of the North Sea Basin, *Journal of Quaternary Science* 2017, 32(2), doi: 10.1002/jqs.2932.

Prins LT, Andresen KJ, Buried late Quaternary channel systems in the Danish North Sea – Genesis and geological evolution, *Quaternary Science Reviews* 2019, 223, doi: 10.1016/j.quascirev.2019.105943.

SCIENTIFIC OUTPUT

LIST OF PUBLICATIONS

Andresen KJ, Hepp DA, Keil H, Spiess V, Seismic morphologies of submerged late glacial to early Holocene landscapes at the eastern Dogger Bank, central North Sea Basin – implications for geo-archaeological potential. *Geological Society London* 2022, Special Publication 525. doi.org/10.1144/SP525-2021-155.

Römer-Stange N, Morales Hernandez PN, Wenau S, et al., From Interface to Layer Characterisation: Stochastic Near Surface Seismic Impedance Inversion in the German North Sea, subm. 2023.

DATA

Seismic and acoustic data:

Data-Server of working group of Marine Technology and Environmental Sciences, University of Bremen, Contact authors for details on data access.

Continuous Thermosalinograph measurements:

<https://doi.pangaea.de/10.1594/PANGAEA.944487>

CRUISE REPORT

HE569: doi: 10.48433/cr_he569

HE570

Fjord Export – Characterizing the Biological Carbon Pump using imaging approaches

AUTHORS

GEOMAR Helmholtz Centre for Ocean Research | Kiel, Germany

H.Hauss (now NORCE Norwegian Research Centre | Bergen, Norway)

HEREON | Geesthacht, Germany

K.O. Möller

The cruise HE570 was applied for by members of the pelagic imaging consortium (PIC) from GEOMAR, HEREON and AWI, who all use *in situ* camera systems to enumerate, size and classify organisms and particles in the ocean. The aim was to produce a process study of the Biological Carbon Pump (BCP) in two Norwegian Fjords that are close to each other and feature similar dimensions and little advection, but a fundamentally differing structure of the pelagic ecosystem and are thus ideal environments as Natural Mesocosms. While Masfjorden sustains populations of mesopelagic fishes and has negligible populations of jellyfish, Lurefjorden is characterised by year-round mass abundance of the deep sea jellyfish *Periphylla periphylla*, which may be a dead end to the food web and an important contributor to carbon export by deposition of moribund/dead individuals. We aimed to quantify the respective contribution to export flux by different zooplankton taxa by respiration, faecal pellet production and subsiding of individuals as well as characterising particle-zooplankton interactions. The spatial and temporal variability of these processes has thus far only been partially captured and understood, nor is it well quantified. To change this, we deployed a suite of different state-of-the-art *in situ* imaging systems to cross-calibrate and harmonise output data, to resolve a broad size spectrum, and to ensure intercomparability between instruments. We combined this high-resolution *in situ* imaging approach with complementary traditional methods, such as vertical net hauls, sediment traps, and shipboard experiments using material collected with a marine snow catcher.

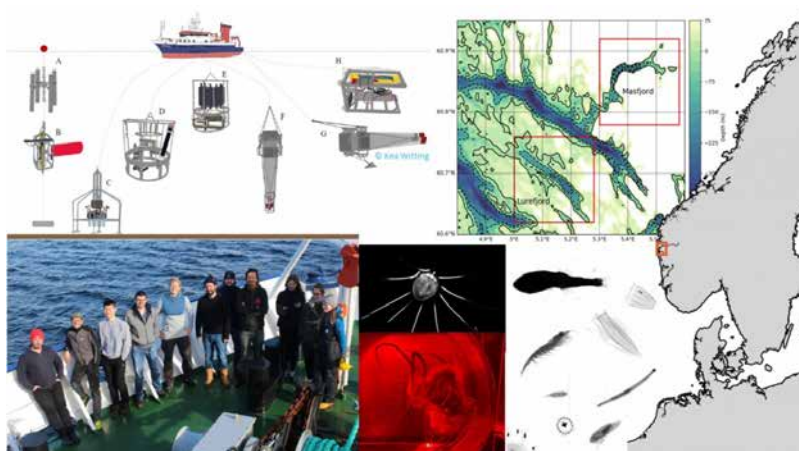


Figure 1: Visual summary of working area, gear used, scientific team and example images of pelagic organisms, both in situ and in experiments in the ship's climate chamber.

In each fjord, a transect of twelve stations was visited as planned and day/night work carried out at the central station of each fjord. The particle size spectra obtained by the different camera systems agreed well in those parts where sizes overlap, and instantaneous flux estimations seem robust. Results from all instruments indicate major differences between the fjord ecosystems. Gear-dependent differences in organism detection, both due to sampling volume and optical method, were evident. High abundances of fragile appendicularia abundances in Masfjorden were found mainly by the data collected with the UVP5/UVP6, which was validated by video material gathered with the PELAGIOS. Copepods could mainly be detected using the MultiNets and UVPs as they were too small to identify exactly using the PELAGIOS. Despite the confirmed presence of the small mesopelagic fish species *Maurolicus muelleri* and *Benthosema glaciale* in Masfjorden, their DNA could not be traced in sediment samples while other demersal and pelagic fish species were detected. All findings suggest a lower carbon sequestration rate in the *Periphylla* – dominated Lurefjord due to BCP pathway alterations. These findings may provide a look into the future where warming and deoxygenation cause jelly-dominated foodwebs with reduced BCP efficiency.

As an add-on to the work program that was applied for, and because a land-based expedition to Norway using submersible JAGO had to be cancelled due to the covid-19 pandemic, also experimental work on *Periphylla* was conducted on this cruise, testing their response to warming and simulated deep sea mining plumes as an exemplary cosmopolitan midwater species. Through a series of ex situ experiments in bottles (different temperatures) and kreisel tanks (five different concentrations of abyssal sediment collected by R/V Sonne near Madeira), we measured the metabolic response (ammonium excretion and respiration, measured on board), electron transport system activity and expression of stress related genes as well as the microbial composition associated to the

jellies (in the home lab). Three temperatures (in situ, +2°C, +4°C for 7–9 hours) and five abyssal sediment concentrations (0, 16.7, 33.3, 166.7, 333.3 mg·L⁻¹ for 24 hours) were tested. Our results, published in Stenvers, Hauss et al. (2023) confirm that an increase in temperature (which scales all metabolic rates in ectotherms) led to increased respiration rates and ammonium excretion. Suspended particle load, however, showed a visible negative effect on *P. periphylla* at concentrations >16.7 mg·L⁻¹, and also led to increased respiration rate (Figure 2). Additionally, jellyfish showed marked expression of genes related to respiration, innate immunity and wound repair in the highest sediment treatments, further signaling stress. Our results are concerning since stressors leading to increased energy expenditure will have to be met with increased food intake. Since food in the deep sea is generally scarce, this could ultimately lead to starvation. Although more data from different midwater species are needed to better understand the environmental impacts of deep-sea mining, the stress response in helmet jellyfish may be representative of other gelatinous animals. The overall results show that caution should be taken to proceed with deep-sea mining, as many of the important ecosystem services of the deep ocean may be compromised.

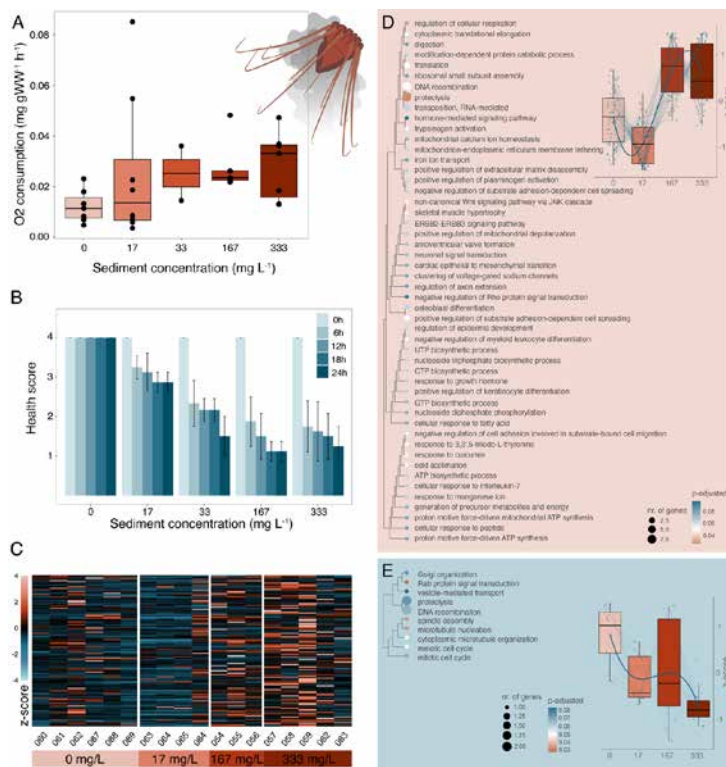


Figure 2: Weight-specific respiration rate of *Periphylla* exposed to five different sediment concentrations based upon ETS measurements (A) and physical health scores (mean±SD) determined at five different time points in individuals exposed to different sediment concentrations.

SCIENTIFIC OUTPUT

LIST OF PUBLICATIONS

Stenvers VI, Hauss H, Bayer T, Havermans C, Hentschel U, Schmittmann L, Sweetman A, & Hoving HJT, Experimental mining plumes and ocean warming trigger stress in a deep pelagic jellyfish, *Nature Communications* 2023, doi:10.1038/s41467-023-43023-6.

Witting K, Characterizing Pathways of the Biological Carbon Pump in two Fjords with Contrasting Pelagic Food Web Structures, *Master thesis 2022*, Christian-Albrechts-Universität zu Kiel, Kiel, Germany, 66 pp.

Witting K, Hoving H-J, Kim D-G, Möller KO, Rogge A, Stenvers VI, Iversen M, Niehoff B, Hauss H, Pathways of the Biological Carbon Pump in two Fjords with Contrasting Food Web Structure, In preparation for *Frontiers in Marine Science*.

LIST OF CONFERENCE PRESENTATIONS

2023 | **Fjord Export Cruise** PIC meets HI workshop, DESY Hamburg, Germany.

2023 | **Characterizing Pathways of the Biological Carbon Pump** WKFISHCARBON (ICES), Copenhagen, Denmark.

2023 | **Characterizing Pathways of the Biological Carbon Pump** ASLO Aquatic Sciences Meeting, Palma de Mallorca, Spain.

2023 | **Towards Identifying Knowledge Gaps in the Mesopelagic Biological Carbon Pump** Ocean Twilight Zone Symposium, Woods Hole (MA), USA.

2023 | **Impacts of global warming and deep-sea mining induced sediment plumes on midwater animals** iAtlantic General Assembly, Edinburgh, UK (online).

2022 | **Impacts of global warming and deep-sea mining induced sediment plumes on midwater animals** iAtlantic General Assembly, Cape Town, South Africa (online).

2022 | **Comparing particle spectra across a suite of pelagic imaging systems** Marine Imaging Workshop, Brest, France.

2022 | **Characterizing Pathways of the Biological Carbon Pump in two Fjords with Contrasting Pelagic Food Web Structure** Marine Imaging Workshop, Brest, France.

2022 | **Impacts of global warming and mining induced sediment plumes on the midwater medusae *Periphylla periphylla*** Smithsonian NMNH No Bones Lunch Seminar, Washington D.C., USA.

2022 | **Impacts of global warming and mining induced sediment plumes on the midwater medusa *Periphylla periphylla*** Ocean Science Meeting, all-online.

2021 | **Impacts of global warming and mining induced sediment plumes on the midwater medusa *Periphylla periphylla*** 16th Deep-Sea Biology Symposium, Brest, France.

DATA

Physical oceanography (CTD):

<https://doi.org/10.1594/PANGAEA.931411>

Thermosalinograph:

<https://doi.org/10.1594/PANGAEA.944723>

Periphylla behaviour and physiology:

<https://doi.org/10.1594/PANGAEA.957367>

Multinet Maxi:

<https://ecotaxa.obs-vlfr.fr/prj/5765>

Multinet Midi:

<https://ecotaxa.obs-vlfr.fr/prj/6056>

UVP5:

<https://ecotaxa.obs-vlfr.fr/prj/4105>

UVP6HF:

<https://ecotaxa.obs-vlfr.fr/prj/4515>

UVP6LP sn109:

<https://ecotaxa.obs-vlfr.fr/prj/4205>

UVP6LP sn111:

<https://ecotaxa.obs-vlfr.fr/prj/4206>

UVP6LP sn112:

<https://ecotaxa.obs-vlfr.fr/prj/4207>

UVP6LP sn123:

<https://ecotaxa.obs-vlfr.fr/prj/4208>

CRUISE REPORT

HE570: submitted, not published yet

HE578

Fluxes and fate of microplastics in northern European waters: Large Scale Transport – South to North (JPI-O FACTS)

AUTHORS

Alfred Wegener Institute Helmholtz Centre for Polar and Marine Research (AWI) |
Helgoland, Germany

G. Gerdtz, F. Wu, H. Jebens

Aalborg University (AAU) | Aalborg, Denmark

A. Vianello

National Research Council of Italy Institute Marine Science (CNR) | Lerici, Italy

G. Suaria, A. Paluselli

GEOMAR Helmholtz Centre for Ocean Research | Kiel Germany

J. Roa, C. Fink

MARUM Center for Marine Environmental Sciences

C. Zonneveld, G. Vertseegeh

Technical University Berlin (TUB) | Berlin, Germany

C. Georgi

JPI-O FACTS (Fluxes and Fate of Microplastics in Northern European Waters). Increasing numbers of studies on the occurrence of microplastics reflect the interest and urgency linked with this topic. The reliability of reported data has improved significantly since more emphasis is put on contamination control, chemical identification of polymer particles and removal of human biases by automation (Primpke et al. 2018, 2020). Methods such as μ -FTIR and Raman microscopy with particle detection limits of 11 and 1 μ m are now routinely applied (Cabernard et al., 2018). Based on these and emerging methods with even lower detection limits, a more complete description of sources, transport and fate of small MP is now accessible. However, further research is needed to understand them at different scales and to detect challenging particle classes.

Large Scale Transport – South to North (JPI-O FACTS workpackage 1). The Norwegian Coastal Current (NCC) is a potentially important transport route of microplastics (MP) that links the population dense areas of northern Europe to the Barents Sea (Cózar et al. 2017), and the Arctic Ocean. The NCC consists of multiple water sources, mixed in on the way towards the high Arctic. Perhaps the most important water mass (at least in

volume) is the Atlantic water, flowing into the Nordic Seas between Shetland and the Faroes (Winther & Johannessen, 2006) and arriving into the Arctic flowing along western Svalbard. Other water masses that mix into the NCC originate from the Baltic, German Bight, and Norwegian rivers (Kristiansen & Aas, 2015). Disentangling the contribution of MP from this array of water masses is tantamount to understand the flow dynamics of MP within the NCC, and quantification of MP in as many sources as possible is needed to allow models to assess the overall transport to the Barents Sea realistically. It has been estimated that 100 – 1200 tons of plastic float in Arctic regions (Cozar et al., 2017) and low resolution surface-circulation models suggest that ocean currents carried the litter to these areas from the North Atlantic that accumulate in the Arctic. Although marine debris has been reported in surface waters along the NCC from continental Europe to Fram strait (Lusher et al., 2015), the pathways and transport to the Fram Strait, which is the gateway to the high Arctic, have not been studied so far. The Skagerrak shores of Denmark, Sweden and Norway have for many years been known to accumulate marine litter and its shores along the Sweden-Norway border are amongst the most heavily impacted by marine litter on beaches from Gibraltar to North Cape (Gutow et al., 2018). Atmospheric air currents are some of the most important transport routes for organic contaminants from lower latitudes to the North. Precipitation, and especially snow is regarded as the most efficient scavenger of organic contaminants and black carbon (Doherty et al., 2010). Also dry deposition can be an important sink for atmospheric particles over ice in the Central Arctic, while vertical transfer from the ocean to the atmosphere can be a local particle source in open leads and ocean waters (Held et al., 2011). Recently, MP have been found in indoor and outdoor air in Paris, France (Dris et al., 2017), outdoor air in Dongguan city, China (Cai et al., 2017) and deposited dust in Tehran, Iran (Dehghani et al., 2017) proving the capability of MPs to travel via air. Also, recent findings of MP in sea ice collected at the HAUSGARTEN stations close to Svalbard as well as the Arctic Central Basin point towards sources by air-transport (Peeken et al., 2018). To link the airborne impact of MP into and vice versa, the ocean the sea surface microlayer (SML), covering the whole ocean (Wurl et al. 2011) plays a key role, since it is a discrete boundary between atmosphere and ocean, a trapping and concentration layer of atmospheric deposition as well as a potential transition vehicle for pollutants and particles as MP (Ng & Obbard, 2006).

Heincke cruise 578. During the cruise we successfully sampled in total 23 stations from the coast of Bergen to the arctic island Bjornoya. In figure 1 an overview of the geographic area and the sampling stations is displayed, figure 2 illustrates the applied sampling instruments. The DSHIP station 2 was sampled twice (DSHIP 24) due to bad weather conditions during the first attempt. With respect to the initial cruise application, five further stations (one of the Faroe Shetland Channel box and two of the Svinoy box and Gimsoy box respectively) were also not performed due to weather or time limitations. On transects between stations, “on the way” air and water sampling was successfully performed by using high and low volume air samplers (TUB) and the newly developed automated COMPASS water filtration system (AAU). Air samplers were installed on the

compass bridge and only operated while the ship was moving. The Intake of water for COMPASS was realized by applying a submersible pump in the Moon Pool of the Heincke. The COMPASS system consists of three so called UFO units with three filtration units each (2 x 300 µm & 1 x 15 µm), providing three integrative samples of up to 1000 L. During He578, the maximum filtration time was set to 3 h per UFO unit. As a consequence on longer transects (e. g. DSHIP 7; transect from Faroe Shetland Channel box to Bjornoya W box), several subsets of the respective transect were sampled. On all stations of the Faroe Shetland Channel box, the Bjornoya W box and the most westerly or southerly stations of the Gimsoy, Svinoy and Fugloya Bjornoya boxes, the COMPASS system was operated in parallel to surface water sampling (by catamaran or buoy) and the < 15 µm filtrate was further filtered on 0.5 µm metal-sinter membranes for enrichment of submicron plastic particles (or even nanoplastics). All stations were started with a CTD cast to get an overview on the oceanographic conditions and the different water bodies present. Based on these information, sampling depths were defined (e. g. below pycnocline, below Chl a maximum, different waterbodies) for CTD (CNR), in situ pump (MARUM) and Marine Snow catcher (GEOMAR) samples which were taken subsequently. By using the in situ pumps equipped with stainless steel 15 µm meshes, it was possible to filter ~500 L at each station and depth. Surface water samples were then taken by using either a Neuston catamaran or a sampling buoy (depending on the weather conditions). The Neuston catamaran (AWI) was equipped with a 300 µm net for enrichment of larger MP particles and a newly developed on board (air driven, PTFE) pumping and filtration system for particles < 300 µm > 15 µm. An identical pumping and filtration system was used on the Heincke for water samples taken by the sampling buoy (AWI, during heavy weather). With both devices between 350–650 L were successfully sampled (and filtered). In total on 5 stations it was possible to take undisturbed sediment cores by using a Multicorer (MARUM). The MUC was equipped with Perspex and stainless steel coring pipes. The stainless steel coring pipes facilitate contamination free samples, enabling slicing of cores and analyses of different sediment horizons for microplastics (AWI) and ²¹⁰Pb based sediment chronology (MARUM, HEREON). All samples were stored cooled or frozen on board the Heincke. Most of the samples are currently still analyzed in the laboratories of the cooperating partners by using FTIR Imaging/FTIR microscopy (AWI, AAU, CNR) or PyGCMS (ICBM). Submicron microplastics (or nanoplastics) will be analyzed by Raman microscopy or nanoFTIR (AWI). Marine Snow Catcher samples (aggregates, water) will be subjected to in deep microbiological and microscopical analyses (GEOMAR).

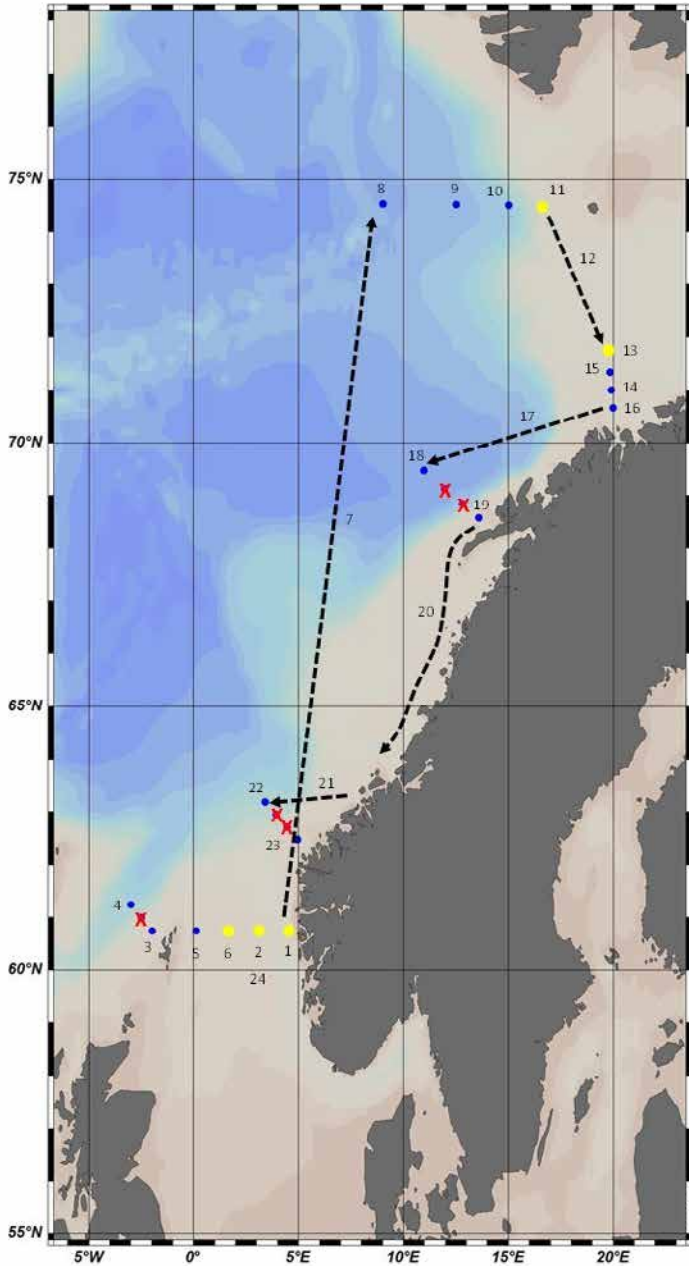


Figure 1: Station map of He578. Blue circles: CTD (up to 5 depths), in situ pumps (up to 3 depths), neuston catamaran (net & on board pump/filtration setup) or sampling buoy with separate on ship pump/filtration setup (surface), marine snow catcher (2 depths). Yellow circles: All devices deployed (blue circles) and Multicorer (sediment). Red crosses: Stations not performed. Dashed lines: Transects between stations used for “on the way sampling” of water and air. Stations 1, 2, 24, 5, 6: Fedje / Shetland box; Stations 3 & 4: Faroe Shetland Channel box; Stations 22 & 23: Svinoy box; Stations 18 & 19: Gimsoy box; Stations 13, 14, 15, 16: Fugjvoja Bjornoya box; Stations 8, 9, 10, 11: Bjornoya W box.

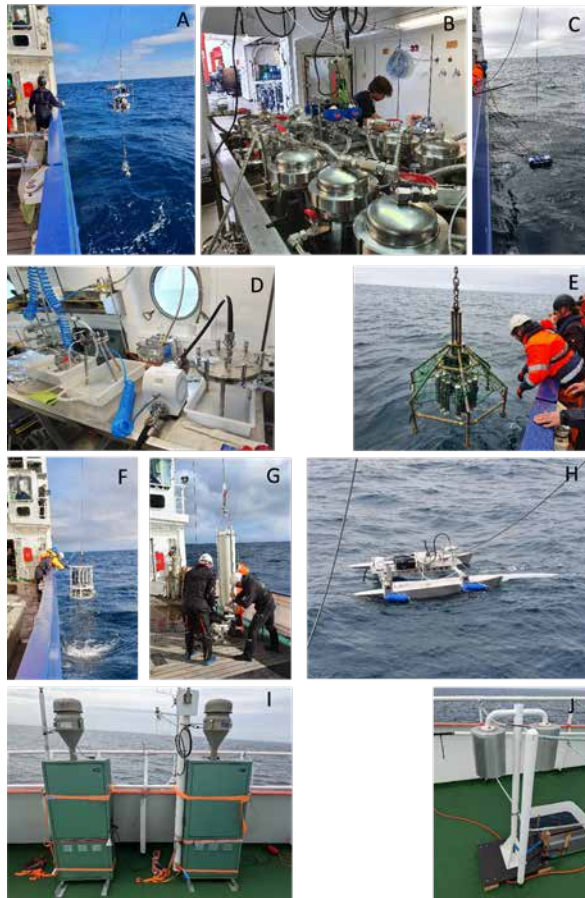


Figure 2: Sampling devices used on He578. A: in situ pumps; B: COMPASS filtration system; C: Sampling buoy with separate on ship pump/filtration set up (D); E: Multicorer; F: CTD; G: Marine Snow Catcher; H: Neuston catamaran with net and on board pump/filtration setup; I & J: High (I) and low volume (J) air sampler.

REFERENCES

Cabernard L, Roscher L, Lorenz C, Gerdtz G, Primpke S, Comparison of Raman and Fourier transform infrared spectroscopy for the quantification of microplastics in the aquatic environment, *Environmental science & technology* 2018, 52(22), 13279–13288.

Cai L, Wang J, Peng J, Tan Z, Zhan Z, Tan X, Chen Q, Characteristic of microplastics in the atmospheric fallout from Dongguan city, China: preliminary research and first evidence, *Environmental Science and Pollution Research* 2017, 24, 24928–24935.

Cózar A, Martí E, Duarte CM, García-de-Lomas J, Van Sebille E, Ballatore TJ, et al., The Arctic Ocean as a dead end for floating plastics in the North Atlantic branch of the Thermohaline Circulation, *Science advances* 2017, 3(4), e1600582.

Dehghani S, Moore F, Akhbarizadeh R, Microplastic pollution in deposited urban dust, Tehran metropolis, Iran, *Environmental Science and Pollution Research* 2017, 24, 20360–20371.

Doherty SJ, Warren SG, Grenfell TC, Clarke AD, Brandt, RE, Light-absorbing impurities in Arctic snow, *Atmospheric Chemistry and Physics* 2010, 10(23), 11647–11680.

Dris R, Gasperi J, Mirande C, Mandin C, Guerrouache M, Langlois V, Tassin B, A first overview of textile fibers, including microplastics, in indoor and outdoor environments, *Environmental pollution* 2017, 221, 453–458.

Gutow L, Ricker M, Holstein JM, Dannheim J, Stanev EV, Wolff JO, Distribution and trajectories of floating and benthic marine macrolitter in the south-eastern North Sea, *Marine pollution bulletin* 2018, 131, 763–772.

Held A, Brooks IM, Leck C, Tjernström M, On the potential contribution of open lead particle emissions to the central Arctic aerosol concentration., *Atmospheric Chemistry and Physics* 2011, 11(7), 3093–3105.

Kristiansen T & Aas E, Water type quantification in the Skagerrak, the Kattegat and off the Jutland west coast, *Oceanologia* 2015, 57(2), 177–195.

Lusher AL, Tirelli V, O'Connor I, Officer R, Microplastics in Arctic polar waters: the first reported values of particles in surface and sub-surface samples, *Scientific reports* 2015, 5(1), 14947.

Ng KL, & Obbard JP, Prevalence of microplastics in Singapore's coastal marine environment, *Marine pollution bulletin* 2006, 52(7), 761–767.

Peeken I, Primpke S, Beyer B, Gütermann J, Katlein C, Krumpfen T, Bergmann M, Hehemann L, Gerdtz G, Arctic sea ice is an important temporal sink and means of transport for microplastic, *Nature communications* 2018, 9(1), 1505.

Primpke S, Cross RK, Mintenig SM, et al., Toward the Systematic Identification of Microplastics in the Environment: Evaluation of a New Independent Software Tool (siMPle) for Spectroscopic Analysis, *Applied Spectroscopy* 2020, 74(9), 1127–1138, doi:10.1177/0003702820917760.

Primpke S, Wirth M, Lorenz C, et al., Reference database design for the automated analysis of microplastic samples based on Fourier transform infrared (FTIR) spectroscopy, *Anal Bioanal Chem* 2018, 410, 5131–5141, <https://doi.org/10.1007/s00216-018-1156-x>.

Winther NG, & Johannessen JA, North Sea circulation: Atlantic inflow and its destination, *Journal of Geophysical Research: Oceans* 2006, 111 (C12).

Wurl O, Wurl E, Miller L, Johnson K, Vagle S, Formation and global distribution of sea-surface microlayers, *Biogeosciences* 2011, 8(1), 121–135.

SCIENTIFIC OUTPUT

LIST OF PUBLICATIONS (SO FAR)

Goßmann I, Herzke D, Held A, Schulz J, Nikiforov V, Georgi C, Evangeliou E, Gerdt G, Wurl O, Scholz-Böttcher, BM, Occurrence and backtracking of microplastic mass loads including tire wear particles in northern Atlantic air, *Nature Communications* 2023, 14(1), 3707.

Wu F, Reding L, Starckenburg M, Leistenschneider C, Primpke S, Vianello A, Zonneveld K, Huserbråten M, Versteegh G, Gerdt G, Spatial distribution of small microplastics in the Norwegian Coastal Current 2024, *Environmental Science & Technology* (submitted).

HE582

The fate of organic matter in sandy sediments

AUTHORS

Alfred-Wegener-Institute, Helmholtz Centre for Polar- und Marine Research | Bremerhaven/Sylt, Germany

M. Holtappels, Z. Zhou, U. Hanz, S. Henkel, S. Kasten, L. Sanders

Helmholtz-Zentrum Hereon | Geesthacht, Germany

F. Minutolo, A. Neumann, K. Dähnke

Max-Planck-Institute for Marine Microbiology | Bremen, Germany

S. Ahmerkamp, F. Lange

Institute for Chemistry and Biology of the Marine Environment, University of Oldenburg | Oldenburg, Germany

H. Waska, T. Dittmar

Center for Marine Environmental Sciences – MARUM, University of Bremen, | Bremen, Germany

M. Holtappels, S. Kasten, S. Ahmerkamp

SANDY SEDIMENTS

Despite the high primary production in shelf waters, more than 50% of the global shelf seafloor is composed of sands that do not accumulate organic matter (Emery, 1968; Wilson et al., 2008). Long regarded as rather inactive sediments, a new paradigm emerged in the 1990s, which found increased mineralization of organic matter in sands similar to or even higher than those in coastal muddy sediments (Huettel and Gust, 1992; Huettel and Rusch, 2000; Huettel et al., 1998). It was shown that mass transport in sands is driven by pore water advection which is often 1-2 orders of magnitude more effective than the diffusive transport in cohesive sediments (Boudreau et al., 2001; Huettel et al., 2014) supplying a versatile microbial community that lives attached to the sand grains (Probandt et al., 2017, Ahmerkamp 2020). Porewater advection in sands is driven by bottom flows over ubiquitous bedforms through Bernoulli's principle (Figure 1), and further depends on the permeability of the sandy seabed (Thibodeaux and Boyle, 1987). The supply of electron acceptors for the oxidation of organic matter can be significantly enhanced leading to high oxygen uptake and denitrification rates (de Beer et al., 2005; Gao et al., 2012; Marchant et al., 2016). Especially the benthic N-loss via denitrification is of utmost importance for the North Sea, and in general for coastal environments, which receive much of the anthropogenic nitrate via riverine and atmospheric input (Beusekom

et al., 1999). It is assumed that coastal permeable sediments act as an efficient natural filter system for reactive nitrogen and thereby provide an important ecosystem service (Seitzinger et al., 2006).

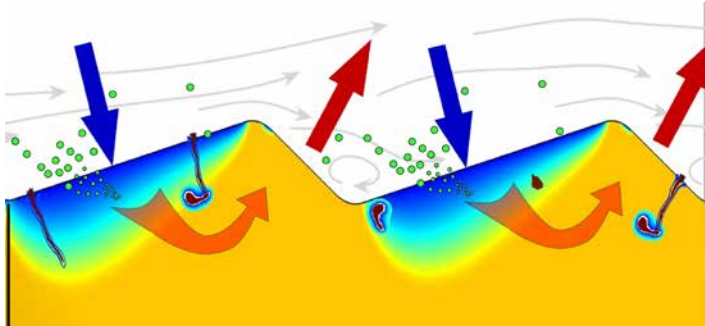


Figure 1: Schematic drawing of advective pore water transport. Blue arrows denote electron acceptors (e. g. O_2 , NO_3^-). Red arrows denote reduced substances and waste products. Green dots denote particulate organic matter.

Much of the early mechanistic understanding was derived from laboratory studies. Recent field campaigns to the North Sea focused on studying these processes under natural conditions using novel benthic observatories equipped with oxygen pore water lances, seabed topography scanners and current meters to measure the oxygen dynamics in the pore water during tidal cycles and for various different sediment types (Ahmerkamp et al., 2017). It was found that the sediment mobility (i.e. current induced ripple migration) has an impact on the oxic turnover rates, as predicted by Ahmerkamp et al. (2015). Most importantly it was shown that the measured mean penetration depth of oxygen could be predicted by a mechanistic model (Ahmerkamp et al., 2017).

These findings represented an important step forward in our understanding of the transport and turnover of electron acceptors such as oxygen and nitrate. However, the supply of organic matter (OM) is still poorly understood. A particular problem is posed by the separate transport routes of the OM fractions. In sand, OM is divided into a mobile dissolved fraction (DOM) and an immobile particulate fraction (POM) that is retained by the sand filter. The conditions for the transport and degradation of either DOM or POM remain speculative. Associated research questions are:

- › Which size fraction of POM is relevant for the OM supply into the pore space?
- › Does the presence of POM in the pore space has a potential feedback on the stability and permeability of sandy sediments?
- › How much DOM is adsorbed to particles and iron phases?

- › How much of the DOM is labile and can be taken up by the benthic microbes, which live attached to the sand grains?

It was shown that sediment grain size and permeability had a clear influence on the microbial abundance (Ahmerkamp et al., 2020) and community composition (Probandt et al., 2017) and it is possible that the porewater advection in sand increases the substrate-microbe encounter rates and favors microbial uptake even of those DOM molecules whose concentrations are otherwise too diluted to match the required energetic investment for their uptake and degradation (Arrieta et al., 2015). The potential of sandy sediments to remove such persistent compounds from the environment needs to be investigated as it is of great interest for the understanding and management of coastal environments.

R/V HEINCKE EXPEDITION HE582

From August 23rd until September 9th 2021, six main stations were surveyed within the German Bight (Figure 2), selected for their different sediment properties, water depths, and nutrient concentrations. At each station, two benthic observatories for high-resolution measurements of currents, sediment topography, benthic O₂ penetration, and turbulent O₂ fluxes were deployed over a full tidal cycle to relate hydro- and morphodynamics with benthic O₂ uptake. Complementing the observatory deployments, the water column and sediments were sampled by CTD, grab, and multi-corer (MUC). In particular, turnover rates of O₂, as well as nitrification and denitrification rates in the sands were experimentally determined. Samples for concentration profiles of pore water and solid phase compounds, such as organic carbon and iron, were taken. Sediment resuspension and leaching experiments were performed to investigate the concentrations and reactivities of dissolved and particulate organic matter. Meanwhile, the large-scale topography and sediment characteristics around the stations were determined using multibeam and side-scan sonar surveys.

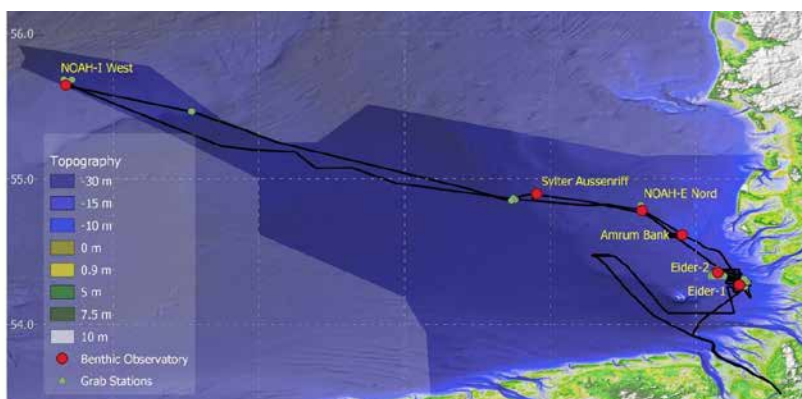


Figure 2: Track chart of the cruise HE582. Bathymetry from GEBCO and EasyGSH. Six main working areas where Benthic Observatory were deployed are marked in red, additional grab stations are marked in green.

ORGANIC MATTER IN SANDY SEDIMENTS

Of the various investigations that make use of HE582 data, three studies are presented here in more detail.

Adsorbed DOM, the overlooked OM pool in sands

Dissolved organic matter (DOM) was collected from bottom water and porewater, and the adsorbed and iron-bound DOM was leached from the sediment using ultra-pure water and 0.5 M HCl, respectively. DOC concentrations were measured with a TOC-VCPH analyzer and molecular composition was analyzed with Fourier transform ion cyclotron resonance mass spectrometry (FT-ICR-MS). It was found that the concentration of adsorbed and iron-bound DOC was about 50 times the concentration of porewater DOC, representing a considerable fraction (2-20%) of the total organic carbon in the sediment. Also, the molecular composition was significantly different between the two leached DOM fractions and the DOM in bottom and pore waters, pointing towards adsorption and iron-coprecipitation as selective processes for the retention of DOM in sandy sediments. Interestingly, both leached DOM fractions exhibited significantly higher H/C ratios and more terrigenous signatures compared to the DOM in bottom and porewaters. From nearshore to offshore stations and correlating with increasing bottom water salinities, the DOM of bottom and pore waters showed a decreasing trend of terrigenous signatures. The massive seawater filtration by sandy sediments in combination with the high DOC concentrations and the selectivity for terrigenous material in the adsorbed and iron-bound DOM suggest that coastal sands play an important role in retaining terrigenous DOM, possibly representing a selective sink for water column DOM. The study by Zhou et al. has been submitted to Environmental Science and Technology.

Comparing predictors for sediment reactivity

In a parallel study, sediments from 4 of the stations were incubated to quantify oxygen, ammonium, and nitrate turnover as a function of a number of different sediment properties, specifically grain size distribution, mud content, total organic carbon, chlorophyll-a, phaeophytin-a, and carbohydrate concentrations. With the aim to assess their potential to predict sediment reactivity, multiple linear regression analysis was used. From all variables, mud content and phaeophytin-a were identified as the best proxies for sediment reactivity showing significant correlations ($R^2 > 0.8$). The correlation with total organic carbon content was also significant but less pronounced and the correlation with chlorophyll-a was weak. Especially mud content is a valuable predictor for sediment reactivity because of the many available data sets. However, the conclusions about the form of organic matter (DOM or POM) that controls the turnover of oxygen, ammonium and nitrate are not straight forward. Phaeophytin-a could be seen as representative for particulate organic carbon derived from algae aggregates, whereas mud content is a grain size fraction ($< 63 \mu\text{m}$), which is known to provide also a large surface area for DOM adsorption. Nevertheless, the reported correlations can be used to extrapolate reaction rates to regions for which proxy values have been reported. The study by Minutolo et al. is in review at Continental Shelf Research.

WHEN BIOLOGY CONTROLS PHYSICS

It is well known that permeability controls the porewater advection and thus the flow of dissolved compounds to the microbial community that lives attached to sand grains. It is less clear to what degree biofilms formed by microorganism and benthic diatoms reduce the flow-regime in the pore space. To investigate the effect of polymers on sediment-water exchange processes, volumetric oxygen consumption rates and permeabilities were measured in combination with the quantification of various forms of sugars that can form gel-like colloids. Indeed, the content of these sugar fractions explained more than 40% of the variance of all measured physical and biological properties, and interestingly, this sugar fraction reveals strong correlations with key parameters of benthic-pelagic exchange fluxes such as permeability, which makes it an excellent predictor for benthic-pelagic exchange fluxes. The results reveal an important feedback of sediment microbiology on the sediment permeability that adds to the physical properties that control the advective porewater flow. The study by Lange et al. is in preparation for submission to *Biogeosciences*.

REFERENCES

Ahmerkamp S, Winter C, Janssen F, Kuypers MMM, and Holtappels M, The impact of bedform migration on benthic oxygen fluxes, *Journal of Geophysical Research: Biogeosciences* 2015, 120(11), 2229-2242, doi:10.1002/2015jg003106.

Ahmerkamp S, Winter C, Krämer K, de Beer D, Janssen F, Friedrich J, Kuypers MMM, and Holtappels M, Regulation of benthic oxygen fluxes in permeable sediments of the coastal ocean, *Limnology and Oceanography* 2017, 62(5), 1935-1954, doi:10.1002/lno.10544.

Ahmerkamp S, Marchant H, Peng C, Probandt D, Littmann S, Kuypers MMM, and Holtappels M, The effect of sediment grain properties and porewater flow on microbial abundance and respiration in permeable sediments, *Scientific reports* (accepted).

Arrieta JM, Mayol E, Hansman RL, Herndl GJ, Dittmar T, and Duarte CM, Dilution limits dissolved organic carbon utilization in the deep ocean, *Science* 2015, 348(6232), 331-333, doi:10.1126/science.1258955.

van Beusekom JEE, Brockmann UH, Hesse KJ, Hickel W, Poremba K, and Tillmann U, The importance of sediments in the transformation and turnover of nutrients and organic matter in the Wadden Sea and German Bight, *Deutsche Hydrografische Zeitschrift* 1999, 51(2-3), 245-266.

Boudreau BP, et al., Permeable marine sediments: Overturning an old paradigm, *Eos, Transactions American Geophysical Union* 1982, 82, 133-136, doi:10.1029/EO082i011p00133-01.

de Beer D, Wenzhöfer F, Ferdelman TG, Boehme SE, Huettel M, von Beusekom JEE, Böttcher ME, Musat N, and Dubilier N, Transport and Mineralization Rates in North Sea Sandy Intertidal Sediments, Sylt-Römö Basin, Wadden Sea, *Limnology and Oceanography* 2005, 50(1), 113-127.

Emery KO, Relict sediments on continental shelves of world, *American Association of Petroleum Geologists Bulletin* 1968, 52(3), 445-464.

Gao H, Matyka M, Liu B, Khalili A, Kostka JE, Collins G, Jansen S, Holtappels M, Jensen MM, Badewien TH, Beck M, Grunwald M, de Beer D, Lavik G, Kuypers MMM, Intensive and extensive nitrogen loss from intertidal permeable sediments of the Wadden Sea, *Limnology and Oceanography* 2012, 57(1), 185-198, doi:10.4319/lo.2012.57.1.0185.

Huettel M, Berg P, and Kostka JE, Benthic Exchange and Biogeochemical Cycling in Permeable Sediments, *Annual Review of Marine Science* 2014, 6(1), 23-51, doi:10.1146/annurev-marine-051413-012706.

Huettel M, and Gust G, Impact of Bioroughness on Interfacial Solute Exchange in Permeable Sediments, *Marine Ecology-Progress Series* 1992, 89(2-3), 253-267, doi:10.3354/meps089253.

Huettel M, and Rusch A, Transport and Degradation of Phytoplankton in Permeable Sediment, *Limnology and Oceanography* 2000, 45(3), 534-549.

Huettel M, Ziebis W, Forster S, and Luther GW, Advective transport affecting metal and nutrient distributions and interfacial fluxes in permeable sediments, *Geochimica Et Cosmochimica Acta* 1998, 62(4), 613-631, doi:10.1016/s0016-7037(97)00371-2.

Marchant HK, Holtappels M, Lavik G, Ahmerkamp S, Winter C, and Kuypers MMM, Coupled nitrification–denitrification leads to extensive N loss in subtidal permeable sediments, *Limnology and Oceanography* 2016, 61(3), 1033–1048, doi:10.1002/lno.10271.

Probandt D, Knittel K, Tegetmeyer HE, Ahmerkamp S, Holtappels M, and Amann R, Permeability shapes bacterial communities in sublittoral surface sediments, *Environmental Microbiology* 2017, 19(4), 1584-1599, doi:10.1111/1462-2920.13676.

Seitzinger S, Harrison JA, Bohlke JK, Bouwman AF, Lowrance R, Peterson B, Tobias C, and Van Drecht G, Denitrification across landscapes and waterscapes: A synthesis, *Ecological Applications* 2006, 16(6), 2064-2090.

Thibodeaux LJ, and Boyle JD, Bedform-Generated Convective-Transport in Bottom Sediment, *Nature* 1987, 325(6102), 341-343, doi:10.1038/325341a0.

Wilson AM, Huettel M, and Klein S, Grain size and depositional environment as predictors of permeability in coastal marine sands, *Estuarine Coastal and Shelf Science* 2008, 80(1), 193-199, doi:10.1016/j.ecss.2008.06.011.

SCIENTIFIC OUTPUT

LIST OF PUBLICATIONS

Zhou Z, Waska H, Henkel S, Dittmar T, Kasten S, Holtappels M, Iron promotes terrigenous dissolved organic matter retention in subtidal permeable sediments, submitted to *Environmental Science and Technology*.

Minutolo F, Dähnke K, Metzke M, Holtappels M, Neumann A, Benthic oxygen and nitrogen process rates in the southern North Sea: Sedimentary mud and phaeophytin-a are reliable predictors of oxygen consumption and nitrogen turnover, in review at *Continental Shelf research*.

Lange F, Ahmerkamp S, Jalaluddin F, Mundanatt A, Ferdelman T, Hehemann J, Winter C, Holtappels M, Kuypers M, Self-sustaining biophysical interactions control benthic-pelagic exchange fluxes on sandy continental shelves, for submission to *Biogeosciences*.

LIST OF CONFERENCE PRESENTATIONS

2022 | **Application of stable isotope dilution to identify novel proxies of sediment reactivity** Jesium Conference, Kuopio, Finland.

2023 | **Self-sustaining biophysical interactions control benthic-pelagic exchange fluxes on sandy continental shelves** AGU, San Francisco, USA.

2023 | **Parameterizing sediment reactivity in the southern North Sea: New proxies for benthic nitrogen turnover** ASLO Aquatic Sciences Meeting, Palma de Mallorca, Spain.

DATA

Master track and station list:

<https://doi.pangaea.de/10.1594/PANGAEA.938529>

Physical oceanography (CTD):

<https://doi.pangaea.de/10.1594/PANGAEA.937791>

Physical oceanography (Thermosalinograph):

<https://doi.pangaea.de/10.1594/PANGAEA.944736>

CRUISE REPORT

HE582: https://doi.pangaea.de/10.48433/cr_he582

M144

Eastern Mediterranean Paleoclimate and Ecosystems during the Rise of Early Civilizations

AUTHORS

Heidelberg University | Heidelberg, Germany

J. Pross, A. Bahr, O. Friedrich, J. Lippold

GEOMAR | Kiel, Germany

D. Nürnberg

Throughout the Holocene, Mediterranean civilizations have closely interacted with their environment. However, it has yet remained unclear to what extent climatic and environmental changes have influenced their evolution. At the same time, the onset, early extent and consequences of anthropogenic impact on terrestrial and notably on marine ecosystems has yet remained poorly constrained. In light of these uncertainties, the main scientific objective of R/V METEOR cruise M144 (EMPIRE – “Eastern Mediterranean Paleoclimate and Ecosystems during the Rise of Early Civilizations”) was the recovery of core material from high-deposition-rate, coastal settings of the E Mediterranean Sea that allows to investigate changes in terrestrial and marine ecosystems during the rise of human civilizations. The coring locations were selected strategically with respect to archeological sites; therefore, they were predominantly from near-coastal settings in the Aegean and Adriatic Seas (Pross et al., 2021).

This approach allows to shed light on how climate and human resource demands have interacted over the course of the Holocene; specifically, it allows (i) to unravel how environmental change has affected socioeconomic evolution during the Holocene, and (ii) to quantitatively assess the growing impact of settled societies and industrialized economies on the structure and biodiversity of Mediterranean ecosystems. Notably, this approach yields terrestrial climate and ecosystem data within a high-quality marine-based age frame and allows a first-order land-sea correlation.

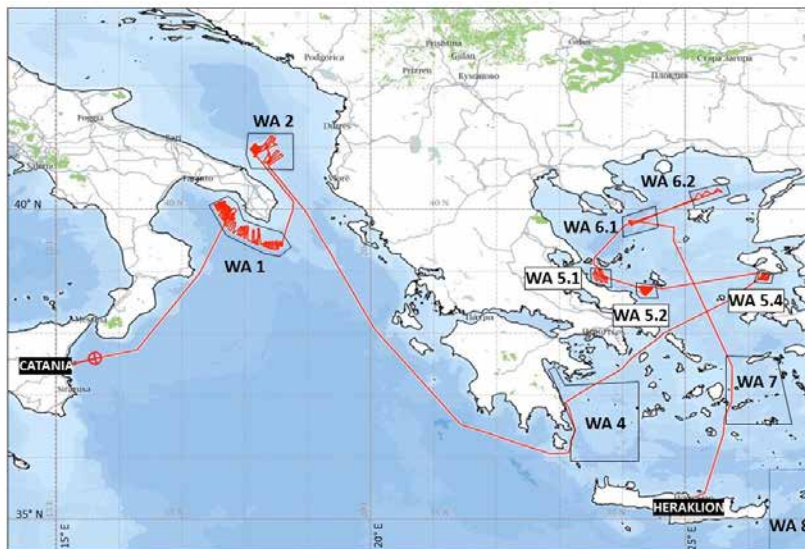


Figure 1: Track of R/V METEOR Cruise M144. Individual Work Areas (WA) are indicated.

Over the course of cruise M144, 215 m of gravity cores at 24 stations and 51 m of kasten cores at eight stations were obtained from the Aegean Sea, the Adriatic Sea, and the Gulf of Taranto (Figs. 1–3). The average recovery across all working areas amounted to between 5 and 6 m for gravity cores, and between 4 and 5 m for kasten cores, with recovery being generally slightly lower in the Aegean Sea than in the Adriatic Sea and the Gulf of Taranto. The positions of coring stations were determined after extensive hydroacoustic surveys, partially based on previous work of collaboration partners from the Hellenic Center for Marine Research (HCMR). For proxy-calibration studies and geochemical analyses of recent upper sea-floor sediments, surface sediments were sampled via multicorer at 24 stations. Water samples for the analysis of water chemistry (i. e., vertical temperature, salinity and oxygen variabilities) were retrieved via 23 CTD/Rosette casts. In addition, double multinet-hauls were run at eight stations to investigate the planktonic foraminiferal communities in the water column down to 700 m water depth, complemented by filtering water from the ship's pump after each haul. After the cruise, all core material was transported to the Institute of Earth Sciences, Heidelberg University, Germany, where it is being stored at 4 °C and has been made available for further research.

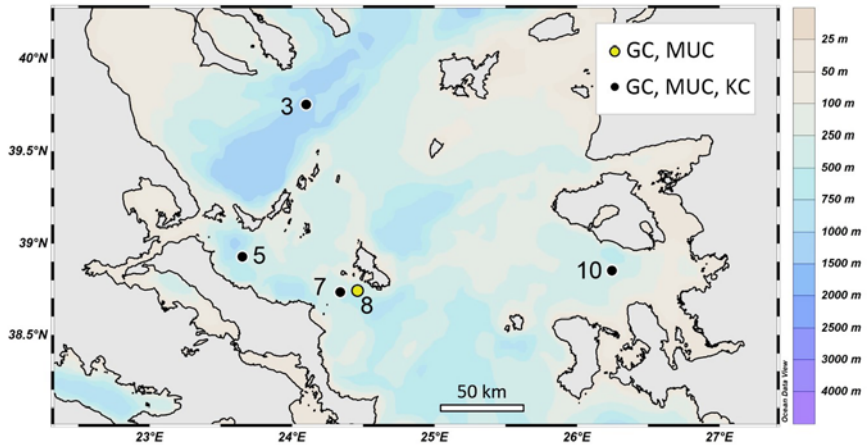


Figure 2: Locations of M144 gravity (GC), kasten (KC), and multicore (MUC) stations in the Aegean Sea. Stations with employment of all three devices are marked by black circles, and stations with GC and MUC employment only by yellow circles.

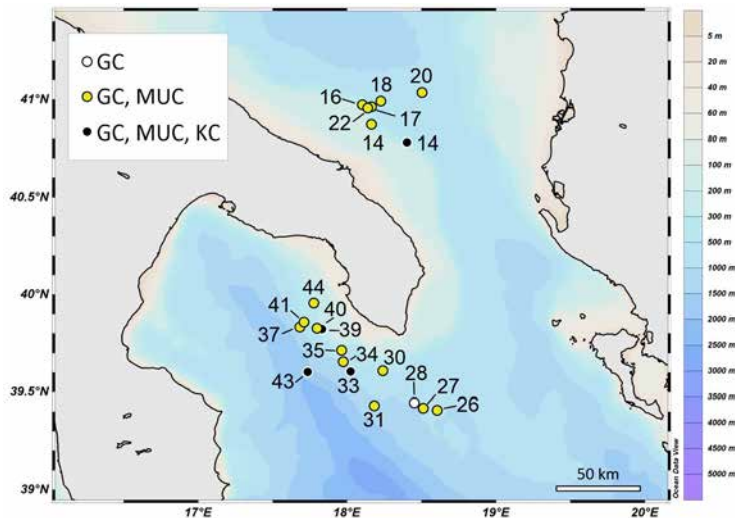


Figure 3: Locations of M144 gravity (GC), kasten (KC), and multicore (MUC) stations in the Southern Adriatic Sea and the Gulf of Taranto. Stations with employment of all three devices are marked by black circles, stations with GC and MUC employment only by yellow circles, and stations with GC employment only by white circles.

Following the establishment of radiocarbon-, color-scanning- (i. e., lightness, L^* ; Figure 4), XRF-scanning-, and tephrostratigraphy-based age models for the individual cores at Heidelberg University, the obtained material is currently being analyzed for signals from terrestrial and marine proxies by members of the M144 Science Party. Despite a substantial delay due to the restrictions in laboratory access, conference attendance, and travel possibilities due to anti-Covid measures from 2020 to 2022, first results are, e. g.,

available on the population dynamics of meso- and epipelagic pelagic fish throughout the past ~11.4 kyr and notably across sapropel S1 based on a fish-otolith record from kasten core M144 KC 5-6 in the western Aegean Sea (Pallacks et al., subm.). The analysis of the Ba/Ca ratios in live and dead specimens of the benthic foraminifer species *Uvigerina mediterranea* and *Melonis affinis* from marginal marine settings in the Central and Northern Aegean Sea has yielded new insight into the geochemical processes underlying the Ba incorporation in the carbonate shell of foraminifers (Petersen et al., subm.). Further studies have been initiated, and additional momentum in the evaluation of M144 material will develop upon the availability of material from R/V METEOR cruise M195 (November-December 2023). This cruise has been designed to probe proximal, high-deposition-rate settings in the Aegean and Ionian Seas that could partially not be visited during cruise M144 due to the Aegean dispute between Greece and Turkey and thus strategically complements the core material collected during cruise M144.

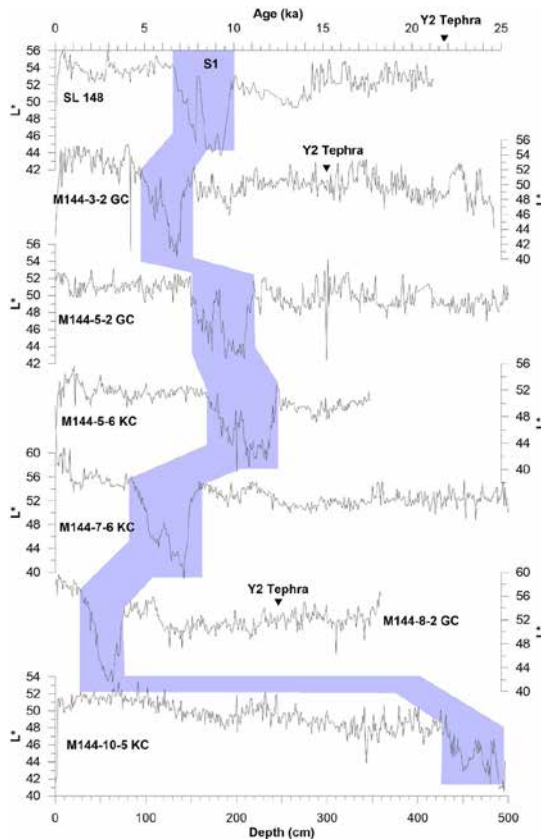


Figure 4: North-south site-to-site correlation of sediment cores recovered from the Aegean Sea during Cruise M144 based on downcore lightness profiles (L^*). The relative location of the Sapropel S1 layer in each core is marked by the blue bar. The ages referenced in the upper x-axis refer to the lightness profile (L^*) of reference record SL148 (Northern Aegean Sea, Ehrmann et al., 2007).

REFERENCES

Ehrmann W, Schmiedl G, Hamann Y, Kuhnt T, Hemleben C, Siebel W, Clay minerals in late glacial and Holocene sediments of the northern and southern Aegean Sea, *Palaeogeography, Palaeoclimatology, Palaeoecology* 2007, 249, 36–57.

Pallacks S, Ziveri P, Jannke H, Lin C-H, Subhas AV, Galbraith E, Kaboth-Bahr S, Friedrich O, Bahr A, Koutsodendris A, Pross J, Norris R, Ocean deoxygenation linked to ancient mesopelagic fish decline. Submitted.

Petersen J, Schmiedl G, Mojtahid M, Raddatz J, Bahr A, Pross J, Grunert P, Controls on barium incorporation into tests of benthic foraminifera – a proxy calibration from the Aegean Sea. Submitted.

Pross J, Bahr A, Berke M, Blum M, Brzelinski S, Campos H, Catunda MC, Evers F, Kaboth S, Kotthoff U, Koutsodendris A, Krengel T, Lange D, Lippold J, Mächtle B, Manta K, Maicher D, Norris RD, Pöppelmeier F, Ravani A, Schulz H, Süfke F, Sugla R, Vakhrameeva P, Vannacci M, Otte F, Raeke A, Eastern Mediterranean paleoclimate and ecosystems during the rise of early civilizations, Cruise No. M144, December 27, 2017 – January 18, 2018, Heraklion (Greece) – Catania (Italy). *METEOR-Berichte M144* 2021, 1, 1–40, doi: 10.48433/cr_m144.

SCIENTIFIC OUTPUT

LIST OF PUBLICATIONS

Numikou P, Papanikolu D, Lampridou D, Blum M, Huebscher C, The active tectonic structures along the southern margin of Lesbos Island, related to the seismic activity of July 2017, Aegean Sea, Greece, *Geo-Marine Letters* 2021, 41(4), 1–11 <https://doi.org/10.1007/s00367-021-00723-6>.

Pallacks S, Ziveri P, Jannke H, Lin C-H, Subhas AV, Galbraith E, Kaboth-Bahr S, Friedrich O, Bahr A, Koutsodendris A, Pross J, Norris R, Ocean deoxygenation linked to ancient mesopelagic fish decline. Submitted.

Petersen J, Schmiedl G, Mojtahid M, Raddatz J, Bahr A, Pross J, Grunert P, Controls on barium incorporation into tests of benthic foraminifera – a proxy calibration from the Aegean Sea. Submitted.

Pross, J, Friedrich O. Die Bücher der Erdgeschichte; Offenbarungen vom Grund des Meeres. *Ruperto Carola Forschungsmagazin* 2019, 15, 44–51.

LIST OF CONFERENCE PRESENTATIONS

Due to Covid restrictions there have not yet been conference presentations on M144 results.

DATA

Raw multibeam EM122 data:

<https://doi.org/10.1594/PANGAEA.887862>

CRUISE REPORT

M144: [doi:10.48433/cr_m144](https://doi.org/10.48433/cr_m144)

M152/2

Persistent organic pollutants in air and surface waters of the Equatorial Atlantic – distributions and air-sea exchange

AUTHORS

Max Planck Institute for Chemistry | Mainz, Germany

G. Lammel¹, B. Nillius

Masaryk University, RECETOX Centre | Brno, Czech Republic

B. Vrana, P. Kukučka, J. Martiník, P. Příbylová, J. Sobotka

Federal Maritime and Hydrographic Agency (BSH), Marine Chemistry | Hamburg, Germany

L. Kretzschmann

¹also at Masaryk University

INTRODUCTION

Many man-made chemicals are long-lived i. e., resist degradation in the environment and are globally cycling between atmosphere, ocean and other compartments. These persistent organic pollutants (POPs) have been reaching the global marine environment through atmospheric deposition and riverine sources since decades, but are not regularly monitored and data from the open oceans are very rare. Following bans, hence, decline of the concentration in air or seasonal variation, the direction of air-sea exchange may reverse in relaxation to chemical equilibrium and turn seas into secondary sources of the pollutant (Bidleman & Connell, 1995; Stemmler & Lammel, 2013; Lammel et al., 2016). Along with Saharan dust and biomass burning plumes, pollutants can be transported with the trade winds from Africa to the Caribbean and parts of South America, not yet verified for POPs (Garrison et al., 2014).

In the project Intercontinental transport of POPs with trade winds into the Caribbean (ITTWIC, M152/2), we have studied distributions and cycling of numerous organic trace pollutants along a north-south transect from the Canary Islands (Las Palmas) to Namibia (Walvis Bay).

METHODS

Air sampling was on an upper deck on polyurethane foam plugs (PUFs, precleaned, 2 in series) and quartz fibre filter (QFF, prebaked) using a Digital high volume sampler (Figure 1a). Surface seawater sampling was done through absorption and concentration on a passive sampling medium (silicon rubber sheet, Altesil, SR), enabled by an immersible

pump generating a jet within a barrel continuously flushed with seawater from the underkeel inlet (Figure 1b-cd; Vrana et al., 2019; Sobotka et al., 2021).

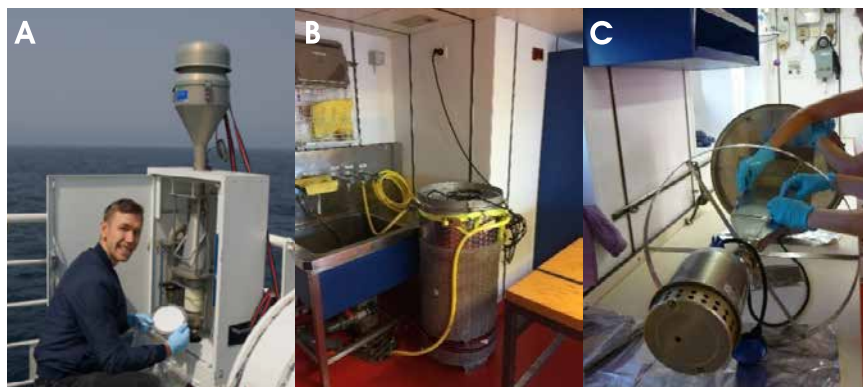


Figure 1: Sampling of (a) air (Digital high-volume air sampler) and (b-c) surface seawater (barrel continuously flushed with seawater with pump and sampler holder) on board R/V Meteor along an equatorial Atlantic transect (M152/2).

Gas-phase (PUFs), particulate phase (QFFs) and surface seawater (SRs) samples, were spiked with isotopically labeled extraction recovery standards and then extracted using automated warm Soxhlet extraction. The extracts were cleaned on modified silica columns and solvent eluted, volume-reduced (TurboVap) and syringe internal standards were added. For PAHs, GC-MS (7890A GC, Agilent, Rxi-5Sil MS column, 7000B MS, Agilent) was used. Nitro- and oxy- PAHs were analysed by atmospheric pressure chromatography tandem mass spectrometry (APGC-MS/MS, Waters Xevo TQ-S MS coupled to Agilent 7890 GC, same column). For PCBs and OCPs, GC-MS/MS was used (7890A GC, HT8 column of SGE, coupled to 7000B MS, Agilent, in EI+ multiple reactions monitoring mode). Cyclodiene pesticides were analysed by GC-APCI-MS/MS (Waters Xevo TQ-S MS coupled to Agilent 7890 GC).

In total 107 and 131 substances were quantified in air and water samples i. e., 54 polycyclic aromatic compounds, 9 polychlorinated biphenyls, 30 organochlorine pesticides, and 14 brominated flame retardants (BFRs) in air and water, and another 23 BFRs in water only.

The direction of air-sea exchange is indicated by the fugacity ratio, f_w/f_o , with $f_w = c_w H(T_w, S) = c_s H(T_w) 10^{S^* [0.04 \log K_{OW} + 0.114]}$, $f_o = c_o R T_o$, Henry's law constant $H(T_w)$ ($\text{Pa m}^3 \text{mol}^{-1}$), salinity S (mol L^{-1}), octanol-water partition coefficient K_{OW} , universal gas constant R , and temperature T (Bidleman & McConnell, 1995), and considered to be upward for $f_w/f_o > 3$, downward for $f_w/f_o < 1/3$ and close to phase equilibrium for $1/3 < f_w/f_o < 3$.

Large-scale atmospheric transports were characterized by wind fields (FLEXPART and HYSPLIT inverse Lagrangian models).

RESULTS AND DISCUSSION

Concentrations observed in equatorial Atlantic air and surface water of 39 organochlorine pesticides, PCBs and organobromine flame retardants (including some metabolites) as well as 25 polycyclic aromatic hydrocarbons (PAHs) and 31 oxygenated and nitrated derivatives thereof (OPAH, NPAH) are summarized in Table 1.

Table 1: Concentrations in air (pg m^{-3}) and freely dissolved concentrations in surface water (pg L^{-1}) (median (min-max)) along an equatorial Atlantic transect, $23.0^{\circ}\text{N}/17.6^{\circ}\text{W}\rightarrow 22.2^{\circ}\text{S}/9.9^{\circ}\text{E}$, January-February 2019 (M152/2). $\Sigma_6\text{DDX} = p,p'$, o,p' -DDT + -DDE + -DDD, $\Sigma_3\text{endosulfan} = \alpha$, β -endosulfan + endosulfan sulfate, $\Sigma_3\text{HCH} = \alpha$, β , γ -HCH, $\Sigma_3\text{heptachlor} = \text{heptachlor} + \text{cis-}, \text{trans-heptachlor epoxide}$, $\Sigma_3\text{chlordanes} = \alpha$, γ -chlordanes + oxychlordanes, $\Sigma_7\text{PCB} = \text{sum of indicator congeners}$, $\Sigma_3\text{PBDE} = \text{sum of major PBDE congeners without BDE209}$.

	Air (n=31)	Water (n=6)
PeCB	6.25 (4.0–11.6)	2.1 (1.9–2.7)
HCB	0.69 (0.25–1.86)	3.3 (3.1–3.6)
$\Sigma_3\text{HCH}$	0.22 (0.08–0.51)	<1.0
Aldrin	0.016 (<0.02–0.08)	<3.8
$\Sigma_3\text{chlordanes}$	0.094 (0.011–0.22)	<0.6
$\Sigma_3\text{heptachlor}$	0.10 (0.07–0.22)	0.97 (<0.36–1.15)
$\Sigma_6\text{DDX}$	0.40 (<0.07–1.20)	0.57 (<0.3–3.84)
$\Sigma_3\text{endosulfan}$	0.15 (<0.06–0.57)	<1.5a
$\Sigma_7\text{PCB}$	1.09 (0.15–3.21)	0.77 (0.26–3.14)
$\Sigma_3\text{PBDE}$	0.41 (0.06–1.62)	<0.08b
$\Sigma_{25}\text{PAHc}$	1260 (139–6600)	1620 (910–3530)
$\Sigma_{13}\text{OPAH}$	82 (0.88–397)	9950 (8290–11800)
$\Sigma_{18}\text{NPAH}$	1.0 (0.035–7.0)	35 (21–45)

a endosulfan sulfate ranged <0.16-0.37

b n=2

c naphthalene not included

The air-sea exchange flux of the chlorobenzenes C_6Cl_6 and C_6HCl_5 , of DDT and its major metabolite DDE were upward i. e., volatilizational, in the equatorial Atlantic, of the metabolite endosulfan sulfate and of the PBDE congeners 28, 47 and 100 mostly close to equilibrium or upward, and of γ -HCH downward i. e., depositional.

Acknowledgements: We thank the crew and chief scientist of M152/2, Christian Hübscher (U Hamburg). This research was supported by the Max Planck Society, the Czech Ministry for Education, Youth and Sports (projects LM2023069 and -030), and the DFG.

REFERENCES

Bidleman TF, McConnell LL, A review of field experiments to determine air–water gas-exchange of persistent organic pollutants, *Science of the Total Environment* 1995, 159(2-3), 101–107, doi:10.1016/0048-9697(95)04255-Y.

Garrison VH, Majewski MS, Foreman WT, et al., Persistent organic contaminants in Saharan dust air masses in West Africa, Cape Verde and the eastern Caribbean, *Science of the Total Environment* 2014, 468-469(1), 530–543 doi: 10.1016/j.scitotenv.2013.08.076.

Lammel G, Meixner FX, Vrana B, et al., Bi-directional air-sea exchange and accumulation of POPs (PAHs, PCBs, OCPs and PBDEs) in the nocturnal marine boundary layer, *Atmospheric Chemistry and Physics* 2016, 16(10), 6381–6393 doi: 10.5194/acp-16-6381-2016.

Sobotka J, Slobodnik J, Schink A, et al., Dynamic passive sampling of hydrophobic organic compounds in surface seawater along the South Atlantic Ocean east-to-west transect and across the Black Sea, *Marine Pollution Bulletin* 2021, 168(7), 112375, doi:10.1016/j.marpolbul.2021.112375.

Stemmler I, Lammel G, Evidence of the return of past pollution in the ocean – a model study, *Geophysical Research Letters* 2013, 40(7), 1373–1378 doi: 10.1002/grl.50248.

Vrana B, Rusina T, Okonski K, et al., Chasing equilibrium passive sampling of hydrophobic organic compounds in water, *Science of the Total Environment* 2019, 664(9), 424–435 doi:10.1016/j.scitotenv.2019.01.242.

SCIENTIFIC OUTPUT

LIST OF PUBLICATIONS

Lammel G, Iakovides M, Kretzschmann L, Kukučka P, Příbylová P, Prokeš R, Sobotka J, Wietzoreck M, Degrendele C, Palátová Nežiková B, Schink A, Pozo K, Stephanou EG, Vrana B, Endosulfan, DDT and other organochlorine pesticides in the Atlantic and Middle East Seas atmosphere, surface waters and air-sea gas exchange, *Organohalogen Compounds* 2023, in press.

Sobotka J, Slobodnik J, Schink A, Prokeš R, Lammel G, Okonski K, Vrana B, Dynamic passive sampling of hydrophobic organic compounds in surface seawater along the South Atlantic Ocean east-to-west transect and across the Black Sea, *Marine Pollution Bulletin* 2021, 168(7), 112375, doi:10.1016/j.marpolbul.2021.112375.

LIST OF CONFERENCE PRESENTATIONS

2019 | **Dynamic passive sampling of POP in surface seawater along a South Atlantic Ocean east-to-west transect and across the Black Sea** 17th EuChemS International Conference on Chemistry and the Environment, Thessaloniki, Greece.

2019 | **Contamination of open ocean waters by persistent organic pollutants and air-sea gas exchange** 6th Conference on Monitoring and Water Analysis, Przysiek, Poland.

2023 | **Endosulfan, DDT and other organochlorine pesticides in the Atlantic and Middle East Seas atmosphere, surface waters and air-sea gas exchange** 43rd International Symposium on Halogenated Persistent Organic Pollutants, Maastricht, Netherlands.

2023 | **Polycyclic aromatic compounds in the environment – distribution and transports** 5th International Environmental Chemistry Conference, Antalya, Turkey.

CRUISE REPORT

M152/2: doi:10.2312/cr_m152_2

M157

Persistent organic pollutants in air and surface waters of the Equatorial Atlantic – distributions, air-sea exchange and trans-Atlantic transport

AUTHORS

Max Planck Institute for Chemistry | Mainz, Germany

G. Lammel¹, M. Wietzoreck, J. Kim, S. Hildmann, B. Nillius

Masaryk University, RECETOX Centre | Brno, Czech Republic

B. Vrana, P. Kukučka, J. Martiník, P. Přibylková, J. Sobotka

Atmo Guyane | Cayenne, French Guyana, France

L. Luttringer

¹also at Masaryk University

INTRODUCTION

Many man-made chemicals are long-lived i. e., resist degradation in the environment and are globally cycling between atmosphere, ocean and other compartments. These persistent organic pollutants (POPs) have been reaching the global marine environment through atmospheric deposition and riverine sources since decades, but are not regularly monitored and data from the open oceans are very rare. Following bans, hence, decline of the concentration in air or seasonal variation, the direction of air-sea exchange may reverse in relaxation to chemical equilibrium and turn seas into secondary sources of the pollutant (Bidleman & Connell, 1995; Stemmler & Lammel, 2013; Lammel et al., 2016). Along with Saharan dust and biomass burning plumes, pollutants can be transported with the trade winds from Africa to the Caribbean and parts of South America, not yet verified for POPs (Garrison et al., 2014).

In the project Intercontinental transport of POPs from western and central Africa (ITWIA, M157), we have studied distributions and cycling of numerous organic trace pollutants along a north-south transect (Figure 1a) from Cabo Verde (Mindelo) to Namibia (Walvis Bay) in combination with coastal measurements.

METHODS

Air sampling was on an upper deck on polyurethane foam plugs (PUFs, precleaned, 2 in series) and quartz fibre filter (QFF, prebaked) using a Digital high volume sampler. Surface seawater sampling was done through absorption and concentration on a passive sampling medium (silicon rubber sheet, Altesil, SR), enabled by an immersible pump

generating a jet within a barrel continuously flushed with seawater from the underkeel inlet (Vrana et al., 2019; Sobotka et al., 2021).

Gas-phase (PUFs), particulate phase (QFFs) and surface seawater (SRs) samples, were spiked with isotopically labeled extraction recovery standards and then extracted using automated warm Soxhlet extraction. The extracts were cleaned on modified silica columns and solvent eluted, volume-reduced (TurboVap) and syringe internal standards were added. For PAHs, GC-MS (7890A GC, Agilent, Rxi-5Sil MS column, 7000B MS, Agilent) was used. Nitro- and oxy- PAHs were analysed by atmospheric pressure chromatography tandem mass spectrometry (APGC-MS/MS, Waters Xevo TQ-S MS coupled to Agilent 7890 GC, same column). For PCBs and OCPs, GC-MS/MS was used (7890A GC, HT8 column of SGE, coupled to 7000B MS, Agilent, in EI+ multiple reactions monitoring mode). Cyclodiene pesticides were analysed by GC-APCI-MS/MS (Waters Xevo TQ-S MS coupled to Agilent 7890 GC).

In total 107 and 131 substances were quantified in air and water samples i. e., 54 polycyclic aromatic compounds, 9 polychlorinated biphenyls, 30 organochlorine pesticides, and 14 brominated flame retardants (BFRs) in air and water, and another 23 BFRs in water only.

The direction of air-sea exchange is indicated by the fugacity ratio, f_w/f_a , with $f_w = c_w H(T_w, S) = c_s H(T_w) 10^{S \cdot [0.04 \log K_{OW} + 0.114]}$, $f_a = c_a R T_a$, Henry's law constant $H(T_w)$ (Pa m³ mol⁻¹), salinity S (mol L⁻¹), octanol-water partition coefficient K_{OW} , universal gas constant R , and temperature T (Bidleman & McConnell, 1995), and considered to be upward for $f_w/f_a > 3$, downward for $f_w/f_a < 1/3$ and close to phase equilibrium for $1/3 < f_w/f_a < 3$.

Large-scale atmospheric transports were characterized by wind fields (FLEXPART and HYSPLIT inverse Lagrangian models) and chemical transformations along transport were quantified using oxidant fields (ECMWF, Copernicus Atmosphere Monitoring Service).

RESULTS AND DISCUSSION

Concentrations observed in equatorial Atlantic air and surface water of 39 organochlorine pesticides, PCBs and organobromine flame retardants (including some metabolites) as well as 25 polycyclic aromatic hydrocarbons (PAHs) and 31 oxygenated and nitrated derivatives thereof (OPAH, NPAH) are summarized in Table 1 and selected pollutants' concentrations illustrated in Figure 1 together with data from 8 other campaigns in the Atlantic and 1 in the Mediterranean (2016-22), and in Figure 2 together with data of 2 campaigns in the Atlantic and 1 in the Mediterranean and Middle East seas (2016-19).

Table 1: Concentrations in air (sum of gaseous and particulate, $\mu\text{g m}^{-3}$) and freely dissolved concentrations in surface water ($\mu\text{g L}^{-1}$) (median (min-max)) along an equatorial Atlantic transect, 13.4°N/21.7°W→21.3°S/12.7°E, August 2019 (M157). $\Sigma_2\text{DDX} = p,p', o,p'-\text{DDT} + -\text{DDE} + -\text{DDD}$, $\Sigma_3\text{endosulfan} = \alpha, \beta\text{-endosulfan} + \text{endosulfan sulfate}$, $\Sigma_3\text{HCH} = \alpha, \beta, \gamma\text{-HCH}$, $\Sigma_3\text{heptachlor} = \text{heptachlor} + \text{cis-, trans-heptachlor epoxide}$, $\Sigma_3\text{chlordanes} = \alpha, \gamma\text{-chlordanes} + \text{oxychlordanes}$, $\Sigma_7\text{PCB} = \text{sum of indicator congeners}$, $\Sigma_9\text{PBDE} = \text{sum of major PBDE congeners without BDE209}$.

	Air (n=11)	Water (n=3)
PeCB	5.97 (3.2–8.1)	2.9 (2.0–3.0)
HCB	0.63 (0.25–0.97)	5.3 (3.3–6.8)
$\Sigma_3\text{HCH}$	0.11 (0.04–0.54)	<1.2
aldrin	<0.01	<18
$\Sigma_3\text{chlordanes}$	0.040(0.014–0.29)	0.09 (0.07–0.16)
$\Sigma_3\text{heptachlor}$	0.044(0.017–0.21)	1.8 (<1.4–2.6)
$\Sigma_6\text{DDX}$	0.28 (0.11–1.20)	0.55 (0.26–2.0)
$\Sigma_3\text{endosulfan}$	0.34 (<0.01–0.84)	<1.0 _a
$\Sigma_7\text{PCB}$	0.30 (0.11–1.68)	2.7 (<0.5–7.5)
$\Sigma_9\text{PBDE}$	0.082(0.038–0.47)	0.46 (0.26–0.85)
$\Sigma_{25}\text{PAHs}$	191 (98–2110)	672 (511–7800)
$\Sigma_{13}\text{OPAH}$	100 (74–318)	26000(23300–33900)
$\Sigma_{18}\text{NPAH}$	0.65 (0.38–1.6)	31 (13–41)

a endosulfan sulfate ranged <0.19–0.75 | b naphthalene not included

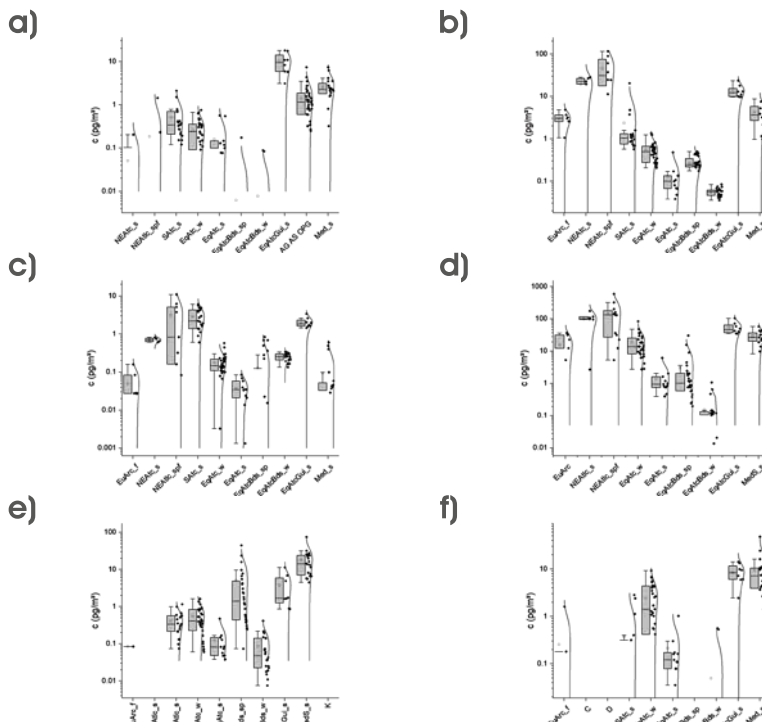


Figure 1: Distributions of the pesticides (a) DDT (sum of 2 isomers), (b) $\Sigma_3\text{HCH}$ (c) $\Sigma_3\text{endosulfan}$, (d) PCB (sum of 9 congeners, $\Sigma_9\text{PCBs}$), (e) the flame retardant PBDE (sum of 9 congeners, $\Sigma_9\text{PBDE}$) and (f) the PAH benzo(a)pyrene in Atlantic air samples (sampled on board ships and at coastal sites, f = fall, s = summer, sp = spring, w = winter; M124 = SAtc_s, M152/2 = EqAtl_w, M157 = EqAtl_s).

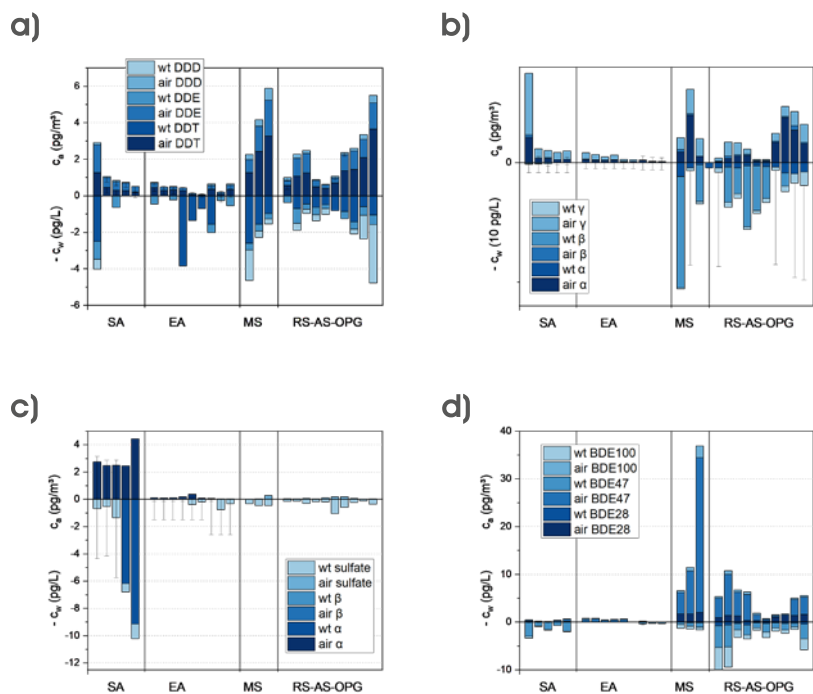


Figure 2: Concentrations of the pesticides (a) DDT and metabolites ($\Sigma 6DDX$), (b) $\Sigma 3HCH$, (c) $\Sigma 3$ endosulfan and (d) $\Sigma 9PBDE$ in Atlantic Ocean, Mediterranean and Middle East seas air and surface waters. SA = South Atlantic (M124), EA = Equatorial Atlantic (M152/2, M157), MS = Mediterranean Sea, RS = Red Sea, AS = Arabian Sea, OPG = Oman and Persian Gulfs.

The air-sea exchange flux of the chlorobenzenes C_6Cl_6 and C_6HCl_5 , of DDT and its major metabolite DDE were upward i. e., volatilizational, in the equatorial Atlantic, of the metabolite endosulfan sulfate and of the PBDE congeners 28, 47 and 100 mostly close to equilibrium or upward, and of γ -HCH downward i. e., depositional. The flux of α -endosulfan is close to equilibrium / about to reverse in the western south Atlantic (as determined during M124 in 2016).

The intercontinental transport of polycyclic aromatic compounds emitted with biomass burning in equatorial and southwest Africa to South America was studied by sampling the same air mass on the north-south transect in the eastern equatorial Atlantic (M157) and 7–8 days later at the Guyana coast ($4.95^\circ N/52.28^\circ W$), verified by atmospheric modelling (Figure 3).

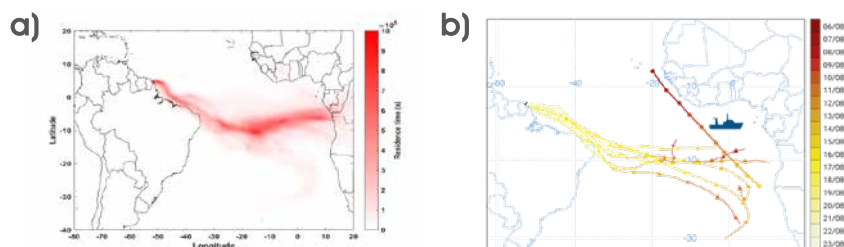


Figure 3: Tracking intercontinental atmospheric transport using (a) FLEXPART and (b) HYSPLIT inverse Lagrangian models. Route of M157 dated in (b).

ACKNOWLEDGEMENTS

We thank the crew and chief scientist of M157, Matthias Zabel (U Bremen), furthermore Alejandro Spitzky (U Hamburg), Kathy Panechou-Pulcherie (Atmo Guyane), Luke Jones and Xiabo Yang (ECMWF) for logistic and technical help. This research was supported by the Max Planck Society, the Czech Ministry for Education, Youth and Sports (projects LM2023069 and -030), and the DFG.

REFERENCES

Bidleman TF, McConnell LL, A review of field experiments to determine air–water gas-exchange of persistent organic pollutants, *Science of the Total Environment* 1995, 159(2-3), 101–107, doi:10.1016/0048-9697(95)04255-Y.

Garrison VH, Majewski MS, Foreman WT, et al., Persistent organic contaminants in Saharan dust air masses in West Africa, Cape Verde and the eastern Caribbean, *Science of the Total Environment* 2014, 468–469(1), 530–543 doi: 10.1016/j.scitotenv.2013.08.076.

Lammel G, Meixner FX, Vrana B, et al., Bi-directional air-sea exchange and accumulation of POPs (PAHs, PCBs, OCPs and PBDEs) in the nocturnal marine boundary layer, *Atmospheric Chemistry and Physics* 2016, 16(10), 6381–6393 doi: 10.5194/acp-16-6381-2016.

Sobotka J, Slobodnik J, Schink A, et al., Dynamic passive sampling of hydrophobic organic compounds in surface seawater along the South Atlantic Ocean east-to-west transect and across the Black Sea, *Marine Pollution Bulletin* 2021, 168(7), 112375, doi:10.1016/j.marpolbul.2021.112375.

Stemmler I, Lammel G, Evidence of the return of past pollution in the ocean – a model study. *Geophysical Research Letters* 2013, 40(7), 1373–1378 doi: 10.1002/grl.50248.

Vrana B, Rusina T, Okonski K, et al., Chasing equilibrium passive sampling of hydrophobic organic compounds in water, *Science of the Total Environment* 2019, 664(9), 424–435 doi:10.1016/j.scitotenv.2019.01.242.

SCIENTIFIC OUTPUT

LIST OF PUBLICATIONS

Lammel G, Iakovides M, Kretzschmann L, Kukučka P, Příbylová P, Prokeš R, Sobotka J, Wietzoreck M, Degrendele C, Palátová Nežiková B, Schink A, Pozo K, Stephanou EG, Vrana B, Endosulfan, DDT and other organochlorine pesticides in the Atlantic and Middle East Seas atmosphere, surface waters and air-sea gas exchange, *Organohalogen Compounds* 2023, in press.

Sobotka J, Slobodnik J, Schink A, Prokeš R, Lammel G, Okonski K, Vrana B, Dynamic passive sampling of hydrophobic organic compounds in surface seawater along the South Atlantic Ocean east-to-west transect and across the Black Sea, *Marine Pollution Bulletin* 2021, 168(7), 112375, doi:10.1016/j.marpolbul.2021.112375.

LIST OF CONFERENCE PRESENTATIONS

2019 | **Dynamic passive sampling of POP in surface seawater along a South Atlantic Ocean east-to-west transect and across the Black Sea** 17th EuChemS International Conference on Chemistry and the Environment, Thessaloniki, Greece.

2019 | **Contamination of open ocean waters by persistent organic pollutants and air-sea gas exchange** 6th Conference on Monitoring and Water Analysis, Przysiek, Poland.

2023 | **Endosulfan, DDT and other organochlorine pesticides in the Atlantic and Middle East Seas atmosphere, surface waters and air-sea gas exchange** 43rd International Symposium on Halogenated Persistent Organic Pollutants, Maastricht, Netherlands.

2023 | **Polycyclic aromatic compounds in the environment – distribution and transports** 5th International Environmental Chemistry Conference, Antalya, Turkey.

CRUISE REPORTS

M157: doi:10.2312/cr_m157

M162

Fluid flow along the Gloria Fault, central North Atlantic

AUTHORS

GEOMAR – Helmholtz Centre for Ocean Research Kiel | Kiel, Germany
C. Hensen, M. Schmidt, T. Müller

Faculty of Geosciences, University of Bremen | Bremen, Germany
N. Kaul

IPMA – Portuguese Institute for Sea and Atmosphere | Lisbon, Portugal
P. Terrinha, L. Batista, M. Neres, V. Magalhães

IDL – Dom Luiz Institute, University of Lisbon | Lisbon, Portugal
J. Duarte

Marine and Environm. Sciences Centre – University of Évora | Évora, Portugal
H. Adao

Department of Geosciences – University of Évora | Évora, Portugal
P. Nogueira

Integrated Geochemical Interpretation Ltd. | Bideford, Great Britain
M. Nuzzo

Eawag – Swiss Federal Institute of Aquatic Science and Technology | Dübendorf,
Switzerland
R. Kipfer

Department of Marine Science, The University of Texas at Austin | Austin, USA
M. Lever

R/V Meteor cruise M162 was conducted as a systematic continuation of ongoing work along the Azores-Gibraltar Fault Zone (AGFZ). It was dedicated to understand if and how fluid flow through crust and sediments continues along transform-type plate boundaries and fracture zones away from mid-ocean ridges and continental margins. The western (Azores Plateau) and eastern (Gulf of Cadiz and Horseshoe Abyssal Plain) ends of the AGFZ have been extensively studied with respect to fluid flow based on the results of a number of scientific cruises (e. g. SO175, MSM1-3, M86, M141, M186).

While – due to the proximity of the region to the Mid-Atlantic Ridge – fluids on the Azores Plateau are obviously affected by hydrothermal activity (Schmidt et al., 2020; Schmidt et al., 2019), previous findings along the eastern continuation of the Gloria Fault revealed fault-controlled fluid advection and mud volcanism along strike-slip faults in the Horseshoe Abyssal Plain and the Gulf of Cadiz, where fluid geochemistry revealed the admixture of fluids from deeply buried oceanic crust and oldest sediments on top of it (Hensen et al., 2019; Hensen et al., 2007; Hensen et al., 2022; Hensen et al., 2015; Scholz et al., 2009).

The target region of M162 was the central part of Gloria Fault. The region is highlighted in the bathymetric map shown in Figure 1. The Gloria Fault is an old, reactivated, and seismically active oceanic fracture zone (Hensen et al., 2019).

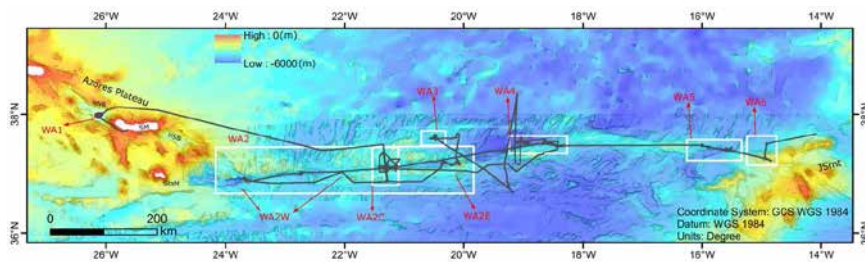


Figure 1: Bathymetric map of the central Gloria Fault region. Black line shows the cruise track, white boxes indicate the working areas of M162.

On cruise M162, a systematic survey was carried out along the main trace of the Gloria Fault between the Azores Plateau and the Madeira-Tore Rise, including sub-bottom profiler surveys, heat flow transects, gravity corer sampling, as well as video-guided CTD and multicorer deployments. In accordance to recently recorded seismic activity along the fault, there is evidence for tectonic motion both in sub-bottom profiler records and sediment cores.

Heat flow transects and sites for gravity coring where typically placed at and across conspicuous seafloor features, such as dome structures or faults, often accompanied by blanking zones in the hydroacoustic record, which, among other reasons, may be indicative for active upward fluid migration. Figure 2 shows the hydroacoustic record of working area (WA) 2 along with selected pore water data from GC 20 and 22. While Ca and Sr concentrations remain at background levels at GC 20, there is a clear concentration gradient in GC 22 indicating enhanced alteration processes at subsurface depths below the cored sediment depth. The most obvious explanation for the observed pore water Ca and Sr excursions is the alteration of oceanic crust or volcanic ash in combination with recrystallization of carbonates (Schmidt et al., 2020).

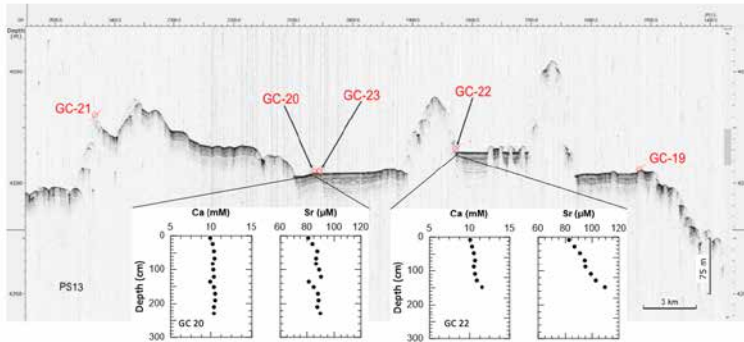


Figure 2: Combined hydroacoustic record and GC locations of working area (WA) 2. Selected pore water plots are shown for GC 20 and 22.

A similar pore fluid signature can be observed at station GC 33, located north of the main fault trace in WA 1C (Figure 3). Interestingly, a heat flow station in the vicinity of the coring station revealed the highest value (226 mW m^{-2}) of the entire cruise. The coincidence of elevated heat flow and geochemical gradients (creating an obvious difference from the regional background of pore water composition) substantiates the hypothesis of slight upward fluid migration at specific sites.

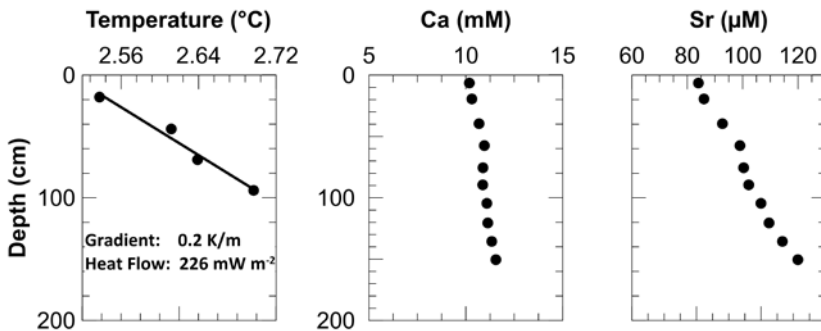


Figure 3: Heat flow measurement at station HF2006P03 and selected pore water data from station GC 33, north of the Gloria Fault (WA 1C).

The relation of Sr and Ca in the pore water can further be used to characterize the two major diagenetic pore water trends observed in sediments retrieved on cruise M162 (Figure 4). As mentioned before, the increase in Ca and Sr likely reflects the alteration of crustal material or volcanic ash and the recrystallization of carbonates. An opposing trend is found in locations of thicker sediment accumulations, where larger amounts of organic material are buried. The decrease in Ca can be ascribed to the formation of

authigenic carbonates, driven by the anaerobic oxidation of methane, presently occurring at an estimated sediment depth of 30–40 m.

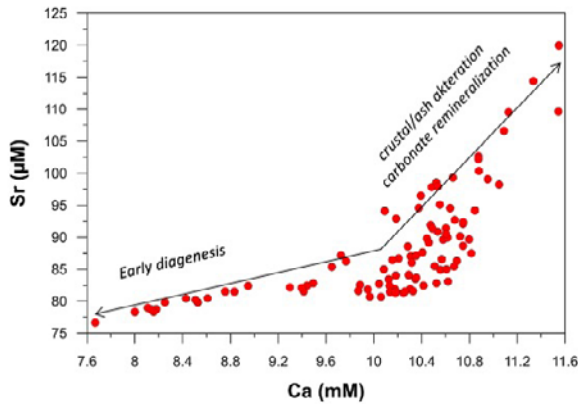


Figure 4: Ongoing work on available data obtained on cruise M162 aims at a combined analysis of geochemical, microbiological and geophysical data in order to generate a profound interpretation and synthesis with respect to magnitude and spatial extent of sub-seafloor fluid flow along the Gloria Fault.

REFERENCES

Hensen C, Duarte JC, Vannucchi P, Mazzini A, Lever MA, Terrinha P, Géli L, Henry P, Villinger H, Morgan J, Schmidt M, Gutscher MA, Bartolome R, Tomonaga Y, Polonia A, Gràcia E, Tinivella U, Lupi M, Çağatay MN, Elvert M, Sakellariou D, Matias L, Kipfer R, Karageorgis AP, Ruffine L, Liebetrau V, Pierre C, Schmidt C, Batista L, Gasperini L, Burwicz E, Neres M, Nuzzo M, Marine Transform Faults and Fracture Zones: A Joint Perspective Integrating Seismicity, Fluid Flow and Life, *Frontiers in Earth Science* 2019, 7.

Hensen C, Nuzzo M, Hornibrook E, Pinheiro LM, Bock B, Magalhães VH, Brückmann W, Sources of mud volcano fluids in the Gulf of Cadiz—indications for hydrothermal imprint, *Geochimica et Cosmochimica Acta* 2007, 71, 1232–1248.

Hensen C, Scholz F, Liebetrau V, Kaul N, Nuzzo M, Schmidt M, Batista L, Villinger H, Terrinha P, Oceanic strike-slip faults represent active fluid conduits in the abyssal sub-seafloor, *Geology* 2022, 50, 189–193.

Hensen C, Scholz F, Nuzzo M, Valadares V, Gràcia E, Terrinha P, Liebetrau V, Kaul N, Silva S, Martínez-Loriente S, Bartolome R, Piñero E, Magalhães VH, Schmidt M, Weise SM, Cunha M, Hilario A, Perea H, Rovelli L, Lackschewitz K, Strike-slip faults mediate the rise of crustal-derived fluids and mud volcanism in the deep sea, *Geology* 2015, 43, 339–342.

Schmidt C, Hensen C, Hübscher C, Wallmann K, Liebetrau V, Schmidt M, Kutterolf S, Hansteen TH, Geochemical characterization of deep-sea sediments on the Azores Plateau – From diagenesis to hydrothermal activity, *Marine Geology* 2020, 429, 106291.

Schmidt C, Hensen C, Wallmann K, Liebetrau V, Tatzel M, Schurr SL, Kutterolf S, Haffert L, Geilert S, Hübscher C, Lebas E, Heuser A, Schmidt M, Strauss H, Vogl J, Hansteen T, Origin of High Mg and SO₄ Fluids in Sediments of the Terceira Rift, Azores-Indications for Caminite Dissolution in a Waning Hydrothermal System, *Geochemistry, Geophysics, Geosystems* 2019, 20, 6078–6094.

Scholz F, Hensen C, Reitz A, Romer RL, Liebetrau V, Meixner A, Weise SM, Haeckel M, Isotopic evidence (⁸⁷Sr/⁸⁶Sr, $\delta^{7}\text{Li}$) for alteration of the oceanic crust at deep-rooted mud volcanoes in the Gulf of Cadiz, NE Atlantic Ocean, *Geochimica et Cosmochimica Acta* 2019, 73, 5444–5459.

SCIENTIFIC OUTPUT

LIST OF PUBLICATIONS

Amadinho M, Large-scale distribution patterns of nematode assemblages along the Oceanic Plate boundary (Glória fault), Mestrado (Master) em Biologia da Conservação, Universidade de Évora, in progress.

Bakker L, The microbial community composition of abyssal plain sediments in relation to oxygen, the N-cycle and metals, Master Thesis, ETH Zürich, 2021.

Bakker L, Glombitza C, Deng L, Hensen C, Lever MA, The microbiome of abyssal fracture zone sediments, to be submitted to *Frontiers in Microbiology*.

Ferreira T, Megafauna large-scale distribution patterns along the Gloria fracture zone (NE Atlantic), Mestrado (Master) em Gestão e Conservação de Recursos Naturais, mestrado em parceria entre a Universidade de Évora e Universidade de Lisboa-Instituto Superior de Agronomia, 2022, <http://hdl.handle.net/10174/31464>.

Koppe M, Evidence for fluid flow? Compilation of geochemical and geophysical data of sediments along the Gloria Fault zone, NE Atlantic. Master Thesis, Faculty of Mathematics and Natural Science, Christian-Albrechts University, Kiel, 2022.

Schmidt J-N, Analysis of marine heat flow signatures across the Gloria Fault – a 2D and 3D numerical topographic correction using COMSOL Multiphysics, Master Thesis Faculty of Geosciences, Bremen, 2022.

LIST OF CONFERENCE PRESENTATIONS

2021 | **Megafauna communities from abyssal sites along the Gloria Fracture Zone (NE Atlantic)** 16th DSBS Deep-Sea Biology Symposium, Brest, France.

<http://hdl.handle.net/10174/31104>

2021 | **Occurrence of marine litter along abyssal areas of the Gloria Fracture Zone (NE Atlantic)** 16th DSBS Deep-Sea Biology Symposium, Brest, France.

<http://hdl.handle.net/10174/31116>

DATA

Event list:

<https://www.pangaea.de/expeditions/events/M162>

Multibeam bathymetry raw data:

<https://doi.org/10.1594/PANGAEA.933327>

Pore water and gas geochemistry data:

https://portal.geomar.de/kdmi;jsessionid=B0D5DC925421426C73B5C047A13AB29E#_48_INSTANCE_5P8d_=metadata%2Fleg%2Fshow%2F351718

Heat Flow:

HF2001: doi.org/10.1594/PANGAEA.926962

HF2002: doi.org/10.1594/PANGAEA.927330

HF2004: doi.org/10.1594/PANGAEA.927317

HF2005: doi.org/10.1594/PANGAEA.927318

HF2006: doi.org/10.1594/PANGAEA.927319

HF2007: doi.org/10.1594/PANGAEA.927320

HF2008: doi.org/10.1594/PANGAEA.927321

HF2010: doi.org/10.1594/PANGAEA.927323

HF2011: doi.org/10.1594/PANGAEA.927324

HF2012: doi.org/10.1594/PANGAEA.927325

HF2013: doi.org/10.1594/PANGAEA.927326

HF2014: doi.org/10.1594/PANGAEA.927327

HF2015: doi.org/10.1594/PANGAEA.927328

HF2016: doi.org/10.1594/PANGAEA.927329

HF2017: doi.org/10.1594/PANGAEA.927331

Processed multibeam bathymetry, hydroacoustic, and core scan data are presently uploaded (submission ID PDI-36603) to Pangaea by Portuguese partners from IPMA.

CRUISE REPORT

M162: https://doi.pangaea.de/10.48433/cr_m162

<https://oceanrep.geomar.de/51612>

M164

AMOC components at 47°N

AUTHORS

IUP – Institute of Environmental Physics, University of Bremen | Bremen, Germany
R. Steinfeldt, D. Kieke, C. Mertens, M. Rhein

MARUM – Center for Marine Environmental Sciences, University of Bremen | Bremen, Germany
M. Rhein, D. Kieke, S. Wett, H. Nowitzki

BSH – Federal Maritime and Hydrographic Agency | Hamburg, Germany
M. Moritz, K. Jochumsen, B. Klein

The Atlantic meridional Overturning Circulation (AMOC) is a main part of the earth's climate system. It plays an important role for the heat transport from the tropics to the higher northern latitudes and also provides a means for the removal of anthropogenic carbon from the atmosphere and its storage in the deep ocean. Whereas there is low confidence in changes in the AMOC since 1850 (IPCC, 2021), models show a substantial weakening of the AMOC under ongoing climate warming until the end of the century.

The NOAC (North Atlantic Changes) array, funded via the BMBF Verbundvorhaben RACE, was established to measure the AMOC strength along 47°N in the Atlantic, close to the boundary between subpolar and subtropical gyre. It consisted of moorings at the eastern and western boundary (measuring temperature, salinity and current speed) as well as pressure inverted echo sounders (PIES) at the ocean bottom, which allow to infer the geostrophic transport in the interior (Figure 1). The deployment period of the NOAC array ended with the cruise M164, which means that all moorings and PIES were recovered on this cruise. The only exception were the two moorings at the eastern boundary, which had been redeployed under the responsibility of the BSH.

First results from the different components of the NOAC array have proven that the transports at the eastern and western boundaries as well as in the interior could be correlated with sea surface height measure by satellite altimetry (Rhein et al., 2019, Nowitzki et al., 2021, and Moritz et al., 2021). This allows to extend the calculated transports backwards in time until 1993. Wett et al. (2023) combined the transports of the different segments in order to infer the total AMOC transport. For the shelf regions, which had not been covered by moorings and shipboard measurements, geostrophic transports have been calculated from the observational based ARMOR3D data set (Guinehut 2021). The AMOC strength at the NOAC array over the period 1993–2018

amounts to 17.2 ± 5.2 Sv. It is significantly correlated with the transport at the RAPID array further south with a time shift of about one year (Wett et al., 2023).

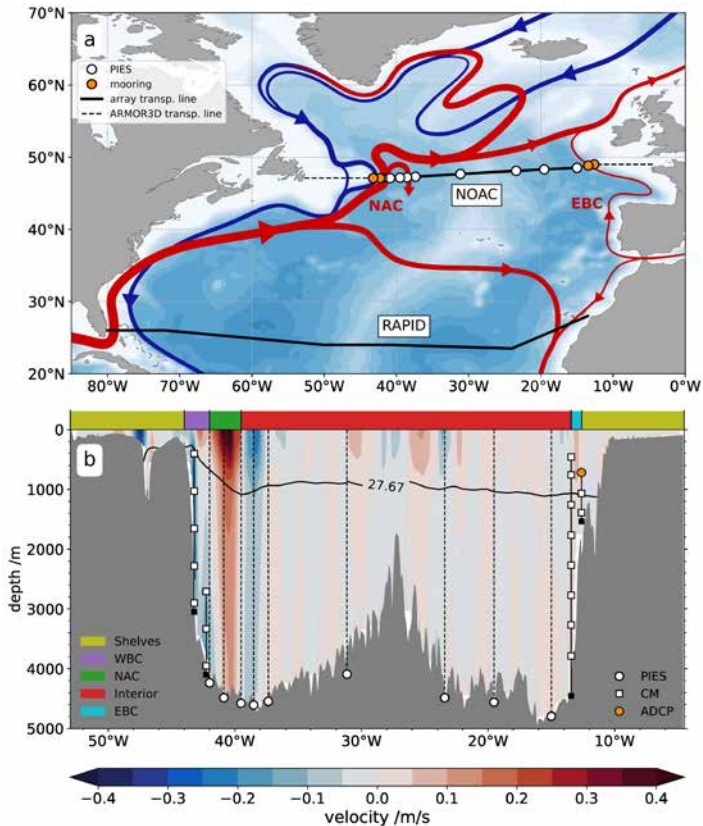


Figure 1a: Schematic representation of the major currents in the North Atlantic. Red (blue) arrows mark upper (deep) circulation pathways. Acronyms: NAC: North Atlantic Current, EBC: Eastern Boundary Current. b: Mean geostrophic velocity (2003–2020) along the NOAC array, based on CTD data and ARMOR3D (on the shelves). Markers indicate the positions of PIES, single-point acoustic current meters (CM) and upward-looking Acoustic Doppler Current Profilers (ADCP). The black line shows the mean depth of the $\sigma_\theta = 27.67$ kg m⁻³ isopycnal, separating the upper and lower AMOC branch (from Wett et al. (2023)).

Another aim of the cruise M164 and previous expeditions along the 47°N line was to investigate changes in the properties of North Atlantic Deep water, especially Labrador Sea Water (LSW). Due to the variability of the convective activity in the Labrador Sea, the rate and the properties (salinity, temperature, oxygen, anthropogenic tracers and carbon) of the newly formed LSW vary (Rhein et al., 2017). The densest LSW was formed between 1987 and 1994 ($27.74 \text{ kg m}^{-3} < \sigma_\theta < 27.8 \text{ kg m}^{-3}$). After that period, mainly the upper LSW with densities $27.68 \text{ kg m}^{-3} < \sigma_\theta < 27.74 \text{ kg m}^{-3}$ has been ventilated. The thickness of this layer increased, and the concentration of anthropogenic

tracers like SF_6 was higher than in the deeper LSW layers (Figure 2a). Since 2014, the convection depth in the Labrador Sea increased again (Rhein et al., 2017). In 2020, the SF_6 concentration over the density range $27.74 \text{ kg m}^{-3} < \sigma_\theta < 27.77 \text{ kg m}^{-3}$ was comparable to that in the upper LSW, whilst the thickness of the deeper layer increased considerably after 2015 (Figure 2b). The densest LSW layer ($27.77 \text{ kg m}^{-3} < \sigma_\theta < 27.8 \text{ kg m}^{-3}$), however, was not ventilated since the mid-1990s and has shrunken in volume.

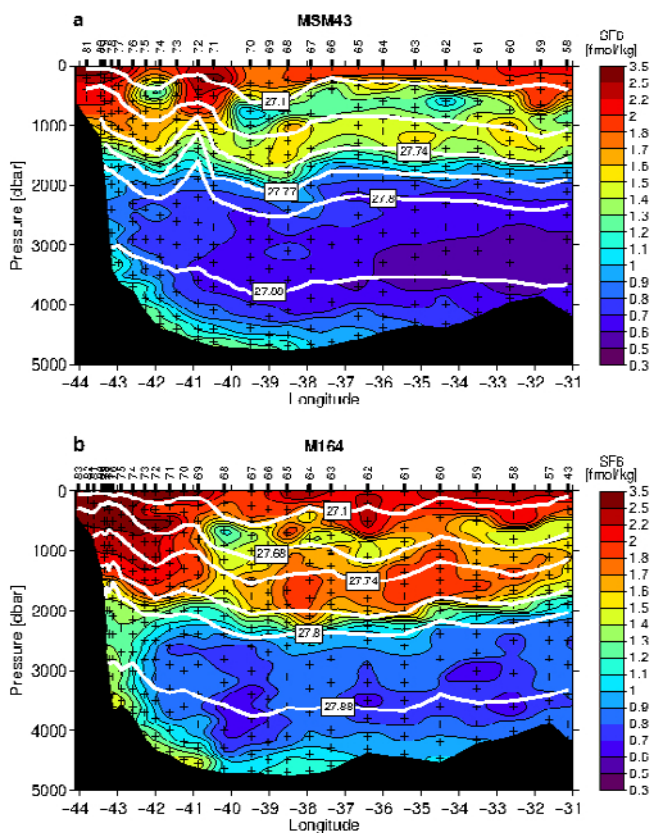


Figure 2: SF_6 concentration along $47^\circ N$ in the western Atlantic, a: in 2015 (cruise MSM43), b: in 2020 (cruise M164).

REFERENCES

Guinehut, S., Multi observation global ocean 3D temperature salinity heights geostrophic currents and MLD product MULTIOBS_GLO_PHY_TSUV_3D_MYNRT_015_012 2021, Copernicus Marine Service.

IPCC, Climate change 2021: The physical science basis. contribution of working Group I to the sixth assessment report of the intergovernmental panel on climate change. Cambridge University Press 2023, doi:10.1017/9781009157896.

Moritz, M., Jochumsen, K., Kieke, D., Klein, B., Klein, H., Köllner, M., Rhein, M., Volume transport time series and variability of the North Atlantic eastern boundary current at goban spur. *Journal of Geophysical Research: Oceans* 2021, 126(9), e2021JC017393, doi:10.1029/2021JC017393.

Nowitzki, H., Rhein, M., Roessler, A., Kieke, D., Mertens, C., Trends and transport variability of the circulation in the subpolar eastern North Atlantic. *Journal of Geophysical Research: Oceans* 2021, 126(2), e2020JC016693, doi:10.1029/2020JC016693.

Rhein, M., Steinfeldt, R., Kieke, D., Stendardo, I., Yashayaev, I., Ventilation variability of Labrador Sea water and its impact on oxygen and anthropogenic carbon: A review. *Philosophical Transactions of the Royal Society A: Mathematical, Physical & Engineering Sciences* 2017, 375(2102), 20160321, doi:10.1098/rsta.2016.0321.

Rhein, M., Mertens, C., Roessler, A., Observed transport decline at 47°N, western Atlantic. *Journal of Geophysical Research: Oceans* 2019, 124(7), 4875–4890, doi:10.1029/2019JC014993

Wett, S., Rhein, M., Kieke, D., Mertens, C., Moritz, M., Meridional connectivity of a 25-year observational AMOC record at 47°N. *Geophysical Research Letters*, 50, e2023GL103284, doi:10.1029/2023GL103284.

M165

Marine Particle off Northwest Africa; from source to sink

AUTHORS

MARUM, Center for Marine Environmental Sciences, University of Bremen |
Bremen, Germany

K.A.F. Zonneveld, O. Romero, S.E.V. Roza, G.J.M. Versteegh

The scientific activities of cruise M165 focus on particulate and dissolved organic carbon (POM/DOM) and processes that steer its turnover. It is well known that carbon dioxide is an important greenhouse gas affecting our climate and that the ocean plays an important role in the global carbon cycle, notably as storage of organic carbon in ocean floor sediments. Apart from storage of organic carbon the ocean floor is likely to store anthropogenic pollutants such as microplastic. However, many aspects are still unclear on influencing processes and mechanisms that shape the organic-matter, (bio-)mineral and micro-plastic vertical particulate flux, the vertical and lateral displacement of particles and their transformation as well as the influence these aspects have on selected environmental proxy signals.

During cruise M165 the formation, sinking, lateral advection, alteration and storage of organic matter, bio-mineral and micro-plastic particles have been studied in the active upwelling area off Cape Blanc at times of low upwelling activity. Mechanisms and processes that shape the vertical POM flux have been investigated with drifting traps. The plankton and export flux succession has been followed for 4 days with an 24h interval in an active upwelling cell and 2 days with an 24h interval in an offshore upwelling filament.

To obtain insight into the vertical/lateral POM flux we compared the association of POM particles of known origin (dinoflagellate cysts) collected by the drifting traps with associations and concentrations in the subsurface nepheloid layer, bottom nepheloid layer and deeper water column. We observed that light limitation hampered phytoplankton production in the active upwelling whereas export flux was increased at the rim of the upwelling cell. In the offshore drifting upwelling filament cyst export production was up to 3 times lower than at the rim of active upwelling cells. Lateral transport of particles was observed in the bottom nepheloid layer and in deeper waters (800–1200m depth) with a maximal extension of about 130km off the shelf break.

Processes of the turnover, transport, degradation and alteration of OM during the settling process, the effect of these processes on selected OM based palaeoceanographic proxies as well as the relationship between dissolved and particulate organic matter

(DOM/POM) have been investigated as well. For this water and suspended matter from the water column and surface sediments have been sampled with Rosette and In-situ pumps, notably in relationship to the presence and extension of nepheloid layers in the deeper water column and the oxygen minimum zone. To study the turnover, degradation and alteration of OM as a result of early aerobic and anaerobic diagenetic processes in upper ocean floor sediments, sediment samples have been collected by multi coring in the oxygen minimum zone as well as in moderately and well ventilated bottom water environments. By investigating the molecular composition of particles of known biological origin from surface waters, deeper water layers, first results show no alteration in molecular composition but species specific differences with species more sensitive against biological degradation processes. This is confirmed by earlier studies on material from MSM48 (Versteegh and Zonneveld, 2022) that show that particular organic matter being extremely sensitive and slightly resistant against aerobic degradation in natural settings show C=N, N-H, N-O, C-N bending/stretching, as well as the presence of C=O and C-O bounds in their micro-FTIR spectra. Somewhat less sensitive particles have a strong indication of the presence of nitrogen in their macromolecules. More resistant species lack nitrogen whereas the most resistant cyst species show low amounts of C=O.

Apart from this, long term sampling stations in the form of two sediment trap moorings have been serviced. The MARUM executes a long-term monitoring program to investigate the seasonal, annual and long-term variability in downward particle flux and carbon sequestration. already since the years 1988 and 2001. This unique series allowed us to investigate the export succession of key organisms of the upwelling ecosystem off Cape Blanc (diatoms and dinoflagellate cysts) between 2003 and 2020 (Romero et al., 2022, Rosa et al., *subm.*) The export production has been compared with variability in environmental parameters that strongly influence the upper water upwelling intensity and environmental conditions such as wind speed, wind direction, atmospheric dust concentration, sea surface temperature (SST), SST difference between trap location and open ocean (SSTa), and sea surface chlorophyll-a concentration (Chl-a). The total export production of diatoms and cysts fluctuated in line with changes in upwelling intensity which maxima notably in spring – summer and upwelling relaxation notably in autumn. Both organisms groups showed large annual- and interannual variability, even with upwelling event unique species composition. Nevertheless we could determine 5 species groups that showed comparable variability in export production related to changes in environmental conditions: (1) upwelling indicators (2) dust/upwelling indicators (3) upwelling relaxation indicators (4) warm water indicators (5) cosmopolite species. The long record of this sediment trap documented a gradual shift in the species associations that co-occurred with the gradual increase of Saharan dust input, notably after the year 2008. This environmental change might be driven by the southern movement of Inter Tropical Convergence Zone (ITCZ) annual migration that carried the rain belt southward to the tropics making the Sahara region more arid.

REFERENCES

Romero O, Ramondenc S, A 17-year time-series of diatom populations flux and composition in the Mauritanian coastal upwelling, *Frontiers in Marine Sciences Section Marine Ecosystems* 2022, 1–14.

Roza SEV, Versteegh GJM, Zonneveld KAF, Environmental control of organic-walled dinoflagellate cyst export production succession in the upwelling off Cape Blanc (Mauretania); a 18 years sediment trap study, *subm. to Frontiers in Marine Science* 2023.

Versteegh GJM, Zonneveld KAF, Micro-Fourier Infrared Spectroscopy of degradation resistant organic microfossils influence of preservation, environment and phylogeny, *Frontiers in Marine Science* 2022, doi.org/10.3389/fmars.2022.1040543.

SCIENTIFIC OUTPUT

LIST OF PUBLICATIONS

Zonneveld KAF, Grotheer H, Versteegh GJM, Dinoflagellate cysts production, excystment and transport in the upwelling off Cape Blanc (NW Africa), *Frontiers in Marine Science* 2022, [10.3389/fmars.2022.915755](https://doi.org/10.3389/fmars.2022.915755).

Romero O, Ramondenc S, A 17-year time-series of diatom populations' flux and composition in the Mauritanian coastal upwelling, *Frontiers in Marine Sciences Section Marine Ecosystems* 2022, 1–14.

Roza SEV, Versteegh GJM, Zonneveld KAF, Environmental control of organic-walled dinoflagellate cyst export production succession in the upwelling off Cape Blanc (Mauretania); a 18 years sediment trap study, *subm. to Frontiers in Marine Science* 2023.

Grotheer H, Hammes J, Gentz T, Castrillejo M, Hansman RL, Mollenhauer G, Radiocarbon measurements of marine dissolved inorganic carbon (DIC) at the AWI Micadas, *subm to Radiocarbon* 2023.

Jaeger D, Dissolved organic matter in the upwelling zone off Mauritania: novel insights in bulk and molecular composition from quantitative analyses and ultrahigh-resolution mass spectrometry, *Master Thesis Sept 2021, University of Oldenburg*.

Kotzem K, Vertikaler und lateraler Transport von Dinoflagellatenzysten in Nepheloidschichten im Auftriebsgebiet vor Cape Blanc. Bachelor Thesis 2021, University of Bremen.

Kirchner J, Lateraler und vertikaler Transport von dinoflagellatenzysten im Sommer 2020 vor Cape Blanc, Bachelor Thesis 2021, University of Bremen.

LIST OF CONFERENCE PRESENTATIONS

2023 | **Time series analysis of the cyst production of toxic dinoflagellates in the Cape Blanc upwelling region, NW Africa between 2003 and 2020** 20th International Conference on Harmful Algae Hiroshima, Japan. Roza et al. (oral presentation)

2023 | **Environmental factors influencing the dinoflagellate cysts production and their preservation in the bottom sediment in the upwelling region off Cape Blanc, Mauritania: a comparison of sediment trap with down-core sediment cyst record** International Conference for Young Marine Researcher, Oldenburg. Roza et al. (oral presentation)

2023 | **Dinoflagellate cysts: A journey from the upper water column to the ocean floor** Bremen PhD Days, Visselhövede. Roza et al. (poster)

2023 | **Connecting the molecular composition and radiocarbon age of dissolved organic matter in the Mauritanian sub-region of the Canary Upwelling System** ICYMARE 2023 Oldenburg, Fenna Alfke (oral presentation)

2022 | **Dissolved organic matter cycling in the coastal upwelling zone off Cap Blanc, Mauritania** ASLO Ocean Sciences Meeting, online. Michael Seidel et al. (oral presentation).

2022 | **Seasonal, annual, and multi-annual variability of dinoflagellate cyst export production in the upwelling area off Cap Blanc based on 18 years sediment trap time series** 12th International Conference on Modern and Fossil Dinoflagellates (DINO12) Las Palmas, Spain. Roza et al. (oral presentation)

2022 | **Dissolved organic matter cycling in the coastal upwelling zone off Cap Blanc, Mauritania** MARUM Ocean Floor Symposium 2022 Bremen, Michael Seidel et al. (poster)

2022 | **Particulate organic matter export flux and ecosystem change in the Cape Blanc upwelling region during the last 18 years reflected by dinoflagellate cysts: a sediment trap study** MARUM Ocean Floor Symposium 2022 Bremen, Roza et al. (poster)

2022 | **New ecological insight of calcareous dinoflagellate cysts export production based on 18 years sediment trap study in the Cap Blanc upwelling area (NW: Africa)**
12th International Conference on Modern and Fossil Dinoflagellates (DINO12) Las Palmas, Spain. Roza et al. (poster)

DATA

Dinoflagellate cyst export flux data:

<https://doi.org/10.1594/PANGAEA.948701>

Diatom Flux data

<https://doi.org/10.1594/PANGAEA.904390>

CRUISE REPORT

M165: [doi:10.48433/cr_m165](https://doi.org/10.48433/cr_m165)

M168

Magmatic and geodynamic evolution of the King's Trough Complex – the “Grand Canyon” of the North Atlantic

AUTHORS

GEOMAR Helmholtz Centre for Ocean Research Kiel | Kiel, Germany

A. Dürkefalden, J. Geldmacher, F. Hauff, J. Schenk, K. Hoernle

Institute of Geosciences and Geography, Martin-Luther-University Halle-Wittenberg | Halle/Saale, Germany

M. Stipp

Institute of Geosciences, Kiel University | Kiel, Germany

D. Garbe-Schönberg

Department of Geoscience, University of Wisconsin-Madison | Madison, USA

B. Jicha

INTRODUCTION AND GEOLOGICAL BACKGROUND

The King's Trough Complex (KTC), located around 700 km NE of the Azores (Figure 1a), is a prominent canyon-like structure in the eastern North Atlantic Ocean and consists of a ~500 km long series of roughly parallel deep basins. The huge King's Trough (KT) has elongated seamount-like structures on its NE and SW margins. Adjoining it in the east are the smaller but deeper (up to 6,000 m) Peake and Freen Deeps, which are separated by the steep and narrow Palmer Ridge (Figure 1b). The KT is located in an area of elevated, plateau-like seafloor, which gradually transitions to the Mid-Atlantic Ridge (MAR) flank in the west and is covered with numerous seamounts (e. g., the Gnitsevich Seamounts).

Despite its remarkable size and structure, the KTC has only been sparsely sampled thus far (Chernysheva et al., 2013; Lisitsyn et al., 1996; Stebbins and Thompson, 1978), and its origin has been a subject of debate for more than five decades. Early seismic refraction profiles revealed abnormally thick oceanic crust beneath the KTC area, which is interpreted to reflect excess lava production due to raised upper mantle temperatures caused by a mantle plume (Searle and Whitmarsh, 1978). The elevated seafloor as well as the abundant seamounts and the ridge-like structures flanking the KT could therefore also reflect the influence of a mantle plume during crustal formation. Furthermore, a melting anomaly on the MAR at 45°N with geochemical compositions more enriched than normal MORB, which was also sampled at DSDP drill site 410 slightly further west (Figure 1b), points to the presence of a mantle plume in this area (e. g., White and Schilling, 1978).

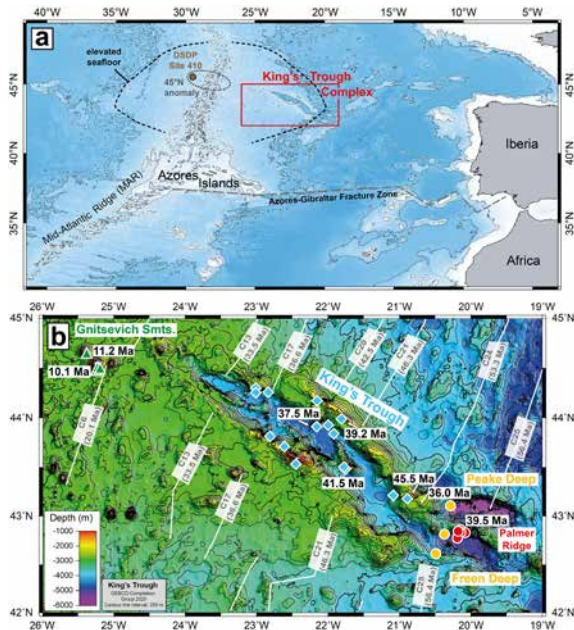


Figure 1a: Overview map of the eastern North Atlantic showing the location of the King's Trough Complex and the 45°N melting anomaly at the Mid-Atlantic Ridge including DSDP Site 410. Map data from www.gebco.net. b Bathymetric map (The GEBCO_2020 Grid, www.gebco.net) of the King's Trough, Peake and Freen Deeps - separated by the Palmer Ridge, and the Gnitsevich Seamounts to the northwest of the trough. $^{40}\text{Ar}/^{39}\text{Ar}$ ages in black are from this study, magnetic anomalies (white lines) and corresponding ages are from Klitgord and Schouten (1986).

Based on plate-kinematic models, the Iberian plate acted as an independent plate between ~84 and 28 Ma. After several plate boundary jumps, it was welded to the Eurasian Plate. Between ~42 and 36 Ma, the plate boundary located at the Bay of Biscay axis presumably jumped to the region of the KTC and eventually to the Azores-Gibraltar Fracture Zone (AGFZ) in the south at ~28 Ma (Macchiavelli et al., 2017; Srivastava and Roest, 1992; Srivastava et al., 1990). Therefore, formation of the troughs may be explained by extension along this transient plate boundary.

During R/V METEOR cruise M168 in 2020, we carried out extensive sampling by dredging as well as bathymetric mapping of the KTC and the Gnitsevich Seamounts (Smts.). Subsequently, we conducted major and trace element and radiogenic isotope (Sr-Nd-Hf-Pb) analyses as well as $^{40}\text{Ar}/^{39}\text{Ar}$ age dating in order to decipher the magmatic and geodynamic evolution of the area.

RESULTS AND DISCUSSION

Rock samples from the KT and Gnitsevich Smts. are mainly alkali basalts and show predominantly enriched trace element compositions typical for ocean island basalts (OIBs) and resemble those from the nearby Azores but also from DSDP drill site 410 belonging to

the 45°N melting anomaly (Figure 2a). In contrast, samples from the Peake and Freen Deeps and Palmer Ridge are tholeiitic and have trace element compositions similar to normal (N-)MORB. The Palmer Ridge lavas, however, extend to enriched (E-)MORB-like signatures similar to the 45°N anomaly directly at the MAR axis. On radiogenic isotope diagrams, the KTC samples span an array between moderately depleted and enriched compositions (Figure 2b). Whereas the lavas from the two deeps plot at the more depleted end within the North Atlantic MORB field, the KT, Gnitsevich Smts. and Palmer Ridge samples are more enriched and overlap with the common mantle source region of the Azores plume. Our results indicate that the KT and Gnitsevich Smts. lavas are derived from an enriched mantle plume source, whereas the Peake and Freen Deep samples likely represent normal oceanic crust generated at a mid-ocean ridge. The Palmer Ridge samples are transitional pointing to mixing of normal upper mantle and plume material.

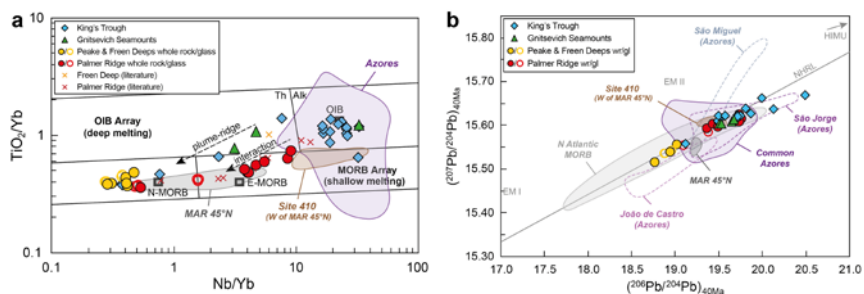


Figure 2a Nb/Yb versus TiO_2/Yb diagram after Pearce [2008] showing that most of the King's Trough samples have enriched OIB type compositions and overlap with the Azores field (www.earthchem.org/petldb; <https://georoc.eu/>; compilation from Béguelin et al., 2017; Larrea et al., 2013; Romer et al., 2018; Romer et al., 2019; Storch et al., 2020). The Gnitsevich Seamounts samples display a wider range but are generally also enriched. Samples from the Peake and Freen Deeps are similar to N-MORB, whereas those from the Palmer Ridge range between depleted and more enriched compositions. Also shown are literature data from Freen Deep and Palmer Ridge (Chernysheva et al., 2013) and fields for the 45°N melting anomaly and DSDP Site 410 (www.earthchem.org/petldb; Brandl et al., 2016). Included are only mafic samples with $MgO > 3.5$ wt.%. b Initial $^{206}Pb/^{204}Pb$ versus $^{207}Pb/^{204}Pb$ diagram (calculated to 40 Ma). The samples form an array between moderately depleted (Peake and Freen Deeps) and enriched (King's Trough) compositions and are similar to the Azores except for the two deeps. North Atlantic MORB data are from www.earthchem.org/petldb.

$^{40}Ar/^{39}Ar$ ages of lava samples from the KT, Peake Deep and Palmer Ridge range between 45.5 Ma and 37.5 Ma, whereas the Gnitsevich Smts. lavas reveal ages of ~10 Ma (Figure 1b). The dated samples from the KT show progressively decreasing ages from east to west consistent with the seafloor ages becoming younger to the west based on the magnetic lineations but being consistently slightly younger (~2-4.5 Ma) at any given location. In contrast, the dated Gnitsevich Smts. lavas are 6–8 Ma and the Peake Deep and Palmer Ridge lavas even 16–18 Ma younger than the surrounding crust.

The combination of geochemical and age data and tectonic considerations suggests that the KTC probably formed at a triple junction (two arms of the MAR, one fault zone/rift)

at ~45°N when the plate boundary between the Iberian and Eurasian plates jumped to this region and dissected the newly formed oceanic crust to the east of the MAR. The graben structure (initially Peake and Freen Deeps) could have formed by merely N-S directed extension, since the magnetic lineations are not significantly offset along this fault zone (Figure 1b). At ~53 Ma ago (indicated by the magnetic chron age, see Figure 1b), activity of a mantle plume, probably the early Azores plume located beneath or near the MAR, started and created thicker oceanic crust at the MAR as still reflected by the elevated seafloor bathymetry (outlined by dashed line in Figure 1). Ongoing extension along the fault zone led to further opening of the graben toward the west, cutting progressively into the newly formed, plume-influenced, oceanic crust successively forming the bulk of the KT. The geochemically enriched nature of the dredged rocks from the KT reflects this plume influence, and the flanking ridge-like structures on both sides of the trough could represent the tops of tilted blocks of oceanic crust. However, since the rocks dredged from these structures are apparently slightly younger than the adjacent crust, they might have formed along a westward propagating fracture by plume-generated late-stage volcanism somewhat off-axis. This would also explain their depletion in heavy rare earth elements indicating an on average deeper melting origin. Extension along this fracture, postdating the volcanism, would split the ridge on top of the fracture in half, such that the trough has half of the ridge volcanism on its NE and the other half on its SW side.

The easternmost part of the fracture must have experienced the strongest and longest-lasting extension due to opening of the graben from east to west, resulting in the extraordinary depths of the Peake and Freen Deeps graben floor. Since the lithosphere/asthenosphere beneath this area was presumably formed before the arrival of the 45°N/Azores plume, the geochemical composition of these lavas resembles normal MORB (Figure 2). In order to explain the significantly younger ages (compared to the surrounding seafloor) of our two dated dredge samples from these structures (Figure 1b), we assume that this ongoing thinning eventually led to decompression melting of the upper mantle.

At ~28 Ma ago, the plate boundary jumped further south to the AGFZ, which probably caused deflection of the upwelling plume and development of a new branch, and formation of the Azores Plateau started (Figure 3). However, the northern branch, although waning, is still active beneath the 45°N melting anomaly at the MAR. Minor intraplate volcanism, fed by this waning plume branch, could then explain the young Gnitsevich Smts. volcanism erupting on more major oceanic crust. Similar models for plume-splitting are proposed elsewhere (e. g., at the Tristan-Gough hotspot, Homrighausen et al., 2023; Rohde et al., 2013).

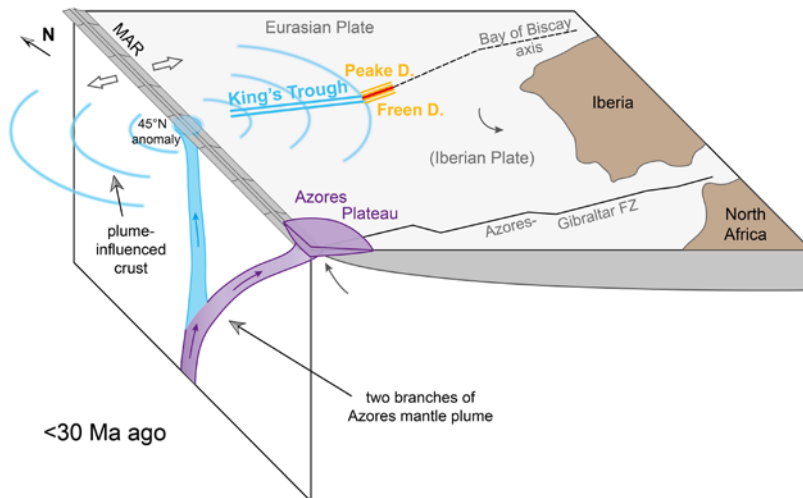


Figure 3: Model showing the eastern North Atlantic region shortly after the plate boundary had jumped from the KTC further south to the Azores-Gibraltar FZ. The northern branch of the Azores mantle plume is assumed to be still active at 45°N, whereas development of the southern branch led to formation of the Azores Plateau.

ACKNOWLEDGMENTS

We would like to thank Captain Hammacher and his crew for their great support during R/V METEOR cruise M168 and we acknowledge funding of the cruise by the German Research Foundation (DFG) and the Federal Ministry of Education and Research (BMBF) and funding of this study by the DFG (grant DU2237/1-1 to A.D.).

REFERENCES

- Béguelin P, Bizimis M, Beier C, Turner S, Rift-plume interaction reveals multiple generations of recycled oceanic crust in Azores lavas, *Geochimica et Cosmochimica Acta* 2017, 218, 132–152, doi:<https://doi.org/10.1016/j.gca.2017.09.015>.
- Brandl PA, Regelous M, Beier C, O'Neill HSC, et al., The timescales of magma evolution at mid-ocean ridges, *Lithos* 2016, 240–243, 49–68, doi:<https://doi.org/10.1016/j.lithos.2015.10.020>.
- Chernysheva EA, Kuz'min MV, Kharin GS, Medvedev AY, Compositional variations of spreading basalts of the King's trough (Central Atlantic) and possible reasons for them, *Doklady Earth Sciences* 2013, 448, 194–199, doi:[10.1134/S1028334X13020037](https://doi.org/10.1134/S1028334X13020037).
- Homrighausen S, Hoernle K, Hauff F, Hoyer PA, et al., Evidence for compositionally distinct upper mantle plumelets since the early history of the Tristan-Gough hotspot, *Nature Communications* 2023, 14, 3908, doi:[10.1038/s41467-023-39585-0](https://doi.org/10.1038/s41467-023-39585-0).

Klitgord KD, Schouten H, Plate kinematics of the central Atlantic, In: Vogt PR and Tucholke BE (Eds.), *The Western North Atlantic Region*, Vol. M. Geological Society of America 1986.

Larrea P, França Z, Lago M, Widom E, et al., Magmatic Processes and the Role of Antecrysts in the Genesis of Corvo Island (Azores Archipelago, Portugal), *Journal of Petrology* 2013, 54, 769–793, doi:10.1093/petrology/egs084.

Lisitsyn AP, Zonenshain LP, Kuz'min MI, Kharin GS, Igneous and metamorphic rocks of the King's Trough and Palmer Ridge, *Oceanology* 1996, 36, 398.

Macchiavelli C, Vergés J, Schettino A, Fernández M, et al., A New Southern North Atlantic Isochron Map: Insights Into the Drift of the Iberian Plate Since the Late Cretaceous, *Journal of Geophysical Research: Solid Earth* 2017, 122, 9603–9626, doi:10.1002/2017jb014769.

Pearce JA, Geochemical fingerprinting of oceanic basalts with applications to ophiolite classification and the search for Archean oceanic crust, *Lithos* 2008, 100, 14–48, doi:http://dx.doi.org/10.1016/j.lithos.2007.06.016.

Rohde J, Hoernle K, Hauff F, Werner R, et al., 70 Ma chemical zonation of the Tristan-Gough hotspot track, *Geology* 2013, 41, 335–338.

Romer RHW, Beier C, Haase KM, Hübscher C, Correlated changes between volcanic structures and magma composition in the faial volcanic system, azores, *Frontiers in Earth Science* 2018, 6, doi:10.3389/feart.2018.00078.

Romer RHW, Beier C, Haase KM, Klügel A, et al., Progressive Changes in Magma Transport at the Active Serreta Ridge, Azores, *Geochemistry, Geophysics, Geosystems* 2019, 20, 5394–5414, doi:https://doi.org/10.1029/2019GC008562.

Searle RC, Whitmarsh RB, The structure of King's Trough, Northeast Atlantic, from bathymetric, seismic and gravity studies, *Geophysical Journal of the Royal Astronomical Society* 1978, 53, 259–287, doi:10.1111/j.1365-246X.1978.tb03742.x.

Srivastava SP, Roest WR, King's Trough: reactivated pseudo-fault of a propagating rift, *Geophysical Journal International* 1992, 108, 143–150, doi:10.1111/j.1365-246X.1992.tb00845.x.

Srivastava SP, Schouten H, Roest WR, Klitgord KD, et al., Iberian plate kinematics: a jumping plate boundary between Eurasia and Africa, *Nature* 1990, 344, 756–759, doi:10.1038/344756a0.

Stebbins J, Thompson G, The nature and petrogenesis of intra-oceanic plate alkaline eruptive and plutonic rocks: King's Trough, Northeast Atlantic, *Journal of Volcanology and Geothermal Research* 1978, 4, 333-361, doi:[https://doi.org/10.1016/0377-0273\(78\)90021-5](https://doi.org/10.1016/0377-0273(78)90021-5).

Storch B, Haase KM, Romer RHW, Beier C, et al., Rifting of the oceanic Azores Plateau with episodic volcanic activity, *Scientific Reports* 2020, 10, doi:[10.1038/s41598-020-76691-1](https://doi.org/10.1038/s41598-020-76691-1).

White WM, Schilling J-G, The nature and origin of geochemical variation in Mid-Atlantic Ridge basalts from the Central North Atlantic, *Geochimica et Cosmochimica Acta* 1978, 42, 1501–1516, doi:[https://doi.org/10.1016/0016-7037\(78\)90021-2](https://doi.org/10.1016/0016-7037(78)90021-2).

SCIENTIFIC OUTPUT

LIST OF PUBLICATIONS

Dürkefälden A, Geldmacher J, Hauff F, Stipp M, et al., Origin of the King's Trough Complex in the North Atlantic: Interplay between a temporary plate boundary and a mantle plume (in preparation).

LIST OF CONFERENCE PRESENTATIONS

2023 | **Magmatic and geodynamic evolution of the King's Trough Complex – The Grand Canyon of the North Atlantic (Poster)** Goldschmidt2023, Lyon, France.

2023 | **Magmatic and geodynamic evolution of the King's Trough Complex – the "Grand Canyon" of the North Atlantic (Poster)** GeoBerlin 2023, Berlin, Germany.

2023 | **The King's Trough Complex: magmatic and geodynamic evolution of the Grand Canyon of the North Atlantic (Talk)** Oceanic Volcanism Workshop, Kiel, Germany.

DATA

Thermosalinograph oceanography (TSG):
<https://doi.pangaea.de/10.1594/PANGAEA.928768>

Multibeam bathymetry raw data (EM 122 working area dataset):
<https://doi.pangaea.de/10.1594/PANGAEA.930095>

Multibeam bathymetry raw data (EM 122 transit dataset):
<https://doi.pangaea.de/10.1594/PANGAEA.928916>

CRUISE REPORT

M168: doi:10.48433/cr_m168

M169

Tracing Origin and Distribution of Geogenic and Anthropogenic Dissolved and Particulate Critical High-technology Metals in the Southern North Sea

AUTHORS

Constructor University | Bremen, Germany

A. Koschinsky, M. Bau, A. Hollister, F. Klimpel, E. Kurahashi

Bundesanstalt für Geowissenschaften und Rohstoffe (BGR) | Hannover, Germany

D. Krämer, K. Schmidt

GEOMAR Helmholtz Centre for Ocean Research Kiel | Kiel, Germany

S. Paul

NARRATIVE OF CRUISE M169

The increasing application of rare trace metals in enabling technologies and in medicine has resulted in a rapidly growing and mostly unconstrained input of many of these metals from anthropogenic sources into the environment, often significantly overprinting their geogenic background concentrations. Estuaries serve as interfaces between land and ocean and play a key role in modulating terrestrial metal input into coastal oceans and beyond. However, so far, only very little data are available for both natural and anthropogenic inputs of emerging critical metals from rivers and modification of riverine fluxes by estuarine processes. The goal of cruise M169 was to determine the concentrations of these metals in the river waters of Elbe, Weser and Ems as well as North Sea water endmembers and in samples along the salinity gradients in the mixing zone of river water and seawater within the German Bight. The metals in the focus of this study were rare earth elements (REE), scandium (Sc), gallium (Ga), germanium (Ge), platinum (Pt), zirconium (Zr), tungsten (W), molybdenum (Mo), and vanadium (V) as well as the “traditional” metals such as iron (Fe), manganese (Mn), lead (Pb), cadmium (Cd), copper (Cu) and nickel (Ni) for comparison.

OPERATION AND WORK PROGRAM OF CRUISE M169

The work program consisted of continuous salinity monitoring in the surface water along the 1900 nm cruise track to follow the river plumes and 191 discrete water sampling stations of surface and deeper water layers using the stainless-steel rosette of R/V METEOR as well as trace-metal clean GoFlo bottles on a Kevlar wire and a pump system (Figure 1). The recording of CTD data, nitrate and suspended solids with an optic sensor complemented our work. Suspended matter was collected on 0.2 µm membrane filters in parallel to the dissolved fractions. In all three rivers, a 12-hours tidal cycle was sampled

at one specific location to account for temporal variability of the parameters. In addition to different size fractions separated by sequential filtration and ultrafiltration of the river-, estuary-, and seawater samples, we deployed passive sampler probes *ex situ* in large-volume water samples of selected stations (diffusive gradients in thin film – DGT). The probes selectively accumulate labile bound dissolved metals from solution over time, which is thought to mimic mechanisms of bioavailability/bio-uptake. Accompanying the M169 cruise, additional DGTs were deployed for a period of four to eight weeks on underwater observatory platforms maintained by different research institutions within the Coastal Observing System for Northern and Arctic Seas (COSYNA).

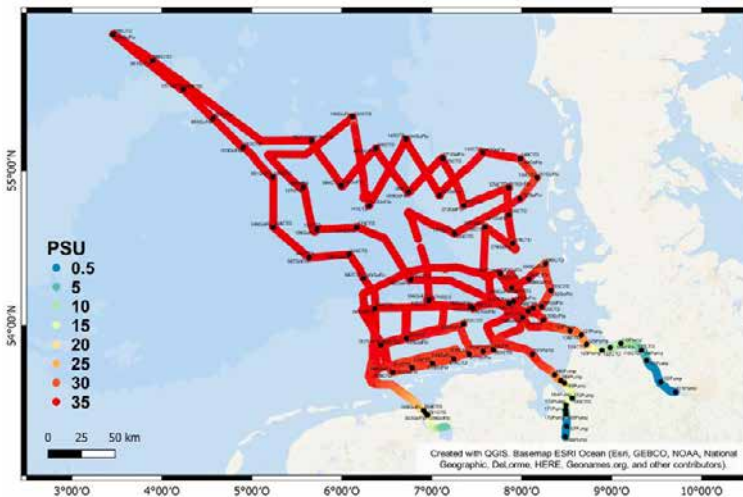


Figure 1: Track chart of R/V METEOR Cruise M169 showing salinities measured with the vessel's TSG and sampling stations (black dots).

RESULTS

Onboard sensor measurements were used as indicators for riverine input, freshwater-seawater mixing and tidal cycles. Salinity records from the ship's thermosalinograph along the complete sampling track represented the river water – North Sea water mixing ratios. Nitrate concentrations showed winter maxima, related to low biological activity and advanced remineralisation and reflected the (anthropogenic) input via rivers. Total suspended solids reflected intense colloidal flocculation (which controls many trace metals via sorption) in the estuaries and strong tidal fluctuations. Dissolved organic carbon (DOC) co-varied with nitrate and suspended solids. pH values varied only slightly between 7.7 in the Elbe River and 8.2 in the open North Sea.

Water samples filtered onboard ship were stored acidified until analyses in the home labs took place. Trace metals are usually present at ultra low concentrations in natural

waters, and for most metals, we applied matrix separation and pre-concentration, e. g., by using a SeaFAST system prior to analyses with ICP-MS. Platinum concentrations were analysed by a highly sensitive voltametric method (see poster by Hollister et al.). At six master stations, we additionally conducted sequential (ultra)filtration to assess the size distribution of target metals and further deployed passive samplers to assess the labile-bound metal fractions that are potentially bioavailable (see poster by Schmidt et al.).

As expected, conservative elements such as alkaline and earth-alkaline metals (Na, K, Ca, Mg, Sr, etc.) increase nearly linearly with increasing salinity and can be considered conservative elements only influenced by binary mixing between river water and seawater endmembers. This reveals that additional freshwater seepage, if present, did not significantly affect the input of the elements considered. In contrast, most trace metals show significantly higher concentrations in river water (mostly bound to nanoparticles and colloids, NPCs), originating from geogenic sources such as weathering of rocks and leaching of soils, (partial) decomposition of organic material, and anthropogenic sources from domestic, industrial and agricultural activities. As an example, Pt concentrations were highest in the Elbe River close to Hamburg and were still 2–10 times higher in the North Sea compared to Atlantic seawater (see poster by Hollister et al.). Mixing with seawater dilutes the trace metal concentrations, but at the same time active loss to the sediment due to the sorption on particles, flocculation of NPCs and sedimentation was observed, indicating non-conservative behavior of these metals especially in the low-salinity mixing zones where NPCs flocculation is most pronounced (Figures 2, 3). In contrast, mid salinity regions are partly characterized by desorption processes and metal transformation from the (suspended) particulate pool into the dissolved pool (e. g., Mn, light REE; see Figure 3).

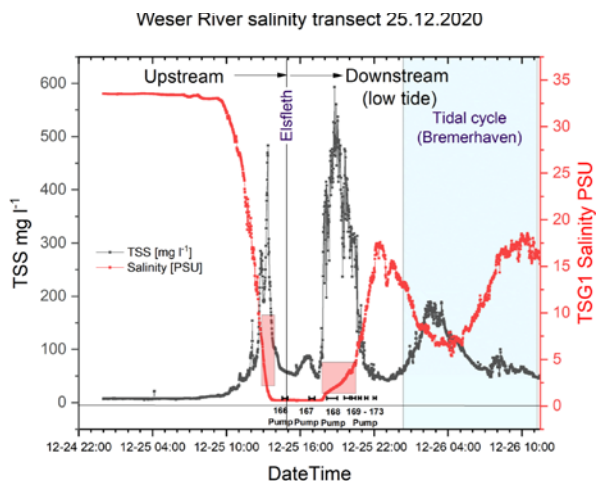


Figure 2: Recording of salinity [with vessel's TSG] and total suspended solids (TSS, with OPUS sensor) during the Weser estuary sampling and Weser tidal cycle.

The size distribution of dissolved trace elements provides insight into the phase association with NPCs and the truly dissolved pool and can be used to deduce the geochemical behavior and fate during fresh water – seawater mixing in estuaries. As an example, Fe and Cu are significantly bound to large, mainly inorganic colloids with more than 40% occurring in the >10 KDa pool, while less than 20–30% is truly dissolved. Cobalt, Ni, V, heavy REE and Mn predominantly occur in the size fraction <10 KDa (more than 80%), with only minor variations with changing salinity. Manganese is further predominantly truly dissolved <1 KDa throughout the salinity region, but its strong concentration drop in low-salinity regions confirms the known particle reactivity related to the complex redox chemistry of Mn (e. g., Jones and Tebo 2021). With increasing salinity, the relative proportions of the smaller size fractions increase for some elements (e. g., REY, Pb, Ga, Cd). The observed mobilization of trace metals into the dissolved phase in mid salinity regions is mainly associated with a transformation from (nano)particulate phases into the truly dissolved (<1 KDa) and small colloidal (1 KDa–10 KDa) phases.

While for many metals our river water concentration data are higher than reported for pristine rivers, which can be seen as an indicator of anthropogenic input, it is generally not trivial to distinguish between geogenic background concentrations and anthropogenic overprinting. However, if geogenic and anthropogenic metals show different chemical forms, i. e. different chemical speciation resulting in different mixing behaviors in estuaries, they may be disentangled from each other. This is the case for the rare earth element gadolinium (Gd). Our data for REE provide evidence for the widespread anthropogenic input and distribution of wastewater-derived Gd in the southern North Sea. Complementary ultrafiltration and DGT passive sampling data show that the anthropogenic Gd exclusively occurs in the truly dissolved element pool (< 1KDa) of the discharged riverine and estuarine waters and is mostly bound in highly stable, inert chemical complexes most of which are not bioavailable. In the river water endmembers, >95% of the Gd is of anthropogenic origin while in the remotest locations from the coast it was only <5%. A comparison with data from the Weser River from 2005 (Kulaksiz and Bau, 2007) showed that the fraction of anthropogenic Gd nearly doubled until 2020. Our results corroborate the notion that the inert Gd-based contrast agents used during MRI scans pass wastewater treatment plants with only minor removal and show a very conservative behavior during estuarine mixing (see Figure 3), effectively enabling its transport to the open sea.

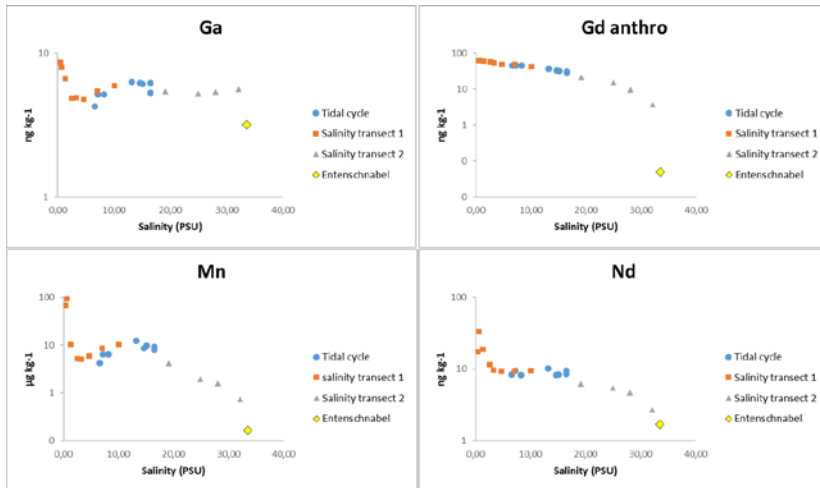


Figure 3: Concentrations (<0.2 μm fraction) of Ga, Mn, the anthropogenic fraction of Gd, and Nd against salinity in the Weser mixing transect. "Entenschnabel" is the northwesternmost point of the German EEZ (Figure 1). Note the log scale of the y axes. While the anthropogenic fraction of Gd shows conservative mixing, the other trace metals show a strong loss at initial estuarine mixing and some remobilization from particles at mid-salinity.

ACKNOWLEDGEMENT

Special thanks to the Captain and crew of R/V METEOR, the scientific team for their dedicated onboard work and the German Science Foundation DFG for funding for cruise M169 and the first evaluation phase.

REFERENCES

Jones MR, Tebo BM, Novel manganese cycling at very low ionic strengths in the Columbia River Estuary, *Water research* 2021, 207, doi: 10.1016/j.watres.2021.117801.

Kulaksiz S, Bau M, Contrasting behaviour of anthropogenic gadolinium and natural rare earth elements in estuaries and the gadolinium input into the North Sea, *Earth and Planetary Science Letters* 2007, 260, doi: 10.1016/j.epsl.2007.06.016.

SCIENTIFIC OUTPUT

LIST OF CONFERENCE PRESENTATIONS

2023 | **Elbe, Weser and Ems rivers as sources of platinum to the southern North Sea**
International Estuarine Biogeochemistry Symposium XVI IEBS2023, Sibenik, Croatia.

2023 | **Tracing wastewater input into the North Sea using anthropogenic Gd anomalies: Evidence for widespread MRI contrast agent contamination of river estuaries of Elbe, Ems and Weser and the southern North Sea including the German Bight**
Goldschmidt Conference, Lyon, France.

2023 | **First indication of platinum input into the southern North Sea via German rivers**
Aquatic Sciences Meeting, Mallorca, Spain.

2022 | **Anthropogenic gadolinium and other emerging contaminants in the southern North Sea and the Elbe, Ems and Weser estuaries** GeoMinKöln, Cologne, Germany.

CRUISE REPORT

M169: doi: 10.48433/cr_m169

M170 AND M175

On the formation of deep valleys at oceanic transform faults – constraints from M170 and M175

AUTHORS

GEOMAR Helmholtz Zentrum für Ozeanforschung | Kiel, Germany

I. Grevemeyer, D. Lange, L.H. Rüpke, I. Klaucke, A. Beniest, L. Gómez de la Peña, Y. Ren, H.-S. Hilbert, Y. Li, L. Murray-Bergquist, K. Unger Moreno, T. Hansteen, C. W. Devey

ABSTRACT

In plate tectonics, oceanic transform faults are featured as simple conservative strike slip plate boundaries, but the theory fails to predict why their fault traces run within wide and deep transform valleys. At the Oceanographer transform at the Mid-Atlantic Ridge near 35°N, micro-earthquakes captured by a network of ocean-bottom-seismometers operated during R/V METEOR cruise M170 reveal a diffuse activity over a broad area, cutting across the inside corner domain between the spreading centre and the transform fault before focusing along the trace of the fault. In the vicinity of the ridge-transform intersection (RTI), focal mechanisms reveal transform-normal extensional tectonics instead of showing transcurrent motion, while strike-slip tectonics occurs only >15 km away from adjacent spreading segments. These observations support a scenario based on numerical simulations showing that at RTIs the right-angular plate boundary at the seafloor develops into an oblique shear zone at depth, causing crustal thinning and consequently forming transform valleys. Away from RTIs, seismicity is focused at a narrow and segmented strike-slip fault system as predicted by plate tectonics. However, tectonic processes shaping transforms are diverse, arguing for a revision of the concept of conservative plate boundaries to account for their morphology and strong lateral differences in seismic behaviour.

BACKGROUND, AIMS AND KEY RESULTS

Fracture zones were recognized to be an integral part of the seabed long before plate tectonics was established. Later, plate tectonics linked fracture zones to oceanic transform faults, suggesting that they are the inactive and hence fossil trace of transforms. Yet, scientists have spent little time surveying them in much detail over the last three decades. Recent evidence (Grevemeyer et al., 2021) suggests that the traditional concept of transform faults as being conservative (non-accretionary) plate boundary faults might be wrong. Instead, transform faults are always deeper than the associated fracture zones (Grevemeyer et al., 2021; Ren et al., 2022) and numerical modelling results suggest that transform faults seem to suffer from extensional tectonics below their strike-slip surface fault zone. Furthermore, deep transform valleys seem to be buried at ridge-transform

intersection, suggesting that a phase of magmatic activity overprints magmatically starved crust in transform faults (Grevemeyer et al., 2021; Guo et al., 2023).

The cruise M170 of the German research vessel METEOR was conducted during the Covid-19 pandemic and aimed to tackle the above outlined features, challenging the concept that oceanic transform faults are conservative plate boundaries. Especially the idea that transform faults suffer from extensional tectonics can be tested studying micro-earthquakes in a transform fault. Therefore, we set out to test this hypothesis by collecting, in a pilot study, micro-seismicity data from the Oceanographer transform fault which offsets the Mid-Atlantic Ridge by 120-km south of the Azores near 35°N.

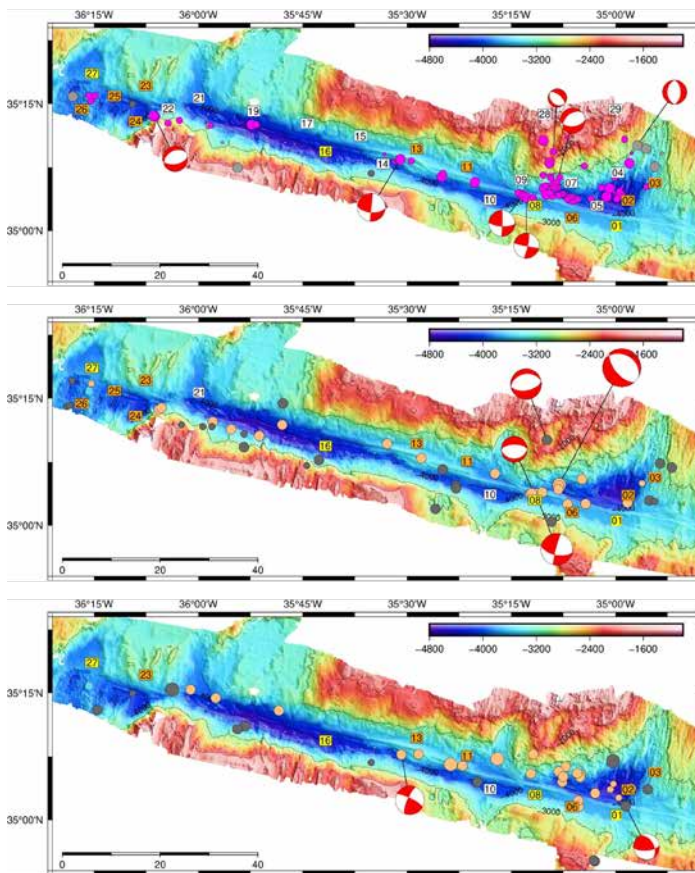


Figure 1: Micro-seismicity and focal mechanisms along Oceanographer transform fault; but events and available OBS for the three periods with 26, 14, and 10 OBS, respectively. (top) 26 OBS/H recorded with the full network in the first 12-days; (middle) with 14 OBS/H February to mid-March of 2021; (bottom) 10 OBS recording between mid-March to 6th of July 2021; colored circles: events $GAP \leq 180^\circ$; gray: $GAP > 180^\circ$; numbered squares are OBS/H stations (white: OBH; orange: short period OBS; yellow: broadband OBS); depth scale in meters and distance scale in kilometers.

Originally, the seismological network was planned to be operated between 21st of January to 2nd of February 2021, monitoring seismicity along the Oceanographer Transform Fault using ocean-bottom-seismometers (OBS) and hydrophones (OBH). The network consisted of 6 Trillium Compact OBS, 12 short-period (4.5 Hz geophone) OBS and 11 OBH from GEOMAR'S OBS pool. Unfortunately, two short-period OBS recorded due to wrongly connected sensors only on the hydrophone channel, leaving effectively 10 short-period OBS and 13 OBH. An unforeseen medical incident on 31th of January 2021 forced us to leave the study area earlier than planned. We therefore recover only those stations that would automatically surface on 4th of February 2021. Due to bad weather conditions and poor weather predictions, we decided to use the automatic (safety) release times on 1st of July 2022 for all OBS. This gave us more flexibility in case another low-pressure system was to enter the area, hindering recovery of the instruments. Consequently, the seismic network was only degraded after the 2nd of February, but the remaining OBS stayed on the seabed, and 10 OBS recorded until their recovery during the cruise M175 of the R/V METEOR in early June of 2021. Four OBS stopped recording in March, but those were equipped with an absolute clock, and therefore timing was available without correction. For the other OBS/H, clocks were synchronized before and after recovery and the time drift was corrected assuming a linear drift. The detection threshold dropped after the degradation of the network from ~11 events per day to less than one event per day after only 10 OBS were available. This also resulted in a change in the magnitude of completeness dropping from $M_w \sim 2.2$ to $M_w \sim 2.8$.

Spatial distribution of micro-earthquakes support earthquakes occurring along the trace of the fault, showing strike-slip motion of the transform away from its intersections with the Mid-Atlantic Ridge. However, in the vicinity of its both ridge-transform intersections seismicity does not mimic a right-angular plate boundary; instead, seismicity occurs below the inside corner and focal mechanism indicate extensional tectonics. Therefore, micro-seismicity supports features found in numerical simulations, revealing that transform faults have an extensional as well as a strike-slip component.

REFERENCES

Grevemeyer I, Rüpke, L H Morgan J P, Iyer K, Devey C W, Extensional tectonics and two-stage crustal accretion at oceanic transform faults, *Nature* 2021, 591, 402–407, doi:10.1038/s41586-021-03278-9

Ren Y, Geersen J, Grevemeyer I, Impact of spreading rate and age-offset on oceanic transform fault morphology, *Geophys. Res. Lett.* 2022, 49, e2021GL096170, doi:10.1029/2021GL096170.

Guo Z, Liu S, Rüpke L H, Grevemeyer I, Morgan J P, Lange D, Ren Y, Tao C, Disparate crustal thicknesses beneath oceanic transform faults and adjacent fracture zones revealed by gravity anomalies, *Geology* 2023, 51, 300-304, doi:10.1130/G50429.1.

SCIENTIFIC OUTPUT

LIST OF PUBLICATIONS

Grevemeyer I, Lange D, Ruepke L H, Klaucke I, Beniast A, Gómez de la Peña L, Ren Hilbert H-S, Li Y, Murray-Bergquist L, Unger Moreno K, Hansteen T, Devey CW, Extensional tectonics at ridge-transform intersections governs the formation of transform valleys, *Geology*, in review

Unger Moreno K, Devey C W, Hansteen T H, Beniast A, Rüpke L H, Grevemeyer, I, Geological overview of the Oceanographer Transform Fault, North Atlantic Ocean, submitted

LIST OF CONFERENCE PRESENTATIONS

2022 | **The Oceanographer transform fault revisited – preliminary results from a micro-seismicity survey reveals extensional tectonics at ridge-transform intersections**
European Geoscience Union, Vienna, Austria.

DATA

Master track of M170:

<https://doi.pangaea.de/10.1594/PANGAEA.933796>

Underway bathymetric data:

<https://doi.pangaea.de/10.1594/PANGAEA.942779>

Bathymetric (EM122) raw data:

<https://doi.pangaea.de/10.1594/PANGAEA.942780>

ADCP current measurements:

<https://doi.pangaea.de/10.1594/PANGAEA.938252>

Thermosalinograph data:

<https://doi.pangaea.de/10.1594/PANGAEA.940645>

Seismological event data:

<https://doi.pangaea.de/10.1594/PANGAEA.xxxxxx> (available after paper is accepted)

CRUISE REPORT

M170: https://doi.pangaea.de/10.48433/cr_m170

M174

Composition, function and environmental controls of the microbiome in the epipelagic Atlantic and Pacific Ocean

AUTHORS

Leibniz Institute for Baltic Sea Research Warnemünde | Rostock, Germany
M. Voss, N. Choisnard, V. Mohrholz, J. Umbricht

Lamont Doherty Earth Observatory | New York, USA
A. Subramaniam

Georgia Institute of Technology | Atlanta, USA
J. P. Montoya

GOALS AND APPROACH

The Amazon, the largest River on Earth in terms of freshwater discharge, has seen its catchment area change over the past decades as a result of deforestation, damming and land use. These changes are thought to impact the riverine nutrient and organic matter loads, which could have consequences on the nitrogen (N) cycling far beyond the estuary, in the western tropical North Atlantic (WTNA). The M174 cruise took place from April 21st to May 13th during peak outflow starting from Las Palmas (Gran Canarias) to Emden (Germany), to improve our understanding of the N-cycling in the region. For the first time, the rates and regulation of N cycle processes that determine sources and sink functions were studied and combined to the physical conditions. As such, rates of N-source processes (riverine N inputs and dinitrogen fixation) were studied together with primary production and dissolved N assimilation (ammonium, nitrate and amino acids), and rates of N recycling (nitrification), along varying degrees of water column structures. The transit to the Amazon and Pará River mouths took 9 days and we worked for 21 days from almost freshwater conditions to fully saline Bajan waters until May 13th thus covering the Amazon River Plume (ARP) and parts of the WTNA. Underway samples were also collected until the Azores to establish a broader picture of dinitrogen fixation across the Atlantic Ocean.

We identified four different water masses and could clearly see the North Brazil current in more offshore waters. The extremely high turbidity in the Amazon waters leads to visible bottom plumes at the river mouths (~0 °N) and across the shelf up to 5 °N. Horizontal convergence enhanced the northward transport on the shelf while the meandering front of the plume caused surface divergence. Current velocities of 15–30 cm s⁻¹ could be roughly translated to water travel times of several days from the Amazon mouth to the French Guyana border. Despite this dynamic processes, the plume remained stable on top of the

bottom water with very little exchange processes, leading euphotic zone N pathways to be isolated from the ones of underlying waters. This information proved very useful for the interpretation of the rate measurements through the water column.

HABITATS, PRIMARY PRODUCTION AND NITROGEN ASSIMILATION

Using the approach of (Weber et al., 2019) and expanding it to the river mouth (Anh et al. submitted) we could distinguish 8 habitats depending on the structure of the water column, depth of the chlorophyll maximum and phytoplankton group composition. Nitrate, silicate and phosphate were consumed and diluted rapidly in the estuarine area, but degradation and nitrification processes were also involved in the regeneration of the nutrients. The uptake rates of inorganic N were maximal close to the coast. Nitrate uptake was only important for primary production, where nutrients from the Amazon River were available at high concentrations or additionally supplied by upwelled waters off French Guyana. Interestingly, inorganic nutrients are a more important driver of the productivity in the plume compared to dinitrogen fixation. The most abundant phytoplankton group in habitats with strong plume influence were the diatoms (Umbricht et al. sub.), which was also described by (Goes et al., 2014). Cryptophytes occurred at low salinities as well, together with dinoflagellates, while haptophytes and smaller species such as *Synechococcus* and *Prochlorococcus* prevailed at higher salinities and lower nutrient concentrations associated with reduced productivity. Only under fully saline conditions typical dinitrogen fixing species like diatom-diazotroph associations (DDAs) and colonial cyanobacteria were found. Primary production rates were partly elevated in these waters, but were maximal in the estuary in areas, where turbidity was reduced. Overall, we could show that remineralization of nitrogen within the surface layer is important to sustain the high primary production rates in the ARP.

RECYCLING AND LOSSES OF NITROGEN

The Amazon River estuary has long been described as a reactor likely dominated by losses of N forms, depending on the preservation of organic matter and its remineralization pathways in the water column and benthic environments. In the water column, our analysis of the dual isotopes of nitrate along with the composition of ambient water oxygen isotopes revealed signs of recycling, mainly via nitrification in the river mouth. Signs of denitrification at the river mouth were found with increasing depth, and signs of nitrate assimilation were visible in the nitrate isotope signature at the surface of more distal, less turbid stations. Our analysis of 8 short cores (Figure 1) confirmed the occurrence of intense recycling of mostly terrestrial material (>60 %) at the river mouth, and little organic carbon was remaining in shelf sediments. We measured a sediment oxygen demand of ~23 mmol m⁻² d⁻¹ (Figure 2) which can explain the ammonification and nitrification of all the organic N reaching the sediment, underlining the importance of the seabed as a sink for organic N species. However, the recycling of organic N to dissolved inorganic N (DIN) seem to be balanced by denitrification in the sediment or overlying water, as no DIN diffused out of the sediment (Figure 2). These results are in line with larger studies conducted in the

80s, suggesting that in spite of the changes in the Amazon Basin, the benthic N cycle so far remained unaltered (Choisnard et al., 2023).

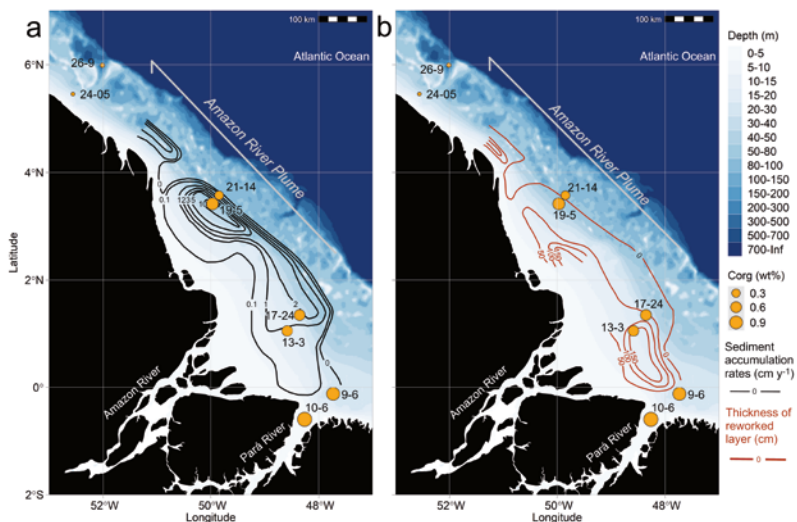


Figure 1: Eight short sediment cores were collected on the Amazon shelf, an area influenced by the outflow of the Pará and Amazon River. Kuehl et al., (1986) demonstrated that the particles delivered by the two rivers are transported along the Amazon River Plume and accumulate at high rates (black line, in cm y^{-1}) around 3°N relative to the rest of the shelf (a). Their study also highlighted the dynamicity of the seabed, with maximum reworked layer thicknesses (red line) of at least 150 cm on the Amazon shelf (b). The surface sediment of small cores collected in both river's estuaries and along the Amazon River Plume presented different Corg content (%wt), as represented by the point area. Figure from Choisnard et al., (2023).

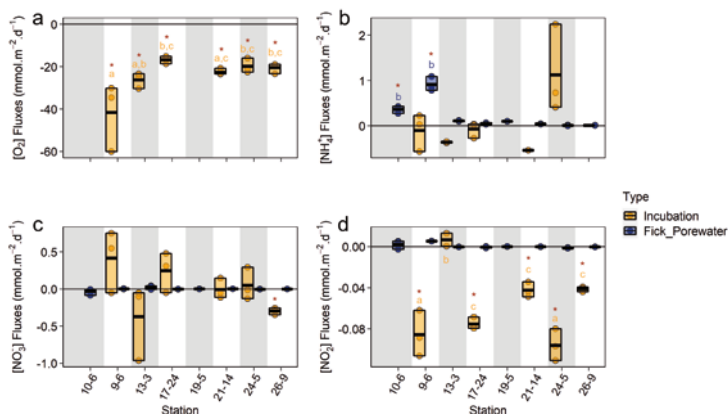


Figure 2: O_2 consumption and DIN fluxes obtained from the cores incubation (yellow) and the pore water profiles (dark blue) revealed that no clear source or sink of NH_4^+ and NO_3^- was detectable on the Amazon shelf, as measurements gathered around the zero-line, which represent the absence of fluxes. A negative flux accounts for a flux into the sediment and a positive flux represents diffusion in the overlying water. The boxes highlight the data range and the average of triplicate measurements. Letters group the stations that are not significantly different from each other (according to a Tuckey test), and red stars highlight fluxes that are significantly different from 0 (according to a one-sample student test). Figure from Choisnard et al., (2023).

IMPLICATIONS

Combining all our data, our results indicate that the Amazon currently supplies tenfold more ammonium (NH_4^+) and nitrate (NO_3^-) than the Pará. We found that while nutrient uptake is light limited by high turbidity near the mouth. As soon as nutrients are transported to regions with reduced turbidity, NH_4^+ assimilation picks up to 0.5 to $6.6 \times 10^8 \text{ mol N d}^{-1}$ and nitrification becomes reduced. We speculate that under increasing anthropogenic pressure, the hydrology, weathering, turbidity, and biogeochemistry of the Amazon and Pará River catchments are likely changing, potentially affecting the concentration and speciation of N entering the estuary. This study provides an invaluable baseline for N cycle pathways not only in the river mouth, but along the river plume, paving the way to monitoring studies of the impact of future changes in the Amazon/Pará catchments on phytoplankton communities and biogeochemical processes in the WTNA.

REFERENCES

Choisnard N, Burtscher E, Forster S, Frey C, Moros M, Voss M, The Amazon shelf sediments, a reactor that fuels intense nitrogen cycling at the seabed, *Limnology and Oceanography* 2023, doi:<https://doi.org/10.1002/lno.12416>.

Goes JI, Gomes HdR, Chekalyuk AM, Carpenter EJ, Montoya JP, Coles VJ, Yager PL, Berelson WM, Capone DG, Foster RA, Steinberg DK, Subramaniam A, Hafez MA, Influence of the Amazon River discharge on the biogeography of phytoplankton communities in the western tropical north Atlantic, *Progress in Oceanography* 2014, 120, 29–40.

Weber SC, Subramaniam A, Montoya JP, Doan-Nhu H, Nguyen-Ngoc, Dippner JW, Voss M, Habitat Delineation in Highly Variable Marine Environments, *Frontiers in Marine Science* 2019, 6, 10.3389/fmars.2019.00112.

SCIENTIFIC OUTPUT

LIST OF PUBLICATIONS

Choisnard N, Burtscher E, Forster S, Frey C, Moros M, Voss M, The Amazon shelf sediments, a reactor that fuels intense nitrogen cycling at the seabed, *Limnology and Oceanography* 2023, doi:<https://doi.org/10.1002/lno.12416>.

Einbock A, Burtscher E, Frey C, Conen F, Export of ice-nucleating particles from watersheds: results from the Amazon and Tocantins river plumes, *Royal Society Open Science* 2023, 10:220878 doi:[doi:10.1098/rsos.220878](https://doi.org/10.1098/rsos.220878).

LIST OF CONFERENCE PRESENTATIONS

2022 | **Nitrification contribution to the N-budget of the Amazon Estuary** Ocean Science Meeting (virtual), Hawaii, USA

2022 | **Nitrous oxide cycling within the Amazon River plume** Ocean Science Meeting (virtual), Hawaii, USA

2022 | **Changes in photo-, mixo- and heterotrophy at the base of the aquatic food web along the Amazon River plume** Ocean Science Meeting (virtual), Hawaii, USA

2023 | **Physical observations and fate of nutrients in the Amazon River plume** ASLO Conference, Palma de Mallorca, Spain

2023 | **Ammonium fuels a large proportion of the primary production in the Amazon River plume** ASLO Conference, Palma de Mallorca, Spain

2023 | **Nitrate dual isotopes reveal the source and cycling of Nitrate in the Amazon River Mouth** ASLO Conference, Palma de Mallorca, Spain

2023 | **Lagrangian Transport and Connectivity in Oceanic Flows: Applications to Ocean Dynamics and Marine Ecosystems** ASLO Conference, Palma de Mallorca, Spain

2023 | **Alternation of Autotrophs and Mixotrophs at surface in the habitats along the Amazon River Plume** ASLO Conference, Palma de Mallorca, Spain

2023 | **Oxidative and reductive nitrous oxide production within the Amazon River plume** ICON – International Conference on Nitrification, Princeton, USA

2023 | **Organophosphate Esters Along the Atlantic Ocean and into the Amazon River Plume** Biosphere 2, Tucson, Arizona, USA

DATA

M174 Master track:

<https://doi.pangaea.de/10.1594/PANGAEA.935041>

M174 Physical Oceanography CTD and nutrient chemistry data:

<https://doi.org/10.1594/PANGAEA.942346>

M174 Sediment (solid phase characteristics):

<https://doi.org/10.1594/PANGAEA.961264>

M174 Chemistry (Porewater nutrients):
<https://doi.org/10.1594/PANGAEA.961274>

M174 Chemistry (nutrient fluxes at sediment water interface):
<https://doi.org/10.1594/PANGAEA.961275>

CRUISE REPORT

M174: [doi:10.48433/cr_m174](https://doi.org/10.48433/cr_m174)

M176

Are the opening of the Bay of Biscay and the origin of the Azores-Biscay Rise linked to the Azores mantle plume?

AUTHORS

GEOMAR Helmholtz Centre for Ocean Research Kiel | Kiel, Germany

J. Geldmacher, A. Dürkefälden, J. Schenk, F. Hauff, S. Homrighausen, K. Hoernle

Institute of Geosciences, Kiel University | Kiel, Germany

D. Garbe-Schönberg

GeoZentrum Nordbayern, Erlangen University | Erlangen, Germany

K. Haase

INTRODUCTION AND GEOLOGICAL BACKGROUND

The margins of the North Atlantic Ocean between Iberia and Newfoundland are generally described as being typical (magma-starved) passive margins. It is all the more astonishing that numerous features of excess volcanism, apparently formed shortly after continental breakup, dot the respective ocean basins including the Bay of Biscay (Figures 1 and 2). The opening of the Bay of Biscay during the late Mesozoic and early Cenozoic and the associated kinematics of the Iberian plate have long been a subject of considerable debate (e. g., Srivastava et al., 1990; Canérot, 2016). Understanding both processes is fundamental for reconstructing the propagation and evolution of the North Atlantic Ocean. A key region for unraveling this opening history is the intersection of the former Biscay spreading axis with the early Mid-Atlantic Ridge. The magnetic lineations of this area show a peculiar confluence at around 45°N /14°30'W between the roughly N-S oriented Atlantic and the E-W trending Biscay A34 and A33 magnetic anomalies (Figure 2a) implying the existence of a former triple junction, which was first proposed by Williams (1973). The existence of this triple junction and a three-plate geometry in the North Atlantic Ocean implies that Iberia and its adjoining oceanic crust formed a separate plate at this time. Immediately to the east of the presumed triple junction lies an elongated ~400 km long seamount complex, composed of the North Charcot Seamount and the South Charcot Seamount, separated by a parallel valley (Figure 2b). Its dominant E-W trending bathymetry, aligned with the magnetic lineations, implies that this complex could represent vestiges of the Biscay mid-ocean ridge spreading center, with the central valley marking the last spreading axis of the Bay of Biscay at chron A33r (~80 Ma; Sibuet et al., 2004).

To the west, however, the two crests of the Charcot seamounts appear to merge into the NE-SW trending, ~750 km long Azores Biscay Rise (ABR), a prominent feature in the

Northeast Atlantic Ocean of unknown origin. Since the ABR runs oblique to seafloor magnetic fabric and fracture zones, it has been speculated that it represents an intraplate hotspot track, possibly generated by a mantle plume (early Azores hotspot?).

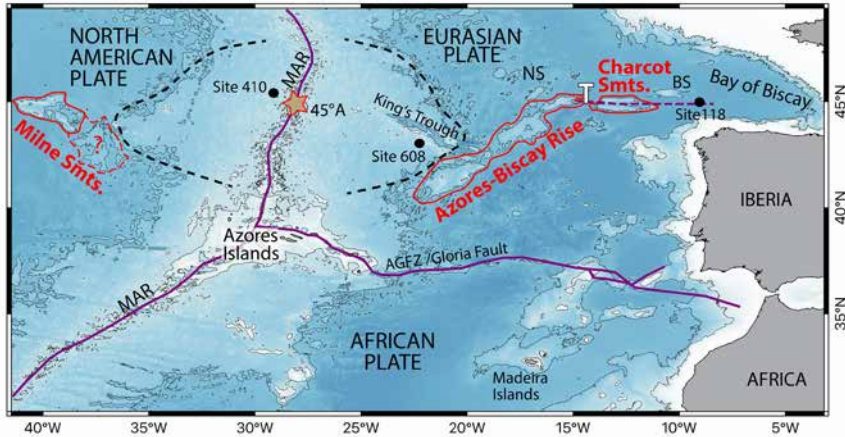


Figure 1: Bathymetric/tectonic map of the central NE Atlantic. The Azores-Biscay Rise (ABR) and the Milne Seamounts could be interpreted as paired aseismic ridges (e. g., Whitmarsh et al., 1982). Their formation terminated at c. 52 Ma contemporaneously with the beginning of the buildup of the Azores platform (from c. 50 Ma on, Searle, 1980) and the creation of an area of thickened oceanic crust to its north (encircled by black stippled line), forming a bulge in the Mid-Atlantic Ridge (MAR) flanks (starting c. 55 Ma ago, Searle and Whitmarsh, 1978). In the center of the latter, at around 45°N (star symbol), a geochemically enriched melting anomaly is recognized (e. g., White and Schilling, 1978). "T" marks former location of inferred triple junction (see Figure 2). NS= Seamounts north of the ABR, BS= Biscay Seamount. Map data from www.gebco.net.

A number of geophysical investigations have been conducted in the Bay of Biscay in the last decades leading to several geodynamic theories (see summary in Nirrengarten et al., 2017). However, almost no ground truthing by rock sampling, in particular from the critical transition between the Biscay and the Atlantic seafloors, was carried out before the recent METEOR expedition M176 (and partly during M168 (reconnaissance dredging)).

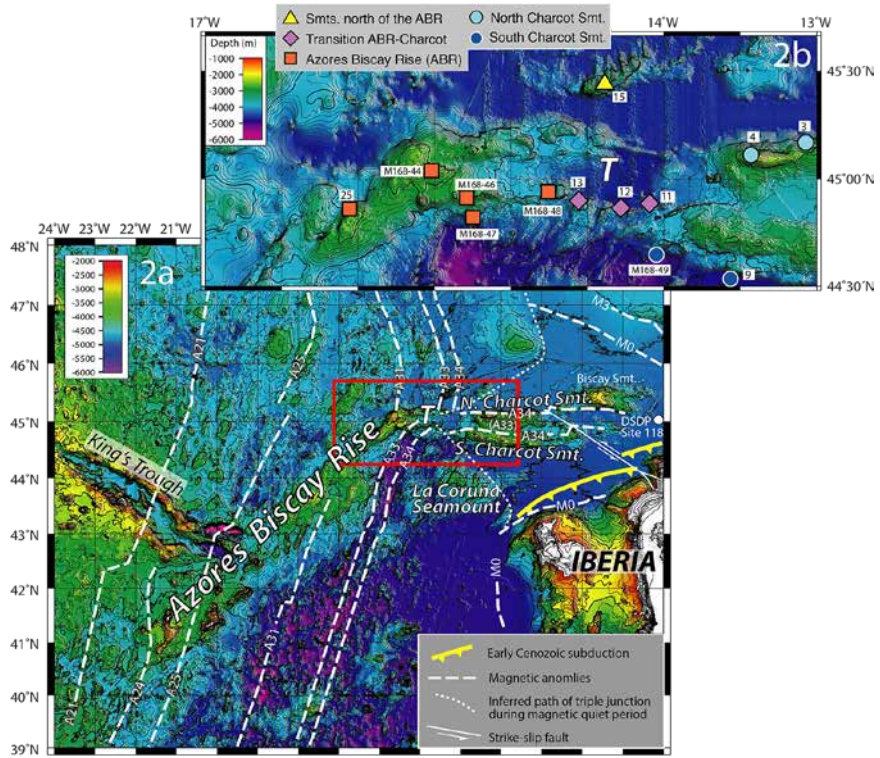


Figure 2a: Close-up of Figure 1 with selected magnetic anomalies after Klitgord and Schouten (1986) and Sibuet et al. (2004). Final site of triple junction between the Bay of Biscay and the Atlantic spreading ridges at ~75 Ma marked with the letter “T”. The youngest anomaly A33 is proposed to underlie the axial valley between the ridge-like North Charcot and South Charcot Seamounts. For clarity, color scale only applied below 2,000 m water depths. Figure 2b. Close-up of 2a (red frame) with location of M168 and M176 dredge sites (the latter without cruise number) from which first (igneous) samples were analyzed (Dürkefalden et al., 2020; Geldmacher et al., 2021). “T” marks inferred location of triple junction at ~75 Ma.

FIRST, PRELIMINARY RESULTS

Although the post-cruise analyses/evaluation of the rock samples obtained during M176 has not started yet (proposal for project funding (including isotope studies and Ar/Ar dating) is under review), we are able to present a few reconnaissance results. These preliminary data indicate that the lavas recovered from the ABR and from the transitional zone towards the Charcot Seamounts to the east are predominantly composed of geochemically depleted to moderately enriched tholeiitic basalt (e. g., $(Ce/Y)_n = 0.7-0.9$, $Zr/Nb < 3.5$; Figures 3 and 4). At the Charcot Seamounts, the presumed fossil spreading center, we see a slightly different picture: While the South Charcot lavas possess (with one exception) a similarly depleted, tholeiitic composition, the North Charcot samples are geochemically more enriched ($Zr/Nb > 5$). All samples (including the tholeiites) plot within the so called “Iceland array” after Fitton et al. (2003) indicating involvement of enriched mantle plume material in the genesis of all lavas analyzed so far

(Figure 3b). The few data obtained from the solitary seamounts located north of the ABR and north of the Charcot complex classify as alkaline basalts showing an enriched ocean island basalt (OIB) signature ($(\text{Ce}/\text{Y})_n = \text{up to } 19.5$; Figure 4). While these alkaline lavas compositionally overlap with the Azores Islands, the tholeiitic samples (ABR, transitional zone and South Charcot Smt.) plot within the compositional field of the 45°N melting anomaly of the Mid-Atlantic Ridge (Figures 3 and 4). This anomaly is characterized by geochemical compositions more enriched than normal mid-ocean ridge basalts (N-MORBs) found in lavas from the ridge flanks and indicates derivation from an enriched mantle source, presumably a mantle plume (e. g., White and Schilling, 1978).

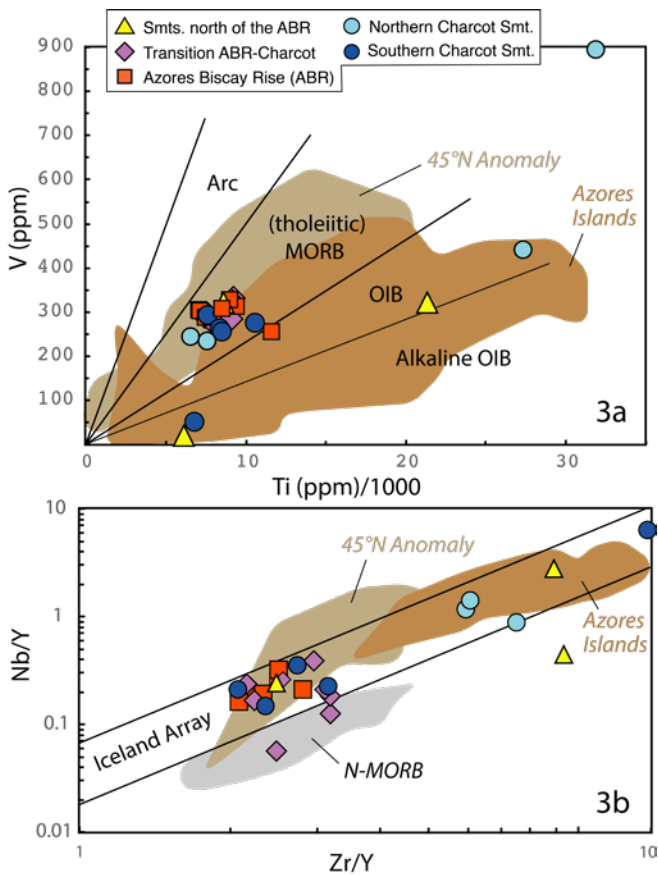


Figure 3a: Ti vs. V discrimination diagram after Shervais et al. (2022) with Azores and 45°N MORB data from <https://georoc.eu/>. Most analyzed samples classify as tholeiitic basalts (XRF data only) overlapping with MORB lavas currently erupted at the 45°N anomaly. Lavas from seamounts north of the ABR and from North Charcot Smt. include alkaline ocean island basalts. Figure 3b. "Fitton diagram" for discriminating mantle plume influenced Icelandic basalt and N-MORB (Fitton et al., 2003). Almost all samples (including the tholeiites) indicate involvement of mantle plume material. Rocks from seamounts north of the ABR and from North Charcot Smt. overlap with OIB compositions from the Azores Islands.

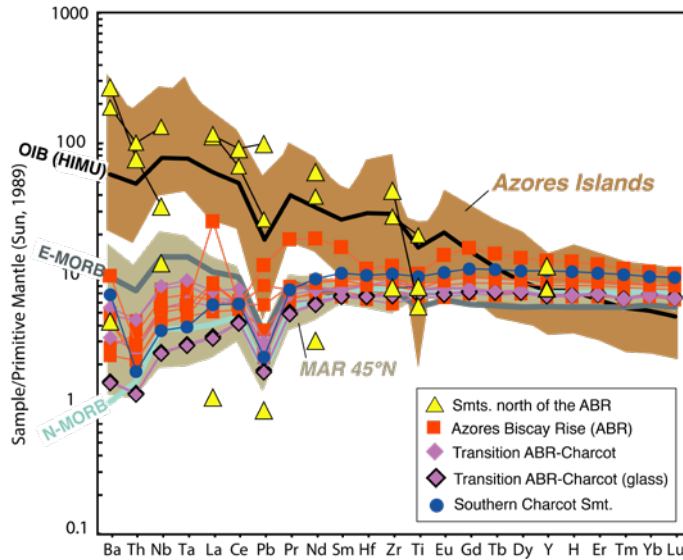


Figure 4: The multi-element diagram confirms compositions ranging from N-MORB to E-MORB for ABR and Charcot Seamounts samples and transitional structures. Lavas from seamounts north of the ABR possess enriched ocean island basalt (OIB)-like compositions (only XRF data available for these samples so far).

In summary, the preliminary results indicate involvement of enriched (mantle plume?) material at least during the final spreading phase in the Bay of Biscay and during the formation of the Azores-Biscay Rise. Because of the tholeiitic composition of the recovered lavas, it is tentatively suggested that the rise does not represent a true intraplate hotspot track but rather formed as aseismic ridge by plume-ridge interaction. It is likely that the same (plume) source has formed true intraplate seamounts (and contributed to seafloor production?) in the Bay of Biscay. Planned radiogenic isotope analyses will be used to test this hypothesis and to constrain the involved magma source(s) (e. g., 45°N anomaly or Azores hotspot).

ACKNOWLEDGMENTS

We would like to thank Captain Detlef Korte and his crew for their great support during expedition M176 and acknowledge funding by the German Research Foundation (DFG) and the GEOMAR Helmholtz Centre for Ocean Research Kiel.

REFERENCES

Canérot J, The Iberian Plate: myth or reality?, *Boletín Geológico y Minero* 2016, 127, 563–574.

Dürkefälden A, Geldmacher J, Hauff F, Werner R (eds.), Origin and Geodynamic Evolution of King's Trough: The Grand Canyon of the North Atlantic, Cruise No. M168 (GPF 20-3_080) 2020, Emden (Germany) - Emden (Germany), METEOR-Berichte 2020, M168, Gutachterpanel Forschungsschiffe, Bonn.

Fitton JG, Saunders AD, Kempton PD, Hardarson BS, Does depleted mantle form an intrinsic part of the Iceland plume?, *Geochem. Geophys., Geosyst.* 2003, 4 (3), doi: 10.1029/2002GC000424.

GEBCO Compilation Group, GEBCO 2020 Grid: doi:10.5285/a29c5465-b138-234d-e053-6c86abc040b9.

Geldmacher J, Werner R (eds.), Azores-Biscay Rise and Bay of Biscay: A key area for the reconstruction of the geodynamic evolution of the early North Atlantic, Cruise No. M176 (GPF 21-2_048), 2021, Emden (Germany) – Emden (Germany). METEOR-Berichte M168, Gutachterpanel Forschungsschiffe, Bonn, doi: 10.48433/cr_m176.

Klitgord KD, Schouten H, Plate kinematics of the central Atlantic. In: Vogt, PR, Tucholke, BE (Eds.), *The Geology of North America 1986, Volume M, The Western North Atlantic Region*, Geol. Soc. Am., 351–378.

Nirrengarten M, Manatschal G, Tugend J, Kuszniek N, et al., Kinematic evolution of the southern North Atlantic: Implications for the Formation of hyperextended rift systems, *Tectonics* 2017, 37, 89–118.

Searle R, Tectonic pattern of the Azores spreading centre and triple junction, *Earth Planet. Sci.* 1980, Lett. 51, 415–434.

Searle R, Whitmarsh RB, The structure of King's Trough, Northeast Atlantic, from bathymetric, seismic and gravity studies, *Geophys. J. R.* 1978, 53, 259–287.

Shervais JW, The petrogenesis of modern and ophiolitic lavas reconsidered: Ti-V and Nb-Th, *Geosciences Frontiers* 2022, 13, doi.org/10.1016/j.gsf.2021.101319.

Sibuet JC, Srivastava SP, Spakman W, Pyrenean orogeny and plate kinematics, *J. Geophys. Res.* 2004, 109, B08104, doi:10.1029/2003JB002514.

Sun S-S, McDonough WF, Chemical and isotopic systematic of oceanic basalts: implications for mantle composition and processes. In: Saunders, A.D. & Norry, M.J. (eds.), *Magmatism in the Ocean Basins*, Geol. Soc. Spec. Pub. 1989, 42, 313-345.

Srivastava SP, Schouten H, Roest WR, Klitgord KD, et al., Iberian plate kinematics: a jumping plate boundary between Eurasia and Africa, *Nature* 1990, 344, 756-759.

White WM and Schilling J-G, The nature and origin of geochemical variation in Mid-Atlantic Ridge basalts from the Central North Atlantic, *Geochimica et Cosmochimica Acta* 1978, 42, 1501–1516, doi:https://doi.org/10.1016/0016-7037(78)90021-2.

Williams C, A fossil triple junction in the northeast Atlantic west of Biscay, Nature 1973, 244, 86–88.

SCIENTIFIC OUTPUT

LIST OF CONFERENCE PRESENTATIONS

2023 | **Are the opening of the Bay of Biscay and the origin of the Azores-Biscay Rise linked to the Azores mantle plume?** Oceanic Volcanism Workshop, 13.09–15.09. Kiel, Germany.

DATA

Physical oceanography: Continuous thermosalinograph data:
<https://doi.org/10.1594/PANGAEA.945706>

CRUISE REPORT

M176: doi: 10.48433/cr_m176

M176/2

Rainbow non-buoyant hydrothermal plume GEOTRACES study

AUTHORS

GEOMAR Helmholtz Centre for Ocean Research Kiel | Kiel, Germany
E.P. Achterberg, X.G. Chen

Constructor University | Bremen, Germany
A. Koschinsky

The Rainbow hydrothermal vent field is situated outside the Portuguese EEZ at 36°13.80' N, 33°54.14' W (Figure 1) and its hydrothermal activity is well studied. The hot discharging fluids show a strong metal enrichment, especially of Fe, and form a pronounced plume in the water column (German et al., 1996). The Rainbow hydrothermal vent field is located at ~2300 m depth on the western flank of the non-volcanic Rainbow ridge situated along the mid Atlantic Ridge (MAR) (Douville et al., 2002). The hydrothermal vent field is composed of multiple (at least 13) black smokers discharging high temperature fluids (up to 370°C) in an area of approximately 100 by 300 m (Edmonds and German, 2004). The surface waters in the study region over the Rainbow field site are influenced by an eastward flowing component of the N Atlantic anticyclonic nutrient depleted subtropical gyre, the Azores Current, which has split from the Gulf Stream in the western North Atlantic. The water masses encountered in our study region include tropical surface waters, with below the North Atlantic Central Water (NACW) which forms the main pycnocline in the subtropical ocean. Mediterranean Water (MW) is found below NACW as a salty warm layer between ~800–1200 m, with Labrador Sea Water (LSW) down to ~2 km. The North Atlantic Deep Water (NADW) is situated below the LSW (Talley et al., 2011) and forms the waters (S ~34.95 and Pot. T ~2.5°C) surrounding the hydrothermal plume at Rainbow.

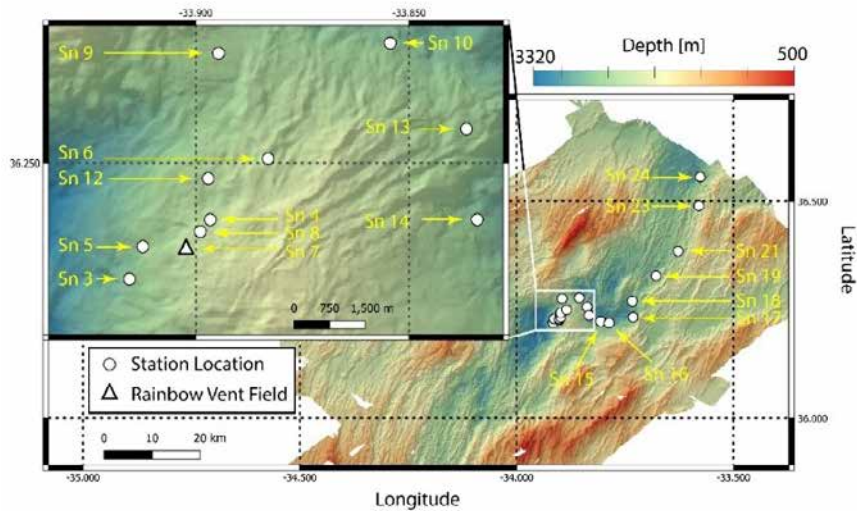


Figure 1: Bathymetric map of the study region. Rainbow vent field is marked with a triangle. CTD stations are marked with white circles.

It had been hypothesized in the early 1990s that hydrothermal vents would impact global ocean biogeochemistry (Kadko, 1993), but not until the emergence of GEOTRACES was clear evidence provided. GEOTRACES revealed in recent years that there is a widespread release of dissolved Fe and a range of other elements from hydrothermal vents to the deep ocean (Saito et al., 2013). Iron is a micronutrient that limits primary productivity of phytoplankton in about 40% of the world's surface oceans and manganese (Mn) has recently been shown to be co-limiting alongside Fe in the Southern Ocean (Browning et al., 2021). Supply of hydrothermally-sourced Fe/Mn through isopycnal upwelling could hence potentially stimulate productivity in Fe/Mn limited regions. This mechanism was indicated for the Fe limited North Pacific and Southern Ocean based on GEOTRACES observations and biogeochemical model studies (Resing et al., 2015).

There is currently a lack of understanding of the processes that set the fluxes of hydrothermally sourced trace elements. The initial consideration of full removal of Fe in the direct vicinity of hydrothermal vents (German C. R. et al., 1991) appears incorrect, with processes appearing more complex. In addition, the older studies (1980-1990s) focused on processes occurring within tens to hundreds of meters from individual vents and thereby missing the processes that determine distal plume spread. The more recent GEOTRACES studies have a spatial resolution of ca. 100 km and therefore miss the key processes that result in removal and stabilization of trace elements occurring in the first kilometers away from the vents. The Rainbow Plume cruise has conducted detailed sampling of the Rainbow hydrothermal plume system over a distance up to 60 km, using state of the art GEOTRACES protocols and laboratory techniques, complemented by supporting analyses (e. g. He, Th and Ra isotopes, metal-binding ligands, metal

redox speciation, Fe isotopes, O₂, POC, DOC). The new knowledge will be combined with a global biogeochemical model (University of Liverpool) to obtain new understanding of the impact of hydrothermal TEI supply on ocean biogeochemistry. Slow-spreading ridges are a much more significant oceanic Fe source than 3He fluxes and spreading rates had previously suggested based on relationships at the East Pacific Rise. Since slow-spreading ridges account for more than half of the submarine ridge system, such a constant emanation of hydrothermal fluids would make hydrothermal vent systems on slow spreading ridges a medium- to long-term stable source of Fe and other micronutrients to the ocean.

On a daily basis we sampled in detail the non-buoyant hydrothermal plume emanating from the Rainbow vent field using the trace metal clean titanium GEOMAR CTD. This CTD is operated by a dedicated winch system with a Kevlar cable, thereby preventing contamination of the samples during the sample collection. We sampled just above and just below the plume, which means between 1700 m and 2300 m, with the plume maxima being at ca. 2100 m. On our Ti rosette with 24 bottles, we sampled 2 bottles at each depth, and therefore 12 depths above, in and below the plume. Once on deck, 12 Niskin bottles are removed from the frame and taken to our trace metal clean container where the water is filtered into a large number of different bottles for analysis at sea and in the home laboratories. We collected particles from the plume for trace element and synchrotron analyses, and we collected waters that were subsequently filtered on-board through various different filter pore sizes. The collection of various size fractions along the plume will provide detail on chemical transformations and allow us to decipher how much material (e. g. iron) is removed by sinking and remains in solution and may ultimately be available to phytoplankton growth in the surface ocean.

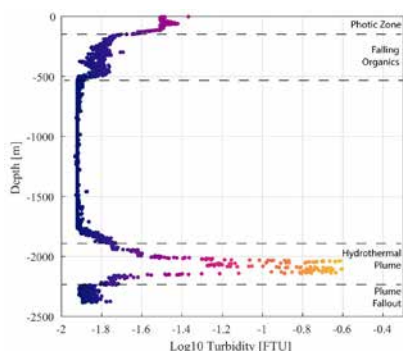


Figure 2: An example of a 1D turbidity distribution with depth, from Station 12. Turbidity varies due to physical and biological processes through the water column, with the signal of a hydrothermal plume sharply standing out.

We sampled the other 12 Niskins from the titanium CTD for helium isotopes, DIC, DOC, oxygen, which we will use as a tracer of the hydrothermal fluid inputs to the ocean. Helium is a conservative tracer and allows us to follow the plume and determine the fluxes of elements.

We deployed CTDs for the collection of Ra and Th isotopes to allow us to assess time scales of plume movement and trace element scavenging processes. Large volume samples (110 L) were obtained from these deployments for Ra isotopes and pumped over Mn cartridge for short-lived Ra analysis on board and long-lived Ra in Kiel. For Th isotopes, we also measured on-board (Th 234) and subsequently on land (Th 230).

An additional titanium CTD was deployed daily to 300 m depth for collection of samples for biological variables. Biological rate experiments of nitrification and di-nitrogen fixation were conducted using the water from the titanium CTD and tow fish. Phytoplankton resource limitation experiments were conducted in the ship-board laboratory and also in incubation tanks on the aft deck.

Each afternoon, a MUC deployment was conducted to obtain sediment cores. These deployments were successful for all stations in obtaining surface sediments. However, the collection of intact cores was not successful in all instances. Nevertheless, on ten occasions we obtained cores which could be used for porewater extraction and slicing.

At night, we conducted CTD Tow-Yo deployments with the CTD to obtain a 3 dimensional picture of the spreading plume (Figure 3).

Our first results of the trace metal analysis show strongly enhanced dissolved Fe concentrations in the immediate vicinity of the Rainbow vent systems, with decreasing concentrations with distant from the vents.

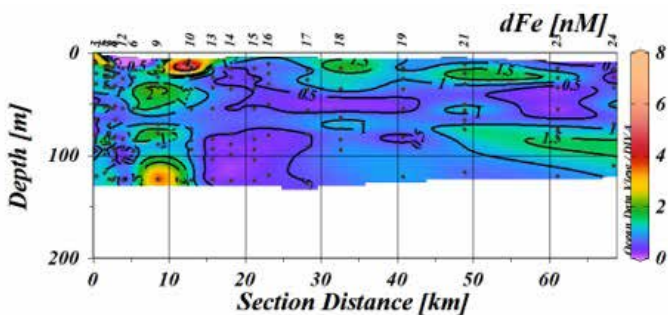


Figure 3: Tow-Yo CTD sections indicating the turbidity signal for 12.09. to 13.09.2021; Line T1-6. The profile started on top of Rainbow ridge and was oriented in a SE-NW direction, crossing over the Rainbow vent field.

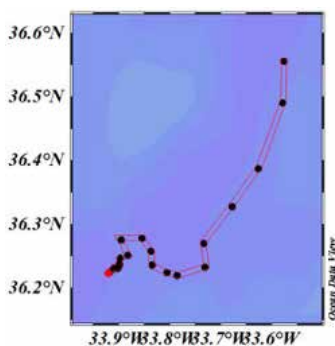


Figure 4: Section of dissolved Fe (top) along the spreading plume .

REFERENCES

Browning T, Achterberg E, Engel A, Mawji E, Manganese co-limitation of phytoplankton growth and major nutrient drawdown in the Southern Ocean, *Nature Communications* 2021, 12, 1–9.

Douville E, Charlou J, Oelkers E, Bienvu P, et al., The rainbow vent fluids (36°14'N, MAR): The influence of ultramafic rocks and phase separation on trace metal content in Mid- Atlantic Ridge hydrothermal fluids, *Chemical Geology* 2002, 184, 37–48.

Edmonds H, German C, Particle geochemistry in the Rainbow hydrothermal plume, Mid-Atlantic Ridge, *Geochimica et Cosmochimica Acta* 2004, 68, 759–772.

German C, Klinkhammer G, Rudnicki M, The Rainbow Hydrothermal Plume, 36°15'N, MAR, *Geophysical Research Letters* 1996, 23, 2979–2982.

Kadko D, Moore W, Radiochemical constraints on the crustal residence time of submarine hydrothermal fluids: Endeavour Ridge, *Geochimica et Cosmochimica Acta* 1988, 52, 659–668.

Resing J, Sedwick P, German, C, Jenkins W, et al., Basin-scale transport of hydrothermal dissolved metals across the S Pacific, *Nature* 2015, 523, 200–203.

Saito M, Noble A, Tagliabue A, et al., Slow-spreading submarine ridges in the South Atlantic as a significant oceanic iron source, *Nature Geoscience* 2013, 6, 775–779.

SCIENTIFIC OUTPUT

LIST OF PUBLICATIONS

Zhongwei Y, Achterberg E, Engel A, Wen Z, Zhou L, Zhu X, Dai M, Browning T, Phytoplankton community response to episodic wet and dry aerosol deposition in the subtropical North Atlantic, *Limnology and Oceanography* 2023. DOI 10.1002/lno.12410.

LIST OF CONFERENCE PRESENTATIONS

2023 | **Is the Rainbow ultramafic hydrothermal system a poor source of radium isotopes to the Atlantic Ocean?** Goldschmidt, Lyon, France.

2023 | **Nanoparticulate iron oxyhydroxides aggregated in carbon matrices dominate iron speciation in hydrothermal plumes over the 1–100 km distance from vent source** Goldschmidt, Lyon, France.

2023 | **Regulation of hydrothermal vent contribution to ocean chemistry by hydrothermally influenced sediments, the Rainbow field case study** Goldschmidt, Lyon, France.

DATA

Mastertrack:

<https://doi.pangaea.de/10.1594/PANGAEA.940195>.

Continuous TSG data:

<https://doi.org/10.1594/PANGAEA.946388>.

ADCP data:

<https://doi.org/10.1594/PANGAEA.946027>

Dissolved and particulate barium and their isotopes:

<https://doi.org/10.1594/PANGAEA.961129>.

Helium and neon isotope data:

<https://doi.org/10.1594/PANGAEA.961104>

CRUISE REPORT

M176/2: http://doi.org/10.48433/cr_m176_2

M177

Fluids migrate across Paleozoic rock and the Quaternary sediments and escape from the seafloor in the eastern Gotland Basin/Baltic Sea

AUTHORS

Institute for Geophysics, University of Hamburg | Hamburg, Germany

C. Hübscher, A. Warwel, M. Hartge, M. Lackner, K. Uhl, J. Preine

Institute for Geology, University of Hamburg | Hamburg, Germany

M. Artschwager, C. Betzler, T. Lüdmann

The Baltic Basin is renowned for its numerous Paleozoic hydrocarbon reservoirs. While there is published evidence of hydrocarbons leaking from the seafloor, our understanding of the pathways through which hydrocarbons migrate from Paleozoic source and reservoir rocks to reach the seafloor and escape structures remains limited. To investigate these processes, we conducted extensive data collection during the RV METEOR expedition M177 within the Exclusive Economic Zones (EEZ) of Estonia, Latvia, and Lithuania (see Figure 1). Unfortunately, the planned research in Swedish territory had to be postponed as the research permit was not granted.

The Baltic Sedimentary Basin is a synclinal depression located within the continental crust of the East European Craton. This basin is filled with Paleozoic deposits and has experienced significant tectonic activity and other reshaping mechanisms, including syn- or post-sedimentary processes. Two prominent features, Leba Ridge and Liepaja-Saldus Ridge, bear witness to this active geological history. The basin extends beneath the Baltic Sea, Northern Poland, and the Baltic States, with its central axis running in a southwest-northeast direction, roughly beneath the east coast of the Baltic Sea. Notably, the sediments within the basin exhibit a unique dip, resulting in parallel but inclined strata, particularly along the northern and western margins. These strata are exposed beneath a thin Quaternary sediment cover, with sediment age increasing from southeast to northwest.

In his 2023 MSc thesis, Hartge utilized exploration wells to establish an initial seismic-stratigraphic framework for the entire M177 study area. Seismic amplitude and attribute plots suggest the migration of fluids from hydrocarbon generation zones in the southwest to early-stage oil generation areas in the central basin, ultimately moving northward. The primary fluid-conducting units consist of Ordovician limestones and Lower Devonian sandstone formations. The integrated interpretation of seismic profiles, diffraction imaging, and bathymetric maps, as conducted by Warwel et al. in 2023, enabled the

identification of a hydrocarbon migration system within the Silurian and Devonian strata. This system includes layer-parallel and up-dip migration beneath sealing layers, migration across seals along fault lines, and the presence of seafloor escape structures in the form of elongated depressions. The general migration trend is directed up-dip, moving from the Paleozoic reservoirs in the southeastern Baltic Sea toward the Gotland Depression in the northwest. The Silurian reefs, meticulously mapped from M177 seismic data by Uhl in her 2023 BSc thesis, represent potential reservoir rocks.

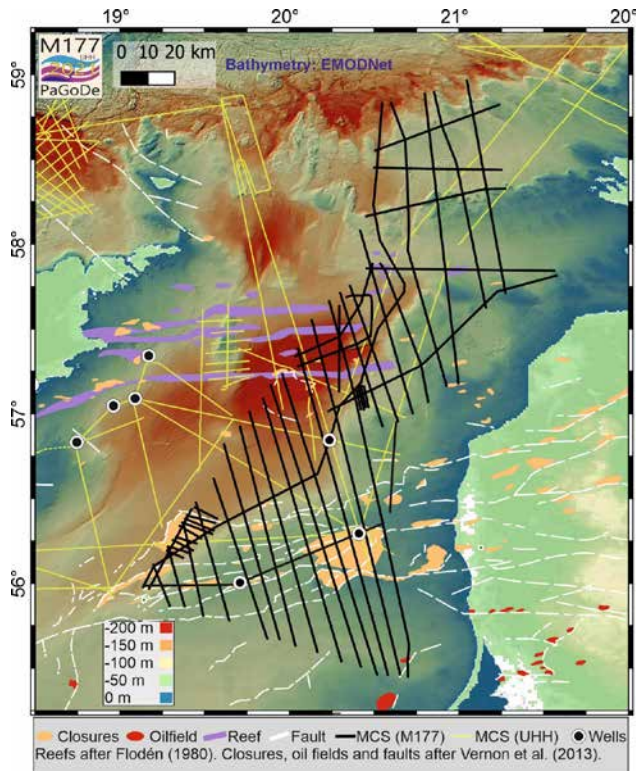


Figure 1: Geophysical profiles collected during R/V METEOR expedition M177.

These reefs typically exhibit an upper reflection with a wavy pattern, sometimes displaying a chaotic reflection pattern or a velocity pull-up underneath due to their relatively high seismic velocity.

As shown by Warwel et al. (2023), the locations of the hydrocarbon escape structures at the seafloor and their elongated shape are mainly controlled by the regional geological setting of outcropping Paleozoic layers. Lackner (2023) interpreted the outcropping sub-Quaternary cuesta-type erosional unconformity and linked the unconformity to the general topography of the Gotland Basin. In addition, iceberg scouring may have

facilitated hydrocarbon migration through the Quaternary deposits. The description of this hydrocarbon migration system fills the gap between the known reservoirs and the observed hydrocarbon accumulations and seepages. With regard to potential Carbon Capture and Storage projects, the identification of this hydrocarbon migration system is of great importance, as potential storage sites may be leaking.

In her 2023 MSc thesis, Artschwager employed multibeam and parametric echosounder data to investigate Quaternary deposits. The research involved the differentiation of five seismic units based on their seismic properties, which were used to create thickness and lateral maps, highlighting distinctive features. These seismic units, associated with the Quaternary epoch, primarily consist of glacial and postglacial sediments deposited during the Weichselian glaciation and deglaciation.

Notably, the Weichselian till exhibits significant thicknesses in the eastern Gotland Basin and flanks, believed to have formed as moraines during a slowdown or readvance of the ice shield between 14,000 and 12,000 years BP. Erosional features from the last glaciation are also evident in the seismic data, manifesting as tunnel valleys in the Gotland Basin and the Hoburg Channel. Furthermore, the postglacial varves, overlying the Weichselian till, can be categorized into four stages corresponding to the Baltic Sea's evolution after the initial deglaciation: the Baltic Ice Lake, Yolida Sea, Ancylus Lake, and Litorina Sea. A major unconformity, detectable throughout the entire study area, separates sediments from the Baltic Ice Lake to the Ancylus Lake from those of the Litorina Sea.

REFERENCES

Artschwager M, Quaternary seismic stratigraphy of the Eastern Gotland Basin (Baltic Sea), MSc-thesis at University of Hamburg (unpublished) 2023.

Flodén T, Seismic stratigraphy and bedrock geology of the central Baltic. Stockholm Contributions in Geology 1980, 35, 1–240.

Hartge M, Seismic Study on the Fluid System in Paleozoic Bedrocks in the Eastern Gotland Basin (Baltic Sea). MSc-thesis at University of Hamburg (unpublished), 2023.

Lackner M, Reflexionsseismische Studie zum Einfluss der Lithologie auf glaziale Erosion im Gotland Becken/zentrale Ostsee. BSc-thesis at University of Hamburg (unpublished), 2023.

Uhl K, Reflection seismic mapping of Silurian Reefs in the eastern Gotland Basin (Baltic Sea). BSc-thesis at University of Hamburg (unpublished), 2023.

Vernon R, O'Neil N, Pasquali R, Nieminen M, Screening of prospective sites for geological storage of CO₂ in the Southern Baltic Sea. VTT, 2013.

Warwel A, Hübscher C, Hartge M, Artschwager M, Schäfer W, Preine J, Häcker T, Strehse V, Karušs J, Lüdmann T, The Paleozoic Hydrocarbon System in the Gotland Basin (central Baltic Sea) leaks. Earth and Space Science 2023, 10, doi: 10.1029/2023EA002883.

SCIENTIFIC OUTPUT

LIST OF PUBLICATIONS

Warwel A, Hübscher C, Hartge M, Artschwager M, Schäfer W, Preine J, Häcker T, Strehse V, Karušs J, Lüdmann T, The Paleozoic Hydrocarbon System in the Gotland Basin (central Baltic Sea) leaks, Earth and Space Science 2023, 10, doi: 10.1029/2023EA002883.

DATA

Seismic reflection data: <https://doi.pangaea.de/10.1594/PANGAEA.957436>

Multibeam data: <https://doi.pangaea.de/10.1594/PANGAEA.956740>

Echsounder data: <https://doi.pangaea.de/10.1594/PANGAEA.957422>

CRUISE REPORT

M177: doi:10.48433/cr_m177

M178

Hazards off Etna: Landslide Nucleation under Tremor (HazELNUT)

AUTHORS

Kiel University | Kiel, Germany

F. Gross, F. Petersen, H. Kolling, R. Barrett, S. Heinrich, M. Hundsdörfer, L. Morgenweck, P. Matzerath, J. Wolf, J. Vollert

GEOMAR Helmholtz Centre for Ocean Research | Kiel, Germany

M. Urlaub, M. Heinrich, C. Filbrandt

Alfred-Wegener-Institute for Polar Research | Bremerhaven, Germany

E. Hadré

University of Catania | Catania, Italy

S. Gambino

Istituto Nazionale di Geofisica e Vulcanologia, sezione di Catania | Catania, Italy

A. Bonforte

Mt Etna, located on the east coast of Sicily, Italy, is one of the world's most well-known volcanoes. Since historical times, Mt Etna's flanks have been and continue to be densely populated and are presently home to up to one million inhabitants. Mt Etna has become increasingly active over the past few decades, with several eruptions per year, which are predominantly of a rather mild Strombolian nature. Since 2018, volcanic activity has twice manifested impressively, with paroxysms and significant seismic activity over Christmas 2018 and in February 2021. In addition to frequent Strombolian eruptions, Mt Etna's south-eastern flank slides seawards at a rate of several centimetres per year (Bonforte et al., 2011, Borgia et al., 1992). This deserves attention because it is known from the geological and historical record that volcano flanks can collapse catastrophically and that the resulting tsunamis are extremely destructive (Ramalho et al., 2015, Paris et al., 2017). Seaward motion of Mount Etna's southeastern flank manifests in continuous deformation as well as episodic 'slow slip' events that are aseismic and occur irrespective of volcanic activity (Palano, 2016). Hence, displacement rates are highly variable over time, averaging about 30-50 mm/year. While vertical ground deformation due to magma overpressure reaches a maximum at the volcano summit, flank subsidence and seaward movement is concentrated along the coast (Bonforte et al., 2011), and even increases below sea-level as revealed by a seafloor geodetic survey over two years (Urlaub et al., 2018). Prior to the February 2021 volcanic activity, a cluster of magnitude

1-2 earthquakes occurred beneath the unstable sector. These earthquakes are however unlikely to be related to the subsequent eruptions because the magma feeder system is located southwest of the summit (Neri et al., 2011). Instead, their occurrence demonstrates clear connections between flank deformation (earthquakes) and the magmatic system (eruptions). It is well known that flank instability and eruptive activity interact with each other through the delicate balancing of lithostatic and magmatic pressures. Flank motion can promote eruptive activity, while eruptive activity results in gravitational loading and over-steepening, and repeated rift zone intrusions and pressurization of a magmatic system can “push” a flank closer to failure. Although the eastern flank seismicity appears to have subsided for now, it is unclear what hazards are evolving from it. What is clear is that Etna defines a highly complex system, wherein changes in one part of the system can strongly influence other parts. While a collapse of Etna’s entire flank may not be imminent, a variety of other hazards may occur along with strong eruptions. Tephra layers immediately on top of mass transport deposits (MTDs) collected with gravity corers from Etna’s flank suggest a close link between emerging volcanic activity and slope failure (Gross et al., 2014). Small to medium scale landslides along the steep submerged slopes of Etna’s eastern flank are capable of generating local but large tsunamis and hence pose a realistic threat to coastal communities. Over the past decade, Kiel scientists have intensely studied the submerged sector of the volcano and its continental margin. These findings show that the well-known flank instability proceeds far into the sea (Gross et al. 2016) and is measurable using marine geodetic networks (Urlaub et al. 2018). Nevertheless, the relation between volcanic activity and deformation of the continental margin remains unclear, and various scenarios ranging from small-scale disintegration over geological time periods to abrupt catastrophic failure have been drawn.

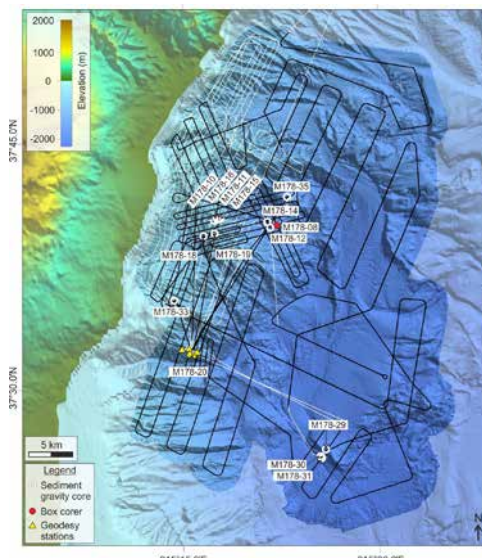


Figure 1: Working area of the R/V Meteor M178 cruise offshore Mount Etna.

During cruise M178 (HazELNUT), we investigated how Mt Etna's recent activity and large-scale instability have reshaped the continental margin over the last ten years. To investigate larger-scale changes of morphology, we used RV Meteor's hull-mounted multibeam echosounders. The resulting bathymetric maps will be compared with previous campaigns offshore Mt Etna to identify hotspots of geomorphological changes on the continental margin. A sediment gravity corer was used to retrieve archives of the sedimentary record in order to validate potential zones of instability offshore Etna. The sediment cores host a variety of tephra layers, which are related to previous volcanic eruptions of Mt Etna and other volcanoes nearby. Some of the sediment cores, particularly those recovered from the headwall of the prominent amphitheater structure in the central part of the continental margin, show intense patterns of deformation, which indicate compressional as well as extensional regimes at the margin. We also performed maintenance work on a marine geodetic network that was deployed in 2020 by GEOMAR Helmholtz Centre for Ocean Research, Kiel. The data upload and retrieval of six stations went smoothly and five stations were redeployed at the same locations again. In addition to the working program offshore Mt Etna, we also had the opportunity to investigate the continental margin offshore La Palma (Canary Islands, Spain). Unfortunately, our permit for a multibeam survey offshore La Palma required that we had at least six independent Marine Mammal Observers onboard, which we were not able to fulfil within the single day between receiving the permit and arriving in the working area. Instead, we used the allocated time to carry out a dedicated CTD Survey with multiple casts across the volcanic flanks of La Palma. The long transit times during M178 HazELNUT were used to collect a unique dataset of 360° 8K images and videos of the research vessel METEOR. This footage and additional videos and recordings were merged to a virtual tour, which can be used for research to research communication formats as well as the information of the general public on marine research and especially the research vessel METEOR.

REFERENCES

- Bonforte A, Guglielmino F, Coltelli M, Ferretti A, Puglisi G, Structural assessment of Mount Etna volcano from Permanent Scatterers analysis, *Geochemistry, Geophysics, Geosystems* 2021, 12(2). <https://doi.org/10.1029/2010GC003213>.
- Borgia A, Ferrari L, Pasquarè G, Importance of gravitational spreading in the tectonic and volcanic evolution of Mount Etna, *Nature* 1992, 357(6375), 231–235.
- Gross F, Krastel S, Chiocci L F, Ridente D, Bialas J, Schwab J, Beier J, Cukur D, Winkelmann D, Evidence for Submarine Landslides Offshore Mt. Etna, Italy, *Advances in Natural and Technological Hazards Research* 2014, <https://doi.org/10.1007/978-3-319-00972-8>.
- Gross F, Krastel S, Geersen J, Behrmann J H, Ridente D, Chiocci F L, Bialas J, Papenberg C, Cukur D, Urlaub M, Micallef A, The limits of seaward spreading and slope instability

at the continental margin offshore Mt Etna, imaged by high-resolution 2D seismic data, *Tectonophysics* 2015, DOI 10.1016/j.tecto.2015.11.011.

Neri M, Acocella V, Behncke B, Giammanco S, Mazzarini F, Rust D, Structural analysis of the eruptive fissures at Mount Etna (Italy), *ANNALS OF GEOPHYSICS* 2011, 54(5).

Ramalho, RS, Winckler G, Madeira J, Helffrich GR, Hipolito A, Quartau R, et al., Hazard potential of volcanic flank collapses raised by new megatsunami evidence, *Science Advances* 2015, 1(9), e1500456. <https://doi.org/10.1126/sciadv.1500456>.

Urlaub M, Petersen F, Gross F, Bonforte A, Puglisi G, Guglielmino F, Krastel S, Lange D, Kopp H, Gravitational collapse of Mount Etna's southeastern flank, *Science Advances* 2018, 4 (10), eaat9700.

Paris R, Bravo JJC, Gonzalez MEM, Kelfoun K, Nauret F, Explosive eruption, flank collapse and megatsunami at Tenerife ca. 170 ka, *Nature Communication* 2017, 8, 15246. <https://doi.org/10.1038/ncomms15246>.

Palano M, Episodic slow slip events and seaward flank motion at Mt. Etna volcano (Italy), *Journal of Volcanology and Geothermal Research* 2016, 324, 8–14.

SCIENTIFIC OUTPUT

LIST OF PUBLICATIONS

Lippert A, Sampling Tephra Layers of Etna's explosive activities of the last 15.000 years, Master Thesis 2023, Kiel University

LIST OF CONFERENCE PRESENTATIONS

2022 | **Repeated mapping and geological sampling of Mt Etna's submerged continental margin: First results from RV Meteor expedition M178** EGU General Assembly, Vienna, Austria.

2022 | **Flank instability at Mount Etna: new insights from seafloor deformation monitoring** EGU General Assembly, Vienna, Austria.

2022 | **How to detect slow slip and long-term seafloor deformation? Lessons from two acoustic ranging campaigns on the submerged flank of Mt Etna** EGU General Assembly, Vienna, Austria.

2022 | **Repeated bathymetric mapping offshore Mt Etna: First results from RV Meteor Expedition M178 HazELNUT** DGG, Munich, Germany.

2023 | **Holocene onshore/offshore tephra correlation of Mt. Etna, Sicily** Oceanic
Volcanism Workshop, Kiel, Germany.

DATA

Hydroacoustics:

data are uploaded to the PANGAEA data repository

Sediment samples:

sediment cores are stored in the GEOMAR Core & Rock repository

Geodesy:

sensor and travelttime data are held at GEOMAR.

CRUISE REPORT

M178: submitted – not published yet

MSM81

Onset and modifications in intensity and pathways of water mass exchange between the Southeast Pacific and the South Atlantic with focus on the Falkland Plateau

AUTHORS

Alfred-Wegener-Institut Helmholtz-Zentrum für Polar- und Meeresforschung |
Bremerhaven, Germany

G. Uenzelmann-Neben, B. Najjarifarizhendi

Analysing a set of 30 high-resolution (1 ms sample rate, 500 Hz max frequency, 80 Hz dominant frequency \cong 9 m vertical resolution, 240 channels, 25 m shot interval) seismic profiles on the Falkland Ridge between the Falkland Islands and the MEB (Figure 1) we were able to reconstruct the oceanic circulation in the southwest Atlantic from the late Cretaceous to the present (Najjarifarizhendi and Uenzelmann-Neben, 2021). In contrast to restricted erosion indicating a quiet circulation for the late Cretaceous, the increased formation of sediment drifts and large erosional surfaces point towards an enhanced circulation in the Paleocene/early Eocene. Three activity levels of water masses are observed and interpreted to correspond to proto-UCDW, proto-LCDW, and Southern Ocean Deep Water. This provides evidence for a multi-layered ocean already in the Paleocene/early Eocene. Sediment drift formation bears witness to overspill of the F/MP by proto-LCDW already in the Paleocene/early Eocene (Najjarifarizhendi and Uenzelmann-Neben, 2021). Erosion of the southern and northern flanks shows that the MEB has acted as an obstacle steering the water masses. A significant increase in erosional surfaces in the late Eocene/Oligocene indicates the onset of a highly dynamic circulation regime mainly in two activity levels corresponding to proto-UCDW and proto-LCDW. Overspill of the F/MP appears increased in the late Eocene/Oligocene but decelerated in the early Miocene resulting in sediment drift formation. A deceleration of proto-UCDW in combination with an eastward relocation can also be observed in the early Miocene. Since the middle Miocene both water masses, proto-UCDW and -LCDW, appear to have remained uniform in intensity (within the limits of seismic resolution), maintaining both erosional features and sediment drifts but extending farther eastward. This attests to the strong control of the MEB's topography on the pathways of deep water masses flowing within the ACC (Najjarifarizhendi and Uenzelmann-Neben, 2021).

Two high amplitude cross-cutting reflectors of normal (non-reversed) polarity are identified across the Falkland/Malvinas Basin and Trough (Najjarifarizhendi and Uenzelmann-Neben, 2023). Reflector XR-F/MB appears as a BSR, observed at about 500 ms TWTbsf. In contrast, reflector XR-F/MT is an NBSR, which shows correlation with the geometry of a shallower reflector (reflector R-EMM), an Early-Middle Miocene unconformity that also

shapes the seafloor in the F/MB. The seismic and geometrical properties of reflectors XR-F/MB and XR-F/MT, together with lithological indications from DSDP Sites 327, 329, 330, and Site 511, allow these two cross-cutting reflectors to be associated with the Opal-A to Opal-CT transition zone. However, estimated temperatures at the present depth for these two reflectors based on regional geothermal gradients lie below the minimum temperatures known for the onset of silica diagenesis. The geometrical characteristics of the two cross-cutting reflectors relative to the seafloor, as well as the presence of deformation features in strata between these reflectors and the seafloor reflector (polygonal faults and differential compaction folds) supports their interpretation as fossilized or arrested silica diagenetic fronts (Najjarifarizhendi and Uenzelmann-Neben, 2023). The arrest of this boundary can be explained by a temperature drop due to widespread erosion and sediment removal by the action of abyssal water masses. It is hypothesized that the erosional action of intensified deep and bottom water masses at Early-Middle Miocene subsequent to Antarctic glaciations may have driven the fossilization of the diagenetic front in the study area. Erosion of a minimum of 270 m of overburden is estimated to have occurred, accounting for thermal conditions leading for the fossilization of the silica diagenetic fronts (Najjarifarizhendi and Uenzelmann-Neben, 2023).

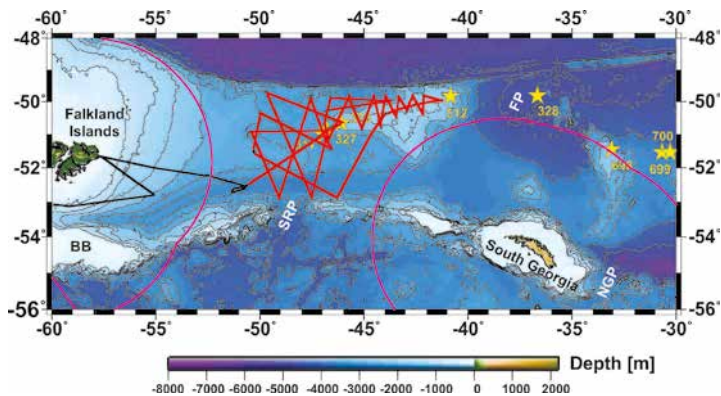


Figure 1: Bathymetry of the Falkland Plateau showing the location of the seismic lines collected during expedition MSM81.

Opening of the Drake Passage-Scotia Sea zone contributed to the completion of a full circumpolar pathway, the establishment of the ACC, and consequently to the vast oceanographic and climatic modifications of the Cenozoic. Investigation of the sedimentary strata across the southern sector of the F/MB and the F/MT using the newly acquired high-resolution 2D seismic reflection data, provided insight into the development of structural and morphological features, coeval with the tectonic and oceanographic evolution in the southwest South Atlantic (Najjarifarizhendi et al., in review). At the southernmost sector of the F/MB and the northern flank of the F/MT, Mesozoic normal faults show reactivation during the Cenozoic. These subvertical faults affect the strata as

young as early to mid-Miocene times (reflector R-EMM). This renewed tectonic activity has occurred subsequent to the underthrusting of the South American Plate below the Scotia Plate, in relation with the development of the Drake Passage and the Scotia Sea.

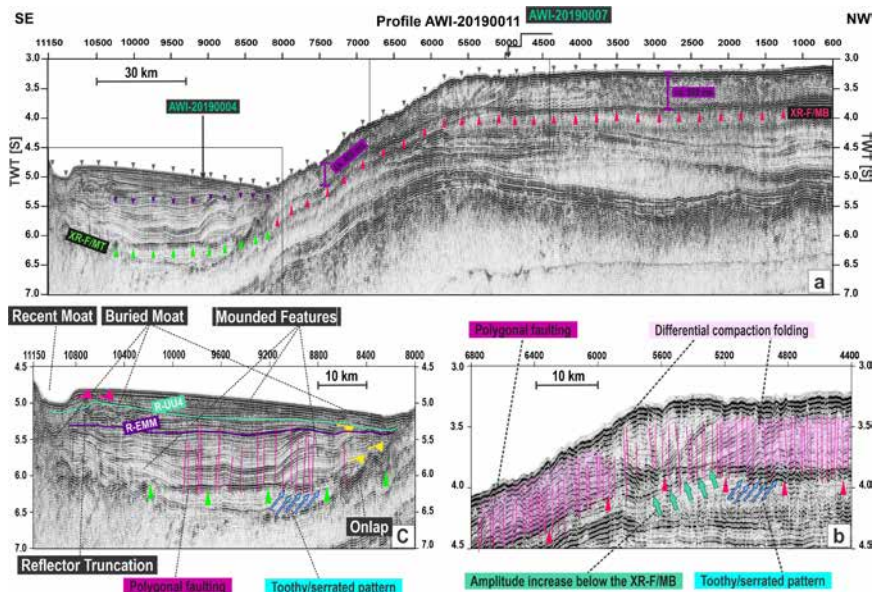


Figure 2: (a) Interpreted seismic profile AWI-20190011. Superimposed is the defined seismic stratigraphy and the marker horizons. The gray and violet triangles respectively mark the seafloor reflector (R-SF) and the Early-Middle Miocene unconformity (R-EMM). The pink and purple triangles respectively mark the cross-cutting reflectors XR-F/MB and XR-F/MT. The black boxes mark the zoomed sections shown in (b) and (c). Arrows show the location of crossing seismic profiles. (b) and (c) Zoomed sections respectively showing the peculiar structural features in proximity of the cross-cutting reflectors XR-F/MB and XR-F/MT (Najjarifarizhendi and Uenzelmann-Neben, 2023).

A package of deformational folds to the south of the F/MT, at the foot of the accreted strata of the NSR, resulted from the transpressional system active in the Cenozoic at the South American Scotian plate boundary (Najjarifarizhendi et al., in review). The strata of Oligocene to early Miocene age underwent deformation in association with the main tectonism of the opening of the Drake Passage-Scotia Sea zone. Prior to mid-Miocene times, sediment waves and minor drift deposits in the F/MT hint at deposition under quiescent abyssal bottom water conditions. The evolution of the Drake Passage by this time, may have allowed for early circulation, however the complete full-depth circum-Antarctic pathway was realized with the end of the magmatism in the Central Scotia Sea and the slab back of the ASSA to the present location of the active South Sandwich Islands volcanic arc.

Since mid-Miocene times, a highly dynamic circulation with action of water masses analogous to today's WSDW has shaped a confined sediment drift at the central floor of

the F/MT (Najjarifarizhendi et al., in review). This vigorous abyssal current activity can be attributed to the full development of the ACC with the tectonic development of the Drake Passage-Scotia Sea zone. This was realized by the deepening of the Drake Passage, the slab-back and demise of the ASSA leading to the opening of the East Scotia Sea, as well as the deep North Georgia Passage. This vast oceanographic reorganization in the Southern Ocean would have contributed to the continent-wide Antarctic glaciation and the enhanced production of bottom water masses below the expanding ice-shelves. Correlation of depth and pathway characteristics of the palaeo-water mass with the present regional oceanographic layout suggests that a branch of proto-WSDW has entered the F/MT through the Georgia Basin since mid-Miocene times; taking a westward path at the southern flank, there making a turn as it overspilled the F/MP confined to the northern slope of the F/MT (Najjarifarizhendi et al., in review).

REFERENCES

Najjarifarizhendi B, Uenzelmann-Neben G, Footprints of palaeocurrents in sedimentary sequences of the Cenozoic across the Maurice Ewing Bank, *Marine Geology* 2021, 438, 106525, doi:<https://doi.org/10.1016/j.margeo.2021.106525>.

Najjarifarizhendi B, Uenzelmann-Neben G, Fossilized silica diagenetic fronts: Implications for palaeoceanographic evolution across the Falkland/Malvinas plateau, *Marine and Petroleum Geology* 2023, 148, 106035, doi:<https://doi.org/10.1016/j.marpetgeo.2022.106035>.

Najjarifarizhendi B, Uenzelmann-Neben G, Gruetzner J, Falkland/Malvinas Trough: Indications for Cenozoic Tectonic and Oceanographic Evolution in the Southwestern South Atlantic, G3 in review.

Wise SW Jr, Schlich R, et al., *Proc. ODP, Sci. Results* 1992, 120: College Station, TX (Ocean Drilling Program), doi:10.2973.odp.proc.sr.120.1992.

SCIENTIFIC OUTPUT

LIST OF PUBLICATIONS

Gutscher M-A, Quétel L, Murphys S, Ricobene G, Royer J-Y, Barreca G, Aurnia S, Klingehoefer F, Petersen F, Urlaub M, Krastel S, Gross F, Kopp H, Detecting strain with a fiber optic cable on the seafloor offshore Mount Etna, Southern Italy, *Earth and Planetary Science Letters* 2023, 616, doi:10.1016/j.epsl.2023.118230.

Jegen A, Lange D, Karstensen J, Pizarro O, Kopp H, Deep-ocean heterogeneity inferred from oceanographically calibrated data of offshore geodetic experiments, *Science Advances* 2023, submitted.

Ma B, Geersen J, Lange D, Klaeschen D, Grevemeyer I, Contreras-Reyes E, Petersen F, Riedel M, Xia Y, Tréhu A, Kopp H, Megathrust reflectivity reveals the updip limit of the 2014 Iquique earthquake rupture, *Nature Communications* 2022, doi:10.1038/s41467-022-31448-4.

LIST OF PUBLICATIONS

Najjarifarizhendi B, Cenozoic Palaeoceanographic evolution of the southwestern South Atlantic: indications from the Falkland/Malvinas Plateau, PhD Thesis 2023, 169 pp, Bremen, Bremen.

Najjarifarizhendi B, Uenzelmann-Neben G, Footprints of palaeocurrents in sedimentary sequences of the Cenozoic across the Maurice Ewing Bank, *Marine Geology* 2021, 438, 106525, doi:<https://doi.org/10.1016/j.margeo.2021.106525>.

Najjarifarizhendi B, Uenzelmann-Neben G, Fossilized silica diagenetic fronts: Implications for palaeoceanographic evolution across the Falkland/Malvinas plateau, *Marine and Petroleum Geology* 2023, 148, 106035, doi:<https://doi.org/10.1016/j.marpetgeo.2022.106035>.

Najjarifarizhendi B, Uenzelmann-Neben G, Gruetzner J, Falkland/Malvinas Trough: Indications for Cenozoic Tectonic and Oceanographic Evolution in the Southwestern South Atlantic, *G³* in review.

LIST OF CONFERENCE PRESENTATIONS

2023 | **Early throughflow of Proto Weddell Sea Deep Water in the Falkland/Malvinas Trough** IODP/ICDP Kolloquium, Hannover, Germany.

2022 | **Active versus arrested silica diagenetic front: Implications on the palaeoceanographic evolution across the Falkland/Malvinas Plateau** IODP/ICDP Kolloquium, Potsdam, Germany.

2022 | **Active versus arrested silica diagenetic front: Implications on the Palaeoceanographic evolution across the Falkland Plateau** EGU, Vienna, Austria & Online. doi:10.5194/egusphere-egu22-3751.

2021 | **Footprints of palaeocurrents in sedimentary sequences of the Cenozoic across the Maurice Ewing Bank** EGU Online. doi:10.5194/egusphere-egu21-10739.

DATA

Multibeam bathymetry raw data:<https://doi.org/10.1594/PANGAEA.902359>

Multibeam bathymetry processed data:<https://doi.org/10.1594/PANGAEA.953877>

Sediment echo sounding data: <https://doi.org/10.1594/PANGAEA.900482>

Seismic profiles:

<https://doi.org/10.1594/PANGAEA.925650>

<https://doi.org/10.1594/PANGAEA.925644>

<https://doi.org/10.1594/PANGAEA.925651>

<https://doi.org/10.1594/PANGAEA.925474>

<https://doi.org/10.1594/PANGAEA.925469>

<https://doi.org/10.1594/PANGAEA.925473>

<https://doi.org/10.1594/PANGAEA.925478>

<https://doi.org/10.1594/PANGAEA.925643>

<https://doi.org/10.1594/PANGAEA.925479>

<https://doi.org/10.1594/PANGAEA.925486>

<https://doi.org/10.1594/PANGAEA.925645>

<https://doi.org/10.1594/PANGAEA.925480>

<https://doi.org/10.1594/PANGAEA.925647>

<https://doi.org/10.1594/PANGAEA.925481>

<https://doi.org/10.1594/PANGAEA.925646>

<https://doi.org/10.1594/PANGAEA.925250>

<https://doi.org/10.1594/PANGAEA.925649>

<https://doi.org/10.1594/PANGAEA.925472>

<https://doi.org/10.1594/PANGAEA.925477>

<https://doi.org/10.1594/PANGAEA.925467>

<https://doi.org/10.1594/PANGAEA.925641>

<https://doi.org/10.1594/PANGAEA.925648>

<https://doi.org/10.1594/PANGAEA.925476>

<https://doi.org/10.1594/PANGAEA.925470>

<https://doi.org/10.1594/PANGAEA.925642>

<https://doi.org/10.1594/PANGAEA.925640>

<https://doi.org/10.1594/PANGAEA.925639>

<https://doi.org/10.1594/PANGAEA.925653>

<https://doi.org/10.1594/PANGAEA.925462>

<https://doi.org/10.1594/PANGAEA.925468>

CRUISE REPORT:

MSM81: doi: 10.2312/cr_msm81

MSM93

Submesoscale Dynamics in Fram Strait

AUTHORS

Alfred Wegener Institute, Helmholtz Centre for Polar and Marine Research | Bremerhaven, Germany

W.-J. von Appen, T. Kanzow, A. Bracher

MARUM Center for Marine Environmental Sciences | Bremen, Germany

M.H. Iversen, M. Walter

The cruise originally had been applied, granted, and planned to take place on R/V HEINCKE as HE558, but that had to be cancelled during the early days of the pandemic. After complete cancellation of cruise activities of the German research fleet in spring 2020, R/V MERIAN supplied R/V POLARSTERN in Svalbard as part of the Mosaic experiment. Afterwards, the first restarted independent science cruise was this cruise, MSM93. This entailed a number short term replanning activities regarding personnel and equipment. Furthermore, it should be noted that the number of cruise participants at 13 was much smaller than for a typical R/V MERIAN cruise.

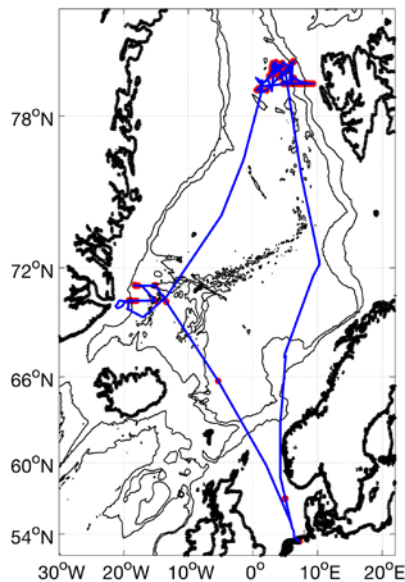


Figure 1: Track chart of R/V MERIAN Cruise MSM93. Bathymetry from GEBCO. Stations in red with two main working areas in Fram Strait and offshore of Scoresby Sund.

Due to Corona, all participants of MSM93 had to stay in a hotel in Leer from 21 June onwards and get tested. After the negative test results had arrived, we were taken to R/V MERIAN in the port of Emden by bus on 24 June. Our containers and non-containerized cargo were loaded and we were able to set up some of our equipment and start testing it. On June 26 we departed Emden and started the 6-day transit to the working area. Most of the transit was smooth, but on one day most scientists were sea-sick.

July 2 to July 6 constituted the first part of the cruise in the eastern Fram Strait. We used it for the testing of various instrument and laboratory procedures and we completed a CTD section across the West Spitsbergen Current. But the majority of that time was dedicated to mooring work. We recovered 5 moorings that are part of a long-term observation program of the AWI to monitor the warm Atlantic Water which flows into the Arctic Ocean. The recoveries went well and even included a so-called trawl resistant bottom mount, something which had eluded us in previous years for a multitude of different technical reasons. After the recoveries, we deployed 4 moorings. On one day we even had perfect sunny calm summer weather.

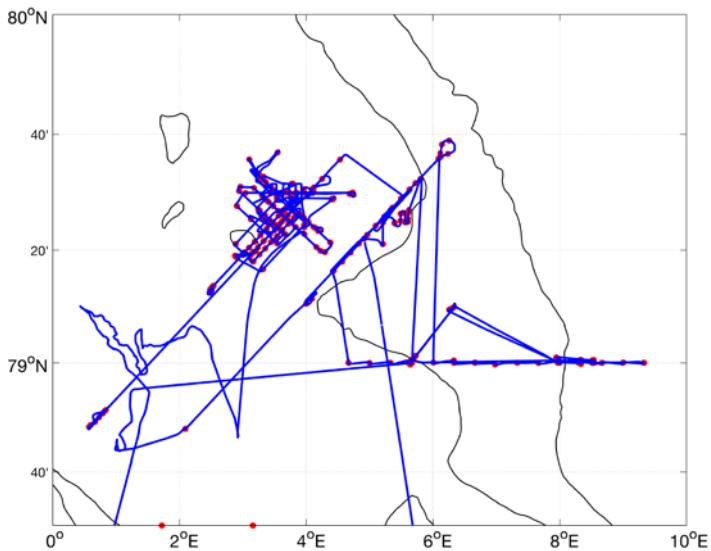


Figure 2: Track chart of RV MERIAN Cruise MSM93 in Fram Strait.

July 7 and July 8 marked the transition to the small-scale work that was the second part of the cruise. We occupied an in-situ camera transect parallel to the ice-edge comprised of 10 stations at a 4 km horizontal resolution. This was followed by the first extensive deployment of the Triaxus towed system. A 100 km section was occupied three times with measurements at three different constant depths. During this transect we identified a region of extremely strong horizontal gradients: a front.

We returned to that front near the ice-edge and sampled it extensively from July 9 to July 16. At that front warm salty Atlantic Water was subducted below cold fresh Polar Water. The goal of the survey was to map the front's complete spatial structure and how it evolved over time. For this we deployed all our gears with a rough separation of towed observations during night-time and stations during day-time. We towed the Triaxus as well as the underway CTD and observed the currents with the vessel mounted ADCP. We made profiles with the CTD-rossette, in-situ camera, and light optical package. Water was collected from the CTD-rossette, marine snow catcher and the ship's sea water intake and samples were collected for nutrient concentrations, primary production, particle properties (e. g. sinking speed and oxygen consumption), phytoplankton concentrations and functional group composition, CFCs, noble gases, and tritium. We deployed surface drifters and drifting sediment traps. During transit, optical properties of the surface water were also measured and we monitored the ship's radar which showed the line at which the subduction took place.

After completion of the front study, we celebrated the cruise's half time (Bergfest) and left Fram Strait. July 17 to July 19 was a transit to the shelf in front of Scoresby Sund in eastern Greenland. Unfortunately, those days were also marked by a storm which did not play out as forecast. Rather it pushed thick multi-year sea ice in front of the entrance of Scoresby Sund. We attempted to get into the fjord on July 19 and July 20. But at nearly 100% concentration the ice was too thick for R/V MERIAN and we had to abort late on July 20. Therefore, we were not able to recover two oceanographic moorings deep in Scoresby Sund, one oceanographic mooring at the entrance of Scoresby Sund, and one passive acoustics mooring in front of the fjord.

By the end of July 21 we were back at the shelfbreak and until July 25, while waiting for better ice conditions, we proceeded to occupy two transects somewhat longer than 100 km from the ice-edge across the East Greenland Current to the open ocean. We periodically returned to the ice-edge to check whether the ice conditions had improved which they however had not.

On July 25 we started the transit home and occupied a last deep station in the international waters east of Iceland. Parts of the remainder of the transit home were windy enough to cause some sea-sickness again, but we were able to store all our equipment and samples and to save and document the collected data. On July 30 the cruise successfully commenced in the port of Emden.

The cruise serviced the AWI physical oceanography moorings in the West Spitsbergen Current. They are long-term observations maintained since 1997 to observe the transport and properties of the Atlantic Water entering the Arctic Ocean. Given the nature of long-term observations, additional two years of recovered data rarely directly lead to new studies, but over the course of several years/decades various studies add up, e. g. <https://www.awi.de/en/science/climate-sciences/physical-oceanography/long-term-observations/long-term-observations-arctic.html>.

The majority of the cruise was spent on the process study in Fram Strait heavily modeled upon the conclusions of von Appen et al (2018). This process study primarily provided data for the PhD theses of Z. Hofmann and W. Körtke (both funded from (AC)3) and for the BSc and MSc theses of B.-L. Duong. The main results from this process study can be summarized as follows.

At high latitudes, submesoscale dynamics act on scales of $O(100\text{m}-1\text{km})$ and are associated with the breakdown of geostrophic balance, vertical velocities, and energy cascading to small scales. Submesoscale features such as fronts, filaments, and eddies are ubiquitous in marginal ice zones forced by the large horizontal density gradients. In July 2020, we identified multiple fronts and filaments using a towed undulating vehicle near the sea ice edge in central Fram Strait, the oceanic gateway to the Arctic Ocean between Greenland and Svalbard. Sea ice covered the entire study region 1–2 weeks earlier, and a stratified meltwater layer was present. We observed a front between warm and saline Atlantic Water and cold and fresh Polar Water at 30–85 m depth, where we identified a subsurface maximum in chlorophyll fluorescence and other biogeochemical properties extending along the tilted isopycnals down to 75 m, indicating subduction of Atlantic Water (mixed with meltwater), which had previously occurred. The meltwater layer also featured multiple shallow fronts, one of which exhibited high velocities and a subsurface maximum in chlorophyll fluorescence, possibly indicating subduction of Polar Water below the meltwater layer. The fronts at different depth levels suggest a stepwise subduction process near the ice edge, where water subducts from the surface below the meltwater and then further down along subsurface fronts. The submesoscale features were part of a larger-scale mesoscale pattern in the marginal ice zone. As sea ice continuously retreats, such features may become more common in the Arctic Ocean.

The last part of the cruise aimed to recover moorings in Scoresby Sund, but this could not be achieved due to the sea ice conditions. These moorings were subsequently recovered during PS131 in 2022 and the associated data evaluation has only started.

REFERENCES

von Appen W-J, Wekerle C, Hehmann L, Schourup-Kristensen V, Konrad C, Iversen M-H, Observations of a submesoscale cyclonic filament in the marginal ice zone, *Geophysical Research Letters* 2018, <https://doi.org/10.1029/2018GL077897>.

SCIENTIFIC OUTPUT

LIST OF PUBLICATIONS

Hofmann Z, von Appen W-J, Kanzow T, Becker H, Hagemann J, Hufnagel L, Iversen MH, Stepwise Subduction Observed at a Front in the Marginal Ice Zone in Fram Strait, Journal of Geophysical Research, submitted.

Hufnagel L, Ramondenc S, Konrad C, von Appen W-J, Hofmann Z, Torres Valdés S, Stefels J, Moradi N, Bracher A, Waite A, Iversen MH, Carbon export in an Arctic frontal system in Fram Strait, Frontiers of Marine Research, in preparation.

Duong BL, Statistics of horizontal density gradients in the ocean. MSc Thesis, Univ. Oldenburg, in preparation.

Duong BL, Identification of fronts in Fram Strait near the Marginal Ice Zone. BSc Thesis, Univ. Bremen, 2021.

LIST OF CONFERENCE PRESENTATIONS

2023 | **Independent validation of EUMETSAT OLCI aspirational inherent optical properties' products** Sentinel-3 Validation Team Meeting, Darmstadt, Germany

2023 | **Hijacking other sensors for ocean colour** Sentinel-3 Validation Team Meeting, Darmstadt, Germany

2023 | **Hijacking other sensors for ocean colour** International Ocean Colour Science Meeting, St. Petersburg, FL, USA

2023 | **The biological carbon pump in changing polar regions** Gordon Research Conference, Polar Marine Science, Ventura, CA, USA

2022 | **Subduction as Observed at a Submesoscale Front in the Marginal Ice Zone in Fram Strait** European Geosciences Union General Assembly, Wien, Austria

2022 | **Subduction as Observed at a Submesoscale Front in the Marginal Ice Zone in Fram Strait** Ocean Sciences Meeting, Honolulu, HI, USA

2021 | **Upper ocean processes in Fram Strait and the central Arctic** (AC)3 Science Conference on Arctic Amplification, Potsdam, Germany

2020 | **The MSM93 cruise** Oceanography Seminar Univ. Bremen, Bremen, Germany

DATA

Raw data from surface drifters:

<https://doi.org/10.1594/PANGAEA.939736>

Raw data from 38kHz VM-ADCP (vessel-mounted Acoustic Doppler Current Profiler):

<https://doi.org/10.1594/PANGAEA.940074>

Raw data from 75kHz VM-ADCP (vessel-mounted Acoustic Doppler Current Profiler):

<https://doi.org/10.1594/PANGAEA.940037>

Continuous ocean current profiles measured with 75kHz VM-ADCP (vessel-mounted Acoustic Doppler Current Profiler):

<https://doi.org/10.1594/PANGAEA.940023>

Raw data of physical oceanography:

<https://doi.pangaea.de/10.1594/PANGAEA.941682>

Physical oceanography measured with UCTD (Underway CTD):

<https://doi.org/10.1594/PANGAEA.939712>

Raw data from UCTD (Underway CTD):

<https://doi.org/10.1594/PANGAEA.939733>

Raw data from Triaxus topAWI (towed ocean profiler of the AWI):

<https://doi.org/10.1594/PANGAEA.940002>

Physical Oceanography measured with CTD on Triaxus topAWI (towed ocean profiler of the AWI):

<https://doi.org/10.1594/PANGAEA.940010>

Metadata of mooring F4-OZA in the Fram Strait, September 2018 - July 2020:

<https://doi.org/10.1594/PANGAEA.942179>

Raw physical oceanography and ocean current velocity data from mooring F2-19 in the Fram Strait, September 2018 - July 2020:

<https://doi.org/10.1594/PANGAEA.942172>

Raw physical oceanography and ocean current velocity data from mooring F1-17 in the Fram Strait, September 2018 - July 2020:

<https://doi.org/10.1594/PANGAEA.941161>

Raw physical oceanography and current meter data from mooring F5-18 in the Fram Strait, September 2018 - July 2020:

<https://doi.pangaea.de/10.1594/PANGAEA.942176>

Raw physical oceanography and ocean current velocity data from mooring F3-18 in the Fram Strait, September 2018 – July 2020:

<https://doi.org/10.1594/PANGAEA.942178>

CRUISE REPORT

MSM93: https://doi.org/10.48433/cr_msm93

MSM94

Subpolar North Atlantic transport variability

AUTHORS

GEOMAR Helmholtz Zentrum für Ozeanforschung Kiel | Kiel, Germany
J. Karstensen

OVERVIEW

The scientific program of the MARIA S. MERIAN MSM94 expedition was dedicated to studies on the intensity of water mass transformation and the transport of water masses in the boundary current systems off Labrador and at the southwestern tip of Greenland. During the expedition we re-deployed 11 moorings and recovered 1 ocean bottom lander. Measurements of the vertical structure of temperature, salinity, density, oxygen, optical properties and the currents along selected sections have been surveyed during the MSM94 expedition. Close to the surface, permanent registrations are carried out with the thermosalinograph (temperature, salinity) and meteorological data are quasi continuously collected. Current measurements from the surface to approximately 1000m depth have been recorded with the ships installed ADCPs (75kHz, 38kHz) (Figure 1). Argo floats (IFREMER, BSH) and surface drifter (NOC, UK) were also deployed. The expedition was a contribution to international projects (OSNAP, Blue Action, EuroSea). Because this expedition was conducted during the COVID-19 pandemic and start/end-port was Emden, Germany, some modifications to the science program were needed because of reduced science crew and respective cut's in data acquisition).

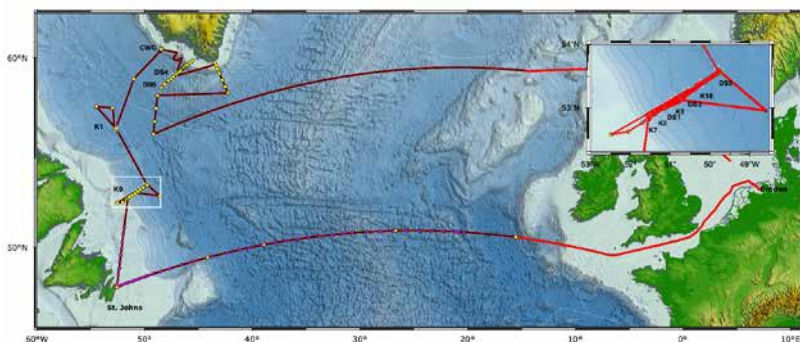


Figure 1: Track chart of R/V MARIA S MERIAN MSM94 cruise track (red) and station overview. Black line: ADCP/TSG Underway data; red dots uCTD; yellow dots: CTD stations; cyan stars: Mooring location.

TRANSPORT

One important objective of the cruise was the re-deployment of moorings as part of the 53°N observatory at the exit of the Labrador Sea (Zantopp et al. 2017). Integrating the current data from these moorings across the area of Deep Western Boundary Current (DWBC) provides estimate of volume transport for the water leaving the Labrador Sea and eventually turning southward, towards the equator (Figure 2). The transport is estimated in two compartments: the upper part (400m to 1850m) can be attributed to the Labrador Sea, the lower part (1850m to seafloor) to the lower North Atlantic Deep Water (LNADW). Through the recovery and the new deployment of the moorings array that belongs to the 523°N observatory, the cruise MSM94 was instrumental for acquiring 4 years of data (2018–2020 and 2020–2022). The data complements the time series that is maintained since 1997 at this location. One important finding is the quasi-decadal transport variability in the boundary current (Figure 2) that has been attributed to North Atlantic Oscillation (NAO) forcing (wind, buoyancy).

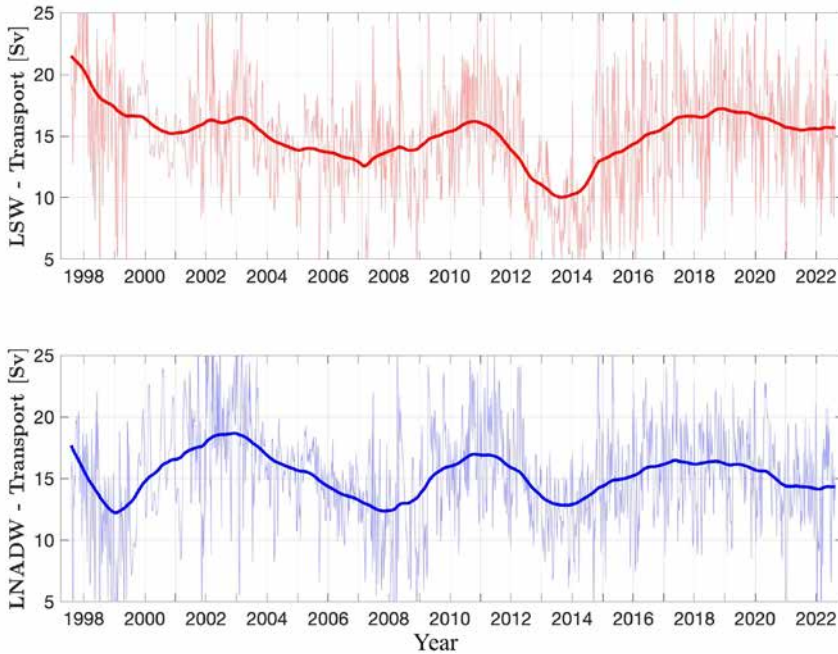


Figure 2: Export from the Labrador Sea at 5-day resolution and without gaps; black lines are for periods of full array coverage; green lines for periods with reduced coverage but with central mooring K9 in place, and magenta lines for gaps filled by SSA (EOF) modes. The low-frequency variation is dominated by a pair of SSA modes at quasi-decadal time scales. For the (a) Labrador Sea water (400m to 1850m) and the (c) LNADW extending from 1850 to the bottom. Recent years (F. Dilmahamod, pers. comm.) are added to the published transport (Zantopp et al. 2017).

Data from the moored sensors also have been combined with data from various other moored sensors from within the OSNAP international consortium that create an array

crossing the full subpolar North Atlantic, from Labrador, via the southern tip of Greenland to Scotland (Lozier et al. 2019). The MSM94 recovered data provides a significant contribution to constraining the western Subpolar North Atlantic overturning transport (volume, heat, freshwater). In the most recent publication of the full array and covering six years of data, from 2014 to 2020 (Figure 3), Fu et al. (2023) could isolate a seasonal cycle of the AMOC transports (Figure 4).

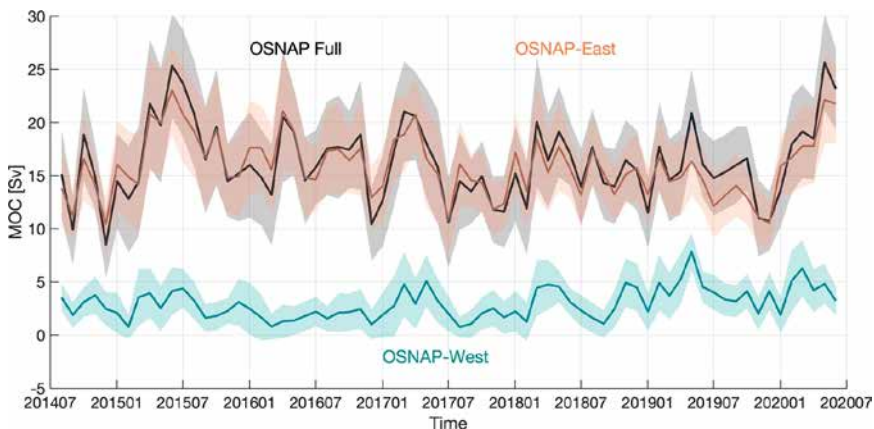


Figure 3: Monthly overturning circulation time series across the full OSNAP array (black), OSNAP East (orange), and OSNAP West (cyan) from Fu et al. (2023). Shading indicates monthly uncertainty estimated from a Monte Carlo analysis (Lozier et al. 2019).

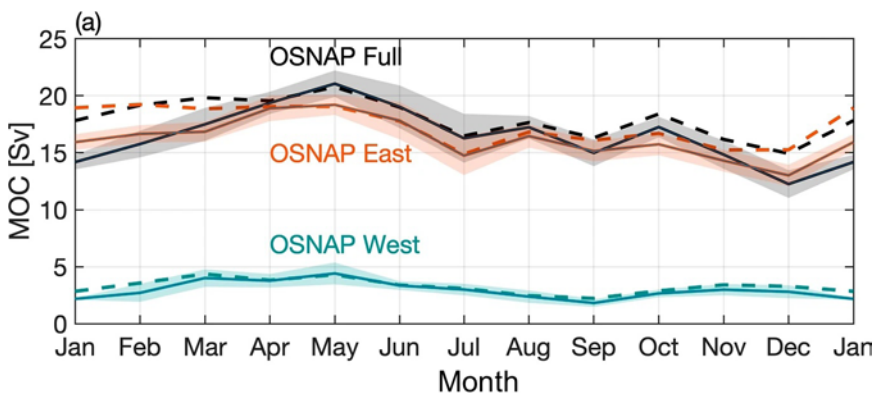


Figure 4: Monthly climatology of the MOC across the full OSNAP array (solid black), OSNAP East (solid orange), and OSNAP West (solid cyan). Shading indicates the standard error of the monthly climatology over the 6-year OSNAP observation period. Dashed lines indicate the MOC seasonal cycle with both the Ekman transport and Ekman transport return flow removed (see Fu et al. 2023).

SYNOPTIC SURVEYS

Hydrographic surveys were done during MSM94 (see Figure 1) but not the full section from Labrador to Greenland (called “OSNAP West”) as proposed because of time limitations as a consequence out of the COVID pandemic. However, importantly a high-resolution synoptic state of currents, hydrography, and other properties (e. g. particles via the Underwater Vision profiler or nutrients via the OPUS ultraviolet spectral sensor) along the 53°N observatory was recorded as well as section through the Deep Western boundary current at two locations off southern Greenland.

REFERENCES

Fu Y, et al., Seasonality of the Meridional Overturning Circulation in the Subpolar North Atlantic, *Nature Communications* 2023, <https://doi.org/10.1038/s43247-023-00848-9>.

Lozier MS, et al., A Sea Change in Our View of Overturning – First Results from the Overturning in the Subpolar North Atlantic Program, *Science* 2019, 363, 516–521, February 1, doi: 10.1126/science.aau6592.

Zantopp R, Fischer J, Visbeck M, and Karstensen J, From interannual to decadal: 17 years of boundary current transports at the exit of the Labrador Sea, *J. Geophys. Res. Oceans* 2017, 122, doi:10.1002/2016JC012271.

SCIENTIFIC OUTPUT

LIST OF PUBLICATIONS

Han, Exploring the AMOC Connectivity Between the RAPID and OSNAP Lines With a Model-Based Data Set, *Geophysical Research Letters* 2023, doi: 10.1029/2023GL105225

Petit T, Lozier MS, Rühs S, Handmann P, Biastoch A, Propagation and transformation of upper North Atlantic Deep Water from the subpolar gyre to 26.5°N, *Journal of Geophysical Research: Oceans* 2023, 128, e2023JC019726. <https://doi.org/10.1029/2023JC019726>

Petit T, Robson J, Ferreira D, Jackson LC, Understanding the sensitivity of the North Atlantic subpolar overturning in different resolution versions of HadGEM3-GC3.1, *Journal of Geophysical Research: Oceans* 2023, 128, e2023JC019672. <https://doi.org/10.1029/2023JC019672>

Wimart-Rousseau C, Steinhoff T, Klein B, Bittig H, Körtzinger A, Technical note: Enhancement of float-pH data quality control methods: A study case in the Subpolar Northwestern Atlantic region, *Biogeosciences Discuss.* [preprint], <https://doi.org/10.5194/bg-2023-76>, in review, 2023.

Fu Y, et al., Seasonality of the Meridional Overturning Circulation in the Subpolar North Atlantic, *Nature Communications* 2023, <https://doi.org/10.1038/s43247-023-00848-9>, (for citations see: https://scholar.google.com/scholar?cites=15419068475962288039&as_sdt=2005&sciodt=0,5&hl=en).

Kiko R, et al., A global marine particle size distribution dataset obtained with the Underwater Vision Profiler 5, *Earth Syst. Sci. Data* 2022, 14, 4315–4337, <https://doi.org/10.5194/essd-14-4315-2022>.

Koelling J, Atamanchuk D, Karstensen J, Handmann P, Wallace DWR, Oxygen export to the deep ocean following Labrador Sea Water formation, *Biogeosciences* 2022, 19, 437–454, <https://doi.org/10.5194/bg-19-437-2022>, 2022.

Knaack C, Investigating the Exchange between Labrador Sea and Irminger Sea using Hydrographic Data, BSc thesis 2023, CAU Kiel.

Kunst T, Characterizing mesoscale eddies in the Labrador Sea based on data from moored observations, MSc thesis 2023, CAU Kiel.

Gößling P, Dynamics of Transport Variability in the Deep Western Boundary Current of the Subpolar North Atlantic, BSc thesis 2023.

Losch P, Biogeochemical characteristics in subpolar deep convection regions, MSc. Thesis 2022, CAU Kiel.

Leimann I, Temporal and spatial variability of the Deep Western Boundary. Current, MSc. Thesis 2022, CAU Kiel.

LIST OF CONFERENCE PRESENTATIONS

2023 | **Updating Lower North Atlantic Deep Water transports in the sub-polar North Atlantic** IAPSO, Berlin, Germany

2023 | **The 53°N observatory: 25 years time series data from the exit of the Labrador Sea (Invited)** The Sixth Xiamen Symposium on Marine Environmental Sciences, Xiamen, China

2023 | **Deep Western Boundary Current variability in the Labrador Sea and its link with sea surface height variability** CLIVAR Workshop, Hamburg, Germany

2023 | **Wind driven Ekman transport vs eddies – ultimate fight or peaceful cooperation in the Labrador Sea?** EGU GA 2021, Vienna, Austria

2022 | **25 years of Eulerian time series observations at the exit of the Labrador Sea – the 53°N array** AGU Fall meeting, San Francisco, USA

2022 | **The 53°N array from remote sensing: Combining in situ data and satellite altimetry** OSNAP Workshop, online

DATA

Physical oceanography (CTD):

<https://doi.pangaea.de/10.1594/PANGAEA.963675> (in review)

IADCP:

<https://doi.pangaea.de/10.1594/PANGAEA.963646> (in review)

Underway CTD:

<https://doi.pangaea.de/10.1594/PANGAEA.963681> (in review)

ADCP (38kHz, 75kHz):

<https://doi.pangaea.de/10.1594/PANGAEA.963542> (in review)

UVP5 particle dataset:

<https://doi.org/10.1594/PANGAEA.924375>

Multibeam bathymetry raw:

<https://doi.pangaea.de/10.1594/PANGAEA.927311>

Multibeam bathymetry processed:

<https://doi.pangaea.de/10.1594/PANGAEA.952415> (in review)

Thermosalinograph data:

<https://doi.pangaea.de/10.1594/PANGAEA.958451>

Drifter data is part of GDP dataset:

<https://doi.org/10.25921/x46c-3620>

Argo Float data:

<http://doi.org/10.17882/42182#96550>

Meridional Overturning transport:
<https://doi.org/10.35090/gatech/70342>

CRUISE REPORT

MSM94: doi:10.48433/cr_msm94

MSM95

Mapping, fauna and trawling impacts of the deep Arctic seafloor

AUTHORS

Alfred Wegener Helmholtz Centre for Polar and Marine Research | Bremen, Germany
A. Purser

THE MSM95 (GPF 19-2_05) 2020 ARCTIC EXPEDITION – A COVID-19 CRUISE

The MSM95 (GPF 19-2_05) expedition was an RV Maria S. Merian expedition which was proposed during the first year of the COVID-19 pandemic, and as such focused on research which could be conducted within reasonable vicinity of Emden, Germany. A young scientific team of scientists, engineers and technologists took part in this multidisciplinary expedition during the global period of concern, with exemplary support from the Deutsche Forschungsgemeinschaft (DFG) who kindly funded this cruise (replacing a planned AWI led cruise intended for R/V Heincke before the crisis). The Leitstelle Deutsche Forschungsschiffe in Hamburg, Germany and Briese Schifffahrts GmbH & Co. KG and the AWI ship coordination team who all supplied their support and assistance throughout. NASA-JPL had originally been intended as participants for the expedition, but unfortunately COVID-19 conditions prevented two engineers joining the shipboard party, but good relations were maintained throughout and after the cruise, which have assisted in the construction of the 'Remora' class ROVs currently in operation within the Deep Sea Ecology and Technology group in AWI.

THE MAIN AIM OF THE MSM95 (GPF 19-2_05) EXPEDITION

The main aim of the MSM95 research expedition was to investigate and map physical impacts on the arctic seafloor in two distinct and contrasting Arctic areas – 1) The western Svalbard shelf edge and 2) the HAUSGARTEN time series stations in the FRAM strait. A 'nested' data approach was conducted in each research area, with broad seafloor mapping conducted initially with the R/V MARIA S. MERIAN onboard acoustic systems (The EM122 and EM712 bathymetric systems), followed by focused subsequent mapping conducted by PAUL 3000 automated underwater vehicle (AUV) sidescan and camera deployments, Ocean Floor Observation and Bathymetry System (OFOBS) towed sidescan and camera trawls and finally with very high resolution investigations conducted with a new mini-ROV launched directly from the OFOBS for close seafloor visual analysis. These data will be used to produce spatial distribution maps of iceberg and fishery impacts on the seafloor at three locations to the north, south and west of the Svalbard Archipelago, as well as maps of drop stone and topography variations across several of the HAUSGARTEN stations.

One of the key reasons for investigating the Svalbard seafloor with AUV and OFOBS acoustic systems was to determine whether or not seafloor trawl marks could be gauged readily with these systems. By also conducting the camera surveys concurrently, the aim was to collect data to determine whether or not any mapped trawl features impacted negatively on seafloor fauna.

ADDITIONAL AIMS OF THE MSM95 (GPF 19-2_05) EXPEDITION

Further aims of the expedition were to conduct water column work across our research areas. We conducted numerous water column camera trawls to image inhabitants at various depths, with a focus on identifying squid populations throughout the Arctic water column. We also sampled waters via CTD from throughout the water column, to continue the microbial observatory work (MicrObs) time series work carried out as part of the FRAM project by AWI and MPI researchers, to investigate the eDNA composition of the waters for analysis of squid presence / absence and bacterial community structure.

Further opportunistic work was conducted between stations, with floating litter surveys conducted to input into the ongoing records being collated by the AWI. An inspection of the NOMAD tracked vehicle, deployed last year in the HAUSGARTEN area was made, which observed the vehicle to be stuck on a stone obstruction. By reconfiguring OFOBS with hooked ropes, the NOMAD was manually freed from the obstruction by the captain and crew of MSM95.

MAPPING AND IMAGING RESULTS OF THE MSM95 (GPF 19-2_05) EXPEDITION

Good weather and ice conditions were prevalent during the expedition, and excellent acoustic data was collected with the RV Maria S. Merian integrated systems as well as with the AUV and towed OFOBS systems brought by the cruise participants. The maps generated during the MSM95 expedition (Figure 1) are a great improvement on those used in the Fram Strait area by the annual HAUSGARTEN expeditions run by AWI. These new maps have allowed new benthic research topics on methane seepage to be carried out during the last two years with RV Polarstern. The maps also indicate numerous pockmark features to the south of Svalbard, which showed distinct seafloor communities in bottom photographs.

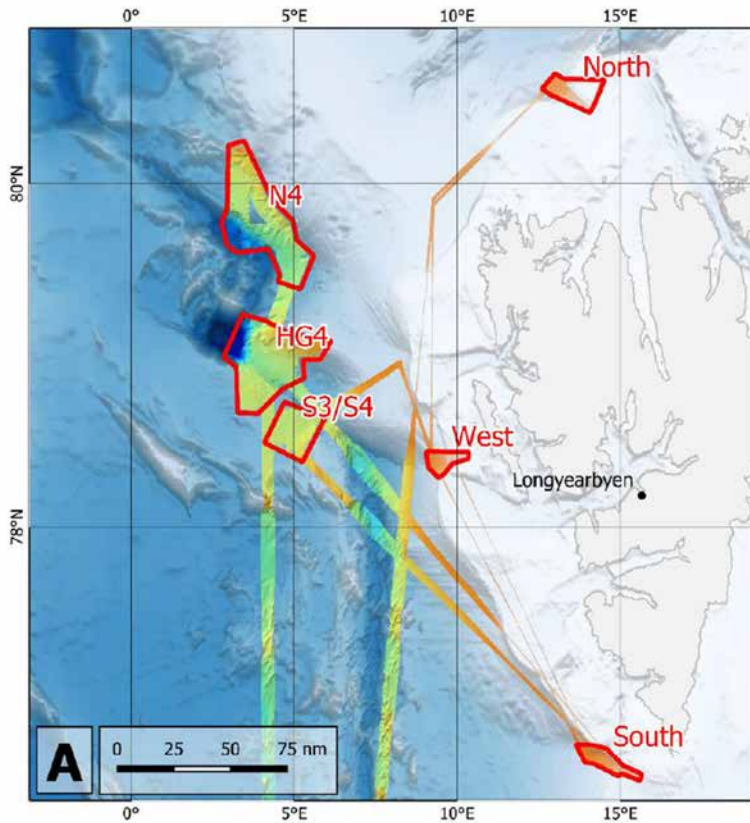


Figure 1: Map showing the regions of seafloor mapped with the R/V Maria S. Merian EM122 and EM712 bathymetric systems during the MSM95 expedition. AUV and OFOBS sidescan data and video and still camera imagery was also collected from within these regions.

High resolution mapping carried out by AUV and OFOBS showed abundant trawl marks around the Svalbard area, down to depths of approximately 1000 m (Figure 2).

Imaging results from these platforms confirmed a reduction in seabed fauna in the trawl tracks. These images are currently forming part of a EU Erasmus+ pilot citizen science project developing interfaces to allow the interested public to directly assist monitoring efforts – the ‘Into The Deep’ project. Within this project, the MSM95 data will allow citizens to log animals in images, to aid in quantifying image abundances in trawled and untrawled areas.

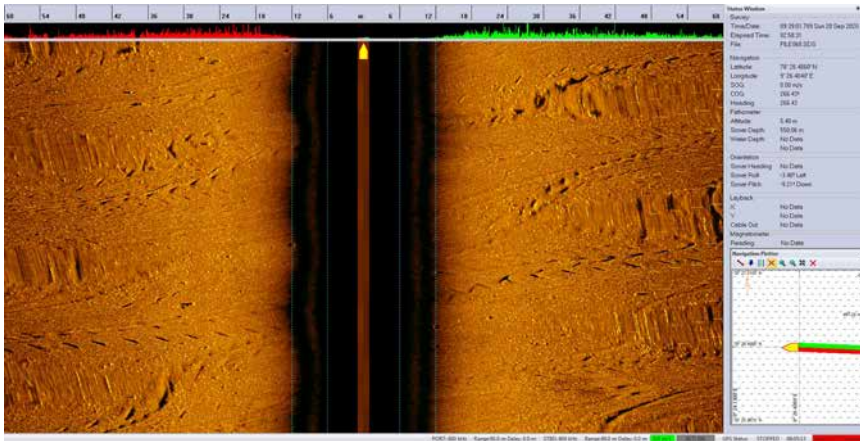


Figure 2: Sidescan data collected from 550m depth with the AUV "Paul 3000" on the continental margin. A 60 m swathe either side of the vehicle can be seen in this waterfall diagram. Numerous trawl door impacts and drag marks are visible.

FURTHER RESEARCH HIGHLIGHTS

To aid in seafloor analysis, and lost equipment recovery, the MSM95 expedition was the first real test cruise for the AWI 'Remora' class ROV platform. This small robot was successfully used to aid in the freeing of a trapped seafloor crawler on the seafloor, and for the biological analysis of the animals within a pockmark at the southern station.

Seafloor floating litter was logged during the expedition, data which has already seen publication. Useful time series physical oceanographic data was collected to augment the HAUSGARTEN time series work carried out annually by AWI. Opportunistic observations of octopi have also led to incorporation of imaging data into a paper outlining octopus feeding behaviour in the Arctic. Various other papers are foreseen in the next years, on habitat integrity post-fishing impacts, further behavioural and distribution studies and papers on deep sea microbial life.

SCIENTIFIC OUTPUT

LIST OF PUBLICATIONS

Golikov AV, Stauffer JB, Schindler SV, Taylor J, et al., Miles down for lunch: deep-sea in-situ observations of Arctic finned octopods *Cirroteuthis muelleri* suggest pelagic-benthic feeding migration, Proc R Soc B 2023, 290, 20230640, doi: 10.1098/rspb.2023.0640.

Merten V, Puebla O, Bayer T, Reusch TBH, et al., Arctic nekton uncovered by eDNA metabarcoding: Diversity, potential range expansions, and pelagic-benthic coupling, *Environmental DNA* 2023, 5, 503–518, doi: 10.1002/edn3.403.

Priest T, Vidal-Melgosa S, Hehemann J-H, Amann R, et al., Spatial heterogeneity in carbohydrates and their utilization by microbes in the high North Atlantic, *bioRxiv preprint*, 2023, doi: 10.1101/2023.05.11.540373

Tekman MB, Gutow L, Berbmann M, Marine debris floating in Arctic and Temperate Northeast Atlantic Waters, *Mar Sci* 2022, 9, 933768, doi: 10.3389/fmars.2022.933768

LIST OF CONFERENCE PRESENTATIONS

2023 | **Into The Deep** Ocean Training 2023, Ghent, Belgium.

DATA

Metagenomic and metatranscriptomic data:

<https://www.ebi.ac.uk/ena/browser/view/PRJEB58071>

Monosaccharine concentrations:

<https://doi.org/10.1594/PANGAEA.957737>

Multibeam EM122 raw bathymetry:

<https://doi.org/10.1594/PANGAEA.924922>

Multibeam EM712 raw bathymetry:

<https://doi.org/10.1594/PANGAEA.924923>

Multibeam EM122 processed bathymetry:

<https://doi.org/10.1594/PANGAEA.950421>

Multibeam EM712 processed bathymetry:

<https://doi.org/10.1594/PANGAEA.950422>

Physical oceanography:

<https://doi.pangaea.de/10.1594/PANGAEA.943220>

Seabed photographs:

<https://doi.org/10.1594/PANGAEA.928815>

CRUISE REPORT

MSM95: doi:10.48433/cr_msm95

MSM96

Metal geochemistry meets machine learning: Assessing sedimentary and pore-water rare earth element variability from local to basin scale across the NE Atlantic Ocean

AUTHORS

GEOMAR Helmholtz Centre for Ocean Research Kiel | Kiel, Germany
S. Paul, F. Scholz, T. Schoening

Cruise MSM96 sailed to assess small- and large-scale geochemical and seafloor substrate heterogeneity across the NE Atlantic basin (Schoening and Paul 2021). We employed a hierarchical surveying strategy at three spatial scales: local, regional, and basin, to investigate trace metal and specifically Rare Earth Element and Yttrium (REY) concentrations and patterns. At each of the survey sites Porcupine Abyssal Plain (PAP) and Iberian Abyssal Plain (IAP), we sampled covering three data resolution scales: centimeter (TV-MUC), meter (OFOS), and kilometer scale (MBES). Our objective was to quantify the impact of topography on the geochemistry within and between regions and to establish the link – across resolution scales – between geochemistry, imagery, and bathymetry to facilitate spatial extrapolation of seafloor geochemical data and substrate characteristics to kilometer-scale. We studied three topography types: valleys, plains, and hills. Their location was objectively chosen by a geomorphons terrain classification and the topographical height was approximately +/- 100 m for hills and valleys, respectively. By studying heterogeneity on the local and regional scales, we focused on topographic heterogeneity because spatial heterogeneity with respect to particle and organic matter flux from the sea surface can be expected to be minimal. As a basis, solid-phase and pore-water samples were taken for on-shore lab analyses of porosity, major elements, total organic carbon (TOC) and total nitrogen (TN), nutrients (nitrate, phosphate, silicate), and dissolved Mn and Fe. This basic data helps to assess REY controls in the solid phase and pore water. All geochemical parameters together will be used to assess local- to basin-scale heterogeneity and how it is linked to topography. In the future, this should be extended to also incorporate, e. g., oceanography, mineralogy, microbiology, and eventually link all these parameters across scales.

Cruise MSM96 was designed to acquire data for our research hypotheses that: - seafloor substrate and habitats as well as geochemistry of plains is less variable on each spatial scale than in valleys and hills, - shale-normalized REY patterns are less variable across topography types and scales than REY concentrations, - varying image-derived seafloor features of substrates and habitats can be linked with point-based geochemistry measurements to extrapolate those to larger areas, - automated and well-documented data acquisition and processing workflows from sea to public archives speed up data analysis and FAIR data publication.

The hierarchical surveying strategy employed during cruise MSM96 was designed to: - assess the heterogeneity within one topography type at local scale (100 m), - assess heterogeneity within one topography type as well as between topography types at regional scale (20 km), - assess heterogeneity within one topography type between regions (basin scale, 1000 km), - assess heterogeneity between topography types (basin scale, 1000 km).

We investigated two deep-sea plains, the PAP and the IAP, see Figure 1. The northern PAP area consists of mainly plain seafloor with slopes less than one degree at a mean depth of ca. 4800 m. The area is additionally covered by North-South facing ridges, rising up to 600 m above the plains. One seamount feature in the wider area even rises to 1000 m above the plain. In this area, the multicorer sampling and on board ex-situ oxygen analysis revealed suboxic conditions of the sediment (Froehberg and Paul, 2021). The southern IAP area is located North of the "Gloria Fracture Zone" separating the European and African plates. The hydro-acoustic map of this area shows narrow and steep valleys in the North-West section, also mainly in a North-South direction as in PAP. Towards the West, wider and up to 6000 m deep plains exist and the fracture zone itself lies to the South which is rising up to 2500 m above the plains we sampled. The oxygen measurements on board revealed predominantly oxic conditions in the sediments in the area. More geochemical data on TOC and TN content, nutrients, porosity, trace metals with a focus on REY, were measured in the home lab on shore after the cruise.

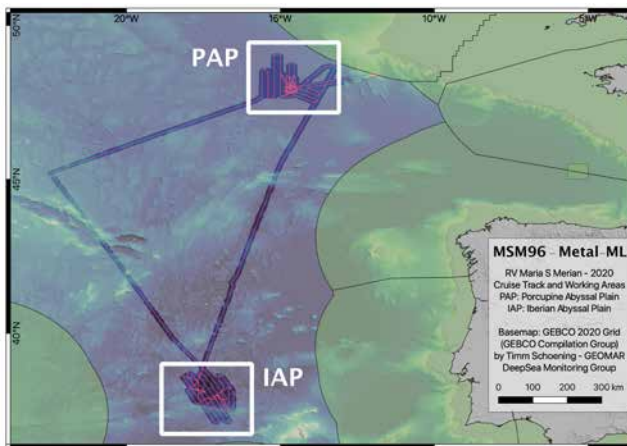


Figure 1: MSM96 cruise track and overview of work areas (PAP: Porcupine Abyssal Plain, IAP: Iberian Abyssal Plain).

All data of cruise MSM96 was immediately published openly and FAIR for public use in the context of the data management projects DAM "Underway data" and the Helmholtz "DataHub" and by other interested parties. Already in late 2020, data has been quality-

controlled and subsequently uploaded to OSIS and PANGAEA [1].

During MSM96 also several data management activities were tested – some for the first time – and improved. We were guided in this effort by making our marine data more FAIR (Schoening, 2021) and thus employ the use of persistent identifiers: ORCID for people, RORs for institutes, URNs, handles and Equipment IDs for platforms and sensors, IGSNs for physical samples, FAIR Digital Objects for images (Schoening et al., 2022), DOIs for published datasets. Openly published bathymetry data sets have already been taken up by the newest releases of GEBCO and derived data products (GEBCO, 2023).

Since the end of the cruise, geochemical lab work on sediment and water samples is ongoing. The deep-sea sediments at the PAP and IAP sites are characterized by low organic matter degradation rates which is why they are oxic up to a depth of ca. 20 cm (PAP) or more (IAP). No elevated dissolved Mn concentrations were detected in any core, because conditions do not become sufficiently reducing to reduce Mn oxides. Pore water and bottom water nutrient (nitrate, phosphate, silicate) concentrations were analyzed by Melanie Schnohr (BSc thesis) to assess whether topography has an impact on nutrient fluxes across the sediment-water interface. For the different topography types a trend from higher fluxes in valleys and lower fluxes in hills was found in both working areas (and for all the measured nutrients) (see Poster by Melanie Schnohr et al.). The comparison of the examined working areas provides some evidence for variable benthic nutrient fluxes as a function of topography (at least between hills and valleys). To further assess organic matter turnover, C-14 analyses were conducted on one core from each topography type from each work area to quantify sedimentation and mass accumulation rates. REY data show that benthic fluxes are widespread across both work areas and that they contribute REY to the bottom seawater. Calculated fluxes are, however, small, with on average $-0.9 \text{ pmol cm}^{-2} \text{ yr}^{-1} \text{ Nd}$ in the PAP ($n=10$) and $-0.6 \text{ pmol cm}^{-2} \text{ yr}^{-1} \text{ Nd}$ in the IAP ($n=9$), using Nd as an example for REY (see Poster by Sophie Paul et al.). Differences between topography types are small and based on the only partly analyzed data set so far, a comparison between topography types is not yet possible.

REFERENCES

[1] Cruise Data available in PANGAEA: <https://pangaea.de/?q=msm96>.

GEBCO Compilation Group (2023) GEBCO 2023 Grid (doi:10.5285/f98b053b-0cbc-6c23-e053-6c86abc0af7b).

Froehberg N, & Paul S, Porewater oxygen profiles in surface sediments of the North Atlantic Basin during RV Maria S. Merian cruise MSM96 2021, <https://doi.org/10.1594/PANGAEA.931647>.

Schoening T, & Paul S, Metal geochemistry meets machine learning: Assessing sedimentary and pore-water rare earth element variability from local to basin scale across the NE Atlantic Ocean, 10.10. 2020–10.11. 2020, Emden (Germany)–Emden (Germany) Metal-ML 2021, https://doi.org/10.48433/cr_msm96.

Schoening T, Image curation and publication, Version 1.0.0 and Supplement, Version 1.0.0. MareHub of the Helmholtz Association 2021, 5pp. DOI: <https://doi.org/10.5281/zenodo.5704846> & Supplement, Version 1.0.0, 7pp. DOI: [10.5281/zenodo.5704844](https://doi.org/10.5281/zenodo.5704844) <https://repository.oceanbestpractices.org/handle/11329/1781>.

Schoening T, Durden JM, Faber C, Felden J, Heger K, Hoving HJT, Zurowietz M, Making marine image data FAIR, *Scientific data* 2022, 9(1), 414. <https://www.nature.com/articles/s41597-022-01491-3>.

SCIENTIFIC OUTPUT

LIST OF PUBLICATIONS

Schoening T, Durden JM, Faber C, Felden J, Heger K, Hoving HJT, Zurowietz M, Making marine image data FAIR. *Scientific data* 2022, 9(1), 414. <https://www.nature.com/articles/s41597-022-01491-3>.

LIST OF CONFERENCE PRESENTATIONS

2023 | Paul, Sophie, et al. The Neodymium isotopic composition in oxic pore waters from the Atlantic and Pacific: implications for the use of Nd isotopes as a past water mass proxy Goldschmidt 2023 Conference, Lyon, France.

DATA

Schoening, Timm; Paul, Sophie Anna Luise (2021): Raw data of physical oceanography during Maria S. Merian cruise MSM96. PANGAEA: <https://doi.org/10.1594/PANGAEA.928600>

Schoening, Timm; Schlundt, Michael (2021): Continuous thermosalinograph oceanography along Maria S. Merian cruise MSM96. PANGAEA: <https://doi.org/10.1594/PANGAEA.927951>

Mohrmann, Jochen; Gazis, Iason-Zois; Schoening, Timm; Wölfl, Anne-Cathrin (2021): Multibeam bathymetry raw data (Kongsberg EM 122 entire dataset) of RV MARIA S. MERIAN during cruise MSM96. PANGAEA: <https://doi.org/10.1594/PANGAEA.929091>

Gazis, Iason-Zois; Mohrmann, Jochen; Schoening, Timm; Wöfl, Anne-Cathrin (2021): Multibeam bathymetry processed data (Kongsberg EM 122 working area dataset) of RV MARIA S. MERIAN during cruise MSM96. PANGAEA:
<https://doi.org/10.1594/PANGAEA.930063>

Schoening, Timm; Gazis, Iason-Zois; Mohrmann, Jochen (2021): Sediment echosounder raw data (Atlas Parasound P70 echosounder entire dataset) of RV MARIA S. MERIAN during cruise MSM96. PANGAEA:
<https://doi.org/10.1594/PANGAEA.929548>

Fröhberg, Nico; Paul, Sophie Anna Luise (2021): Porewater oxygen profiles in surface sediments of the North Atlantic Basin during RV Maria S. Merian cruise MSM96. PANGAEA:
<https://doi.org/10.1594/PANGAEA.931647>

Schoening, Timm; Kopte, Robert; Mohrmann, Jochen; Gazis, Iason-Zois (2020): ADCP current measurements (38 kHz) during Maria S. Merian cruise MSM96. PANGAEA:
<https://doi.org/10.1594/PANGAEA.925936>

Schoening, Timm; Kopte, Robert; Mohrmann, Jochen; Gazis, Iason-Zois (2020): ADCP current measurements (75 kHz) during Maria S. Merian cruise MSM96. PANGAEA:
<https://doi.org/10.1594/PANGAEA.925938>

CRUISE REPORT

MSM96: https://doi.org/10.48433/cr_msm96

MSM97

High Resolution Reflection Seismic Imaging of the Cenozoic Barrier | Structures of the West-Schleswig Block and the Fluid Migration | System of the blowout structure 'Figge Maar'

AUTHORS

Bundesanstalt für Geowissenschaften und Rohstoffe (BGR) | Hannover, Germany
A. Ehrhardt, G. Kuhlmann, H. Stück

GEOMAR Helmholtz-Zentrum für Ozeanforschung | Kiel, Germany
J. Karstens

INTRODUCTION

Regarding the use of renewable energy and the reduction of greenhouse-gas emissions, the usage of geological storage sites for fluids is of particular interest. Therefore, reservoir and barrier formations in the German North Sea come into focus. Due to the widespread distribution of storage and barrier rocks at suitable depths and in combination with a relatively low tectonic overprint, the West Schleswig Block region in the German North Sea is one of the highest prospective regions for CO₂ storage in the German EEZ.

By means of 1500 km of high-resolution 2D reflection seismic profiles, we investigate the potential impairment of geological barriers at the top of geological storage formations (i. e. claystones/mudstones and salt of the Upper Buntsandstein, mudstone dominated formations of the Lower Cretaceous and the Tertiary). The seismic acquisition setup with a 2400 m active streamer cable with 384 channels allowed a precise image of near-surface structures, such as tunnel valleys, seismic pipe structures, chimneys, polygonal fault systems and crestal faults. The high-resolution seismic data image the sediments from the seafloor down to the base of the Zechstein. The imaged fault systems will be investigated regarding their ability to build seal bypass systems. In addition, we acquired seismic data across the Figge Maar blowout crater and analyzed these data regarding the fluid migration pathway for the blowout.

METHODS

The seismic data acquisition was carried out with two GI-Guns with 45 in³ generator chamber volume each and 105 in³ injector chamber volume each in true GI mode, which suppressed the bubble energy well and produced a sharp and well broadband seismic signal. For the registration, we used a 2400 m 384 channel streamer cable with a channel distance of 6.25 m. We used a special stretch section, only 17.5 m long, which made it possible to realize a near trace offset of only 30 m, which was essential to image

the seafloor and the uppermost sediment layers. Figure 1 shows the basemap of the seismic lines in the area of the southern 'West-Schleswig Block' (WSB) and the star shaped survey across the Figge Maar (see cruise report MSM97/2 Ehrhardt et al., 2021). The processing of the data included designation, de-bubbling, de-multiple (including 3D-SRME, 3D-shallow water demultiple, radon demultiple), several velocity analysis iterations, prestack Kirchhoff migration, stacking with angle mute, poststack predictive deconvolution. An example seismic section shows the image of the sediments from the base of the Zechstein up to the seafloor.

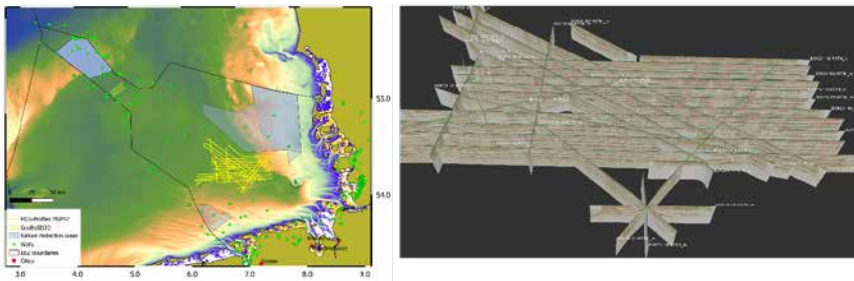


Figure 1: (Left) Overview map of the German EEZ and the location of the GeoHifi seismic survey in the area of the West-Schleswig Block. (Right) 3D aerial view from south to north of the seismic lines of the project.

RESULTS

The dense coverage of seismic lines across the southern WSB and the high-resolution approach enables us to identify prospective areas for the geological storage of fluids and to analyze the integrity of the seal layers above potential reservoir layers. Prospective reservoirs are identified in Mesozoic sediments in the top of salt anticlines, like Henni (Figure 2). There, the analyzed moderate burial depth, seal integrity and calculated reservoir volume of the evaluated Middle Bunter reveal very good storage conditions (Fuhrmann et al. 2023).

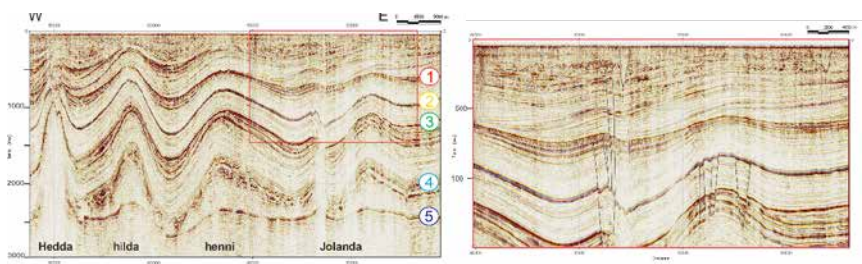


Figure 2: (Left) 2D seismic profile from West to East across the WSB. The profile crosses the salt diapirs 'Hedda' and 'Jolanda' and the salt pillows 'Hilda' and 'Henni'. Numbers 1-5 show the main horizons (1) Mid-Miocene unconformity, (2) Base Paleogene, (3) Base Cretaceous, (4) Base Triassic, (5) Base Zechstein. (Right) Close-up of the red box, black lines show faults. Dashed lines show the outline of tunnel valleys.

Mudstones and evaporites of the Upper Triassic and Lower Cretaceous are the main seal layers (Bense & Jähne-Klingberg, 2017), which we analyze regarding their integrity. Different sets of faults were detected in the survey area, especially crestal faults above salt structures, polygonal faults within the Rupel Clay layer and faults related to tunnel valleys. Most of the deeper crestal faults do not puncture Mid Miocene Unconformity (MMU), except in the areas of salt diapirs. In some areas, however, crestal faults cut through the MMU and can be traced up to the seafloor (Figure 2). Faults terminating at the MMU could build a seal bypass system in combination with the polygonal faults.

A fluid migration system was triggered in 1963 by drilling into a high-pressure dolomite reservoir in 2925 m depth (Kornfeld, 1964), resulting in a major blow-out of Nitrogen. After the closing of the well with a blow-out preventer, the blow-out of Nitrogen was initiated about 500 m away from the rig, leading to the formation of a 500 m wide and 30 m deep crater in the seafloor, which was called later on 'Figge-Maar'. A star-shaped survey across the Figge-Maar (see Figure1) enabled us to present a model of the fluid migration system (Karstens, et al., 2022). The model shows that the drill hole vertically connected different hydraulic permeable faults or layer interfaces, thus forming a 'human-triggered' seal-bypass system.

REFERENCES

Bense FA, Jähne-Klingberg F, Storage Potential in the deeper subsurface of the Central German North Sea, *Energy Procedia* 2017, 114, 4595-4622.

Karstens J, Schneider von Deimling J, Berndt C, Böttner C, Kühn M, Reinardy B, Ehrhardt A, Gros J, Schramm B, Klaeschen D, Elger J, Haeckel M, Schmidt M, Heinrich S, Müller P, Bense F, Formation of the Figge Maar Seafloor Crater During the 1964 B1 Blowout in the German North Sea, *Earth Science, Systems and Society* 2022, 2, doi: 10.3389/esss.2022.10053.

Kornfeld JA, Wild Blowout Taps First North Sea Gas. *World Oil* 1964.

SCIENTIFIC OUTPUT

LIST OF PUBLICATIONS

Karstens J, Schneider von Deimling J, Berndt C, Böttner C, Kühn M, Reinardy B, Ehrhardt A, Gros J, Schramm B, Klaeschen D, Elger J, Haeckel M, Schmidt M, Heinrich S, Müller P, Bense F, Formation of the Figge Maar Seafloor Crater During the 1964 B1 Blowout in the German North Sea, *Earth Science, Systems and Society* 2022, 2, doi: 10.3389/esss.2022.10053.

LIST OF CONFERENCE PRESENTATIONS

2023 | **Analysis of fluid migration pathways in the context of CO₂ underground storage in the German North Sea using high-resolution 3D and 2D seismic data**
Ahlrichs N, Ehrhardt A, Schnabel M, Fuhrmann A, Stück H, GeoBerlin, Germany

2023 | **CO₂ storage potential of the Middle Buntsandstein in the Exclusive Economic Zone (EEZ) of the German North Sea** Fuhrmann A, Knopf S, Ahlrichs N, Stück H, Kästner F, Thöle H, Kuhlmann G, GeoBerlin, Germany

2023 | **Potential CO₂ Storage Sites in the German North Sea? A Reservoir-Modelling and Parametrization Study**, Schlieder-Kowitz A, Kästner F, Fuhrmann A, Thöle H, Kuhlmann G, Stück H, f Bense F, Zehner B, GeoBerlin, Germany

DATA

The data from MSM97/2 is available according to GeolDG:

https://www.bgr.bund.de/DE/Themen/Geodatenmanagement/GeolDG/Downloads_Daten_AWZ/downloads_daten_AWZ_node.html

CRUISE REPORT

MSM97: doi:10.48433/cr_msm97

MSM98

Project VARIOSEEP – Variability, amount and fate of methane seepage in the German North Sea

AUTHORS

MARUM – Center for Marine Environmental Sciences, University of Bremen |
Bremen, Germany

M. Römer

BGR – Federal Institute for Geosciences and Natural Resources | Hanover, Germany

M. Blumenberg, K. Schwalenberg

SUMMARY

R/V Maria S. Merian cruise MSM98 focused on hydrocarbon fluid emissions in the German North Sea. The presence of seepage in the 'Entenschnabel'-area has been proven during R/V Heincke cruise HE537 in July 2019. During MSM98 the newly detected gas emissions should be investigated in detail regarding its quantities, temporal and spatial variability, source and fate. Besides using ship-based hydroacoustic methods, sediment sampling with multicorer and water sampling with the onboard CTD, we brought an air-analyzer for detecting light hydrocarbon emissions above the sea-air interface, a miniROV for gas bubble sampling, and a towed electromagnetic measurement system (Golden Eye) as a new tool for the detection of shallow gas accumulations in sediments, as well as a sonar lander for gas bubble variability monitoring on board. During the two-week cruise, the work schedule has been fulfilled and sampling has been successfully finished. A comprehensive hydroacoustic mapping approach revealed the presence and distribution of numerous gas emission sites, which could partly be quantitatively analyzed and sampled. The Sonar Lander was deployed at two different emission sites for several days each, revealing variable emission intensities. The Golden Eye had in total four deployments and gas samples were successfully taken with the miniROV at two different emission sites, which were analyzed for their gas composition and isotopic signatures revealing its source. Finally, also six well locations were investigated to prove its integrity. Regarding the scientific work plan to answer the proposed questions and objectives, cruise MSM98 was highly successful and revealed many new results regarding the shallow gas system in the North Sea.

AGENDA OF THE CRUISE

Our research focus was planned to be conducted in the southern part of the Entenschnabel. The major part of the cruise was therefore passed in this area (Figure 1b). However, due to very heavy weather conditions towards the end of the cruise, it was decided to finish some part of our planned studies closer to the coast, where wind and wave conditions

still allowed mapping and station work (Figure 1a). As numerous wells are located in the entire North Sea and one of our research questions focused on well integrity, the time could be successfully used for our research expedition, despite the very bad weather in our proposed work area in the Entenschnabel.

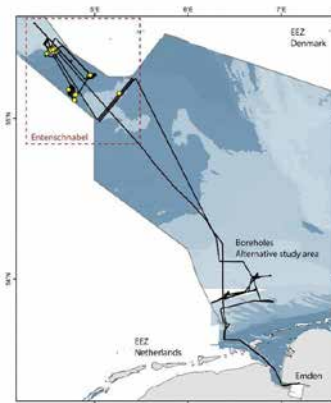


Figure 1a: Overview of the ships track (black line) and stations (yellow dots) of MSM98.

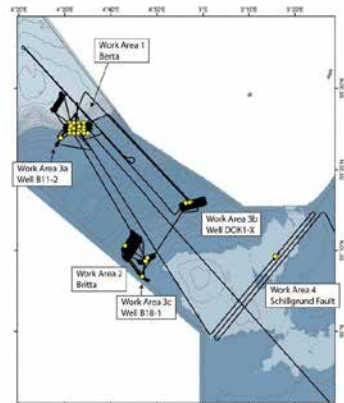


Figure 1b: Map of the primary work area in the Entenschnabel in the German North Sea.

HYDROACOUSTIC MAPPING

The main purpose of most of the surveys was the better understanding of the flares found during the previous HE537 cruise in the Entenschnabel (Römer et al., 2021) but also the expansion of high-resolution bathymetry in the Entenschnabel. Another goal was the detection and mapping of gas bubble emissions and the impact of the tides and the seasons of already known seeps. For this purpose, the EM712 and the EK60 were used for flare visualization and seep activity analysis.

CONTINUOUS AIR MEASUREMENTS WITH A GREENHOUSE GAS ANALYZER (GGA)

Measurements were taken continuously throughout the entire cruise. They were interrupted only during the measurements for the CTD water samples. Besides that, the GGA ran continuously for 24 hours at a rate of one measurement per second. Background measurements for methane in the air are typically between 1.8 and 2.1 ppm. These values were achieved on all measurement days. Higher methane values could not be detected during the entire cruise. Except for the measurements at the near coast area, at the beginning and towards the end of the cruise, no increasing methane concentrations were measured.

HYDROGRAPHY

A total of 43 CTD stations was realized. As expected, only minor or no stratification was observed throughout the water column unlike to measurement in summer 2019 where a

strong thermocline was observed between 20 and 25 m water depth. As a result the oxygen saturation was uniform throughout the water column.

ELECTROMAGNETICS

Electromagnetic measurements with the Golden Eye system have been carried out to study the electrical signatures of the shallow seafloor. For the Varioseep project, cruise MSM98 Golden Eye deployments focused on the flare cluster at salt diapir Berta with the aim to identify possible shallow gas accumulations in the sediments below the flares, and at the pockmark area found in bathymetry data and previous electromagnetic data collected during cruise HE537 near salt diapir Britta. Two deployments have been carried out over the flare cluster, one over the pockmark area and one SW of the pockmark area across some chimney structures detected in the sub-bottom profiler.

SONAR LANDER

The sonar lander is an autonomous, battery-powered instrument designed to monitor the variations of methane gas emissions from the seabed over several days. The sonar lander was deployed twice in the vicinity of known gas bubble emissions located within the Berta salt diapir study area, at a water depth of about 43 m. For each deployment, we used the ROV to confirm visually the position and orientation of the sonar lander in relation to the bubble streams. The first deployment lasted about 5 days and targeted a site, referred to as "Berta Chimney", where numerous recurrent gas bubble streams occur. The sonar lander was placed facing East and few meters to the southwest of active bubble streams. The second deployment lasted about 4 days and took place at the site of a recurrent bubble plume, referred to as "Berta Fault", because of its location atop, or near, a known fault in the sediments. The deployments were successful, in that active bubble plumes are clearly visible on the sonar records. For each deployment, the sonar data show that at least two to three recurrent gas bubble streams occurred within the scanning sector of the sonar. Some were not detected in every scan, indicating that the bubble release was intermittent. Used for groundtruthing, camera footage confirms that some bubble plumes at Berta Fault were not continually active. Unfortunately, because of the poor visibility, bubble plumes are hardly visible on the camera footage from Berta Chimney. Nevertheless, separate ROV observations made at Berta Chimney before the sonar lander deployment showed bubbles being released in pulses. Preliminary results suggest that the variations of bubble release might be tidally modulated.

MINI ROV

In total, 11 dives and a number of shorter test deployments (for reasons such as control system check, buoyancy tuning or sensor check) were successfully carried out during MSM98. Seeping gas bubbles were sampled at two sites near Berta salt dome with a funnel-bag system. Gas samples were transferred into the BGR home laboratory, where they were analysed for gas composition and isotopic signatures of methane and other hydrocarbons. Data demonstrate that the seep gases consist mainly of methane with a biogenic origin.

REFERENCES

Römer M, Blumenberg M, Heeschen K, Schloemer S, Müller H, Müller S, Hilgenfeldt C, Barckhausen U, Schwalenberg K, Seafloor Methane Seepage Related to Salt Diapirism in the Northwestern Part of the German North Sea, *Front. Earth Sci.* 2021, doi: 10.3389/feart.2021.556329.

SCIENTIFIC OUTPUT

LIST OF PUBLICATIONS

Blumenberg M, Schlömer S, Reinhardt L, Scheeder G, Pape T, Römer M. Biomarker insights into a methane-enriched Holocene peat-setting from “Doggerland” (central North Sea). *The Holocene* 2022, 32(10), 1015-1025.
<https://doi.org/10.1177/09596836221106958>

LIST OF CONFERENCE PRESENTATIONS

2021 | **Biomarker insights into a methane-enriched Holocene peat-setting from “Doggerland” (Central North Sea)** – Preliminary Data 39th International Meeting on Organic Geochemistry, online.

DATA

Master tracks in different resolutions:

<https://doi.pangaea.de/10.1594/PANGAEA.933697>

Continuous thermosalinograph oceanography:

<https://doi.pangaea.de/10.1594/PANGAEA.937864>

Sediment echosounder raw data (Atlas Parasound P70 echosounder):

<https://doi.pangaea.de/10.1594/PANGAEA.937631>

Multibeam bathymetry raw data (Kongsberg EM712):

<https://doi.pangaea.de/10.1594/PANGAEA.937616>

<https://doi.pangaea.de/10.1594/PANGAEA.928946>

Physical oceanographic profiles of 43 CTD casts:

<https://doi.pangaea.de/10.1594/PANGAEA.937826>

CRUISE REPORT

MSM98: doi:10.48433/cr_msm98

MSM98/2

Submarine landslides, tunnel valleys, and pits – results from seismo-acoustic studies

AUTHORS

Kiel University – Institute for Geoscience | Kiel, Germany

J. Schneider von Deimling, A. Lohrberg, R. Barrett, H. Grob, F. Lenz, Sebastian Krastel

The results of the cruise MSM98/2 with R/V Merian comprise three independent research topics. Two objectives were pursued beforehand, and one topic exposed during the cruise.

TAMPEN SLIDE AND THE AEGIR RIDGE, OFFSHORE NORWAY

In the first part of the cruise, the Tampen submarine landslide on the Norwegian continental slope was mapped using high-resolution seismic data to determine its lateral extent and volume. In particular, we were interested in whether the Tampen Slide deposits correlate with mega-slide deposits previously identified in the Aegir Ridge, an extinct spreading ridge, to the north. Initially, the slide could be clearly traced in the multi-channel seismic data collected during MSM98/2 downslope from the headwall; however, the corresponding deposits terminate abruptly at an up-to-200 m high (buried and previously unknown) escarpment at the boundary between the proximal and distal deposits of the North Sea Fan (Barrett, Bellwald et al., in prep). Multiple profiles were collected across this buried escarpment using hull-mounted EM122 (12 kHz) multibeam and Parasound systems and Kiel University's high-resolution seismic system. Additional seismic surveys in and along the Aegir Ridge revealed several multiple meter-thick megaturbidite layers. Hydroacoustic data show that these layers thin towards the sides of the Aegir Ridge and seven gravity cores (4.5–7.5 m in length) were successfully taken here and in a small basin north of the Ridge. These gravity cores penetrate through multiple turbidites, including that related to the Storegga Slide. Dating and correlating these turbidite layers will provide critical information for understanding the frequency and volume of mass transport processes in the region, which is important for constraining the ongoing risk posed by these processes (Barrett, Hunt et al., in prep.).

HELIGOLAND GLACIOTECTONIC COMPLEX

In the second cruise section, the Heligoland Glaciotectonic Complex (HGC) was targeted using seismic and hydroacoustic methods to reconstruct the advances and retreats of ice sheets in the southeastern North Sea during the Quaternary. Aiming for a combined profile line spacing of only 400 m, we were able to generate a very high-density subbottom data set. Thrust sheets and faults are imaged well in our data, although further

processing is needed to reduce shallow water artefacts. From the new data, we know that the HGC extends farther than previously thought and we established a seamless connection to the previous high-resolution data set in the region. Some thrust sheets were cut and eroded by subglacial meltwater channels (so-called tunnel valleys) providing the relative temporal sequence. Sporadically, we were able to identify small near-surface channels that lie only 1–2 m below the seafloor and are cut only few meters into the ground and likely served as a drainage system during the late Pleistocene. Further investigation of these channels is planned during project TRAPA on MSM128. The data set acquired on MSM98/2 provides the basis to further analyse the formation of the HGC and its interaction with the large tunnel valley in the region. We will be able to update the spatial distribution of tunnel valleys in the area (Lohrberg et al., 2022). Additionally, we sailed dedicated profiles along the course of these tunnel valleys. Such data has been non-existent for tunnel valleys and holds the potential to shed light on their formation and infill mechanisms (Lohrberg et al., 2022). This analysis will result in a detailed 3D subsurface model, which will be used as a basis for a groundwater model as part of DFG project 524639242 (“More than buried valleys: Do tunnel valleys serve as conduits for preferential freshened groundwater flow within the North Sea?”). Furthermore, we examined the seafloor surface and shallow subsurface for possible degassing structures, but no evidence of fluid seepage and pockmark genesis was found.

MACRO-BIOTURBATION BY VERTEBRATES

Early in the cruise, while calibrating the MBES system, we discovered some enigmatic seafloor depressions. We hypothesized that these features were caused by whales feeding on the seafloor. At the very end of the cruise, additional data were collected to test this hypothesis. This and subsequent analyses including follow up cruises and data mining of legacy multibeam data provide evidence that the hypothesis gathered during MSM98/2 was correct (Schneider von Deimling et al., 2023).

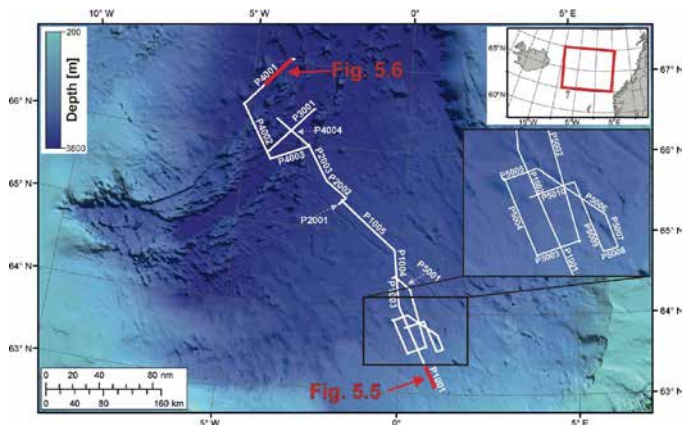


Figure 1: Seismic lines acquired in the Tampen study area. The GEBCO bathymetry grid is used for background bathymetry (Barrett et al., in prep.).

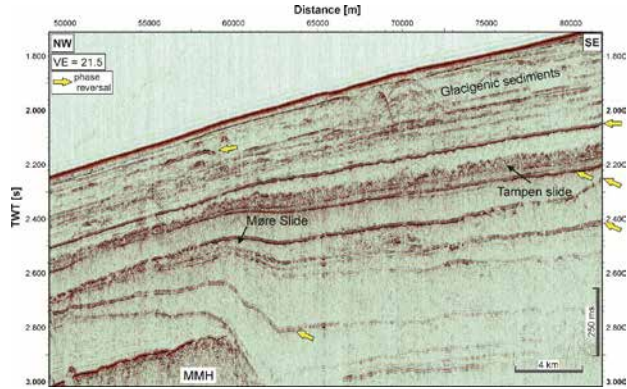


Figure 2: A part of profile P1001 at the continental slope west of Norway. The profile runs from southeast to northwest and crosses the Møre Marginal High (Barrett et al., in prep.).

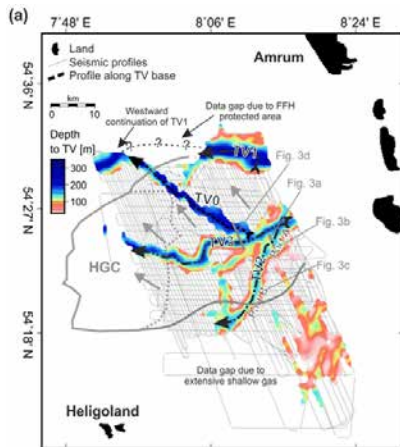


Figure 3: Overview of the study area. Detailed distribution of large tunnel valleys (TVs) in the study area in the form of a depth grid based on all available high-resolution 2D reflection seismic profiles (Lohrberg et al., 2022).

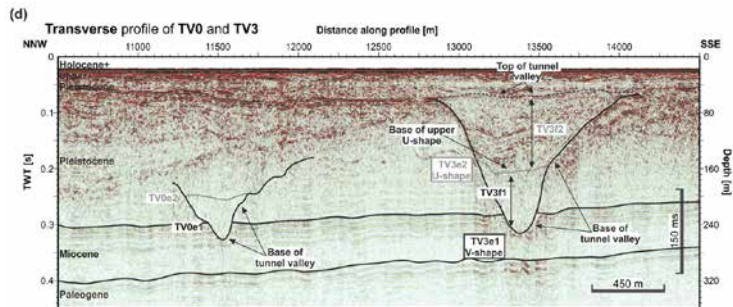


Figure 4: Seismic sections showing transverse profile imaging TV0 and TV3 perpendicular to their thalweg (Lohrberg et al., 2022).

REFERENCES

Barrett R, Bellwald B, Talling P, Hunt J, Grob H, Lenz F, Lohrberg A, Schneider von Deimling J, Krastel S, 2D seismic reflection data reveal a previously unknown headwall in the North Sea Fan, offshore Norway (in prep).

Barrett R, Hunt J, Lenz F, Talling P, Kolling H, Schneider von Deimling J, Krastel S, Mass transport in the Aegir Ridge, northern Atlantic Ocean (in prep.).

Lohrberg A, Schneider von Deimling J, Grob H, Lenz KF, Krastel S, Tunnel valleys in the southeastern North Sea: more data, more complexity, E&G Quaternary Sci. J. 2022, 71, 267–274, <https://doi.org/10.5194/egqsj-71-267-2022>.

Schneider von Deimling J, Hoffmann J, Geersen J, Koschinski S, Lohrberg A, Gilles A, Belkin I, Böttner C, Papenmeier S, Krastel S, Millions of seafloor pits, not pockmarks, induced by vertebrates in the North Sea, Nature Communications Earth and Environment (in press).

SCIENTIFIC OUTPUT

LIST OF PUBLICATIONS

Barrett R, Bellwald B, Talling P, Hunt J, Grob H, Lenz F, Lohrberg A, Schneider von Deimling J, Krastel S, 2D seismic reflection data reveal a previously unknown headwall in the North Sea Fan, offshore Norway (in prep).

Barrett R, Hunt J, Lenz F, Talling P, Kolling H, Schneider von Deimling J, Krastel S, Mass transport in the Aegir Ridge, northern Atlantic Ocean (in prep.).

Lohrberg A, Schneider von Deimling J, Grob H, Lenz KF, Krastel S, Tunnel valleys in the southeastern North Sea: more data, more complexity, E&G Quaternary Sci. J. 2022, 71, 267–274, <https://doi.org/10.5194/egqsj-71-267-2022>.

Schneider von Deimling J, Hoffmann J, Geersen J, Koschinski S, Lohrberg A, Gilles A, Belkin I, Böttner C, Papenmeier S, Krastel S, Millions of seafloor pits, not pockmarks, induced by vertebrates in the North Sea, Nature Communications Earth and Environment (in press).

LIST OF CONFERENCE PRESENTATIONS

2022 | **Tunnel valleys in the southeastern North Sea: Complex incision patterns dating back to MIS16?** INQUA2023, Rome, Italy.

2022 | **Investigating the origin, frequency, and extent of submarine mass wasting processes in the Aegir Ridge, offshore Norway** International Conference on Seafloor Landforms, Processes and Evolution, Malta.

2023 | **Whales cause millions of seafloor pits** GEOHAB, Saint Paul Réunion, France.

2023 | **Identification and mapping of an up to 200 m high, buried escarpment within the North Sea Fan, offshore Norway** DGG Jahrestagung, Bremen, Germany.

DATA

Seismo-acoustic data (Multibeam, Parasound, Airgun Seismics):
Data availability is still restricted due to a moratorium.

Tracklines:

<https://doi.pangaea.de/10.1594/PANGAEA.957181>

Thermosalinigraph data:

<https://doi.pangaea.de/10.1594/PANGAEA.943866>

Seafloor Samples (Gravity Core, Grab Sampler): Samples stored at Kiel University.

CRUISE REPORT

MSM98/2: [doi:10.48433/cr_msm98_2](https://doi.org/10.48433/cr_msm98_2)

MSM99

Baltic Sea Deep Water Ventilation

AUTHORS

Institute of Geosciences, Kiel University | Kiel, Germany

R. Schneider

Leibniz Institute for Baltic Sea Research | Rostock-Warnemuende, Germany

M. Moros, T. Neumann

Cruise MSM99 into the central and northern Baltic Sea executed multibeam bathymetry and sediment echosounder surveys, as well as sampling of Holocene sediments, water column, and sea ice in the central and northern basins of the Baltic Sea. The main goals were to investigate the water column wintertime mixing underneath the winter sea-ice and how deeper water masses originating in the northern basins may ventilate also central basins at cold or warm climate conditions. Hydroacoustic surveys, sediment coring and hydrographic measurements, as well as winter sea-ice probing should fill important gaps in existing data sets. Together with numerical modeling the new data will provide better understanding about past and future variations in the ventilation of the deeper Baltic Sea by northern water masses. Next to the detailed study of the importance of wintertime deep mixing for oxygenation of northern and central basins, we investigate erosional processes of early to mid-Holocene sediments in the western and northern regions that are transported into the deeper central basins. The response of deeper ventilation and overall ecosystem conditions to such an erosional activity, e. g., organic matter re-suspension and transport of contaminants, cannot be predicted with available data and models.

The water depths of the erosion basis seem to be linked to the individual sub-basin's size, configuration and location. The reconstruction of the spatial linkage and the timing of erosional processes in greater detail was thus the first goal for the post-cruise work. Based on hydroacoustic profiling along basin-wide transects new gravity cores were taken for visual description directly onboard and for detailed post-cruise investigation. In parallel MSM99 research is dedicated to the physical (hydrographic) processes leading to deep water formation probably linked to winter-time climate cooling and sea-ice formation with massive brine formation which is still not well understood on temporal and spatial scales. The effect of sea-ice formation in the Bay of Bothnia was studied performing sea ice coring and brine sampling, as well as water column studies beneath the sea ice, including, two hydrographic moorings for continuous water column measurements that after one year. As already partly suggested based on results from the former Baltic cruises MSM51 and 62, it became apparent, that the Eastern Gotland Basin is probably

very suitable to study past changes in surface and subsurface water conditions entraining from the Central Baltic from the North. However, this time the more northward located two Åland Deep sub-basins, critical for the water exchange between the central and northern Baltic Sea were targeted in greater detail based on new hydroacoustic surveying of these basins during MSM99. It is very likely, that during colder periods newly formed bottom waters caused widespread re-suspension of organic carbon-rich laminated sediments, originally deposited during the preceding warm periods in shallower areas. Probably, this material was transported to and re-deposited in the deeper parts of the Baltic Sea sub-basins north of the Baltic Sea Klint, a topographic high, that acted as a hydrographic barrier for deep-water formed in the northern Baltic. Nonetheless, in the past 7,000 years, deep-water formation produced bottom currents that not only led to the formation of sediment contourite drifts at water depths of > 200 m in the Bothnian Sea and the Åland Deep but also northern central Baltic Sea sub-basins.

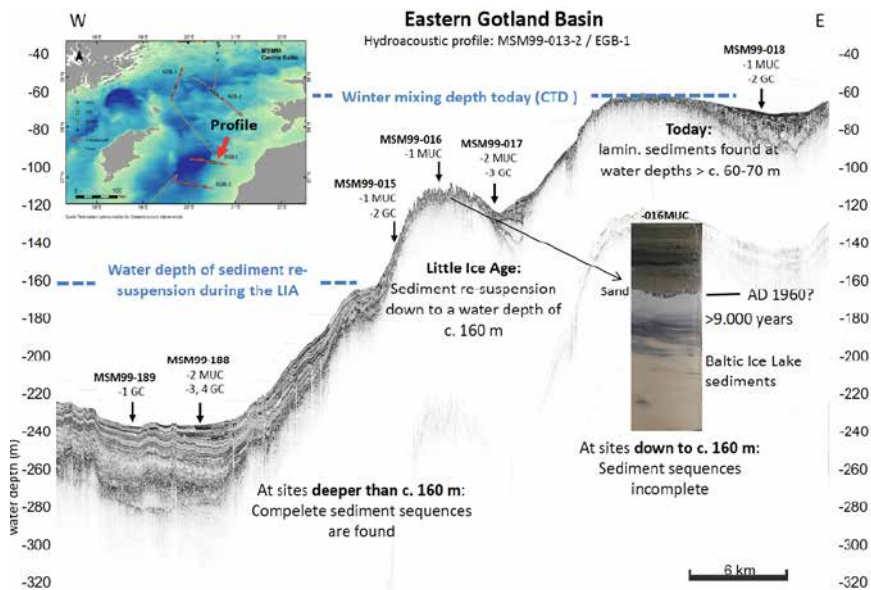


Figure 1: Schematic sketches of deep-water formation processes on sediment accumulation during.

As already suggested before (Moros et al. 2020) also the preliminary results of MSM99 strongly support the hypothesis, that during colder periods newly formed bottom waters caused widespread re-suspension of organic carbon-rich laminated sediments, originally deposited during the preceding warm periods in shallower areas. Such features are not observed for the warm climate intervals implying a much weaker deep convection and ventilation in the northern basins then. Furthermore, since bottom water ventilation in the Baltic Sea is generally assumed to be determined solely by the inflow of oxygen-rich, saline water from the North Sea, our findings postulate that deep-water formation during

winter-time sea ice formation is a key process for ventilation and spread of anoxia of bottom waters in the northernmost basins. However, if this process was much weaker during warm climate periods as the data suggests, this raises the immediate question about the conditions of deep basin ventilation under even warmer conditions in the future. Now the overarching post-cruise goal is the modelling of the modern physical processes and the reconstruction at larger temporal and spatial scales in order to investigate recent and past ecosystem changes in an integrated palaeoceanographic proxy and modelling approach. The combination of state-of-the-art proxy reconstructions and advanced numerical simulations will elucidate cause-effect relationships of the changing Baltic Sea environment, disentangling effects of external forcing from internal feedbacks or drivers, and allow to extrapolate the rather point proxy investigations to the whole Baltic.

SCIENTIFIC OUTPUT

LIST OF PUBLICATIONS

Moros M, Kotilainen TP, Snowball I, et al., Is 'deep-water formation' in the Baltic Sea a key to understanding seabed dynamics and ventilation changes over the past 7,000 years?, *Quat. Intern.* 2020, 550, 55–65, doi.org/10.1016/j.quaint.2020.03.031.

Moros M, Kotilainen A, Snowball I, et al., Giant saltwater inflow in AD 1951 triggered Baltic Sea hypoxia, *Boreas* 2023, in review.

LIST OF CONFERENCE PRESENTATIONS

2022 | **Winter-time deep-water formation / convection in the Baltic Sea: a key to understand seabed dynamics and ventilation changes over the past 150 years**

Kotilainen, A., Moros, M., Snowball, I., Neumann, T., Perner, K., Meier, H. E. M., Leipe, T., Sinninghe Damsté, J., and Schneider, R., 4th Baltic Earth Conference, Jastarnia, Poland.

2023 | **Winter-time deep-water formation / convection in the Baltic Sea – affecting seabed dynamics and ventilation changes over the past** Kotilainen, A., Moros, M.,

Snowball, I., Neumann, T., Perner, K., Meier, H. E. M., Sinninghe Damsté, J., and Schneider, R., EGU General Assembly 2023, Vienna, Austria.

CRUISE REPORT

MSM99: https://doi.org/10.48433/cr_msm99

MSM99/2

The enigmatic pockmarks of the southeastern North Sea

AUTHORS

Aarhus University | Aarhus, Denmark

C. Böttner

Kiel University | Kiel, Germany

D. Unverricht, C. Böttner

GEOMAR Helmholtz Centre for Ocean Research | Kiel, Germany

M. Schmidt, T. Spiegel, T. Müller, C. Schmidt

INTRODUCTION

Fluid flow through marine sediments manifests itself on the seafloor in numerous ways. Seepage can involve the discharge of gas, oil, water and sediments (Judd & Hovland, 2009).

Submarine cold seeps have been in the focus of scientific investigation since King and MacLean discovered pockmarks (“cone-like depressions”) in 1970 on the Nova Scotia Shelf, offshore Canada (King & MacLean, 1970), as they are often related to methane discharge and thereby to global biogeochemical cycles as well as local environmental conditions (Judd & Hovland, 2009). Increasing seismic and hydroacoustic data coverage and quality revealed the abundance and nature of different seepage and venting types, but also documented the ubiquitous appearance of pockmarks. Pockmarks have been found in almost all subaqueous geologic settings spanning from the deep ocean trenches to shallow lakes (Judd & Hovland, 2009)

Pockmarks are often interpreted as the surface manifestation of hydrocarbon venting but may also result from freshwater flow in coastal regions, compaction induced sediment dewatering, or bottom scouring. Pockmarks can be meters to hundreds of meters in diameter, meters to tens of meters in depth and affect the local environment, morphodynamics, biochemistry and ecology (e. g., Berndt, 2005). The morphology and size of pockmarks vary largely, and they are often reshaped by local bottom-currents (e. g., King & MacLean, 1970; Judd & Hovland, 2009).

Pockmarks are so far mostly identified in areas with soft, fine-grained sediments and can remain here, even inactive, for tens of thousands of years if no sediment supply fills them in (Feng et al., 2010; Paull et al., 2002). Their tendency to primarily occur in muddy sediments is likely the result of higher preservation potential rather than less fluid migration

or activity in sandy regions, similar to the preservation time of trawl marks on the seafloor (Bruns et al., 2020). Pockmarks can thus even be preserved over geologic time scales (Andresen et al., 2008, 2011). In soft sediments, there is a direct relationship between depth and perimeter or the diameter of the pockmarks (e. g., Andrews et al., 2010; Gafeira et al., 2012). In sandy environments very few pockmarks have been described. Only small and short-lasting depressions of 10s of cm depth have been reported from Gullfaks field and Tommeliten site (Judd & Hovland, 2009).

POCKMARKS IN THE SOUTHEASTERN NORTH SEA

The aim of the MSM99/2 cruise was to investigate the formation of pockmarks in the south-eastern North Sea, where high-resolution bathymetry systems were able to resolve pockmarks of only a few tens of centimeters depth (Krämer et al., 2017). These pockmarks occur in medium to fine sands. The formation of these pockmarks has been linked by Krämer et al. (2017) to gas expulsion during large storm events. During these events, wave motions lead to pressure changes in the sediment and thus gas pockets in the upper sedimentary succession could be stimulated to rise. We have investigated this hypothesis by means of numerical model calculations (Gupta et al., 2022) and came across an alternative process that could explain the formation of the pockmarks. Extending the original hypothesis, the model calculations show that wave-induced pressure changes can lead to spontaneous degassing and accumulation of free gas in the subsurface, which is possible because the solubility of gas in pore water is pressure and temperature dependent. Our numerical data suggest that this wave-induced degassing and subsequent pockmark formation is dependent on a sufficiently high initial gas saturation in the pore water, and a high permeability. These parameters can vary considerably and on different spatial scales in the investigated area, which can influence the local occurrence of pockmarks. MSM99/2 was designed to fill in the knowledge gaps on these parameters and shed light on the pockmark formation in the southeastern North Sea.

DATA AND METHODS

The work program included hydroacoustic mapping of the seafloor and geological sampling for sediment properties and pore water analysis (Figure 1). We investigated two working areas, with distinct sediment characteristics: The sandy environments north of Heligoland and the Heligoland Mud Area south of Heligoland (Figure 1). During the cruise, we mapped about 1100 NM of seafloor and took at 35 stations sediment samples. We were able to identify > 50,000 pockmarks across a large area north of Heligoland and measured geochemical parameters across three individual sites. No pockmarks could be found in the Heligoland Mud Area.

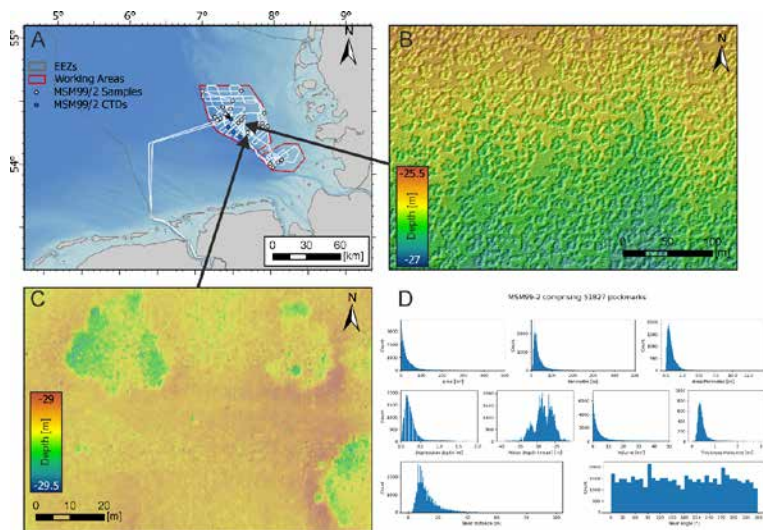


Figure 1: (A) A map of the cruise track of MSM99/2 (white line). The two survey areas are indicated with red outlines. Sediment samples (grey dots) and CTD stations (blue dots) are indicated. (B) Map of hundreds of coalescing pockmarks in the survey area north of Heligoland, west of the windfarm areas “Meerwind Süd/Ost”. (C) Map of pockmarks showing the distinct evolutionary steps from small circular features to intermingled mega-structures (“cauliflower pockmark”). (D) Geomorphological analyses of >50,000 pockmarks in the area showing distribution of Area, Perimeter, Area/Perimeter, Depth, Water depth, Volume, Thickness of underlying Holocene sediments, Nearest neighboring pockmark distance and angle.

WHY DO THESE POCKMARKS FORM?

The primary model for pockmark formation is the venting of hydrocarbons (Judd & Hovland, 2009). However, this predominant model may lead to a very inclined interpretation of all pockmarks to be associated with hydrocarbon venting (Paull et al., 2002). Our seismic analyses of the shallow subsurface indicate no major vertical fluid migration pathways and only sparsely distributed shallow gas is imaged at the Holocene/Pleistocene boundary. Our geochemical analyses show minor abundances of methane in very low saturations (<1%). The small amount of methane in our cores are likely derived from shallow buried peat. We conclude that the formation of more than 50,000 pockmarks in this part of the North Sea cannot be caused by methane emissions alone and estimates on the contribution of this system to the methane budget of the North Sea by Krämer et al. (2017) are likely to be highly overestimated.

Pockmarks may also form and/or be maintained by groundwater discharge or pore-water expulsion (e. g., Hoffmann et al., 2020; Andresen et al., 2021). Groundwater discharge in the southeastern North Sea may be sourced from buried glacial tunnel valleys or fluvial paleo-channels. However, we do not see a spatial correlation of pockmarks with the potential groundwater-bearing sedimentary units at depth. In addition, our radon analyses do not show indications for groundwater discharge above the pockmarks. Thus, active groundwater seepage is unlikely to cause pockmark formation in our survey area.

In the absence of evidence for fluids below the seafloor, pockmark formation may potentially be initiated from above it. Fish and other benthic fauna are known to form crater-like structures (up to meters deep), which could be termed pockmarks as well (e. g., Mueller, 2015). Schneider von Deimling et al. (in press) link the pockmark formation in the southeastern North Sea to harbor porpoises hunting for prey. This process may cause initial dents at the seafloor, which get subsequently eroded by the strong tidal currents. However, we find that pockmarks cluster in distinct depth horizons, indicating some geological control on the formation.

HOW DO THESE POCKMARKS FORM?

According to (Judd & Hovland, 2009) “the key factors that distinguish pockmarks from other, morphologically similar features are that they are erosive, and that the eroding agent comes from beneath the seabed”. Since many studies worldwide describe seafloor depressions as pockmarks although their origin remains unknown (Paull et al., 2002; Hoffmann et al., 2019; Hillman et al., 2023;) and to conform with previous terminology used in the southeastern North Sea, we will use the term pockmark here to describe seafloor depressions of unknown origin.

All above mentioned hypotheses rely on a model where small irregularities (dents) in the seafloor develop into a much bigger structure over time. The modification of pockmarks by subsequent ocean current interaction and scouring is a common process described in various marine settings (e. g., Brothers et al., 2011; Gafeira et al., 2012). Pockmarks generally develop an elongation over time depending on the primary ocean current direction. Here we observe a multidirectional growth of the pockmarks rather than an elongation. Our data suggests a distinct spatiotemporal evolution in four distinct evolutionary steps: (1) formation as small (semi-) circular feature of less than 1 m diameter, (2) modulation by strong tidal bottom currents, (3) intermingling and coalescence of pockmarks (4) vanishing of pockmarks. Based on our findings, we define a new type of pockmark that forms solely in sandy environments.

CONCLUSION

We have analyzed more than 50,000 pockmarks and derived geomorphological parameters to characterize a new type of pockmark that is solely formed in sandy shallow water environments. We find that this type of pockmark is highly dynamic. Our data suggest a life cycle of these pockmarks in four distinct evolutionary steps. Pockmarks wax and vanish over short periods of time (days to weeks). However, we cannot confirm any formation processes at the current stage. With the lack of conclusive evidence for any of the hypotheses on pockmark formation, we neither can rule out or confirm process to answer the remaining questions regarding the source that fuels these pockmarks, more and deeper geochemical data on the subsurface, reconnaissance surveys at higher rates or cabled-monitoring sites and/or benthic monitoring are needed to confirm any of the theories beyond doubt.

REFERENCES

Andresen KJ, Huuse M, Clausen OR, Morphology and distribution of Oligocene and Miocene pockmarks in the Danish North Sea-implications for bottom current activity and fluid migration, *Basin Research* 2008, 20. Jg., Nr. 3, S. 445–466.

Andresen KJ, Huuse M, 'Bulls-eye' pockmarks and polygonal faulting in the Lower Congo Basin: Relative timing and implications for fluid expulsion during shallow burial, *Marine Geology* 2011, 279. Jg., Nr. 1-4, S. 111–127.

Andresen KJ, et al., The longevity of pockmarks – A case study from a shallow water body in northern Denmark, *Marine Geology* 2021, 434. Jg., S. 106440.

Andrews BD, Brothers LL, Barnhardt WA, Automated feature extraction and spatial organization of seafloor pockmarks, Belfast Bay, Maine, USA, *Geomorphology* 2010, 124. Jg., Nr. 1–2, S. 55-64.

Berndt C, Focused fluid flow in passive continental margins, *Philosophical Transactions of the Royal Society A: Mathematical, Physical and Engineering Sciences* 2005, 363. Jg., Nr. 1837, S. 2855–2871.

Brothers LL, et al., More than a century of bathymetric observations and present-day shallow sediment characterization in Belfast Bay, Maine, USA: implications for pockmark field longevity, *Geo-Marine Letters* 2011, 31. Jg., S. 237–248.

Bruns I, et al., Identifying trawl marks in north sea sediments, *Geosciences* 2020, 10. Jg., Nr. 11, S. 422.

Feng D, et al., Authigenic carbonates from methane seeps of the northern Congo fan: microbial formation mechanism, *Marine and Petroleum Geology* 2010, 27. Jg., Nr. 4, S. 748–756.

Gafeira J, Long D, Diaz-Doce D, Semi-automated characterisation of seabed pockmarks in the central North Sea, *Near Surface Geophysics* 2012, 10. Jg., Nr. 4, S. 301–312.

Gupta S, et al., Spontaneously exsolved free gas during major storms as an ephemeral gas source for pockmark formation, *Geochemistry, Geophysics, Geosystems* 2022, 23. Jg., Nr. 8, S. e2021GC010289.

Hoffmann JLL, et al., Complex eyed pockmarks and submarine groundwater discharge revealed by acoustic data and sediment cores in Eckernförde Bay, SW Baltic Sea, *Geochemistry, Geophysics, Geosystems* 2020, 21. Jg., Nr. 4, S. e2019GC008825.

Judd A; Hovland M., Seabed fluid flow: the impact on geology, biology and the marine environment, Cambridge University Press 2009.

King LH; MacLean B, Pockmarks on the Scotian shelf, Geological Society of America Bulletin 1970, 81. Jg., Nr. 10, S. 3141–3148.

Krämer K, et al., Abrupt emergence of a large pockmark field in the German Bight, southeastern North Sea, Scientific reports 2017, 7. Jg., Nr. 1, S. 5150.

Mueller RJ, Evidence for the biotic origin of seabed pockmarks on the Australian continental shelf, Marine and Petroleum Geology 2015, 64. Jg., S. 276–293.

Paull C, et al., Pockmarks off Big Sur, California, Marine Geology 2002, 181. Jg., Nr. 4, S. 323–335.

Schneider von Deimling J, et al., Millions of seafloor pits, not pockmarks, induced by vertebrates in the North Sea, Nature Communications Earth & Environment in press.

SCIENTIFIC OUTPUT

LIST OF PUBLICATIONS

Böttner C, Hoffmann J, Unverricht D, Geersen J, Krämer K, Schmidt M, Karstens J, Spiegel T, Müller T, Sander L, Schmidt C, et al., The enigmatic seafloor depressions of the southeastern North Sea, in prep. for Frontiers in Earth Sciences.

DATA

Continuous thermosalinograph oceanography:
<https://doi.pangaea.de/10.1594/PANGAEA.938269>

Bathymetric data set: To be published soon.

CRUISE REPORT

MSM99/2: [doi:10.48433/cr_msm99_2](https://doi.org/10.48433/cr_msm99_2)

MSM100

Geophysical Investigations for Barrier Structures and their Integrity in the subsurface of the German North Sea by means of 3D-Seismic data

AUTHORS

Bundesanstalt für Geowissenschaften und Rohstoffe (BGR) | Hannover, Germany
A. Ehrhardt, M. Schnabel, H. Stück

Institute of Geophysics, University Hamburg | Hamburg, Germany
C. Hübscher

Department of Geoscience, University Bremen | Bremen, Germany
H. Keil, S. Wenau

INTRODUCTION

Within the transition to renewable energy and the reduction of greenhouse gas emissions, the integrity of barriers and seals in the deep underground becomes increasingly important for storage purposes, e. g. for CO₂ in the framework of CCS or for synthetic energy gases in the course of the change to renewable energy (Power2Gas). With this project, we study the integrity of barrier formations of Cenozoic mudstone layers in the German North Sea. If the barrier formation is not closed, either because of abandoned drill holes or along natural pathways it enables discharge of fluids into the North Sea. Thus, the second topic is the understanding of migration of fluids along pathways through seal formations. For the first time we will use high resolution multi-channel seismic 3D and OBS data to image the Cenozoic sediments in detail, in order to identify and interpret the fault systems that may enable fluid migration to the surface and to transfer the interpretation into a 3D geological model. By means of the high-resolution approach, we image fault systems that were previously postulated in the "sub-seismic" domain. The data cover in close proximity different fault systems, seeps, and undisturbed strata. The outcome of this study will be a profound understanding of fault systems and structures in the Cenozoic sediments like polygonal-, crestal- or step faults as well as tunnel valleys and especially how they communicate.

METHODS

The 3D reflection seismic acquisition was carried out with two streamer cables (each 1050 m long with 168 channels) and two sources (each with two GI guns in true GI mode). For the high-resolution setup streamer cables were separated by 50 m, the guns by 25 m. This lead to the inline cdp separation of 3.125 m and crossline separation of 12.5 m. In total an area of 94 km² was covered by the 3D seismic acquisition, in

addition we acquired several 2D seismic lines during a bad weather time window (see Figure 1). The processing of the data included designation, de-bubbling, de-multiple (including 3D-SRME, 3D-shallow water demultiple, radon demultiple), regularization of the seismic traces, several velocity analysis iterations including velocity autopicker, prestack Kirchhoff migration, stacking with angle mute, poststack predictive deconvolution. The resulting 3D high resolution image will not only give the opportunity to track small scale structures laterally but also improve the vertical resolution significantly compared to conventional 2D HRS data (Games and Wakefield, 2014; Games and Self, 2017). With this 3D high-resolution approach, we can image and analyze faults that were previously postulated as “sub-seismic” faults (e. g. Seebeck et al., 2015).

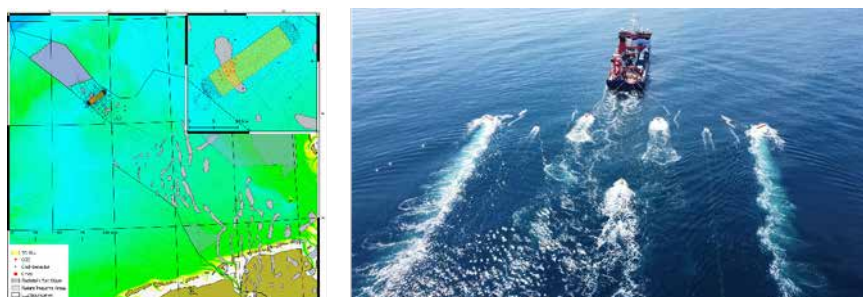


Figure 1: (Left) Overview map of the German EEZ and the location of the GeoBasis-3D seismic survey in the area of the Entenschnabel (Ducks Beak). The inset in the top-right corner shows the 3D area above the salt diapir “Belinda” (Right) 3D aerial view of the 3D seismic acquisition aboard R/V Maria S. Merian. The setup consists out of 2 streamer cables (each 1050 m long and 2 sources (2x GI gun) which were triggered in flip-flop mode.

RESULTS

The 3D seismic volume shows the sedimentary succession in the area of salt diapir Belinda (Figure 1) from the seafloor down to the Zechstein. Maximum signal penetration is about 4 seconds TWT, so that the base of the Zechstein is not imaged continuously. The vertical resolution shows even smallest faults after comparing the vertical and lateral coherency. The uppermost 300–400 ms TWT of the seismic volume (approx. 500 m) are mainly affected by various generations of tunnel valleys and in the southern part by the near surface parts of the crestal faults above Belinda (Figure 2). In the context of potential fluid migration systems, tunnel valleys and crestal faults coincide spatially and are in contact to each other (Figure 2). Whether there is a true genetic relationship between these structural elements, such as between the formation of tunnel valleys and the lithology or permeability of Cenozoic sediments in the Danish North Sea (Huuse and Lykke-Andersen, 2000), was not analyzed so far in the present study. Apart from the crestal faults we observe isolated phase reversed bright spots within very recent and very shallow valley structures (see Ahlrichs et al. this volume).

The interval of 400–1400 ms TWT shows a regular sedimentation pattern, only affected by the rise of salt diapir Belinda and the corresponding crestal faults. In the southeastern part of the survey area we observe an active fluid migration system with a stacked pattern (Christmas tree pattern) of bright spots (Figure 2 and Figure 3; see also Müller et al. 2018). Römer et al. (this volume) sampled several active seeps in the area of the southern Entenschnabel (mainly the neighboring salt diapir Berta) and analyzed the nature of the fluids as of biogenic origin. It is likely that we observe at Belinda also a biogenic fluid migration system.

Between 1400 and 2000 ms TWT we observe a thick layer with polygonal faults (Figure 3). This layer is overprinted by the rise of salt diapir Belinda but most likely not affected by faults. The small scaled pattern of round and sickle shaped polygonal faults that formed during the dewatering process of the clay sediments (e. g. Cartwright et al. 2003), seems to be not permeable for fluids as we do not observe any bright spots within or above the polygonal faults. However, the clay sediments are unusually thick in this area, e. g. compared to the Westschleswig Block, where we observe a thickness of 50–100 ms TWT (see MSM97/2 Ehrhardt et al. this volume).

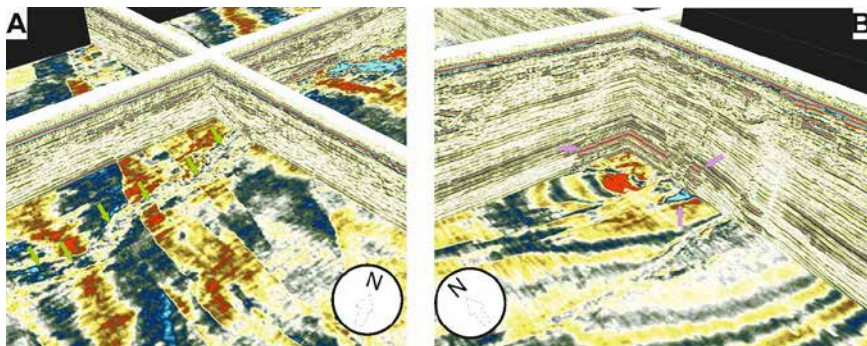


Figure 2: (A) 3D view to the crestal faults of salt diapir Belinda at time slice 280 ms showing a through cutting tunnel valley (green arrows). (B) 3D view to the bright spot pattern (pink arrows) above the crestal faults of Belinda (time slice at 630 ms).

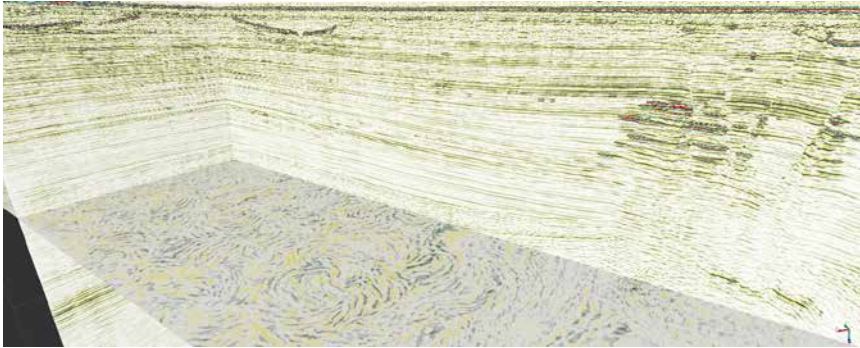


Figure 3: 3D view of the GeoBasis-3D volume. On the right hand side bright spots in the Christmas tree like pattern show an active fluid migration system along the crestal faults over the salt diapir Belinda. The time slice at 1568 ms TWT shows the circular pattern of the polygonal faults of the Rupel Clay.

REFERENCES

Cartwright JA, Bolten AJ, James DM, The Genesis of polygonal fault systems: A review, Geological Society London Special Publications 2023, 216(1), DOI:10.1144/GSL.SP.2003.216.01.15.

Games KP, Wakefield NP, The Successful Design, Development and Acquisition of a UHRS 3D Seismic Dataset, Near Surface Geoscience 2014, EAGE, DOI: 10.3997/2214-4609.20142132.

Games KP, Self E, HRS 3D data — a fundamental change in site survey geohazard interpretation, First Break 2017, 35, p 39–47.

Huuse M, Lykke-Andersen H, Overdeepened Quaternary valleys in the eastern Danish North Sea: morphology and origin, Quat. Sci. Rev. 2000, 19 (12), 1233–1253.

Schurr B, Asch G, Hainzl S, Bedford J, et al., Gradual unlocking of plate boundary controlled initiation of the 2014 Iquique earthquake, Nature 2014, 512, doi: 10.1038/nature13681.

Seebeck H, Tenthoery E, Consoli C, Nicol A, Polygonal faulting and seal integrity in the Bonaparte Basin, Australia, Marine and Petroleum Geology 2015, 60, 120–135, Elsevier

SCIENTIFIC OUTPUT

LIST OF PUBLICATIONS

Ahlich N, Ehrhardt A, Schnabel M, et al., Vertical acoustic blanking in seismic data from the German North Sea: a spotlight to shallow gas-bearing incised channels, Journal of Quaternary Science Reviews, in Review.

LIST OF CONFERENCE PRESENTATIONS

2023 | **Analysis of fluid migration pathways in the context of CO₂ underground storage in the German North Sea using high-resolution 3D and 2D seismic data**
Ahlich N, Ehrhardt A, Schnabel M, Fuhrmann A, Stück H, GeoBerlin, Germany

2023 | **New insights into the formation and distribution of Pleistocene tunnel valleys in northern Germany** Breuer S, Bebiolka A, Ehrhardt A, Noack V, Lang J, GeoBerlin, Germany

2023 | **Tunnel valley formation in the “Entenschnabel” area of the German EEZ – results from a High Resolution 3D Seismic Dataset**, Ehrhardt A, Schnabel M, Ahlich N, DGG Bremen, Germany.

DATA

The data from MSM100 will be available according to GeolDG from 01.06.2024:
https://www.bgr.bund.de/DE/Themen/Geodatenmanagement/GeolDG/Downloads_Daten_AWZ/downloads_daten_AWZ_node.html

CRUISE REPORT

MSM100: doi: 10.48433/cr_msm100

MSM101

Paleoclimate and Biogeochemistry Nova Scotia Margin

AUTHORS

Institute of Geosciences, Kiel University | Germany

R. Schneider

Cruise MSM101, on the one hand, conducted sediment coring for paleoceanographic investigations, oriented along four inner shelf basin transects on the Scotian Shelf and one on the southern Newfoundland Shelf (Figure 1). On the other hand, three cross-shelf-slope transects were executed. This sampling setup was designed to reconstruct (i) the climatic variability of the main cold subpolar water masses originating from the Labrador Sea, (ii) directly compare it with the warm North Atlantic Circulation (NAC) in the Northwest Atlantic, and (iii) also link it in the same setting with subsurface water mass changes (Figure 2). The latter include the Scotian Slope Water Mass, and those related to the Deep Western Boundary Circulation (DWBC), the third major element of the Atlantic Meridional Overturning Circulation (AMOC). Since all important oceanic surface and subsurface water masses are merging along the Scotian Margin, this region is pivotal to directly disentangle climate changes in the Labrador Sea from those in the Subtropical Gyre circulation of the North Atlantic. The latter is much less affected by meltwater than the LC and generally much warmer due to the northward heat transport by the Gulf Stream. At intermediate and deeper water depths, the reconstruction of the formation and variability in the Scotian Slope Water Mass, a mixture of subsurface NAC and LC / Gulf of St. Lawrence waters, is the second goal of the post-cruise work, because it is important for biogeochemical cycling of, e. g., carbon, oxygen, and trace element and nutrient fluxes, thus controlling offshore planktonic and benthic ecosystems.

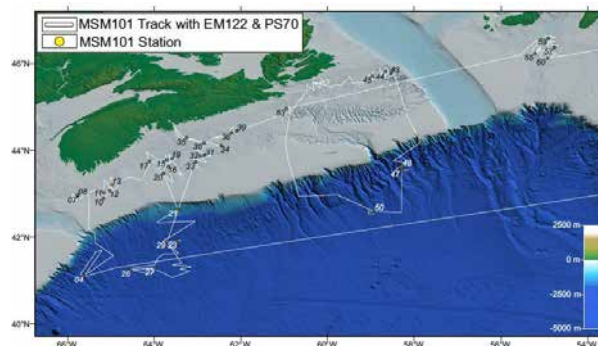


Figure 1: MSM101 cruise track in the originally planned working areas with geological and water column sampling stations. Numbers refer to individual station coding.

During the cruise the inner shelf basin hydroacoustic surveys and cross-shelf-slope transects assisted to identify the best locations of thickest young mud deposits most suited for our aim to reconstruct Postglacial to Latest Holocene time-transgressive gradients of changes in water mass variability, benthic nutrient, freshwater and terrigenous material fluxes by paleoceanographic proxy records. The retrieved sediments are characterized by an enhanced continental material supply from the Gulf of St. Lawrence and Gulf of Maine, either trapped as thick Deglacial to Holocene sediment sequences in the inner shelf basins and in morphological depressions or in channel-levee systems on the upper slope, mainly forming terrigenous to hemipelagic muds, silty sands, or sands with a pelagic component from marine biological productivity. With about 250 m of new gravity corer sediment sequences and more than 5500 1 cm thick sediment slices from multicorer deployments at the interface of bottom waters and surface sediments, we have gained an unprecedented archive to address the research questions described above.

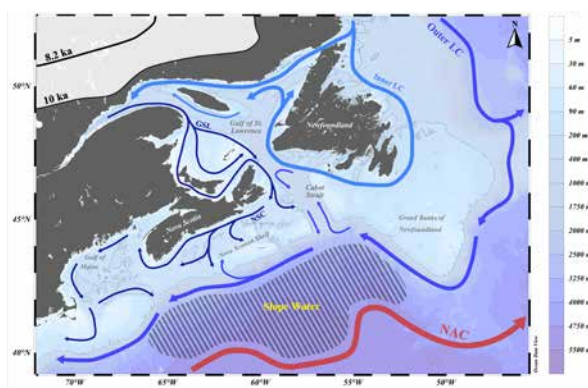


Figure 2: Location map of the Nova Scotian and Newfoundland region with recent surface circulation pattern and reconstructed LIS retreat. Cold currents (blue) on the eastern Canadian margin are shown delineating the Gulf of St. Lawrence waters (GSL), the Nova Scotian Current (NSC), and the inner and outer Labrador Currents (LC). The North Atlantic Current (NAC) transports warm waters (red) northeast-wards also in greater water depths (taken from P. Matzerath, Master Thesis, Kiel, May 2023).

First results from post-cruise work will be presented based on two sediment cores from the northeastern cold water and the southwestern warm water end on the Nova Scotia margin that have been XRF scanned and radiocarbon dated. Moreover, sediment core MSM101-44-3 retrieved from the Scatarie Basin on the northeastern Nova Scotian Shelf, an area strongly influenced by the Gulf of St. Lawrence outflow waters, was investigated in the frame of two Master Thesis studies. One focused on the reconstruction of sea-ice dynamics and their influence on marine productivity on the during the Holocene, based analyses of the total organic carbon content and several geochemical proxies, including biomarkers indicative of sea ice cover, phytoplankton productivity and terrigenous inputs. The second investigated the variance of planktonic foraminifera assemblages, investigating particularly the occurrence warm versus cold water species.

SCIENTIFIC OUTPUT

LIST OF PUBLICATIONS

Günther L, Abundance of planktonic foraminifera in Holocene sediments off Nova Scotia. Master Thesis, Institute of Geosciences, Kiel University, 2023.

Matzerath P., Biomarker and TOC based reconstruction of Holocene changes in sea ice and productivity on the Nova Scotian Shelf. Master Thesis, Institute of Geosciences, Kiel University, 2023.

CRUISE REPORT

MSM101: submitted to GPF, in review

MSM102

Morphology, stratigraphy and sedimentary record of the Northwest Atlantic Mid-Ocean Channel, Labrador Sea

AUTHORS

Institute for Geoscience – Kiel University | Kiel, Germany

S. Krastel, R. Barrett, K.-F. Lenz, G. v. Rönn

Geological Survey of Canada | Dartmouth, Canada

D. Mosher, K. Boggild

University of Liverpool | Liverpool, UK

C. Stevenson

INTRODUCTION

The Northwest Atlantic Mid-Ocean Channel (NAMOC) is the longest known deep sea channel in the World located between Greenland and Canada. NAMOC was first discovered in the early 1950s (Ewing et al., 1953) and stretches for ~4000 km offshore Hudson Strait through the Labrador Sea, circumnavigating the Grand Banks of Newfoundland and terminating at the northern limit of the Sohm Abyssal Plain (Heezen et al., 1969; Hesse et al., 1990; Klaucke and Hesse 1996). It was a major sediment transport pathway during Quaternary glacial cycles, directing sediment from the subaerial to the deep-sea environment. NAMOC exhibits features similar to fluvial systems with tributaries, channel meanders, levees, point bars, Yazoo channels, and a prominent thalweg. NAMOC is unique in respects other than just its length. It is not associated with a river system, did not form on a delta or deep-water fan and has no evident source of sediment that would account for its formation. The main aim of R/V MARIA S. MERIAN Cruise MSM102 was to enable the quantitative reconstruction of fundamental flow properties (e. g. thickness, speed and concentration) that created and maintained NAMOC. To achieve this aim, we: i) mapped the NAMOC over a distance of ~2000 km with the hydroacoustic systems of the vessel, ii) acquired high-resolution reflection seismic data crossing the NAMOC at several locations, and iii) collected sediment cores at 24 stations.

MORPHOLOGICAL ANALYSIS OF THE NAMOC

Continuous coverage of multibeam bathymetry and subbottom profiler data acquired during MSM102 facilitate detailed analysis of NAMOC to investigate factors that contribute to its unusually long and straight morphology. Cross-channel and downstream morphometrics measured every 500 m along length of the mapped channel (1800 km) distinguish three major segments characterized by variations in channel floor width.

Sinuosity values calculated at multiple scales are highest where the channel path is steered by bedrock exposures and rare tributary confluences (Figure 1). Where the channel path is unaffected by these external factors, the channel maintains a low sinuosity path. Most of these ‘equilibrium’ (low-sinuosity) channel segments are also characterized by extensive channel wall failures, as evidenced by scars in bathymetry and subbottom profiles. This observation suggests that instability of the levee sediments may play an important role in minimizing sinuosity growth through channel wall collapses that reset amplification of meanders. Between channel walls, the channel floor shows numerous bar-like features located upstream of inner bends, forming a ‘stepped’ downstream bathymetry. The location of these features relative to channel bends is contrary to what is expected for conventional models of submarine channels, which typically develop bars laterally or immediately downstream of inner bends (Peakall and Sumner, 2015). Narrow bedforms at the crests of these bar-like features suggest their geometry is resculpted by currents in the channel axis (Figure 1). This interplay of channel wall collapse and current resculpting was likely, therefore, an important factor in establishment of the unique morphology of NAMOC.

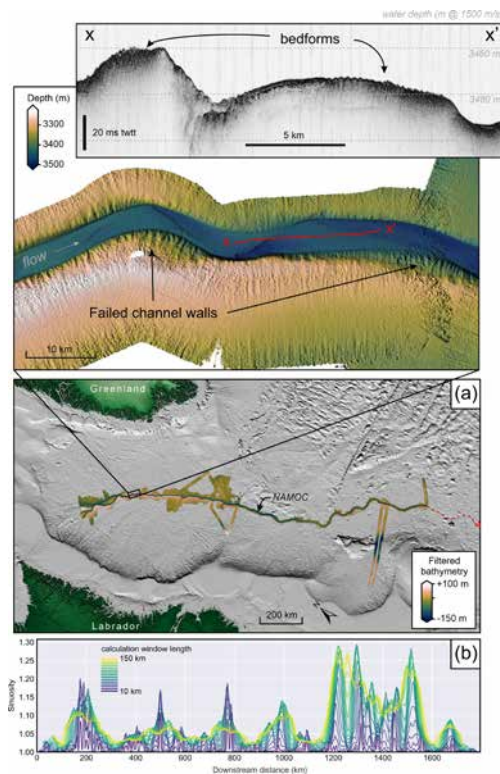


Figure 1: (a) Bathymetry from MSM102 over the Northwest Atlantic Mid-Ocean Channel (NAMOC) with enlarged inset (top) showing the presence of failed channel walls; subbottom profiler data ($x - x'$) shows narrow bedforms atop bar-like features in the channel axis. Sinuosity along the mapped channel path is shown in (b).

ARCHITECTURE OF THE NAMOC

Seismic profiles were recorded to image the architecture of the channel system with a focus on the levee structure and channel migration. The crossing profile P504 shows multiple buried channels (Figure 2). The NAMOC itself appears to have undergone little lateral migration over time. Further buried channels are visible on both sides of the main channel, which points to a buried braided channel system rather than Yazoo Channels. The entire channel is bounded by well developed levees. Profil P504 (Figure 2) shows two well developed, typical wedge-shaped levees on the eastern and western sides of the NAMOC. The western right-hand levee is better developed along the entire channel due to Coriolis Forces. Levee height decreases significantly with increasing distance to the continental margin. Flows are losing energy leading to less overspill of the turbidity currents resulting in a large variety of levee shapes along the channel.

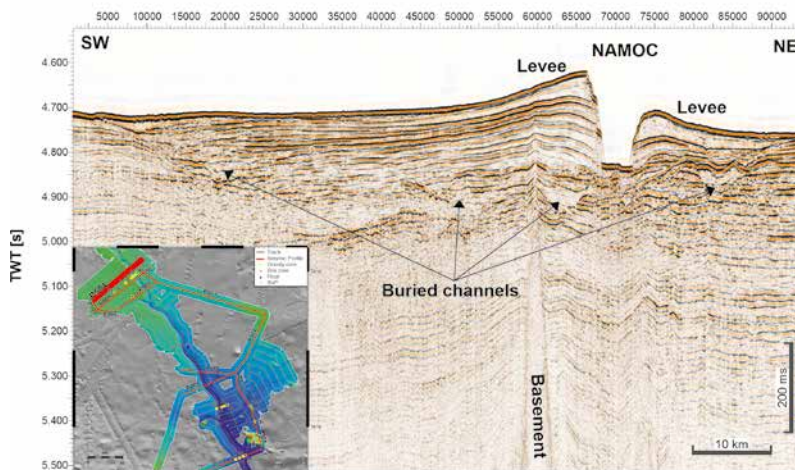


Figure 2: Seismic profile P504 crossing the NAMOC. The righthand levee is very well developed at this location. Several buried channels indicate an ancient braided channel system.

MASS TRANSPORT ADJACENT TO THE NAMOC

The structure of a submarine channel is controlled by the competing processes of erosion and deposition within the channel, with turbidity currents and channel wall (levee) collapses playing a central role in channel development. Mass wasting adjacent to the NAMOC, however, also plays a role in the development of the channel. The acoustic data collected during cruise MSM102 image a series of stacked debris flows along the western side of the NAMOC. These debris flows, sourced from the Canadian continental shelf and each up to 25 m thick in our study area, run parallel to the NAMOC for tens or even hundreds of kilometres before locally breaching the channel levee and continuing within the NAMOC itself (Figure 3). Our data show that the debris flows only breach the levees where they are less than 20 m high and have slope gradients less than 1.3° . Two

tributaries have been completely (and repeatedly) infilled by these debris flows. The striking bathymetric steps at the junctions of the tributaries with the NAMOC (Figure 3 inset) provide evidence of erosion and re-establishment of these infilled channel tributaries. In their in-prep manuscript, Barrett et al. map out the minimum extent of these debris flows; characterize their internal morphology using acoustic data (sub-bottom profiles) and sediment gravity cores (Figure 4); and constrain the timing of emplacement of the uppermost of these debris flows using radiocarbon dating. These findings highlight the importance of external processes on channel development.

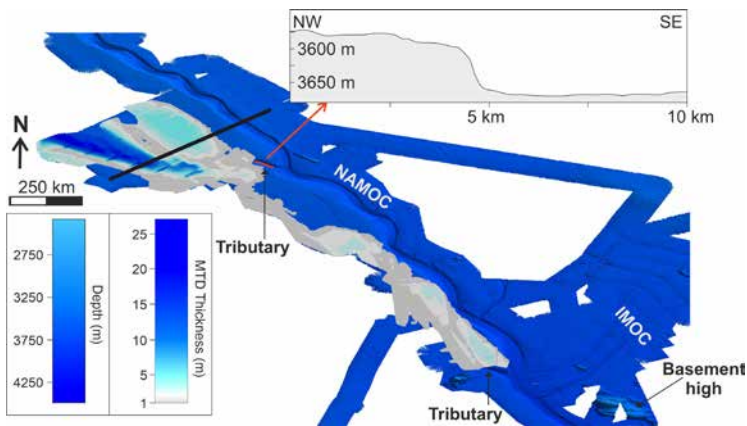


Figure 3: The distribution of the uppermost of a series of laterally-extensive mass transport deposits mapped adjacent to the NAMOC in acoustic data collected during cruise MSM102. IMOC = Imarsuak Mid-Ocean Channel.

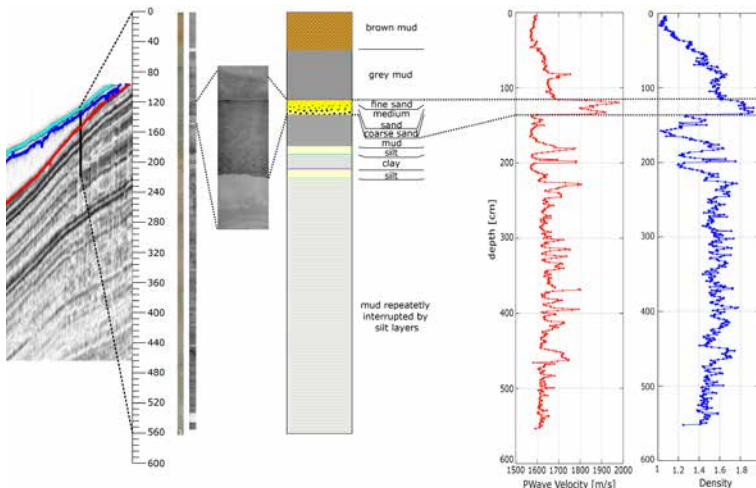


Figure 4: Core MSM102-44 penetrated through the uppermost of the mass transport deposits (MTDs) adjacent to the NAMOC. The MTD follows a classic Bouma sequence, with a coarse (erosive) base and upwardly fining character, and is clearly demarcated in the along-core P-velocity and density data collected after the cruise.

REFERENCES

Ewing M, Heezen BC, Ericson DB, Northrop J, Dorman J, Exploration of the northwest Atlantic mid-ocean canyon, *GSA Bulletin* 1953, 64(7), 865–868, [https://doi.org/10.1130/0016-7606\(1953\)64\[865:EOTNAM\]2.0.CO;2](https://doi.org/10.1130/0016-7606(1953)64[865:EOTNAM]2.0.CO;2).

Hesse R, Rakofsky A, Chough SK, The central Labrador Sea: facies and dispersal patterns of clastic sediments in a small ocean basin, *Marine and Petroleum Geology* 1990, 7, 13–28, [https://doi.org/10.1016/0264-8172\(90\)90052-l](https://doi.org/10.1016/0264-8172(90)90052-l).

Heezen BC, Johnson GL, Hollister CD, The northwest Atlantic mid-ocean canyon, *Canadian Journal of Earth Sciences* 1969, 6(6), 1969, <https://doi.org/10.1139/e69-146>.

Klaucke I, Hesse R, Fluvial features in the deep-sea: new insights from the glacial sub-marine drainage system of the Northwest Atlantic Mid-Ocean Channel in the Labrador Sea, *Sedimentary Geology* 1996, 106, 223–234, [https://doi.org/10.1016/S0037-0738\(96\)00008-5](https://doi.org/10.1016/S0037-0738(96)00008-5).

Peakall J, Sumner EJ, Submarine channel flow processes and deposits: A process-product perspective. *Geomorphology* 2015, 244, 95–120, <https://doi.org/10.1016/j.geomorph.2015.03.005>

SCIENTIFIC OUTPUT

LIST OF PUBLICATIONS

Krastel S, Mosher DC, Mapping a river beneath the sea, *EOS* 2022, 103, <https://doi.org/10.1029/2022EO220052>.

Mosher DC, Dickson ML, Shimeld J, Jackson HR, et al., Canada's maritime frontier: the science legacy of Canada's extended continental shelf mapping for UNCLOS, *Canadian Journal of Earth Sciences* 2023, 60, 1–51, <https://doi.org/10.1139/cjes-2022-0069>.

LIST OF CONFERENCE PRESENTATIONS

2021 | **A River Beneath the Sea: mapping the Northwest Atlantic Mid-Ocean Channel**
Lecture to the Geological Survey of Canada, Atlantic, Canada.

2022 | **A River Beneath the Sea: Morphological Investigations of the Northwest Atlantic Mid-Ocean Channel (NAMOC)** 82. Jahrestagung der Deutschen Geophysikalischen Gesellschaft, München (online), Germany.

2022 | NAMOC; **A River Beneath the Sea** World River and Delta Systems S2S talk series; North Carolina State Univ., USA.

2023 | **Building (and rebuilding) a submarine channel: Mass transport processes in the Northwest Atlantic Mid-Ocean Channel, Labrador Sea** 83. Jahrestagung der Deutschen Geophysikalischen Gesellschaft, Bremen, Germany.

DATA

Hydroacoustic data:

https://www.bsh.de/EN/DATA/Climate-and-Sea/Oceanographic_Data_Center/Surveying_data/surveying_data_node.html, DOD-Referenz: 20210011

Seismic data: stored on servers at Kiel University, no central data base available

Cores: stored in the repository of Kiel University

Argo Floats:

<https://argo.ucsd.edu/>

<https://www.ocean-ops.org/board?t=argo>

Thermosalinograph:

<https://doi.org/10.1594/PANGAEA.946415>

Physical oceanography (ADCP):

<https://doi.org/10.1594/PANGAEA.945842>

<https://doi.org/10.1594/PANGAEA.945800>

CRUISE REPORT

MSM102: [doi:10.48433/cr_msm102](https://doi.org/10.48433/cr_msm102)

MSM103

Investigation of Potential Offshore Groundwater in the Gulf of St. Lawrence, Canada

AUTHORS

GEOMAR Helmholtz Centre for Ocean Research | Kiel, Germany

S. Hölz, G. Franz, J. Klein, M. Kühn, J. Elger, M. Schmidt, T.H. Müller, C. Berndt, M. Jegen, A. Haroon, Hensen, C., Lenz, N.

Dalhousie University | Halifax, Canada

F. Córdoba-Ramírez, I. Schulten, G. Cairns, V. Maselli, M. Nedimović, B. Kurylyk, A. Hay, C. Brown, J. MacFadyen

University of Malta | La Valletta, Malta

A. Micallef

University of Delaware | Newark, USA

H. Michael

Groundwater represents the world's largest freshwater resource and provides drinking water for two billion people globally and over 10 million Canadians. Groundwater resources in Prince Edward Island (PEI) have faced compounding stresses in recent years due to the extensive agricultural industry and the impacts of climate change on sea-level and the hydrological cycle. Freshened Offshore Aquifers (FOAs) could represent a new freshwater resource for PEI, and for similar island settings worldwide. SOURCE, the first exploratory study of fresh submarine groundwater resources in Canada, aims to test the hypothesis that ice sheet dynamics and landscape evolution during the last glacial-interglacial cycle(s) contributed to the recharge of FOAs hosted in fractured consolidated clastic sediments offshore PEI and to explore the interaction between submarine groundwater discharge, ocean biogeochemistry and benthic eco-systems.

During the 9-week long research expedition MSM103 (12.9.–15.11.2021), carried out with R/V Maria S. Merian as part of the SOURCE project, multidisciplinary investigations were carried out in the Gulf of St. Lawrence north of Prince Edward Island (PEI) to identify and quantify offshore aquifers in the region (see Figure 1). Investigations were carried out with a variety of geophysical and geological methods, including multibeam echosounder data, high-resolution sub-bottom profiles and 2D multi-channel seismic profiles to gather information on the water column, the seafloor, and the upper 500m of sediments and sedimentary rocks. These acoustic measurements were complemented by nine controlled source electromagnetic (CSEM) experiments at locations around PEI,

which were chosen based on preliminary results from the acoustic methods. Finally, sediment samples with a gravity corer were collected at various locations around the island and – at one location – potentially gave the first direct indication for the existence of OFG in the region.

A large number of channel structures could be detected in acoustic / seismic sections, which are interpreted as parts of glacial or post-glacial drainage systems. It is not yet possible to say whether these are connected to any existing deeper groundwater systems. In the hydroacoustic data, only subtle evidence for the escape of fresh water or gas could be observed in the water column. In several places, however, a blanking was evident in the seafloor, which indicates the occurrence of gases and could hint at potential pathways for gas and / or freshwater within the seafloor. In sediment samples taken at a location north of PEI, a significant drop in salinity and resistivity could be detected in the upper 3m of the sediment, which provided a first direct indication of the presence of fresher groundwater. From the electromagnetic measurements carried out in seven working areas, first evidence is available that high resistivities may show a FOA within the seafloor.

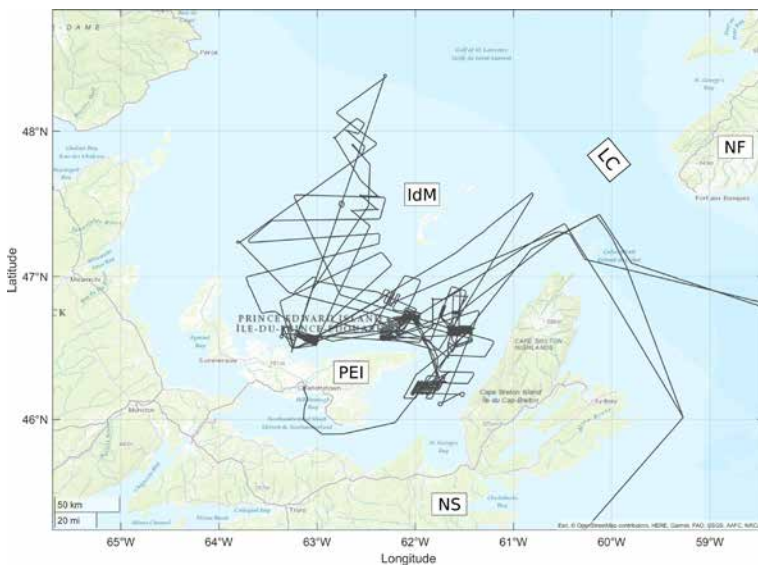


Figure 1: Overview map of working area in the Gulf of St. Lawrence, which is located between (clockwise) Newfoundland (NF), Cape Breton Island, Nova Scotia (NS) and mainland Canada. The ship-track, which is mostly along the seismic and hydroacoustic lines, outlines the main working area to the N and E of Prince Edward Island (PEI) and around the Îles de la Madeleine (IdM). To the N, profiles were terminated at the Laurentian Channel (LC).

The first half of the cruise was mainly used for seismic and bathymetric measurements. In order to comply with environmental restrictions in the working area, which were monitored by Canadian marine mammal observers (MMOs), seismic measurements were carried out

along a total profile length of 2166km with a short (150m), bird-controlled streamer with dense hydrophone spacing (1,56m) in combination with a small source (GI-Gun, 45 in³ generator and 45 in³ injector chamber). Due to the shallow water depth in the working area (<100m), the seismic sections were strongly influenced by multiples (Figure 2, top), which could be significantly reduced with suitable fk-filtering with or without including dip information (Figure 2, middle and bottom, respectively). In the above example, gently dipping layers represent middle to upper Paleozoic sandstone formations (Ryan et al., 1991; St. Peter, 1993), partially influenced by tectonics (left part of section), which can host large groundwater aquifers in fractures (Paradis et al., 2016). They often directly crop out at the seafloor, some-times covered by a thin veneer of marine sediments or glacial deposits. In some parts of the sections (e. g. right edge of section in Figure 2), the sandstones are incised by channels, which most likely formed during the last ice age when the whole area was fully glaciated (Shaw 2005; Shaw et al., 2006).

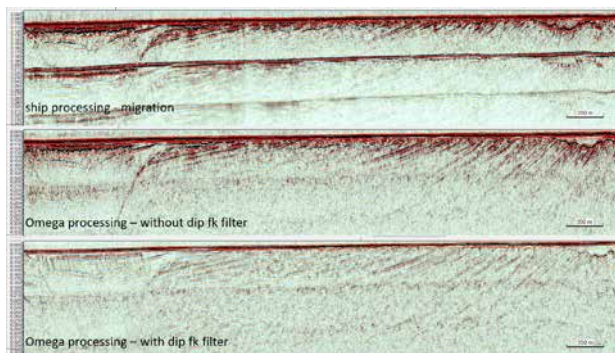


Figure 2: Exemplary seismic section with different levels of processing.

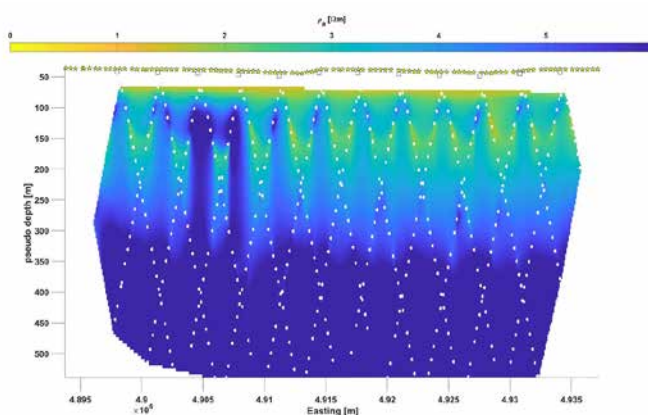


Figure 3: Pseudo section of CSEM data (based on Swidinsky et al., 2015) acquired with the CAGEM transmitter system and OBEM receivers in the main working area to the N of PEI (Survey 7 in Hölz, 2022). The pseudo-section shows elevated apparent resistivities in the shallow part at one of the channel incisions identified by seismics. See text for further details.

Channels identified in the seismic sections during the first half of the cruise, were then investigated in more detail with controlled source electromagnetic experiments and detailed bathymetric mapping in the second half of the cruise. The original plan of using a bottom-towed CSEM system for investigations along profiles had to be abandoned after a first try, because the hard seafloor, partially covered by coarse glacial deposits, led to substantial damage of the system, thus, not allowing for a save operation in the working area. As alternative experiment, we used the novel CAGEM transmitter system (Hölz et al., 2019), which is operated a few meters above the seafloor, in combination with OBEM receiver nodes deployed stationary to the seafloor. While this style of experiment did not allow for measurements along extended profile lines, it was good for detailed investigation with flexible array layouts of six channel structures previously identified in seismic data. Figure 3 shows a first pseudo-section derived from the data measured to the N of PEI (Survey 7 in Hölz, 2022), which shows a significant increase in the apparent resistivity in the westerly part of the section at shallow depth, which coincides with one of the channel structures identified in the seismic data. Please note, that while pseudo-sections of CSEM data can give a first impression of the overall resistivity structure (e. g. lateral resistivity contrasts), they are generally not suitable for a detailed structural interpretation. Such an interpretation should instead rely on the inversion of data, which by the time of writing this abstract is work in progress.

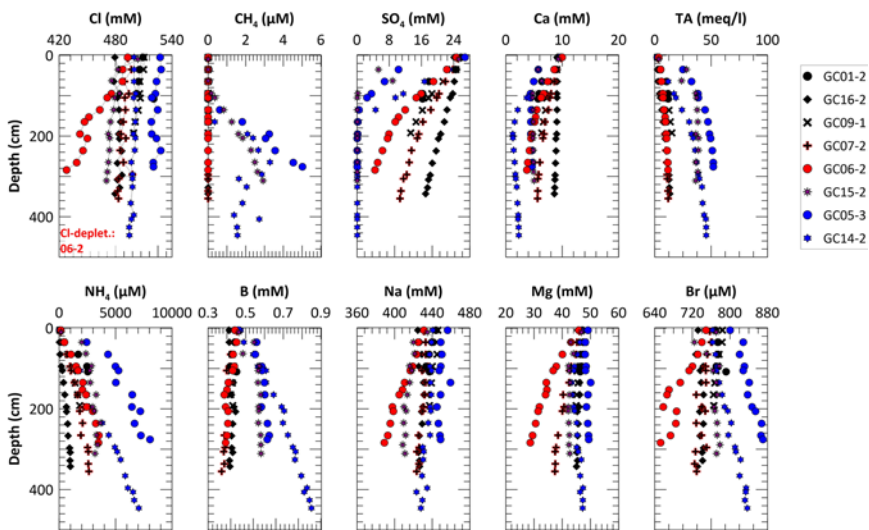


Figure 4: Porewater composition of gravity cores from cruise MSM103.

Figure 4 shows porewater chemical data from eight gravity cores with variable seawater chloride concentrations, which is clearly less saline than Atlantic Ocean water. The chloride content in most of the pore water profiles differs from Atlantic Seawater (~540 mM) by up

to 10–15 % but variability with depth is about <5%. This variability is probably induced by seawater/freshwater mixing conditions in the St. Lawrence Bay (e. g. Frank, 2015). However, chloride, sodium and other tracer concentrations of GC06 markedly decline with depth (red dots), which rather indicates a sub-bottom freshwater source than changing oceanographic conditions. Since gravity core GC06 was taken in the close vicinity to the anomaly observed in the CSEM data, we consider this a first direct indication for freshened offshore groundwater in the working area.

REFERENCES

Frank A, A Hydrographic Climatology of the Gulf of St. Lawrence. (Master's thesis 2015). Retrieved from <https://scholarcommons.sc.edu/etd/3120>.

Hölz S, Haroon A, Martins S eds., RV POSEIDON Fahrtbericht / Cruise Report POS535 – Loki2GrimseyEM: Geophysical and geological investigations of massive sulfides at and in the vicinity of Loki's Castle (Norway) and similar experiments around the Grimsey Hydrothermal Field (Iceland) for the assessment of the geothermal potential and the exploration for potential mineralizations within the seafloor. Akureyri (Iceland) – Bremerhaven (Germany), 09.06–03.07.2019, GEOMAR Report 2019, N. Ser. 0053. GEOMAR Helmholtz-Zentrum für Ozeanforschung, Kiel, Germany, 89pp. DOI 10.3289/GEOMAR_REP_NS_53_2019.

Hölz S (ed), Groundwater Resources Offshore Prince Edward Island, Canada Cruise No. MSM103, 12.9.–15.11.2021 Emden (Germany) – Halifax (Canada) – Emden (Germany). Maria S. Merian Berichte 2022, MSM103, Begutachtungspanel Forschungsschiffe, Bonn, Germany, 121 pp. DOI 10.48433/cr_msm103.

Ryan RJ, Boehner RC, Calder JH, Lithostratigraphic revisions of the upper Carboniferous to lower Permian strata in the Cumberland Basin, Nova Scotia and the regional implications for the Maritimes Basin in Atlantic Canada, *Bulletin of Canadian Petroleum Geology* 1991, 39, 289–314.

Shaw J, Geomorphic Evidence of Postglacial Terrestrial Environments on Atlantic Canadian Continental Shelves, *Géographie physique et Quaternaire* 2005, 59, 141–154.

Shaw J, Piper DJW, Fader GBJ, King EL, Todd BJ, Bell T, Batterson MJ, Livermanc DGE, A conceptual model of the deglaciation of Atlantic Canada, *Quaternary Science Reviews* 2006, 25, 2059–2081.

St. Peter C, Maritimes Basin evolution: key geologic and seismic evidence from the Moncton Subbasin of New Brunswick, *Atlantic Geology* 1993, 29, 233–269.

SCIENTIFIC OUTPUT

LIST OF CONFERENCE PRESENTATIONS

2022 | **Preliminary results from the first study for offshore groundwater exploration in Atlantic Canada** INTERNATIONAL WORKSHOP ON OFFSHORE FRESHENED GROUNDWATER RESEARCH, Valletta, Malta.

2023 | **Determination of Orientation of Marine Magnetometers by Means of Modelled Local Field Variations Derived from Spherical Elementary Current Systems** EGU, Vienna, Austria.

2023 | **Determination of Orientation of Marine Magnetometers by Means of Modelled Local Field Variations Derived from Spherical Elementary Current Systems** IUGG, Berlin, Germany.

2023 | **CSEM investigations for freshened offshore groundwater, challenges, and solutions** EMTF, St. Marienthal, Germany.

DATA

Ship data (ship track):

<https://doi.pangaea.de/10.1594/PANGAEA.941874>

Ship data (ship track):

<https://doi.org/10.1594/PANGAEA.941885>

Physical oceanography (ADCP, 38kHz):

<https://doi.org/10.1594/PANGAEA.945365>

Physical oceanography (ADCP, 75kHz):

<https://doi.org/10.1594/PANGAEA.945370>

Physical oceanography (thermosalinograph):

<https://doi.org/10.1594/PANGAEA.946385>

Bathymetry: MSM103 Transit-Bathymetrie has been handed over to the data-management team but publication is still pending.

CRUISE REPORT

MSM103: DOI 10.48433/cr_msm103

MSM104

Sinking particles, their production, transfer and preservation

AUTHORS

MARUM, Center for Marine Environmental Sciences, University of Bremen |
Bremen, Germany
K.A.F. Zonneveld

During the cruise MSM104, scientists from the MARUM at the University of Bremen and Carl von Ossietzky University of Oldenburg, the Alfred-Wegener-Institute Heilmholz-Zentrum für Polar- und Meeresforschung in Bremerhaven and the Royal Netherlands Institute for Sea Research have performed joint investigations to study natural and anthropogenic formed particular and dissolved organic matter and mineral particles off NW Africa. Main focus was the study the of the input/formation, the sinking/lateral advection and alteration in the water column and surface sediments of organic matter, (bio)mineral and micro-plastic particles and their environmental proxies in relationship to different environmental conditions. Furthermore, the relationship between production/aggregation of dissolved and particular organic matter as well as their residence time in ocean waters was studied. Apart from this the relationship between mineral dust input and upper ocean bioproduction, aggregate formation and water column winnowing has been investigated. Results of these process studies shall be compared to long-term flux records in sediment-trap series and dust collection. These processes have been studied in an active upwelling cell, offshore drifted upwelling filaments and the open ocean off the highly dynamic Cape Blanc region off Blanc d'Arquin (Mauretania) in comparison to the open ocean conditions off southeast Cape Verde.

To obtain insight into how signals of the watercolumn are being preserved in the sediments, we have conducted a comparison study where we compared the export organic particle flux of particles of known origin and species specific morphology (dinoflagellate cysts) collected during an 18 years sediment trap survey, with particle composition of an undisturbed sediment core from the vicinity area of the trap. The core was subsampled per 3 mm to produce a high-resolution and dated with ^{210}Pb that showed that a sedimentation rate of ca. 0.1 cm/year. Our preliminary results indicated that the association of species resistant against aerobic degradation, follow the flux variations over time as registered by the sediment trap. Particles that are known to be sensitive for microbial degradation are highly affected by degradation in relationship to their exposure to oxygenated pore waters.

To obtain insight into the molecular alterations of particles sensitive to aerobic decay, we studied the molecular change of the wall of the dinoflagellate cysts *Stelladinium stellatum* as reflected by micro-Fourir transform infrared (micro-FTIR) from its production in the

upper water column, during the sinking process in the deeper water column and after embedding in the sediments. First results show that no molecular alteration takes place during the transport and settling process and that degradation in the sediments is most probably the result of microbial decay and not of a chemical process.

SCIENTIFIC OUTPUT

LIST OF PUBLICATIONS

Alfke F, Connecting the molecular composition and radiocarbon age of dissolved organic matter in the Mauritanian sub- region of the Canary Upwelling System, Master Thesis 2023, University of Bremen.

LIST OF CONFERENCE PRESENTATIONS

2023 | **Environmental factors influencing the dinoflagellate cysts production and their preservation in the bottom sediment in the upwelling region off Cape Blanc, Mauritania: a comparison of sediment trap with down-core sediment cyst record** International Conference for Young Marine Researcher, Oldenburg. Roza et al. (oral presentation)

2023 | **Micro-FTIR spectroscopy of dinoflagellate cysts-a step towards better understanding of selective organic matter transformation in the water column?** TMS Annual Conference 2023 Southampton Reuter et al. (oral presentation)

2023 | **Connecting the molecular composition and radiocarbon age of dissolved organic matter in the Mauritanian sub-region of the Canary Upwelling System** ICYMARE 2023 Oldenburg, Fenna Alfke (oral presentation)

2023 | **Dinoflagellate cysts: A journey from the upper water column to the ocean floor** Bremen PhD Days, Visselhövede. Roza et al. (poster)

2022 | Grotheer, H., Hammes, J., Gentz, T., Castrillejo, M., Hansman, R. L., Mollenhauer, G. **DIC radiocarbon measurements at the AWI-MICADAS facility Current method development and validation** Radiocarbon 2022 Zürich, CH

DATA

ADCP current measurement: <https://doi.org/10.1594/PANGAEA.952407>

Continuous thermosalinographs measurements
<https://doi.org/10.1594/PANGAEA.946413>

CRUISE REPORT

MSM 104: http://doi.org/10.48433/cr_msm104

MSM106

WASCAL students meet science – Educating West-African students by Training-Through-Research

AUTHORS

GEOMAR Helmholtz Centre for Ocean Research Kiel | Kiel, Germany

B. Fiedler, E. Borchert, T. Fischer, H. Hauss, T. Steinhoff

Thünen Institute for Sea Fisheries | Bremerhaven, Germany

H. Fock, M. Schaber

Instituto do Mar | Mindelo, Cabo Verde

N. Vieira

Universidade Técnica do Atlântico | Mindelo, Cabo Verde

C. Almeida

MARIA S. MERIAN Cruise MSM106 was conceptualized as a joint research and curricular education cruise. The training component of MSM106 was part of the curriculum of the international Master program "Climate Change and Marine Sciences", which is currently being implemented at Universidade Técnica do Atlântico (UTA) in Cabo Verde within the framework of the BMBF-funded WASCAL program ("West African Science Service Centre on Climate Change and Adapted Land Use"). Students from 12 West African countries participated in this cruise. Several modules of the curriculum were taught theoretically and practically at sea. Throughout the cruise West African students got involved in the different research components of MSM106 (physical oceanography, biogeochemistry, marine ecology, marine pollution) but were also tasked to carry out science communication exercises. As such, a livestream from the vessel as part of the UN Ocean Decade Laboratory "A Healthy and Resilient Ocean" has been produced by the student cohort.

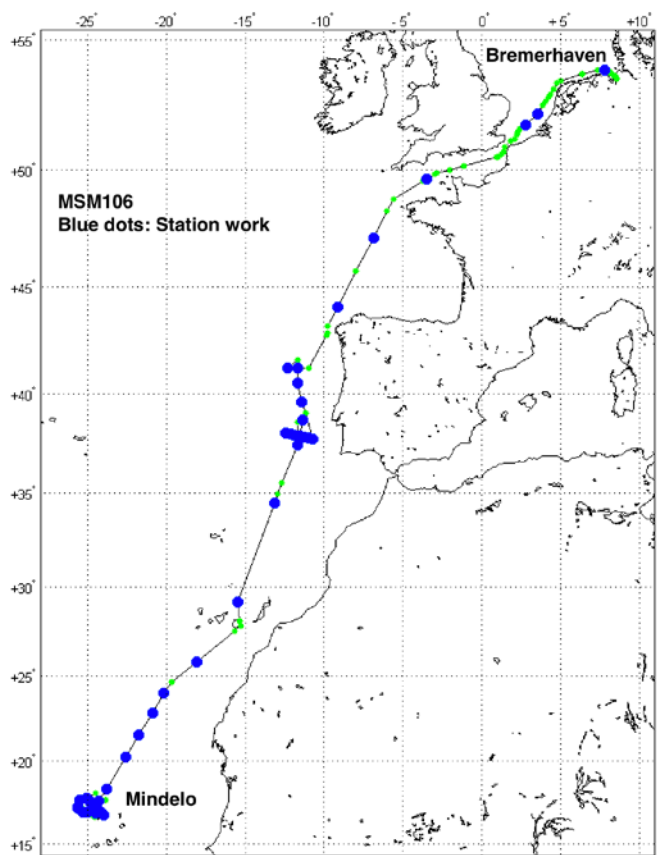


Figure 1: Cruise track of MSM106 from Mindelo, Cabo Verde until Bremerhaven, Germany. Blue dots denote station work, green dots navigational waypoints.

As part of the scientific program a mooring and an autonomous surface vehicle equipped with novel instrumentation for $p\text{CO}_2$ analysis got deployed at Nola Seamount near the Cabo Verdean Island Santo Antao to carry out a 3-month long test deployment. The objective of this deployment was to assess the quality and robustness of a new $p\text{CO}_2$ measurement system on an open-ocean buoy. The aim was to install this buoy later at the Cabo Verde Ocean Observatory (CVOO) which is part of the European Integrated Carbon Observing System (ICOS). Data obtained from both platforms showed very promising results. High accuracy has been achieved by onboard automatic calibration using certified reference gases.

After targeted ADCP and hydroacoustic biomass surveys north of the archipelago an anticyclonic mode-water eddy near CVOO was precisely located. This special type of eddies has not been surveyed often in the past, therefore an intense sampling survey incl. CTD sections, biogeochemical & ecological samplings was carried out. A pronounced

oxygen minimum in its core at a depth of approx. 150 m was found. High resolution ADCP data across the island's underwater slopes covered the moment when this eddy hit the archipelago, thereby causing strong horizontal shear at the slopes.

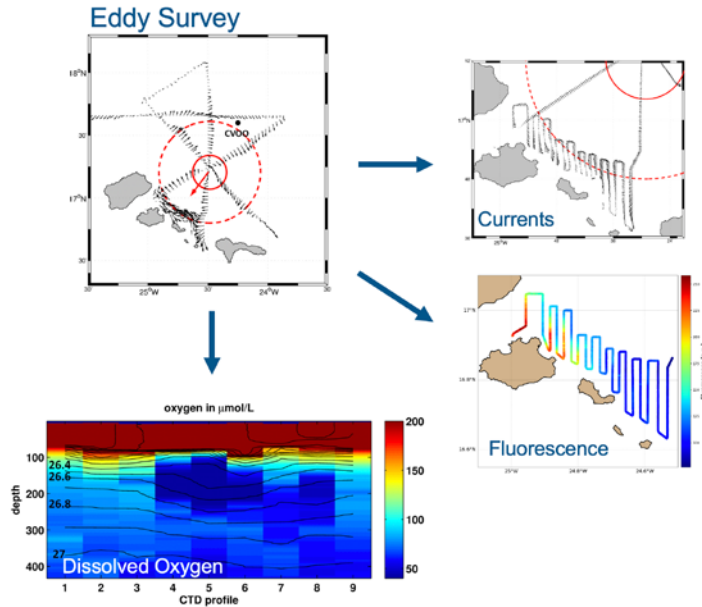


Figure 2: Results from the eddy survey (upper left) during MSM106. High resolution ADCP observations investigated interactions between the eddy and the island's slopes (upper right). Current Data were combined with biogeochemical underway measurements (lower right) and a CTD section along a northwest to southeast transect revealed a distinct minimum of dissolved oxygen beneath the mixed layer (lower left).

After the eddy survey a full time-series sampling was conducted at CVOO. After this, daily stations along the transit towards Germany were carried out. Off Canary Islands a biogeochemical and ecological sampling at the ESTOC time-series site was conducted, followed by another eddy survey off Portugal main land. The daily station scheme was continued along the transit to Bremerhaven. Off the Rhine River delta an extended sampling for microplastics has been conducted. MSM106 also contributed to the international Argo program by deploying 4 core Argo floats and one biogeochemical Argo float between Cabo Verde and Canary Islands.

SCIENTIFIC OUTPUT

LIST OF PUBLICATIONS

Schütte F, et al., Mesoscale Eddy-Island interactions in the Eastern Tropical North Atlantic, in prep.

LIST OF CONFERENCE PRESENTATIONS

2022 | **WASCAL Floating University** UN Ocean conference, Lisbon, Portugal.

DATA

Physical oceanography (Thermosalinograph):

<https://doi.org/10.1594/PANGAEA.953846>

Physical oceanography (ADCP):

<https://doi.org/10.1594/PANGAEA.952429>

Physical oceanography (CTD):

<https://portal.geomar.de/>

Biogeochemical sensor data (buoy):

<https://socat.info/index.php/data-access/> (id: 069920220226)

CRUISE REPORT

MSM106: report submitted to GPF, accepted

PS121

Supplementary Users IMMIPlanS 2019 „Innovative Molecular Methods in Plankton Studies“ and CARCASS „Carbon Transport via Arctic Pelagic Animals Sinking to the Deep-Sea Seafloor“

AUTHORS

Universität Bremen | Bremen, Germany

H. Auel, P. Kaiser

GEOMAR Helmholtz-Zentrum für Ozeanforschung Kiel | Kiel, Germany

H.-J. Hoving

The presentation covers only the two supplementary user proposals IMMIPlanS 2019 – „Innovative Molecular Methods in Plankton Studies“ by scientists from the University of Bremen and CARCASS – „Carbon Transport via Arctic Pelagic Animals Sinking to the Deep-Sea Seafloor“ by researchers from GEOMAR, since the main user proposal for PS121 covering the AWI HAUSGARTEN LTER monitoring had been already approved before the establishment of the GPF management scheme for German research vessels and, hence, is not a topic of the Status Conference Research Vessels.

The Arctic Ocean and adjacent ice-covered seas are the areas most rapidly and strongly affected by global warming over the coming decades. Climate models predict a rise in air temperature in the Arctic by 3 to 6°C over the coming 50 years. In the Arctic marginal seas, such as Fram Strait, closely related zooplankton sister species of polar vs. boreal-Atlantic origin occur sympatrically. It is expected that the polar representatives will be replaced by boreal-Atlantic congeners in the course of global climate change and warming. IMMIPlanS 2019 focused on the dynamics and potential effects of this shift in species composition. Species-specific sensitivities of polar vs. boreal-Atlantic species to temperature increase were determined experimentally by optode respirometry.

Zooplankton are particularly suitable as indicators of environmental change due to their rapid response (generally short life-cycles), direct coupling to physical forcing (relatively passive drifters) and the fact that they are not subject to targeted harvesting, which could bias or obscure other environmental impacts. In the North Atlantic, a northward shift of several hundred kilometers of the distribution ranges of many zooplankton species has been observed with more southerly species replacing northerly relatives at higher latitudes. Climate change induced impacts on species composition also occur in the Arctic. Repetitive analyses of zooplankton community structure demonstrate substantial changes in species composition and biodiversity between the 1990s and 2006, both in

Fram Strait and in Svalbard fjord systems. Boreal-Atlantic species have shifted in distribution further north and now dominate plankton communities in Fram Strait. Shifts in the Arctic pelagic community of mesozooplankton have been noted among pelagic gastropods and amphipods captured in sediment traps at the HAUSGARTEN LTER site. High abundance of gelatinous fauna has been observed under the ice at HAUSGARTEN suggesting importance of this faunal group in Arctic ecosystems.

Such changes in species composition will have a strong impact on secondary production of Arctic seas, pelagic-benthic coupling processes and sedimentation rates, in particular as most of the boreal-Atlantic species are smaller and have a lower lipid content than their polar relatives. This has profound consequences for marine food chains in the Arctic. Often the larger, more lipid-rich polar species are the preferred prey for fish and seabirds. However, predictions are still highly controversial and the effects of an increasing Atlantic inflow on pelagic biodiversity and productivity represent key questions for ecological research in the Arctic. Studies on the physiological and ecological response of key species to ocean warming and an increasing Atlantic inflow are needed to assess and forecast potential impacts of global change on marine pelagic ecosystems in Arctic seas.

Pelagic organisms play an important role in the flux of organic matter to the deep sea, which is essential both, for the global carbon cycle and the provision of food to benthic deep-sea inhabitants. An ecological paradox that exists for many deep ocean carbon budgets is the fact that the amount of carbon associated with the organic material captured in sediment traps does not account for the biomass and respiration rates of deep ocean benthic communities. In some regions the shortage is as much as 30–70% of the carbon budget. This suggests that there must be other carbon sources reaching the seafloor that are currently not measured. One of the problems with understanding the connection between the seafloor and overlying water column is that baseline information on diversity, distribution and abundance of pelagic communities of larger organisms (> 1 cm) is missing for many regions. As a result the potential role of larger pelagic organisms such as jellyfish, cephalopods and fish, in the carbon flux remains unknown for most ocean basins including the Arctic Ocean. The overall goal of CARCASS during PS121 was to unravel the role of large pelagic organisms in subsidizing deep-sea benthic communities.

Particulate matter and carcasses of mesozooplankton can be quantified in sediment traps, but these traps do not properly quantify macrozooplankton, nekton and megafauna. The deposition of such larger carcasses on the seafloor results in foodfalls, and may provide local enrichments and attract a variety of benthic scavengers. The rapid consumption of medium size carcasses (1–100 cm) results in rarity of observations of these foodfalls. While bottom surveys are the most widely used method to document natural foodfalls they are labour-intensive, time consuming and success is not guaranteed. Therefore additional techniques should be tried to reveal scavenged foodfalls and support visual observations.

The sequencing of environmental DNA (genetic material obtained directly from environmental samples without any obvious signs of biological source material) can reveal the identity of the organism based on the DNA in the traces that were left behind by that particular organism. The method has been successfully applied to study distribution and diversity of pelagic organisms. In addition to water samples, eDNA can also be isolated from sediment samples. Sediment preserves eDNA well, and it has enabled the detection of historic and contemporary biodiversity. CARCASS analyzed eDNA from sediment samples to test its suitability for the detection of pelagic foodfalls. In order to investigate scavenging communities and determine scavenging rates of foodfalls, artificial foodfalls were deployed via the attachment of bait on deep-sea landers.

During PS121, IMMIPlanS 2019 focussed on the biodiversity and ecophysiology of zooplankton communities in Fram Strait with special focus on polar vs. boreal-Atlantic sister species in order to establish at which temperature thresholds changes in zooplankton species composition will occur and what consequences they will have. In detail, IMMIPlanS 2019 studied how polar and boreal-Atlantic zooplankton sister species differed in their temperature tolerance and thresholds and how they differed in lipid content, fatty acid composition and, hence, nutritional value for potential predators. In addition IMMIPlanS focussed on the evaluation and applicability of novel molecular methods for zooplankton studies. This included both, eDNA techniques and MALDI-TOF protein fingerprinting. In particular, MALDI-TOF proved to be highly useful for ecological studies on Arctic zooplankton, such as the analysis of vertical distribution, species and stage composition of closely related sister species (i. e. with high taxonomic resolution), where classical morphological approaches reach their limit (juveniles lack secondary sex characters, which are important features for species identification in many copepods) and molecular genetic techniques are too expensive and time-consuming to screen a substantial fraction of the specimens.

At each IMMIPlanS 2019 sampling station, a CTD/rosette water sampler cast was conducted to record depth profiles of temperature, salinity and fluorescence, which are important to relate zooplankton abundance and species composition to different water masses. For the analysis of abundance, biomass and species composition of mesozooplankton, stratified vertical hauls with a multiple opening/closing net system were conducted. Mesozooplankton was sampled by stratified vertical hauls down to 1,500 m with opening and closing nets (Hydro-Bios MultiNet Midi, 0.25 m² mouth opening, 150 µm mesh size) at 11 stations. Sampling concentrated on a transect across Fram Strait at 79°N coinciding with the majority of the HAUSGARTEN stations and extending from the Atlantic-influenced West Spitsbergen Current to the polar East Greenland Current along the East Greenland continental rise. Zooplankton individuals were sorted alive immediately after the catch in a temperature-controlled lab container and either used for respiration measurements onboard at increasing ambient temperatures or deep-frozen at -80°C to provide material for genetic and biochemical analyses in the home lab (MALDI-TOF mass spectrometry, reference material for DNA analysis, stable isotope and fatty acid trophic biomarkers).

To establish species-specific temperature sensitivities, ca. 250 respiration measurements were conducted onboard with polar and boreal-Atlantic zooplankton species at different ambient temperatures (0°C, 4°C, 8°C, and 10°C). Individuals were placed in gas-tight incubation bottles, filled with filtered and oxygenated sea water, and kept in a water bath in a temperature-controlled incubator usually for 10 to 24 hours. Respiration rates were recorded by high resolution optode respirometry throughout the incubation at different temperatures. In order to establish differences in lipid content, composition and nutritional value, individuals of polar and boreal-Atlantic zooplankton species were collected and deep-frozen at -80°C onboard for determination of dry mass and lipid content at Bremen University. A quantitative assessment of the different caloric and nutritional values of polar vs. boreal-Atlantic zooplankton will help to better understand the effects of shifts in zooplankton species composition on higher trophic levels such as fish and seabirds and for the structure and secondary production of Arctic marine ecosystems in general. In total, more than 500 deep-frozen zooplankton samples have been collected during the research cruise.

CARCASS combined in-situ observations and net catches as well as molecular means via eDNA to obtain baseline information on community composition, species distributions and abundance in order to identify potential species of large gelatinous zooplankton and nekton (>1 cm) that have an important role in the carbon flux in the Arctic, and to increase our knowledge on pelagic biodiversity at HAUSGARTEN. CARCASSES's objectives were to detect naturally deposited pelagic foodfalls (using visual and molecular genetic tools), to compare scavenging rates and communities of foodfalls from different pelagic species, and to collect baseline information on abundance, distribution and diversity of macrozooplankton and nekton that may form significant source of nutrition for deep-sea benthic communities.

For the detection of pelagic foodfalls, we obtained 148 sediment samples with the multicorer for extraction of eDNA from the sediment to detect traces of organisms with a pelagic origin. From each core we have taken samples from the sediment surface to detect recent deposition, as well as at different depths to investigate the deposition over time. Deep-sea bottom landers equipped with a time-lapse camera, CTD, current meter, ADCP and a food plate with bait were used to perform artificial foodfall experiments with different species of pelagic bait including jellyfish and cephalopods. By identifying and quantifying the attracted scavenging bottom communities, the scavenging rates, and successional stages were determined allowing an analysis of how different kinds of foodfalls impact seafloor communities. We have also deployed amphipod traps with bait on landers to collect specimens for identification.

To identify potential sources of pelagic foodfalls and to increase our knowledge on the biodiversity in the area, horizontal pelagic video transect surveys using the pelagic in situ observation system (PELAGIOS) and discrete net sampling (Multinet Maxi) were performed. At the same depths as the video and net surveys, water samples were

collected with a CTD for eDNA for metabarcoding of specific taxonomic groups of potential foodfall species (fish, jellyfish and cephalopods). Net samples were used for DNA barcoding and as a reference library for the eDNA analysis.

In total, 24 CTD and 11 multicorer stations were sampled during PS121 for CARCASS covering different hydrographic regimes of the HAUSGARTEN long-term observatory station grid and resulting in 380 eDNA samples. Nine lander deployments were performed. Five lander deployments involved bait experiments, where we put 300 g of bait (squid or jellyfish) on a bait plate, and the bait plate and the attracted scavengers were photographed every 2.5 minute. Three such camera lander deployments were done with squid as bait and another two were done with jellyfish (*Periphylla periphylla*) as bait. Specimens of the scavenging communities were captured using amphipod traps on a lander. The landers were deployed in water depths from 2,388–2,732 m for at least 24 hours. The towed camera system PELAGIOS was deployed five times in waters exceeding 2,000 m, resulting in approximately 25 hours of video. To complement the video surveys, we used a Multinet Maxi to capture micronekton and zooplankton. This net allows for discrete sampling of particular depths in oblique tows. Amphipods and medusa were picked out of the sample and frozen for genetic studies.

Additional observations were done by ROV. We tested a D-sampler, which is a hydraulically powered sampling system consisting of an acrylic, cylindrical chamber with sliding lids. The chamber gets positioned over an organism by the ROV, and then the sliding lids are closed using a hydraulically powered arm. This allows for the capture of living deep-sea organisms. During the test, the ROV pilots captured a large ctenophore. We also deployed two artificial foodfalls, with jellyfish and squid, during an ROV dive and observed the attracted scavengers after 3.25 hours, and recovered the foodfalls.

Despite delays and challenges related to the Covid-19 pandemic after PS121, which affected both, laboratory analysis and international travel to conferences, IMMIPanS 2019 and CARCASS could be carried out successfully. Together, the two small research teams of only three cruise participants each already published six scientific publications related to PS121 with more to follow and presented the results at an international conference in the USA.

SCIENTIFIC OUTPUT

LIST OF PUBLICATIONS

Golikov AV, Stauffer JB, Schindler SV, Taylor J, Boehringer L, Purser A, Sabirov RM, Hoving HJT, Miles down for lunch: deep-sea in situ observations of Arctic finned octopods *Cirroteuthis muelleri* suggest pelagic–benthic feeding migration, Proceedings of the Royal Society B 2023, 290(2001), 20230640.

Kaiser P, Hagen W, Bode-Dalby M, Auel H, Tolerant but facing increased competition: Arctic zooplankton versus Atlantic invaders in a warming ocean, *Frontiers in Marine Science* 2022, 9:908638. doi: 10.3389/fmars.2022.908638.

Merten V, Puebla O, Bayer T, Reusch TBH, Fuss J, Stefanschitz J, Metfies K, Stauffer JB, Hoving HJT, Arctic nekton uncovered by eDNA metabarcoding: Diversity, potential range expansions, and pelagic-benthic coupling, *Environmental DNA* 2023, 5(3), 503-518.

Pantiukhin D, Verhaegen G, Kraan C, Jerosch K, Neitzel P, Hoving HJT, Havermans C, Optical observations and spatio-temporal projections of gelatinous zooplankton in the Fram Strait, a gateway to a changing Arctic Ocean, *Frontiers in Marine Science* 2023, 10, 987700.

Rohlfen EK, Scheer SL, Bergmann M, Sweetman AK, Hoving HJT, Contrasting residence time and scavenging communities of experimental invertebrate food falls in the Arctic deep sea, *Deep Sea Research Part I: Oceanographic Research Papers* 2022, 189, 103832.

Rossel S, Kaiser P, Bode-Dalby M, Renz J, Laakmann S, Auel H, Hagen W, Martínez Arbizu P, Peters J, Proteomic fingerprinting enables quantitative biodiversity assessments of species and ontogenetic stages in *Calanus* congeners (Copepoda, Crustacea) from the Arctic Ocean, *Molecular Ecology Resources* 2023, 23, 382–395.

LIST OF CONFERENCE PRESENTATIONS

2020 | **Turning up the Heat – Implications of Rising Temperatures for Arctic Zooplankton**, Ocean Sciences Meeting, San Diego, USA.

DATA

Pelagic observations with PELAGIOS PS121:

<https://doi.pangaea.de/10.1594/PANGAEA.953752>

Raw sequencing data of cephalopods and fishes:

<https://doi.org/10.5061/dryad.5qfttdz92>

Video observations of bathypelagic *cirrate* *Cirroteuthis muelleri*:

<https://doi.pangaea.de/10.1594/PANGAEA.957196>

Raw counts of scavenger fauna attracted to experimental food falls deployed during PS121 in the Arctic deep sea: <https://doi.pangaea.de/10.1594/PANGAEA.947588>

CRUISE REPORT

PS121: doi:10.2312/BzPM_0738_2020

PS124

Occurrence of microplastics in the southern Weddell Sea

AUTHORS

Man-Society-Environment Program, Department of Environmental Sciences, University of Basel | Basel, Switzerland

P. Burkhardt-Holm, C. Leistenschneider

Department of Microbial Ecology, Biologische Anstalt Helgoland, Alfred-Wegener-Institut Helmholtz-Zentrum für Polar- und Meeresforschung | Helgoland, Germany

G. Gerds, S. Primpke

The Atlantic and Pacific Ocean cover ~80% of the world's oceans and thus are extremely widespread. The widespread presence of microplastics (MPs; < 5 mm in size; Arthur et al., 2009) in the marine environment is a significant concern. It's increasingly clear that even the Southern Ocean below 60°S is affected by this issue. Possible sources of MPs include local human activities (e. g., Cincinelli et al., 2017; Leistenschneider et al., 2021; Munari et al., 2017) as well as long-range transportation through the ocean (Fraser et al., 2018; Wilson et al., 2023).

Despite increased research efforts, most studies in the Southern Ocean waters south of 60°S have not focused on MPs smaller than 300 µm. However, these smaller particles have been shown to be more prevalent in the marine environment (e. g., Lindeque et al., 2020; Peeken et al., 2018) and may pose greater ecological risks due to their higher bioavailability (Vroom et al., 2017). Hence, our primary aim during the PS124 expedition was to examine the presence of small MPs, specifically plastics ranging from 11 to 500 µm (Roscher et al., 2021). This investigation sought to address knowledge gaps regarding small MPs in the Southern Ocean and the relatively unexplored region of the Weddell Sea.

We collected seventeen surface water samples (average volume: 0.84 ± 0.15 m³) using a custom-designed sampling system comprising an immersion pump and a stainless-steel tank. After each station, seawater was filtered directly from the tank through a series of stainless-steel filters. This process involved a 500-µm pre-filter and a final 10 µm filter to capture small particles. All equipment underwent thorough rinsing with seawater from the respective station to prevent any cross-contamination. Subsequently, the 500 µm filter was examined under a stereo microscope to identify any large MPs (> 500 µm), which, however, were not found.

In our laboratory, filters containing particles ranging from 11 to 500 µm underwent a multi-step process. This process involved oxidative digestion and one to two density

separation steps to isolate the MPs. Chemical identification was then carried out using Focal Plane Array micro-Fourier-transform infrared spectroscopy (FPA- μ FTIR). Subsequent polymer identification involved using the SiMPle software (Primpke et al., 2020) along with reference polymer databases.

The analysis of a significant volume of surface water revealed a notable presence of microplastics (MPs), namely approximately 500 particles after adjusting for potential contamination from sample processing. Total MP concentrations varied significantly, peaking in the two samples taken offshore, north of the southern Weddell Sea continental shelf, while MP concentrations in samples collected in the surface waters above the continental shelf were considerably lower. This trend was consistent for both particle-like and fiber-like MPs. The mean concentration was estimated, as well as the median value. Regarding the MP shapes, the majority of all MPs were particles, while a minor part were fiber-like MPs.

Polypropylene (PP) and polyamide (PA) emerged as the predominant polymers identified among the MPs, suggesting potential sources related to maritime activities and synthetic textiles. The majority of MPs were smaller than 300 μ m, indicating a prevalence of smaller-sized particles and fibers in the studied area. There were observable correlations between MP concentrations and natural particles like chitin and quartz, hinting at potential links between MPs and natural particulate matter, however, this statement is statistically limited due to small sample size.

The findings emphasized the need to include smaller MP size classes in future studies in the Southern Ocean to better understand their occurrence and ecological risks. The differences in MP concentrations between offshore and nearshore samples might be influenced by regional ocean currents. While the identified polymer types suggest possible sources from maritime activities and synthetic textiles, establishing exact sources remains challenging. Other local or long-range transport mechanisms could also contribute to MP presence in the studied area.

REFERENCES

Arthur C, Baker J, Bamford HA, Proceedings of the International Research Workshop on the Occurrence, Effects, and Fate of Microplastic Marine Debris, University of Washington Tacoma, Tacoma, WA, USA, September 9-11, 2008, URL: <https://www.paper/Proceedings-of-the-International-Research-Workshop-Arthur-Baker/7f8c9dd6437a34f96812836c66ca83d69f7ea9eb> (accessed November 30, 2020).

Cincinelli A, Scopetani C, Chelazzi D, Lombardini E, Martellini T, Katsoyiannis A, Fossi MC, Corsolini S, Microplastic in the Surface Waters of the Ross Sea (Antarctica): Occurrence, Distribution and Characterization by FTIR, *Chemosphere* 2017, 175, 391–400, doi:10.1016/j.chemosphere.2017.02.024.

Fraser CI, Morrison AK, Hogg AM, Macaya EC, Ryan PG, Padovan A, Jack C, Valdivia N, Waters JM, Antarctica's Ecological Isolation Will Be Broken by Storm-Driven Dispersal and Warming, *Nature Climate Change* 2018, 8, 704–708, doi: 10.1038/s41558-018-0209-7.

Leistenschneider C, Burkhardt-Holm P, Mani T, Primpke S, Taubner H, Gerdts G, Microplastics in the Weddell Sea (Antarctica): A Forensic Approach for Discrimination between Environmental and Vessel-Induced Microplastics, *Environ. Sci. Technol.* 2021, 55, 15900–15911, doi: 10.1021/acs.est.1c05207.

Lindeque PK, Cole M, Coppock RL, Lewis CN, Miller RZ, Watts AJR, Wilson-McNeal A, Wright SL, Galloway TS, Are we underestimating microplastic abundance in the marine environment? A comparison of microplastic capture with nets of different mesh-size, *Environmental Pollution* 2020, 265, doi: 10.1016/j.envpol.2020.114721.

Munari C, Infantini V, Scoponi M, Rastelli E, Corinaldesi C, Mistri M, Microplastics in the sediments of Terra Nova Bay (Ross Sea, Antarctica), *Marine Pollution Bulletin* 2017, 122, 161–165, doi: 10.1016/j.marpolbul.2017.06.039.

Peeken I, Primpke S, Beyer B, Gütermann J, Katlein C, Krumpfen T, Bergmann M, Hehemann L, Gerdts G, Arctic sea ice is an important temporal sink and means of transport for microplastic, *Nature Communications* 2018, doi: 10.1038/s41467-018-03825-5.

Primpke S, Cross RK, Mintenig SM, Simon M, Vianello A, Gerdts G, Vollertsen J, Toward the Systematic Identification of Microplastics in the Environment: Evaluation of a New Independent Software Tool (siMPle) for Spectroscopic Analysis, *Appl. Spectrosc.* 2020, 74, 1127, <https://doi.org/10.1021/acs.est.1c05207>.

Roscher L, Fehres A, Reisel L, Halbach M, Scholz-Böttcher B, Gerriets M, Badewien T H, Shiravani G, Wurpts A, Primpke S, Gerdts G, Microplastic pollution in the Weser estuary and the German North Sea, *Environmental Pollution* 2021, 288, 117681, doi: 10.1016/j.envpol.2021.117681.

Vroom RJE, Koelmans AA, Besseling E, Halsband C, Aging of microplastics promotes their ingestion by marine zooplankton, *Environmental Pollution* 2017, 231, 987–996. doi: 10.1016/j.envpol.2017.08.088.

Wilson DR, Sheen KL, Clark JR, Thorpe S, Young EF, Modelling the transport of microplastic pollution across the Antarctic Circumpolar Current, *EGU-5971* 2023, doi: 10.5194/egusphere-egu23-5971.

SCIENTIFIC OUTPUT

LIST OF PUBLICATIONS

Dzurisin D, A comprehensive approach to monitoring volcano deformation as a window on the eruption cycle, *Reviews of Geophysics* 2003, 41(1), 1.1–1.29, doi:10.1029/2001RG000107.

Schurr B, Asch G, Hainzl S, Bedford J, et al., Gradual unlocking of plate boundary controlled initiation of the 2014 Iquique earthquake, *Nature* 2014, 512, doi: 10.1038/nature13681.

CRUISE REPORT

PS124: https://doi.org/10.48433/BzPM_0755_2021

PS126

Time-Series Studies at the LTER (Long-Term Ecological Research) Observatory HAUSGARTEN

AUTHORS

Alfred-Wegener-Institute Helmholtz Center for Polar and Marine Research |
Bremerhaven, Germany
T. Soltwedel

RATIONALE

The R/V Polarstern expedition PS126 (24th May–27th June 2021, Bremerhaven – Bremerhaven) to the Fram Strait between Greenland and the Svalbard archipelago contributed to various large national and international research and infrastructure projects (FRAM, INTAROS, ICOS, SIOS, ARCHES) as well as to the new research programme „Changing Earth – Sustaining our Future“ of the AWI. Within Topic 6 “Marine and Polar Life: Sustaining Biodiversity, Biotic Interactions and Biogeochemical Functions” (Subtopics 6.1 “Future ecosystem functionality” and 6.3 “The future biological carbon pump”) of the new research programme, ecosystem shifts in the pelagic and deep ocean associated with water temperature increase and sea ice retreat were identified and quantified, and feedback processes on oceanographic processes were investigated. These studies included the identification of spatial and temporal developments in the function of selected pelagic and benthic communities. Within Subtopic 6.4 “Use and misuse of the ocean: Consequences for marine ecosystems”, the input of plastic waste into the ocean, the vertical fluxes of plastic from the sea surface to the seafloor, and the interaction between plastic and marine biota were investigated.

The work supported the time-series studies at the LTER (Long-Term Ecological Research) observatory HAUSGARTEN (Soltwedel et al., 2016), where we document Global Change induced environmental variations on a polar deep-water ecosystem. This work was carried out in close co-operation between the HGF-MPG Research Group on Deep-Sea Ecology and Technology, the Working Group PEBCAO (“Phytoplankton Ecology and Biogeochemistry in the Changing Arctic Ocean”) at AWI and the Helmholtz Young Investigators Group SEAPUMP (“Seasonal and regional food web interactions with the biological pump”), representing a joint effort between the AWI, the MARUM – Center for Marine Environmental Sciences and the University of Bremen.

The expedition was further used to accomplish installations for the HGF infrastructure project FRAM (FRontiers in Arctic marine Monitoring; Soltwedel et al., 2013). The FRAM Ocean Observing System aims at permanent presence at sea, from surface to depth, for the provision of near real-time data on Earth system dynamics, climate variability and

ecosystem change. It serves national and international tasks towards a better understanding of the effects of change in ocean circulation, water mass properties and sea-ice retreat on Arctic marine ecosystems and their main functions and services. FRAM implements existing and next-generation sensors in observatory platforms, allowing synchronous observation of relevant ocean variables as well as the study of physical, chemical and biological processes in the ocean. Experimental and event-triggered platforms complement the observational platforms. Products of the infrastructure are continuous long-term data with appropriate resolution in space and time, as well as ground-truthing information for ocean models and remote sensing.

ECOLOGICAL LONG-TERM STUDIES IN THE MARINE ARCTIC

The marine Arctic has played an essential role in the history of our planet over the past 130 million years and contributes considerably to the present functioning of the Earth and its life. The past decades have seen remarkable changes in key variables, including a decrease in sea-ice extent and sea-ice thickness, changes in temperature and salinity of arctic waters, and associated shifts in nutrient distributions. Since arctic organisms are highly adapted to extreme environmental conditions with strong seasonal forcing, the accelerating rate of recent climate change challenges the resilience of arctic life. The stability of a number of arctic populations and ecosystems is probably not strong enough to withstand the sum of these factors, which might lead to a collapse of subsystems.

To detect and track the impact of large-scale environmental changes in the transition zone between the northern North Atlantic and the central Arctic Ocean, and to determine experimentally the factors controlling deep-sea biodiversity, the Alfred Wegener Institute Helmholtz Center for Polar and Marine Research (AWI) established the deep-sea observatory HAUSGARTEN, which constitutes the first, and until now only open-ocean long-term observatory in a polar region (Soltwedel et al., 2005).

HAUSGARTEN is located in the eastern Fram Strait and includes 21 permanent sampling sites along a depth transect (250 - 5500 m) and along a latitudinal transect following the 2500 m isobath crossing the central HAUSGARTEN station (Figure 1). Multidisciplinary research activities at HAUSGARTEN cover almost all compartments of the marine ecosystem from the pelagic zone to the benthic realm. Regular sampling as well as the deployment of moorings and different stationary and mobile free-falling systems (Bottom-Lander, Benthic Crawler), which act as local observation platforms, have taken place since the observatory was established in 1999. Frequent visual observations with towed photo/video systems allow the assessment of large-scale epibenthic distribution patterns as well as their temporal development.

years after the cruise. All data retrieved during PS126 will be archived, published and disseminated according to international standards by the World Data Center PANGAEA Data Publisher for Earth & Environmental Science (www.pangaea.de). The CC-BY license will be applied after publication. Benthic data was also deposited in CRITTERBASE at AWI, seafloor still images were uploaded to the online image database BIIGLE to enable access by other parties, and DNA sequences of benthic larvae and recruits collected during PS126 will be archived in GenBank. Molecular data (DNA, RNA) from the cruise will be archived, published and disseminated within one of the repositories of the International Nucleotide Sequence Data Collaboration (INSDC, www.insdc.org) comprising of EMBL-EBI/ENA, GenBank and DDBJ.

REFERENCES

Soltwedel T, Bauerfeind E, Bergmann M, Budaeva N, Hoste E, Jaeckisch N, Juterzenka K v, Matthießen J, Mokievsky V, Nöthig E-M, Quéric N, Sablotny B, Sauter, E, Schewe I, Urban-Malinga B, Wegner J, Wlodarska-Kowalczyk M, Klages M, HAUSGARTEN: multidisciplinary investigations at a deep-sea, long-term observatory in the Arctic Ocean, *Oceanography* 2005, 18 (3), 46-61, doi: 10.5670/oceanog.2005.24.

Soltwedel T, Schauer U, Boebel O, Nöthig E-M, Bracher A, Metfies K, Schewe I, Klages M, Boetius A, FRAM – FRontiers in Arctic marine Monitoring: Permanent Observations in a Gateway to the Arctic Ocean, *OCEANS - Bergen* 2013, MTS/IEEE, doi: 10.1109/OCEANS-Bergen.2013.6608008.

Soltwedel T, Bauerfeind E, Bergmann M, Bracher A, Budaeva N, Busch K, Cherkasheva A, Fahl K, Grzelak K, Hasemann C, Jacob M, Kraft A, Lalande C, Metfies K, Nöthig E-M, Meyer K, Quéric NV, Schewe I, Wlodarska-Kowalczyk M, Klages M Natural variability or anthropogenically-induced variation? Insights from 15 years of multidisciplinary observations at the arctic open-ocean LTER site HAUSGARTEN, *Ecological Indicators* 2016, 65, 89-102, doi: 10.1016/j.ecolind.2015.10.001.

SCIENTIFIC OUTPUT

LIST OF PUBLICATIONS

(Selected peer-reviewed publications from the time-series work at LTER HAUSGARTEN for the last 5 years)

Priest T, von Appen W-J, Oldenburg E, Popa O, Torres-Valdés S, Bienhold C, Metfies K, Boulton W, Mock T, Fuchs BM, Amann R, Boetius A, Wietz M, Atlantic water influx and sea-ice cover drive taxonomic and functional shifts in Arctic marine bacterial communities, *ISME Journal* 2023, doi: 10.1038/s41396-023-01461-6.

Cardozo-Mino M, Salter I, Nöthig E-M, Metfies K, Ramondenc S, Wekerle C, Krumpen T, Boetius A, Bienhold C, A decade of microbial community dynamics on sinking particles during high carbon export events in the eastern Fram Strait, *Frontiers in Marine Science* 2023, doi: 10.3389/fmars.2023.1173384.

Salter I, Bauerfeind E, Fahl K, Iversen MH, Lalande C, Ramondenc S, Von Appen W-J, Wekerle C, Nöthig E-M, Interannual variability (2000–2013) of mesopelagic and bathypelagic particle fluxes in relation to variable sea ice cover in the eastern Fram Strait, *Front Earth Sci* 2023, 11 (1210213), doi: 10.3389/feart.2023.1210213.

Gorska B, Gromisz S, Legeżyńska J, Soltwedel T, Włodarska-Kowalczyk M., Macrobenthic diversity response to the atlantification of the Arctic Ocean (Fram Strait, 79°N) – A taxonomic and functional trait approach, *Ecological Indicators* 2022, 144 (109464), doi: 10.1016/j.ecolind.2022.109464.

Ramondenc S, Nöthig E-M, Hufnagel L, Bauerfeind B, Busch K, Knüppel N, Kraft A, Schröter F, Seifert M, Iversen MH, Effects of Atlantification and changing sea-ice dynamics on zooplankton community structure and carbon flux between 2000 and 2016 in the eastern Fram Strait, *Limnology and Oceanography* 2022, doi: 10.1002/lno.12192.

Nöthig E-M, Ramondenc S, Haas A, Hehemann L, Walter A, Bracher A, Lalande C, Metfies K, Peeken I, Bauerfeind E, Boetius A, Summertime Chlorophyll a and Particulate Organic Carbon Standing Stocks in Surface Waters of the Fram Strait and the Arctic Ocean (1991–2015), *Frontiers in Marine Science* 2020, 7 (350), doi: 10.3389/fmars.2020.00350.

Soltwedel T, Grzelak K, Hasemann C, Spatial and temporal variation in deep-sea meiofauna at the LTER Observatory HAUSGARTEN in Fram Strait (Arctic Ocean), *MDPI – Diversity* 2020, 12 (279), 1–23, doi: 10.3390/d12070279.

Parga Martínez KB, Tekman MB, Bergmann M, Temporal trends in marine litter at three stations of the HAUSGARTEN observatory in the Arctic deep sea, *Frontiers in Marine Science* 2020, 7 (321), doi: 10.3389/fmars.2020.00321.

Engel A, Bracher A, Dinter T, Endres S, Grosse J, Metfies K, Peeken I, Piontek J, Salter I, Nöthig E-M, Inter-Annual Variability of Organic Carbon Concentration in the Eastern Fram Strait During Summer (2009–2017), *Frontiers in Marine Science* 2019, doi: 10.3389/fmars.2019.00187.

Schröter F, Havermans C, Kraft A, Knueppel N, Beszczynska-Möller A, Bauerfeind E, Nöthig E-M Pelagic Amphipods in the Eastern Fram Strait With Continuing Presence of *Themisto compressa* Based on Sediment Trap Time Series, *Frontiers in Marine Science* 2019, 6 (311), doi: 10.3389/fmars.2019.00311.

Kröncke I, Neumann H, Dippner J, Holbrook S, Lamy T, Miller R, Padedda B, Pulina S, Reid D, Reinikainen M, Satta C, Sechi N, Soltwedel T, Suikkanen S, Lugliè A, Comparison of biological and ecological long-term marine trends related to northern hemisphere climate in different marine ecosystems, *Nature Conservation* 2019, 34, 311–341, doi: 10.3897/natureconservation.34.30209.

Meyer K, Bergmann M, Soltwedel T, Klages M, Recruitment of Arctic deep-sea invertebrates: results from a long-term hard-substrate colonization experiment at the LTER observatory HAUSGARTEN, *Limnology and Oceanography* 2019, doi: 10.1002/lno.11160.

Vedenin A, Mokievsky V, Soltwedel T, Budaeva N, The temporal variability of the macrofauna at the deep-sea observatory HAUSGARTEN (Fram Strait, Arctic Ocean), *Polar Biology* 2019, 42 (3), doi: 10.1007/s00300-018-02442-8.

Taylor J, Staufenbiel B, Soltwedel T, Bergmann M, Temporal trends in the biomass of three epibenthic invertebrates from the deep-sea observatory HAUSGARTEN (Fram Strait, Arctic Ocean), *Marine Ecology Progress Series* 2018, 602, 15–29, doi: 10.3354/meps12654.

Buttigieg P, Fadeev E, Bienhold C, Hehemann L, Offre P, Boetius, A, Marine microbes in 4D — using time series observation to assess the dynamics of the ocean microbiome and its links to ocean health, *Current Opinion in Microbiology* 2018, 43, 169–185, doi: 10.1016/j.mib.2018.01.015.

LIST OF CONFERENCE PRESENTATIONS

(featuring the scientific output of PS126)

2021 | **Exploring the role of gelatinous zooplankton in Tomorrow's Arctic Ocean** 16th Deep-Sea Biology Symposium, Brest, France.

2021 | **More jellyfish (and less fish) in Tomorrow's Arctic? Exploring jellyfish' range shifts, their role in pelagic and benthic food webs and interactions with fish stocks** Svalbard Science Conference, Oslo, Norway.

2021 | **Trophic ecology of Arctic gelatinous zooplankton** ICYMARE International Conference for Young Marine Researchers, Berlin, Germany.

2021 | **Modelling of Arctic gelatinous zooplankton distribution and abundance based on data from pelagic video transects in Fram Strait** ICYMARE International Conference for Young Marine Researchers, Berlin, Germany.

- 2021 | **Genetic connectivity of the widespread hydrozoan *Aglantha digitale* from temperate to central Arctic regions** ICYMARE International Conference for Young Marine Researchers, Berlin, Germany.
- 2021 | **Zooplankton in an ocean of change: a molecular & modelling toolkit to study diversity, trophic links and range shifts** BreMarE Symposium "Future Trends and Hot topics in Marine Zooplankton research, Bremen, Germany.
- 2022 | **Identifying hidden sinks of Arctic plastic pollution: Fram Pollution Observatory** 7th International Marine Debris Conference, Busan, South Korea.
- 2022 | **Microplastics in the atmosphere and cryosphere in the circumpolar North: A case for multi-compartment monitoring** 7th International Marine Debris Conference, Busan, South Korea.
- 2022 | **Floating marine debris in Arctic and temperate Northeast Atlantic waters** 7th International Marine Debris Conference, Busan, South Korea.
- 2022 | **Benthic megafauna in the Arctic Ocean – Dynamics in temporal community composition** 4th Marine Imaging Workshop, Brest, France.
- 2022 | **Trophic role of gelatinous zooplankton in the Arctic marine food web** 28th International Polar Conference, Potsdam, Germany.
- 2022 | **Predicting spatio-temporal distributions of Arctic gelatinous zooplankton in Fram Strait in a changing environment** ICYMARE International Conference for Young Marine Researchers, Bremerhaven, Germany.
- 2022 | **Who's there? A comprehensive eDNA metabarcoding survey of gelatinous zooplankton biodiversity in the Fram Strait** ICYMARE International Conference for Young Marine Researchers, Bremerhaven, Germany.
- 2022 | **Wiggling in the deep – Diversity of Arctic deep-sea nematodes at the long-term ecological research observatory HAUSGARTEN** ICYMARE International Conference for Young Marine Researchers, Bremerhaven, Germany.
- 2022 | **Benthic megafauna in the Arctic Ocean – Future dominion by sea cucumbers?** ICYMARE International Conference for Young Marine Researchers, Bremerhaven, Germany.
- 2022 | **The phylogeography of two *Beroe* species in the Arctic Ocean based on one mitochondrial and one ribosomal marker** ICYMARE International Conference for Young Marine Researchers, Bremerhaven, Germany.

2022 | **Range expansions of scyphozoan jellyfish – the case study of *Periphylla periphylla* and *Cyanea capillata*** ICYMARE International Conference for Young Marine Researchers, Bremerhaven, Germany.

2022 | **Zooplankton in an ocean of change: evaluating the likelihood and consequences of poleward range expansions for pelagic ecosystems** Polar Genomics Workshop, Bielefeld, Germany.

2022 | **Seasonality of microbial genetic functions in the Arctic Ocean revealed by autonomous sampling** Ocean Sciences Meeting, online event.

2022 | **Seasonal, interannual and spatial patterns of bacterial taxonomy and genetic functions in the Arctic Ocean** 18th Symposium of the International Society for Microbial Ecology (ISME18), Lausanne, Switzerland.

2023 | **Macrobenthic diversity response to the atlantification of the Arctic Ocean (Fram Strait, 79°N)** Polar Symposium, Sopot, Poland.

2023 | **Winners and losers of Atlantification: The degree of ocean warming affects the structure of Arctic microbial communities** ASLO Aquatic Sciences Meeting, Palma de Mallorca, Spain.

DATA

Master track in 1 sec resolution:

<https://doi.org/10.1594/PANGAEA.935580>

Master track in different resolutions:

<https://doi.org/10.1594/PANGAEA.935582>

Continuous thermosalinograph:

<https://doi.org/10.1594/PANGAEA.949666>

Raw data continuous VM-ADCP:

<https://doi.pangaea.de/10.1594/PANGAEA.938056>

Raw data physical oceanography:

<https://doi.pangaea.de/10.1594/PANGAEA.940754>

Raw physical oceanography, bio-optical and ocean current data from mooring:

<https://doi.pangaea.de/10.1594/PANGAEA.959812>

Gelatinous zooplankton annotations of pelagic video transects:

<https://doi.org/10.1594/PANGAEA.953888>

Raw physical oceanography, ocean current velocity and particle export data from mooring HG-N-FEVI-39:
<https://doi.org/10.1594/PANGAEA.946533>

Raw physical oceanography, bio-optical and biogeochemical data from mooring HG-IV-S-4:
<https://doi.org/10.1594/PANGAEA.946507>

Raw physical oceanography, bio-optical and biogeochemical data from mooring F4-W-2:
<https://doi.org/10.1594/PANGAEA.946447>

Raw physical oceanography, ocean current velocity and bio-optical data from mooring HG-IV-SWIPS-2019 (HG-IV-W-4):
<https://doi.org/10.1594/PANGAEA.946537>

Raw physical oceanography and ocean current data from mooring HG-IV-FEVI-40:
<https://doi.org/10.1594/PANGAEA.946514>

Raw physical oceanography and ocean current velocity data from mooring F4-19:
<https://doi.org/10.1594/PANGAEA.946530>

Raw physical oceanography and ocean current velocity data from mooring HG-N-S-1:
<https://doi.org/10.1594/PANGAEA.946513>

Raw physical oceanography, bio-optical and biogeochemical data from mooring F4-S-4:
<https://doi.org/10.1594/PANGAEA.946508>

Raw physical oceanography, ocean current velocity, bio-optical and biogeochemical data from mooring HG-EGC-6:
<https://doi.org/10.1594/PANGAEA.946539>

Video observations of a bathypelagic cirrate octopod *Cirroteuthis muelleri*:
<https://doi.org/10.1594/PANGAEA.957196>

Metadata for incubation experiment testing temperature effects on a microbial community:
<https://doi.org/10.1594/PANGAEA.960624>

CRUISE REPORT

PS126: [doi:10.48433/BzPM_0757_2021](https://doi.org/10.48433/BzPM_0757_2021)

PS128

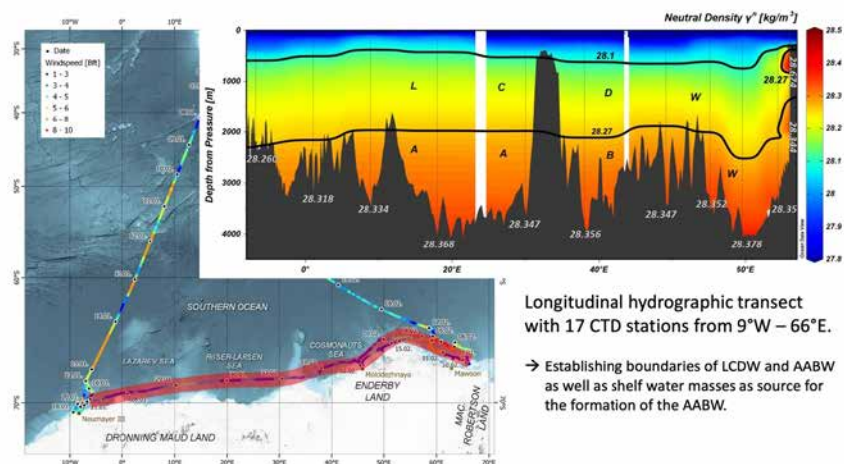
East Antarctic Ice Sheet Instability (EASI-1): History of the East Antarctic Ice Sheet

AUTHORS

Alfred-Wegener-Institut, Helmholtz-Zentrum für Polar- und Meeresforschung |
Bremerhaven, Germany

R. Tiedemann, J. Müller, B. Dorschel, Shipboard Scientific Party

Expedition EASI-1 was carried out to investigate the history of the Antarctic ice sheet and its interaction with changes in Southern Ocean (SO) circulation. The behaviour of the East Antarctic Ice Sheet (EAIS) under projected anthropogenic warming is a key uncertainty in predicting future sea level rise due to the influence of strong ice-ocean feedbacks, which are poorly understood. Reconstructing and disentangling these feedbacks during past warmer-than-present climate states is considered to provide an enhanced basis for improved prediction of future changes in the ice-ocean-climate system. Our work focused on the East Antarctic continental margin between the Weddell and Cooperation Seas (Figure 1). The overall goal was to acquire marine and terrestrial sediment records, in combination with oceanographic, marine-geophysical and continental-geodetic data. This goal was successfully achieved. The combination of parasound profiling and high-resolution bathymetric mapping played a key role in sampling and identifying (sub-)seafloor structures such as lineations, iceberg plough marks and recessional moraines, which are indicative of palaeo-ice streams and deglacial retreat patterns. The future processing of the samples and data collected will expand our knowledge of changes in the following topics: Transport of Warm Deep Water across the continental shelf, formation and export of Antarctic Bottom Water, behaviour of the grounding line, sea ice cover, meltwater input and oceanic stratification.



Longitudinal hydrographic transect with 17 CTD stations from 9°W – 66°E.
 → Establishing boundaries of LCDW and AABW as well as shelf water masses as source for the formation of the AABW.

Figure 1: Cruise track and longitudinal hydrographic transect along the East Antarctic continental margin, 9°W – 66°E.

PRELIMINARY GEOPHYSICAL RESULTS

A network of seismic profiles, most of them by vibroseis technique, was acquired on the Ekström Ice Shelf in various previous seasons (summary in Oetting et al. 2022), revealing a sequence of northward dipping, pre-glacial sediments overlain by glacial deposits. The geophysical campaign during PS128 successfully connected the seismic ice shelf network to the marine seismostratigraphic network. This allows the dating of the sediment succession below Neumayer Station, which comprises stratigraphic units from the ~Jurassic to the Neogene. This result provides a basic prerequisite for planned continental drilling at Neumayer.

PRELIMINARY OCEANOGRAPHIC RESULTS

The zonal section with 17 CTD (Conductivity, Temperature, Depth) stations from 9° W to 66° E allowed to establish the boundaries of the Lower Circumpolar Deep Water (LCDW) and the Antarctic Bottom Water (AABW) as well as the water masses from the surface and shelf water masses as sources for the formation of the AABW (Figure 1).

PRELIMINARY PALEOCEANOGRAPHIC RESULTS

An important geological achievement of EASI-1 was the recovery of sediment cores along a north-south profile from the Antarctic upper continental slope near Aika Bay to the Bungenstock Plateau (Tiedemann and Müller, 2022). It thus allows us to reconstruct the influence of warm deep-water masses on the upper continental slope that can penetrate the cavities below the Ekström Ice Shelf. Warm Deep Water incursions onto the Antarctic continental shelf during the last glacial termination are generally not well constrained. Compared to other sediment archives from the Antarctic continental margin, this archive contains exceptionally high amounts of biogenic carbonate (foraminifera shells). This significantly increases the library of proxies to be used for reconstructing

oceanographic and climatic changes as well as establishing a reliable stratigraphic framework for this region. At station PS128_2 (and _20), 20 AMS 14C datings on planktic foraminifers in combination with a high resolution $\delta^{18}\text{O}$ stratigraphy were carried out. As a result, these archives provide for the first-time detailed insights into environmental changes offshore Neumayer Station III on time scales of centuries to millennia:

- › à Presence of an open-ocean polynya within the perennial sea-ice zone during glacial times from 90–15 ka.
- › à Glacial subsurface temperatures are warmest during Marine Isotope Stage (MIS) 4 and from 38–21 ka due to atmosphere-ocean interactions and/or bathymetric-deep ocean feedbacks (polynya, topographic rise)
- › à Extreme minima in $\delta^{13}\text{C}$ values (-0.4 ‰) indicate old, nutrient-enriched and warm CDW during meltwater pulse (MWP) 1A (14.7–14.3 ka) and more clearly during MWP 1B (11.5–11.2 ka).

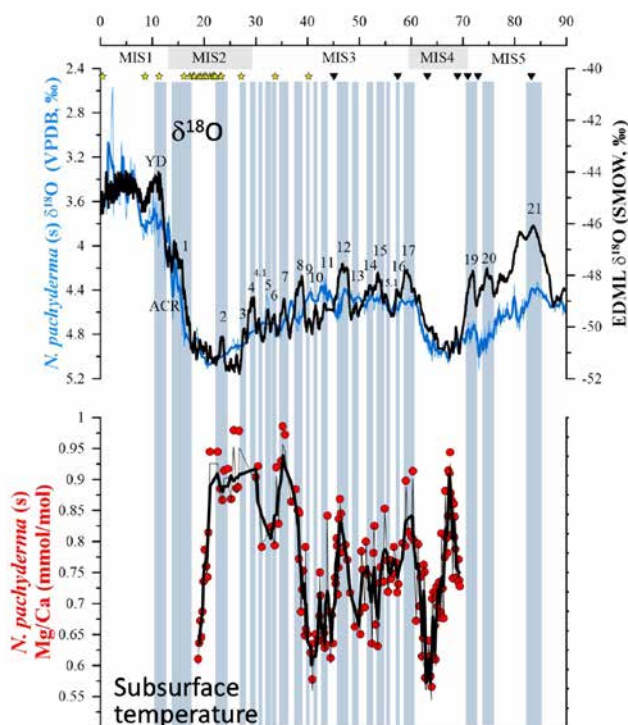


Figure 2: $\delta^{18}\text{O}$ data of ice core EDML (black, air temperatures) in comparison to the planktic $\delta^{18}\text{O}$ signal (blue, temperature and salinity) at Site PS128_2/_20 (upper panel). Mg/Ca subsurface temperature at Site PS128_2/_20 (lower panel).

REFERENCES

Oetting A, Smith EC, Arndt JE, Dorschel B, Drews R, Ehlers TA, Gaedicke C, Hofstede C, Klages JP, Kuhn G, Lambrecht A, Läufer A, Mayer C, Tiedemann R, Wilhelms F, Eisen O, Geomorphology and shallow sub-sea-floor structures underneath the Ekström Ice Shelf, Antarctica, *The Cryosphere* 2022, 16, <https://tc.copernicus.org/articles/16/2051/2022/>.

Hidayat, SR, Environmental changes on the Bungenstock Plateau offshore Dronning Maud Land during the last 70,000 years – Antarctic cryosphere-ocean interactions, Bachelor Thesis 2023, Department of Geoscience, University of Bremen.

SCIENTIFIC OUTPUT

CRUISE REPORT

PS128: <https://epic.awi.de/id/eprint/57028/>

SO272

Kerguelen Plateau Drift Deposits: outstanding high-resolution chronicle of Cenozoic climatic and oceanographic changes in the southern Indian Ocean

AUTHORS

Alfred-Wegener-Institut Helmholtz-Zentrum für Polar- und Meeresforschung |
Bremerhaven, Germany

G. Uenzelmann-Neben, B. Najjarifarizhendi, M. Schneider

MARUM – Zentrum für Marine Umweltwissenschaften, Universität Bremen |
Bremen, Germany

T. Westerhold, El. Zircks

The overarching objectives of the project Kerguelen Plateau Drift Deposits (KPDD) were twofold: 1) to study variations in flow paths and intensities of deep and bottom water masses in response to tectonic movements and climate variability; this is the major focus of the cruise, and 2) to collect critical pre-site survey data for the preparation of an IODP drilling proposal.

OBJECTIVE 1: VARIATIONS IN PATHWAYS AND INTENSITIES OF DEEP AND BOTTOM WATER MASSES

The tectonic development of the Kerguelen Plateau during the late Cretaceous and Cenozoic has led to significant modifications in the flow paths of deep and bottom water masses that can be reconstructed studying sediment drifts in great detail. Opening, widening and deepening of the Tasman gateway and the Drake Passage have had a significant effect on flow paths of Antarctic Bottomwater (AABW) and the Antarctic Circumpolar Current (ACC) in particular. Development and modifications in the ACC itself primarily influenced the location of the oceanographic frontal system around Antarctica relocating sedimentary depocentres. The seismic data collected allow the identification and mapping of these depocentres, and to reconstruct changes in water mass pathways and intensities through time. Major focus in the analysis of the data will be on the climate dynamics and tectonic development in the Eocene to Oligocene when climate shifted from greenhouse to icehouse conditions. Seismic mapping of the above mentioned depocentres will provide unique insight into effects of tectonic movements and modifications in climate during that time. Our detailed study will focus on the Eocene opening of the Tasman Gateway, the Oligocene opening of the Drake Passage, the late Eocene ephemeral glaciations, and the Eocene-Oligocene Transition. As a second focus, the seismic survey in the Labuan Basin (LB) provides unprecedented information on variations in water mass flows and movements in the Antarctic frontal system from the

Mid-Miocene Climatic Optimum, the late Miocene cooling, and Pliocene warming. Especially this latter interval is of high significance because it might provide new views on the dynamics of both the East and West Antarctic Ice Sheets on ocean circulation when atmospheric $p\text{CO}_2$ was as high as today (~400 ppm).

The following hypotheses are to be tested:

Hypothesis 1: Tectonic movements were the major factors controlling the pathway of AABW/DWBC during the Cenozoic, while the intensity of the ACC was mainly influenced by modifications in climate.

Hypothesis 2: While colder bottom water activity can be observed east of the Tasman gateway already in the early Paleogene, warm water masses, and hence no bottom water, prevailed west of the gateway in the southern Indian Ocean prior to the Eocene-Oligocene boundary.

To test those hypotheses, we collected a grid of 18 seismic profiles (1 ms sample rate, 500 Hz max frequency, 80 Hz dominant frequency \cong 9 m vertical resolution) and a set of 11 sediment cores carefully selected during the cruise on the eastern KP between the central Kerguelen Plateau (CKP) and Williams Ridge (WR) (Figure 1). This area is perfectly suitable for the objectives of this study because topographic highs like the KP and Williams Ridge reduce the speed of deep water masses flowing within the ACC and the AABW causing the deposition of large sediment piles. The structure (geometry, internal unconformities, reflection characteristics) of these sediment drifts represent an extraordinary archive documenting modifications in the flow paths as well as intensity variations of the water masses in great detail. The new high-resolution seismic lines will enable the detection and detailed imaging of sediment drifts shaped by AABW and the Deep Western Boundary Current (DWBC) in the LB and east of WR and by the ACC in the gap between the CKP and southern Kerguelen Plateau (SKP). Sediment drifts located in the LB and the gap between the CKP and SKP are particularly important targets because they should be sensitive recorders of past relocations of the powerful southern ACC front (SACCF) retroflexion (Dezileau et al., 2000; Fukamachi et al., 2010; Mazaud et al., 2010; Sokolov and Rintoul, 2009). The seismic lines further cross ODP Leg 120 Sites 748, 750, and 751. Those sites recovered sedimentary rocks going back towards the Cretaceous (Schlich and Wise Jr, 1992; Wise et al., 1992), were used for dating regional seismic reflections (Fritsch et al., 1992; Munschy et al., 1992), and have thus allowed to correlate the acquired seismic data with geological information (lithology, sediment composition, grain sizes, etc) and to develop age-depth models via the computation of synthetic seismograms. Since the newly collected seismic data are of higher resolution than the previously existing data additional horizons could be identified: the top Paleogene, an Eocene chert reflector, and the Eocene-Oligocene boundary. This enables a palaeoceanographic interpretation of the seismic reflection data as required to address the objectives of this project. Recovery of sediment cores located off the ODP

sites are required to characterize the sediment composition and dating of outcropping sediment layers to facilitate and support the interpretation of seismic profiles.

OBJECTIVE 2: PRE-SITE SURVEY FOR AN IODP3 PROPOSAL

Supported by the proposed seismic survey and geological sampling of the surface deposits we plan to write an IODP drilling proposal to recover the drift deposits in the Ragatt Basin on the northern SKP and in the Labuan Basin.

Carbonate rich sediments from the SKP are ideal to monitor changes in geochemical properties driven by climate throughout the Cenozoic at high resolution. The SKP is a key area to document the evolution of the Antarctic cryosphere, the ACC and the surface frontal system in the southern Indian Ocean. Previous drill cores provided low resolution and spotty windows into Cenozoic climate history of the region. Based on the information to be collected in the proposed survey a much more focused expedition could be planned to retrieve stratigraphic complete successions. In combination with the results from previous drilling at the Tasman Gateway (Leg 189), Wilkes Land (Exp. 318), and IODP 862-Pre proposal (PI Westerhold, Bohaty et al.) to drill in the subantarctic South Atlantic Ocean on the eastern Falkland Plateau (Maurice Ewing Bank and Georgia Basin), the planned IODP drilling proposal for the SKP will focus on climate change, biotic shifts, and deep-sea chemistry during the Paleogene in important southern Indian Ocean sectors, testing the following hypotheses:

Hypothesis 1: the magnitude of temperature change across transient warming events in the Paleogene is driving the response of high-latitude plankton groups.

Hypothesis 2: southern high latitude cooling causing changes in deep and bottom water circulation preceded the major onset of Antarctic Peninsula glaciation at the Eocene-Oligocene Transition.

Hypothesis 3: opening of the Drake Passage and Tasman Gateway paced the development of the Antarctic Circumpolar Current (ACC), AABW and DWBC.

Hypothesis 4: changes in high-latitude and global climate during the Cenozoic are coupled to variations in the ACC circulation.

The seismic grid and the sediment cores collected during cruise So272 will help to characterise lithology and age of layers outcropping at the flanks of the drift deposits. We have collected a set of seismic profiles covering the locations of ODP Leg 120 Sites 748, 750 and 751 and allowing the choice of appropriate sites for an IODP proposal in the Ragatt and Labuan basins (Figure 1). Parasound, providing detailed seismostratigraphic information about the upper 100-200 m of the sedimentary column, and multibeam bathymetric data have also been collected to fulfil the site survey guidelines of IODP's Science Evaluation Panel. We envision IODP drilling at KP and the

Labuan Basin in a way to retrieve complete carbonate rich key records spanning Paleogene to Neogene time and to drill across important structural changes in the drift deposits for highly precise age determination. Synthesis of the here proposed seismics data and future IODP drilling would unfold the detailed history of southern high latitude climate development over the last 66 million years.

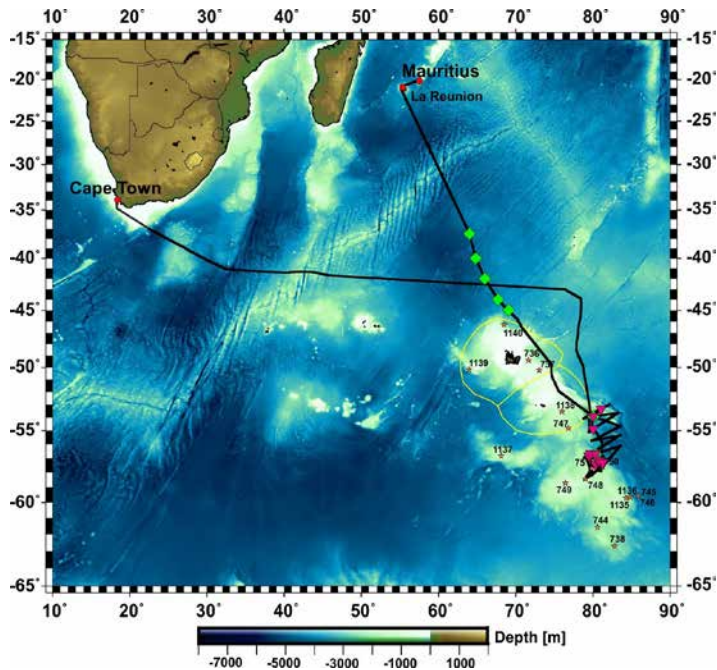


Figure 1: Track chart of R/V SONNE Cruise SO 272. Bathymetry from Smith and Sandwell [1997]. The green diamonds show the locations of deployed ARGO floats, and the purple inverted triangles show the locations of geological sampling carried out during the cruise. Orange stars show the locations of ODP drill sites on the Kerguelen Plateau.

REFERENCES

Dezileau L, Bareille G, Reyss JL, Lemoine F, Evidence for strong sediment redistribution by bottom currents along the southeast Indian ridge, *Deep Sea Research Part I: Oceanographic Research Papers* 2000, 47(10), 1899–1936, doi:[http://dx.doi.org/10.1016/S0967-0637\(00\)00008-X](http://dx.doi.org/10.1016/S0967-0637(00)00008-X).

Fritsch B, Schlich R, Munsch M, Fezga F, Coffin MF, Evolution of the Southern Kerguelen Plateau deduced from seismic stratigraphic studies and drilling at Sites 748 and 750, in *Proceedings of the Ocean Drilling Program, Scientific Results 1992*, edited by Wise Jr S.W., Schlich R., et al., pp. 895–906, Ocean Drilling Program, doi:[10.2973/odp.proc.sr.120.125.1992](https://doi.org/10.2973/odp.proc.sr.120.125.1992).

Fukamachi Y, Rintoul SR, Church JA, et al., Strong export of Antarctic Bottom Water east of the Kerguelen plateau, *Nature Geosci* 2010, 3(5), 327–331, doi:10.1038/ngeo842.

Mazaud A, Michel E, Dewilde F, Turon JL, Variations of the Antarctic Circumpolar Current intensity during the past 500 ka, *Geochem. Geophys. Geosyst* 2010, 11(8), Q08007, doi:10.1029/2010GC003033.

Munsch M, Fritsch B, Schlich R, et al., (1992), Structure and Evolution of the Central Kerguelen Plateau deduced from Seismic Stratigraphic studies and drilling at Site 747, in *Proceedings of the Ocean Drilling Program, Scientific Results 1992*, edited by Wise Jr S.W., Schlich R. et al., pp. 881–893, Ocean Drilling Program, doi:10.2973/odp.proc.sr.120.125.1992.

Schlich R, Wise Jr SW, The geologic and tectonic evolution of the Kerguelen Plateau: An introduction to the scientific results of Leg 120, in *Proceedings of the Ocean Drilling Program, Scientific Results 1992*, edited by Wise Jr S.W., Schlich R. et al., pp. 5–30, Ocean Drilling Program, doi:10.2973/odp.proc.sr.120.125.1992.

Smith WHS, Sandwell DT, Global Sea Floor Topography from Satellite Altimetry and Ship Depth Soundings, *Science* 1997, 277, 1956–1962.

Sokolov S, Rintoul SR, Circumpolar structure and distribution of the Antarctic Circumpolar Current fronts: 1. Mean circumpolar paths, *J. Geophys. Res* 2009., 114, doi:10.1029/2008jc005108.

Wise SW Jr, Schlich R, et al., *Proc. ODP, Sci. Results 1992, 120*: College Station, TX (Ocean Drilling Program), doi:10.2973.odp.proc.sr.120.1992.

SCIENTIFIC OUTPUT

LIST OF PUBLICATIONS

Todd VLG, Williamson LD, Cetacean distribution in relation to oceanographic features at the Kerguelen Plateau, *Polar Biology* 2021, doi: 10.1007/s00300-021-02977-3.

Dorschel B, Hehemann L, Viquerat S, et al., The International Bathymetric Chart of the Southern Ocean Version 2, *Scientific Data* 2022, 9, 275.

Magri L., Whittaker M, Coffin M, et al., Tectono-stratigraphic Evolution of the Kerguelen Large Igneous Province: the Conjugate William's Ridge - Broken Ridge Rifted Margins, *JGR Earth in review*.

Najjarifarizhendi B, Uenzelmann-Neben G, Schneider M, Westerhold T, The Non-Bottom Simulating Reflector across the Raggatt – and Labuan Basin: Evidence for Cenozoic palaeoceanographic changes of the Southern Ocean, in prep.

LIST OF CONFERENCE PRESENTATIONS

2020 | **Kerguelen Plateau Drift Deposits: outstanding high-resolution chronicle of Cenozoic climatic and oceanographic changes in the southern Indian Ocean** EGU General Assembly vEGU2021, online, Vienna, Austria.

2021 | **Sediment drifts at the eastern Kerguelen Plateau: Archives of climate and circulation development** EGU General Assembly vEGU2021, online, Vienna, Austria.

2021 | **Sediment drifts at the eastern Kerguelen Plateau: Archives of climate and circulation development** Ifremer weekly scientific seminar, Plouzane, France.

2021 | **Kerguelen Plateau – outstanding Southern Indian Ocean archives of Cenozoic climate and oceanographic changes** EGU General Assembly vEGU2021, online, Vienna, Austria.

2023 | **Sediment drifts at the eastern Kerguelen Plateau: Archives of climate and circulation development** 4th Deep Water Circulation Research Conference, Edinburgh, UK.

DATA

Multibeam bathymetry raw data:

<https://doi.org/10.1594/PANGAEA.916165>

Multibeam bathymetry processed data:

<https://doi.org/10.1594/PANGAEA.955101>

Sediment echo sounding data:

<https://doi.org/10.1594/PANGAEA.913384>

Seismic profiles:

<https://doi.pangaea.de/10.1594/PANGAEA.935812>

<https://doi.pangaea.de/10.1594/PANGAEA.935752>

<https://doi.pangaea.de/10.1594/PANGAEA.935813>

<https://doi.pangaea.de/10.1594/PANGAEA.935843>

<https://doi.pangaea.de/10.1594/PANGAEA.934739>

<https://doi.pangaea.de/10.1594/PANGAEA.935733>

<https://doi.pangaea.de/10.1594/PANGAEA.935751>

<https://doi.pangaea.de/10.1594/PANGAEA.935738>

<https://doi.pangaea.de/10.1594/PANGAEA.935771>

<https://doi.pangaea.de/10.1594/PANGAEA.935773>

<https://doi.pangaea.de/10.1594/PANGAEA.935840>
<https://doi.pangaea.de/10.1594/PANGAEA.935714>
<https://doi.pangaea.de/10.1594/PANGAEA.935807>
<https://doi.pangaea.de/10.1594/PANGAEA.935731>
<https://doi.pangaea.de/10.1594/PANGAEA.935841>
<https://doi.pangaea.de/10.1594/PANGAEA.935739>
<https://doi.pangaea.de/10.1594/PANGAEA.935842>

Documentation of sediment cores:

<https://doi.pangaea.de/10.1594/PANGAEA.949453>
<https://doi.pangaea.de/10.1594/PANGAEA.949458>
<https://doi.pangaea.de/10.1594/PANGAEA.949457>
<https://doi.pangaea.de/10.1594/PANGAEA.949451>
<https://doi.pangaea.de/10.1594/PANGAEA.949452>
<https://doi.pangaea.de/10.1594/PANGAEA.949448>
<https://doi.pangaea.de/10.1594/PANGAEA.949456>
<https://doi.pangaea.de/10.1594/PANGAEA.949450>
<https://doi.pangaea.de/10.1594/PANGAEA.949455>

Lightness of data extracted from core images:

<https://doi.pangaea.de/10.1594/PANGAEA.949409>
<https://doi.pangaea.de/10.1594/PANGAEA.949403>
<https://doi.pangaea.de/10.1594/PANGAEA.949411>
<https://doi.pangaea.de/10.1594/PANGAEA.949404>
<https://doi.pangaea.de/10.1594/PANGAEA.949405>
<https://doi.pangaea.de/10.1594/PANGAEA.949406>
<https://doi.pangaea.de/10.1594/PANGAEA.949407>
<https://doi.pangaea.de/10.1594/PANGAEA.949408>
<https://doi.pangaea.de/10.1594/PANGAEA.949401>
<https://doi.pangaea.de/10.1594/PANGAEA.949410>

Multi sensor core logging data:

<https://doi.pangaea.de/10.1594/PANGAEA.949516>
<https://doi.pangaea.de/10.1594/PANGAEA.949515>
<https://doi.pangaea.de/10.1594/PANGAEA.949514>
<https://doi.pangaea.de/10.1594/PANGAEA.949517>
<https://doi.pangaea.de/10.1594/PANGAEA.949509>

X-ray fluorescence core scanning:

<https://doi.pangaea.de/10.1594/PANGAEA.948277>
<https://doi.pangaea.de/10.1594/PANGAEA.948287>
<https://doi.pangaea.de/10.1594/PANGAEA.948282>
<https://doi.pangaea.de/10.1594/PANGAEA.948288>

<https://doi.pangaea.de/10.1594/PANGAEA.948281>

<https://doi.pangaea.de/10.1594/PANGAEA.948285>

<https://doi.pangaea.de/10.1594/PANGAEA.948286>

<https://doi.pangaea.de/10.1594/PANGAEA.948284>

<https://doi.pangaea.de/10.1594/PANGAEA.948289>

<https://doi.pangaea.de/10.1594/PANGAEA.948283>

CRUISE REPORT

SO272: doi: 10.2312/cr_so272

SO273

ROV-Sampling and Mapping of the Marion Rises at the Southwest Indian Ridge (SWIR)

AUTHORS

Institute for Mineralogy, Leibniz University Hannover | Hannover, Germany

J. Koepke

Petrologie der Ozeankruste, University Bremen | Bremen, Germany

E. Albers, C. Hansen

Freie Universität zu Berlin | Berlin, Germany

H. Becker

Department of Geosciences and Geography, University of Helsinki | Helsinki, Finland

C. Beier

University of Modena | Modena, Italy

D. Brunelli

University of Wyoming | Wyoming, USA

M. Cheadle

Woods Hole Oceanographic Institution | Woods Hole, MA, USA

H.J.B. Dick, F. Klein, M. Tivey

Institut für Mineralogie, Westfälische Wilhelms-Universität Münster | Münster, Germany

F.S. Genske

GEOMAR Helmholtz-Zentrum für Ozeanforschung | Kiel, Germany

K. Unger-Moreno

Institut für Geo- und Umweltnaturwissensch., Universität Freiburg | Freiburg, Germany

D. Wölki

OBJECTIVES OF THE CRUISE

The "Marion Rise" at the ultra-slow spreading Southwest Indian Ridge (SWIR, full spreading rate of ~14mm/year) in the southern Indian Ocean, is one of the largest oceanic rises in the global oceanic ridge system. Within the framework of the collaborative project SO273, it should be tested whether the Marion Rise was formed by isostatic uplift of an impoverished mantle residuum, or by the rise of a "hot spot" mantle plume. Fine-scale geophysical mapping and detailed ROV sampling should verify that large areas of the Rise are composed of mantle rocks, as well as clarify the crustal architecture. The results of geochemical analysis of basalts, peridotites, and gabbros, as well as the investigation of PGE and Os isotopes on peridotites should clarify whether the lateral heterogeneity of the mantle at SWIR is the result of recycling of different ancient mantle provinces that once formed the complex lithosphere of Gondwana. Also, the distribution of hydrothermal vent areas in the working area should be investigated.

PRELIMINARY WORK; COLLABORATIONS

SO273 is embedded within a two-stage joint project with working groups from Germany, U.S., China, and Italy with the goal of thoroughly investigating the Marion Rise by geological and geophysical methods. SO273 built on the previous successful cooperation of 5 German working groups (Universities of Hannover, Münster, Berlin, Erlangen, Bremen) within this joint project on the U.S.-coordinated cruise TN365 with the RV Thomas G. Thompson to the Marion Rise in 2019. An overall work plan was developed with several work areas, of which the northern area was covered by the US TN365 cruise and the southern area by the German SO273 project, which was designed as collaborative project (Verbundprojekt). Details on the state of science, objectives, and execution of both ship expeditions can be found in the published cruise reports (for links see references).

CRUISE EXECUTION

R/V Sonne cruise SO273 had been subject to several short notice changes in the scientific party due to SARS-COVID19 pandemic related travel restrictions and quarantine bans prior to departure of the vessel in Cape Town, which was especially related to the Chinese group which could not join the cruise. On 07.03.2023, R/V Sonne left the port of Cape Town, transited towards the working area with increasing seas and winds and arrived at 11.03.2020 in the working area. Before the premature termination of the cruise due to the worldwide rampant SARS-COVID-19 pandemic, the project proceeded essentially as described in the project proposal.

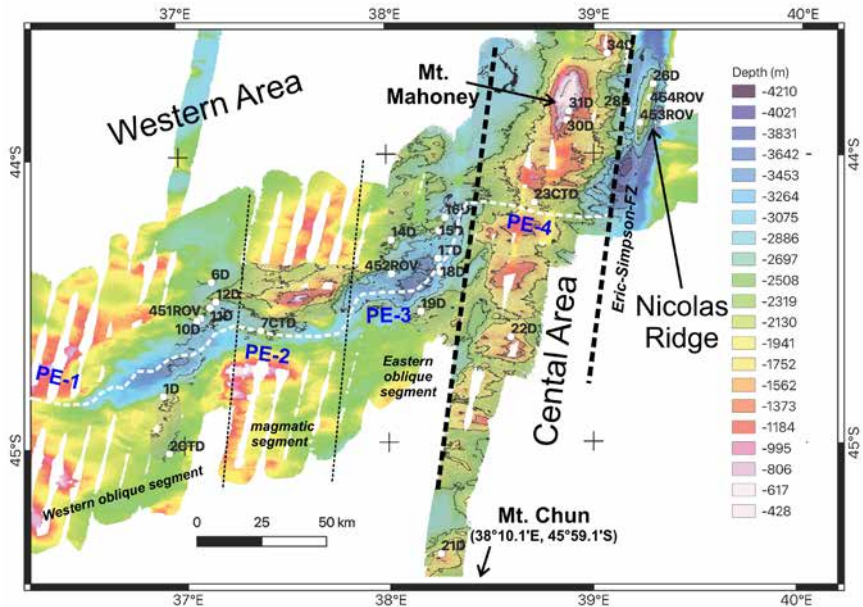


Figure 1: Overview of the SO273 work areas (combination of KH-07-04 and KH-09-05 (Sato et al., 2013) and SO273 bathymetry) consisting of the western area, the central area, and Nicolas Ridge. The western area is divided into the western oblique, magmatic, and eastern oblique segments. Also listed are the locations of the Mt. Mahoney seamounts and Mt. Chun, the location of the current spreading axis (white line), and segment names (in blue) after Sato et al. (2013).

The cruise focused on three working areas of the western segment of the Southwest Indian Ridge (SWIR) between the Prince Edward and Eric Simpson Fracture Zones as well as towards Marion Island: the western area, the central area, and the Nicolas-Ridge (Figure 1). The western segment of the SWIR is dominated by oblique spreading while the central segment is considered magmatically robust. Hydroacoustic imaging revealed that the regular bathymetric anomalies towards Marion Island in the south reflect the frequent changes between magmatically and tectonically dominated spreading, respectively. Additionally, the newly discovered Nicolas transpressional ridge in the Eric Simpson Fracture Zone was targeted. In total, 5 dives using MARUM ROV QUEST 4000 have been performed, 19 rock dredges, 2 CTDs, 1 CTD Tow-Yo and 7 geophysical profiles (hydroacoustics, gravimetry, magnetics). Hydrothermal plumes were determined and investigated using the CTD and Mini Autonomous Plume Recorders (MAPRs) attached to dredges, the ROV and the CTD. During the SO273 cruise, new features were installed and applied to the ROV's video capabilities, which also enabled 3D reconstructions of seafloor outcrops. The new telepresence video streaming system allowed on-shore project participants to participate, with the ability to design details during ongoing dives.

Cruise SO273 was abandoned on the 21.03.2020 due to increasing concerns about the SARS-COVID19 pandemic causing closures of South African ports and worldwide

travel restrictions. Thus, a return voyage of the FS Sonne with scientific crew and crew to Germany was carried out, which ended on 22.04.2020 in Emden Dockyard. Therefore, only a part of the planned program could be carried out. Despite the early termination, the data and samples obtained were sufficient to meet the targeted objectives of the overall project. The post-cruise work in the laboratories of the Universities of Erlangen, Münster, Berlin, Bremen and Hannover went largely without problems, with the restriction that in the project of the University of Hannover, the ultramylonites of the Nicolas Ridge were the subject of the analytical work instead of the targeted gabbros.

RESULTS: CRUSTAL ARCHITECTURE

The studied work area at the ultraslow-spreading SWIR in the vicinity of the Marion Islands provides an excellent opportunity to exemplify the interaction between phases of magma absence, where purely tectonic processes dominate at detachment faults, and those with increasing "magma lubrication". Our geophysical profiles, in conjunction with lithologic "groundtruthing" by dredges and ROV, show that the regular bathymetric anomalies in the work area indicate a rhythmic alternation between magmatic and tectonic dominated extensional movements. The discovered peridotite plateaus were most likely formed during a-magmatic phases by two intersecting (flip-flopping) detachment faults, which explains the uplift of the mantle rocks. Using magnetic mapping, the spreading rate over a period of 30 My could be calculated: This is 7.2 km/My in the south and was relatively constant, while it is slower at 5.9 km/My in the north. Another result of the geophysical mapping is the finding that the volcanic chain north of Marion Island is NOT a hotspot trace. According to the hotspot model, a chain of extinct seafloor volcanoes was expected (similar to the Hawaiian seamounts). In contrast, interpretation of the SO273 mapping implies that this trace represents a series of spine-parallel volcanic mounds formed over the last 30 My by spreading at the SWIR.

RESULTS: ULTRAMYLONITES OF THE NICOLAS RIDGES

Samples recovered from the transpressional Nicolas ridge in the Eric Simpson Fracture Zone are fresh ultramylonitic peridotites covered with thick carbonate sequences. From the evaluation of the mineral analyses and from the microstructural studies of the Nicolas Ridges ultramylonites, it was possible, for the first time for such an oceanic transpressional massif, to determine precisely the temperature and pressure conditions of the reforming. The results clearly show that the ultramylonites were formed at very high temperatures (850 to 1000°C), from peridotites that were very likely already serpentinized before the transformation. Here, the determined pressures indicate depths for the formation of 3 and 15 km, with a peak of 30 km. Relatively high Cl contents in the amphiboles of the ultramylonites imply that a seawater-derived hypersaline fluid was present during the formation of the ultramylonites. These results indicate that seawater intrusion along detachment faults on slow-spreading ridge systems is possible to very great depths during a-magmatic periods. Such a finding for recent oceanic ridge systems is presented here for the first time. So far, only microseismic investigations have indicated such great depths in the vicinity of detachment faults.

RESULTS: GEOCHEMISTRY OF THE BASALTS

The sampling program during SO273 revealed that the exposures in the oblique, magmatically inactive segment consist of volatile-rich pillow basalts with a minor volume of peridotites exposed on the inside corner high. The magmatically robust segment and newly discovered Mahoney seamount North of the axis (Figure 1) shows subtle evidence for active hydrothermal activity. The recovered lavas are fresh, volatile-rich alkali basalts indicating that the off-axis seamount has recently been active. Highly vesicular basalts from the Mahoney Seamount have unradiogenic Nd-Hf together with radiogenic Sr isotopic compositions (Woelki et al., 2023). Their distinct low $^{206}\text{Pb}/^{204}\text{Pb}$ isotope signature combined with high $^{207}\text{Pb}/^{204}\text{Pb}$ and $^{208}\text{Pb}/^{204}\text{Pb}$ is best explained by melting of a mantle that has been strongly influenced by stranded lower continental crust. The geographic distribution of the isotopic variability favors the idea of shallow re-cycling of lower continental crust isolated for a longer period contributing to melts forming Mahoney Seamount through off-axis fault systems. The isotopic composition of Mahoney Seamount lavas shares many characteristics with EM-1 sources and the DUPAL signature. Previous isotopic studies of the SWIR basalts proposed recycling of ancient subcontinental lithospheric mantle (SCLM) or pelagic sediments with oceanic crust to be responsible for this enriched isotopic signature. Lu/Hf and Sm/Nd ratios of pelagic sediments would result in decoupled $^{143}\text{Nd}/^{144}\text{Nd}$ and $^{176}\text{Hf}/^{177}\text{Hf}$ ratios. However, Mahoney Seamount shows no decoupling in those isotopic systems and the restricted occurrence of the extreme lower continental crustal signature at Mahoney Seamount implies that the enriched isotopic signature has a different origin.

REFERENCES

- Dick HJB, Zhou H, Koepke J, et al., Cruise Report: Marion Rise, Southwest Indian Ridge, Cruise No. TN365, 21.02.2019–28.03.2019, Durban – Cape Town (South Africa), <https://www.marine-geo.org/tools/search/entry.php?id=TN365#documents>.
- Koepke J, Beier C, Dick HJB, et al., Cruise Report: ROV-Sampling and Mapping of the Marion Rises at the Southwest Indian Ridge (SWIR), Cruise No. SO273, 06.03.2020–22.04.2020, Cape Town (South Africa) – Emden (Germany). SONNE-Berichte, SO273, 1-80, http://doi.org/10.2312/cr_so273.
- Sato T, Okino K, Sato H, Mizuno M, Hanyu T, Seama N, Magmatic activities on the Southwest Indian Ridge between 35°E and 40°E, the closest segment to the Marion hotspot, *Geochemistry, Geophysics, Geosystems* 2013, 14, 5286–5307, doi:10.1002/2013GC004814.
- Woelki D, Salters V, Beier C, Dick HJB, Koepke J, Romer R, Shallow recycling of lower continental crust: The Mahoney Seamount at the Southwest Indian Ridge, *Earth and Planetary Science Letters* 2023, 602, 117968 <https://doi.org/10.1016/j.epsl.2022.117968>.

SCIENTIFIC OUTPUT

LIST OF PUBLICATIONS

Woelki D, Salters V, Beier C, Dick HJB, Koepke J, Romer R, Shallow recycling of lower continental crust: The Mahoney Seamount at the Southwest Indian Ridge, Earth and Planetary Science Letters 2023, 602, 117968, <https://doi.org/10.1016/j.epsl.2022.117968>.

In the "Schlussbericht" from 30.10.2022 are 6 manuscripts listed with the status "to be submitted". This is still the case. We plan the submission of these papers to Journals within the next 6 months.

LIST OF CONFERENCE PRESENTATIONS

2023 | **Highly siderophile element composition of mantle domains at the Southwest Indian Ridge near Marion Rise correlate with geologic setting** Becker H, Waag M, Fleming WL, Gastescu A, Stammeier JA, Gleissner P, Hoffmann JE, Dick HJB, Koepke J, AGU Fall Meeting, San Francisco, US.

2023 | **The Marion Hotspot Track Isn't** Dick HJB, Koepke J, Tivey MA, Beier C, South African GeoCongress, Stellenbosch, South Africa.

2023 | **Ancient residual lithosphere at the Marion Rise: Evidence from Hf-Nd isotope systematics in basalts and peridotites** Woelki D, Beier C, Dick HJB, Stracke A, Salters VJM, Goldschmidt Conference, Lyon, France.

2023 | **Oceanic mylonites: a wet origin story** Urann BM, Cheadle MJ, John BE, Brunelli D, Dick HJB, Koepke J, AGU Fall Meeting, San Francisco, US.

2022 | **Highly siderophile elements reveal ancient subarc mantle beneath the Southwest Indian Ridge at Marion Rise** Waag M, Fleming WL, Gastescu A, Becker H, Stammeier JA, Gleissner P, Hoffmann JE, Dick HJB, Koepke J, GeoMinKöln, Cologne, Germany.

2022 | **Shallow recycling of lower continental crust: The Mahoney Seamount at the Southwest Indian Ridge** Woelki D, Salters V, Beier C, Dick HJB, Koepke J, Romer HW, Goldschmidt Conference, Hawaii, US.

2021 | **Exhumation at the Southwest Indian Ridge: constraints on temperature and depth of water ingress during detachment faulting** Colwell DJ, Cheadle MJ, John BE, Dick HJB, Swapp SM, Brunelli D, Urann BM, Conference of the Geological Society of America, Portland, US.

2021 | **Widespread alkaline explosive volcanism and mantle outcrops on the SW Indian Ridge** Dick HJB, Zhou Y, Koepke J, AGU Fall Meeting, New Orleans, US.

2021 | **Highly siderophile element-depleted mantle beneath the Southwest Indian Ridge at the Marion Rise** Fleming W, Waag M, Gastescu A, Becker H, Schleicher A, Stammeier J, Dick HJB, Koepke J, AGU Fall Meeting, New Orleans, US.

DATA

Bathymetry:

https://www.bsh.de/DE/DATEN/Klima-und-Meer/Ozeanographisches_Datenzentrum/Vermessungsdaten/Indischer_Ozean/indischer_ozean_node.html (bathymetric data centre of the Bundesamt für Seeschifffahrt und Hydrografie).

Petrological samples:

<https://www.geosamples.org/>.

For all petrological samples, IGSN (International Geo Sample Number) codes have been assigned. All samples are registered in the System for Earth Sample Registration SESAR. The corresponding links for access to each sample in the IGSN system are given in the table of the detailed sample characterization in Appendix A2 of the cruise report (http://doi.org/10.2312/cr_so273).

Images of the petrological samples:

http://doi.org/10.2312/cr_so273 (Appendix 3).

Description of the petrological samples:

http://doi.org/10.2312/cr_so273 (Appendix 2).

Gravimetric and magnetic data:

currently in the process of being archived at WHOI (Woods Hole Oceanographic Institution). Responsibility: M. Tivey (mtivey@whoi.edu).

Rock samples:

are stored and available in the Institutes of the Universities of the collaboration partners:

Basaltic samples:

U Erlangen-Nürnberg, responsibility K. Haase (karsten.haase@fau.de) and C. Beier (christoph.beier@helsinki.fi).

Peridotite samples:

U Münster and FU Berlin, responsibility A. Stracke (astra_01@uni-muenster.de) and H. Becker (hbecker@zedat.fu-berlin.de).

Fluid samples:

U Bremen, responsibility W. Bach (wbach@uni-bremen.de)

CRUISE REPORT

SO273: http://doi.org/10.2312/cr_so273

SO276

Depth transects and connectivity along gradients in the North Atlantic and Nordic Seas in the frame of the IceAGE project (Icelandic marine Animals: Genetics and Ecology) (IceAGE3)

AUTHORS

Senckenberg am Meer, Deutsches Zentrum für Marine Biodiversitätsforschung (DZMB) | Wilhelmshaven & Hamburg, Germany
S. Brix

Originally applied for R/V Meteor and scheduled for Meteor in early 2020, MerMet17-6 became SO276 due to pandemia-related changes in the usage of the German research fleet. The focus of the expedition were the subarctic waters North and South of the Greenland-Faroe Ridge including selected habitat like abyssal plains, the shelf break along the Ridge, cold-water coral reefs East of Iceland as well as geothermal activity on the Reykjanes Ridge. Each habitat was mapped via dives with the ROV Kiel6000 (GEOMAR) and sampled with various gear (CTD, Plankton nets, multinet, multicorer, boxcorer or smaller grabs as well as epibenthic sledge). The video surveys via ROV led to habitat descriptions (Brix et al. 2022, Brix et al. in preparation) as well as descriptions of species new to science (Lörz et al. in review) or unknown observations (Golikov et al. 2023). Within this talk, the results per working area along the cruise track are summarized and highlights presented.

NORWEGIAN BASIN (AREA 1)

During IceAGE3, the main objectives were exploration, documentation, and sampling of fauna and sediments. The first stations were located in the Norwegian Basin, where mainly video-mapping of small areas of the seafloor, fauna sampling, and sediment sampling was carried out. This station could be considered as a classical arctic "abyssal plain station" with large quantities of holothurians (*Elpidia* sp.), crinoids (cf. *Bathycrinus* sp.), burrowing crustaceans, anemones, *Hymenaster*, benthic fish species, and even two appearances of *Grimptoteuthis* (dumbo) octopuses (Golikov et al. 2023).

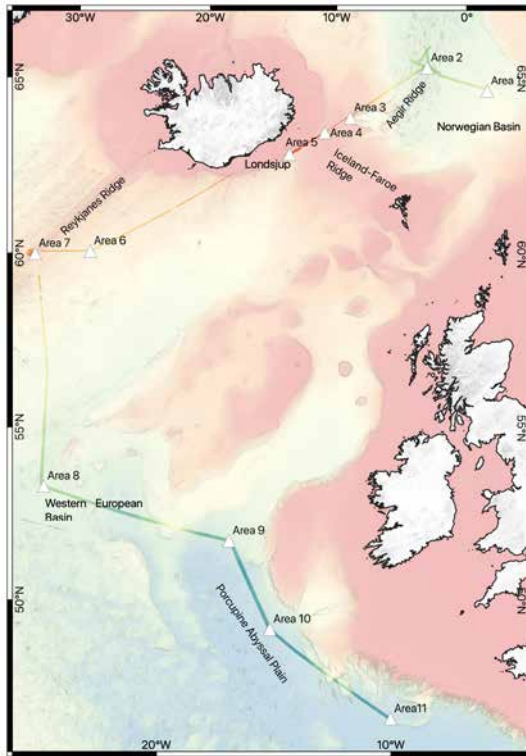


Figure 1: Total map of the surface covered by SO276 (MerMet17-6) over the faded GEMCO map. Working areas are located by a white triangle (Norwegian Basin and Aegir Ridge, Iceland-Faroe Ridge, Lónsjúp coral reef, Reykjanes Ridge, East Atlantic Abyssal plains). Figure is visible in the cruise report as 3.1 (Brix et al. 2020).



Figure 2: Glass sponge *Cauliphacus arcticus* with a reddish *Bythocaris* shrimp (right), a pantopod (middle) and the amphipod species new to science *Halirages spongiae* sp. nov. Lörz et al. in review (left). Picture taken by Solvín Zankl on board of R/V Sonne in the cool room with life specimens.

AEGIR RIDGE (AREAS 2 & 3)

According to Brix et al. (2022), the Ægir Ridge System (ARS) is an ancient extinct spreading axis in the Nordic seas extending from the upper slope east of Iceland (~550 m depth), as part of its Exclusive Economic Zone (EEZ), to a depth of ~3,800 m in the Norwegian basin. Geomorphologically a rift valley, the ARS has a canyon-like structure that may promote increased diversity and faunal density. The main objective was to characterize benthic habitats and related macro- and megabenthic communities along the ARS, and the influence of water mass variables and depth on them. Benthic communities of the ARS were surveyed by means of ROV and epibenthic sledge (EBS). For this purpose, two working areas (2, 3) were selected, including abyssal stations in the northeast and bathyal stations in the southwest of the ARS. Patterns of diversity and community composition of the soft-sediment macrofauna, retrieved from the EBS and a variety of grabs. At each station, CTD and plankton sampling complemented the data. Additionally, high-resolution bathymetric maps using the vessel's multi-beam echosounder system were created. A biological "canyon effect" became evident in dense aggregates of megafaunal filter feeders and elevated macrofaunal densities (Brix et al. 2022, Kaiser et al. submitted).

ICELAND-FAROE RIDGE (AREA 4)

During the station work in area 4, we deployed EBS, multicorer, boxcorer, and plankton nets. A total of 19 samples were obtained from the West Iceland-Faroe Ridge. At present, mainly EBS data are currently input in Kaiser et al. (submitted).

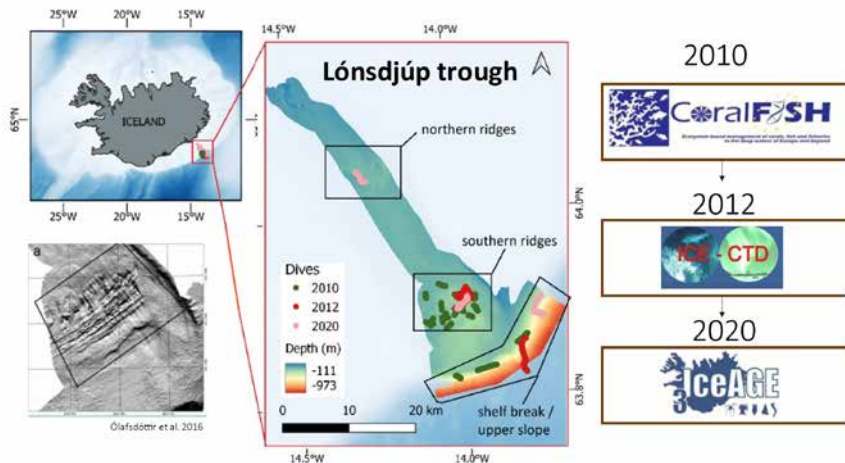


Figure 3: Lónsdjúp trough is approximately 50 km long, 6 km wide and has a depth ranging from 100 to 300 m, beyond the shelf break below 900 m. Over the last 20 years, a total of 74 hours of video footage were collected spanning a total of 51 Km in length from different expeditions (right) allowing a time series and applying species distribution models for coral mounts (DeClippele et al. in preparation).

LÓNDSJÚP TROUGH (AREA 5)

On the south and southeastern continental slope of Iceland, reef-forming cold-water corals such as *Desmophyllum pertusum* (aka *Lophelia pertusa*) have been found (Figure 3,4). Cold-water coral reefs are nurseries, home to economically important species and are hotspots of biodiversity and carbon cycling. The Lónsdjúp trough, located off southeastern Iceland, is of particular interest due to its commercial importance and its pristine cold-water coral reefs present on ridges in the southern part of the trough. Due to risk from disturbances such as fishing and climate change, it is important that we understand where these reefs occur, what drives their presence and how we can use this information as a tool in marine ecosystem management. A Species Distribution Modelling (SDM, Figure 3) approach was used as a method to answer these questions.

REYKJANES RIDGE (AREAS 6 & 7)

One of the goals of the SO276 (MerMet 17-6) expedition was to locate the potential hydrothermal vents responsible of the redox anomaly evidenced by several AUV dives during the MSM75 expedition in 2018 (Devey et al., 2018). This led to the discovery of the newly named IceAGE vent field on 12th June 2020 during the 103ROV08 dive (607 m - 730 m). The IceAGE vent field is the second known hydrothermal vents along the 900 km of the Reykjanes Ridge. Whilst there was no megafauna directly visible at the chimneys, there was “a ring of life” present (see Figure 5). Especially barnacles of the species *Bathylasma hirsutum* were discovered as indicator species for geothermal activity (Neuhaus et al. submitted).



Figure 4: The most prominent coral species at Lónsdjúp are *Madrepora oculata* Linnaeus, 1758 and *Desmophyllum pertusum* (Linnaeus, 1758). This picture taken by ROV Kiel 6000 shows the middle reefs in the rose area shown in figure 3.

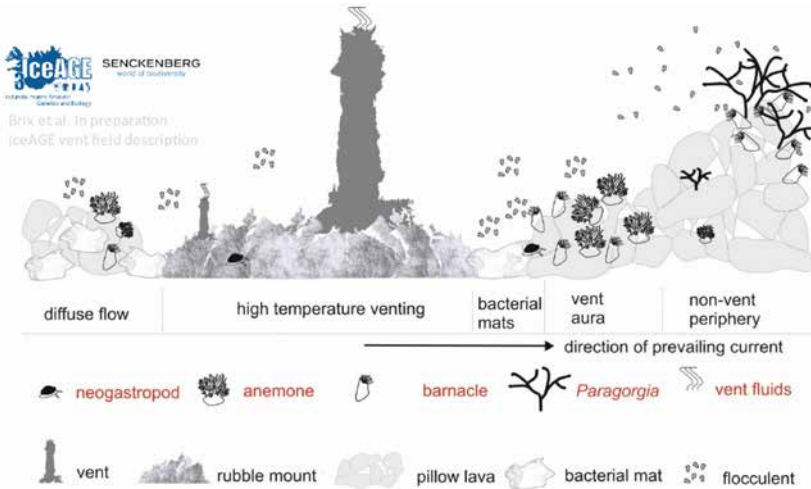


Figure 5: Schematic drawing of the IceAGE vent field by Katrin Linse for the joint paper in preparation shows the “ring of life” using the produced food source (“fluff” from bacterial mats, hot, but clear fluids).

ABYSSAL PLAINS SOUTH OF ICELAND (AREAS 8–11)

The final sampling of the expedition took place in the European Basin and the Porcupine Abyssal Plain (PAP) at depth of about 4000-4500 m. These sampling areas laid the background for a standardized gear deployment carried out in follow-up expeditions SO280 and SO286. A total of 69 samples were obtained. The results are partly linked to the follow-up expeditions SO280 (IceDivA1) and SO286 (IceDivA2) dealing with connectivity of deep-sea invertebrates (IceDivA: Icelandic marine Animals: Genetics and Ecology meets Diversity along latitudinal gradients in the deep sea of the Atlantic Ocean).

REFERENCES

Brix S, Taylor J, Le Saout M, Mercado-Salas N, Kaiser S, Lörz A-N, Gatzemeier N, Jeskulke K, Kürzel K, Neuhaus J, Paulus E, Uhlir C, Korfhage S, Bruhn M, Stein T, Wilsenack M, Siegler V, Schumacher M, Lux T, Gärtner L, Abegg F, Pieper M, Bodendorfer M, Cuno P, Huusmann H, Matthiessen T, Bischof F, Suck I, Depth transects and connectivity along gradients in the North Atlantic and Nordic Seas in the frame of the IceAGE project (Icelandic marine Animals: Genetics and Ecology), Cruise No. SO276 (MerMet17-06), 22.06.2020–26.07.2020, Emden (Germany) – Emden (Germany), Open Access, Sonne-Berichte, SO276. Leitstelle Deutsche Forschungsschiffe 2020, Bonn, Germany, 48 pp. DOI 10.48433/cr_so276.

Brix S, Kaiser S, Lörz A-N, Le Saout M, Schumacher M, Bonk F, Egilisdottir H, Olafsdottir SH, Tandberg AHS, Taylor J, Tewes S, Xavier JR, Linse L, Habitat variability and faunal zonation at the Ægir Ridge, a canyon-like structure in the deep Norwegian Sea, PeerJ 2022, <https://doi.org/10.7717/peerj.13394>.

Brix S, Linse K, Taylor J, LeSaout M, Palgan M, Petersen S, Abegg F, Devey C, et al., IceAGE vent field description, in preparation.

De Clippele LH, Gafeira J, Robert K, Hennige S, Lavaleye MS, Duineveld GCA, ... & Roberts JM, Using novel acoustic and visual mapping tools to predict the small-scale spatial distribution of live biogenic reef framework in cold-water coral habitats, *Coral Reefs* 2017, <https://doi.org/10.1007/s00338-016-1519-8>.

Devey, et al., 2018

Golikov AV, Stauffer JB, Schindler SV, Taylor J, Boehringer L, Purser A, Sabirov RM, Hoving H-J, Miles down for lunch: deep- in situ observations of Arctic finned octopods *Cirroteuthis muelleri* suggest pelagic-benthic feeding migration, *Proceedings of the Royal Society* 2023, <https://doi.org/10.1098/rspb.2023.0640>.

Kaiser S, Brix S, Kolb M, Kürzel K, Linse K, Tandberg AHS, Rich to ridges - Diversity and composition of benthic Isopoda from continental shelves to the abyss into the Norwegian Sea, submitted to *Diversity*.

Lörz A-N, Nack M, Tandberg AHS, Brix S, Schwentner M, A new deep-sea species of Halirages (Crustacea: Amphipoda: Calliopiidae) inhabiting sponges, *European Journal of taxonomy*, in review.

SCIENTIFIC OUTPUT

LIST OF PUBLICATIONS

Baco, A.R., Ross, R., Althaus, F., Amon, D.J., Bridges, A., Brix, S. et al., and the DOSI working group on VMEs from Imagery, Towards a scientific community consensus on designating Vulnerable Marine Ecosystems from imagery. *PeerJ* 2023, <https://doi.org/10.7717/peerj.16024>.

Ballesteros, J.A., Setton, E.V.W., Santibáñez-López, C.E., Arango, C.P., Brenneis, G., Brix, S., et al., & Sharma, P.P., Phylogenomic Resolution of Sea Spider Diversification through Integration of Multiple Data Classes, *Molecular Biology and Evolution* 2022, <https://doi.org/10.1093/molbev/msaa228>.

Brix, S., Kaiser, S. Lörz, A.-N., Le Saout, M., Schumacher, M., Bonk, F. Egilisdottir, H., Olafsdottir, S.H., Tandberg, A.H.S., Taylor, J., Tewes, S., Xavier, J.R., Linse, L., Habitat variability and faunal zonation at the Ægir Ridge, a canyon-like structure in the deep Norwegian Sea. *PeerJ* 2022, <https://doi.org/10.7717/peerj.13394>.

Eichsteller, A., Taylor, J. Stöhr, S., Brix, S., Martínez Arbizu, M., DNA Barcoding of Cold-Water Coral-Associated Ophiuroid Fauna from the North Atlantic. *Diversity* 2022, <https://doi.org/10.3390/d14050358>.

Golikov, A.V., Stauffer, J.B., Schindler, S.V., Taylor, J., Boehringer, L., Autun Purser, A., Sabirov, R.M., Hoving, H.J., Miles down for lunch: deep- in situ observations of Arctic finned octopods *Cirroteuthis muelleri* suggest pelagic–benthic feeding migration. *Proceedings of the Royal Society* 2023, <https://doi.org/10.1098/rspb.2023.0640>.

Jażdżewska, A.M., Tandberg, A.H.S., Horton, T., Brix, S., Global gap-analysis of amphipod barcode library. *PeerJ* 2021, <https://doi.org/10.7717/peerj.12352>.

Kaiser S., Brix S., Kolb M., Kürzel K., Linse K., Tandberg A.H.S., Rich to ridges – Diversity and composition of benthic Isopoda from continental shelves to the abyss into the Norwegian Sea, submitted to *Diversity*.

Korfhage, S. A., Rossel, S., Brix, S., McFadden, C. S., Ólafsdóttir, S. H., & Martínez Arbizu, P., Species delimitation of Hexacorallia and Octocorallia around Iceland using nuclear and mitochondrial DNA and proteome fingerprinting, *Frontiers in Marine Science* 2022, 304, Doi: 10.3389/fmars.2022.83820.

Kürzel K, Kaiser S, Lörz A.-N, et al, Correct Species Identification and Its Implications for Conservation Using Haploniscidae (Crustacea, Isopoda) in Icelandic Waters as a Proxy, *Frontiers in Marine Science* 2022, 8, doi:10.3389/fmars.2021.795196.

Kürzel K, Brix S, Brandt A, Brenke N et al., Pan-Atlantic Comparison of Deep-Sea Macro- and Megabenthos, *Diversity* 2023; 15(7):814. <https://doi.org/10.3390/d15070814>.

Lörz AN, Oldeland J, Kaiser S, Niche breadth and biodiversity change derived from marine Amphipoda species off Iceland. *Ecology and Evolution* 2022. doi: 10.1002/ece3.8802.

Lörz AN, Horton T., Investigation of the Amathillopsidae (Amphipoda, Crustacea), including the description of a new species, reveals a clinging lifestyle in the deep sea worldwide. *ZooKeys* 2021, 1031:19–29. <https://doi.org/10.3897/zookeys.1031.62391>.

Lörz A.-N., Nack, M. Tandberg, A.H.S., Brix, S., Schwentner, M., A new deep-sea species of *Halirages* (Crustacea: Amphipoda: Calliopiidae) inhabiting sponges, *European Journal of taxonomy*, in review.

Lörz A.-N., Kaiser S, Oldeland J, Stolter C, Kürzel K, Brix S, Biogeography, diversity and environmental relationships of shelf and deep-sea benthic Amphipoda around Iceland (2021). PeerJ 9:e11898 <https://doi.org/10.7717/peerj.11898>.

Le Saout, M., Palgan, D., Devey, C., Lux, T., Petersen, S., Thorhallsson, D., Tomkowicz, A., Brix, S., Variations in Volcanism and Tectonics Along the Hotspot-Influenced Reykjanes Ridge. *Geochemistry, Geophysics, Geosystems* 2023, <https://doi.org/10.1029/2022GC010788>.

Neuhaus J, Linse K, Brix S, Martínez Arbizu P, Taylor J, Shedding light on the deep-sea acorn barnacle *Bathylasma hirsutum* (Hoek, 1883) and its affiliation with a hydrothermal vent field on the Reykjanes Ridge, submitted.

Paulus, E., Brix, S., Siebert, A., Martínez Arbizu, P., Rossel, S., Peters, J., Svavarsson, J., Schwentner, M., Recent speciation and hybridization in Icelandic deep-sea isopods: An integrative approach using genomics and proteomics. *Molecular Ecology* 2021, <https://doi.org/10.1111/mec.16234>.

Xu, Y.-T., Taylor, J., Liu, H.-C., Zhang, Y., Guo, S.-F., Brix, S., Wong, Y.H., The shell proteome of the deep-sea barnacle *Bathylasma hirsutum* and the convergency in barnacle and molluscan shell proteins. 26 September 2023, (Version 1) available at Research Square. <https://doi.org/10.21203/rs.3.rs-3287643/v1>.

LIST OF CONFERENCE PRESENTATIONS

2023 | **The North Atlantic Gateway as natural experimental area for marine benthic long-term observation – case studies in various habitats and future perspectives** 56th EMBS, Reykjavik, Iceland, – TALK

2023 | **Filter feeding on filter feeders viewed by the integrative taxonomy perspective: Arcturidae Dana, 1849 on Paramuricea placomus Linnaeus, 1758** 56th EMBS, Reykjavik, Iceland, – TALK

2023 | **Icelandic cold-water coral reefs: using data collected over a 20-year period to understand their distribution** 56th EMBS, Reykjavik, Iceland, – TALK

2023 | **Amazing deep-sea Amphipoda off Iceland** 56th EMBS, Reykjavik, Iceland, – TALK

2023 | **Tricky species identification: corals, proteomic fingerprints and solving taxonomic riddles** 56th EMBS, Reykjavik, Iceland – TALK

2023 | **Strong indications for linear concatemeric mitochondrial DNA in Octocorallia** 56th EMBS, Reykjavik, Iceland – POSTER

- 2023 | **IceDivA post IceAGE, a project update focussing on peracarid crustaceans**
International Crustacean Conference, Wellington, New Zealand – TALK
- 2023 | **A cosmopolitan predator in the abyssal depth- really?** International Colloquium on Amphipoda, Djerba, Tunisia – TALK
- 2023 | **Strong indications for linear concatemeric mitochondrial DNA in Octocorallia**
ISDSC8, Edinburgh, United Kingdom – RESEARCH HIGHLIGHT
- 2022 | **The deep-sea acorn barnacle *Bathylasma hirsutum* (Hoek, 1883): first record from a hydrothermal vent field at the Reykjanes Ridge** 24th Annual Meeting of the Society of Biological Systematics, Hamburg, Germany – TALK
- 2022 | **Connectivity of deep-sea basins in the North-Atlantic using invertebrate taxa as surrogates – preliminary results** 23rd Annual Meeting of the Society of Biological Systematics, Hamburg, Germany – TALK
- 2022 | **The Deep-Sea Acorn Barnacle *Bathylasma hirsutum* (Hoek, 1883): An Indicator for Geothermal Activity Along the Reykjanes Ridge?** iAtlantic 4th General Assembly, Florianópolis, Brazil – TALK
- 2022 | **Complete mitochondrial genomes of three octocorals from a geothermal area off Iceland** iAtlantic General Assembly, Florianópolis, Brazil – POSTER
- 2022 | **Species delimitation of Hexacorallia and Octocorallia around Iceland using nuclear and mitochondrial DNA and proteome fingerprinting** International Coral Reef Symposium, Bremen, Germany – POSTER
- 2022 | **Species delimitation of Hexacorallia and Octocorallia around Iceland using nuclear and mitochondrial DNA and proteome fingerprinting** Annual Meeting of the Society of Biological Systematics, online – TALK
- 2022 | **A suprabenthic predatory amphipod showing a global distribution in the abyss**
20^{te} Crustaceologentagung im Zoologischen Museum Kiel, Germany – POSTER
- 2022 | **Living on sponges: A new amphipod species in the Deep Sea of the North Atlantic** Crustaceologentagung im Zoologischen Museum Kiel, Germany – POSTER
- 2021 | **Species delimitation of Hexacorallia and Octocorallia around Iceland using nuclear and mitochondrial DNA and proteome fingerprinting** International Deep Sea Biology Symposium, Brest, France – POSTER

2021 | **Interactive keys as a tool to assess biodiversity in selected deep-sea isopods**

Iceymare online forum: Marine Biodiversity in the Anthropocene, online – TALK

2021 | **The Aegir Ridge – a canyon-like structure** Deep Sea Biology Symposium (DSBS)

Brest, France: hybrid – TALK

2021 | **A biological approach on CTD data along with EBS tracks to assign water masses to marine benthic species distribution data** Deep Sea Biology Symposium

(DSBS) Brest, France: hybrid, – POSTER

2021 | **New species of Amathillopsidae (Amphipoda, Crustacea) from the deep sea worldwide reveal a clinging lifestyle** Deep-Sea Biology Symposium, digital

participation- Brest, France: hybrid, – POSTER

2020 | **Interactive keys in selected deep-sea isopods** World Marine Biodiversity

Conference (WMBC) Auckland (New Zealand), online, – TALK

2020 | Poster – The status quo of the IceAGE project”, World Marine Biodiversity Conference, digital participation -Auckland, New Zealand.2023 | **Pan-Atlantic**

comparison of deep-sea macro- and megabenthos 56th EMBS, Reykjavik, Iceland – TALK

2020 | **Necessity of reliable identification as a baseline for conservation – an isopod case study on the genus Haploniscus Richardson 1908** 4th Annual Meeting in

Conservation Genetics, Frankfurt – POSTER

DATA

Water column data:

Continuous thermosalinograph oceanography along R/V SONNE cruise SO276:

<https://doi.org/10.1594/PANGAEA.943865>

Multibeam data:

Multibeam bathymetry raw data (Kongsberg EM 122 transit dataset) of R/V SONNE during cruise SO276. PANGAEA: <https://doi.org/10.1594/PANGAEA.945674>

Multibeam bathymetry processed data (Kongsberg EM710 entire dataset) of R/V SONNE during cruise SO276: <https://doi.org/10.1594/PANGAEA.954158>

Multibeam bathymetry raw data (Kongsberg EM710 entire dataset) of R/V SONNE during cruise SO276: <https://doi.org/10.1594/PANGAEA.956873>

Multibeam bathymetry raw data (Kongsberg EM 122 transit dataset) of R/V SONNE during cruise SO276: <https://doi.org/10.1594/PANGAEA.945674>

Multibeam bathymetry raw data (Kongsberg EM 122 working area dataset) of R/V SONNE during cruise SO276: <https://doi.org/10.1594/PANGAEA.952306>

Water column raw data (Kongsberg EM710 entire dataset) of R/V SONNE during cruise SO276: <https://doi.pangaea.de/10.1594/PANGAEA.957391>

Species distribution data:

Video observations of a bathypelagic cirrate octopod *Cirroteuthis muelleri*:
<https://doi.org/10.1594/PANGAEA.957196>

Discovery Metadata System. Pan-Atlantic comparison of deep-water macrobenthos diversity collected by epibenthic sledge sampling and analysis of patterns and environmental drivers:
<https://doi.org/10.5285/58080F33-884C-4E13-A419-C00CF1BAB6A6>.

Benthic Haploniscidae (Isopoda) from Icelandic waters:
<https://doi.org/10.5281/zenodo.5710069>.

Benthic Haploniscidae (Isopoda) collected around Iceland during the BIOICE, IceAGE, IceAGE2, IceAGE_RR and IceAGE3 expeditions in 1992–2020:
<https://dx.doi.org/10.14284/551>

Marine Amphipoda and environmental occurrence around Iceland. PANGAEA:
<https://doi.org/10.1594/PANGAEA.931959>

Marine Data Archive. North Atlantic and Arctic Amphipoda sampled during IceAGE project: <https://ipt.vliz.be/eurobis/resource?r=north-atlantic-artic-amphipoda-iceage>

Sequence data:

Barcode of Life Database (BoLD): Dataset – DS-HALIRAGE North Atlantic and Arctic *Halirages* species

Barcode of Life Database (BoLD): Dataset – DS-HAPLB Recent speciation and hybridization in *Haploniscus bicuspis* around Iceland

Barcode of Life Database (BoLD): Dataset – DS-IACIR The deep-sea acorn barnacle *Bathylasma hirsutum* (Hoek, 1883) collected in the frame of the IceAGE project

Barcode of Life Database (BoLD): Dataset – DS-IAORR DNA Barcoding of cold-water coral associated ophiuroid fauna from the North Atlantic

Barcode of Life Database (BoLD): Dataset – DS-OPHNA Ophiuroids from the North Atlantic Ocean

Barcode of Life Database (BoLD): Dataset - DS-PGCNA Nuclear and mitochondrial DNA sequences of Icelanddic Hexacorallia and Octocorallia

CRUISE REPORT

SO276: https://doi.org/10.48433/cr_so276

SO277

Seafloor processes in the central Mediterranean region – results from SO277 OMAX

AUTHORS

GEOMAR Helmholtz Centre for Ocean Research Kiel | Kiel, Germany

C. Berndt, M. Jegen, M. Schmidt, M. Urlaub, Z. Faghih, A. Haroon, M. Kühn, T. Müller, B. Schramm, B. Weymer

University of Malta | Valetta, Malta

A. Micallef

SO277 OMAX served two scientific projects. The objectives of the first project, SMART, were to develop multi-disciplinary methodologies to detect, quantify, and model offshore groundwater reservoirs in regions dominated by carbonate geology such as the Mediterranean Sea (Figure 1). To this end we acquired controlled-source electromagnetic, seismic, hydroacoustic, geochemical, seafloor imagery data off Malta. Preliminary evaluation of the geophysical data show that there are electrical resistivity anomalies that may represent offshore freshwater aquifers. The absence of evidence for offshore springs means that these aquifers would be confined and that it will be difficult to use them in a sustainable manner. The objective of the second project, MAPACT-ETNA, is to monitor the flank of Etna volcano on Sicily which is slowly deforming seaward. Here, we deployed six seafloor geodesy stations and six ocean bottom seismometers for long-term observation (1–3 years). In addition, we mapped the seafloor off Mt. Etna and off the island of Stromboli to constrain the geological processes that control volcanic flank stability.

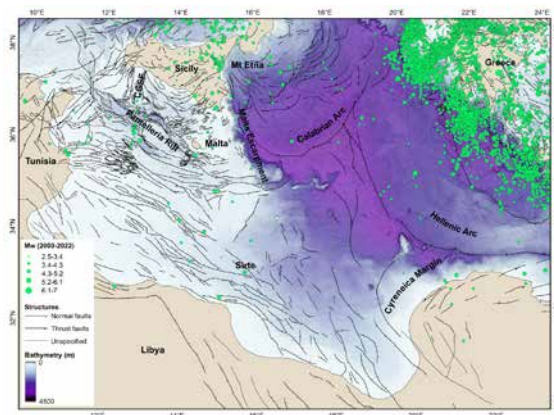


Figure 1: Regional tectonic map of the central Mediterranean region. CGSF, Capo Granitola-Sciaccà Fault zone.

TECTONIC SETTING OFF MALTA

During SO277 we acquired high-resolution 2D and 3D seismic data with a GI gun source and a 200 m long streamer and a 16-streamer set up, respectively. These data have been fully processed and analyzed within the SMART project including the interpretation of extensional structures and the picking of key horizons. The data image the proximal parts of the shelf around Malta within the 12 nm zone. Numerous extensional faults strike predominantly in NE-SW direction (Figure 2) and similar to other graben structures that are perpendicular to the main Pantelleria Rift in this area, e. g. the Comino Graben between Malta and Gozo. The new data document two unexpected discoveries: (1) all faults terminate at the Messinian Unconformity suggesting that the tectonic forces abruptly changed at that time and that the area around Malta is now tectonically almost inactive. This is consistent with the lack of seismicity in the Sicily Channel where most earthquakes are confined to the Capo Granitola-Sciacca Fault zone. (2) the data do not support the existence of a normal fault beneath the shelf break north of Malta making Malta a half graben structure and not a horst. This is significant as a normal fault in this area would have posed a significant hydraulic barrier to any offshore groundwater system.

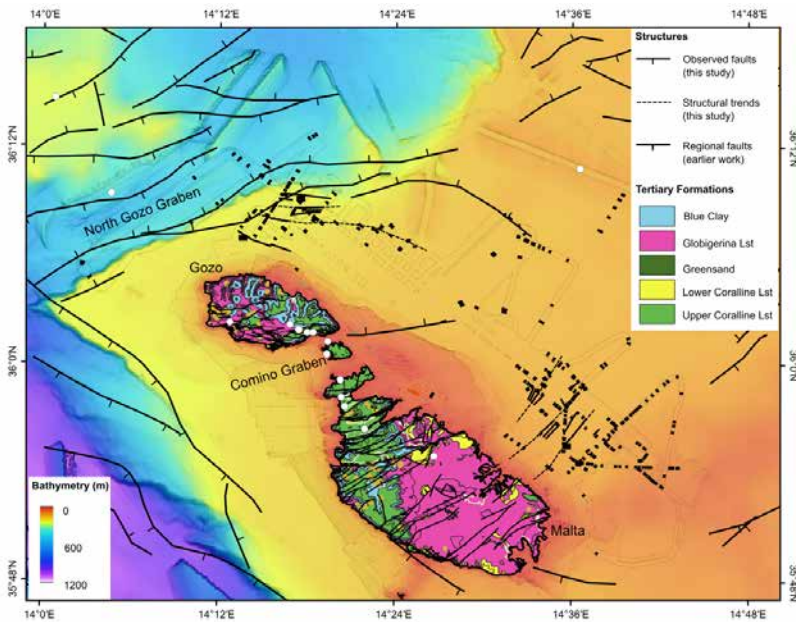


Figure 2: Structural map of the offshore region of Malta based on SO277 and legacy data.

INDICATIONS FOR OFFSHORE FRESHENED GROUNDWATER OFF MALTA

The time-domain step-off controlled source electromagnetic (CSEM) data were processed for stationary waypoints using MARE2DEM (Key, 2016; Haroon et al., 2018) to conduct

an inversion of the CSEM data. To quantify groundwater salinity and estimate associated uncertainties, we implemented a 1-D trans-dimensional Markov Chain Monte Carlo (MCMC) approach (Mosegaard & Tarantola 1995; Sambridge & Mosegaard 2002).

2D resistivity models along CSEM profiles are shown in 3 (left column). To quantify the uncertainties of these results, we conducted 1D Bayesian inversion at selected waypoints along each profile and plotted the posterior probability density (PPD) profiles overlaid by extracted 2D resistivity model at the same waypoint (right column in Figure 3). The electrical resistivity models reveal localized resistive anomalies ($> 10 \Omega\text{m}$) at depths of tens of meters below sea level within the highly permeable Upper Coralline Limestone formation offshore the northeastern coast of Gozo (Figure 2). Furthermore, a deeper resistive body is observed at depths 250–300 m below sea level near the coast of Gozo (Figure 3, CSEM-L3), extending northeastwards and diminishing at approximately 8 km offshore (Figure 1, CSEM-L1). So far, no onshore drilling for groundwater in Malta has reached this depth and thus these results cannot be independently linked to groundwater anomalies, but the results are consistent with offshore freshened groundwater occurrences. This will be further investigated with hydrological modeling.

SLOPE STABILITY OFF MT ETNA, SICILY

The target of the side-user project MAPACT-ETNA was the submerged parts of Mount Etna at the east coast of Sicily, Italy. We deployed a seafloor geodetic network for long-term measurements of acoustic distances. The six instruments measure distances between each other across a strike slip fault, which is kinematically related to the movement of the southeast flank of the Etna volcano (Urlaub et al., 2018). The measurements are a continuation of two-years of seafloor geodetic measurements with a similar set-up (2016–2018). Together with the new data set (2020-2022), the network detected several episodic slip events (~4 cm of slip over 8 days in May 2017, ~2 cm of slip in less than 2 hours and ~3 cm of slip over 3 days both in August 2022), as well as near-continuous creep (~1 cm over a period of 15 months from September 2020 – November 2021). Neither a submarine fibre optic strain cable deployed along the presumable offshore extension of the fault, nor onshore ground deformation measurements detected simultaneous fault movement, demonstrating that this specific transient behaviour is inherent to the here monitored fault segment. Hence, multiple deformation processes affect one segment of a submarine strike slip fault. The transient episodes of various slip mechanisms of this fault segment make it a highly interesting target to study the physical processes and mechanical interactions between slow slip, low-frequency earthquakes, and creep directly at an offshore site in a logistically convenient location 14 km off the coast in 1000 m water depth.

Hydroacoustic surveys at Etna and Stromboli during SO277 provided high-quality seafloor maps. Comparisons to maps acquired in previous and following cruises show significant changes along the slopes of both volcanoes. Strong erosion dominates the submerged continuation of the Sciara del Fuoco at Stromboli. At Etna, we observe both erosion and deposition.

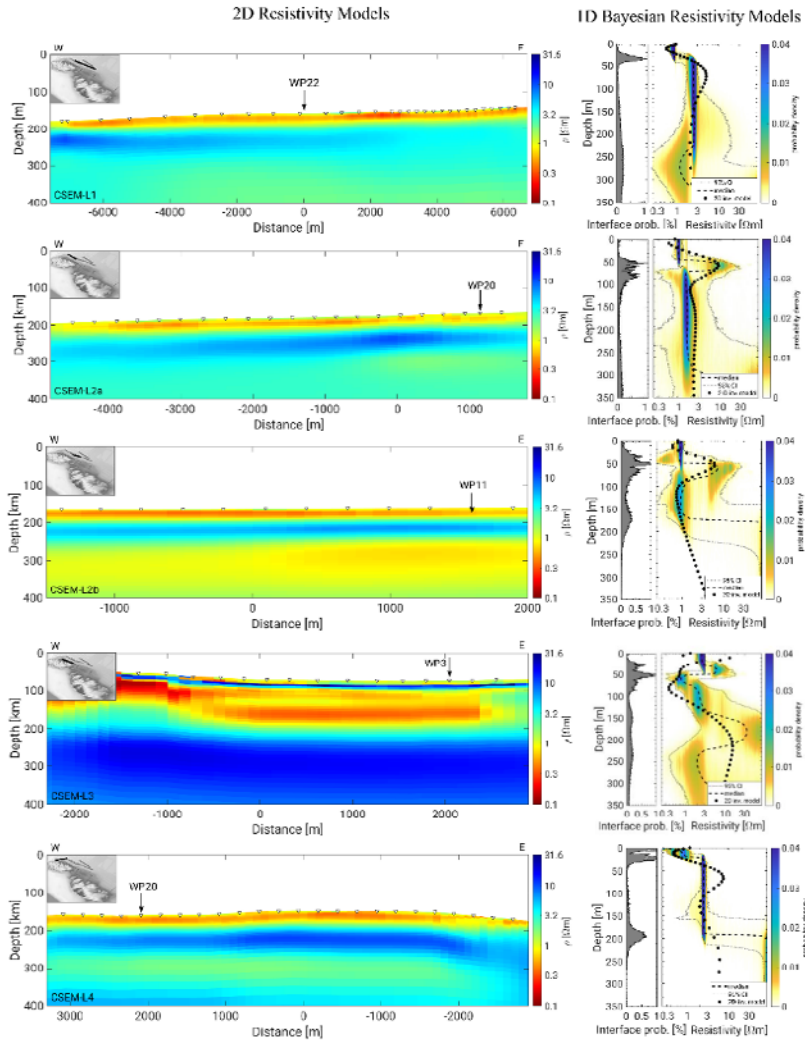


Figure 3: 2D inversion of the controlled-source electromagnetic data collected during expedition SO277 (left) and 1D Bayesian resistivity models (right). For location see insets in the 2D profiles.

REFERENCES

Haroon A, Hölz S, Weymer BA, Tezkan B, & Jegen M, Calculating Time-Domain Controlled Source Electromagnetic Signals with MARE2DEM. 2018(1), 1–5.

Key K, MARE2DEM: a 2-D inversion code for controlled-source electromagnetic and magnetotelluric data, *Geophysical Journal International* 2016, 207(1), 571–588. <https://doi.org/10.1093/gji/ggw290>.

Mosegaard K, and Tarantola A, Monte Carlo sampling of solutions to inverse problems, *Journal of Geophysical Research: Solid Earth* 1995, 100(B7), 12431–12447.
<https://doi.org/https://doi.org/10.1029/94JB03097>.

Sambridge M, and Mosegaard K, Monte Carlo methods in geophysical inverse problems, *Reviews of Geophysics* 2002, 40(3), 3-1-3–29.
<https://doi.org/https://doi.org/10.1029/2000RG000089>.

Urlaub M, Petersen F, Gross F, Bonforte A, Puglisi G, Guglielmino F, Krastel S, Lange, D, and Kopp H, Gravitational collapse of Mount Etna’s southeastern flank, *Open Access Science Advances* 2018, 4 (10). eaat9700. DOI 10.1126/sciadv.aat9700.

SCIENTIFIC OUTPUT

LIST OF PUBLICATIONS

Bialik OM, Varzi AG, Durán R, Le Bas T, Gauci A, Savini A, Micallef A, Mesophotic Depth Biogenic Accumulations (“Biogenic Mounds”) Offshore the Maltese Islands, Central Mediterranean Sea, *Frontiers in Marine Science* 2022, 9.

Gutscher MA, Quetel L, Murphy S, Riccobene G, Royer JY, Barreca G, Aurnia S, Klingelhoefer F, Cappelli G, Urlaub M, Krastel S, Gross F, & Kopp H, Detecting strain with a fiber optic cable on the seafloor offshore Mount Etna, Southern Italy, *Earth and Planetary Science Letters* 2023, 616, 118230.
<https://doi.org/10.1016/j.epsl.2023.118230>.

Köser K, Kwasnitschka T, & Urlaub M, Fusion seismischer, akustischer und optischer Unterwasserdaten und Modelle zur Analyse submariner Hangrutschungen an Vulkansystemen, *Informatik Spektrum* 2022, 45(5), 319–322.
<https://doi.org/10.1007/s00287-022-01494-9>.

Müller T, Gros J, Leibold P, Al-Balushi H, Petermann E, Schmidt M, Brückmann W, Al Kindi M, Al-Abri OS, Autonomous Large-Scale Radon Mapping and Buoyant Plume Modeling Quantify Deep Submarine Groundwater Discharge: A Novel Approach Based on a Self-Sufficient Open Ocean Vehicle, *Environmental Science & Technology* 2023, 57(16), 6540-6549, <https://doi.org/10.1021/acs.est.3c00786>.

Pandolpho BT, Urlaub M, Berndt C, & Bialas J, Identification and differentiation of vertical movement through morphological changes and stratigraphic imprint: Two distinct uplifting mechanisms in the upper Calabrian accretionary wedge, western Ionian Sea, *Basin Research* 2023, <https://doi.org/10.1111/bre.12819>.

Schulten I, Micallef A, Krastel S, Urlaub M, Gutscher MA, & Kopp H, Reconstruction of the 1908 Messina gravity flow (central Mediterranean Sea) from geophysical and sedimentological data, *Marine Geology* 2023, 459, 107047. <https://doi.org/10.1016/j.margeo.2023.107047>.

Urlaub M, Geersen J, Petersen F, Gross F, Bonforte A, Krastel S, & Kopp H, The submarine boundaries of Mount Etna's unstable southeastern flank, *Frontiers in Earth Science* 2022, 10, 810790. <https://doi.org/10.3389/feart.2022.810790>.

Weymer BA, Everett ME, Haroon A, Jegen M, Micallef A, Berndt C, Michale HA, Evans RL, Post V, The coastal transition zone is an underexplored frontier in hydrology and geoscience, *Commun Earth Environ* 2022, 3, 323.

LIST OF CONFERENCE PRESENTATIONS

2021 **Can Offshore Groundwater help mitigate water scarcity in arid coastal communities?** DGGV Seminar Series: Geo-scientific contributions to sustainable development, online.

2021 **Hydro-geophysical investigations using controlled-source electromagnetic methods in near-coastal environments** Joint Scientific Assembly IAGA-IASPEI 2021, online.

2021 **Integrating Marine Controlled Source Electromagnetic Data to Characterize Coastal Groundwater Resources** International Virtual Course of Applied GeoEM and Indonesian Association of Geophysicists (HAGI) Near Surface Webinar, online.

2021 **Sub-seafloor Pore-fluid Salinity Estimation in the Canterbury Bight**, New Zealand, based on Bayesian Inversion of Controlled-source Electromagnetic Data 81. Jahrestagung der Deutschen Geophysikalischen Gesellschaft (DGG), Kiel, Germany.

2021 **Interplay of volcanotectonic, sedimentary, and regional tectonic processes at Mount Etna's submerged south-eastern flank** EGU General Assembly, Vienna, Austria.

2022 **State of the art in the study of volcanic flank collapses** International Conference on Seafloor Landforms, Processes and Evolution, Valetta, Malta.

2022 **Flank collapse mechanisms at coastal and ocean island volcanoes: Insights from shoreline-crossing investigations** Cities on Volcanoes 11, Heraklion, Greece.

2022 **Flank instability at Mount Etna: new insights from seafloor deformation monitoring** EGU General Assembly, Vienna, Austria.

2022 **How to detect slow slip and long-term seafloor deformation? Lessons from two acoustic ranging campaigns on the submerged flank of Mt Etna** EGU General Assembly, Vienna.

2023 **Slow slip, stick slip, continuous slip – the spectrum of underwater flank movements measured by the Etna GeoSEA array** DGG Annual Meeting, March 2023, Bremen, Germany.

SO277 DATA

All data are uploaded in OSIS, findable with the links below, but they remain under moratorium until 12.12.2024 as there are still PhD students working on the data.

Video CTDs (VCTDs):

[https://portal.geomar.de/web/guest/
kdmi#_48_INSTANCE_5P8d_=metadata%2Fleg%2Fshow%2F356226](https://portal.geomar.de/web/guest/kdmi#_48_INSTANCE_5P8d_=metadata%2Fleg%2Fshow%2F356226)

Geochemical analysis of gravity cores:

[https://portal.geomar.de/web/guest/
kdmi#_48_INSTANCE_5P8d_=metadata%2Fleg%2Fshow%2F356226](https://portal.geomar.de/web/guest/kdmi#_48_INSTANCE_5P8d_=metadata%2Fleg%2Fshow%2F356226)

Magneto-telluric impedance data:

[https://portal.geomar.de/web/guest/
kdmi#_48_INSTANCE_5P8d_=metadata%2Fleg%2Fshow%2F356226](https://portal.geomar.de/web/guest/kdmi#_48_INSTANCE_5P8d_=metadata%2Fleg%2Fshow%2F356226)

Controlled source electromagnetic data:

[https://portal.geomar.de/web/guest/
kdmi#_48_INSTANCE_5P8d_=metadata%2Fleg%2Fshow%2F356226](https://portal.geomar.de/web/guest/kdmi#_48_INSTANCE_5P8d_=metadata%2Fleg%2Fshow%2F356226)

Hydroacoustic data (Parasound, EM710, EM122):

[https://portal.geomar.de/web/guest/
kdmi#_48_INSTANCE_5P8d_=metadata%2Fleg%2Fshow%2F356226](https://portal.geomar.de/web/guest/kdmi#_48_INSTANCE_5P8d_=metadata%2Fleg%2Fshow%2F356226)

Multichannel seismic data:

[https://portal.geomar.de/web/guest/
kdmi#_48_INSTANCE_5P8d_=metadata%2Fleg%2Fshow%2F356226](https://portal.geomar.de/web/guest/kdmi#_48_INSTANCE_5P8d_=metadata%2Fleg%2Fshow%2F356226)

TSG (surface ocean) data:

[https://portal.geomar.de/web/guest/
kdmi#_48_INSTANCE_5P8d_=metadata%2Fleg%2Fshow%2F356226](https://portal.geomar.de/web/guest/kdmi#_48_INSTANCE_5P8d_=metadata%2Fleg%2Fshow%2F356226)

Ocean bottom seismometer data:

[https://portal.geomar.de/web/guest/
kdmi#_48_INSTANCE_5P8d_=metadata%2Fleg%2Fshow%2F356226](https://portal.geomar.de/web/guest/kdmi#_48_INSTANCE_5P8d_=metadata%2Fleg%2Fshow%2F356226)

Sediment cores are stored in the GEOMAR core repository:
<https://geomar.maps.arcgis.com/apps/webappviewer/index.html?id=602b8f04d28147469080417af087cf27>

CRUISE REPORT

SO277: http://dx.doi.org/10.3289/GEOMAR_REP_NS_57_20

SO278

Mud volcanoes along the Euro-African collision zone in the eastern Mediterranean Sea

AUTHORS

MARUM – Center for Marine Environmental sciences, University of Bremen |
Bremen, Germany

G. Bohrmann, T. Pape, M. Römer, M. Doll, N. Behrendt, N. Kaul, V. Kürzinger,
K. Streuff, Y. Tseng, M. Kölling, C. dos Santos Ferreira, M. Zabel, A. Kopf, W.
Menapace

GEOMAR – Helmholtz Center for Ocean Research | Kiel, Germany
M. Riedel

OGS – Istituto Nazionale di Oceanografia e di Geofisica | Sgonioco, Italy
S. Ceramicola

Marine Geology and Physical Oceanography Laboratory, University of Patras |
Patras, Greece
G. Ferentinos

Mud volcanoes are surface eruption sites on land or in the ocean at the sea floor where water and gaseous soft mud is often piled up with rock clasts from deeper underground. While about 1,100 mud volcanoes are known on land, their number in the oceans is unknown because there is no complete, high-resolution mapping of the seafloor. Marine geologists estimate the number of marine mud volcanoes very differently, at 1,000 to 100,000. A particular concentration of mud volcanoes lies in the eastern Mediterranean, where at least 500 mud volcanoes are known to date (Masclé et al. 20214). Most of these mud volcanoes are very clearly tied to the collision zone between Europe and Africa, with microplates playing an important role in the Aegean and Turkey. The comparison of the discovered mud volcanoes (Figure 1 above) with the plate tectonic elements (Figure 1 below) shows that mud volcanoes are particularly concentrated in the 3 collision areas, the Calabrian Arc, the Mediterranean Ridge and the Cyprus Arc. Apart from these convergent plate margins, mud volcanoes occur in the Nile deep-sea fan area, where particularly thick sediments are deposited.

During the R/V SONNE expedition SO278 we examined mud volcanoes in the Calabrian Arc and the Mediterranean Ridge (Figure1). To date, around 70 positive morphological structures known as mud volcanoes are known in the Calabrian Arc of the Ionian Sea. There we examined the Sartori MV, whose mud flows were separated into 5 distinct

eruption phases of different ages using very different backscatter intensities of the seafloor from multibeam mapping (Figure 2). Five eruption phases over the last 50 ka could be worked out by combining sediment core data with the different backscatter pattern. The basis for the temporal classification of individual mud flow units was based on the sedimentological analysis of the cores, with temporally classified volcanic ash layers and ¹⁴C dating of foraminifera forming the stratigraphic framework.

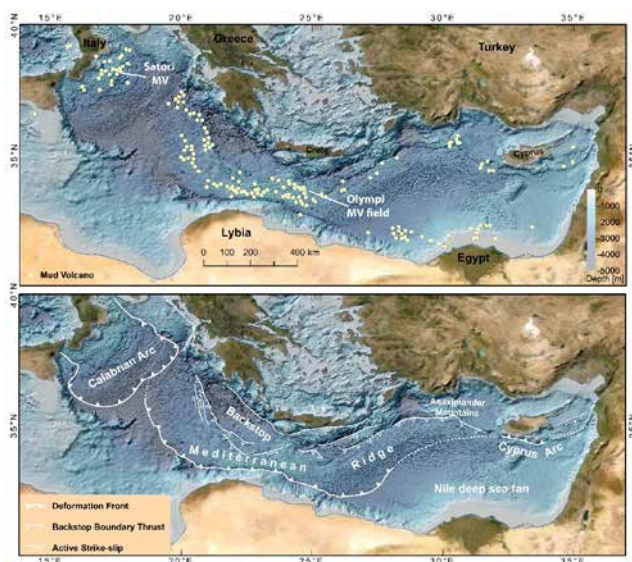


Figure 1: Maps of the Eastern Mediterranean with bathymetric data from the EMODnet project (www.emodnet.eu/en/bathymetry). The upper map contains the locations of known mud volcanoes (according to Mascle et al. 2014). Satori MV is situated within the Calabrian Arc and the Olimpi Mud Volcano Field is part of the Mediterranean Ridge. The lower map shows important plate tectonic elements of the collision zone between the Eurasian and African plates (after Rabaute and Chamot-Rooke 2007).

Gas bubble releases in the form of acoustic anomalies in the multibeam and single echosound data were not observed during the expedition and a previous expedition in 2016, so no recent mud release exists. However, subrecent mud episodes are to be expected based on the pore water analyzes in both chimneys of the Satori mud volcano. Pore water modelling suggests that seawater has penetrated the surface sediments to a greater extent within the last few years. In contrast, cm-thick layers of hemipelagic sediments overlying mud breccia in sediment cores taken from both eruption centers show that no solid material has been ejected in recent times. Sediment core analyses combined with high-resolution seafloor mapping show an absence of rim-passing mudflows over the past ~10 ka. It is concluded that Satori MV is an episodically active MV from which fluids with a comparatively low flux were released into the bottom water in recent times.

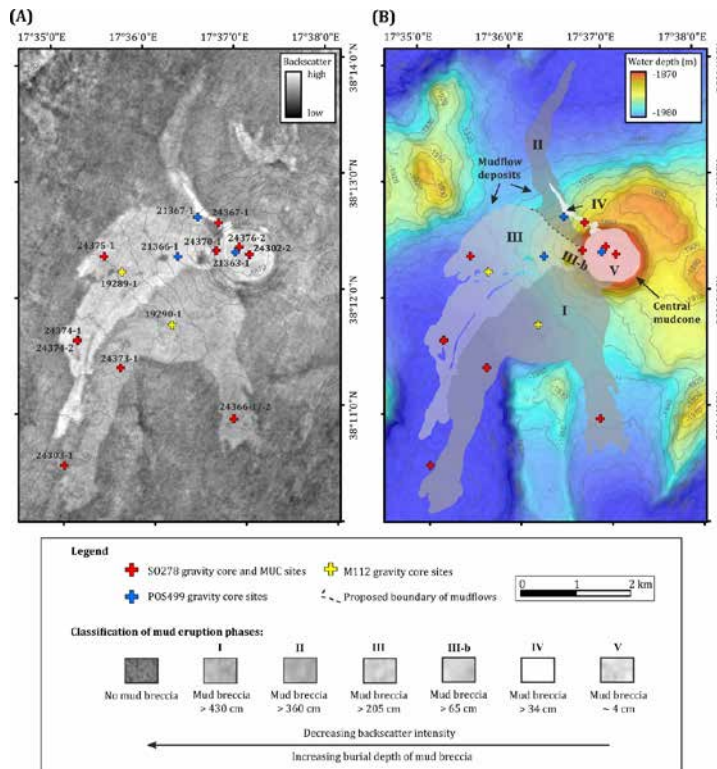


Figure 2: (A) Ship-derived backscatter map of Sartori MV and its surrounding seafloor area. Different backscatter intensities (light = high backscatter intensity and dark = low backscatter intensity) indicate mud flows of different ages. Locations of sediment core sites are shown. (B) Ship-bathymetry of Sartori MV and major mud flow units. Numbers I to V are represent individual mud flow eruption phases (Doll et al. unpublished).

Investigations on mud volcanoes along the Mediterranean Ridge were carried out divided into 2 working areas known as the Cobblestone Area and the Olimpi mud volcano field (Figure 2) including the United Nation Ridge. With the MARUM AUV SEAL 11 dives were successfully carried out to create high-resolution detailed maps of certain seafloor structures (Figure 3). In total 16 mud volcanoes were examined, 10 of which are characterized by pore waters that show a distinct freshening. The data highlight strong depletion in Cl (<200 mM), Na (~200 mM), Mg and K (with concentrations ~0 mM) and striking water isotope ratios ($\delta^{18}\text{O}$ of +9.79‰ V-SMOW and δD of -26.33‰ V-SMOW), indicating dehydration of clay minerals at depth. Three mud volcanoes, Napoli, Heraklion and Gelendzhik, are characterized by very high salt concentrations. The interstitial waters are characterized by extremely high salinities (Cl > 5000 mM and Na >6500 mM). The salt accumulations in these structures are derived from the Messinian salt deposits in the subbed, from which salty brines arise through subsrosion, which interact in various ways with the mud volcanoes.

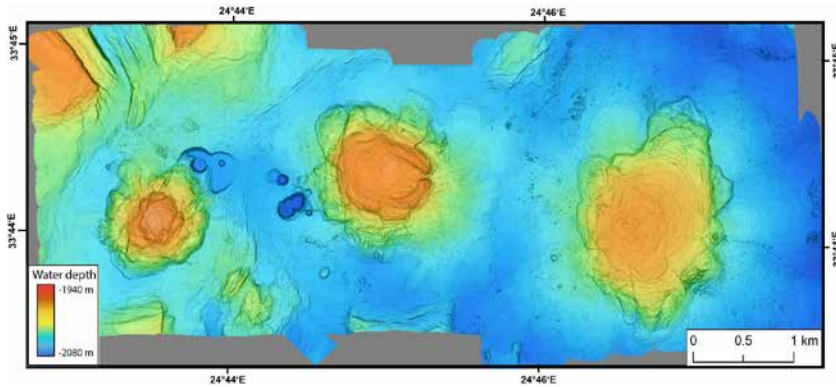


Figure 3: High-resolution micro-bathymetry of the three mud volcanoes Monza MV, Bergamo MV and Milano MV (from left to right). Circular sinkhole-like subrosion structures are formed between Monza MV and Bergamo MV.

The pore water measurements further reveal that Gelendzhik mud volcano, located in the western part of the Olimpi Mud Volcano Field along a major strike-slip fault, shows an unusual pore water downcore profile and its water isotopes signature differ strongly from the other structures ($\delta^{18}\text{O}$ of +13.63‰ and δD of +1.83‰). Upon calculations of the hydrates stability zone, we tied the anomalous low salinity values of the Gelendzhik MV pore waters results from the presence of gas hydrates in the sediments. This is the first, indirect evidence of gas hydrates in the Olimpi Mud Volcano Field. The presence of hydrate in sediments of the Mediterranean is very limited because of the high temperature of Mediterranean deep water close to 14°C and known locations are mud volcanoes of the Anaximander Mountains (Figure 1) and the Nile deep sea fan.

REFERENCES

Masclé J, Mary F, Praeg D, Brosolo L, Camera L, Ceramicola S, et al., Distribution and geological control of mud volcanoes and other fluid/free gas seepage features in the Mediterranean Sea and nearby Gulf of Cadiz. *Geo-Marine Letters* 2014, 1–22. <https://doi.org/10.1007/s00367-014-0356-4>.

Rabaute A, Chamot-Rooke N, Quantitative mapping of active mud volcanism at the western Mediterranean Ridge-backstop contact, *Mar Geophys Res* 2007, 28:271–295. [doi:10.1007/s11001-007-9031-8](https://doi.org/10.1007/s11001-007-9031-8).

SCIENTIFIC OUTPUT

LIST OF PUBLICATIONS

Behrendt N, Menapace W, Bohrmann G, Zabel M and Kopf AJ, Pore water signatures and gas hydrates occurrence in and around the Olimpi mud volcano field, south of Crete, *Marine and Petroleum Geology* 2023, 156. 106429. doi:10.1016/j.marpetgeo.2023.106429.

Doll M, Römer M, Pape T, Kölling M, Kaul N, dos Santos Ferreira C, and Bohrmann G, Recent and episodic activity of decoupled mud/fluid discharge at the Sartori mud volcano in the Calabrian arc, Mediterranean Sea. *Front. Earth Sci.* 2023, 11:1181380. doi: 10.3389/feart.2023.1181380.

MASTER'S AND BACHELOR'S THESES

Krahl J, Mass wasting at the southern continental margin of Crete – Results from two gravity cores (Expedition SO278), Master thesis at University Greifswald 2020, 60 pages.

Feddersen G, Ursprung Methan-haltiger Fluide zweier Schlammvulkane des Mediterranean Ridge Accretionary Complex - Geochemische und geothermische Signaturen, Bachelor Arbeit am Fachbereich Geowissenschaften der Universität Bremen 2021, 57 Seiten.

LIST OF CONFERENCE PRESENTATIONS

2022 | Behrendt N., Menapace W., Bohrmann G., Kopf A. (2022). **The Mediterranean Ridge 25 years after ODP Leg 160 drilling: New discoveries on mud volcanism and fluid-rock interactions in the Olimpi mud volcano field** Talk presented at 2022 EGU Meeting, Vienna, Austria, 23–27 May.

2023 | Doll, M., Römer, M., Pape, T., Klügel, A., Kaul, N., Kölling, M., Bohrmann, G. **Recent activity and evolutionary reconstruction of Sartori mud volcano in the Calabrian Arc, Mediterranean Sea** Talk presented at 2023 GIMS15 Meeting, Cadiz, Spain, 23–27 October.

2023 | Menapace W., Kopf A. **The Mediterranean Ridge 25 years after the ODP160 expedition: new discoveries on mud volcanism and future research trajectories** Poster presented at 2023 GIMS15 Meeting, Cadiz, Spain, 23-27 October.

DATA

A total of 59 data sets have so far been stored in the PANGAEA database related to the SO278 expedition. Data sets in PANGAEA will be expanded in parallel with further publications.

Heat flow data: e. g.
<https://doi.org/10.1594/PANGAEA.936442>

Physical oceanography (CTD): e. g.
<https://doi.org/10.1594/PANGAEA.927863>

Multibeam bathymetry raw data (EM122): e. g.
<https://doi.org/10.1594/PANGAEA.927272>

Sediment echosounder raw data (Atlas Parasound P70):
<https://doi.pangaea.de/10.1594/PANGAEA.927444>

Continuous thermosalinograph oceanography:
<https://doi.org/10.1594/PANGAEA.943794>

Concentrations of methane in sediment cores: e. g.
<https://doi.org/10.1594/PANGAEA.953915>

Concentrations and stable C and H isotopic compositions of methane in sediment cores: e. g. <https://doi.org/10.1594/PANGAEA.953918>

Sediment core descriptions: e. g.
<https://doi.pangaea.de/10.1594/PANGAEA.956320>

C/N, TC, TIC and TOC values of sediment cores:
e. g. <https://doi.org/10.1594/PANGAEA.953756>

Chloride and sulfate concentrations of pore water sediment cores:
e. g. <https://doi.pangaea.de/10.1594/PANGAEA.956544>

Stable oxygen and hydrogen isotopic composition of pore water ($\delta^{18}\text{O}$; δD) of sediment cores: e. g. <https://doi.org/10.1594/PANGAEA.959922>

X-ray fluorescence (XRF) data of sediment cores: e. g.
<https://doi.org/10.1594/PANGAEA.959863>

Pore water geochemistry of sediment cores: e. g.
<https://doi.org/10.1594/PANGAEA.959820>

CRUISE REPORT

SO278: doi:10.48433/cr_so278

SO279

NAPTRAM: North Atlantic plastic transport mechanisms, sinks, and interactions with biota

AUTHORS

GEOMAR Helmholtz Centre for Ocean Research Kiel | Kiel, Germany

A. Beck, E. Achterberg, M. Haeckel, U. Hentschel-Humeida, M. Lenz

BACKGROUND

Currently, 5–13 MT (mega tons, 10^6 tons) of plastic debris are believed to enter the oceans every year (Jambeck et al., 2015), but only about 0.27–1.00 MT have been observed in the surface ocean (Eriksen et al., 2014; Lebreton et al., 2018). This discrepancy has been explained by various processes, for instance by the fact that 40% of the introduced plastic debris has negative buoyancy and sinks to the seafloor soon after release. A further, much smaller part with positive buoyancy is deposited along the coastlines, while the remaining material is assumed to reach the open ocean where it fragments into particles too small to be recognized by monitoring and/or gets transferred by vertical transport from the sea surface to deeper water layers and finally to the seafloor. This vertical pathway presumably constitutes the largest sink for plastic debris on the planet. However, no observational data exist on the export of this material to the deep sea and the mechanisms facilitating this transport, including biota-plastics interactions.

Consequently, no quantitative models exist that could help to assess vertical transport rates in the oceanic environment. Furthermore, little knowledge exists on the trophic transfer of plastic debris in open ocean food webs and on the environmental impact it may have on deep sea ecosystems. In summary, we are currently unaware of the ultimate fate of the largest part of the marine plastic debris and of the effects it may have on the world's largest ecosystem.

The working area for the research cruise is located within the inner accumulation zone of the North Atlantic garbage patch (Figure 1), where debris loads of up to 2500 g per km² have been documented at the sea surface (Cózar et al., 2014). On the basis of these data, a permanent and substantial vertical transport of plastic debris from the surface to the seafloor was expected.

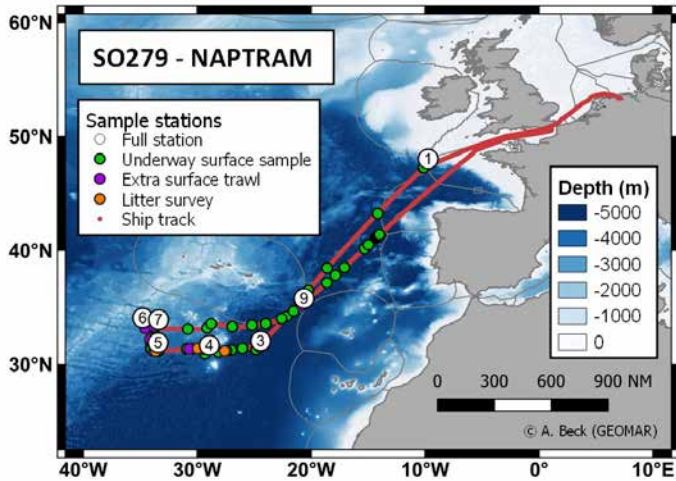


Figure 1: Track chart of R/V SONNE cruise SO279. Primary sampling stations and additional sampling locations are indicated. Bathymetry from GEBCO 2019.

Long distance transport of MP from coastal sources to the open ocean is poorly understood, in part, because little is known regarding transport mechanisms from the coast to accumulation areas in the centre of subtropical gyres. Given current estimates of plastic input to the ocean, at least 1.71 MT should reach the gyres in the North Atlantic, North Pacific, South Atlantic, South Pacific and Indian Oceans per year (Eriksen et al., 2014). Despite these theoretical reflections, it is still not known how much plastic debris actually floats at the ocean surface, or what mechanisms control plastic transport and fate from land to the open ocean. Lebreton et al. (2018) concluded that there remains a major discrepancy between the amount of buoyant plastic that enters the oceans every year (i. e., millions of tons) and the amount that can be observed at the ocean surface (i. e., hundred thousands of tons). Furthermore, data from time series revealed no significant increase in plastic debris concentrations in the surface ocean since the 1980s (Law et al., 2010; Law et al., 2014).

This prompts a fundamental question: what has become of the missing plastic? Several, mutually non-exclusive mechanisms have been proposed to explain the apparent loss of plastic debris from surface waters. These include transfer into the ocean interior by biota-plastic interactions, fragmentation into pieces too small to be captured by current monitoring schemes, or coagulation with suspended biogenic particles and accelerating removal by sinking. While all of these processes are possible explanations, quantitative data on these mechanisms and their relative contribution to plastic debris loss from ocean surface waters do not exist.

SAMPLE COLLECTION METHODS

NAPTRAM was part of connected research cruises to build an understanding of the transport pathways of plastic and microplastic debris in the North Atlantic, from the input through rivers and air across coastal seas into the accumulation spots in the North Atlantic gyre and the vertical export to its final sink at the seabed.

NAPTRAM builds on a preliminary cruise to the study region (R/V Poseidon, POS536; Aug–Sep 2019), expanding its smaller study area and extending into deeper waters. NAPTRAM also complements R/V Alkor cruise AL534/2 (March 2020) that focused on microplastic inputs from rivers and estuaries to coastal waters.

The sample collection agenda during SO279 was identical for all stations. Deployments of net trawls (Catamaran Neuston, Bongo, Multi-net) constituted core activities during SO279 in order to map plastic pollution at the sea surface and throughout the water column. When time allowed, additional catamaran samples were collected between the primary stations. Sediment coring was conducted with a box corer (BC) after unsuccessful attempts with the multiple corer (MUC). Sediment subsamples from the BC were taken for microplastic analyses of the sediment and sediment-dwelling fauna. At each station about 1500 L of water were filtered at 5 different depths using in situ pumps. Vertical CTD profiles complemented the work to collect small-volume water samples and relevant oceanographic data for the investigation of the particle export. Observations of macrolitter on the seafloor were made with the ship's OFOS system.

In addition, water and particle samples were collected along the cruise track from the ship's underway seawater supply, a pump system deployed in the moonpool, and a metal-clean towfish deployed in surface waters. Visual litter surveys were conducted during the few periods when seas were calm enough for reliable observations.

SELECTED RESULTS

Samples of net-collected MPs (catamaran neuston trawls at the surface, and multi-net and bongo net trawls within the water column) were analyzed using a novel benchtop near-infrared hyperspectral imaging system. As an example, a total of 27 neuston net tows sampled 2534 suspected MP particles that were imaged and analyzed at sea (Figure 2). Approximately 77.1% of particles were identified as polyethylene, followed by polypropylene (9.2%). A small fraction of polystyrene was detected only at one station. Approximately 13.6% of particles were either other plastic polymers or were natural materials visually misidentified as plastics. These results provide the basis for modelling lateral transport and accumulation in the central North Atlantic gyre, as well as vertical fluxes and accumulation in sediments.

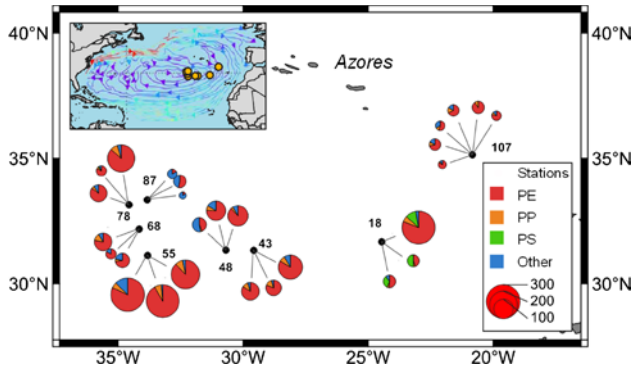


Figure 2: Floating microplastic particles. Filled circles indicate net sampling locations, and numbers are station IDs. Pie charts indicated for each station are the triplicate individual net tows, except station 107, which had six tows (polyethylene, PE; polypropylene, PP; polystyrene, PS). The size of the pie charts indicates the total number of microplastic particles collected in each respective tow. The inset shows the location of the sample locations within the North Atlantic Ocean, with the gyre surface currents.

Sediments were collected by box corer at all stations, as the carbonate-rich sediments were highly compact and not possible to sample with the multi-core device. Sediment samples for further processing were either collected from the surface or sub-sampled by hand with core liners (Figure 3). The cores were sampled on board and the samples were stored for land-based analyses of infauna, microplastic abundance, and geochemical parameters.

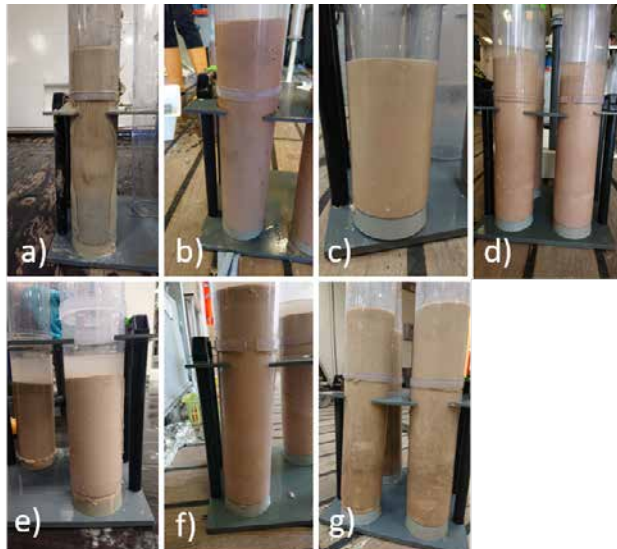


Figure 3: Photos of sediment samples that were extracted from box cores: a) 8BC2, b) 27BC5, c) 40BC7, d) 60BC9, e) 73BC11, f) 89BC14, g) 105BC16.

Given the scarcity and heterogeneity of plastic debris on the deep seafloor, traditional sediment sampling gear (e. g., box coring) cannot provide information appropriate to catalog this debris. To survey seafloor debris, we used the RV SONNE Ocean Floor Observation System (OFOS). This system consisted of a towed platform with high-resolution video and still cameras and illumination (maintained, prepared, and deployed by the SONNE WTD). High-resolution video footage was continuously recorded, and high-resolution still images were recorded every 5–8 seconds, the frequency limited by the recharge time of the flash bulbs.

No macrolitter objects were observed on the first dive, but one piece of rope was found on the second dive. Several items were observed on each of the subsequent dives. Images of some of the macrolitter objects are shown in Figure 4. Individual still images from each dive will be compiled into calibrated photomosaics to allow estimation of the macrolitter spatial density. These estimates can then be extrapolated to an inventory of plastic litter within the study area.



Figure 4: Selected images of macrolitter on the seafloor captured by OFOS.

The first results indicate strong accumulation of microplastics within surface waters of the North Atlantic gyre. The transport timescales and accumulation in the deep sea and sediments will provide a comprehensive picture of the fate of plastics debris in the ocean.

REFERENCES

Cózar A, Echevarría F, González-Gordillo JJ, Irigoien X, Úbeda B, Hernández-León S, Duarte CM, Plastic debris in the open ocean, *Proceedings of the National Academy of Sciences* 2014, 111(28), 10239–10244.

Eriksen M, Lebreton LCM, Carson HS, Thiel M, Moore CJ, Borerro JC, Galgani F, Ryan PG, Reisser J, Plastic pollution in the world's oceans: more than 5 trillion plastic pieces weighing over 250,000 tons afloat at sea, *PLoS ONE* 2014, 9, e111913.

Jambeck JR, Geyer R, Wilcox C, Siegler TR, Perryman M, Andrady A, Narayan R, Law KL, Plastic waste inputs from land into the ocean, *Science* 2015, 347, 768–77.

Law KL, et al., Distribution of surface plastic debris in the eastern Pacific ocean from an 11-year data set, *Environ Sci Technol* 2014, 48(9):4732–4738.

Law KL, et al., Plastic accumulation in the North Atlantic subtropical gyre, *Science* 2010, 329(5996):1185–1188.

Lebreton LCM, Slat B, Ferrari F, Sainte-Rose B, Aitken J, Marthouse R, Hajbane S, Cunsolo S, Schwarz A, Levivier A, Noble K, Debeljak P, Maral H, Schoeneich-Argent R, Brambini R, Reisser J, Evidence that the Great Pacific Garbage Patch is rapidly accumulating plastic, *Nature* 2018, 8, 4666.

SCIENTIFIC OUTPUT

LIST OF PUBLICATIONS

Beck A J, Kaandorp M, Hamm T, Bogner B, Kossel E, Lenz M, Achterberg EP, Rapid shipboard measurement of net-collected marine microplastic polymer types using near-infrared hyperspectral imaging, *Analytical and Bioanalytical Chemistry* 2023, 1–10.

Hansen J, Hildebrandt L, Zimmermann T, El Gareb F, Fischer EK, Pröfrock D, Quantification and characterization of microplastics in surface water samples from the Northeast Atlantic Ocean using laser direct infrared imaging, *Marine Pollution Bulletin* 2023, 190, 114880.

LIST OF CONFERENCE PRESENTATIONS

2021 | **Analysis of Nanoplastics by Raman Microspectroscopy-based Methods** SETAC, Virtual.

DATA

Continuous thermosalinograph oceanography along RV SONNE cruise SO279:
<https://doi.org/10.1594/PANGAEA.946377>

CTD sensor data:

<https://portal.geomar.de/metadata/leg/show/357846>

CRUISE REPORT

SO279: [10.3289/CR_SO279](https://doi.org/10.3289/CR_SO279).

SO280

Icelandic marine Animals: Genetics and Ecology meets Diversity along latitudinal gradients in the deep sea of the Atlantic Ocean (IceDivA)

AUTHORS

Senckenberg am Meer, Deutsches Zentrum für Marine Biodiversitätsforschung (DZMB) | Wilhelmshaven & Hamburg, Germany

S. Brix, J. Taylor, K.-H. George

IceDivA aims to be the link between the two previous deep-sea programs, IceAGE (Icelandic marine Animals: Genetics and Ecology) and DIVA (Latitudinal Gradients in BioDiversity in the deep Atlantic) in the deep Atlantic Ocean, and connect to the recent EU project iAtlantic and furthermore the follow-up expedition IceDivA2 (SO286). The IceAGE3 (SO276; MerMet 17-06) expedition in summer 2020 extended the project's station network, with stations in the Icelandic Basin of >3,000 m depth and extended the depth transect southward of Iceland. Continuing from the southernmost IceAGE3 station, during IceDivA we sampled a N-S transect towards the Azores ending at 32°N, therefore also being linked with the BIODIAZ (Controls in benthic and pelagic BIODiversity of the AZores) and MAPS (Madeiran Archipelago Pre-Seamount Stages) projects. The research area is located within the target regions of the EU project iAtlantic (among others: the Porcupine Abyssal Plain and the Azores platform). To map the species diversity and answer questions on the connectivity of deep-sea fauna along latitudinal gradients in the Atlantic Ocean, we sampled in 4,000 m to 5,000 m water depth from the Icelandic Basin to the Azores and Madeira, bridging the knowledge gap between prior expeditions. The faunal analysis follows an integrative approach, combining modern genomic methods with traditional, morphological taxonomy. In total, we were able to sample five working areas in a standardized approach. At each working area we deployed a full set of plankton and benthos gear and based the station planning on the ship's bathymetry and the challenging weather conditions. This talk summarizes the results of the expedition obtained so far and provides some extra attention to the results of the PhD and master students on board.

ARGO FLOAT DEPLOYMENTS

As part of the project "DArgo2025", a total number of 10 ARGO floats were deployed on the SO280 cruise. One main objective of this project is the diversification of CTD ("conductivity, temperature depth") sensors that these floats are equipped with. Therefore, five floats of each available manufacturer (RBR, SeaBird) were deployed to compare their respective performances on measurements of salinity, temperature and pressure. To make a direct comparison of the measuring parameters possible the floats were released as a

swarm in one single position. As a reference data set, the onboard CTD SBE911 measured alternately until 2000 m depth and until maximum water depth at the deployment position as well as at four positions in the area around it. Additionally two deep ARVOIR floats from IFREMER were deployed at two separate locations. These floats are able to descend to a depth of 4000 m and also measure oxygen. Furthermore, at each working area, deployment of Argo floats complimented the research program. Each working area started with a standardized CTD deployment.

A HIGHLIGHT IN HIGH DIVERSITY –SMALL BIVALVES CONTRADICTING A DEEP-SEA PARADIGM

Next to the macrofauna paper of Kürzel et al. (2023, see extended abstract SO286), a highlight in sample analysis of the SO280 expedition was the student work about population structure and genetic diversity of the bivalve *Ledella ultima* (E. A. Smith, 1885). Diversity in the deep-sea have been found to decrease along with depth. This pattern has been formulated in the Depth-Differentiation Hypothesis (DDH), which states that differentiation decreases with greater depth. Based on this hypothesis, the diversity in abyssal areas below 3000 m declines significantly (Etter et al. 2005, 2011). They based the DDH hypothesis on population structure of *Ledella ultima*. When comparing the population structure of this pan-Atlantic mollusk to more bathyal protobranch bivalve species, *L. ultima* was consistently less diversified. Based on IceDivA material and a complementary Atlantic dataset, we attempted to recreate these results with samples fixed in ethanol as opposed to formalin, whilst also adding a different marker (COI) to the original (16S). Our results confirmed many of the previous findings, but highlighted a clear degree of underestimation. This underestimation was likely caused by a combination of the degenerative effect of formalin on DNA, as well as the choice of marker. We discovered a clear population structure across latitude and little to no effect of the Mid-Atlantic Ridge (MAR) on the geneflow of *L. ultima*. Additionally, we discovered several consistently divergent mitochondrial lineages, indicating possible speciation. Alternatively, and more fitting with our additional analyses, these mitochondrial lineages could be considered several sex-specific mitochondrial lineages. However, our findings indicated a contradiction of the DHH based on the same model organism as previously used by Etter et al. (2011).

MEIOFAUNA IN THE NORTH-EAST ATLANTIC USING A METABARCODING APPROACH

The IceDivA expedition SO280 enabled a unique multicorer sampling for metabarcoding building up on previous samples from the IceAGE expeditions. Highlighting the importance of standardized deep-sea sampling and the value of continuous sampling campaigns, samples were obtained during three cruises, IceAGE2 (POS456), IceAGE3 (SO276) and IceDivA (SO280) between 2013 and 2021. Based on this unique dataset, Bonk et al. (in preparation) investigated the meiofaunal diversity and distribution in the North-East Atlantic, with a special attention to benthic Copepoda, using a molecular metabarcoding approach. Two gene regions were targeted, the V1V2 hyper variable region of 18S rDNA and CO1 mtDNA. In total 139 samples were analyzed, revealing significant differences between the

deep-sea basins for all encountered meiofaunal taxa. Many delimited species could not be linked to any public stored sequences, demonstrating the need for reference libraries and further barcoding of meiofaunal organisms. This would aid further investigations of the deep sea and help to monitor areas with increasing anthropogenic pressure.

REFERENCES

Bonk F, Khodami S, Martinez Arbizu PM, Analysis of distribution and diversity of deep sea Copepoda (Crustacea) and Meiofauna in the North-East Atlantic using a metabarcoding approach, in preparation.

Etter R, Rex MA, Chase MR, Quattro JM, Population differentiation decreases with depth in deep-sea bivalves, *Evolution* 2005, 59(7), 1479–1491.

Etter RJ, Boyle EE, Glazier A, Jennings RM, Dutra E, Chase MR, Phylogeography of a pan-Atlantic abyssal protobranch bivalve: Implications for evolution in the Deep Atlantic, *Molecular Ecology* 2011, 20(4), 829–843.

<https://doi.org/10.1111/j.1365-294X.2010.04978>.

Kürzel K, Brix S, Brandt A, Brenke N, Enderlein P, Griffiths HJ, Kaiser S, Svavarsson J, Lörz A-N, Frutos I, Taylor J, Linse K, Pan-Atlantic Comparison of Deep-Sea Macro- and Megabenthos, *Diversity* 2023, 15, 814, <https://doi.org/10.3390/d15070814>.

Neuhaus J, de Wilt ME, Linse K, Etter RJ, Jennings RM, Martínez Arbizu P, Brix S, The ecological enigma of *Ledella ultima* (E.A. Smith, 1885): An in-depth assessment of genetic diversity and population structure in an abyssal protobranch, in preparation.

SCIENTIFIC OUTPUT

LIST OF PUBLICATIONS

Bonk F, Analysis of distribution and diversity of deep sea Copepoda (Crustacea) and Meiofauna in the North-East Atlantic using a metabarcoding approach, Master's Thesis 2022, Carl von Ossietzky University Oldenburg.

De Wilt M, The ecological enigma of *Ledella ultima* (E.A. Smith, 1885): a deep-dive into the population structure of an abyssal protobranch, Master's Thesis 2023, University of Groningen.

Kamyab E, Khodami S, Martinez Arbizu P, Comparison of eDNA and Community Metabarcoding Methodologies for Analyzing the Distribution and Diversity of Deep Sea Meiofauna: A Case Study in the North-West Atlantic Ocean, In the submission process.

Kieneke A, Brix S, IceDivA (SO280) Eine Tiefseeexpedition zur Vernetzung langjähriger Messdaten und Proben. Published 2021 in the Newsletter No. 39 of the "Gesellschaft für Biologische Systematik" (ISSN 1867-6766), pages 16–23.

Kürzel K, Brix S, Brandt A, Brenke N, Enderlein P, Griffiths HJ, Kaiser S, Svavarsson J, Lörz A-N, Frutos I, Taylor J, Linse K, Pan-Atlantic Comparison of Deep-Sea Macro- and Megabenthos, *Diversity* 2023, 15, 814, <https://doi.org/10.3390/d15070814>.

Lörz AN, Schwentner M, Bober S, Jażdżewska AM. Multi-ocean distribution of a brooding predator in the abyssal benthos, *Sci Rep.* 2023, 13(1):15867. <https://doi.org/10.1038/s41598-023-42942-0>.

Neuhaus J, de Wilt ME, Linse K, Etter RJ, Jennings RM, Martínez Arbizu P, Brix S, The ecological enigma of *Ledella ultima* (E.A. Smith, 1885): An in-depth assessment of genetic diversity and population structure in an abyssal protobranch, in preparation.

Schumacher M, Huvenne VA, Devey CW, Arbizu PM, Biastoch A, & Meinecke S, The Atlantic Ocean landscape: A basin-wide cluster analysis of the Atlantic near seafloor environment, *Frontiers in Marine Science* 2022, 9, 936095.

Stoffers T, The Seen and the Unseen: Epipelagic Zooplankton assemblages inferred from integrated Morphological Identification and Environmental DNA Analysis, Master's Thesis 2022, Carl von Ossietzky University Oldenburg.

Trokhymchuk R, Kieneke A, Novel distribution records of marine Tardigrada from abyssal sediments of the Northwest Atlantic Ocean, *Organisms, Diversity and Evolution*, submitted.

LIST OF CONFERENCE PRESENTATIONS

2023 | **IceDivA Project: The Exploration of Deep-Sea Holothurian Diversity in the North Atlantic Ocean Using Molecular Approaches** 11th European Conference on Echinoderms, Lyon, France. – POSTER

2023 | **Comparison of eDNA and Community Metabarcoding Methodologies for Analyzing the Distribution and Diversity of Deep Sea Meiofauna: A Case Study in the North-West Atlantic Ocean** iAtlantic Final Meeting, Edinburgh, UK. – POSTER

2023 | **The ecological enigma of *Ledella ultima* (E. A. Smith, 1885): A deep-dive in the population structure of an abyssal protobranch** iAtlantic 5th General Assembly, Edinburgh, United Kingdom. – POSTER

2023 | **Expanding studies northwards – Benthic deep-water communities from the Filchner Trough to the Fram Strait** UK Arctic Conference 2023, Cambridge, United Kingdom. – POSTER

- 2023 | **Amazing deep sea Amphipoda off Iceland** European Marine Biodiversity Symposium, Reykjavik, Iceland. – TALK
- 2023 | **The ecological enigma of *Ledella ultima* (E. A. Smith, 1885): An in-depth assessment of genetic diversity and population structure in an abyssal protobranch** 56th European Marine Biology Symposium, Reykjavik, Iceland. – POSTER
- 2023 | **A genetic fingerprint of the ophiuroid fauna of the deep North Atlantic Ocean** 56th European Marine Biology Symposium, Reykjavik, Iceland. – POSTER
- 2023 | **IceDivA post IceAGE, a project update focussing on peracarid crustaceans** International Crustacean Conference, Wellington, New Zealand. – TALK
- 2023 | **A cosmopolitan predator in the abyssal depth – really?** International Colloquium on Amphipoda, Djerba, Tunisia. – TALK
- 2022 | **IceDivA Project: Study the Diversity of Deep-Sea Holothurians and Meiofauna in the North Atlantic Ocean using Molecular Approaches** iAtlantic Assembly meeting, Florianopolis, Brazil. – TALK
- 2022 | **Assembling the mosaic: the distribution and phylogeographies of North Atlantic *Gastrotricha*** Invited talk at the Departamento de Oceanografia e Pescas (DOP) / Instituto do Mar (IMAR) of the Universidade dos Açores, Horta (Faial, Azores), Portugal. – TALK
- 2022 | **What is the IceDivA project? Research expeditions and science in the face of Covid-19** 23rd Annual Meeting of the Society of Biological Systematics (GfBS), Greifswald, Germany. – TALK
- 2022 | **Connectivity of deep-sea basins in the North-Atlantic using invertebrate taxa as surrogates – preliminary results** 23rd Annual Meeting of the Society of Biological Systematics, Hamburg, Germany. – TALK
- 2022 | **The IceDivA project: Exploring biogeographic connectivity of deep-sea basins in the North-Atlantic using invertebrate taxa as surrogates** 20. Crustaceologen-Tagung, Kiel, Germany. – TALK
- 2022 | **A suprabenthic predatory amphipod showing a global distribution in the abyss** 20. Crustaceologen-Tagung, Kiel, Germany. – POSTER
- 2022 | **What is the IceDivA project? Research expeditions and science in the face of Covid-19** The Challenger Society Conference 2022, London, United Kingdom. – TALK

DATA

Bathymetry

Master tracks in different resolutions of SONNE cruise SO280, Emden – Emden, 2021-01-08 - 2021-02-07:

<https://doi.org/10.1594/PANGAEA.933686>

Master track of SONNE cruise SO280 in 1 sec resolution (zipped, 16.1 MB):

<https://doi.org/10.1594/PANGAEA.933685>

Multibeam bathymetry processed data (Kongsberg EM122 entire dataset) of RV SONNE during cruise SO280:

<https://doi.org/10.1594/PANGAEA.956572>

Multibeam bathymetry processed data (Kongsberg EM710 entire dataset) of RV SONNE during cruise SO280:

<https://doi.org/10.1594/PANGAEA.955826>

Oceanography

Current measurements (38 kHz) during RV SONNE cruise SO280:

<https://doi.org/10.1594/PANGAEA.935638>

Thermosalinograph oceanography along RV Sonne cruise SO280:

<https://doi.org/10.1594/PANGAEA.938476>

ADCP current measurements (75 kHz) during RV SONNE cruise SO280:

<https://doi.org/10.1594/PANGAEA.935640>

CRUISE REPORT

SO286: Brix, S; Taylor, J; George, K., Tewes, S., Jensen, K. et al. Icelandic marine Animals: Genetics and Ecology meets Diversity along latitudinal gradients in the deep sea of the Atlantic Ocean, Cruise No. SO280, 08.01.2021–07.02.2021, Emden (Germany) – Emden (Germany). SONNE-Berichte, Begutachtungspanel Forschungsschiffe, in review.

SO283

Mooring Rescue in the South Atlantic

AUTHORS

Universität Hamburg, Institute for Geology | Hamburg, Germany

N. Lahajnar, L. Meiritz

Universität Hamburg, Institute of Marine Ecosystem and Fishery Science |

Hamburg, Germany

R. Koppelman, B. Martin

Leibniz Zentrum für Marine Tropenforschung (ZMT) | Bremen, Germany

T. Rixen, T. Dudeck

Leibniz-Institut für Ostseeforschung Warnemünde | Rostock, Germany

B. Sabbaghsideh, M. Schmidt, V. Mohrholz

GEOMAR Helmholtz-Zentrum für Ozeanforschung | Kiel, Germany

M. Dengler

Universität Bremen, Institut für Umweltphysik | Bremen, Germany

C. Mertens

SONNE cruise SO283 was not a classical research cruise based on a single research project, but aimed to continue ongoing mooring programs of different projects in the South Atlantic, i. e. to recover existing moorings or to re-deploy them – hence *Mooring Rescue*. *Mooring Rescue* compensated for the research cruises with R/V METEOR and R/V MARIA S. MERIAN that had been cancelled in 2020 and 2021 due to the Corona pandemic. This lack of ship time meant that the associated research projects could not be continued. However, eight mooring systems had already been deployed in 2019 - prior to the outbreak of the pandemic – as integral components of the respective BMBF research projects off the coasts of South Africa, Namibia and Angola, respectively. There was a risk of total loss of these moorings as they only had a limited battery life and could no longer be actively recovered after a certain deployment period. This would also result in a massive and invaluable loss of recorded data and samples. The goal was therefore to recover existing moorings in good time before they had to be considered technically lost. Since no international flights were feasible at the time of the research cruise and all German research vessels were in their home ports in Germany, all forces were mobilized and a cruise was organized from Emden (Germany) to the southern Atlantic and back to Emden. A total of almost 17,000 nautical miles were covered during 64 days non-stop at sea (see Figure 1).

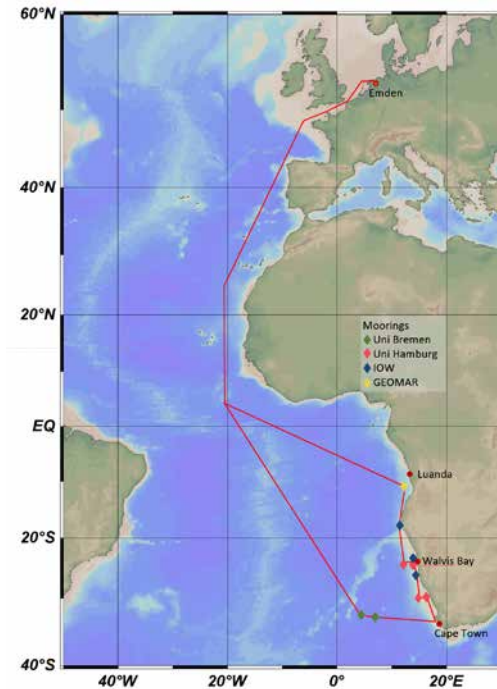


Figure 1: Cruise track of SO283.

In addition, two large mooring systems should have been deployed in 2020 as part of the DFG collaborative research center TRR181 „Energy Transfers in Atmosphere and Ocean“, an interdisciplinary project that aims to better understand the energy transfer between waves, eddies and local turbulence in the ocean and the atmosphere to develop energetically consistent models and thus enhance climate analyzes and forecast accuracy. For TRR181, the lack of ship time would have meant to cancel major parts of the second phase of the research program.

All core objectives of the cruise were achieved. Figure 2 shows the mooring positions:

- › Two deployments of oceanographic moorings in the open South Atlantic as part of the TRR181 program.
- › Two deployments of sediment trap moorings off South Africa (TRAFFIC).
- › Two recoveries and two re-deployments of sediment trap moorings off Namibia (TRAFFIC).
- › Three recoveries and one re-deployment of oceanographic moorings off Namibia (BANINO).

- › One recovery and one re-deployment of an oceanographic mooring off Angola (BANINO).

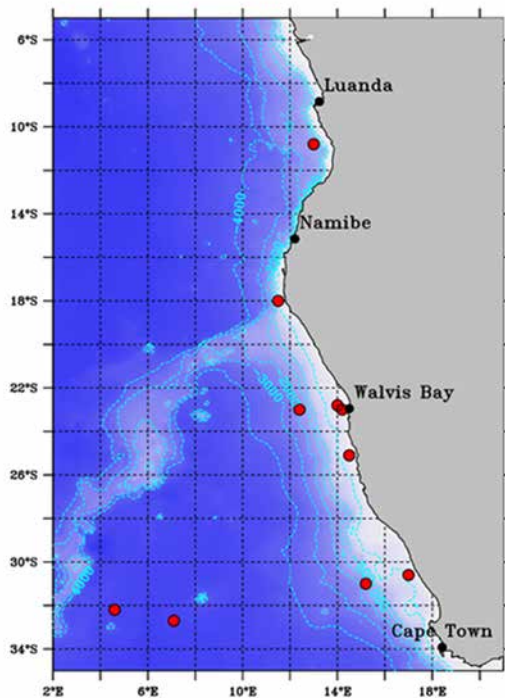


Figure 2: Dedicated mooring positions (red dots) during SO283.

In addition to the anchored moorings, in total seven short-term floating sediment traps systems (“drifter”) were deployed and recovered in the TRAFFIC working area off the coast of South Africa and Namibia.

As part of the DFG program TRR181 (Energy Transfers in Atmosphere and Ocean), two moorings were deployed in the open South Atlantic in approximately 5000 m water depth, flanked by *Pressure Inverted Echo Sounders* (PIES). The BMBF-funded project TRAFFIC (Trophic TRAnSfer eFFICIency in the Benguela Current), was one of the nine large projects funded by the BMBF within the framework of SPACES (Science Partnerships for the Adaptation to Complex Earth System Processes in Southern Africa). The overall objective of TRAFFIC was to investigate climate change and human impacts on ecosystem structure and function, as well as ecosystem services such as fisheries and CO₂ sequestration in the Benguela upwelling system (BUS). For the TRAFFIC project long-term sediment trap moorings were recovered in the Benguela upwelling area and re-deployed at four locations (two South Africa, two Namibia). In addition, seven short-term drifting sediment trap

systems were deployed and successfully recovered during the cruise. This expedition also laid the foundation for the successful accomplishment of the SO285 research cruise (Rixen et al., 2021). In the northern Benguela area off Namibia, three IOW moorings were recovered and one was re-deployed. As part of the BANINO project (Benguela Niños: physical processes and long-term variability), an oceanographic mooring system was successfully recovered and re-deployed off the coast of Angola. The results of the SPACES projects TRAFFIC and BANINO (among others) have been synthesized in the SPACES book "Sustainability of Southern African Ecosystems under Global Change Science for Management and Policy Interventions". This book was written for and from all SPACES projects and will be released by Springer in late 2023 in the prestigious Ecological Studies series. Results are presented in chapters by Brandt et al. (in press), Martin et al. (in press), von Maltitz et al. (in press), Rixen et al. (in press), and Sell et al. (in press).

The project EVAR (The Benguela Upwelling System under climate change – Effects of variability in physical forcing on carbon and oxygen budgets) considered the hydrographic and ecosystem variability on various time scales in the Northern Benguela Upwelling System. As a specific topic of interest, the consequences of intermittent sub- and anoxic conditions on microbial communities are investigated in detail. The considered players in the food web span from archaea and bacteria to macro-zoobenthos living eventually in symbiosis with denitrifying bacteria. One overarching question of EVAR was how the different organisms deal with oxygen conditions varying on short time scales, but undergoing also a seasonal cycle and exhibiting a strong interannual variability. Another issue of interest was the dynamics, sources and sinks of climate relevant trace gases like CO₂, methane and nitrous oxides.

The remaining time in the working areas was used for oceanographic, biogeochemical and biological work as well as for underway measurements. The CTD work was accompanied by APSTEIN- and WP-2 net hauls. This included the investigation of the seasonal variability of trace gas (N₂O, CH₄ and CO₂) along three transects perpendicular to the coast of Namibia at about 17.25°S, 23°S and 25°S. Finally, three ARVOR- and two BIO-ARGO-Floats were released between 33° and 10°S. Throughout the cruise (at least south of the EEZ of Cape Verde Islands), underway measurements for water pH, dissolved inorganic carbon (DIC), total alkalinity (TA), temperature and salinity and other parameters including weather data were conducted providing a unique data set for such a long cruise. The deployment of a total of 282 instruments, gears and systems at 101 stations made the expedition a complete success.

REFERENCES

Brandt P, Bordbar M H, Coelho P, Imbol Koungue R A, Körner M, Lamont T, Lübbecke J F, Mohrholz M, Prigent A, Roch M, Schmidt M, Van der Plas A K, Veitch J, Drivers of climatic variability and change in southern Africa, In: von Maltitz G, et al. (Eds.), Sustainability of southern African ecosystems under global change: Science for management and policy interventions, Springer (in press), Berlin, Heidelberg, New York.

Martin B, Auel H, Bode-Dalby M, Dudeck T, et al., Studies of the ecology of the Benguela Current Upwelling System – the TRAFFIC approach, In: von Maltitz G, et al. (Eds.), Sustainability of southern African ecosystems under global change: Science for management and policy interventions, Springer (in press), Berlin, Heidelberg, New York.

Rixen, T, et al., Trophic Transfer Efficiency in the Benguela Current, Cruise No. SO285, August 20th – November 2nd 2021, Emden (Germany) – Emden (Germany). 2510-764X, Gutachterpanel Forschungsschiffe (2021), Bonn. DOI: 10.48433/cr_so285.

Rixen, T, Lahajnar N, et al., The marine carbon footprint: Challenges in the quantification of CO₂ emissions from southern Africa, In: von Maltitz G, et al. (Eds.), Sustainability of southern African ecosystems under global change: Science for management and policy interventions, Springer (in press), Berlin, Heidelberg, New York.

Sell, A F, Rixen T, Lahajnar N, et al., Unique southern African terrestrial and oceanic biomes and their relation to steep environmental gradients, In: von Maltitz G, et al. (Eds.), Sustainability of southern African ecosystems under global change: Science for management and policy interventions, Springer (in press), Berlin, Heidelberg, New York.

von Maltitz G, et al., Synthesis and outlook on future research and scientific education in southern Africa, In: von Maltitz G. et al. (Eds.), Sustainability of southern African ecosystems under global change: Science for management and policy interventions, Springer (in press), Berlin, Heidelberg, New York.

SCIENTIFIC OUTPUT

LIST OF PUBLICATIONS

Brandt P, Bordbar M H, Coelho P, Imbol Koungue R.A, Körner M, Lamont T, Lübbecke J F, Mohrholz M, Prigent A, Roch M, Schmidt M, Van der Plas A K, Veitch J, Drivers of climatic variability and change in southern Africa, In: von Maltitz G, et al. (Eds.), Sustainability of southern African ecosystems under global change: Science for management and policy interventions, Springer (in press), Berlin, Heidelberg, New York.

Gaye B, Lahajnar N, Rixen T, et al., What can we learn from amino acids about oceanic organic matter cycling and degradation?, Biogeosciences 2022, 19(3): 807-830.

Imbol Koungue R A, Brandt P, Prigent A, Aroucha L C, Lübbecke J, Imbol Nkwinkwa A S N, Dengler M, Keenlyside N, Drivers and impact of the 2021 extreme warm event in the tropical Angolan upwelling system, Scientific Reports 2023 (submitted).

Körner M, Brandt P, Illig S, Dengler M, Subramaniam A, Bachèlery M-L, Krahnmann G, Coastal trapped waves and tidal mixing control primary production in the tropical Angolan upwelling system, *Science Advances* 2023 (resubmitted).

Lamont T, Rixen T, Lahajnar N, New moored observations reveal a contrasting oxygen seasonality along the southern Benguela coast, *Departments of Forestry, Fisheries and the Environment* 2022, RSA Cape Town, South Africa.

Lamont T, van den Berg M A, Lahajnar N, Rixen T., Dissolved oxygen and temperature variability off Hondeclip Bay, *Departments of Forestry, Fisheries and the Environment* 2023, RSA Cape Town, South Africa.

Martin B, Auel H, Bode-Dalby M, Dudeck T, et al., Studies of the ecology of the Benguela Current Upwelling System – the TRAFFIC approach, In: von Maltitz G, et al. (Eds.), *Sustainability of southern African ecosystems under global change: Science for management and policy interventions*, Springer (in press), Berlin, Heidelberg, New York.

Rehder G, Sabbaghzadeh B, Seasonal fluxes of trace gases and their governing physical and microbial controls, *EVAR-Interim report* 2023.

Rixen T, Lahajnar N, et al., The marine carbon footprint: Challenges in the quantification of CO₂ emissions from southern Africa, In: von Maltitz G, et al. (Eds.), *Sustainability of southern African ecosystems under global change: Science for management and policy interventions*, Springer (in press), Berlin, Heidelberg, New York.

Rixen T., Lahajnar N, et al., Oxygen and Nutrient Trapping in the Southern Benguela Upwelling System, *Frontiers in Marine Science* 2021, 8: 1367.

Sabbaghzade B, Arévalo-Martínez D L, Glockzin M, Otto S, Rehder G, Meridional and cross-shelf variability of N₂O and CH₄ in the Eastern-South Atlantic, *Journal of Geophysical Research: Oceans* 2021, 126, e2020JC016878.
<https://doi.org/10.1029/2020JC016878>

Sell, A F, Rixen T, Lahajnar N, et al., Unique southern African terrestrial and oceanic biomes and their relation to steep environmental gradients, In: von Maltitz G, et al. (Eds.), *Sustainability of southern African ecosystems under global change: Science for management and policy interventions*, Springer (in press), Berlin, Heidelberg, New York.

Siddiqui C, Rixen T, Lahajnar N, et al., Regional and global impact of CO₂ uptake in the Benguela Upwelling System through preformed nutrients, *Nature Communications* 2023, 14(1): 2582.

von Maltitz G, et al., Synthesis and outlook on future research and scientific education in southern Africa, In: von Maltitz G, et al. (Eds.), Sustainability of southern African ecosystems under global change: Science for management and policy interventions. Springer (in press), Berlin, Heidelberg, New York.

LIST OF CONFERENCE PRESENTATIONS

2021 | **Music in your data: Hydroacoustic observations and the art of noise removal** Dudeck T, 2nd ZMT Annual Conference (ZAC), Bremen, Germany.

2022 | **Hydroacoustics: Technology, Methods, Applications and Benefits** Dudeck T, TRAFFIC Summer School, Durban, South Africa.

2022 | **Size spectra of zooplankton and mesopelagic fish in the Benguela Upwelling System** Dudeck T, South African Marine Science Symposium (SAMSS), Durban, South Africa.

2022 | **Pinging the Benguela: Revealing deep-scattering layers, krill migrations and fish aggregations with hydroacoustic observations** Dudeck T, Hartkens L, et al., 17th South African Marine Science Symposium (SAMSS), Durban, South Africa.

2022 | **Trophic Transfer Efficiency in the Benguela Current** Ekau W, Rixen, T, TRAFFIC, SPACES Project Synthesis Meeting, Pretoria, South Africa.

2022 | **Biogeochemistry of Trophic Interactions and Impacts on the Ocean Carbon Cycle** Rixen T, TRAFFIC Summer School, Durban, South Africa.

2022 | **Biological Carbon Pump, Regional Graduate Network of Oceanography** Rixen T, RGNO seminar series, online.

2022 | **The Benguela Upwelling System and the CO₂ uptake by the biological carbon pump** Rixen T., Lahajnar N, et al. Open Science Conference on Eastern Boundary Upwelling Systems (EBUS): Past, Present and Future, Lima, Peru.

2022 | **The marine carbon footprint: Challenges in the quantification of CO₂ emissions from southern Africa** Rixen T, Lahajnar N, et al. 17th South African Marine Science Symposium (SAMSS), Durban, South Africa.

2022 | **CO₂ sequestration in the Benguela Upwelling System from a global biological carbon pump perspective** Siddiqui C, Rixen T, Lahajnar N, et al. South African Marine Science Symposium (SAMSS), Durban, South Africa.

2022 | **On the link between CO₂ sequestration in the Benguela Upwelling System and in the Southern Ocean** Siddiqui C, Rixen T, Lahajnar N, et al. Open Science Conference on Eastern Boundary Upwelling Systems (EBUS): Past, Present and Future, Lima, Peru.

2022 | **Role of coastal CO₂ sequestration in the Benguela Upwelling System from a global biological carbon pump perspective** Siddiqui C, Rixen T, 3rd ZMT Annual Conference (ZAC).

2022 | **Seasonal changes in the vertical and biologically mediated particle transport derived from floating sediment traps in the northern and southern Benguela Upwelling System** Meiritz L, Lahajnar N, Rixen T, et al. EBUS 2022 – Open Science Conference on Eastern Boundary Upwelling Systems (EBUS): Past, Present and Future, Lima, Peru.

2022 | **Reactions of microplankton on physical drivers in the northern and southern Benguela Upwelling Systems** Martin B, Koppelman R, et al. SAMSS Vision 2022: Southern African Marine Science Symposium, Durban, South Africa.

2022 | **Short term variability of trace gas and nutrient patterns** Rehder G, Schulz-Vogt H, Mohrholz V, Sabbaghzadeh B, et al. CUSCO/EVAR/REEBUS-Joint annual meeting, Kiel, Germany.

2022 | **Variability in the water column** Mohrholz V, et al. CUSCO/EVAR/REEBUS-Joint annual meeting, Kiel, Germany.

2023 | **Southern African - German Workshop Ocean – Climate – Land Interactions and Feedbacks in southern Africa under Climate Change** Rixen T, et al. Braunschweig, Germany.

2023 | **The Base of the Food Web and Gelatinous Consumers** Koppelman R, Martin B, et al. Southern African – German Workshop Ocean – Climate – Land Interactions and Feedbacks in southern Africa under Climate Change, Braunschweig, Germany.

2023 | **The benefit of long-term moorings** Lahajnar N, Rixen T, Siddiqui C, Meiritz L, et al. Southern African – German Workshop Ocean – Climate – Land Interactions and Feedbacks in southern Africa under Climate Change, Braunschweig, Germany.

2023 | **Why research and monitoring matters?** Lamont T, Lahajnar N, Southern African – German Workshop, Ocean – Climate – Land Interactions and Feedbacks in southern Africa under Climate Change, Braunschweig, Germany.

2023 | **Floating sediment traps – closing a gap: detailed representation of trophic interactions and estimation of carbon sequestration potential in marine high productivity regions** Meiritz L, Lahajnar N, Rixen T, ICYMARE 2023, Oldenburg, Germany.

2023 | **Coastal trapped waves and tidal mixing control primary production in the tropical Angolan upwelling system** Körner M, Brandt P, Illig S, Dengler M, et al. PIRATA-26 / TRIATLAS Conference and General Assembly, Banyuls-sur-Mer, France.

2023 | **Drivers and impact of the 2021 extreme warm event in the tropical Angolan upwelling system** Imbol Koungue R A, Brandt P, Prigent A, et al. PIRATA-26 / TRIATLAS Conference and General Assembly, Banyuls-sur-Mer, France.

DATA

Schmidt, Martin; Mertens, Christian; Lahajnar, Niko (2022): Physical oceanography during Sonne cruise SO283: <https://doi.org/10.1594/PANGAEA.941254>

Brandt, Peter; Imbol Koungue, Rodrigue Anicet; Krahmann, Gerd; Dengler, Marcus (2023): Physical oceanography from mooring KPO_1235: <https://doi.org/10.1594/PANGAEA.962193>

Mertens, Christian; Dengler, Marcus; Lahajnar, Niko (2022): ADCP current measurements (38 kHz) during SONNE cruise SO283: <https://doi.org/10.1594/PANGAEA.940259>

Mertens, Christian; Dengler, Marcus; Lahajnar, Niko (2022): ADCP current measurements (75 kHz) during SONNE cruise SO283: <https://doi.org/10.1594/PANGAEA.940306>

Sabbaghzadeh, B; Otto, S; Rehder, G (2023): Trace gases CH₄, N₂O, and CO₂ measured on discrete water samples during SONNE cruise SO283: <https://doi.org/10.1594/PANGAEA.959646>

Sabbaghzadeh, Bitia; Burmeister, Christian; Meiritz, Luisa; Lahajnar, Niko (2022): Hydrochemistry measured on water bottle samples in the northern Benguela during SONNE cruise SO283: <https://doi.org/10.1594/PANGAEA.941122>

Dudeck, Tim; Heinatz, Knut; Lahajnar, Niko: EK60 raw multi-frequency (18, 38, 120, 200 kHz) acoustic data collected during RV SONNE cruise SO283 in 2021 to the Benguela Upwelling System transit area: <https://doi.org/10.1594/PANGAEA.942185>

Martin, Bettina (2022): Microplankton biomass in the Benguela Upwelling System sampled during the RV SONNE cruise SO283: <https://doi.org/10.1594/PANGAEA.945305>

Martin, Bettina (2022): Stable isotopes ($\delta^{13}\text{C}$ and $\delta^{15}\text{N}$) of microplankton in the Benguela Upwelling System sampled during the RV SONNE cruise SO283:
<https://doi.org/10.1594/PANGAEA.945314>

CRUISE REPORT

SO283: https://doi.org/10.48433/cr_so283

SO284

Tropical Atlantic Circulation and Climate

AUTHORS

GEOMAR Helmholtz Centre for Ocean Research Kiel | Kiel, Germany

P. Brandt, F. P. Tuchen, M. Körner, R. Hummels, M. Dengler, G. Krahnemann, R. Kiko

Max Planck Institute for Meteorology | Hamburg, Germany

J. Windmiller, B. Stevens

R/V Sonne cruise SO284 was set up to rescue long-term moorings in the central and western tropical Atlantic. During the cruise the Cape Verde Ocean Observatory (CVOO), the equatorial mooring at 23°W (in cooperation with the international PIRATA program), and the western boundary current mooring array at 11°S off Brazil were recovered and re-deployed ensuring the continuity of long-term observations of tropical circulation, water-mass distribution, and biogeochemical parameters. During SO284 hydrographic and current measurements along repeat sections at 11°S, 5°S, and 35°W were carried out. CTD measurements along these sections included biochemical measurements using water samples of the CTD rosette and optical measurements for particle counts and phyto- and zooplankton identification with an underwater vision profiler (UVP). The physical oceanography program additionally included a study of upper ocean mixing processes using an autonomous glider and a freely drifting buoy. SO284 was a contribution to the GEOMAR research program OCEANS, to the EU projects TRIATLAS, NextGEMS, and EuroSea, and to the „Make Our Planet Great Again“ project by R. Kiko.

In addition to the oceanographic measurements, a set of atmospheric measurements was performed during SO284. The region of key interest was the Atlantic Intertropical Convergence Zone (ITCZ), which plays a central role for the tropical weather and climate and structures the large-scale circulation. The thermodynamic and dynamic state of the atmosphere was measured by frequent radiosonde launches, providing atmospheric profiles with high vertical resolution extending from the surface through the lower stratosphere. These measurements were complemented by continuous measurements of the atmospheric boundary layer and lower free troposphere, including optical measurements of water vapor, aerosol, precipitation, wind speed and direction as well as cloud base height. The atmospheric measurements specifically addressed the question of how convective scale processes in the atmosphere, and their coupling to the ocean, shape the ITCZ. The collected data help to prepare the strategy for more extensive measurements of the ITCZ planned for the BOW-TIE Cruise and contemporaneous airborne measurements in Aug 2024 through MPI/DFG/DLR led Tropical-Ocean and Organized Convection Field study. In addition, the data serve as a benchmark to the first

international inter-comparison of global storm-resolving models (DYAMOND, Stevens et al., 2019) and support the EU Project NextGEMS.

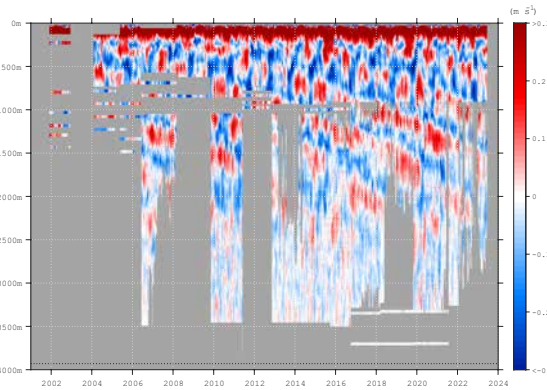


Figure 1: Zonal current velocity time series from the moored observatory at 0°N, 23°W. The long-term observatory was recovered and redeployed during SO284.

REFERENCES

Stevens B, Satoh M, Auger L, et al., DYAMOND: the DYNAMics of the Atmospheric general circulation Modeled On Non-hydrostatic Domains, *Prog Earth Planet Sci* 2019, 6, 61, doi:10.1186/s40645-019-0304-z.

SCIENTIFIC OUTPUT

LIST OF PUBLICATIONS

Bastin S, Claus M, Greatbatch RJ, Brandt P, Factors influencing the meridional width of the equatorial deep jets, *Ocean Sci.* 2023, 19, 923–939, doi:10.5194/os-19-923-2023.

Heukamp FO, Brandt P, Dengler M, Tuchen FP, et al., Tropical instability waves and wind-forced cross-equatorial flow in the central Atlantic Ocean, *Geophys. Res. Lett.* 2022, 49, e2022GL099325, doi:10.1029/2022GL099325.

Körner M, Claus M, Brandt P, Tuchen FP, Sources and pathways of intraseasonal meridional kinetic energy in the equatorial Atlantic Ocean, *J. Phys. Oceanogr.* 2022, 52, 2445-2462, doi:10.1175/JPO-D-21-0315.1, 2022.

Tuchen FP, Brandt P, Hahn J, Hummels R, et al., Two decades of full-depth current velocity observations from a moored observatory in the central equatorial Atlantic at 0°N, 23°W, *Front. Mar. Sci.* 2022, 9, 910979, doi:10.3389/fmars.2022.910979.

Tuchen FP, Perez RC, Foltz GR, Brandt P, et al., Modulation of Equatorial Currents and Tropical Instability Waves during the 2021 Atlantic Niño, *J. Geophys. Res. Oceans* 2023, resubmitted.

Windmiller JM and Stevens B, The inner life of the Atlantic ITCZ, *Q. J. R. Meteorol. Soc.* 2023, doi:10.1002/qj.4610.

LIST OF CONFERENCE PRESENTATIONS

2023 | **Modulation of Equatorial Currents and Tropical Instability Waves during the 2021 Atlantic Niño** TRIATLAS Final Conference and General Assembly / PIRATA-26/TAV Meeting, Banyuls-sur-Mer, France.

2023 | **Seasonal cycle of mixing and upward nutrient supply in the equatorial Atlantic cold tongue** TRIATLAS Final Conference and General Assembly / PIRATA-26/TAV Meeting, Banyuls-sur-Mer, France.

2023 | **The Inner Life of the Atlantic ITCZ [talk]** CFMIP-GASS 2023, Paris, France.

2023 | **Organization of deep convection in the Atlantic ITCZ [invited talk]** 3rd Workshop on Cloud Organisation and Precipitation Extremes – WCO3, Trieste, Italy.

2023 | **Seasonal cycle of mixing and upward nutrient supply in the equatorial Atlantic cold tongue** IUGG/IAPSO, Berlin, Germany.

2023 | **Observations of the Boundary Currents and AMOC at 11°S – the TRACOS Array [poster]** IUGG/IAPSO, Berlin, Germany.

2023 | **Modulation of Tropical Instability Waves and chlorophyll concentration by equatorial waves during the 2021 Atlantic Niño** EGU General Assembly, Vienna, Austria.

2023 | **The Inner Life of the Atlantic ITCZ [poster]** EGU 2023, Vienna, Austria.

2023 | **Investigating long-term variability and trends of Atlantic Tropical Instability Waves with multidecadal satellite observations and mooring data** US CLIVAR Mesoscale and Frontal-Scale Air-Sea Interactions Workshop, Boulder, USA.

2023 | **Observations of the Boundary Currents and AMOC at 11°S – the TRACOS Array [poster]** Helmholtz POF IV Topic 2 Seminar, Kiel, Germany.

2023 | **Detecting the ocean response to climate variability: Long-term observatories of RD1 [poster]**, 12th SAB Meeting, Kiel, Germany.

2023 | **Observations of the Boundary Currents and AMOC at 11°S [talk]** Physical Oceanography Seminar, Bremen, Germany.

2023 | **Observations of the Boundary Currents and AMOC at 11°S – the TRACOS Array [talk]** AMOC Webinar Series #1, online.

2023 | **MSM117: Circulation, flow-topography interaction and ecosystem impact [talk]** VIII Seminar of the Bilateral Cooperation DOCEAN – GEOMAR, Recife, Brazil.

2022 | **Atmospheric measurements of the Atlantic ITCZ during a ship campaign in summer 2021 [talk]** DACH2022, Leipzig, Germany.

2022 | **Investigating long-term changes of equatorial ocean dynamics with 20 years of current velocity observations from a moored observatory at 0°N, 23°W** AGU Fall Meeting, Chicago, USA.

2022 | **Multidecadal Intensification of Atlantic Tropical Instability Waves** TRIATLAS 3rd Conference and General Assembly / PIRATA-25/TAV Meeting, Porto de Galinhas, Brazil.

2022 | **Seasonal cycle of upwelling and upward nutrient supply in the equatorial Atlantic** International Conference Themes 2022, Venice, Italy.

2022 | **Tropical Ocean Processes [talk]** 11th SAB Meeting, Kiel, Germany.

DATA

Physical oceanography (CTD):

<https://doi.pangaea.de/10.1594/PANGAEA.952519>

ADCP current measurements (38 and 75 kHz):

<https://doi.pangaea.de/10.1594/PANGAEA.952102>

Lowered ADCP data:

<https://doi.pangaea.de/10.1594/PANGAEA.941186>

Continuous thermosalinograph oceanography:

<https://doi.pangaea.de/10.1594/PANGAEA.951256>

Physical oceanography from mooring KPO_1210:

<https://doi.pangaea.de/10.1594/PANGAEA.960093>

Radio sonde data:

<https://zenodo.org/records/7051674>

Data product of full-depth current velocity observations at 0°N, 23°W from 2001–2021 (v1.0):

<https://doi.org/10.1594/PANGAEA.941042>

CRUISE REPORT

SO284: doi:10.48433/cr_so284

SO285

TRAFFIC: Trophic TRAnSfer eFFICIency in the Benguela Current (SO285/SO283)

AUTHORS

Leibniz Centre for Tropical Marine Research | Bremen, Germany (ZMT)

T. Rixen, T. Dudeck, W. Ekau

Bremen Marine Ecology, University of Bremen | Germany (BreMarE)

H. Auel, W. Hagen

Institute for Marine Systems and Fisheries Science, University of Hamburg | Germany (IFM)

R. Koppelman, B. Martin

Thünen Institute of Sea Fisheries | Bremerhaven, Germany (TI)

A.F. Sell, H.O. Fock, S.E. Duncan

Institute of Geology, Universität Hamburg | Germany (IFG)

N. Lahajnar

The SO285 cruise is the second field campaign of the TRAFFIC (Trophic TRAnSfer eFFICIency in the Benguela Current) collaborative project. TRAFFIC was one of the nine large projects funded by the BMBF within the framework of SPACES (Science Partnerships for the Adaptation to Complex Earth System Processes in Southern Africa, https://www.fona.de/en/measures/international-cooperation/spaces_ii.php). Due to COVID, our African partners could not participate in the cruise and it had to start and end in Emden, Germany (Figure. 1).

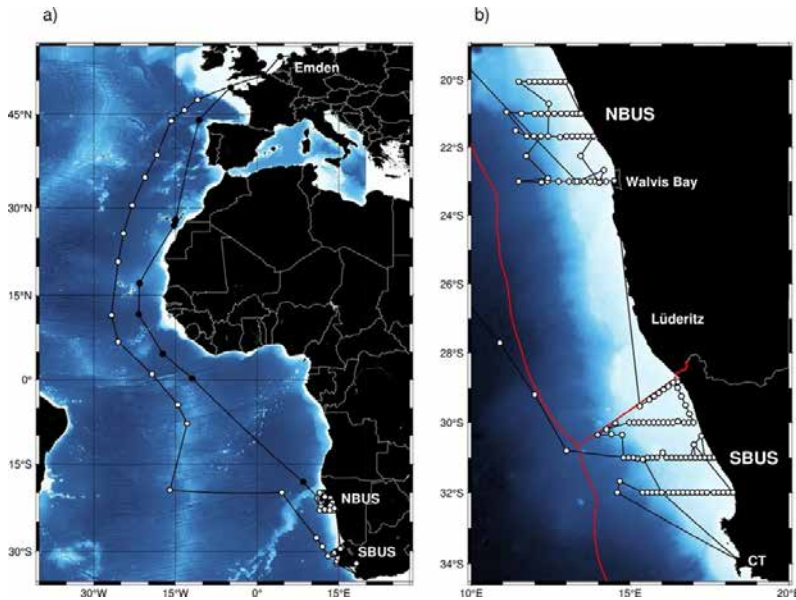


Figure 1: (left) SO285 cruise track. (right) Station grid in the nBUS and sBUS. The red lines mark the EEZs of Namibia and South Africa, respectively.

The overall objective of TRAFFIC was to investigate climate change and human impacts on ecosystem structure and function, as well as ecosystem services such as fisheries and CO₂ sequestration in the Benguela upwelling system (BUS). Unlike the first TRAFFIC cruise with R/V Meteor (M153) in the austral summer/autumn of 2019, cruise SO285 took place in the winter/spring of 2021. The aim was to study ecosystem responses in the BUS to seasonally varying physical conditions. In order to also record data between cruises, moorings have been deployed on the cruise M153 and maintained during the cruise SO283. This was necessary because COVID-related temporal shifts of cruises would have led to a loss of mooring systems (Lahajnar et al., 2021).

The BUS is one of the four highly productive eastern boundary upwelling systems in the ocean and is divided into a southern (sBUS) and northern subsystem (nBUS). To better assess the response of the BUS to global change, the aim of TRAFFIC was to test the following four hypotheses:

1. global climate change affects upwelling intensity differently in the nBUS and sBUS,
2. different lengths of food chains in the nBUS and sBUS cause differences in the stocks of economically relevant species,
3. nBUS and sBUS differ in the abundance of trophic dead ends,

4. differences in pelagic food webs in the nBUS and sBUS influence biological CO₂ uptake efficiency in the ocean.

TRAFFIC results have been summarized in the SPACES book 'Sustainability of Southern African Ecosystems under Global Change Science for Management and Policy Interventions'. This book was written by more than 170 authors from all SPACES projects and will be published by Springer in the renowned 'Ecological Studies' series in late 2023/early 2024. The TRAFFIC results are presented in Rixen et al. (in press), von Maltitz et al. (in press), Sell et al. (in press) and Martin et al. (in press).

Overall, it can be said that southern Africa is one of the regions that is warming disproportionately fast in the course of global warming, which is accompanied by a frequent occurrence of extreme events and first signs of meridionally shifting climate zones. It is becoming apparent that upwelling in the nBUS is weakening, while the sBUS show no clear trend which confirms the 1st TRAFFIC hypothesis.

Although there is evidence that trophic transfer efficiency was lower in the nBUS than in the sBUS, no conclusions can so far be drawn about the length of the food chain. Systematic observations are still lacking here to prove the 2nd TRAFFIC hypothesis.

With respect to hypothesis 3, confirmation is also emerging. Overall, the data density is still too low to show real trends, but our results join a series of observations that increasingly report the mass occurrence of jellyfish in the nBUS. The oxygen minimum zone (OMZ), which is more pronounced in the nBUS than in the sBUS, is discussed - along with fishing - as one reason for this development. The OMZ shows strong seasonal and interannual variations due to which it is difficult to clearly prove an intensification of the OMZ in the nBUS and sBUS. In the sBUS, however, nutrient trapping behind the upwelling front near the coast seems to be a mechanism that decouples the intensity of the OMZ from the strength of upwelling.

We could not confirm our assumptions underlying hypothesis 4 that the influence of ecosystem-immanent processes explains the opposite CO₂ fluxes in the nBUS and sBUS. Instead, we found that the opposite behavior of the nBUS and sBUS in terms of CO₂ fluxes is a consequence of the interaction of the physical solubility pump and biological carbon pump. In both subsystems, the solubility pump favors the CO₂ emission while the biological carbon pump acts as a CO₂ sink but in contrast to the nBUS, the biological carbon pump is stronger than the solubility pump in the sBUS. Decisive factors influencing the strength of the solubility pump and biological carbon pump are physical factors such as the warming of the upwelling water at the sea surface and the delivery of nutrients from the Antarctic Ocean.

Effects of near-bottom fisheries on carbon storage in sediments seems in turn to lower CO₂ storing capacity of biological carbon pump in the BUS. As these processes take

place in the EEZs of Namibia and South Africa, they should also be included in the national greenhouse gas reports (NIR). This has not been done so far due to the lack of agreed methods to quantify the CO₂ uptake and storing capacity of the biological carbon pump. We see a need for action here and for future research projects.

REFERENCES

Lahajnar N, et al., Mooring Rescue, Cruise No. SO283, 19 March 2021 – 25 May 2021, Emden (Germany) – Emden (Germany). 2510-764X, Gutachterpanel Forschungsschiffe 2021, Bonn.

Martin B, et al., Studies of the ecology of the Benguela Current Upwelling System – the TRAFFIC approach. In: von Maltitz, G. et al. (Eds.), Sustainability of southern African ecosystems under global change: Science for management and policy interventions, Springer (in press), Berlin, Heidelberg, New York.

Rixen T, et al., The marine carbon footprint: Challenges in the quantification of CO₂ emissions from southern Africa, Sustainability of southern African ecosystems under global change: Science for management and policy interventions, Springer (in press).

Sell AF, et al., Unique southern African terrestrial and oceanic biomes and their relation to steep environmental gradients. In: von Maltitz, G. et al. (Eds.), Sustainability of southern African ecosystems under global change: Science for management and policy interventions, Springer (in press), Berlin, Heidelberg, New York.

von Maltitz G, et al., Synthesis and outlook on future research and scientific education in southern Africa. In: von Maltitz, G. et al. (Eds.), Sustainability of southern African ecosystems under global change: Science for management and policy interventions. Springer (in press), Berlin, Heidelberg, New York.

SCIENTIFIC OUTPUT

LIST OF PUBLICATIONS

Duncan SE, Sell AF, Hagen W, Fock HO, Environmental drivers of upper mesopelagic fish assemblages in the Benguela Upwelling System. Marine Ecology Progress Series 2022, 688:133–152.

Duncan SE, Fock HO, Sell AF, Hagen W, Trophic ecology of mesopelagic fishes in the northern and southern Benguela Upwelling Systems revealed through stable isotope patterns, Marine Ecology Progress Series (in press).

Gaye B, et al., What can we learn from amino acids about oceanic organic matter cycling and degradation?, *Biogeosciences* 2022, 19(3): 807–830.

Lamont T, Rixen T, Lahajnar N, New moored observations reveal a contrasting oxygen seasonality along the southern Benguela coast, *Departments of Forestry, Fisheries and the Environment* 2022, RSA Cape Town, South Africa.

Lamont T, van den Berg MA, Lahajnar N, Rixen T, Dissolved oxygen and temperature variability of Hondeklip Bay, *Departments of Forestry, Fisheries and the Environment* 2023, RSA Cape Town, South Africa.

Martin B, et al., Studies of the ecology of the Benguela Current Upwelling System – the TRAFFIC approach. In: von Maltitz, G. et al. (Eds.), *Sustainability of southern African ecosystems under global change: Science for management and policy interventions*, Springer (in press), Berlin, Heidelberg, New York.

Rixen T, et al., Trophic Transfer Efficiency in the Benguela Current, Cruise No. SO285, August 20th – November 2nd 2021, Emden (Germany) – Emden (Germany). 2510-764X, *Gutachterpanel Forschungsschiffe 2021a*, Bonn.

Rixen T, et al., The marine carbon footprint: Challenges in the quantification of CO₂ emissions from southern Africa. In: von Maltitz, G. et al. (Eds.), *Sustainability of southern African ecosystems under global change: Science for management and policy interventions*, Springer (in press), Berlin, Heidelberg, New York.

Rixen T, et al., Oxygen and Nutrient Trapping in the Southern Benguela Upwelling System, *Frontiers in Marine Science* 2021b, 8: 1367.

Sell AF, et al., Unique southern African terrestrial and oceanic biomes and their relation to steep environmental gradients. In: von Maltitz, G. et al. (Eds.), *Sustainability of southern African ecosystems under global change: Science for management and policy interventions*, Springer (in press), Berlin, Heidelberg, New York.

Siddiqui C, et al., Regional and global impact of CO₂ uptake in the Benguela Upwelling System through preformed nutrients, *Nature Communications* 2023, 14(1): 2582.

von Maltitz G, et al., Synthesis and outlook on future research and scientific education in southern Africa. In: von Maltitz, G. et al. (Eds.), *Sustainability of southern African ecosystems under global change: Science for management and policy interventions*. Springer (in press), Berlin, Heidelberg, New York.

SO286

Icelandic marine Animals: Genetics and Ecology meets Diversity along latitudinal gradients in the deep sea of the Atlantic Ocean 2 (IceDivA2)

AUTHORS

Senckenberg am Meer, Deutsches Zentrum für Marine Biodiversitätsforschung (DZMB) | Wilhelmshaven & Hamburg, Germany

S. Brix, P. Martinez Arbizu, A.Kieneke

British Antarctic Survey, Biodiversity, Evolution and Adaptation | Cambridge, United Kingdom

K. Linse

IceDivA2 (Icelandic marine Animals meets Diversity along latitudinal gradients in the deep sea of the Atlantic Ocean 2) aimed to investigate the connectivity/biodiversity within key groups of the marine benthic abyssal habitats and their overlaying planktonic communities. IceDivA2 built on the previous work completed during the first IceDivA expedition (SO280) during January 2021 east of the Mid-Atlantic Ridge (MAR), an expedition connecting the IceAGE (Icelandic marine Animals: Genetics and Ecology) and DIVA (Latitudinal Gradients in BioDIiversity in the deep Atlantic) projects. Coinciding perfectly with the beginning of the UN Ocean Decade at the start of 2021, the IceDivA project has been a proud contributor as part of the Challenger 150 program. IceDivA2 also hosted the Satellite event "A floating classroom: Deep-sea science in action towards a clean ocean" for the UN Ocean Decade's Laboratory on 'A Clean Ocean' on 18th November 2021 (Figure 1). This event was conducted live, via satellite, in the middle of the Atlantic Ocean, live on board. During this talk, scientific outcomes of the IceDivA project are highlighted per working area of the expedition SO286.

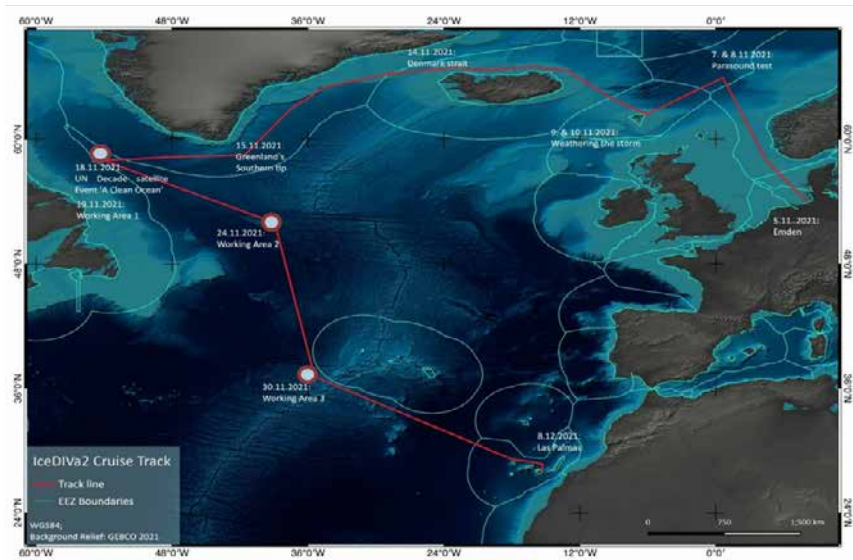


Figure 1: Working areas of SO286. Working Area 1: “Labrador Sea and UN Decade satellite event “A clean Ocean”, Working Area 2: “NACES MPA” with discovery of “Mount Doom”, Working Area 3: Azores fracture zones at the MAR. This figure represents Figure 3.1. of the cruise report showing the track chart of R/V SONNE Cruise SO286 indicating the three working areas (Working Areas 1–3 as indicated below). The date of each station runs along the cruise track (Red line starting in Emden, Germany and ending in Las Palmas, Spain). Turquoise lines are indicating the 200 nautical miles zones of the country’s economic zones.)

LABRADOR SEA AND UN DECADE SATELLITE EVENT “A CLEAN OCEAN”

After 15 days trying to reach a working area as planned and weathering the storm North of Iceland and previously hiding behind the Faroe Islands, we arrived in the Labrador Sea. Selecting a deep-sea abyssal area below 3000 m depth in a storm-free weather window, we got a complete station work done of three days in a row including the public outreach event “A floating classroom” as satellite event of the kick-off event of the UN ocean decade hosted by Germany as online event. Both, science wise and outreach wise, we had full success in the Labrador Sea. A combination of video footage and physical samples (Figure 2) lead to the discovery of species new to science like the *Fissidentallium* species (Scaphopoda) living in symbiosis with an anemone as illustrated already for public outreach in Brix (2022) and now in description in Linse & Neuhaus (in preparation).

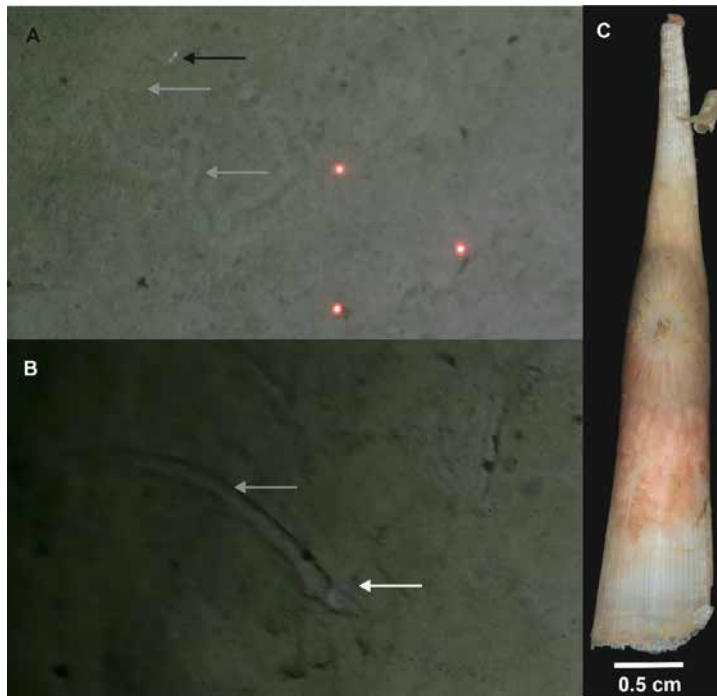


Figure 2: In-situ and life images of scaphopod – actinostolid symbiosis. A) Scaphopod (black arrow) hosting anemone with retracted tentacles and its “Lebensspur” (grey arrows); B) Anemone with extended tentacles (white arrow) and scaphoid created “Lebensspur” (grey arrow); C) Scaphopod (DZMB6509) with epizoic actinostolid anemone. Plate from OFOS dive and sampled reference specimen from Linse & Neuhaus (in preparation).

THE NACES MARINE PROTECTED AREA (MPA)

The NACES MPA was established in 2021 and based on the benthic data retrieved during IceDivA2 the benthos was included in the protection in summer 2023 (OSPAR press release 30th June 2023 about the revised nomination proforma). Additional an – by now in the naming process – volcano, “Mount Doom” (southwest of the Charlie-Gibbs Fracture Zone) was exhaustively mapped for 19.25 h in total at Working Area 2. Down to a depth of 2800 m, the volcano top could be mapped at 30 m resolution, below with 50 m. The seamount also lies within the NACES MPA, that has recently been extended by OSPAR to further include the seafloor. It is mentioned in the revised nomination proforma. Currently, the analysis of the video footage from the OFOS deployments and the final species determination is ongoing. So far, the macrofauna data are included in Kürzel et al. (2023).

ABYSSAL PLAINS AND FRACTURE ZONES SOUTH OF THE AZORES

South of the Azores and close to the fracture zones at the Mid-Atlantic Ridge (MAR), we were able to deploy a full station with all gear comparable to the previous working areas. The area was comparably spectacular hosting abyssal plains next to over 100m high walls, which were not visible in the ship’s bathymetry, and were detected during the

OFOS deployment, clearly colonized by corals and sponges. Working Area3 gave us the opportunity to compare the latitudinal gradient on the West side of the MAR with the East side of the on the same latitude sampled during the first IceDivA expedition SO280. A comparison of image based macrofauna data is currently work in progress.

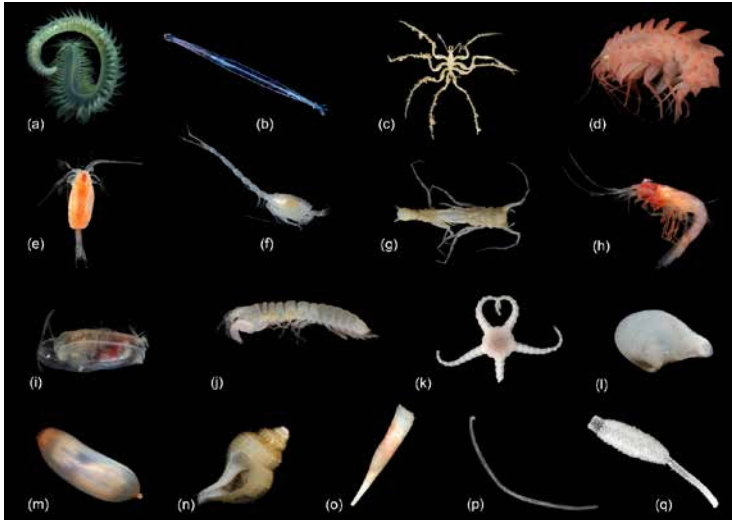


Figure 3: In-situ and life images of scaphopod – actinostolid symbiosis. A) Scaphopod (black arrow) hosting anemone with retracted tentacles and its “Lebensspur” (grey arrows); B) Anemone with extended tentacles (white arrow) and scaphoid created “Lebensspur” (grey arrow); C) Scaphopod (DZMB6509) with epizoic actinostolid anemone. Plate from OFOS dive and sampled reference specimen from Linse & Neuhaus (in preparation).

REFERENCES

Brix S, Taylor J, Forschung für den Ozean, den wir uns wünschen. Das Senckenberg Wissenschaftsmagazin NATUR • FORSCHUNG • MUSEUM 152 | 1 – 3 2022.

Kürzel K, Brix S, Brandt A, Brenke N, Enderlein P, Griffiths HJ, Kaiser S, Svavarsson J, Lörz A-N, Frutos I, Taylor J, Linse K, Pan-Atlantic Comparison of Deep-Sea Macro- and Megabenthos, Diversity 2023, 15, 814, <https://doi.org/10.3390/d15070814>.

Linse L, Neuhaus J, et al., Deep Atlantic Fissidentalium sp (Scaphopoda) in association with an actinostolid anemone. In preparation for Marine Biodiversity.

OSPAR commission press release to the nomination proforma. North-East Atlantic’s biggest Marine Protected Area extended to include the seafloor. 30th June 2023. OSPAR Contact: Lucy Ritchie; Communications Lead, lucy.ritchie@ospar.org; https://www.ospar.org/site/assets/files/38964/01_naces_rev_nomination_proforma_20221201_version_for_consultation.pdf.

SCIENTIFIC OUTPUT

LIST OF PUBLICATIONS

Brix S, Taylor J, Forschung für den Ozean, den wir uns wünschen. Das Senckenberg Wissenschaftsmagazin NATUR • FORSCHUNG • MUSEUM 152 | 1 – 3 2022.

Brix S, Live-Schaltung zu „Sonne“. Das Senckenberg Wissenschaftsmagazin NATUR • FORSCHUNG • MUSEUM 152 | 1 – 3 2022.

Hesemann M, Benthic Foraminifera Diversity of the Abyssal Northwest Atlantic, *Diversity* 2023; 15(3):381. <https://doi.org/10.3390/d15030381>.

Kaiser S, Stransky B, Jennings RM, Kihara TC, & Brix S, Combining morphological and mitochondrial DNA data to describe a new species of *Austroniscus* Vanhöffen, 1914 (Isopoda, Janiroidea, Nannoniscidae) linking abyssal and hadal depths of the Puerto Rico Trench, *Zootaxa* 2023, 5293(3), 401–434.

Kamyab E, Khodami S, Martinez Arbizu P, Comparison of eDNA and Community Metabarcoding Methodologies for Analyzing the Distribution and Diversity of Deep Sea Meiofauna: A Case Study in the North-West Atlantic Ocean, In the submission process.

Kieneke A, Neuhaus J, Taylor J, Brix S, Fortsetzung erfolgt! Nun auch im Nordwest-Atlantik: Expedition IceDivA2 zur Erforschung der Tiefsee-Fauna, *Gesellschaft für Biologische Systematik Newsletter*, 2022, 40, 42–49, https://www.researchgate.net/publication/361275907_Fortsetzung_erfolgt_Nun_auch_im_Nordwest-Atlantik_Expedition_IceDivA2_zur_Erforschung_der_Tiefsee-Fauna.

Kürzel K, Brix S, Brandt A, Brenke N, Enderlein P, Griffiths HJ, Kaiser S, Svavarsson J, Lörz A-N, Frutos I, Taylor J, Linse K, Pan-Atlantic Comparison of Deep-Sea Macro- and Megabenthos, *Diversity* 2023, 15, 814, <https://doi.org/10.3390/d15070814>.

Linse L, Neuhaus J, et al., Deep Atlantic *Fissidentalium* sp (Scaphopoda) in association with an actinostolid anemone, In preparation for *Marine Biodiversity*.

Lörz AN, Schwentner M, Bober S, Jażdżewska AM, Multi-ocean distribution of a brooding predator in the abyssal benthos, *Sci Rep.* 2023, 13(1):15867. <https://doi.org/10.1038/s41598-023-42942-0>.

Neuhaus J, de Wilt ME, Linse K, Etter RJ, Jennings RM, Martínez Arbizu P, Brix S, The ecological enigma of *Ledella ultima* (E.A. Smith, 1885): An in-depth assessment of genetic diversity and population structure in an abyssal protobranch, in prep.

Schumacher M, Huvenne VA, Devey CW, Arbizu PM, Biastoch A, & Meinecke S, The Atlantic Ocean landscape: A basin-wide cluster analysis of the Atlantic near seafloor environment, *Frontiers in Marine Science* 2022, 9, 936095.

James Taylor, et al., IceDivA2 "goes west" of the Mid-Atlantic Ridge! iAtlantic Newsletter Issue4 | 04.01.2022.

Taylor J, Schumacher M, Kamyab E, Neuhaus J, IceDivA2 from the perspective of four iAtlantic Fellows, iAtlantic Project Newsletter 2022, 4, 10–11, https://www.iatlantic.eu/wp-content/uploads/2022/02/iAtlantic_newsletter4_Jan22_FINAL.pdf.

Taylor J, Neuhaus J, Kieneke A, Linse K, Martínez Arbizu P, Brix S, IceDivA2 – Expedition to the abyssal plains west of the MAR, *Deep-Sea Life* 2022, 18, 4–5, https://www.dosi-project.org/wp-content/uploads/DSL18_final.pdf.

Trokhymchuk R, Kieneke A, Novel distribution records of marine Tardigrada from abyssal sediments of the Northwest Atlantic Ocean, *Organisms, Diversity and Evolution*, submitted.

LIST OF CONFERENCE PRESENTATIONS

2023 | **IceDivA Project: The Exploration of Deep-Sea Holothurian Diversity in the North Atlantic Ocean Using Molecular Approaches.** 11th European Conference on Echinoderms, Lyon, France. – POSTER

2023 | **Comparison of eDNA and Community Metabarcoding Methodologies for Analyzing the Distribution and Diversity of Deep Sea Meiofauna: A Case Study in the North-West Atlantic Ocean.** iAtlantic Final Meeting, Edinburgh, UK. – POSTER

2023 | **The ecological enigma of *Ledella ultima* (E. A. Smith, 1885): A deep-dive in the population structure of an abyssal protobranch** iAtlantic 5th General Assembly, Edinburgh, United Kingdom. – POSTER

2023 | **Expanding studies northwards – Benthic deep-water communities from the Filchner Trough to the Fram Strait,** UK Arctic Conference 2023, Cambridge, United Kingdom. – POSTER

2023 | **Amazing deep sea Amphipoda off Iceland,** European Marine Biodiversity Symposium, Reykjavik, Iceland. – TALK

2023 | **The ecological enigma of *Ledella ultima* (E. A. Smith, 1885): An in-depth assessment of genetic diversity and population structure in an abyssal protobranch** 56th European Marine Biology Symposium, Reykjavik, Iceland. – POSTER

2023 | **A genetic fingerprint of the ophiuroid fauna of the deep North Atlantic Ocean.**
56th European Marine Biology Symposium, Reykjavik, Iceland. – POSTER

2023 | **IceDivA post IceAGE, a project update focussing on peracarid crustaceans.**
International Crustacean Conference, Wellington, New Zealand. – TALK

2023 | **A cosmopolitan predator in the abyssal depth – really?** International
Colloquium on Amphipoda, Djerba, Tunisia. – TALK

2022 | **IceDivA Project: Study the Diversity of Deep-Sea Holothurians and Meiofauna in the North Atlantic Ocean using Molecular Approaches.** iAtlantic Assembly meeting,
Florianopolis, Brazil. – TALK

2022 | **Assembling the mosaic: the distribution and phylogeographies of North Atlantic Gastrotricha.** Invited talk at the Departamento de Oceanografia e Pescas (DOP) /
Instituto do Mar (IMAR) of the Universidade dos Açores, Horta (Faial, Azores),
Portugal. – TALK

2022 | **What is the IceDivA project? Research expeditions and science in the face of Covid-19.** 23rd Annual Meeting of the Society of Biological Systematics (GfBS),
Greifswald, Germany. – TALK

2022 | **Connectivity of deep-sea basins in the North-Atlantic using invertebrate taxa as surrogates – preliminary results** 23rd Annual Meeting of the Society of Biological
Systematics, Hamburg, Germany. – TALK

2022 | **The IceDivA project: Exploring biogeographic connectivity of deep-sea basins in the North-Atlantic using invertebrate taxa as surrogates** 20. Crustaceologen-Tagung,
Kiel, Germany. – TALK

2022 | **A suprabenthic predatory amphipod showing a global distribution in the abyss,** 20. Crustaceologen-Tagung, Kiel, Germany. – POSTER

2022 | **What is the IceDivA project? Research expeditions and science in the face of Covid-19** The Challenger Society Conference 2022, London, United Kingdom. – TALK

DATA

Physical oceanography:

ADCP current measurements (75 kHz) during RV SONNE cruise SO286 Size:
12950510 data points, <https://doi.org/10.1594/PANGAEA.956601>

Continuous thermosalinograph oceanography along RV SONNE cruise track SO286, Size:
180062 data points, <https://doi.org/10.1594/PANGAEA.952357>

Species distribution data:

Data from: Pan-Atlantic comparison of deep-water macrobenthos diversity collected by epibenthic sledge sampling and analysis of patterns and environmental drivers. GB/NERC/BAS/PDC/01719

Bathymetry

Master tracks in different resolutions of SONNE cruise SO286, Emden – Las Palmas, 2021-11-05 – 2021-12-08, <https://doi.org/10.1594/PANGAEA.942629>

Master track of SONNE cruise SO286 in 1 sec resolution (zipped, 16.7 MB), <https://doi.org/10.1594/PANGAEA.942626>

Multibeam bathymetry processed data (Kongsberg EM 122 transit dataset) of RV SONNE during cruise SO286, North Atlantic Ocean, Size: 29 data points, <https://doi.org/10.1594/PANGAEA.950893>

CRUISE REPORT

Brix, S; Taylor, J; Kieneke, A et al. (2022): Icelandic marine Animals: Genetics and Ecology meets Diversity along latitudinal gradients in the deep sea of the Atlantic Ocean 2, Cruise No. SO286, 04.11.2021 – 09.12.2021, Emden (Germany) – Las Palmas (Spain). SONNE-Berichte, Begutachtungspanel Forschungsschiffe

Cruise identifier: Link to cruise report

(e. g. SO286: doi:XXX) is unfortunately not possible yet.

SO287

Pan-Atlantic connectivity of marine biogeochemical and ecological processes and the impact of anthropogenic pressures

AUTHORS

GEOMAR Helmholtz Centre for Ocean Research Kiel | Kiel, Germany

B. Quack, D. Arevalo, H. Bange, K. Becker, W. Böhme, D. Booge, A. Engel, H. Hephach, R. Ingeniero, J. Karnatz, C. Marandino, T. Müller, B. Pontiller, L. Scheidemann

Hereon | Geesthacht, Germany

M. Hieronymi, R. Röttgers, G. Schulz

IUP – Institut für Umweltphysik | Bremen, Germany

T. Bösch, M. Latsch, F. Wittrock

ARDITI – Agência Regional para o Desenvolvimento da Investigação, Tecnologia e Inovação | Funchal, Portugal

R. Caldeira, C. Cardoso, J. Reis, A. Rosa

CRODT – Centre de Recherche Océanographique de Dakar Thiaroye | Dakar, Senegal

N. Diogoul

IRD - Institut de Recherche pour le Développement | Dakar, Senegal

P. Brehmer

RSMAS – Rosenstiel School of Marine and Atmospheric Science | Miami, Florida, USA

E. Atlas

SDU – University of Southern Denmark | Odense, Denmark

C. Löscher, P. Xu

CNRS – Centre national de la recherche scientifique, Station Biologique de Roscoff | Roscoff, France

P. Potin

UiO – University of Oslo | Oslo, Norway

S. Auganaes, K. Krüger

SO287-CONNECT FROM LAS PALMAS TO GUAYAQUIL IN WINTER 2021/2022

The transit of R/V SONNE from Las Palmas (11.12.2021) to Guayaquil, Ecuador (11.01.2022) was directly related to the international collaborative project SO287-CONNECT of GEOMAR in cooperation with Hereon and the University of Bremen, supported by the German Federal Ministry of Education and Research (BMBF) between October 2021 and January 2024. The research expedition was conducted to decipher the coupling of biogeochemical and ecological processes and their influence on atmospheric chemistry. A comprehensive work program combined continuous underway water and atmospheric sampling and measurements, incubations, as well as 36 stations from the upwelling zones off Africa into the Sargasso Sea and further to the Caribbean and the equatorial Pacific.

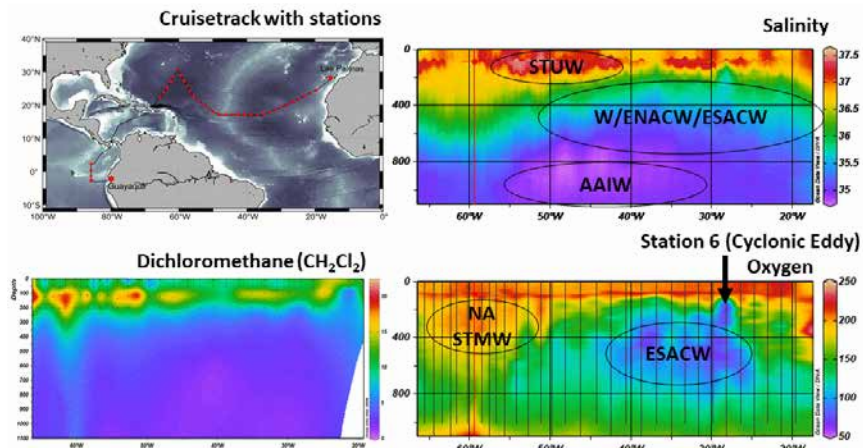


Figure 1: Track chart of R/V SONNE cruise SO287-CONNECT with stations (upper left). Salinity (upper right) and oxygen (lower right), with encountered water masses along the route in the top 1100 m of the Atlantic as North Atlantic Subtropical Mode water (NASTMW), subtropical Underwater (SUW), western and eastern North and South Atlantic Central Waters (W/ENACW/ESACW), Antarctic intermediate water (AAIW), dichloromethane (pM) in the upper water column (lower left).

WATER MASS ANALYSIS ALONG THE NORTH EQUATORIAL CURRENT

With the Extended Multi-parameter analysis (OMP) from Karstensen & Tomczak (1998) with source water types (SWT) based on Liu & Tanhua (2021), eight upper and lower

central water masses, Antarctic Intermediate and Mediterranean Water, as well as North Atlantic Deep Waters, Antarctic Bottom and Northeast Atlantic Bottom Water were analysed in the Atlantic transect. Based on a literature search, it was possible to additionally identify North Atlantic Subtropical Mode water and subtropical Underwater (Goes et al., 2005) in the upper depth ranges. An interesting feature in the OMP analysis is related to the higher proportions of SACW at station 6, which is related to a cyclonic low-oxygen eddy (Figure 1). The water masses sampled at this station were significantly different from the other stations, which underlines the efficiency of eddies formed in the Mauritanian upwelling region in transporting tracers from the coast to the open ocean.

The biogeochemical and ecological processes along the cruise track need to be interpreted on the background of this water mass analysis, e. g. for marine and atmospheric halocarbons during the cruise.

HALOCARBON DYNAMICS

The spatial variations of natural and anthropogenic short-lived bromo-, chloro- and iodocarbons, e. g. bromoform (CHBr_3), methyl iodide (CH_3I), di- and trichloromethane (CH_2Cl_2 , CHCl_3) were highly dynamic in both the ocean and atmosphere. Production of brominated and, surprisingly, chlorinated methanes occurred in the deep chlorophyll maximum (Figure 1), while the chemistry of iodinated compounds was closely related to light. The cycling of anthropogenic chlorinated compounds was coupled to water mass formation and transport. First time incubation experiments of halocarbon release from the floating seaweed species *Sargassum* spp. suggest, that during its extensive blooms in the Atlantic, this brown seaweed plays an important role in the emissions of natural halogens and organic matter.

MARINE CARBON AND NITROGEN CYCLING

Marine carbon cycling was tightly coupled to differences in microbial diversity, activity, and abundance from the Canary current upwelling system into the subtropical gyre. Phosphorus availability was an important driver of shifts in the bacterial community composition along the transect affecting the semi-labile DOM pool, supported by pronounced changes in the relative proportion of transcribed genes associated with the utilization of phosphorus and transcription of carbohydrate-active enzymes.

The vertical distribution of gel particles was investigated along the cruise track from the surface to the deep sea. Significant distinctions were found in terms of particle abundances and sizes between the productive upwelling system at the northwest coast of Africa compared to the open ocean regime in the western north Atlantic.

Ambient atmospheric concentrations of nitrogen dioxide (NO_2 , manmade pollutant) were highly variable, but were typically below 0.1 parts per billion (ppbv) in air from “clean sector” wind directions unperturbed by the ship’s own emissions. Even at night, no molecular iodine (I_2 , natural emissions) above the instrument’s detection limit (~ 1 pptv)

was observed, except for a small iodine signal (~2 pptv) in the equatorial Pacific. Time series measurements of the solar flux, photosynthetically active radiation (PAR), and the photolysis rate coefficients for 16 photolabile atmospheric gases will be used for the interpretation of halocarbon cycling above the subtropical North Atlantic.

As the cruise went through the Equatorial Tropical Pacific (ETP), we took the opportunity to revisit a section at 85.5°W, which covers the ETP oxygen minimum zone (OMZ) that has been sampled and investigated on prior cruises. All ocean surface waters were above or close to equilibrium with respect to the corresponding atmospheric values of nitrous oxide (N₂O) and methane (CH₄). Enhanced N₂O saturations were observed in the vicinity of the Canary current upwelling system and above the OMZ in the ETP. Enhanced CH₄ saturations were also observed in coastal waters of the ETP. N₂O concentrations within the hypoxic zone were twice as high as those in the rest of the water column during SO287. Comparison of depth-integrated concentrations of dissolved N₂O with previous cruises reveals comparatively high values during La Niña years, maximizing during SO287.

SO287 connect was the first study to measure surface dissolved nitric oxide (NO) concentration across the Atlantic Ocean. Dissolved NO concentrations ranged from 9.38 to 48.24 pM (average: 13.89 ± 5.82 pM). Notably higher concentrations were observed in the eastern Tropical North Atlantic Ocean, southeast of the Azores Archipelago, and northwest of the Canary Islands. The sea-to-air-flux ranged from 1.12×10⁻¹⁸ to 4.78×10⁻¹⁷ mol m² s⁻¹ (average: 1.50 ± 0.99×10⁻¹⁷ mol m² s⁻¹), indicating that the open ocean was a notable source of NO to the atmosphere during this campaign.

A metagenomic approach was utilized across a dissolved oxygen (DO) gradient from oxic to suboxic conditions in the ETP. The findings were compared to the Tara Ocean datasets obtained from the same region under a comparable La Niña event in 2011. SO287 observed a decrease in microbial diversity and abundance, coupled with an increase in most nitrogen metabolisms as DO decreased. Dominant microbial groups and key functions displayed varying sensitivities to different DO ranges (5 to >120 μmol/kg). The shift in functional groups occurred when DO dropped below 120, 90, 80, 60, or 12 μmol/kg. A significant reduction in the relative abundance of SAR11, along with an increase in nitrogen metabolisms, e. g., denitrification (N₂O production) and nitrogen fixation, were observed in our datasets comparing to Tara Ocean datasets. The study improves our understanding of the response of microbial diversity, groups, and functions to a future OMZ expansion and how ENSO events impact in-situ microbial community and their roles.

INFLUENCE OF SHIP EMISSIONS ON DMS

Dimethyl sulfide (DMS) biogenically produced in the ocean is an important precursor of cloud condensation nuclei in the remote marine boundary layer and therefore influences the radiation budget of the Earth. The goal during SO287 was to investigate, how ship

emissions (i. e. use of scrubbers) impact the trace gas biogeochemistry in the surface ocean. Incubation experiments revealed a significant difference of DMS concentrations between the scrubber treatment and the controls. DMS concentrations in the scrubber treated water are drastically reduced at the start of the experiment indicating an immediate effect (possibly pH related) of scrubber water addition on the actual DMS concentration. Initial DMSO concentrations in the scrubber treated water were significantly higher than in the control during the experiment with a 2% scrubber addition indicating a pH induced oxidation to DMSO. The overall decrease of the climate relevant trace gas DMS through addition of scrubber effluent could facilitate climate change.

TRANS-ATLANTIC MICRO-PLASTIC

95% of plastic particles along the transect were either polyethylene (PE) or polypropylene, with PE clearly dominating. Furthermore, the distribution of the plastic particles along the transect was defined by a few stations with high concentrations, such as the one in the North Atlantic garbage patch located in the North Atlantic gyre.

UPTAKE OF OZONE TO THE OCEAN

Atmospheric ozone levels and uptake of ozone to the ocean alongside biogeochemical properties of the seawater (including iodine speciation, fatty acid composition, DOC concentrations and surface tension) were measured in order to investigate the mechanisms of ozone uptake. Measured ambient ozone mixing ratios 10 m above sea level were between ~ 5 – 40 ppb. The highest concentrations were observed in the Atlantic (35.0 ± 2.6 ppb), followed by the Caribbean (17.7 ± 2.1 ppb) and ETP (6.5 ± 1.4 ppb). Ozone uptake to seawater was measured for samples from the CTD, underway system and from the sea-surface microlayer (SML). The SML was the most reactive towards ozone, with chemical reactivity to ozone on average 17% higher than in the underlying water. Iodine speciation (iodide, iodate, dissolved organic iodine, total inorganic iodine and total dissolved iodine) was measured for all samples, with the reduced form, iodide, representing the most ozone-reactive fraction. Mean (\pm sd) iodide concentrations in the CTD, SML and underway samples were 140 ± 24 , 59 ± 11 and 139 ± 29 nM, respectively, revealing a significant depletion of iodide in the SML compared to the near-surface CTD sample. Mean total dissolved iodine concentrations were 438 ± 20 , 401 ± 15 and 397 ± 15 nM for CTD, SML and underway samples. The SML samples were enriched in DOC relative to the CTD samples (EF=1.4) and their concentration range was far greater (0.68 – 8.9 mgL⁻¹ vs 1.4 – 2.6 mgL⁻¹). SML surface tensions were depressed relative to the CTD seawater (72.1 ± 1.6 vs 73.5 ± 0.2) indicating enhanced surfactant concentrations in the SML. The DOC and surface tension measurements show that there is increased organic material concentration within the SML. This dataset will help improve our understanding of the mechanism and rates of ozone uptake to the ocean.

PLANKTON DIEL MIGRATION

Sea temperature and dissolved oxygen were identified as primary drivers of SSLs distribution, highlighting their significance in oceanic ecosystems and global climate

regulation. The planktonic sound scattering layer (SSLs) revealed strong regional variations in the Atlantic and Pacific and responses to environmental factors in the North Atlantic Gyre. Sea temperature and DO were identified as primary drivers of SSL distribution, highlighting their significance in oceanic ecosystems and global climate regulation. The Pacific's shallow SSLs were linked to the OMZ.

REFERENCES

Karstensen J, Tomczak M, Age determination of mixed water masses using CFC and oxygen data. *Journal of Geophysical Research: Oceans* 1998, 103(C9), 18599–18609. <https://doi.org/10.1029/98JC00889>.

Liu M, Tanhua T, Water masses in the Atlantic Ocean: Characteristics and distributions. *Ocean Science* 2021, 17(2), 463–486. <https://doi.org/10.5194/os-17-463-2021>.

Goes M, Molinari R, da Silveira I, Wainer I, Retroreflections of the north brazil current during February 2002, *Deep-Sea Res. Pt. I* 2005, 52, 647–667, <https://doi.org/10.1016/j.dsr.2004.10.010>.

SCIENTIFIC OUTPUT

LIST OF PUBLICATIONS

Auganæs, S, Ozone above the tropical Atlantic ocean, 19. June 2023 at the University of Oslo.

Bi S, Hieronymi M, Röttgers R, Bio-geo-optical modelling of natural waters, *Front. Mar. Sci.* 2023, 10, 1196352. doi: 10.3389/fmars.2023.1196352.

Böhme W, On the relationships between dissolved organic matter, inorganic nutrients, and the bacterial community composition in the tropical North Atlantic Ocean", Masterthesis, 06. April 2023 at the Christian-Albrechts-Universität zu Kiel (CAU Kiel).

Karnatz J, Sargassum seaweed in the North Atlantic and its potential contributions to the emissions of halocarbons and DOC", Masterthesis 02. December 2022 at the Christian-Albrechts-Universität zu Kiel (CAU Kiel).

Keß K, Interaction of dimethyl sulphide (DMS) and hypobromous acid (HOBr) in global ocean surface waters, Masterthesis 20. August 2023 at the Christian-Albrechts-Universität zu Kiel (CAU Kiel).

Müller T, Abundance and size distribution of Transparent Exopolymer Particles (TEP) and Coomassie Stainable Particles (CSP) in the North Atlantic Ocean, Masterthesis 29. März 2023 at the Christian-Albrechts-Universität zu Kiel (CAU Kiel).

Offin A J M B, Iodine volatilisation from the ocean, PhD thesis (submitted) 2023, School of Chemistry, University of Leicester (United Kingdom).

Pohlmann M, Nitrous oxide measurements in the western tropical South Pacific, Bachelor thesis, Christian-Albrechts-Universität zu Kiel, 2023, Kiel, Germany, 41 pp.

Xu, P, Microbial Ecology under Ocean Deoxygenation: Diversity, Metabolisms, Environmental Controls, Ph.D. thesis, SDU, 2023, Syddansk Universitet. Det Naturvidenskabelige Fakultet. <https://doi.org/10.21996/nag8-j503>.

Baker et al., Iodine speciation in aerosols over the tropical Atlantic and Pacific Oceans, (working title, ongoing analysis).

Baker et al., Trace metal fractional solubility in aerosols collected over the tropical southeast Pacific Ocean, (working title, ongoing analysis).

Becker K W, Engel A., Variations of the surface ocean microbial lipidome across a biogeochemical continuum from the productive Canary upwelling system to the oligotrophic Sargasso Sea, (working title, ongoing analysis).

Becker K W, Pontiller B, Engel A; Effects of nutrient availability on lipid biosynthesis in marine prokaryotes based on combined metatranscriptomic and lipidomic analysis, (working title, ongoing analysis).

Brown L, Chemical Controls on the Uptake of Ozone to the Ocean, PhD thesis, University of York, to be submitted 2024.

Devresse et al., Size-fractionated plankton respiration and bacterial growth efficiency in the subtropical north Atlantic ocean, (working title, ongoing analysis).

Diogoul et al., Pelagic Sound Scattering Layer distribution and diel vertical migration behavior across the North Est Atlantic & Eastern Tropical Pacific Ocean.

Hepach et al., Tracing organic matter degradation along an East-to-West gradient in the subtropical Atlantic, (working title, ongoing analysis).

Ingeniero et al., Underway Measurement of Dissolved Nitric Oxide in the Tropical North Atlantic Ocean and in the Eastern Pacific Ocean.

Müller T et al., Gel-like particles distribution along a trophic gradient in the North Atlantic Ocean.

Pontiller B, Böhme F W, Hepach H, Engel A, Dissolved organic matter and nutrient availability across the tropical North Atlantic shape microbial community structure (working title, ongoing analysis, writing in progress).

Pontiller B, Böhme F W, Lundin D, Engel A, Expression patterns of carbohydrate, nitrogen, and phosphorus utilization by marine prokaryotes across the tropical North Atlantic, (working title, ongoing analysis, writing in progress).

Pontiller B, Lundin D, Knoop T, Biastoch, A., Engel. A, Tropical North Atlantic resistome: Exploring antibiotic resistance gene abundance, distribution, and connectivity from the eastern to the western tropical North Atlantic, (working title, ongoing analysis).

Quack B, Atlas E, Booge D, Cardoso C, Hepach H., Karnatz J, Potin P, Reis J, Rosa, A, Schmidt L, The biogeochemistry of halocarbons in the subtropical North Atlantic, (working title, ongoing analysis).

Scheidemann L, Schlundt C, Pontiller B, Galgani L, Beck A, Engel A, Abundance of small plastic marine Debris (PMD) in the surface equatorial Atlantic Ocean along an East to west transect and its colonisation by bacteria, (working title, ongoing analysis).

Weddell, Katherine, Links between Oceanic Ozone Uptake and Ocean Biology, PhD thesis, University of York, to be submitted 2024.

Xu, P et al., Metagenomic insights into variability of microbial diversity and functions in the Eastern Tropical Pacific Ocean, (writing in progress).

Xu, P et al., Do sinking particles promote vertical and horizontal connectivity in the ocean, (working title, ongoing analysis).

LIST OF CONFERENCE PRESENTATIONS

2022 | **Vom Startschuss ins Ziel – Die sportliche Expedition SO287-CONNECT**

<https://www.geomar.de/news/>

article/16032022-vortragsreihe-wissenschaften-online-vortragPublic

2022 | **The Chemical Controls on the Uptake of Ozone to the Ocean** iCACGP-IGAC Joint Conference, Manchester, United Kingdom

2023 | **Halocarbon dynamics from Las Palmas to Guayaquil in winter 2021/2022 – Results of SO287-CONNECT** EGU, Vienna, Austria

2023 | **Measurements of trace gases with a MAX-DOAS system during a ship cruise from the Canaries to Ecuador (SO287)** on board of RV Sonne EGU, Vienna, Austria

2023 | **Variations in microbial community and organic matter composition along a coastal upwelling to open ocean continuum in the subtropical North Atlantic ASLO**, Palma de Mallorca, Spain

2023 | **Atmospheric Chemistry On and Over the Ocean** Atmospheric Chemistry GRC Conference, Maine, USA

DATA

Continuous thermosalinograph oceanography along RV SONNE cruise track SO287: <https://doi.org/10.1594/PANGAEA.953082>

Multibeam bathymetry raw data (Kongsberg EM 122 entire dataset) of RV SONNE during cruise SO287: <https://doi.org/10.1594/PANGAEA.943705>

Master tracks in different resolutions of SONNE cruise SO287, Las Palmas - Guayaquil, 2021-12-11 – 2022-01-11. GEOMAR – Helmholtz Centre for Ocean Research Kiel: <https://doi.org/10.1594/PANGAEA.944256>

ADCP current measurements (75 kHz) during RV SONNE cruise SO287: <https://doi.org/10.1594/PANGAEA.945808>

Continuous bio-optical measurements of chlorophyll a and turbidity along RV SONNE cruise SO287 (CONNECT): <https://doi.org/10.1594/PANGAEA.959910>

Physical oceanography (CTD): <https://portal.geomar.de/group/so287-connect/data>

e. g. son_287_1_ctd_rel4.zip, SO287_ADCP_data_38and75KHz(raw), SO287_eddies.zip, SO287_OMPA_water masses

Biogeochemical variables:

<https://portal.geomar.de/group/so287-connect/data>.

e. g. SO287_primaryproduction, SO287_bacphytvir_cellcounts, SO287_bacterialproduction, SO287_POCN_POP_BSi, SO287_pigmente_HEREON.xlsx, SO287_CDOM_ABS_HEREON.xlsx, SO287_DOC__DON_DOP_CTD, SO287_Dissolved_carbohydrates_CTD, size-fractionned respiration rates using the in-vivo electron transport system method

Chemical variables:

<https://portal.geomar.de/group/so287-connect/data>.

e. g. SO287_UW_4ODV_1min_import.xlsx, SO287_UW_Masterfile.xlsx, SO287_CTD_Masterfile.xlsx, SO287_oxygen_and_nutrient_data, DMS_UW.txt, SO287incubation_NO, Underway_measurements_of_N2O_CH4_and_CO2, DMS_CTD.txt

Atmospheric variables:

<https://portal.geomar.de/group/so287-connect/data>.

e. g. Trace_gas_canister_data, SO287-aerosol, SO287_Ozone.zip, SO287_photolysis_rates_Leicester.xlsx, Surface ozone_minutely_clean.csv, IUP-Bremen_MAX-DOAS_and_InSitu_data.zip, SO287_Radiosondes.zip, SO287_AOD.zip

SDU Metagenomic sequence data has been archived in the NCBI Sequence Read Archive (SRA) database under the Bioproject PRJNA983277 from SRR24907232 to SRR24907253, which will be released after the work is published or after 2025.

CRUISE REPORT

SO287: doi:10.48433/cr_so287

SO288

Measuring Tectonic Strain Build-up On The Seafloor With The GeoSEA Array

AUTHORS

GEOMAR Helmholtz Centre for Ocean Research Kiel | Kiel, Germany

H. Kopp, D. Lange, A. Jegen

THE EMERGING FIELD OF SEAFLOOR GEODESY

The ocean floor is the outer solid shell for over 70% of our planet, which is continuously moved and deformed in the course of global plate tectonics. These processes lead to tectonic stresses building up in the seafloor, which over long periods of time become so large that they suddenly and usually unexpectedly discharge in an earthquake. During the past three decades, advances made by using space geodetic systems, such as GPS and InSAR, have revolutionized our ability to precisely track actively deforming areas onshore at high spatial and temporal resolution. In the marine environment, however, the seafloor cannot be studied with the established tools of tectonic geodesy, as water is not a suitable medium for geodetic systems that depend on the relatively unperturbed transmission of electromagnetic waves. Offshore seafloor geodesy aims at precise underwater measurements of interstation distances, absolute positions, water depth, and tilt (Petersen et al., 2019). Seafloor displacement occurs in the horizontal (x,y) and vertical direction (z) as a function of time (t) (Bürgmann and Chadwell, 2014). The vertical displacement is measured by monitoring pressure variations at the seafloor. Horizontal seafloor displacement can be measured either using an acoustic/GPS combination to provide absolute positioning or by long-term acoustic direct-path ranging in-between beacons fixed on the seafloor.

We use the direct-path ranging technique with GEOMAR's GeoSEA Array (Geodetic Earthquake Observatory on the SEAfloor) to record crustal deformation between stations on the seafloor. The GeoSEA array was installed offshore Chile during SO244 in 2015 and was recovered during cruise SO288 in 2022. SO288 was the first expedition of the R/V SONNE to return to the Pacific Ocean from a South American port during the COVID-19 pandemic.

THE GEOSEA ARRAY AND RECOVERY DURING SO288 RECOVERY

The GeoSEA array is a network of seafloor transponders used in direct path measurements at water depths up to 6.000 m. Distance changes are estimated using the travel time observations together with the sound speed of the water. To resolve deformation with mm-resolution, the sound speed is calculated using the pressure and temperature sensors

of the geodetic instruments. Direct path acoustic ranging with baselines up to 2.500 m resolves seafloor deformation at high resolution (< 5mm repeatability). The array is configured for continuous interrogations to monitor the state of seafloor deformation, e. g. active faults or continental slopes. Data retrieval may be conducted via an acoustic modem using a vessel or a surface vehicle (wave glider) as a platform. The GeoSEA array consists of a total of 34 acoustic transponders, which have been deployed in various tectonic settings (Lange et al., 2019; Urlaub et al., 2018). Three networks consisting of 8, 10 and 5 transponders, respectively, were installed in 2015 on the continental slope and outer rise of the North Chilean subduction zone (Figure 1) during SO244 and were recovered during SO288. The arrays were positioned in water depths between 2.400 m and 5.200 m using the deep-sea cable of R/V SONNE (Kopp et al., 2017). The recovery of the instruments from the seabed required using a remotely operated vehicle (ROV). Despite their long service life on the seabed of over 6 years due to the COVID-19 pandemic, the stations showed no signs of corrosion and the technical functionality was fully given for each station.

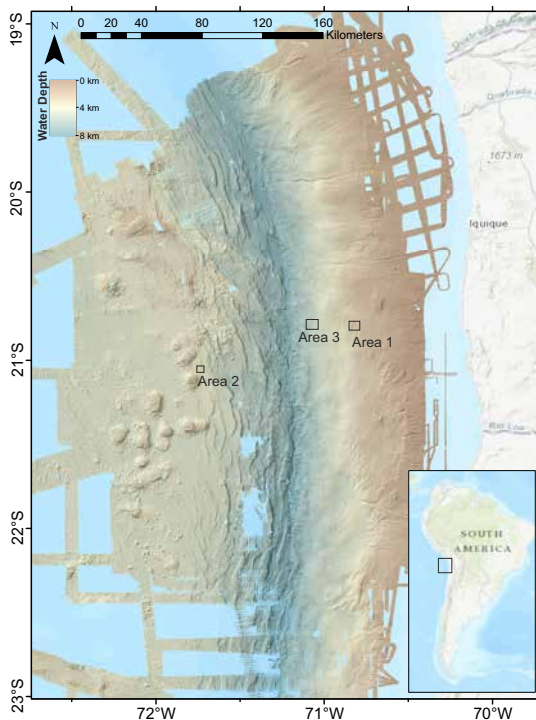


Figure 1: High-resolution seafloor map of the continental slope off northern Chile with the three locations of the GeoSEA array, which are located on the middle and lower slope and on the oceanic plate. The map is based on bathymetric data from several cruises of the research vessels SONNE and METEOR. All 23 GeoSEA transponders were successfully recovered and registered 100% of the time during the monitoring period. The GeoSEA survey represents the first geodetic seafloor transect across a subduction zone extending from the oceanic plate to the lower and middle slopes of the upper continental plate.

The main objective of the GeoSEA investigation is to monitor the surface deformation as a consequence of the tectonic state of the plate boundary. The coupling of the megathrust at depth can be compensated by free slip, creep and complete locking. In AREA3 (Figure 1), where we measure baseline changes with an accuracy of 0.5 mm, our in-situ observation of seafloor deformation shows no change in baseline (Figure 2). An analysis of the directionality of the deformation has further confirmed this observation. Furthermore, the pressure data for all three grids show no deformation and a very high resolution for short-term changes in water depth. The pressure measurements indicate that there are no sudden pressure changes and thus no vertical crustal movement. The initial evaluation of the geodetic GeoSEA dataset retrieved during SO288 shows that the resolution of the 2.5-year survey is sufficient to determine the horizontal strain rate.

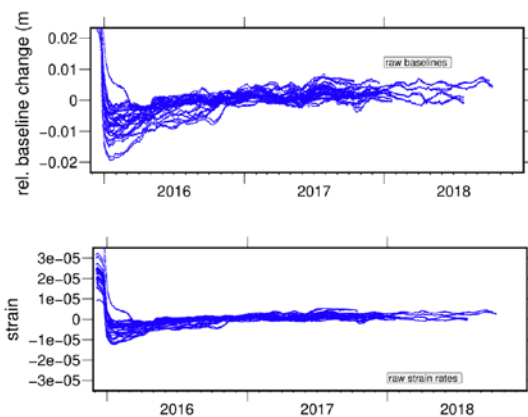


Figure 2: Relative baseline changes in AREA3 (upper graph) for all measured baselines between the intercommunicating eight transponders. The baseline between stations 2306 and 2308 showed an offset in the baseline of ~ 15 mm (not shown), which is associated with a data upload in December 2016 and, therefore, likely represents a data artifact. The signal during the first months after the installation is an adaption effect of the sensors to the deep-sea environment.

SEISMIC SURVEY DURING SO288

During SO288, the subsurface at the three installation locations of the GeoSEA array was investigated (Figure 1) to study the tectonics of the seabed. The active seismic survey using a multichannel streamer and ocean bottom seismometers (OBS) revealed sub-seafloor faulting and deformation as well as the velocity field to a depth of ~ 8 km.

On the continental slope beneath deployment site AREA 1, the seabed and sub-seafloor show a high degree of deformation, which manifests itself in active extensional faults and folds (Figure 3, upper panel). The continental basement is only covered by a thin sediment layer; most sediments are highly compacted. Eight GeoSEA stations were placed over a series of bathymetric lineaments, and the seismic section shows that these are surface traces of active faults.

Below the seafloor reflection on the oceanic plate on the outer rise at deployment site AREA 2 (Figure 3, lower panel) at 5.39 s TWT in the southwestern part of the profile, an approximately 0.1 s TWT thick package of hemi-pelagic / pelagic sediments is visible, indicated by continuous, coherent and parallel reflections. Below these sediments, at 5.5 s TWT, a strong coherent reflection marks the impedance contrast between the sediments and the basaltic crust. Trench-parallel thrusts related to plate bending (black dashed lines in Figure 3) reach distances of ~ 0.1 s TWT. In the northeast of the profile, a tilted crustal block can be recognized under the horizontally layered sedimentary layer.

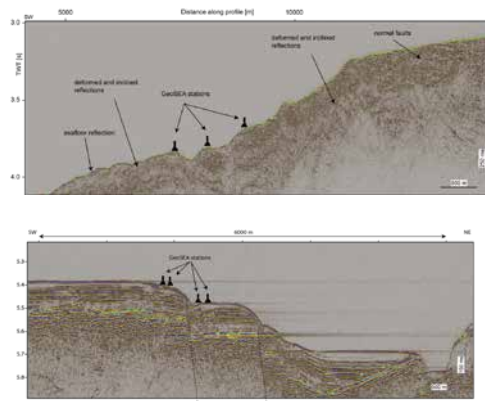


Figure 3: Reflection seismic profile (MCS) over deployment sites at AREA1 (upper panel) and AREA 2 (lower panel). Compare Figure 1 for location. The geodetic stations are marked as black tripods on the seabed. The upper continental slope is characterized by large-scale deformation and fault structures (upper panel). The GeoSEA stations in AREA 2 are positioned on both sides of the surface trace of a crustal-scale normal fault (lower panel) which originates from the bending of the oceanic lithosphere as it enters the deep-sea trench visible on the right side of the seismic section.

CROSS-BENEFICIAL APPROACH TO OCEANOGRAPHIC AND GEODETIC STUDIES

Even though the global ocean has a mean depth of 3.700 m, ocean observations below 2.000 m are sparse compared to the deep ocean's vastness. However, because of the importance of deep-sea observations for accurate climatologic and oceanographic prediction models, as well as for offshore geodesy, better knowledge of the extent and drivers of deep-sea variability is crucial. To this end, data from SO288 were used to quantify regional deep ocean variability. This cross-beneficial approach combining geodetic and oceanographic parameters uses observed temperature, pressure and sound velocity time series. By estimating salinity and density, the full spectrum of the sites' hydrographic variability was quantified from a multi-hourly to multiannual time scale and with average inter-station distances of less than 1 km. The analysis reveals independent dynamical regimes and periodic temperature anomalies overprinting a multi-year warming trend in the deep ocean.

REFERENCES

Bürgmann R, Chadwell D, Seafloor Geodesy, Annual Review of Earth and Planetary Sciences 2014 42:1, 509-534, doi:10.1146/annurev-earth-060313-054953.

Kopp H, Lange D, Steffen K P, Petersen F. Antragsteller/Inhaber: GEOMAR Helmholtz-Zentrum für Ozeanforschung Kiel, Vorrichtung zur lösabaren Verbindung eines Drahtes und Verfahren zum Ausbringen des Gerätes in ein Gewässer mit der Vorrichtung, 2017, DE 102016107558 A1 2017.10.26 (Patent).

Lange D, Kopp H, Royer J-Y, Henry P, et al., Interseismic Strain Build-up on the Submarine North Anatolian Fault Offshore Istanbul, Nature Communications 2019, 10:3006, doi:10.1038/s41467-019-11016-z.

Petersen F, Kopp H, Lange D, Hannemann K, Urlaub M, Invited Review Article: Measuring tectonic seafloor deformation and strain-build up with acoustic direct-path ranging, Journal of Geodynamics 2019, 124, 14-24, doi:10.1016/j.jog.2019.01.002.

Urlaub M, Petersen F, Gross F, Bonforte A, Puglisi G, Guglielmino F, Krastel S, Lange D, and Kopp H, Gravitational collapse of Mount Etna's southeastern flank, Science Advances 2018, 4 (10), eaat9700, doi:10.1126/sciadv.aat9700.

SCIENTIFIC OUTPUT

LIST OF PUBLICATIONS

Gutscher M-A, Quétel L, Murphys S, Ricobene G, Royer J-Y, Barreca G, Aurnia S, Klingehoefer F, Petersen F, Urlaub M, Krastel S, Gross F, Kopp H, Detecting strain with a fiber optic cable on the seafloor offshore Mount Etna, Southern Italy, Earth and Planetary Science Letters 2023, 616, doi:10.1016/j.epsl.2023.118230.

Jegen A, Lange D, Karstensen J, Pizarro O, Kopp H, Deep-ocean heterogeneity inferred from oceanographically calibrated data of offshore geodetic experiments, Science Advances 2023, submitted.

Ma B, Geersen J, Lange D, Klaeschen D, Grevemeyer I, Contreras-Reyes E, Petersen F, Riedel M, Xia Y, Tréhu A, Kopp H, Megathrust reflectivity reveals the updip limit of the 2014 Iquique earthquake rupture, Nature Communications 2022, doi:10.1038/s41467-022-31448-4.

Ma B, Geersen J, Klaeschen D, Contreras-Reyes E, Riedel M, Xia Y, Tréhu A, Lange D, Kopp H, Impact of the Iquique Ridge on structure and deformation of the North Chilean subduction zone, *J. South American Earth Sciences* 2023, 124, 104262, 10.1016/j.jsames.2023.104262 .

LIST OF CONFERENCE PRESENTATIONS

2023 | **Measuring tectonic strain build-up on the seafloor with the GeoSEA array**
IUGG, Berlin, Germany.

2022 | **In-situ monitoring of strain on the seafloor: An overview and results of the GeoSEA projects** EGU, Vienna, Austria.

2022 | **Subduction Zone Research: An Offshore Perspective** Franco-German Subduction Zone Conference/SZ4D Potsdam Coordination Workshop, Potsdam, Germany.

DATA

Multibeam bathymetry:

<https://doi.org/10.1594/PANGAEA.893033>

Physical oceanography (pressure, temperature, sound speed):

<https://doi.pangaea.de/10.1594/PANGAEA.961701>

Physical oceanography (ADCP current measurements):

<https://doi.org/10.1594/PANGAEA.957635>

Physical oceanography (thermosalinograph):

<https://doi.org/10.1594/PANGAEA.956343>

Navigation (Master track):

<https://doi.org/10.1594/PANGAEA.944960> and

<https://doi.org/10.1594/PANGAEA.944957> (zipped)

CRUISE REPORT

SO288: https://doi.org/10.3289/CR_SO288

POSTER

M169

Platinum input from German Rivers into the North Sea

AUTHORS

Constructor University | Bremen, Germany

A. Hollister, M. Schulte, A. Koschinsky

Ruđer Bošković Institute | Zagreb, Croatia

S. Marcinek, D. Omanovic

The aim of METEOR Cruise M169 (TRAM) was to assess in detail the role of the rivers Ems, Weser, and Elbe in the input of high-technology metals into the southern North Sea. These metals are increasingly used in new industries including renewable energy technologies as well as medicinal and cosmetics products and can be assumed to be potential emerging contaminants that affect the coastal North Sea via riverine input. Platinum (Pt) is one of these emerging critical metals with increasing anthropogenic use. 80% of Pt mass transfer in the environment is anthropogenic in origin (Sen and Peucker-Ehrenbrink 2012), with the primary anthropogenic sources being sewage (from the cancer treatment cis-platin) and road runoff (from catalytic converters) (Figure 1). Pt is known to bioaccumulate (e. g. in mussels) and is toxic in high concentrations (Neira et al 2015), but the long-term biological effects remain unknown. Thus far, relatively little estuarine data are available for Pt (e. g., Obato et al 2006, Soyol-Erdene and Huh 2012, Cobelo-García et al 2013, 2014, Pađan et al 2019), and none for the North Sea.

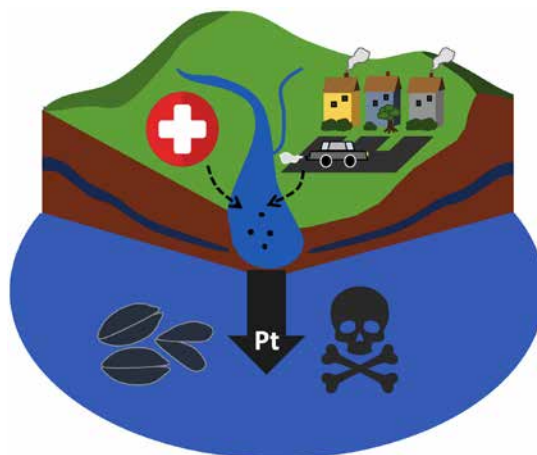


Figure 1: Diagram of Pt sources. Pt emerges from road runoff and sewage, enters rivers, and eventually enters estuaries/oceans, where it has the potential to be bioaccumulated.

This study examined dissolved ($<0.2 \mu\text{m}$) Pt input from three major north-German rivers (Elbe, Weser and Ems) into the southern North Sea (figure 2). Samples were collected with trace-metal clean GoFlo bottles or with a pump from a range of salinities ($S = 0.4 - 34$) from Weser and Elbe endmembers and the southern North Sea extending to Doggerbank, which represented a presumably pristine/unpolluted endmember. The Ems endmember could not be sampled due to locks. Ultrafiltered (10 kDa) samples were also collected at several selected stations. Platinum was analyzed in the home laboratories using voltammetric method (Pađan et al 2019).

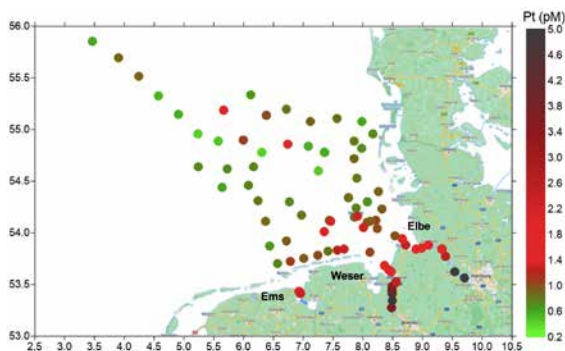


Figure 2: Dissolved ($<0.2 \mu\text{m}$) Pt distribution in the southern North Sea and three German rivers (Ems, Weser and Elbe). Labels at the map are latitude N and longitude E, respectively.

Dissolved Pt concentrations ranged from $\sim 5-6 \text{ pM}$ in the river endmembers ($S \leq 0.5$) to $\sim 0.5-1 \text{ pM}$ in the high-salinity North Sea stations ($S \geq 33$) (figure 3). In general, the Weser stations were highest in Pt, reflecting a different catchment area. Pt concentration followed a mostly – but not fully – conservative distribution, and an increase at $S \sim 3$ in the Elbe and Weser indicated possible desorption from particles.

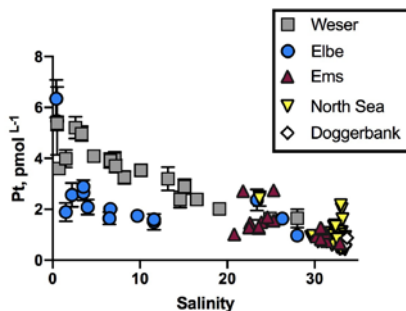


Figure 3: Dissolved ($<0.2 \mu\text{m}$) Pt plotted against salinity (PSU) in the Weser (grey squares), Elbe (blue circles) and Ems (red triangles) rivers and estuary mixing zones, as well as the North Sea ($S \geq 32$, yellow triangles) and Doggerbank ("pristine" northwesternmost point of our transect, white diamonds).

Tidal cycles (figure 4) were also collected in the three rivers and reflected potential non-conservative behavior at low salinity. In general, the Weser and Ems tidal cycles followed an inverse correlation with salinity, while the Elbe (lowest salinity tidal cycle) did not show this trend. All stations were elevated in Pt compared to Atlantic Ocean values of ~ 0.2 pM (López-Sánchez et al. 2019), indicating that the river influence of Pt extends through the southern North Sea. Pt in north German rivers and mixing zones was also higher than most other estuary data (generally ≤ 1 pM, Soyol-Erdene and Huh 2012, Cobelo-García et al 2013, 2014, <https://www.publish.csiro.au/EN/EN19157>), excluding Tokyo Bay (Japan) and the Ara River (Switzerland) (Obata et al. 2006). Further analysis of river endmember samples as well as sediment samples is needed to determine the specific source of the Pt and fully understand the sources, sinks and estuarine processes of this trace metal.

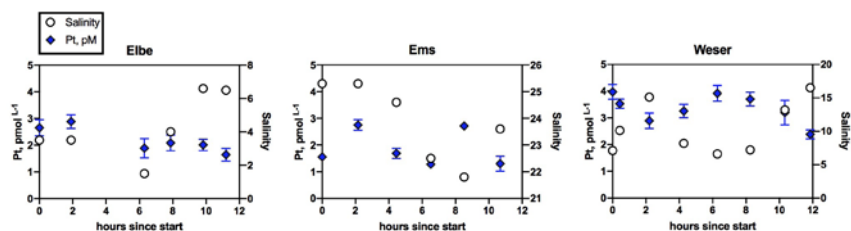


Figure 4: Tidal cycles in the Elbe, Ems and Weser River transects. Dissolved ($<0.2 \mu\text{m}$) Pt and salinity (PSU) are plotted against time. Note the different salinity ranges for the three rivers.

ACKNOWLEDGEMENT

Special thanks to the Captain and crew of R/V METEOR, the scientific team for their dedicated onboard work and the German Science Foundation DFG for funding for cruise M169 and the first evaluation phase.

REFERENCES

Cobelo-García A, López-Sánchez D E, Almécija C, & Santos-Echeandía J. Behavior of platinum during estuarine mixing (Pontevedra Ria, NW Iberian peninsula), *Marine Chemistry* 2013, 150, 11–18, doi: 10.1016/j.marchem.2013.01.005.

Cobelo-García A, López-Sánchez D E, Schäfer J, Petit J C J, Blanc G, Turner A Behavior and fluxes of Pt in the macrotidal Gironde estuary (SW France), *Marine Chemistry* 2014, 167, 93–101, doi: 10.1016/j.marchem.2014.07.006.

López-Sánchez D E, Cobelo-García A, Rijkenberg M J A, Gerringa, L J A, de Baar H J W New insights on the dissolved platinum behavior in the Atlantic Ocean, *Chemical Geology* 2019, 511, 204–211, doi: 10.1016/j.chemgeo.2019.01.003.

Neira P, Cobelo-García A, Besada V, Santos-Echeandía J, Bellas J Evidence of increased anthropogenic emissions of platinum: Time-series analysis of mussels (1991–2011) of an urban beach, *Science of the Total Environment* 2015, 514, 366–370, doi: 10.1016/j.scitotenv.2015.02.016.

Obata H, Yoshida T, Ogawa H Determination of picomolar levels of platinum in Estuarine Waters: A comparison of cathodic stripping voltammetry and isotope dilution-inductively coupled plasma mass spectrometry, *Analytica Chimica Acta* 2006, 580(1), 32–38, doi: 10.1016/j.aca.2006.07.044.

Pađan J, Marcinek S, Cindrić A-M, Layglon N, Garnier C, Salaün P, Cobelo-García A, Omanović D. Determination of sub-picomolar levels of platinum in the pristine Krka River estuary (Croatia) using improved voltammetric methodology, *Environmental Chemistry* 2019, 17(2), 77–84, doi:10.1071/EN19157.

Sen I S, Peucker-Ehrenbrink B Anthropogenic Disturbance of Element Cycles at the Earth's Surface, *Environmental Science and Technology* 2012, 46(16), 8601–8609, doi: 10.1021/es301261x.

Soyol-Erdene T.-O. Huh Y. Dissolved platinum in major rivers of East Asia: Implications for the Oceanic Budget, *Geochemistry, Geophysics, Geosystems* 2012, 13(6), Q06009, doi: 10.1029/2012gc004102.

M169

Geochemical fate of trace metals including high-technology elements during riverine export into the North Sea: results from ultrafiltration and passive sampling

AUTHORS

Bundesanstalt für Geowissenschaften und Rohstoffe (BGR) | Hanover, Germany
K. Schmidt, D. Krämer

Constructor University | Bremen, Germany
A. Koschinsky, M. Bau

INTRODUCTION

The increasing anthropogenic use of technology-critical trace elements (TCEs) such as rare earth elements and yttrium (REY), gallium (Ga), or platinum (Pt) rises concerns about an enhanced input of such contaminants of emerging concern (ICES 2021) into coastal marine environments and related adverse biological effects. However, the present understanding on the occurrence, speciation, mobility and fate of many of these elements in surface fresh and seawaters and the potential risks they pose to marine organisms is strongly limited. No regulations regarding their concentrations in the marine environment exist at present. While at one side, there is the obvious need to obtain high quality geochemical data to study TCEs in the environment and to derive suitable indicator variables for monitoring purposes, the analyses of trace metals especially in seawater is challenging and just now starts to become kind of a routine, at least for total dissolved concentrations. Furthermore, robust tools to discriminate geogenic versus anthropogenic input are required.

In this study, we investigated the geochemical behaviour and fate of selected TCEs (Ga, REY, V) and traditional trace metals (Cd, Co, Cu, Fe, Mn, Ni, Pb, and Zn) in three German estuaries and the present-day net fluxes into the open North Sea. In addition to routine water sampling during M169 (see Koschinsky et al.), we conducted sequential (ultra)filtration at six master stations (open North Sea at "Entenschnabel", Elbe River low salinity, Elbe estuary high salinity, Weser River low salinity, Weser estuary high salinity, Ems estuary high salinity) and at the Ems River station that was sampled by the land-based team, to assess the size distribution of target metals. In high volume water samples from these stations, passive samplers were deployed *ex situ* on board, to assess the labile-bound fractions of these metals that are potentially bioavailable. The passive sampling method uses the diffusive gradients in thin films (DGT) technique with constant accumulation of elements on a binding membrane for the time of deployment. DGT passive sampling is considered as speciation method, as strongly complexed metals do not dissociate in the diffusion layer (i. e., are not labile) and hence will not be enriched

in the binding layer. Besides value for geochemical process studies, the DGT method has gained some attractiveness as it may be used to indicate toxicity-relevant biotic uptake. Recently, research activities to explore the potential of DGTs for environmental monitoring programmes for contaminants in European coastal waters and for the definition of bioavailable Environmental Quality Standards (EQS) for metals significantly increased (e. g., MONITOOL project). However, these studies mainly focus on some traditional elements such as Ni and Cd, and information for TCE is largely missing.

This study contributes to a better understanding on the geochemical cycling of TCEs during estuarine mixing and increases the database for TCEs and other trace elements in coastal areas. It further enhances our knowledge on sampling and analytical aspects and establishes relationships between different assessment methods.

RESULTS

The size distribution of dissolved trace elements provides insight into the phase association with nanoparticles and colloids (NPCs) and the truly dissolved pool and can be used to deduce the geochemical behavior and fate during fresh water – seawater mixing in estuaries. In the German river estuaries of Elbe, Weser, and Ems as well as in the North Sea, Fe and Cu are significantly bound in large NPCs with more than 40% occurring in the >10 KDa pool, and less than 20–30% as truly dissolved (Figure 1). Cobalt, Ni, V, HREE and Mn predominantly occur in the size fraction <10 KDa (more than 80%), with only minor variations with changing salinity (Figure 1). Manganese is predominantly truly dissolved <1 KDa throughout the salinity region, but its strong concentration drop in low salinity regions confirms the known particle reactivity, related to the complex redox chemistry of Mn. Gallium association with different size pools strongly depends on salinity.

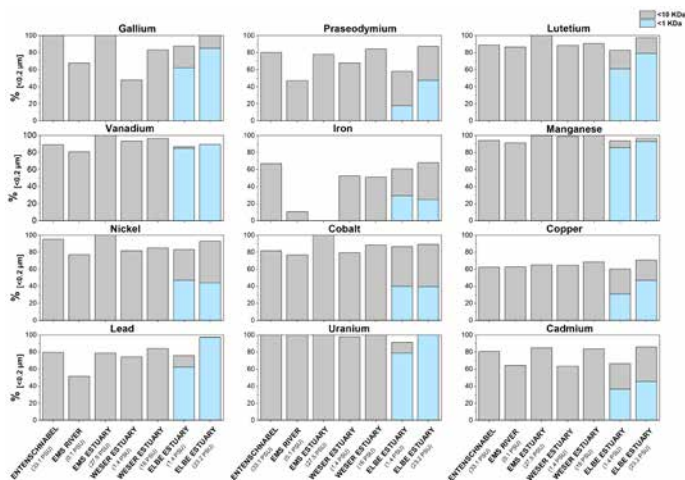


Figure 1: Size distribution of selected target metals between dissolved (<0.2 μm) and 10 KDa pools. Additional 1 KDa filtration was applied in the Elbe estuary.

With increasing salinity in the estuaries, the relative proportions of the smaller size fractions increase for Cd, Ga, REY, and Pb and can be partly related to flocculation of larger-sized colloids and nanoparticles. The observed mobilization of trace metals into the dissolved phase in mid salinity regions (see Koschinsky et al.) is mainly associated with a transformation from (nano)particulate phases into the truly dissolved (<1 KDa) and small colloidal (1 KDa-10 KDa) phases, as observed for example in the Elbe estuary for LREE, Ga, Mn, and Cd.

Within the REY group, we observe systematic differences in the size distribution independent from salinity (Figure 2). The association with the smaller size fractions < 10 KDa and <1 KDa strongly increases from LREE to HREE, with HREE mainly bound in the truly dissolved fraction (80–100%) compared to LREE where a significant proportion is bound to larger NPCs between 10 KDa and 0.2 μm (10–50%), or to smaller colloids between 1 and 10 KDa (>35%). Gadolinium, dominated by anthropogenic compounds (more than 90% in all ultrafiltered samples except for the open North Sea) is almost exclusively truly dissolved. The general distribution patterns reflect the known differences in solution complexation and relative particle reactivity between LREE and HREE. Decreasing LREE/HREE in all size fractions with increasing salinity likely relates to a preferential mobilization of (nano)particulate LREE into the small colloidal and truly dissolved pools along the salinity gradient.

The DGT lability of the investigated elements is complex and varies with salinity. Overall, DGT-labile concentrations display the same concentration trends as total dissolved concentrations. In the estuaries, DGT lability generally increases with increasing salinity (e. g., for REY, Co, Ni, and Cd), reflecting changes in physical and chemical speciation. In the open North Sea, highest DGT lability was observed for V and Cd (>70%). DGT-labile concentrations that are much lower than 0.2 or 10 KDa dissolved concentrations indicate that metals are strongly bound to small-sized organic ligands and are only weakly labile (e. g., Cu, where only about 25% of the <10 KDa fractions and about 50% of the <1 KDa fractions were measured with DGT). Also, the weak HREE lability in low to mid salinity regions is likely controlled by truly dissolved organic complexes. In contrast, DGT-labile LREE concentrations are higher than the 1 KDa dissolved concentrations, which indicates partial mobilization from NPCs and less relevance of organic complexes. Manganese, which is not known to be organically complexed also shows only weak DGT lability. Anthropogenic Gd is fully inert and not measured with DGT. Gallium shows the lowest DGT lability of all elements measured (3–20%), negatively correlating with salinity. This is surprising considering the 50% lability in the Pacific Ocean.

DGTs that were complementary deployed *in situ* using COSYNA underwater observatories off Helgoland (operated by AWI), in the Elbe estuary at Cuxhaven (operated by HZG) and in the tidal channel close to the island of Spiekeroog (operated by ICBM) at the same

time as the cruise took place, provides significantly higher DGT-labile concentrations for some elements compared to the 25L incubations on board. For example, Mn shows almost full lability as also known for the Pacific Ocean. This observation questions the applicability of *ex situ* DGT deployments for longer periods (in our case 3 weeks). Similarly long on-site deployments in well-mixed, partially highly dynamic, tidal settings seem to be more appropriate for assessing the DGT lability of trace metals in coastal areas. For elements such as Cu, Ga, or REY, differences between *ex situ* and *in situ* deployments are only minor.

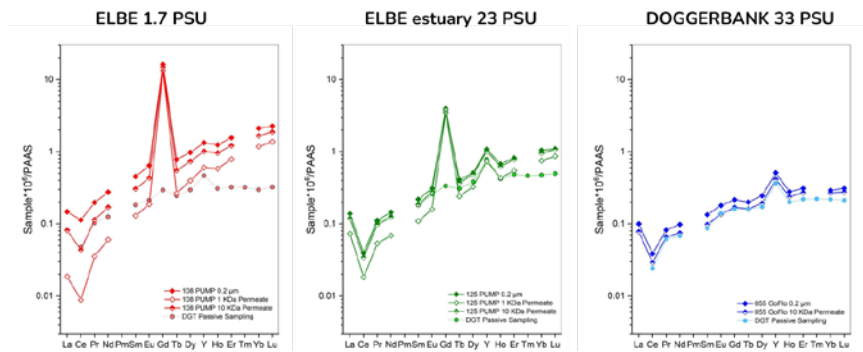


Figure 2: Shale-normalized REY in different size fractions of low and mid salinity samples from the Elbe estuary in comparison with the open North Sea station at Doggerbank.

ACKNOWLEDGEMENT

Special thanks to the Captain and crew of R/V METEOR, the scientific team for their dedicated onboard work and the German Science Foundation DFG for funding for cruise M169 and the first evaluation phase.

We are grateful for the possibility to use the COSYNA monitoring platforms off Helgoland, off Cuxhaven, and off Spiekeroog, and highly acknowledge the help from Philipp Fischer and Laura Eickelmann (AWI), Daniel Proefrock and Burkhard Erbsloeh (HZG), and Thomas Badewien and Helmo Nicolai (U Oldenburg) with organization and DGT handling.

M176/2

Do hydrothermal systems at the Mid-Atlantic Ridge affect the distribution of dissolved Rubidium, Uranium and Vanadium?

AUTHORS

Constructor University | Bremen, Germany

S. Poehle, L. Klose, A. Koschinsky

BACKGROUND AND OBJECTIVE

Hydrothermal systems have been studied in the past though the sampling was most often not done in direct vicinity of the vent sites. Hence, processes occurring in the first few kilometers off the vent site were not examined in detail. Within this framework of research cruise M176/2 (led by GEOMAR, Helmholtz Centre for Ocean Research, Kiel, Germany) a detailed sampling campaign starting at an emanating hydrothermal plume at the Rainbow vent field located at the Mid-Atlantic Ridge (MAR) up to 60 km distance was performed (Figure 1). The flow direction of the plume was assessed by tow-yo-CTD perpendicular to the estimated plume direction recording turbidity as a parameter for the hydrothermal signal. This approach enabled to map the plume dispersion from its vent site towards further downstream.

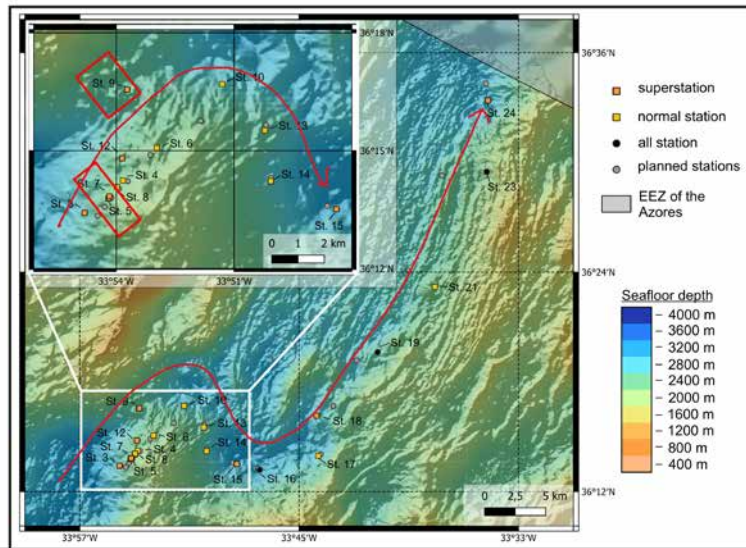


Figure 1: Sampling locations covered during research cruise M176/2 in September 2021. The red arrow sketches the direction of the hydrothermal plume from the Rainbow vent field through submarine valleys towards north-east. Data presented herein are from three stations (station 5, 7 and 9) highlighted in red frames.

A range of trace metals was focused in the past e. g. Fe, Mn (Nishioka et al., 2013; Resing et al., 2015) and are well studied at hydrothermal vent sites.

One focus of our group from Constructor University was trace elements that typically show a largely conservative behavior in the oceans. As a representative for conservative mixing and distribution we selected dissolved Rubidium (Rb) which belongs to the group of major cations in the marine water column.

While most trace elements do not behave conservatively in the ocean, Uranium (U) is known as a largely conservative trace metal (Ku et al., 1977) though variations from its typical depth profile have been observed in specific regimes with oxygen deficiency (Anderson et al., 1989). Since U is of high interest for isotope studies using U as a redox proxy in marine carbonates (Brüske et al., 2020; Clarkson et al., 2018), it is essential to understand the processes controlling the distribution of dissolved U in seawater.

Dissolved Vanadium (V) has been reported to show nutrient-like behavior in the marine water column which, however, mostly does not deviate much from a conservative distribution. Two redox species, V(IV) and V(V), build up the major pool of V species in seawater. Both differ in their physico-chemical behaviour depending on the ambient conditions. Most of the knowledge on these three elements (Rb, U, V) relates to the ambient water column, however, their specific behavior in hydrothermal plumes as potential sources or sinks of elements to the ocean has not been studied in detail. We aim to shed more light into the biogeochemical processes of these selected metals in the Rainbow hydrothermal plume.

SAMPLE COLLECTION AND PROCESSING

Samples have been collected by 24x12 L NISKIN water sampler attached to a trace metal clean rosette equipped with sensors for conductivity, temperature, depth (CTD), and turbidity while the latter one served to trace the hydrothermal plume. According to this signal the NISKIN water samples were closed during upcast of the CTD covering the depth range below, within and above the plume. The CTD set-up with its specific winch and Kevlar coated cable were provided by GEOMAR.

Once on deck again, the NISKIN bottles were immediately brought into a clean lab container (provided by GEOMAR), processed and subsampled therein. Data presented here are from filtered (0.8/0.2 μm , Acropack) and acidified samples (0.02 M HCl, ultrapure, Roth).

RESULTS AND DISCUSSION

Here we present data from three stations with different distances from the hydrothermal source. Station 5 was in close vicinity of an active vent site in the Rainbow vent field showing a peak in turbidity between 1950 m and 2250 m. This feature was even more pronounced at station 7 in the same depth range showing that this station was located

even closer to the venting spot. Station 9 was located further north within the plume flow path though the plume seemed to get less broad since the turbidity peak was detected between 2050 and 2250 m covering only 200 m water layer (Figure 2 A, B, and C). Water samples were taken above, within, and below the plume.

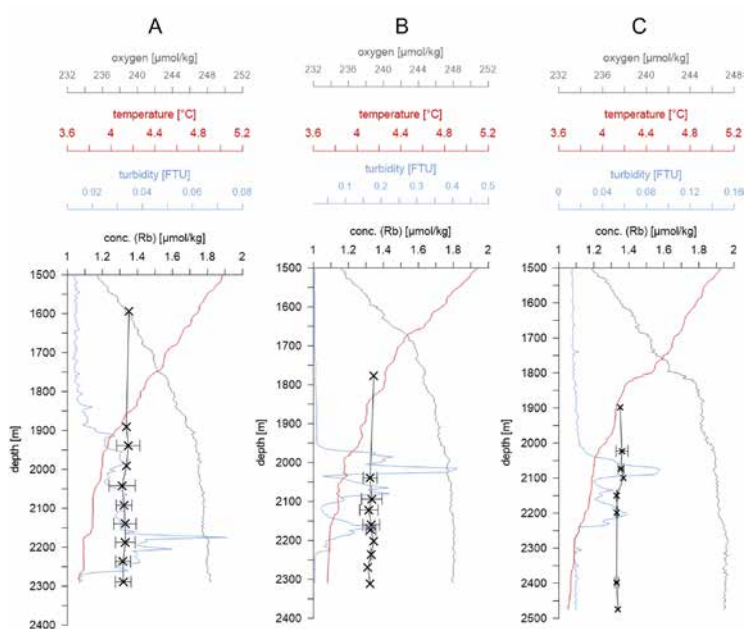


Figure 2: Depth distribution of dissolved Rb at A) station 5, B) station 7, and B) station 9. The data points are average values of up to four replicate measurements and the error bars are calculated from the standard deviation (SD, n= up to 4). Turbidity (blue), temperature (red) and oxygen (grey) are taken from the sensors attached to the trace metal clean rosette frame (TM-CTD).

Dissolved oxygen and temperature did not show anomalies in the plume range but decreased (temperature) and increased (oxygen) with depth as typical for the ambient water column.

The concentrations for Rb observed above and below the plume are similar with no obvious deviation from conservative distribution which means Rb is not controlled by scavenging processes in the hydrothermal plume and the plume is also not a significant source of Rb to the water column (Figure 2A, B, and C).

Also dissolved U did not vary significantly with depth at the three selected locations (Figure 3 A, B, and C); the slight tendency of higher U within the plume is within the range of analytical uncertainty. Hence, the impact from the Rainbow hydrothermal plume as a source of U is negligible, which is in agreement with the expected immobile behavior of U in reducing hydrothermal fluids.

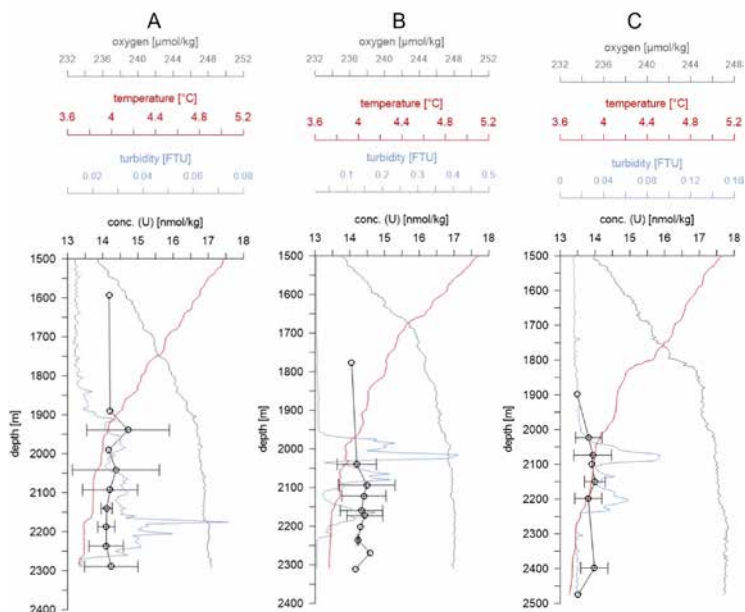


Figure 3: Depth distribution of dissolved U at A) station 5, B) station 7, and B) station 9. The data points are average values of up to four replicate measurements and the error bars are calculated from the standard deviation (SD, $n =$ up to 4). Turbidity (blue), temperature (red) and oxygen (grey) are taken from the sensors attached to the trace metal clean rosette frame (TM-CTD).

Dissolved V showed the most varying signals across the plume (Figure 4 A, B, and C). The significant drop in concentration at station 5 between 2000 and 2100 m water depth covers the upper range of the hydrothermal signal and could be related to adsorption on iron oxyhydroxide particles precipitation in the plume, however, Edmonds and German (2004) described conservative behavior of oxyanions including V and U in the Rainbow plume, based on particle analyses. Dissolved V increased again back to the concentration range detected above the plume. Interestingly, this increase happened in the same depth range as the hydrothermal plume was detected according to the turbidity signal. Since all samples were collected from oxic water layers changes in the redox speciation of V causing the formation of the particle-reactive V(IV) redox species are not very likely to happen. Alternatively, the cause might not be the hydrothermal sink; since this station was located west of the actual vent site we cannot exclude other factors affecting station 5 which were located further south. This hypothesis is supported by the fact that water masses in this underwater valley flow in northerly direction.

Although station 7 was located closer to an active hydrothermal vent site with stronger turbidity signal compared to station 5, the depletion of V within the plume was not observed, but the slight variations with depth are within the error of the applied method. Further north, at station 9, the depth profile of V was similar to the one reported for station 7.

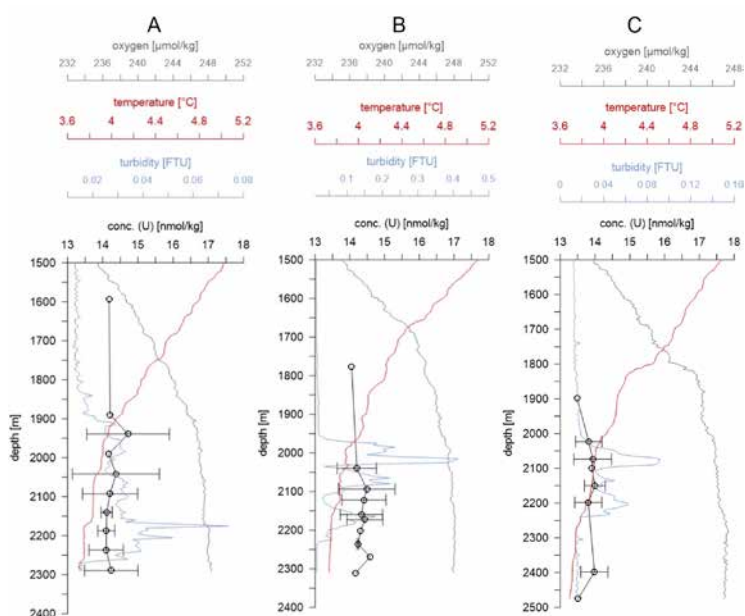


Figure 4: Depth distribution of dissolved V at A) station 5, B) station 7, and B) station 9. The data points are average values of up to four replicate measurements and the error bars are calculated from the standard deviation (SD, n= up to 4). Turbidity (blue), temperature (red) and oxygen (grey) are taken from the sensors attached to the trace metal clean rosette frame (TM-CTD).

To conclude, the distributions of dissolved Rb, U and most likely V are not significantly affected by the hydrothermal plume in the dissolved fraction < 0.2 μm at the Rainbow hydrothermal vent site.

OUTLOOK

During research cruise M176/2 we filtered samples through different pore size filters and collected different size fractions (< 0.8 μm , < 0.2 μm , < 0.015 μm). We aim to analyze these samples prior to this presentation to provide a picture on the physical fractionation of Rb, U and V in the vicinity of hydrothermal vent sites.

REFERENCES

Nishioka J, Obata H, and Tsumune D, Evidence of an extensive spread of hydrothermal dissolved iron in the Indian Ocean, *Earth Planet. Sci. Lett.* 2013, 361, 26–33.

Resing J A, Sedwick P N., German C R, Jenkins W J, Moffett J W, Sohst B M, et al., Basin-scale transport of hydrothermal dissolved metals across the S Pacific, *Nature* 2015, 523, 200–203.

Brüske A, Weyer S, Zhao M Y, Planavsky N J, Wegwerth A, Neubert N, Dellwig O, Lau K V, Lyons T W, Correlated molybdenum and uranium isotope signatures in modern anoxic sediments: Implications for their use as paleo-redox proxy, *Geochim Cosmochim Acta* 2020, 270, 449–474. <https://doi.org/10.1016/j.gca.2019.11.031>.

Clarkson M O, Stirling C H, Jenkyns H C, Dickson A J, Porcelli D, Moy C M, Von Strandmann P P A E, Cooke I R, Lenton T M, Uranium isotope evidence for two episodes of deoxygenation during Oceanic Anoxic Event 2. *Proc Natl Acad Sci U S A* 2018, 115, 2918–2923. <https://doi.org/10.1073/pnas.1715278115>.

Ku T L, Knauss K G, Mathieu G G, Uranium in open ocean: concentration and isotopic composition, *Deep-Sea Research* 1977, 24, 1005–1017. [https://doi.org/10.1016/0146-6291\(77\)90571-9](https://doi.org/10.1016/0146-6291(77)90571-9).

Anderson R F, Fleisher M Q, LeHuray A P, Concentration, oxidation state and particulate flux of uranium in the Black Sea, *Geochim Cosmochim Acta* 1989, 53(9), 2215–2224.

Edmonds H N, German C R, Particle geochemistry in the Rainbow hydrothermal plume, Mid-Atlantic Ridge, *Geochim. Cosmochim. Acta* 2004, 68(4), 759–772.

MSM96

Rare earth element cycling in oxic pore waters from the Northeast Atlantic: benthic fluxes and implications for the use of Nd isotopes as a past water mass proxy

AUTHORS

GEOMAR Helmholtz Centre for Ocean Research Kiel | Kiel, Germany

S. Paul, M. Gutjahr, A. Xu, E. Hathorne, F. Scholz, M. Frank, T. Schoening

Constructor University Bremen | Bremen, Germany

N. Fröhberg

Neodymium (Nd) isotopic signatures (ϵNd) have been widely used as a proxy to reconstruct past water mass mixing and ocean circulation. A variety of archives (e. g., sedimentary Fe-Mn oxyhydroxides, phosphates) have been used to extract authigenic seawater Nd isotopic signatures but recently it has been increasingly questioned which archives can be reliably used and under which environmental conditions primary seawater Nd isotopic signatures are likely to be altered by early diagenesis.

Pore waters of marine sediments are *the* key environment in which early diagenetic exchange processes between seawater-derived Nd and terrigenous solid phases take place. The trace metal budget of marine pore waters hence provides crucial information to understand Nd isotope and Rare Earth Element and Yttrium (REY) cycling between marine sediments and overlying bottom waters. In conjunction with other pore-water constituents (e. g., NO_3^- and Mn_2^+), whose distribution is coupled to organic matter degradation and/or redox processes, underlying controls of REY mobilization can be identified. Due to methodological challenges, pore-water Nd isotopic compositions have only been assessed in few places globally until now, thus providing a non-representative picture.

A second major gap in understanding REY cycling at the seafloor is limited information on benthic REY fluxes. It has been proposed that benthic fluxes of REY are considerable, especially at continental shelf and slope sites and that they can impact bottom water REY concentrations and ϵNd signatures (Abbott et al., 2015a, b). Such a modulation of bottom water ϵNd would lead to an alteration of the seawater signature already during authigenic mineral formation.

Here we present REY and ϵNd data of oxic pore waters at 4500–5500 m water depth from the Northeast Atlantic, sampled during cruise MSM96. Two work areas were visited during the cruise: The Porcupine Abyssal Plain (PAP) and the Iberian Abyssal Plain (IAP).

The deep-sea sediments at both sites are characterized by low organic matter degradation rates which is why they are oxic up to a depth of ca. 20 cm (PAP) or more (IAP). No elevated dissolved Mn concentrations were detected in any core, wherefore conditions do not become sufficiently reducing to reduce Mn oxides. Therefore, these sediments can be used to study REY exchange in an area where the water mass signature would actually likely be studied in authigenic phases (as compared to sites with more reducing and reactive sediments). As the cruise aimed to assess geochemical heterogeneity of abyssal plains, the large number of cores taken per work area led to a robust data set of benthic REY fluxes in the two study areas of the Northeast Atlantic.

Samples were taken with a multi corer and sediments were sliced in the cool room. Ex-situ voltammetric oxygen measurements prior to slicing provided first information on redox-conditions in the sediments and sampling was conducted in a glove bag under an oxygen-free atmosphere if cores reached suboxic conditions. This was only the case in the PAP area. Samples were centrifuged to subsequently extract and filter the pore waters. Samples were acidified on board and later analyzed at GEOMAR using seaFAST offline preconcentration and HR-ICP-MS analysis for REY concentrations and ion chromatography and MC-ICP-MS analyses to measure the Nd isotope compositions. Benthic fluxes were calculated based on the concentration difference of the MUC bottom water and the uppermost pore water sample (usually 0–2 cm) following Fick's first law of diffusion.

Neodymium concentrations in these oxic pore waters range from 10–50 pM in the Northeast Atlantic (overlying bottom seawater 12–22 pM) and are at the low end of published pore-water REY concentrations (27–130 pM Nd in oxic pore waters of the Pacific margin of Antarctica (Wang et al., 2022), 95–310 pM Nd in pore waters of calcareous sediments in the Tasman Sea (Abbott, 2019), 300–800 pM in manganese and 200–400 pM Nd in ferruginous pore waters at the Oregon shelf (Abbott et al., 2015a)).

The pore-water depth profiles at our sites display a concentration peak in the uppermost ca. 2 cm, suggesting a benthic flux of REY. The data show that benthic fluxes are widespread across the study area and contribute REY including Nd to the bottom seawater. Calculated fluxes are, however, small, with on average $-0.9 \text{ pmol cm}^{-2} \text{ yr}^{-1}$ Nd in the PAP ($n=10$) and $-0.6 \text{ pmol cm}^{-2} \text{ yr}^{-1}$ Nd in the IAP ($n=9$). Similar to the Nd concentrations, fluxes are considerably lower than previously published benthic fluxes of REY which were predominantly assessed at ocean margin sites in the past and up to around $-13 \text{ pmol cm}^{-2} \text{ yr}^{-1}$ (Abbott et al., 2015a). Shale normalized (SN) pore-water REY patterns show seawater characteristics including large negative CeSN anomalies, positive YSN anomalies and HREY enrichment. The HREY enrichment decreases with depth in the upper ca. 20 cm at both sites, revealing REY fractionation during interactions of the pore water and the solid phase. ϵNd values of the pore waters range from -9.8 to -12.8 in the Northeast Atlantic and are in the same range as near-bottom seawater values.

Our results show small but widespread benthic fluxes in the Northeast Atlantic deep sea. Even though REYSN patterns indicate slight REY fractionation during early diagenesis, the Nd isotope compositions are in a similar range in the pore water and the overlying seawater potentially indicating no change of the Nd isotopic signature during early diagenesis at the studied sites. The small benthic fluxes also suggest that there is little input of Nd into bottom seawater and a considerable change of the bottom seawater Nd isotopic composition is thus unlikely. Comparison to the authigenic and detrital solid-phase Nd isotopic composition is, however, crucial to fully understand the early diagenetic processes. These analyses are currently being carried out.

REFERENCES

Abbott AN, A benthic flux from calcareous sediments results in non-conservative neodymium behavior during lateral transport: A study from the Tasman Sea, *Geology* 2019, 47, 363–366.

Abbott AN, Haley BA, McManus J and Reimers CE, The sedimentary flux of dissolved rare earth elements to the ocean, *Geochimica et Cosmochimica Acta* 2015a, 154, 186–200.

Abbott AN, Haley BA and McManus J, Bottoms up: Sedimentary control of the deep North Pacific Ocean's ϵ Nd signature, *Geology* 2015b, 43, 1035–1038.

Wang R, Williams TJ, Hillenbrand CD, Ehrmann W, et al., Boundary processes and neodymium cycling along the Pacific margin of West Antarctica, *Geochimica et Cosmochimica Acta* 2022, 327, 1–20.

MSM96

Influence of seafloor topography on benthic nutrient fluxes in deep-sea sediments of the North Atlantic

AUTHORS

GEOMAR – Helmholtz Centre for Ocean Research Kiel | Kiel, Germany

M. Schnohr, S. Paul, F. Scholz

Nutrients like nitrate, phosphate and silicate are consumed by primary producing organisms in the surface ocean. The majority is recycled in the water column or surface sediments and only a small portion is permanently buried at the seafloor. It is generally assumed that benthic nutrient fluxes are similar across vast areas of the deep ocean. However, because of heterogeneous topography, which leads to unequal sedimentation rates, this assumption is questionable. It is already known that water depth is a crucial factor for different nutrient concentrations and fluxes but the exact influence of the seafloor topography on diffusive benthic nutrient fluxes has not been studied yet. For this purpose, measurements of bottom water and pore water nutrient concentrations were carried out in regions with topographical differences that vary around 50–500 m.

Twelve sediment cores were taken with a multiple corer in the working areas Porcupine Abyssal Plain (PAP), located approximately 750 km west of France and the South Western Iberian Abyssal Plain (SWIAP), located 700 km west of Portugal. For each of the topography types (hill, valley, plain) four cores were sampled. The PAP working area is characterized by comparatively little topographical differences, whereas the SWIAP shows more topographical variability. Furthermore, SWIAP is located at greater water depth (between 5200 m and 5700 m) compared to the PAP (between 4700 m and 4900 m). After sampling, the pore water was extracted by centrifugation and nutrient concentrations were analysed using an autoanalyzer at GEOMAR after the cruise. The diffusive fluxes across the sediment-water interface were calculated from the concentration difference between bottom water and uppermost pore water (0–1 cm) sample according to Fick's first law.

Some differences can be observed between the two working areas (Figure 1). The nitrate profile in the PAP is characterized by an increase in concentration in the upper centimetres of the sediment. From a certain depth, the concentration decreases again. In contrast, in the SWIAP, nitrate concentrations continue to increase slightly throughout the recovered depth interval. The nitrate profiles reflect nitrification within the upper centimeters where oxygen is present and denitrification in anoxic sediments below. Since there is more oxygen in the cores of the SWIAP over the entire sediment depth, the nitrate concentration continues to increase slightly (since the nitrogen can be further converted into nitrate,

even as the sediment depth increases). Also, the silicate concentrations increase up to a certain depth in the PAP and stay relatively constant below whereas in the SWIAP, silicate further increases downcore. The silicate concentration within the sediment increases due to the dissolution of biogenic silica until a saturation is reached (Tréguer & De La Rocha, 2013). Phosphate concentrations mostly increase over the entire depth but show higher concentrations in the PAP. The phosphate concentration mainly depends on the amount of accumulated organic material. In the upper sediment, it can be released back to bottom water. The higher phosphate concentration in the PAP can be explained with a greater organic carbon turnover compared to the SWIAP.

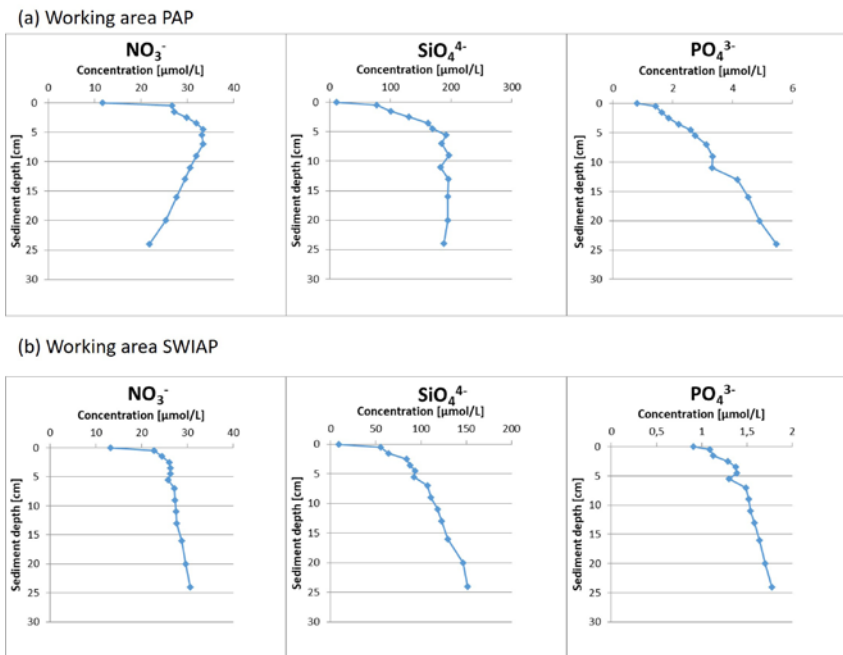


Figure 1: Nutrient concentrations of nitrate (NO₃⁻), phosphate (PO₄³⁻) and silicate (SiO₄⁴⁻) in the working areas (a) PAP (28MUC) and (b) SWIAP (37MUC).

In the PAP, the mean nutrient fluxes amount to -13.45 mmol m² yr⁻¹ for nitrate, -0.32 mmol m² yr⁻¹ for phosphate and -0.07 mmol m² yr⁻¹ for silicate. The mean fluxes in the SWIAP are -9.62 mmol m² yr⁻¹ for nitrate, 0.07 mmol m² yr⁻¹ for phosphate and -0.04 mmol m² yr⁻¹ for silicate. By using mean bottom water concentrations for each working area, the mean difference between hill and valley in the PAP is -0.04 µmol cm² yr⁻¹ for nitrate, -0.01 µmol cm² yr⁻¹ for phosphate and -0.27 µmol cm² yr⁻¹ for silicate. In the SWIAP, the difference for nitrate is -0.18 µmol cm² yr⁻¹, -0.01 µmol cm² yr⁻¹ for phosphate and -0.88 µmol cm² yr⁻¹ for silicate.

The nutrient fluxes correspond well with previous studies in deep sea areas. In general, the working area with the shallower water depth (PAP) is characterized by higher fluxes. The difference of the mean diffusive fluxes between the two working areas can be explained by the lower nutrient concentration in the sediment due to less primary production (NASA, 2020) and lower organic matter accumulation and turnover at greater water depths (Suess, 1980) in the SWIAP. Furthermore, there are differences dependent on the topography. For the different topography types a trend from higher fluxes in valleys and lower fluxes in hills is found in both working areas (and for all the measured nutrients). This trend is more pronounced in the working area with greater topography variability (SWIAP). The reason for the trends of the nutrient fluxes could be the higher organic matter accumulation in the valleys compared to the hills (fine-grained organic material is focused into the deeper areas). The more pronounced trends in the SWIAP can be explained by the more pronounced topographical differences compared to the PAP (difference between the mean water depths of the hills and valleys is 73 m in the PAP and 171 m in the SWIAP).

In conclusion, the comparison of the examined working areas provides some evidence for variable benthic nutrient fluxes as a function of topography (between hills and valleys). The topography should be considered in future benthic fluxes studies and more data is needed to make robust assumptions for the northeast Atlantic and globally.

REFERENCES

NASA, Chlorophyll Concentration (1 month – Aqua/MODIS), retrieved March/ 2022 from https://neo.gsfc.nasa.gov/view.php?datasetId=MY1DMM_CHLORA&year=2020.

Suess E, Particulate organic carbon flux in the oceans — surface productivity and oxygen utilization, *Nature* 1980, 260-263.

Tréguer PJ, De La Rocha CL, The world ocean silica cycle, *Annual review of marine science* 2013, 5, 10.1146/annurev-marine-121211-172346.

MSM98/2

Tunnel valleys in the southeastern North Sea: Complex incision patterns dating back to MIS16?

AUTHORS

Christian-Albrechts-Universität zu Kiel | Kiel, Germany

A. Lohrberg, J. Schneider von Deimling, H. Grob, K.-F. Lenz, S. Krastel

Large Pleistocene ice sheets have produced glacial structures both at and below the surface in northern Europe. Some of the largest and most erosive structures are so-called tunnel valleys. Extensive seismic studies have shown a high abundance of tunnel valleys (TVs) in many regions of the North Sea (Figure 1). TVs typically have widths of 1 to 5 km, incision depths of up to 400 m and lengths of up to 100 km. Widths of up to 10 km and depths of up to 500 m have been observed locally in the North Sea. In the German sector of the North Sea lengths of up to 60 km, widths of up to 8 km and depths of up to 400 m have been reported. Most of these TVs are now filled with sediments and often buried beneath a drape of glacial and interglacial deposits.

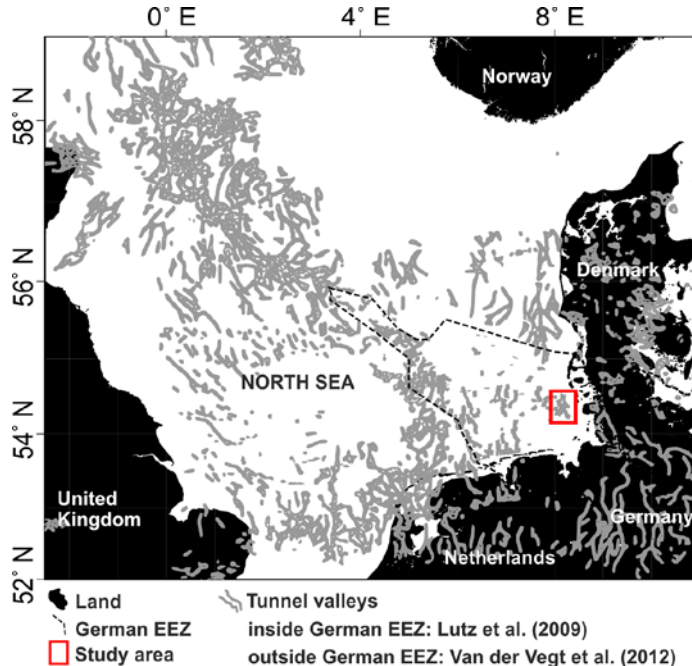


Figure 1: Location of the study area and distribution of tunnel valleys (TVs) in the North Sea and adjacent countries (adapted from Lohrberg et al., 2020).

In this study we provide an update of the tunnel valley distribution between Amrum and Heligoland in the southeastern North Sea based on a very dense grid of high-resolution 2D multi-channel seismic reflection data (Figure 2). Using newly acquired data, the known tunnel valleys in that area can now be traced in greater detail and further westwards, which results in an increased resolution and coverage of their distribution (Figure 2). Due to the increased profile density, we were able to close gaps that previously led to an ambiguous tracing of the TVs. Although similar to earlier results, the updated map allows for the tracing of previously identified TV1, TV2 and TV3 in greater detail and approx. 10 km farther towards the west. Based on the updated map, we are confident that we imaged the westward continuation of TV1 in the northwest of the study area (Figure 2a). Furthermore, TV2 can now be traced along its thalweg over 17 km and TV3 can now be traced along 22 km (Figure 2b). Owing to the increased profile density, we were able to identify a new tunnel valley, TV0, which lies in a deeper stratigraphic level than TV1–TV3. The average depth of its thalweg is around 250 m, and the thalweg shows minor undulation. The fill of TV0 shows less stratification, yet it can be separated into a lower and an upper part in some profiles, despite strongly undulating reflectors in its upper part. TV0 is oriented in a SE–NW direction and therefore parallels the identified thrust direction of the Heligoland Glacitectonic Complex (HGC) towards the northwest postulated in that area.

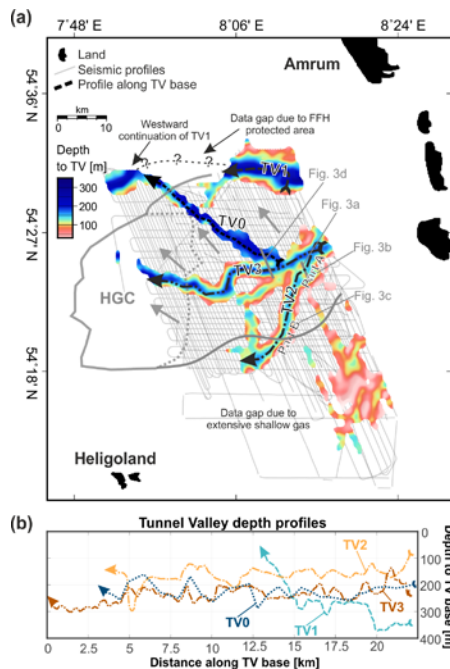


Figure 2: Overview of the study area. (a) Detailed distribution of large tunnel valleys (TVs) in the study area in the form of a depth grid based on all available high resolution 2D reflection seismic profiles (with the sea level as depth reference). (b) Depth profiles for the base of TV1–TV3 inferred from longitudinal seismic profiles following the thalweg of the TVs.

For the first time, we were able to generate high-resolution seismic profiles oriented along the thalweg of TVs by planning surveys based on earlier results. From our data it is evident that TV2's thalweg significantly undulates along the profile. The depth profiles for the thalwegs of TV1–TV3 are shown in Figure 2b for comparison. The longitudinal profiles show that TV2 incised through Miocene and late Paleogene strata while overcoming significant barriers of over 75 m height difference during incision. The dip of the thalweg parallels the dip of the underlying strata in limited areas with frequent deeper incisions on several occasions.

Our high-resolution longitudinal profiles along a single-incision TV show that the incision has overcome significant morphological highs of over 75 m over a 500 m distance, which is a significant gradient when compared to earlier studies, who showed a maximum gradient of approx. 100 m over a 1 km distance. These large gradients are impossible to reconcile with a gravity-driven fluvial erosion, as any water flow would stagnate at either of the morphological barriers. Therefore, we conclude that fluvial erosion is not the primary process that led to the formation of the TVs in our study area. Instead, we conclude and confirm interpretations that bank-full pressurized drainage beneath an ice sheet was responsible for their formation as bankfull conditions would be capable of overflowing such barriers. Following their incision, most TVs of the North Sea have been filled. Contrary to our expectation, we do not observe patterns that are diagnostic for specific sedimentary processes in the fill of the TVs along their thalweg, except for a segmentation into an upper part with increased stratification and a lower part with decreased or absent stratification.

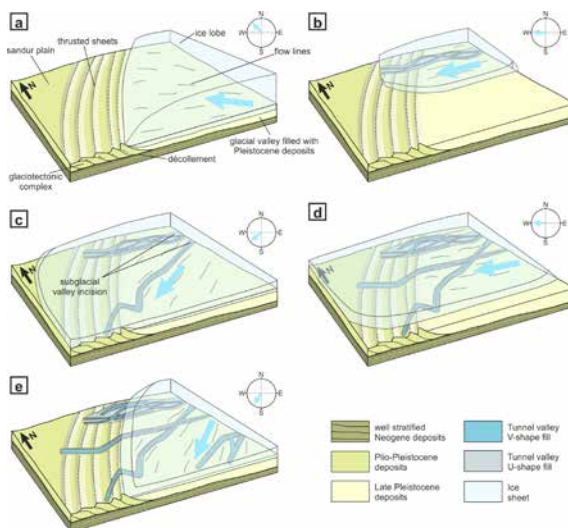


Figure 3: Schematic subplots showing multiple possible ice margins in the study area resulting in glaciotechnic thrust sheets and multiple tunnel valleys with different orientations. Subplots show progressively younger ice margins from (a) to (e).

Owing to the increased density of seismic profiles, we were able to identify the hitherto unknown deep tunnel valley TV0. Likely due to a subsequent overriding ice sheet, TV0's shoulders were eroded, and only its middle and lower parts are preserved. Yet, its NW–SE orientation can be clearly derived from the data. This orientation parallels the thrust direction postulated for the HGC (Winsemann et al., 2020; Lohrberg et al., 2022). Combining its deeper stratigraphic location with thrusts occurring stratigraphically higher/later than the top of TV0, it seems likely that its incision dates back to the same ice lobe responsible for the formation of the HGC or is older (Figure 2a). The clear separation from TV1–TV3, both in depth and in orientation, also indicates a substantial time between the formation of TV0 and TV1–TV3 as observed for other TVs in the North Sea. These observations strengthen the conclusion that an early-Elsterian or pre-Elsterian ice lobe reached the study area from the southeast. Consequently, these chronospatial relationships indicate that TV0 may reflect this early-Elsterian or pre-Elsterian ice advance into the southeastern North Sea (Figure 3). Considering recent modelling results for global ice sheets (Batchelor et al., 2019), we hypothesize that TV0 may be a relic of the Cromer glaciation (MIS 16). Data from all over the North Sea show that the distributions and the depth of TVs are major factors when trying to attribute their formation to specific glaciations in specific regions.

Our results demonstrate that a very dense profile spacing is required to decipher the complex incisions of tunnel valleys during multiple ice advances in a specific region (Figure 3). We also demonstrate that the time- and cost-effective acquisition of high-resolution 2D seismic reflection data holds the potential to further our understanding of the distribution, complexity and incision depths of tunnel valleys in different geological settings.

REFERENCES

Batchelor C L, Margold M, Krapp M, Murton D K, Dalton A S, Gibbard P L, Stokes C R, Murton J B, & Manica A, The configuration of Northern Hemisphere ice sheets through the Quaternary, *Nat. Commun.* 2019, 10, 1–10, doi:10.1038/s41467-019-11601-2.

Lohrberg A, Schwarzer K, Unverricht D, Omlin A, & Krastel S, Architecture of tunnel valleys in the southeastern North Sea: new insights from high-resolution seismic imaging, *Journal of Quaternary Science* 2020, 35(7), 892–906, doi:10.1002/jqs.3244.

Lohrberg A, Schneider von Deimling J, Grob H, Lenz K-F, & Krastel S, Tunnel valleys in the southeastern North Sea: more data, more complexity, *E&G Quaternary Sci. J.* 2022, 71, 267–274, doi:10.5194/egqsj-71-267-2022.

Lutz R, Kalka S, Gaedicke C, Reinhardt L, & Winsemann J, Pleistocene tunnel valleys in the German North Sea: spatial distribution and morphology, *Z. Dtsch. Ges. Geowiss.* 2009, 160, 225–235, doi:10.1127/1860-1804/2009/0160-0225.

van der Vegt P, Janszen A & Moscariello A: Tunnel valleys: current knowledge and future perspectives, *Geol. Soc. London, Spec. Publ.* 2012, 368, 75–97, doi:10.1144/SP368.13.

Winsemann J, Koopmann H, Tanner D C, Lutz R, Lang J, Brandes C & Gaedicke C: Seismic interpretation and structural restoration of the Heligoland glaciotectionic thrust-fault complex: Implications for multiple deformation during (pre-)Elsterian to Warthian ice advances into the southern North Sea Basin, *Quat. Sci. Rev.* 2020, 227, 1–15, doi:10.1016/j.quascirev.2019.106068.

MSM100

Vertical acoustic blanking anomalies in 2D and 3D seismic data from the German North Sea: Imaging artifacts by shallow gas-bearing incised channels

AUTHORS

Bundesanstalt für Geowissenschaften und Rohstoffe (BGR) | Hannover, Germany
N. Ahlrichs, A. Ehrhardt, M. Schnabel

Geomar Helmholtz-Zentrum für Ozeanforschung | Kiel, Germany
C. Berndt

INTRODUCTION

Seismic data interpretation is critical for identifying subsurface structures, particularly in fields like hydrocarbon exploration and underground CO₂ or hydrogen storage. A main aspect of structural interpretation is connecting observable features in seismic images with their geological counterparts using key elements of the seismic image like travel time, reflection characteristics, and irregularities. In the North Sea, chaotic reflection patterns and reduced amplitudes are often linked to fluid conduits, like gas chimneys, associated with faults or deep-seated fluid migration. Shallow structures like tunnel valleys or fluvial channels with gas-charged sediments can produce similar seismic anomalies below them, making it challenging to distinguish true geological features from imaging artifacts.

Patches of vertical acoustic blanking (VAB), where the seismic signal is strongly attenuated and reflections are discontinuous, are a common seismic anomaly in data from the German North Sea. VAB can be caused by shallow gas-charged sediment and is observed in various geological settings (Okyar and Ediger, 1999; Garcia-Gil et al., 2002; Mathys et al., 2005; Laier and Jensen, 2007; Tóth et al., 2014). However, in the German North Sea, the exact origin of these anomalies and their differentiation from fluid conduits is not well understood.

In this work, we reveal that many of these VAB features are imaging artifacts related to shallow gas-bearing incised channels. We systematically analyzed and mapped VAB anomalies in the German North Sea using industry and academic 2D and 3D seismic data. Thereby, this study contributes to a better understanding of acoustic blanking in seismic data and helps to avoid misinterpretation of VAB features as gas chimneys. The findings benefit investigations related to fluid migration, especially in the context of carbon capture and storage (CCS) and other underground utilization applications.

The study area encompasses the German North Sea sector and neighboring regions. This area has a long and complex Paleozoic to Cenozoic geological history shaped by continental rifting, tectonic inversion, and salt tectonics (Ziegler, 1990; Pharaoh et al., 2010). From the Mid-Pleistocene onward, the North Sea region experienced three major glaciations, resulting in the coverage by large ice sheets (e. g. Hughes et al., 2016). During the late Weichselian and early Holocene, falling sea levels led to the emergence of a landmass between Britain and the European mainland termed Doggerland. The landscape featured a periglacial to fluvial environment, providing a habitat for Mesolithic communities (Gaffney et al., 2009). Regional to local studies detected various incised-fluvial channels assembling the Doggerland drainage system (Gaffney et al., 2009; van Heteren et al., 2014; Hepp et al., 2017; Prins and Andresen, 2019).

METHODOLOGY

We use multichannel reflection seismic data from various surveys conducted over the past five decades, involving both academic and industry campaigns. The dataset includes 35.150 km of 2D data and 10.000 km² of 3D data, whereas the latter mostly covers the Ducks Beak area (Figure 1).

In 2021, the Federal Institute for Geoscience and Natural Resources (BGR) and partner institutions conducted a 94 km² 3D seismic survey in the Ducks Beak region as part of the GeoBaSIS-3D project (cruise MSM100, see Ehrhardt et al, this volume). This dataset was acquired with an optimized setup (broad signal spectrum, small initial offsets, hydrophone interval of 6.25 m and a streamer separation (2 seismic cables) of 50 m.). The resulting seismic volume (bin grid spacing 12.5 x 3.125 m) provided a high-resolution image even for the shallow sediment, allowing a 3D analysis of shallow structures and their connection to the deeper subsurface. Additionally, we use sediment echosounder data recorded by the Atlas PARASOUND system DS P70 to investigate the uppermost sedimentary layers and channel fill. For further details on the cruise MSM100, see Ehrhardt et al., this volume.

RESULTS

We detected 30 VAB occurrences across the German North Sea, predominantly affecting the image from below the seafloor reflection to -2 seconds two-way travel time (TWT) (Figure 1). The VAB localities cluster in two main regions: the southwestern part of the German North Sea sector, near the Ems estuary, and the southeastern area of the Ducks Beak and northern German North Sea close to the Danish maritime border (Figure 1).

The new seismic data from cruise MSM100 delivered a 3D image of a shallow, meandering channel which is partly characterized by high-amplitude anomalies (Figure 2). The lateral analysis of this data-set unveiled a clear spatial correlation between VAB patches and the meandering channel below the seafloor. Further 3D data from the Ducks Beak show additional meandering channels across the Ducks Beak. The channels base is formed by a high-amplitude, dipping reflection. Above a VAB patch, this reflection is

phase reversed and forms part of a local bright spot within the channel. By using varying source-receiver distances (offset), we analyzed a possible acquisition dependence on the character and extent of the blanking (Figure 2). Large offsets allow imaging the subsurface below the channel without signal penetrating through it (undershooting). This approach removed the blanking effect uncovering the observed VAB as an imaging artifact (Figure 2). Biogenic gas accumulations within the channels are a potential explanation, with locally trapped gas causing the blanking effect due to the high absorption of acoustic energy. The amount of gas produced, sediment permeability, and local barriers determine the accumulation of gas. The presence of gas is likely not exclusive to the channels but might be trapped within the uppermost sedimentary layers. Parasound data imaging the sedimentary infill of the channels suggest that the accumulation could be controlled by the deposition of floodplain deposits acting as a barrier enhancing increased gas accumulation.

VAB anomalies are mainly clustered in the Ducks Beak region and the northwestern part of the Elbe-Palaeovalley, offering insight into the former river channels and paleo-landscapes in the area.

This research reveals VAB anomalies as imaging artifacts and highlights the potential of using VAB anomalies, initially detected in large-scale datasets from various sources, to identify former river channels or other paleo-landscape features, aiding geoarchaeology and research on prehistoric societies in the North Sea region and beyond.

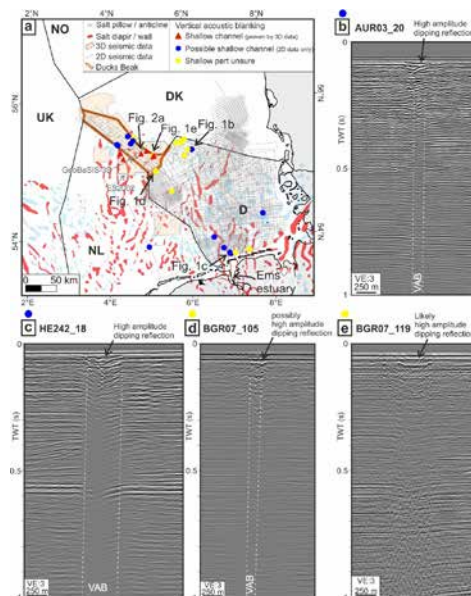


Figure 1: Vertical acoustic blanking occurrences across the German North Sea and representative examples of blanking observed in 2D data (Ahlich et al., in Review).

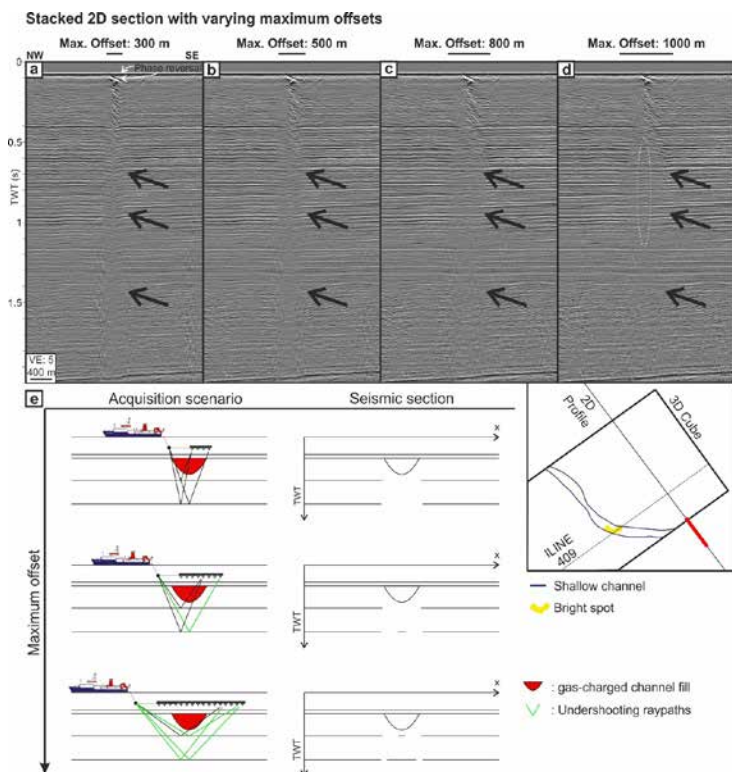


Figure 2: Offset-dependent imaging of a VAB occurrences visible in a 2D seismic section. Note the decrease of VAB, and thus more continuous imaging of reflections within the VAB patch at greater depths with increasing offset (black arrows). e: Sketch showing offset-influence in imaging VAB structures. With larger maximum offset, undershooting of the gas-charged channel fill becomes possible (green raypaths) allowing imaging of deeper strata below the channel without influence from the channel infill on the seismic signal. Figure adapted from Ahlrichs et al. (in Review).

REFERENCES

Ahlrichs N, Ehrhardt A, Schnabel M, et al., Vertical acoustic blanking in seismic data from the German North Sea: a spotlight to shallow gas-bearing incised channels, *Journal of Quaternary Science Reviews*, in Review.

Laier T, Jensen JB, Shallow gas depth-contour map of the Skagerrak-western Baltic Sea region, *Geo-Marine Letters* 2007, 27, 127–141.
<https://doi.org/10.1007/s00367-007-0066-2>.

Gaffney V, Fitch S, Smith D, Europe's Lost World: The Rediscovery of Doggerland, Research Report 2009, York.

Garcia-Gil S, Vilas F, Garcia-Garcia A, Shallow gas features in incised-valley fills (Ria de Vigo, NW Spain): a case study, *Continental Shelf Research* 2002, 22, 2303-2315.
<https://link.springer.com/article/10.1007/s00367-007-0066-2>.

Hepp DA, Warnke U, Hebbeln D, et al., Tributaries of the Elbe Palaeovalley: Features of a Hidden Palaeolandscape in the German Bight, North Sea, in: Bailey G N, Harff, J, Sakellariou, D (Eds.), *Under the Sea: Archaeology and Palaeolandscapes of the Continental Shelf*, Springer International Publishing 2017, pp. 211–222.
https://doi.org/10.1007/978-3-319-53160-1_14.

Hughes ALC, Gyllencreutz R, Lohne Ø S, et al., The last Eurasian ice sheets – a chronological database and time-slice reconstruction, *DATED-1*, *Boreas* 2016, 45, 1–45.
<https://doi.org/10.1111/bor.12142>.

Huuse M, Lykke-Andersen H, Overdeepened Quaternary valleys in the eastern Danish North Sea: morphology and origin, *Quaternary Science Reviews* 2000, 19, 1233–1253. [https://doi.org/10.1016/S0277-3791\(99\)00103-1](https://doi.org/10.1016/S0277-3791(99)00103-1).

Mathys M., Thießen O, Theilen F, et al., Seismic Characterisation of Gas-rich Near Surface Sediments in the Arkona Basin, Baltic Sea, *Marine Geophysical Researches* 2005, 26, 207–224. <https://doi.org/10.1007/s11001-005-3719-4>.

Pharaoh T, Dusar M, Geluk M, et al., Tectonic evolution, in: Doornenbal, H, Stevenson, A G (Eds.), *Petroleum Geological Atlas of the Southern Permian Basin Area*. EAGE Publications 2010, Houten, pp. 25–57.

Prins LT, Andresen KJ, Buried late Quaternary channel systems in the Danish North Sea – Genesis and geological evolution, *Quaternary Science Reviews* 2019, 223, 105943.
<https://doi.org/10.1016/j.quascirev.2019.105943>.

Okyar M, Ediger V, Seismic evidence of shallow gas in the sediment on the shelf off Trabzon, southeastern Black Sea, *Continental Shelf Research* 1999, 19, 575–587.
[https://doi.org/10.1016/S0278-4343\(98\)00111-3](https://doi.org/10.1016/S0278-4343(98)00111-3).

Tóth Z, Spieß V, Jensen J, Seismo-acoustic signatures of shallow free gas in the Bornholm Basin, Baltic Sea, *Continental Shelf Research* 2014, 88, 228–239.
<https://doi.org/10.1016/j.csr.2014.08.007>.

van Heteren S, Meekes JAC, Bakker MAJ, et al., Reconstructing North Sea palaeolandscapes from 3D and high-density 2D seismic data: An overview, *Netherlands Journal of Geosciences* 2014, 93, 31–42. <https://doi.org/10.1017/njg.2014.4>.

Ziegler PA, Tectonic and paleogeographic development of the North Sea Rift System, in: Blundell D, Gibbs A D (Eds.), *Tectonic Evolution of North Sea Rifts*, 1999, Oxford University Press, New York, pp. 1–36.

MSM101

Post-glacial palaeoceanographic changes on the Scotian Shelf – first results

AUTHORS

Institute of Geosciences, Kiel University | Kiel, Germany

H. Kolling, P. Matzerath, R. Schneider

The Scotian Shelf, on the Northwest Atlantic Canadian coast, is a critical climatic region. It lies near the confluence of cold polar waters of the Labrador Current and warmer water masses transported by the North Atlantic Current, originating from the Gulf Stream. Both currents are critical components of the Atlantic Meridional Overturning Circulation, controlling the global water mass exchange and the subsequent distribution of heat on our planet. The Northwest Atlantic, and the Scotian Shelf in particular, is not only a region of the world's ocean expected to be most dramatically affected by ongoing climate change (e. g., Saba et al. 2016, Pepin et al. 2013), but has changed markedly in the past as well. Hence, this area is a key region to study past variations in the Atlantic Meridional Overturning Circulation.

During the Holocene, the Nova Scotian Shelf has undergone various climatic and oceanographic forcing interactions, including the disintegration of the Laurentide Ice Sheet (resulting in meltwater pulses) and changes in solar insolation rates. Despite its importance, the Scotian Shelf has not been studied in great detail, and the existing records do not indicate a consistent climate pattern. To close this knowledge gap, expedition MSM101 sampled continuous Pleistocene and Holocene sediment records, as climate archives to study the past oceanic changes and ocean-atmosphere interactions during events of climate change in a high spatial and temporal resolution.

Here we present first results from sediment cores MSM101_13-3 (SE Scotian Shelf) and MSM101-44-3 (NW Scotian Shelf) (Figure 1). We use XRF core scanning, planktonic foraminiferal assemblages as well as stable isotopes, Mg/Ca thermometry and biomarkers for sea ice, phytoplankton productivity and sea surface temperatures (IP25, dinosterol, e. g., alkenones) to decipher the complex oceanic changes and interactions during the past 10–14 ka on the Scotian Shelf.

In both sediment cores, we find strong evidence that full marine conditions did not prevail until the early Holocene. This is most likely caused by lower sea levels (Edgecombe et al., 1999, Vaccì et al., 2018).

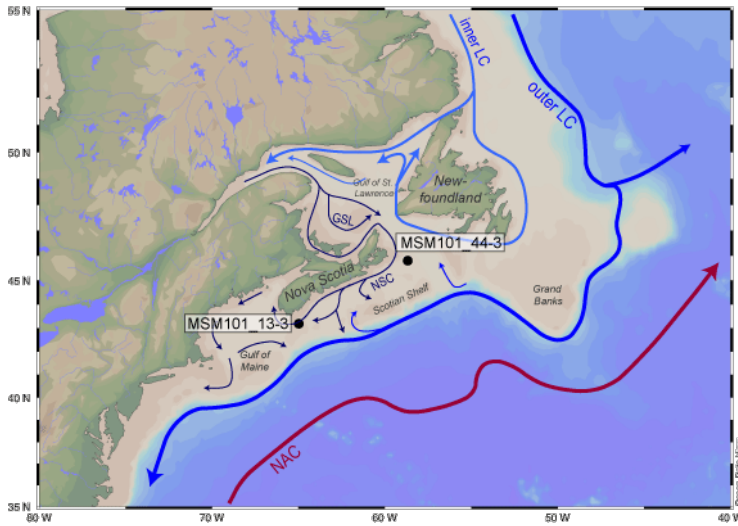


Figure 1: Location map of the Nova Scotia and Newfoundland region with the modern surface circulation pattern after Scott et al. (1984), Drinkwater (1996), Levac (2001). Cold water currents are indicated by blue coloured arrows, namely the Gulf of St. Lawrence waters (GSL), the Nova Scotian Current (NSC) and the inner and outer Labrador Currents (LC). The North Atlantic Current (NAC) transports warm waters (red arrow) flowing north-eastwards in greater water depths. Black dots indicate the location of sediment cores MSM101-13-3 and MSM101-44-3.

The first preliminary results from the SE Scotian Shelf (Roseway Basin) reveal that this record may represent the past 20 kyr and allows to reconstruct the transition from full glacial to modern interglacial conditions. This however, has yet to be confirmed by additional basal radiocarbon dating. Based on the preliminary age model, full marine conditions were established around 12 ka, indicated by a strong colour change in the sediment and the first occurrence of foraminifera. A dominance of cold planktonic foraminifera around 11.4 ka BP may be related to the Younger Dryas cold phase. A following dominance of warm planktonic foraminifera may indicate the first inflow of Atlantic derived waters on the SE Scotian Shelf. This coincides with the Holocene Thermal Maximum, a warm phase reported for the western North Atlantic between 11 and 8 ka BP (e. g., Levac, 2001). This warm phase is, however interrupted by a short dominance of cold planktonic foraminifera around 8.5-8.2 ka, which may be related to the 8.2 ka cold event (e. g., Barber et al., 1999). Further, XRF core scanning revealed a Ca/Ti peak around 8.8 ka BP, which may point towards the inflow of meltwaters derived from the Hudson Bay carrying Paleozoic carbonates underlying the melting ice sheet (Andrews et al., 1995). The Early Holocene is dominated by a continuous cooling trend, associated with the Neoglacial cooling period, following a decrease in solar insolation.

The preliminary results from the NW Scotian Shelf (Scatarie Basin) indicate that this core represents the past 10 ka BP. Prior to 8.6 ka BP, full marine conditions did not prevail over the core site. However, the core site seems to be flooded completely but the exclusive

occurrence of the benthic foraminifera *Brizalina subaenariensis* (Cushman, 1922) indicates hypoxic conditions in the basin. We assume that water mass exchange with the open Atlantic occurred only periodically during this phase. Sea ice biomarkers indicate a heavy sea ice cover over the core site during this phase, which may also contribute to a strong stratification and low productivity. Seasonal sea ice starts to be less severe between 8.6 and 8.4, which may be related by rising sea levels, which increased the sea ice flux southwards, preventing sea ice from being trapped in the basins. Further, the meltwater flow from the drainage of Lake Agassiz had reached the core site, indicated by a Ca/Ti peak during this period. The mid Holocene is dominated by relatively stable intermediate seasonal sea ice conditions, two IRD events, which can be related to short meltwater outbursts of the final disintegration of the Laurentide Ice Sheets. However, Mg/Ca based SST reconstructions from planktonic foraminifera reveal a high variability during the mid-Holocene, indicating short-term Atlantic water intrusions. A continuous cooling trend that can be related to the Neoglaciation is only found during the past 1000 years, by decreasing SST reconstructions and increasing sea ice conditions.

In summary, the first scientific results of expedition MSM101, reveal new insights into the oceanographic changes and indicate a close connection of these changes to climate events. We find a temporal offset between the SE and NW core sites, which has to be investigated further. In the future, a more robust age model will be established for both sediment cores and the proxy record will be completed in the same resolution for both cores.

REFERENCES

- Andrews JT, et al., Final stages in the collapse of the Laurentide Ice Sheet, Hudson Strait, Canada, NWT: 14C AMS dates, seismic stratigraphy, and magnetic susceptibility logs, *Quaternary Science Reviews* 1995, 14. Jg., Nr. 10, S. 983–1004. [https://doi.org/10.1016/0277-3791\(95\)00059-3](https://doi.org/10.1016/0277-3791(95)00059-3).
- Barber DC, Dyke A, Hillaire-Marcel C, Jennings AE, Andrews JT, Kerwin MW, Bilodeau G, McNeely R, Southon J, Morehead MD, Gagnon J-M, Forcing of the cold event of 8200 years ago by catastrophic drainage of Laurentide lakes, *Nature* 1999, 400, 344–348. <https://doi.org/10.1038/22504>.
- Cushman JA, Foraminifera of the Atlantic Ocean, Part III - Textulariidae. United States National Museum Bulletin 1922, Washington, 104, 1–149 p. <https://www.biodiversitylibrary.org/page/7884044>.
- Drinkwater KF, Atmospheric and Oceanic Variability in the Northwest Atlantic during the 1980s and Early 1990s, *Journal of Northwest Atlantic Fishery Science* 1996, 18, 77–97. <https://doi.org/10.2960/J.v18.a6>.

Edgecombe RB, Scott DB, Fader GBJ, New data from Halifax Harbour: paleoenvironment and a new Holocene sea-level curve for the inner Scotian Shelf, *Canadian Journal of Earth Sciences* 1999, 36(5), 805–817. <https://doi.org/10.1139/e99-083>.

Levac E, High resolution Holocene palynological record from the Scotian Shelf, *Marine Micropaleontology* 2001, 43(3–4), 179–197.
[https://doi.org/10.1016/s0377-8398\(01\)00033-0](https://doi.org/10.1016/s0377-8398(01)00033-0).

Pepin, P., G.L. Maillet, D. Lavoie and C. Johnson. 2013. Temporal trends in nutrient concentrations in the northwest Atlantic basin. Ch. 10 (p. 127-150) In: *Aspects of climate change in the Northwest Atlantic off Canada* [Loder, J.W., G. Han, P.S. Galbraith, J. Chassé and A. van der Baaren (Eds.)]. *Can. Tech. Rep. Fish. Aquat. Sci.* 3045: x + 190 p.

Saba VS, Griffies SM, Anderson, WG, Winton M, Alexander MA, Delworth TL, Hare JA, Harrison MJ, Rosati A, Vecchi GA, Zhang R, Enhanced warming of the Northwest Atlantic Ocean under climate change, *J. Geophys. Res. Oceans* 2016, 121, 118–132, doi:10.1002/2015JC011346.

Scott DB, Mudie PJ, Vilks G, Younger DC, Latest Pleistocene–Holocene paleoceanographic trends on the continental margin of eastern Canada: foraminiferal, dinoflagellate and pollen evidence, *Marine Micropaleontology* 1984, 9(3), 181–218.
[https://doi.org/10.1016/0377-8398\(84\)90013-6](https://doi.org/10.1016/0377-8398(84)90013-6).

Vacchi M, Engelhart SE, Nikitina D, Ashe EL, Peltier WR, Roy K, Kopp RE, Horton BP, Postglacial relative sea-level histories along the eastern Canadian coastline, *Quaternary Science Reviews* 2018, 201, 124–146.
<https://doi.org/10.1016/j.quascirev.2018.09.043>.

PS123 AND PS127

Opportunistic collection of bathymetric transit data during Expeditions PS123 and PS127 with R/V Polarstern

AUTHORS

Alfred-Wegener-Institut Helmholtz-Zentrum für Polar- und Meeresforschung |
Bremerhaven, Germany

S. Dreutter, L. Hehemann, B. Dorschel-Herr

World maps give the impression that the global seabed is fully mapped. This is misleading as, according to the General Bathymetric Chart of the Oceans (GEBCO), the authoritative map of the oceans, only about a quarter of the global seabed is constrained by direct measurements (Figure 1 and 2) (GEBCO Bathymetric Compilation Group 2023, 2023). This means that the depth of the seabed is charted with modern echosounders resulting in resolutions of tens to hundreds of metres. In unmapped areas, often referred to as “the gaps in the map”, depth information for the seabed are interpolated from satellite derived predicted bathymetry with corresponding low resolutions of several kilometres.

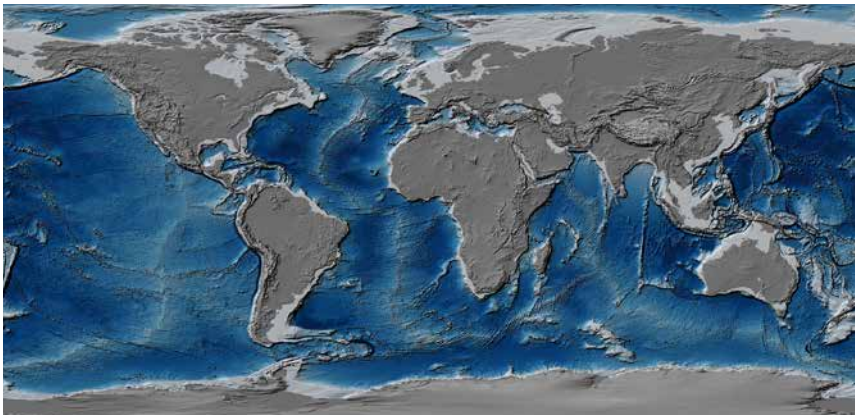


Figure 1: The GEBCO 2023 grid as shaded relief illustration with 12 times vertical exaggeration. The figure shows areas constrained by measured data and areas constrained by satellite derived bathymetry. Below, GEBCO 2023 only showing directly measured data. Interpolated data and satellite derived predicted bathymetry is shown in black.

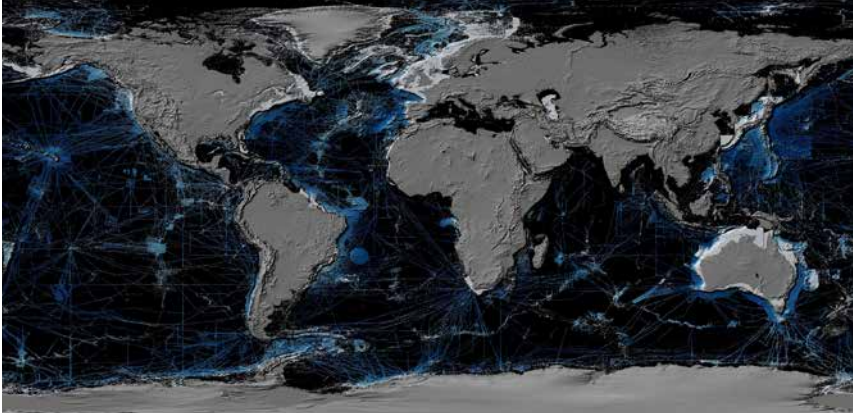


Figure 2: The GEBCO 2023 grid as shaded relief illustration with 12 times vertical exaggeration. The figure only shows areas constrained by measured data. Areas constrained by satellite derived bathymetry, the so-called gaps-in-the-map are shown in black.

This rudimentary state of resolution and coverage of global bathymetric data is outlined in Mayer et al. (2018) and the associated challenges addressed by Wöflfl et al. (2019). At the same time, there is an increasing need for high-quality bathymetric information for e. g. cruise planning, for the interpretation of point measurements in a spatial context, and for conservation and management planning – just to name a few.

Collected over years, bathymetric data can also form the basis for regional bathymetric compilations. Examples are the International Bathymetric Chart of the Arctic Ocean (Jakobsson et al., 2020), the International Bathymetric chart of the Southern Ocean (Dorschel et al., 2022), the Southwest Indian Ocean Bathymetric Compilation (Dorschel et al., 2018), and the Digital Bathymetric Model of the Drake Passage (Bohoyo et al., 2019). These compilations are widely used in various scientific disciplines, are cited in numerous publications, and nicely illustrate the benefit of continuously collected high-quality bathymetric data.

Since 1984, the Alfred Wegener Institute collects bathymetry data with RV Polarstern (Alfred-Wegener-Institut Helmholtz-Zentrum für Polar- und Meeresforschung, 2017) in polar regions and during transit expeditions. Moreover, since 2017, we collect bathymetric transit data with offset cruise tracks thus allowing for the collection of bathymetric data from previously uncharted seabed. Expeditions PS123 and PS127 added to the ever-increasing stripe of mapped seafloor along the transit route from Bremerhaven to Cape Town (Figure 3).

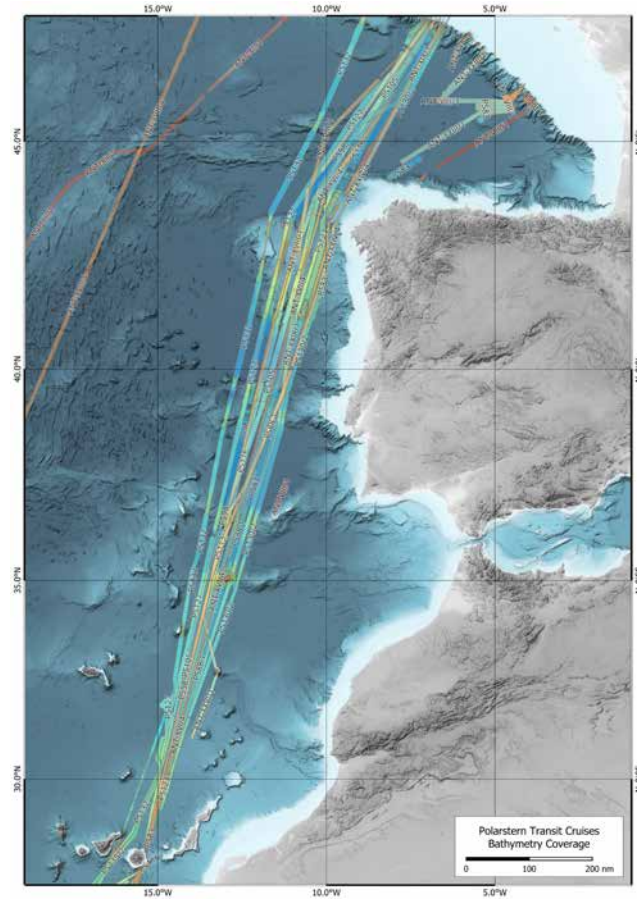


Figure 3: Coverage of opportunistically collected bathymetric transit data with offset cruise tracks for an areas coverage.

Raw and processed bathymetric datasets are publically available in Pangaea (Dreutter et al., 2022, 2023; Hehemann et al., 2023a, b). Furthermore, we provide polygons of the data coverages to the IHO Data Centre for Digital Bathymetry (DCDB) as a web feature service (wfs). We also deliver the processed datasets to the Nippon Foundation – GEBCO Seabed 2030 project, thus supporting the international effort of mapping the entire global seabed by 2030.

REFERENCES

Alfred-Wegener-Institut Helmholtz-Zentrum für Polar- und Meeresforschung, Polar Research and Supply Vessel POLARSTERN Operated by the Alfred-Wegener-Institute, *Journal of large-scale research facilities* 2017, 3, A119, <https://doi.org/10.17815/jlsrf-3-163>.

Bohoyo F, Larter RD, Galindo-Zaldívar J, Leat PT, Maldonado A, Tate AJ, Flexas MM, Gowland EJM, Arndt JE, Dorschel B, Kim YD, Hong JK, López-Martínez J, Maestro A, Bermúdez O, Nitsche FO, Livermore RA, Riley TR, Morphological and geological features of Drake Passage, Antarctica, from a new digital bathymetric model, *Journal of Maps* 2019, 15(2), 49–59, <https://doi.org/10.1080/17445647.2018.1543618>.

Dorschel B, Hehemann L, Viquerat S, Warnke F, Dreutter S, Schulze Tenberge Y, Accettella D, An L, Barrios F, Bazhenova E, Black J, Bohoyo F, Davey C, De Santis L, Escutia Dotti C, Fremand AC, Fretwell PT, Gales JA, Gao J, Gasperini L, Greenbaum JS, Jencks JH, Hogan K, Hong JK, Jakobsson M, Jensen L, Kool J, Larin S, Larter RD, Leitchenkov G, Loubrieu B, Mackay K, Mayer L, Millan R, Morlighem M, Navidad F, Nitsche FO, Nogi Y, Pertuisot C, Post AL, Pritchard HD, Purser A, Rebesco M, Rignot E, Roberts JL, Rovere M, Ryzhov I, Sauli C, Schmitt T, Silvano A, Smith J, Snaith H, Tate AJ, Tinto KJ, Vandenbossche P, Weatherall P, Wintersteller P, Yang C, Zhang T, Arndt JE, The International Bathymetric Chart of the Southern Ocean Version 2, *Scientific Data* 2022, 9(1), 275, <https://doi.org/10.1038/s41597-022-01366-7>.

Dorschel B, Jensen L, Arndt JE, Brummer G-JA, de Haas H, Fielies A, Franke D, Jokat J, Krockner R, Kroon D, Pätzold J, Schneider RR, Spieß V, Stollhofen H, Uenzelmann-Neben G, Watkeys MK, Wiles EA, The Southwest Indian Ocean Bathymetric Compilation (swIOBC), *Geochemistry, Geophysics, Geosystems* 2018, <https://doi.org/10.1002/2017GC007274>.

Dreutter S, Schulze Tenberge Y, Dorschel B, Multibeam bathymetry raw data (Atlas Hydrosweep DS 3 echo sounder entire dataset) of RV POLARSTERN during cruise PS123, 2022, <https://doi.org/10.1594/PANGAEA.948590>.

Dreutter S, Schulze Tenberge Y, Dorschel B, Multibeam bathymetry processed data (Atlas Hydrosweep DS 3 echo sounder entire dataset) of RV POLARSTERN during cruise PS123, Atlantic Ocean, 2023, <https://doi.org/10.1594/PANGAEA.954624>.

GEBCO Bathymetric Compilation Group 2023, The GEBCO_2023 Grid – a continuous terrain model of the global oceans and land, 2023, <https://doi.org/10.5285/f98b053b-0cbc-6c23-e053-6c86abc0af7b>.

Hehemann L, Brehmer-Moltmann J, Dreutter S, Dorschel B, Multibeam bathymetry processed data (Atlas Hydrosweep DS 3 echo sounder entire dataset) of RV POLARSTERN during cruise PS127, Atlantic Ocean, 2023a, <https://doi.org/10.1594/PANGAEA.954699>.

Hehemann L, Brehmer-Moltmann J, Dreutter S, Dorschel B, Multibeam bathymetry raw data (Atlas Hydrosweep DS 3 echo sounder entire dataset) of RV POLARSTERN during cruise PS127, 2023b, <https://doi.org/10.1594/PANGAEA.949989>.

Jakobsson M, Mayer LA, Bringensparr C, Castro CF, Mohammad R, Johnson P, Ketter T, Accettella D, Amblas D, An L, Arndt JE, Canals M, Casamor JL, Chauché N, Coakley B, Danielson S, Demarte M, Dickson M-L, Dorschel B, Dowdeswell JA, Dreutter S, Fremand AC, Gallant D, Hall JK, Hehemann L, Hodnesdal H, Hong J, Ivaldi R, Kane E, Klaucke I, Krawczyk DW, Kristoffersen Y, Kuipers BR, Millan R, Masetti G, Morlighem M, Noormets R, Prescott MM, Rebesco M, Rignot E, Semiletov I, Tate AJ, Travaglini P, Velicogna I, Weatherall P, Weinrebe W, Willis JK, Wood M, Zarayskaya Y, Zhang T, Zimmermann M, Zinglensen KB, The International Bathymetric Chart of the Arctic Ocean Version 4.0, *Scientific Data* 2020, 7(1), 176, <https://doi.org/10.1038/s41597-020-0520-9>.

Mayer LA, Jakobsson M, Allen GL, Dorschel B, Falconer R, Ferrini V, Lamarche G, Snaith H, Weatherall P, The Nippon Foundation—GEBCO Seabed 2030 Project: The Quest to See the World's Oceans Completely Mapped by 2030, *Geosciences* 2018, 8(2), 63, <https://doi.org/10.3390/geosciences8020063>.

Wöfl A-C, Snaith H, Amirebrahimi S, Devey CW, Dorschel B, Ferrini V, Huvenne VAI, Jakobsson M, Jencks J, Johnston G, Lamarche G, Mayer L, Millar D, Pedersen TH, Picard K, Reitz A, Schmitt T, Visbeck M, Weatherall P, Wigley R, Seafloor Mapping – The Challenge of a Truly Global Ocean Bathymetry, *Frontiers in Marine Science* 2019, 6(283), <https://doi.org/10.3389/fmars.2019.00283>

PS127

Autonomous measurement platforms for energy and material exchange between ocean and atmosphere (OCEANET): Atmosphere

AUTHORS

Institute for Tropospheric Research (TROPOS) | Leipzig, Germany
R. Engelmann, K. Ohneiser, R. Hengst, M. Hajipour, A. Macke

The OCEANET-ATMOSPHERE project delivers valuable atmospheric measurement datasets over the oceans – in regions of the world that are not easily accessible. For the last 14 years, a container-based platform is operated regularly at RV Polarstern to obtain measurements and to contrast atmospheric processes between the anthropogenic polluted northern hemisphere and the more undisturbed southern hemisphere.

OCEANET participated already in 22 Polarstern cruises (often on Atlantic transects, including summer schools, PS106 PASCAL, MOSAiC). During MOSAiC in 2019-2020 measurements with OCEANET were extremely successful. The highlight of the lidar measurements was the detection of a 10 km deep wildfire smoke layer over the North Pole region between 7–8 km and 17–18 km height. We published the research on our atmospheric measurements on R/V Polarstern in more than 6 publications. More publications will follow.

Another focus for our poster presentation will be the measurements during PS127 from Bremerhaven to Cape Town (December 2021 – January 2022). The instruments on board were a multichannel microwave radiometer HATRPO, a total-sky imager for cloud-structure measurements, a multiwavelength polarization Raman lidar PollyXT, a handheld sun photometer (Microtops) for aerosol and cloud optical thickness, an automatic Cimel sun photometer, a fully-automated spectral shadow band radiometer (GUVis-3511), and a wind lidar litra that has ship-motion-corrected data. The highlight of our measurements was the detection of a long-lasting optically thick dust plume with our lidar instrument downwind of the African Sahara. In addition, the meanwhile retired ESA satellite Aeolus was in its orbit in late 2021 equipped with a wind lidar on board. We obtained valuable ground-comparison profiles during PS127 in order to calibrate and validate the data within the EVAA project (Experimental Validation and Assimilation of Aeolus observations).

On our poster presentation we will present the highlights of our 14 years of OCEANET on R/V Polarstern with the main focus on PS122 (MOSAIC) and PS127.

REFERENCES

Bohmann S, et al., Ship-borne aerosol profiling with lidar over the Atlantic Ocean: from pure marine conditions to complex dust–smoke mixtures, *Atmos. Chem. Phys.* 2018.

Griesche H, et al., Application of the shipborne remote sensing supersite OCEANET for profiling of Arctic aerosols and clouds during Polarstern cruise PS106, *Atmos. Meas. Tech.* 2020.

Ohneiser K, et al., The unexpected smoke layer in the High Arctic winter stratosphere during MOSAiC 2019–2020, *Atmos. Chem. Phys.* 2021.

Griesche HJ, et al., Contrasting ice formation in Arctic clouds: surface-coupled vs. surface-decoupled clouds, *Atmos. Chem. Phys.* 2021.

Engelmann R, et al., Wildfire smoke, Arctic haze, and aerosol effects on mixed-phase and cirrus clouds over the North Pole region during MOSAiC: an introduction, *Atmos. Chem. Phys.* 2021.

Ansmann A, et al., Ozone depletion in the Arctic and Antarctic stratosphere induced by wildfire smoke, *Atmos. Chem. and Phys.* 2022.

Wendisch M, et al., Atmospheric and surface processes, and feedback mechanisms determining Arctic amplification: A review of first results and prospects of the (AC) 3 project, *BAMS* 2023.

Ansmann, A. et al., Annual cycle of aerosol properties over the central Arctic during MOSAiC 2019–2020—light-extinction, CCN, and INP levels from the boundary layer to the tropopause, *Atmos. Chem. Phys.* 2023.

SO264

SONNE-EMPEROR: The Plio/Pleistocene to Holocene development of the pelagic North Pacific

AUTHORS

GEOMAR Helmholtz Centre for Ocean Research Kiel | Kiel, Germany
D. Nürnberg, L. Jacobi

Alfred-Wegener-Institut Helmholtz-Zentrum für Polar- und Meeresforschung |
Bremerhaven, Germany
R. Tiedemann, L. Lembke-Jene, W.-S. Chao

Universität Bremen, Fachbereich Geowissenschaften | Bremen, Germany
Th. Friederichs

Sediment cores from the volcanic Emperor seamount chain obtained during SO264 (Figure 1) allow us to reconstruct lateral changes in the subarctic and subtropical gyres in the pelagic North Pacific over the last ~3.4 Ma. Sea-surface ($SST_{Mg/Ca}$) and sub-surface ($subSST_{Mg/Ca}$) temperatures and salinities ($\delta^{18}O_{sw}$) were reconstructed using combined Mg/Ca and stable isotope ($\delta^{18}O$) measurements on shallow and deeper dwelling planktonic foraminifera. XRF scanner data illustrate the variability of marine productivity and dust input.

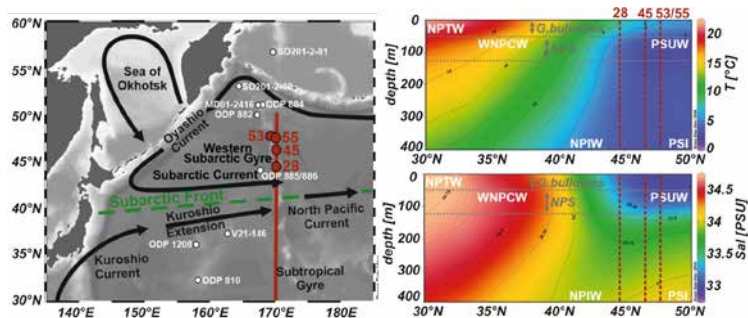


Figure 1: Oceanography of the SO264 SONNE-EMPEROR study area (Emperor seamount chain in the North Pacific). Left: Bathymetric map with the locations of the processed sediment cores SO264-55, -53, -45 and -28, and reference cores. Surface currents and the Subarctic Front are marked. Red line = N-S oriented sections to the right. Right: Temperature and salinity sections from 30°N to 50°N (Schlitzer, 2002). Core locations are marked, as are the habitats of the planktonic foraminifera species studied. NPTW = North Pacific Tropical Water; WNPCW = Western North Pacific Central Water; PSUW = Pacific Subarctic Upper Water; NPIW = North Pacific Intermediate Water.

Sea-surface dynamics during ~3.3–2.73 Ma BP. In the Pliocene period prior to ~2.73 Ma BP, all proxy parameters show laterally different conditions in the oceanic mixed layer

between $\sim 46.5^{\circ}\text{N}$ and 47.5°N (Figure 2). Marine productivity was higher at the southern core locations. At the same time, the $\text{SST}_{\text{Mg/Ca}}$ were warmer by more than $\sim 2^{\circ}\text{C}$. The high mixed layer temperatures demonstrate that our core locations were influenced by the subtropically warm and saline North Pacific Tropical Water (NPTW) (Figure 1), due to a marked northward shift of both subtropical and subarctic frontal systems.

A clear drop in mixed layer temperatures by more than $\sim 4^{\circ}\text{C}$ and a change to lower salinity conditions occurred at ~ 2.73 Ma BP with the intensification of the northern hemisphere glaciation (NHG; Lisiecki & Raymo, 2005), pointing to the southward shift of the subtropically warm Western North Pacific Central Water (WNPCW) and the stronger influence of the cooler and fresher Pacific Subarctic Upper Water (PSUW) (Figure 1) within only a few thousand years. The discrepancy to the alkenone-based $\text{SST}_{\text{UK}^{37}}$ warming indicates a clearly increasing seasonality in the study area (Riethdorf et al., 2013b; Haug et al., 2005). For the period before ~ 2.73 Ma BP, Abell et al. (2021) postulate weaker westerly winds and a northward shift of the westerly wind axis, indicated by low Fe values in our records.

Periods from ~ 2.73 – 1.7 Ma BP and ~ 1.7 – 1.3 Ma BP. The Ca/Ti (calcareous phytoplankton) and Ba/Ti records (siliceous plankton) (Riethdorf et al., 2013a) show a significant decline in marine productivity after ~ 2.73 Ma BP, associated with the NHG-intensification (Figure 2). The decline in marine productivity was associated with the formation of a stable, deep halocline and permanent stratification in the North Pacific, which reduced the transport of nutrient-rich deep water masses into the euphotic zone. After 2.73 Ma BP, enhanced dust fluxes (Abell et al., 2021) and Fe inputs point to the intensification of the atmospheric circulation and the southward shift of the "East Asian Jet Stream" axis across our study area. From ~ 2.1 Ma BP we see a much more dynamic development of the near-surface North Pacific than previously known (Martínez-García et al., 2010). Until ~ 1.7 Ma BP, the $\text{SST}_{\text{Mg/Ca}}$ were 2 – 3°C warmer and the $\text{subSST}_{\text{Mg/Ca}}$ 2 – 3°C cooler than today, while the salinities of the surface layer and their amplitude variations remain comparable, indicating a stable and deep halocline. The gradual but variable trend towards warmer $\text{SST}_{\text{Mg/Ca}}$ (max. 12°C , comparable to $\text{SST}_{\text{Mg/Ca}}$ prior to ~ 2.73 Ma BP) and cooler $\text{subSST}_{\text{Mg/Ca}}$ (min. 1°C) intensified over the period 1.7 – 1.3 Ma BP, resulting in an increasing vertical temperature gradient. The corresponding shallow thermocline is explained by the northward (seasonal) extension of a shallow tongue of subtropical NPTW and WNPCW above the subarctic PSUW. We interpret the significant drop in $\text{subSST}_{\text{Mg/Ca}}$ by ~ 2 – 3°C at ~ 1.7 Ma BP as southward spreading of the PSUW below the shallow WNPCW (Figure 1). The intensified northward net heat transport at surface was likely related to a gradual northwestward expansion of the West Pacific Warm Pool (WPWP) and a shift of the South Pacific Convergence Zone during 1.7 – 1.3 Ma BP (Raddatz et al., 2017), causal for an intensified or northward shifted Kuroshio Current. The continuously decreasing meridional SST gradient between the WPWP and the equatorial East Pacific since ~ 1.7 – 1.3 Ma BP (de Garidel-Thoron et al., 2005) underpins a significant influence of the WPWP on the North Pacific surface hydrography (Figure 1).

Period from 1.3–0.7 Ma BP. After ~1.35 Ma BP, the eolian dust (Fe) input and amplitudes increase significantly, showing glacial/interglacial variations for the last ~800,000 years with systematically lower Fe input during interglacials. Glacial dust maxima are attributed to the "East Asian Jet Stream" (Rack et al., 2014). During ~1.3–0.7 Ma BP, the SST_{Mg/Ca} are persistently 1–2°C higher than today's SST conditions, with pronounced amplitude fluctuations of up to ~6°C (Figure 2). From ~1.3 Ma BP, the vertical temperature gradient in the study area decreases, also with marked glacial/interglacial variations. The correspondingly deepening thermocline is due to an increasing vertical expansion of subtropical water masses (NPTW, WNPCW) to the deeper levels. The phases of pronounced thermocline deepening often appear synchronous with northward expansions of the WPWP (Raddatz et al., 2017; de Garidel-Thoron et al., 2005).

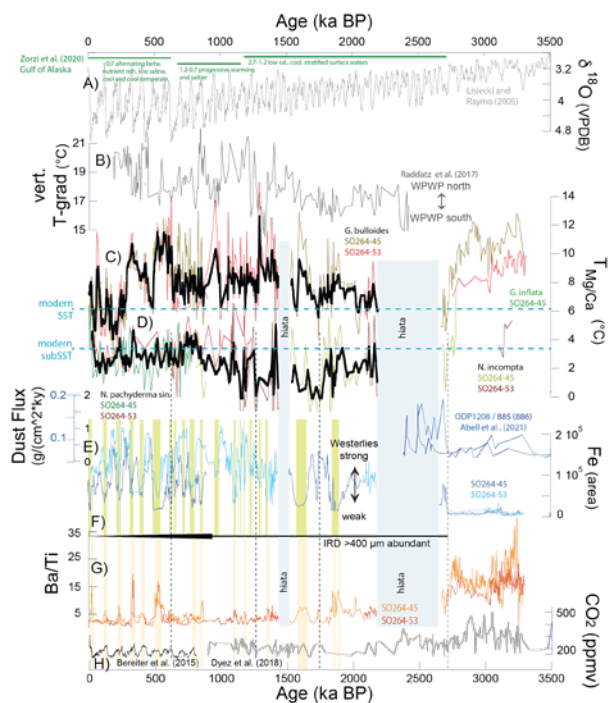


Figure 2: Combined proxy records of cores SO264-45 and -55 of the last ~3.4 Ma compared to reference data sets. A) LR04 $\delta^{18}\text{O}$ climate record (Lisiecki & Raymo, 2005); green annotations from Zorzi et al. (in press) regarding ODP Site 887 (Gulf of Alaska). B) Vertical temperature gradient in the W-Pacific Warm Pool (WPWP; Raddatz et al., 2017) with gradual northward shift of the WPWP from ~1.7–1.35 Ma BP. C) Surface temperatures (SST from $\text{Mg}/\text{Ca}_{G.\text{bulloides}}$; green: core -45; red: core -53) with SST mean curve (black). D) Near-surface temperatures (subSST from $\text{Mg}/\text{Ca}_{N.\text{pachyderma}}$ and $\text{Mg}/\text{Ca}_{N.\text{incompta}}$; green: core -45; brown: core -53) with subSST mean curve (black). Blue dashed lines = today's SST and subSST. E) Fe (light blue = core -53; dark blue = core -45) shows the variability of the aeolian dust input and thus changes in the westerly wind drift. Phases of low Fe input, mainly during warm periods, are highlighted in green. In comparison: Dust inputs at ODP Sites 1208 and 885/886 (Abell et al., 2021). F) Ice transported material (IRD; defined as $>400\ \mu\text{m}$, non-basaltic, partly rounded, lithogenic sediment components). G) Ba/Ti (red = core -53; orange = core -45) reflects changes in marine productivity. Phases of increased productivity (orange shading) appear predominantly during deglaciations and early interglacials. H) Atmospheric CO_2 (Bereiter et al., 2015; Dyez et al., 2018). Blue shading = hiata.

Glacial/interglacial surface dynamics of the last 0.7 Ma. On glacial-interglacial time scales over the last 700 kyrs, export production in the North Pacific varied in concert with atmospheric CO₂ concentrations, implying more effective nutrient utilization during glacials (Galbraith et al., 2008). Marine productivity mostly increased during deglaciations and reached maxima during early interglacials (Figure 2). Because Fe inputs followed productivity maxima and reached maxima during late and outgoing interglacials and early glacials, eolian Fe inputs had negligible impact on marine productivity (Jacobi et al., 2023). Other mechanisms regulating nutrients and the biological utilization, at least in the seasonally sea ice-affected northern regions, are deglacially increasing insolation, thermal stratification with accompanying higher nutrient consumption as sea ice cover loosens and the ice margin retreats. In addition, increased advection of Fe-rich Okhotsk Sea Intermediate Water into the upper subarctic Pacific might have provided nutrients from below.

Clearly independent of glacial/interglacial changes in marine productivity and terrigenous input, the mixed layer temperatures evolve. While the subSST_{Mg/Ca} show little variation ($\pm 1.5^\circ\text{C}$) around a steady mean of $\sim 3^\circ\text{C}$ indicating a continuous presence of deeper subarctic PSUW, the SST_{Mg/Ca} change gradually from relatively high values of $\sim 10\text{--}12^\circ\text{C}$ to $\sim 6\text{--}8^\circ\text{C}$. The initial large vertical temperature gradient suggests a shallow thermocline due to the northward extension of a shallow tongue of warm subtropical water masses (NPTW, WNPCW) during prevailing La Niña-like climate conditions. This heat transfer might have been seasonal (summer) only, as glacial/interglacial variability in productivity and terrigenous proxies at the core location does not suggest a significant shift in the Subarctic Front. Rapid SST_{Mg/Ca} cooling of $\sim 4^\circ\text{C}$ during the "Mid Brunhes Transition" at 480 ka BP and subsequently at ~ 280 ka BP indicating a reduced Kuroshio Current system, occurs synchronously with reductions in marine productivity and increased Fe input. From ~ 280 ka BP, the SST_{Mg/Ca} vary around the present-day SST value of $\sim 6^\circ\text{C}$ with low SST_{Mg/Ca} around $\sim 4\text{--}5^\circ\text{C}$ during glacials and marked SST_{Mg/Ca} warmings during deglaciations.

REFERENCES

Abell J T, Winckler G, Anderson R F, Herbert T D, Poleward and weakened westerlies during pliocene warmth, *Nature* 2021, 589, 70–75. doi: 10.1038/s41586-020-03062-1.

Bereiter B, Eggleston S, Schmitt J, Nehrbass-Ahles C, et al., Revision of the EPICA Dome C CO₂ record from 800 to 600 kyr before present, *Geophysical Research Letters* 2015, 42, 542–549. doi:10.1002/2014GL061957.

de Garidel-Thoron Th, Rosenthal Y, Bassinot F, Beaufort L, Stable sea surface temperatures in the western Pacific warm pool over the past 1.75 million years, *Nature* 2005, 433, 294-298. www.nature.com/nature.

Haug G H, Ganopolski A, Sigman D N, Rosell-Mele A, et al., North Pacific seasonality and the glaciation of North America 2.7 million years ago, *Nature* 3005, 433, 821-825. www.nature.com/nature.

Dyez K A, Hönisch B, Schmidt G A, Early Pleistocene obliquity-scale pCO₂ variability at ~1.5 million years ago, *Paleoceanography and Paleoclimatology* 2018, 33, 1270–1291. <https://doi.org/10.1029/2018PA003349>.

Galbraith E D, Kienast M, Jaccard S L, Pedersen T F, et al., Consistent relationship between global climate and surface nitrate utilization in the western subarctic Pacific throughout the last 500 ka, *Paleoceanography* 2008, 23, PA2212.

Haug G H, Ganopolski A, Sigman D M, Rosell-Mele A, et al., North Pacific seasonality and the glaciation of North America 2.7 million years ago, *Nature* 2005, 433, 821–825. doi:10.1038/nature03332.

Jacobi L, Nürnberg D, Chao W-S, Lembke-Jene L, et al., ENSO vs glacial-interglacial-induced changes in the Kuroshio-Oyashio transition zone during the Pleistocene, *Frontier in Marine Science* 2023, 10:1074431. doi: 10.3389/fmars.2023.1074431.

Lisiecki L E, Raymo M E, A Pliocene-Pleistocene stack of 57 globally distributed benthic $\delta^{18}\text{O}$ records, *Paleoceanography* 2005, 20, 1–17. <http://dx.doi.org/10.1029/2004PA001071>.

Martínez-García A, Rosell-Melé A, McClymont E L, Gersonde R, et al., Subpolar link to the emergence of the modern equatorial Pacific Cold Tongue, *Science* 2010, 328, 1550. doi: 10.1126/science.1184480.

Rack F R, Rutter, N W, Bush A, Rokosh D, et al., Linking ocean and continental records of paleoclimate: Determining accord and discord in the records, *Canadian Journal of Earth Sciences* 2000, 37, 831–848. DOI: 10.1139/cjes-37-5-831.

Raddatz J, Nürnberg D, Tiedemann R, Rippert N., Southeastern marginal West Pacific Warm Pool sea-surface and thermocline dynamics during the Pleistocene (2.5–0.5 Ma), *Palaeogeography, Palaeoclimatology, Palaeoecology* 2017, 471, 144–156.

Riethdorf J R, Nürnberg D, Max L, Tiedemann R, et al., Millennial-scale variability of marine productivity and terrigenous matter supply in the western Bering Sea over the past 180 kyr, *Climate of the Past* 2013a, 9, 1345-1373. doi: 10.5194/cp-9-1345-2013.

Riethdorf J R, Max L, Nürnberg, D, Lembke-Jene L, et al., Deglacial development of (sub) sea surface temperature and salinity in the subarctic northwest Pacific: Implications for upper-ocean stratification, *Paleoceanography* 2013b, 28, 91–104. doi:10.1002/palo.20014.

Schlitzer R, Interactive analysis and visualization of geoscience data with ocean data view, *Computational Geoscience* 2002, 28, 1211–1218.

Zorzi C, Matthiessen M, de Vernal A, Palynology, biostratigraphy, and paleoceanbography of the Plio-Pleistocene at Ocean Drilling Program Site 997, Gulf of Alaska. *Palaeogeography, Palaeoclimatology, Palaeoecology* 2020. <https://doi.org/10.1016/j.palaeo.2020.109605>.

SO264

Tephrostratigraphy for late Pleistocene sediments of the Minnetonka Seamount (~47°N 169°E; Emperor Seamount Chain) based on core SO264-55-1

AUTHORS

Institute of Volcanology and Seismology RAS | Petropavlovsk-Kamchatsky, Russia
V. Ponomareva

Shirshov Institute of Oceanology RAS | Moscow, Russia
N. Bubenshchikova

GEOMAR Helmholtz Centre for Ocean Research Kiel | Kiel, Germany
M. Portnyagin, D. Nürnberg

Alfred Wegener Institute Helmholtz Centre for Polar and Marine Research | Bremerhaven, Germany
L. Lembke-Jene, R. Tiedemann

Quaternary sediments preserved on the Emperor Seamount Chain (ESC) provide a unique opportunity to study variations in the past oceanographic conditions at mid to high latitudes of the Northwest (NW) Pacific relative to glacial to interglacial climate changes (Nürnberg, 2018). Numerous tephra layers interbedded in the ESC sediments and related to the past activity within the Kurile-Kamchatka and Alaska-Aleutian volcanic arcs may help to establish regional stratigraphy, which is a prerequisite for paleoceanographic reconstructions. A detailed tephrostratigraphical framework, including geochemically characterized and dated 119 unique ash layers (labelled DS1 to DS119), has been recently developed for the 6.2 Ma-old sediments of the Detroit Seamount of the northernmost ECS based on study of the ODP Sites 882A and 884B and core MD01-2416 (Ponomareva et al., 2023). To extend the regional tephrostratigraphy for sediments of mid latitude part of the ECS, we here present the results of our research on tephra preserved in core SO264-55-1. The 16.11 m - long core SO264-55-1 (47°10.542N; 169° 25.292E) was recovered from a 2936 m water depth at the Minnetonka Seamount of the ESC during the R/V "Sonne-Emperor" cruise SO264 held in the North Pacific in 2018 (Nürnberg, 2018). The core SO264-55-1 sediments were estimated to cover 450 to 6.8 ka basing on AMS ^{14}C dating, XRF-based chronostratigraphy and stable oxygen isotope ($\delta^{18}\text{O}$) stratigraphy (Chao et al., 2023). The identification near the SO264-55-1 core base of ca. 418 ka Pauzhetka tephra (Bubenshchikova et al., 2024) supported the age of the oldest sediments in the core. The aims of this study are: (1) to establish a tephra record for 450 to 6.8 ka of core SO264-55-1; (2) to date the

tephras by refining of the $\delta^{18}\text{O}$ stratigraphy of the core (Chao et al., 2023); (3) to evaluate potential of the tephras for tephrostratigraphy the NW Pacific sediments. To achieve the study objectives, we obtained new data on major and trace elemental compositions of tephra glass and $\delta^{18}\text{O}$ compositions of benthic foraminifera from core SO254-55-1.

In core SO246-55-1, we detected occurrence of visible tephra layers during the on board lithological description (Nurnberg, 2018) and the post-cruise analysis of high resolution XRF-retrieved K/Ti and K/Fe records (Chao et al., 2023) and re-examination of the sediments. In total, twelve 1.5 to 13.5 cm -thick tephra layers, also forming the prominent concurrent maxima/ minima in the K/Ti and K/Fe records, were recognised and sampled. In addition, using the inconspicuous concurrent maxima/ minima in the K/Ti and K/Fe records as a proxy for presence of invisible by naked eyes volcanic glass in sediments, we identified and sampled fifteen glass enriched horizons (referred to as potential cryptotephra).

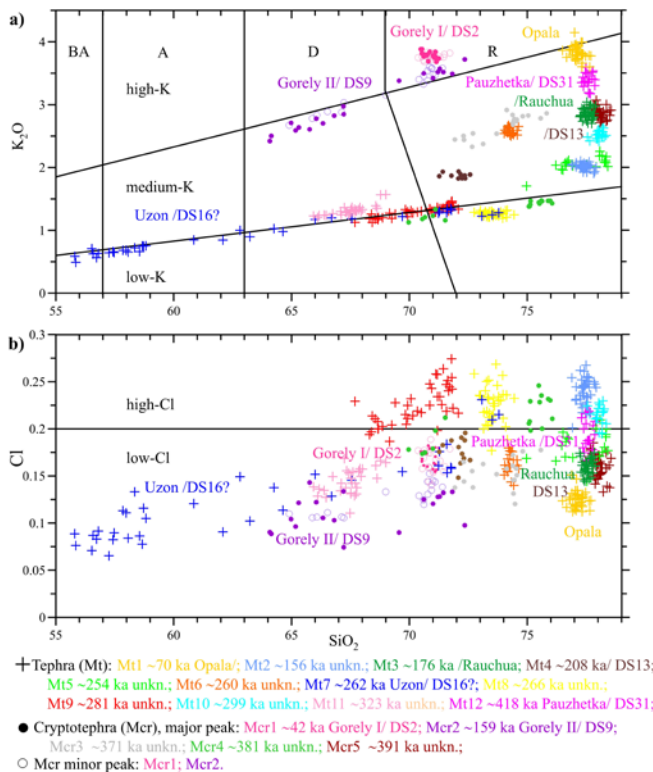


Figure 1: Major elemental compositions for single glass shards from tephras (Mt) 1 to Mt12 and cryptotephra (Mcr) 1 to 5 in core SO264-55-1. The ages are derived from benthic $\delta^{18}\text{O}$ stratigraphy of the core. The tephra correlations to source volcano/ regional tephra or unknown state (= unkn.) are indicated. a: Solid lines divide fields of low- K_2O , medium- K_2O , and high- K_2O basalts (B), basaltic andesites (BA), andesites (A), dacites (D), and rhyolites (R).

Major elements in glass shards of each tephra sample were analysed at the GEOMAR Helmholtz Centre for Ocean Research Kiel (Germany) using JEOL JXA 8200 EPM equipped with 5 wave-length dispersive spectrometers. Twelve tephtras labelled as (Mt)1 to Mt12 and five cryptotephtras marked as (Mcr)1 to Mcr5 were characterised by the EMP data (Figure 1). The identified tephtras and cryptotephtras were further investigated with respect to the trace element compositions of glass shards at the Institute of Geosciences, Christian-Albrecht University of Kiel (Germany) using Agilent 8900 triple quadrupole ICP-MS. In order to define source volcanoes of the Minnetonka tephtra deposits, we compared their geochemical characteristics to the database of the Kamchatka proximal glass compositions (Portnyagin et al., 2020). We also compared the Minnetonka glass compositions to those described in the Detroit Seamount and Meiji Rise sediments and to those of other known terrestrial and submarine tephtras in the studied region.

Because of calcareous benthic foraminifera were rare or absent in a number intervals of core SO264-55-1, the generation of a continuous monospecies-based $\delta^{18}\text{O}$ record was not possible for the core (Chao et al., 2023). The previous core composite benthic $\delta^{18}\text{O}$ record was constructed mainly on $\delta^{18}\text{O}$ values on *Uvigerina* (*U.*) *peregrina* and *U. senticosa*, from the 250–500 μm size fraction (Chao et al., 2023). In order to detail the core $\delta^{18}\text{O}$ record, in particularly its older part, we took sediment samples and collect predominantly *U. auferiana* and *U. peregrina*, and in case of their absence *Melonis* (*M.*) *pompiloides*, *M. barleanum*, or *Gyroidina* spp. from the 250–500 μm size fraction. The $\delta^{18}\text{O}$ measurements were performed at GEOMAR using a Finnigan MAT 253 mass spectrometer coupled to an automatic Kiel carbonate preparation line. In total, we obtained 179 $\delta^{18}\text{O}$ measurements for 147 samples. We constructed a composite $\delta^{18}\text{O}$ record by using uncorrected values on *Uvigerina* spp. and corrected values on all other measured species in the core. We refined depth-age control points for core SO264-55-1 correlating its composite benthic $\delta^{18}\text{O}$ record to LR04 stack (Lisiescki and Raymo, 2005). The ages of all tephtra bottom depth (or cryptotephtra K/Ti or K/Fe maximum depth) were calculated by linear interpolation between the new depth-age control points.

In core SO264-55-1, we have geochemically fingerprinted twelve tephtras and five cryptotephtras with the help of 540 EMP and 135 LA-ICP-MS analyses (Figure 1). Basing on comparison with the proximal Kamchatka deposits (Portnyagin et al., 2020), we related the origin of three tephtras and two cryptotephtras to the activity within the Kamchatka volcanic arc, namely Mt1, Mt7 and Mt12 - to Opala, Uzon and Pauzhetka calderas, respectively, and Mcr1 and Mcr2 to Gorely volcano. The provenance of the other nine tephtras and three cryptotephtras remained unknown. However, high Cl contents in tephtras Mt2, Mt8, Mt9 and Mt10 and cryptotephtra Mcr4 (Figure 1b) suggest their probable origin from the activity within the Kurile volcanic arc. Four tephtras and two cryptotephtras were found to belong to the regional tephtras previously described in terrestrial sites and/ or marine cores of the studied region. Basing on the correlation to the Detroit tephrochronological framework (Ponomareva et al., 2023),

we tied the Mcr1 to DS2, Mcr2 to DS9, Mt4 to DS13, Mt7 to DS16, and MT12 to DS31 (Pauzhetka) tephra. The widespread 418 ka Pauzhetka tephra (Mt12 here) has now known in fourteen cores from the NW Pacific and two cores from the Okhotsk Sea (Bubenshchikova et al., 2024). The Pauzhetka tephra has been suggested as a regional marker for Termination V that is in good agreement with the $\delta^{18}\text{O}$ stratigraphy of SO264-55-1 core. The well-known 175-177 ka Rauchua tephra (Mt3 here) has been described in Arctic coast and later found in the Elgygytgyn Lake sediments (T1 there) and the Meiji Rise sediments (WP14 there) (e.g., Derkachev et al., 2020). The results of our study supports high potential of the identified tephras and cryptotephras for the stratigraphy of the NW Pacific sediments.

This research was funding by the German Ministry of Education and Research (BMBF), grants 03G0264A (GEOMAR) and 03G0264B (AWI). VP and NB gratefully acknowledge support of Russian Science Foundation grant #22-17-10074, <https://rscf.ru/en/project/22-17-00074/>.

REFERENCES

Bubenshchikova N, Ponomareva V, Portnyagin M, et al., The Pauzhetka tephra (South Kamchatka): A key middle Pleistocene isochron for the Northwest Pacific and Okhotsk Sea sediments, *Quaternary Geochronology* 2024, 79 101476, doi.org/10.1016/j.quageo.2023.101476.

Chao W, Jacobi L, Niederbockstruck B, et al., XRF Down-Core Scanning Data, Benthic Oxygen Isotope, Sand Fraction and Geochemistry Data of Sediment Cores from the Subarctic Northwest Pacific during the Last 500,000 Years, *PANGAEA*. 2023, doi.org/10.1594/PANGAEA.955877.

Derkachev AN, Gorbarenko SA, Ponomareva V, Portnyagin M, Middle to late Pleistocene record of explosive volcanic eruptions in marine sediments offshore Kamchatka (Meiji Rise, NW Pacific), *Journal of Quaternary Science* 2020, 35(1-2) 362–379, doi: 10.1002/jqs.3175.

Lisiecki LE, Raymo M, A Pliocene-Pleistocene stack of 57 globally distributed benthic ^{18}O records, *Paleoceanography* 2005, 20, PA1003, doi:10.1029/2004PA001071.

Nürnberg D, Cruise report SO264-SONNE-EMPEROR: the PlioPleistocene to Holocene Development of the pelagic North Pacific from surface to depth – Assessing its role for the global Carbon Budget and Earth's climate, Suva (Fiji) – Yokohama (Japan), 30.6. – 24.8.2018. In: *GEOMAR Report N. Ser 2020*, vol. 46, p. 284, doi.org/10.3289/GEOMAR.

Ponomareva VV, Portnyagin MV, Bubenshchikova NV, Zelenin EA, Derkachev AN, Jicha B, et al. A 6.2 Ma-long record of major explosive eruptions from the NW Pacific volcanic arcs based on the offshore tephra sequences on the northern tip of the Emperor Seamount Chain. *Geochemistry, Geophysics, Geosystems* 2023, 24, e2023GC011126, doi.org/10.1029/2023GC011126.

Portnyagin MV, Ponomareva VV, Zelenin EA, et al., TephraKam: geochemical database of glass compositions in tephra and welded tuffs from the Kamchatka volcanic arc (northwestern Pacific), *Earth System Science Data* 2020, 12, 469–486, doi.org/10.5194/essd-12-469-2020.

SO287

Planktonic and Micronektonic Scattering Layer distribution along latitudinal section: from North East Atlantic to Eastern Tropical Pacific Oceans

AUTHORS

CRODT – Centre de Recherche Océanographique de Dakar Thiaroye | Dakar, Senegal

N. Diogoul

IRD – Institute for Research and Development | Dakar, Senegal

P. Brehmer

IRD – Institute for Research and Development | Brest, France

Y. Perrot

ARDITI – Agência Regional para o Desenvolvimento da Investigação, Tecnologia e Inovação | Funchal, Portugal

J. Reis, A. Rosa

Kiel University – Institute of Geosciences, Coastal Geology And Sedimentology | Kiel, Germany

R. Kopte

GEOMAR Helmholtz Centre for Ocean Research Kiel | Kiel, Germany

B. Quack

Pelagic Sound Scattering Layers (SSLs) are ubiquitous in all oceans (Tont, 1976; Boswell et al., 2020; Geoffroy et al., 2019) and the result of acoustic scattering from extensive aggregations of micronekton and large zooplankton (Proud et al., 2015; Behagle et al., 2017). SSLs appear continuous on the echogram from scientific echosounder (Simmonds and MacLennan, 2006) vertically narrow, tens to hundreds of meters, and horizontally extensive for tens to thousands of kilometers (Proud et al., 2015). In this study, we explore acoustic and environmental data obtained along a cross Atlantic sea survey ending in the Eastern Tropical Pacific Ocean. In our research, we described the distribution patterns of SSLs along the transport pathway of water from the Northwest African EBUS to the Sargasso Sea and, subsequently, to the Caribbean Sea and the Eastern Tropical Pacific Ocean. On this basis, we scrutinized the SSLs spatial variability in response to key environmental factors taking advantage of the contrasted area surveyed.

Our dataset, collected during the SO287 Connect cross-tropical Atlantic cruise, encompassed acoustic and environmental data. We used a Simrad EK60 echosounder to collect acoustic data, as well as Acoustic Doppler Current Profilers (ADCP) to measure backscatter and water velocities. Coupled with this, hydrographic data, including temperature, salinity, and chlorophyll-a concentration, were obtained from a calibrated CTD (Conductivity, Temperature, Depth) rosette-sampler. We used Matlab open source tool (Matecho) to extract SSLs based on echo levels, allowing us to calculate descriptors such as minimum and maximum depth, width, length, and mean Sv (acoustic backscatter).

Data processing involved advanced techniques, including the use of Matlab open source tool (Matecho) to extract SSLs based on echo levels, allowing us to calculate SSLs descriptors. The Weighted Mean Depth (WMD) as a proxy for vertical distribution was also computed. The diel vertical migration (DVM) of SSLs was analyzed, and generalized additive mixed models (GAMMs) were applied to examine the relationships between SSLs metrics and environmental variables.

SSLs ACOUSTIC CHARACTERIZATION

The clustering of SSLs acoustic data (38 kHz) resulted in four clusters, spatially distributed across the survey area (Figure 1). These clusters corresponded to four regions with different SSLs features: Eastern Tropical North Atlantic Ocean, Sargasso Sea, Caribbean Sea and Eastern Tropical Pacific Ocean. The Atlantic and Pacific cluster exhibited the thickest and longest SSLs. The Pacific Ocean cluster also displayed the shallowest SSLs, which corresponded to the areas of greatest acoustic density. The Sargasso Sea had the deepest, shortest and thinnest SSLs, with the lowest acoustic density. The SSLs in the Caribbean Sea exhibited similar characteristics to those of the Sargasso Sea, with the exception of a higher acoustic density.

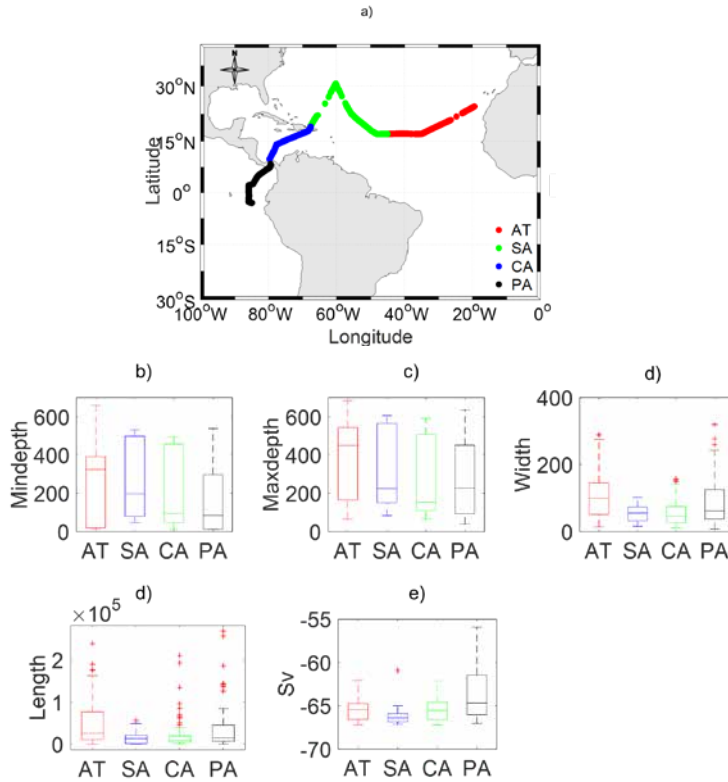


Figure 1: k-means clustering of (38 kHz) discriminated four area along the vessel survey part (Fig 1). a) Map of the daytime survey track with each day colored by its resulting cluster: Atlantic (red); Sargasso (blue); Caribbean (green); Pacific (black). b-f) Boxplots of Sound Scattering Layer (SSLs) metrics for each identified cluster: minimal depth (m), maximal depth (m), width (m) length (m) and Acoustic backscattering strength Sv (dB) used as a micronektonic biomass proxy. AT (Eastern Tropical North Atlantic Ocean), SA (Sargasso Sea), CA (Caribbean Sea) and PA (Eastern Tropical Pacific Ocean).

SSLS VERTICAL DISTRIBUTION

SSLs vertical structuration also differed from region to region (Figure 2). Throughout the studied areas, two main SSLs were observed: epipelagic SSLs between 10–200 m depth and mesopelagic SSLs located between 300–600 m depth during day and at shallower depths during night. The Pacific region, particularly, exhibited a singular feature showing an intermediate SSL appearing at 350–450 m depth between the epipelagic and mesopelagic SSLs.

The vertical profile of mean acoustic volume backscattering strength (Sv in dB) recorded at 38 kHz (Figure 3) exhibited diverse patterns from the surface down to 800 m. Daytime and nighttime effects on the vertical distribution consistently emerged, with elevated values of acoustic backscatter (Sv) generally observed in the epipelagic zone (0–200 m) during the night and in the mesopelagic zone (200–800 meters) during the day. However, there were exceptions, particularly in the Pacific region, where the diel

difference is less clear in the epipelagic layer with day and night profiles overlapping. Notably, in the Sargasso Sea, the daytime biomass slightly exceeded the nocturnal biomass in the mesopelagic zone, occasionally overlapping with the latter.

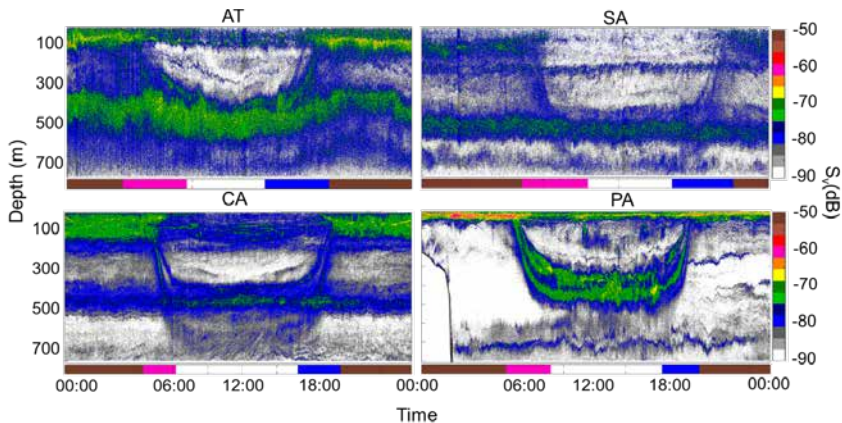


Figure 2: TPM (transcript per million) value of each nitrogen metabolite in the metagenome datasets from Tara Ocean samples and SO287, and their correlations (excluding Tara Ocean datasets) with physiochemical parameters ($p < 0.05$, $|r| > 0.5$).

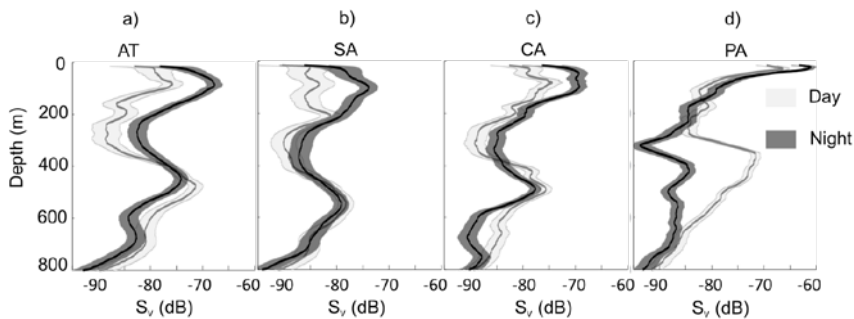


Figure 3: Diel difference of mean acoustic volume backscattering strength (S_v in dB) within the water column in AT (Tropical Atlantic Ocean), SA (Sargasso Sea), CA (Caribbean Sea) and PA (Eastern tropical Pacific Ocean).

ENVIRONMENTAL CONDITIONS ACROSS THE STUDY AREA

Vertical variability of temperature, salinity, dissolved oxygen, and chlorophyll-a along the transects performed in the North Atlantic and in the Pacific Ocean are shown in Figure 4. The variability of the environmental parameters clearly reflects the transport pathway of water from the upwelling zones off Africa into the Sargasso Sea, further to the Caribbean and to the equatorial Pacific. Our results are indicative of the properties of the water masses and the influence of ocean circulation in the tropical Atlantic and Pacific.

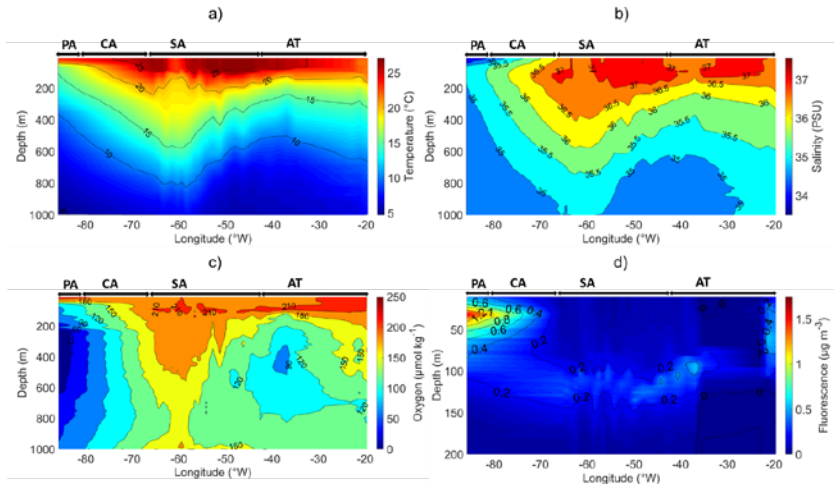


Figure 4: Contour plots of (a) temperature, (b) salinity, (c) dissolved oxygen, and (d) fluorescence in the entire surveyed area, i.e., AT (Eastern Tropical Atlantic Ocean), SA (Sargasso Sea), CA (Caribbean Sea) and PA (Eastern tropical Pacific Ocean).

EFFECT OF ENVIRONMENTAL PARAMETERS ON SSLS

The relationships between the vertical distribution of SSLs and the physical environment are depicted in Figure 5. The vertical variability of temperature, salinity, and dissolved oxygen was found to influence the vertical distribution of the SSLs WMD, shaping their vertical distribution. Thus, the observed variability of WMD seems to be drifted by the water masses characteristic despite no obvious environmental constraint or gradient limiting their vertical extend. The influence of water masses characteristics on SSLs vertical distribution are corroborated by the deepening of the SSLs (Figure 6) in the Sargasso sea coinciding with the deepening of thermocline, oxycline and halocline. Numerous previous studies have investigated the potential environmental factors, including primary production, dissolved oxygen levels, light intensity, temperature, wind-induced mixing and predation pressure, that drive the spatial distribution of SSLs (Escobar-Flores et al., 2013; Diogoul et al., 2020; Irigoien et al., 2009; Klevjer et al., 2016a; Aksnes et al., 2017; Balino and Aksnes, 1993; Proud et al., 2017; Receveur et al., 2019). Our research findings suggest that sea temperature fluorescence and oxygen play a predominant role in determining the vertical distribution of the SSLs while salinity and diel period exerted less influence. On a global or basin scale, the primary influencing factors for SSLs include sea surface temperature, primary productivity, and dissolved oxygen levels (Bianchi et al., 2013; Irigoien et al., 2014a; Escobar-Flores et al., 2013; Klevjer et al., 2016b). The combination of salinity, light, temperature, nutrients, circulation, carbon dioxide, and oxygen collectively determines the physiology of life, ultimately impacting the composition, structure, and functioning of the ecosystem (Röthig et al., 2023)

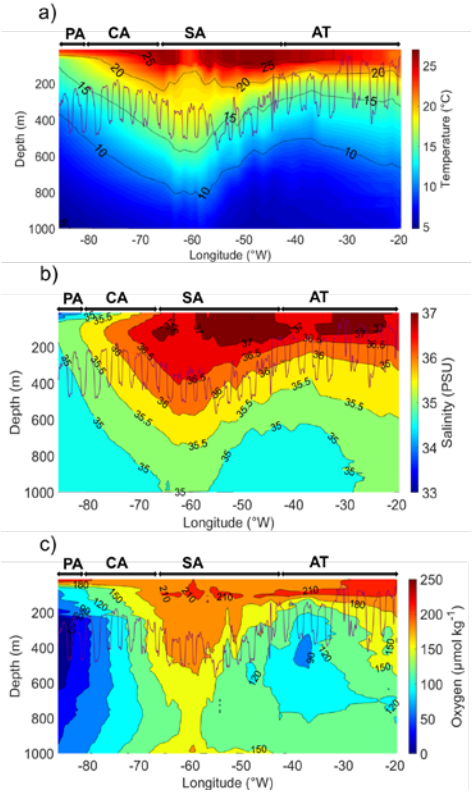


Figure 5: Vertical section along the vessel pathway from CTD probe for (a) sea water temperature, (b) salinity, and (c) dissolved oxygen in the AT (EasternTropical Atlantic Ocean), SA (Sargasso Sea), CA (Caribbean Sea) and PA (Eastern tropical Pacific Ocean). Purple line depict the Weighted Mean Depth (WMD) on each panel.

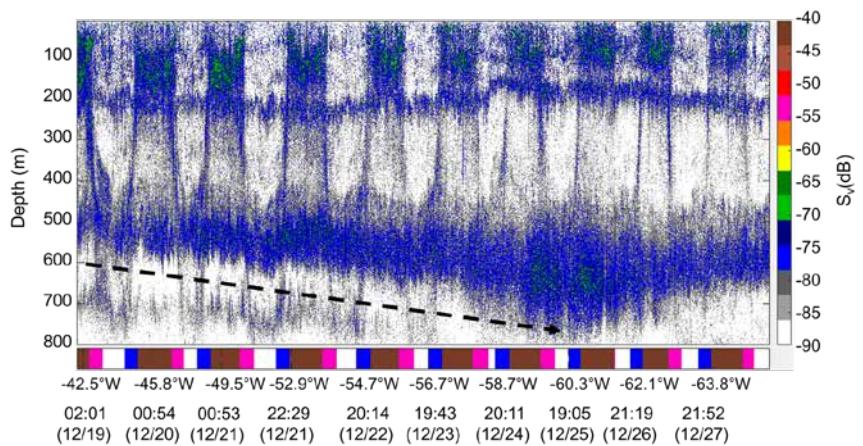


Figure 6: Echogram (38 kHz) in the Sargasso sea depicting the deepening of the mesopelagic layer from 19/12 to 26/12/2021.

REFERENCES

Behagle N, Cotté C, Lebourges-Dhaussy A, Roudaut G, Duhamel G, Brehmer P, Josse E, and Cherel Y, Acoustic distribution of discriminated micronektonic organisms from a bi-frequency processing: The case study of eastern Kerguelen oceanic waters, *Progress in Oceanography* 2017, 156, 276–289.

Boswell KM, D'Elia M, Johnston MW, Mohan JA, Warren JD, Wells RJD, and Sutton TT, Oceanographic Structure and Light Levels Drive Patterns of Sound Scattering Layers in a Low-Latitude Oceanic System, *Frontiers in Marine Science* 2020, 7.

Geoffroy M, Daase M, Cusa M, Darnis G, Graeve M, Santana Hernández N, Berge J, Renaud PE, et al., Mesopelagic Sound Scattering Layers of the High Arctic: Seasonal Variations in Biomass, Species Assemblage, and Trophic Relationships, *Frontiers in Marine Science* 2019, 6.

Proud R, Cox MJ, Wotherspoon S, and Brierley AS, A method for identifying Sound Scattering Layers and extracting key characteristics, *Methods Ecol Evol* 2015, 6, 1190–1198.

Simmonds EJ and MacLennan DN, *Fisheries Acoustics: Theory and Practice*, 2nd edn. FISH and FISHERIES 2006, 7, 227–228.

Tont, SA, Deep scattering layers: patterns in the Pacific, *Rep Calif Coop Ocean Fish Invest* 1976, 18, 112–117.

DATA

Acoustic observations:

<https://portal.geomar.de/group/so287-connect/data>

Physical oceanography (CTD):

<https://portal.geomar.de/group/so287-connect/data>

SO287

Metagenomic insights into variability of microbial diversity and functions in the Eastern Tropical Pacific Ocean

AUTHORS

Department of Biology, University of Southern Denmark | Odense, Denmark
P. Xu, C.R. Löscher

Radboud University | Nijmegen, Netherlands
D.L. Arévalo-Martínez

GEOMAR Helmholtz Center for Ocean Research | Kiel, Germany
H.W. Bange, M. Pohlmann

Department of Biology, Copenhagen University | Copenhagen, Denmark
M. Middelboe

Oxygen minimum zones (OMZs) expand in the ocean and may significantly affect the microbial process which drive major biogeochemical cycles of carbon, nitrogen, sulfur, phosphorus in the ocean (Callbeck et al., 2021; Thamdrup et al., 2019; Ward et al., 2009; Wright et al., 2012). The Eastern Tropical Pacific Ocean (ETP) bears one of the largest perennial OMZ in the present ocean and is strongly influenced by the recurring climate pattern (alternating cold and warm phases) known as El Niño Southern Oscillation (ENSO) (Cappellen et al., 2008; Lavín et al., 2006). However, little is known about how microbial diversity and functions in biogeochemical cycles might shift in associated with oxygen variability and ENSO events. Here we utilized a metagenomic approach to analyze changes in microbial diversity on samples covering a dissolved oxygen (DO) gradient ranging from oxic to suboxic conditions in the ETP. The samples were collected in 2022 through the research expedition, SO287-CONNECT. We then compared our findings to the Tara Ocean datasets obtained from the same region under a comparable La Niña event eleven years earlier in 2011. We observed a decrease in microbial diversity and abundance, coupled with an increase in most nitrogen metabolisms as DO decreases. Dominant microbial groups and key functions displayed varying sensitivities to different DO ranges from 5 to >120 $\mu\text{mol kg}^{-1}$. The shift in functional groups occurred when DO drops below 120, 90, 80, 60, or 12 $\mu\text{mol kg}^{-1}$. The relative abundances of certain groups (SUP05, UBA868, Dehalococcoidia, Nitrospina, Marinisomatota, Thermoproteota) increased while that of others (SAR11, Flavobacteriaceae, Cyanobacteria, Rhodobacteraceae, D2472) decreased as DO decreased, particularly at DO levels below 80 $\mu\text{mol kg}^{-1}$. Furthermore, Thermoproteota dominated the metabolism of N_2O production, and the relative abundance of Thermoproteota encoding *nirK* were

positively associated with N_2O but negatively associated with DO, suggesting the expansion of OMZ might lead to an increase in Thermoproteota-induced N_2O production. However, ENSO events do not seem to have any large effect on microbial diversity or taxonomy in the ETP by comparing the two datasets between 2011 and 2022. We observed a significant reduction in the relative abundance of SAR11, along with an increase in nitrogen metabolisms (e. g., denitrification (N_2O production) and nitrogen fixation) in the ETP between 2011 and 2022. Together, our study helps to improve our understanding on the response of microbial diversity, various groups, and functions to the possible future OMZ expansion in the ETP.

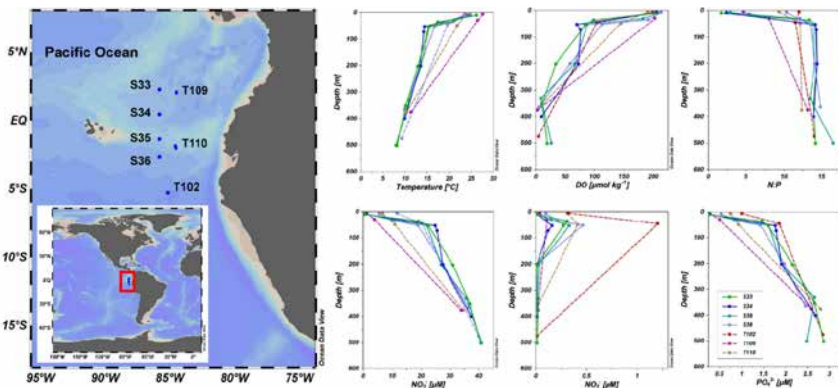


Figure 1: Comparison of depth profiles of physicochemical variables in the same sampling regions of the ETP between the two Cruise periods, SO287 Cruise (S33, S34, S35, S36) and Tara Ocean (T102, T109, T110).

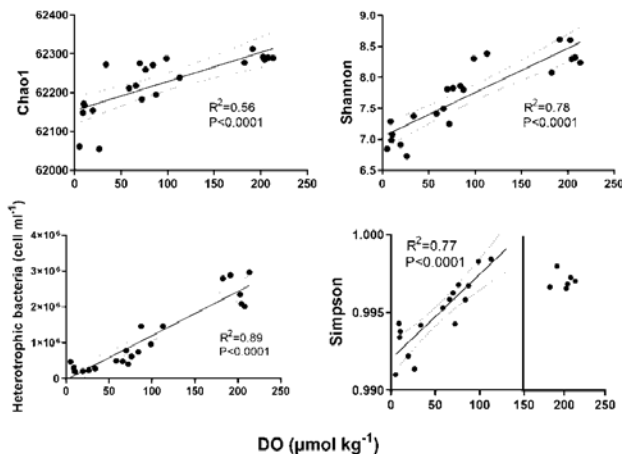


Figure 2: The correlation between DO and alpha diversity of microbial community (Chao1, Shannon, Simpson) and abundance of heterotrophic bacteria (cell counts) with all twenty-two samples in the ETP. *Only for samples from SO287.

Ward BB, Devol AH, Rich JJ, Chang BX, Denitrification as the dominant nitrogen loss process in the Arabian Sea, *Nature* 2009, 461(7260), 78–81, doi:10.1038/nature08276.

Wright JJ, Konwar KM and Hallam SJ. Microbial ecology of expanding oxygen minimum zones, *Nature Reviews Microbiology* 2012, 10(6), 381–394, doi:10.1038/nrmicro2778.

SO288

Monitoring strain on the seafloor offshore Northern Chile using acoustic direct-path ranging techniques

AUTHORS

GEOMAR Helmholtz-Zentrum für Ozeanforschung Kiel | Kiel, Germany

D. Lange, H. Kopp, I. Klauke, M. Kühn

Universidad de Chile | Santiago de Chile, Chile

E. Contreras-Reyes

INTRODUCTION

Since GPS/GSSN does not work in water, stress and strain buildup between earthquakes remain enigmatic for the offshore domain. Here, we use acoustic ranging techniques (Bürgmann and Chadwell, 2014; Petersen et al., 2019) between stations on the seafloor to obtain crustal strain measurements across a subduction zone. Three geodetic networks on the seafloor off northern Chile at $\sim 21^\circ\text{S}$ latitude were installed in 2015 to obtain information on strain in the marine forearc of a subduction zone. We use data from ~ 2.5 years starting in December 2015 using high-resolution acoustic ranging techniques up to 5200 m water depth and distances up to 2 km to the trench. Each of the 23 installed stations measures temperature, pressure and the acoustic travel time between the intercommunicating sensors. The pressure data for all three networks indicate no sudden vertical movement of the marine forearc. The network measured the travel times autonomously during the whole deployment. We find no measurable crustal strain within our measurement precision of $2\text{E}6/\text{yr}$ for our network located on the outer rise and two networks on the marine forearc. Using numerical kinematic modeling of strain build-up for Northern Chile, we detect no strong locking gradient on the plate interface related to the up-dip end of the seismogenic zone.

GEODETIC DATA AND METHOD

We use acoustic ranging techniques to measure distance changes of transponders on the seafloor over three years in three geodetic networks to resolve tectonic deformation. The method of acoustic path-ranging between two sites on the seafloor has become increasingly used in oil exploration (Dunn et al., 2016) and research (McGuire and Collins, 2013; Yamamoto et al., 2019). The acoustic direct path ranging techniques (e. g. Petersen et al., 2019) can resolve relative distance changes between instruments, with a temporal resolution of hours with mm-precision over periods of years. The technique has been used mostly in shallow water (Lange et al., 2019; Yamamoto et al., 2019).

The transponders are manufactured by Sonardyne (www.sonardyne.com) and measure temperature, inclination, pressure, sound velocity in the water, and the two-way travel time between stations on the seafloor. Each station either interrogates the other stations or acts as a replying instrument. Thus, the experiment forms an autonomous intercommunicating network on the seafloor rather than observations at individual positions. The acoustic distance is then calculated from the sound speed in water multiplied by the one-way travel time (Petersen et al., 2019). Each transponder has an integrated sound-velocity sensor (accuracy 0.030 m/s). However, these sensors showed unexpected offsets and long-term drift of up to 0.5 m/s water speed in the time series during previous deployment in shallow water of ~800 m depth (e. g., Lange et al., 2019). They turned out to have artifacts during the installation offshore Northern Chile. Therefore, we estimate the sound speed in water from temperature and pressure measurements (Leroy et al., 2008), assuming a constant salinity similar to other path-ranging experiments (Chadwell et al., 1999; McGuire and Collins, 2013). Table 1 shows the dependency of the baseline lengths on water parameters. The baseline length is mostly dependent on temperature changes. For example, a temperature change of 0.01°C results in baseline changes of 4.1 cm.

The three geodetic networks were installed with R/V SONNE during cruise SO244-2 between Nov. 27 to Dec. 13, 2015, on the marine forearc and outer rise of the South American subduction system around 21°S (Kopp H. and all Cruise Participants, 2015). The GeoSEA Network consists of autonomous seafloor transponders installed on 4 m high tripods, which were lowered to the seabed on the deep-sea cable of RV SONNE. The array in AREA1 (Figure 1, left panel) on the middle continental slope in ~2700 m water depth consists of 8 transponders located in pairs on four topographic ridges. AREA2 (~4000 water depth, Figure 1, central panel) is located on the outer rise seaward of the trench, where five stations monitor extension across plate-bending related normal faults identified in the AUV bathymetry. AREA3 is located at water depths ~5200 m on the lower continental slope (Figure 1, right panel), consisting of 10 stations to measure potential diffuse strain build-up. Data from all networks and all stations were successfully uploaded with an acoustic modem during cruise MGL1610 of RV Marcus Langseth (December 2016). The last upload was with the Offshore Patrol Vessel Cabo Odger (OPV 84) from the Chilean Navy in June 2018. We could communicate with 20 of the 23 geodetic stations during this cruise. Still, we could only upload parts of the data due to the high energy consumption of marine acoustics from the modem (in ~40 m water depth) to the stations located on the seafloor. All transponders were deinstalled during SO288 with the ROV. The eight stations of AREA1 were deinstalled with the tripods, all others (except one station in AREA2) without the tripods.

Baseline change (cm)	Parameter		unit
4.185	Temperature	0.01	°C
1.317	Salinity	0.01	PSU
1.751	Pressure	10	kPa*
*10 kPa = 0.1 bar = m 1 dbar ~ 1 m Water column			

Table 1: Dependency of baseline lengths on water parameters for a 750 m long baseline (e. g., 1.500 m acoustic two-way distance).

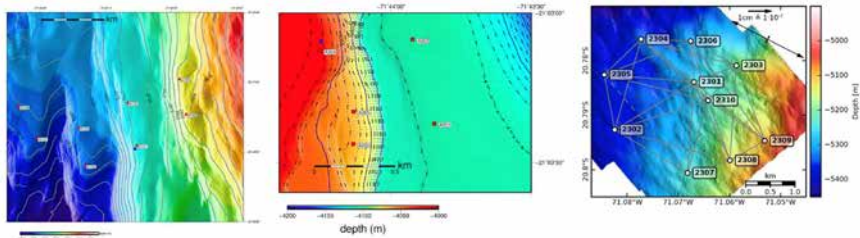


Figure 1: Maps showing the geodetic networks. Left: AREA1, Middle: AREA2, right: AREA3. The bathymetry is from the AUV mapping conducted during SO244, Leg1. The location of the three networks is shown in Figure 1 of the SO288 report (Kopp et al, this issue).

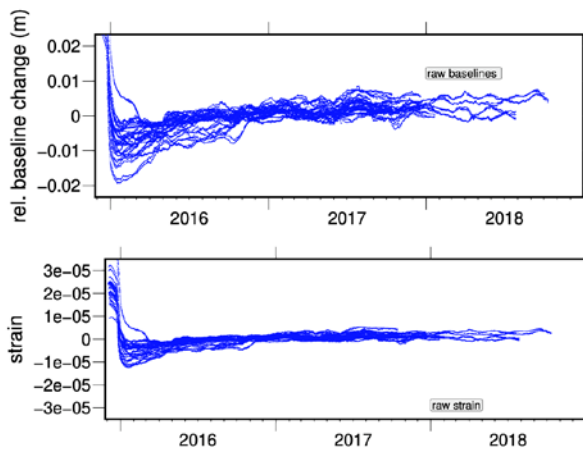


Figure 2: Baseline changes (upper panel) and strain (two week means) estimated for 47 baselines in AREA3 located in ~5200 m water depth. Baselines from and to station 2306 are not shown since the tripod was tilting during the deployment.

BASELINES AND STRAIN

The baselines and strain (Figure 2) were calculated using the estimated sound speed in water and the travel times. The sensor settling effect during the first ~2 months of the travel time measurement (Figure 2) directly maps into the baselines and strain estimates and is an artifact. After March 2016, the baselines were all in a corridor of approx. 10 mm width. Considering strain, all baselines are within a corridor of $10E5$, indicating the upper bound of resolvable strain. Baselines of AREA2 suffer from the loss of high-resolution temperatures that worked only for 1.5 years, but look similar to those of AREA3, although only 14 months long. Baselines for AREA1 show a significantly lower resolution due to large temperature heterogeneities in the water column.

We measure crustal strain with $5E06$ precision for individual baselines at water depths up to 5200 m. The upper bound on the horizontal strain rate on the seafloor of $2E06/yr$ (e. g., no deformation observed larger than 2 mm/yr for a 1 km long baseline) is in line with locking models based on GSSN landstations. Comparing our results with numerical kinematic modeling of strain build-up for Northern Chile, we suggest that there is no strong locking gradient on the plate interface related to the up-dip end of the seismicogenic zone.

REFERENCES

Bürgmann R, Chadwell D, Seafloor Geodesy. *Annu. Rev. Earth Planet. Sci.* 2014, 42, 509–534. <https://doi.org/10.1146/annurev-earth-060313-054953>.

Chadwell CD, Hildebrand JA, Spiess FN, Morton JL, Normark WR, Reiss CA, No spreading across the Southern Juan de Fuca Ridge axial cleft during 1994–1996. *Geophys. Res. Lett.* 1999, 26, 2525–2528, <https://doi.org/10.1029/1999GL900570>.

Dunn S, Hatchell P, Beukel A van den, Vries R de, Frafjord T, A long-term seafloor deformation monitoring campaign at Ormen Lange gas field. *First Break* 2016, 34, 55–64.

Kopp H, all Cruise Participants, RV SONNE Fahrtbericht / Cruise Report SO244/2, GeoSEA: Geodetic Earthquake Observatory on the Seafloor, Antofagasta (Chile) – Antofagasta (Chile), 27.11.–13.12.2015. (cruise report). GEOMAR 2015.

Lange D, Kopp H, Royer J-Y, Henry P, Çakir Z, Petersen F, Sakic P, Ballu V, Bialas J, Özeren MS, Ergintav S, Géli L, Interseismic strain build-up on the submarine North Anatolian Fault offshore Istanbul. *Nature Communications* 2019, 10, 3006. <https://doi.org/10.1038/s41467-019-11016-z>.

Leroy CC, Robinson SP, Goldsmith MJ, A new equation for the accurate calculation of sound speed in all oceans. *The Journal of the Acoustical Society of America* 2008, 124, 2774–2782. <https://doi.org/10.1121/1.2988296>.

McGuire JJ, Collins JA, Millimeter-level precision in a seafloor geodesy experiment at the Discovery transform fault, East Pacific Rise. *Geochem. Geophys. Geosyst.* 2013, 14, 4392–4402. <https://doi.org/10.1002/ggge.20225>.

Petersen F, Kopp H, Lange D, Hannemann K, Urlaub M, Measuring tectonic seafloor deformation and strain-build up with acoustic direct-path ranging. *Journal of Geodynamics* 2019, 124. <https://doi.org/10.1016/j.jog.2019.01.002>.

Yamamoto R, Kido M, Ohta Y, Takahashi N, Yamamoto Y, Pinar A, Kalafat D, Özener H, Kaneda Y, Seafloor Geodesy Revealed Partial Creep of the North Anatolian Fault Submerged in the Sea of Marmara. *Geophysical Research Letters* 2019, 46. <https://doi.org/10.1029/2018GL080984>.

SO288

Deep Ocean Heterogeneity Inferred From Offshore Geodetic Experiments

AUTHORS

GEOMAR Helmholtz Centre for Ocean Research Kiel | Kiel, Germany

A. Jegen, D. Lange, J. Karstensen, H. Kopp

CROSS-BENEFICIAL OCEANOGRAPHIC-GEOPHYSICAL-GEODETTIC APPROACH

The majority of the global ocean volume lies below 2000 m and thus within the deep ocean, which despite being an important heat and carbon sink, and the host to highly specialised ecosystems, energetic currents and resources, remains chronically understudied (Levin et al., 2019). Our knowledge of the deep ocean is restricted further because systematic deep ocean observations are typically limited to address either spatial (ship surveys) or temporal (moored sensors) resolution, with the exception of a few multi-year projects (Sloyan et al., 2019). In recent years, high resolution numerical model simulations have suggested prominent meso- and submesoscale dynamics in the deep ocean (de Lavergne et al., 2017), often related to current-topography interactions. Observations of the kind have led to a notable shift in paradigm, recognizing that mixing processes occurring near the ocean floor play an important role in the large-scale ocean circulation (de Lavergne et al., 2017), particularly in regions with prominent topographic features, such as the continental slope. In recent years, a growing number of offshore geodesy experiments has targeted the deep ocean in order to evaluate marine geohazards by assessing tectonic deformation through strain measurements (Petersen et al., 2019). The resolution of all acoustic-ranging based geodesy methods is limited predominantly by the accuracy of the ambient sound speed information and thus on the correct representation of temporal variations in temperature, pressure, and salinity (Petersen et al., 2019). Therefore, despite having contrasting objectives, oceanographic and offshore geodetic experiments show great overlap in the measured parameter space, evoking the possibility of cross-beneficial studies.

SO288 SEAFLOOR GEODESY EXPERIMENT

A high-resolution (sampling frequencies of 90 min as well as 160 min, respectively) time series of deep in-situ temperature, pressure and sound speed was acquired at three representative locations across the northern Chilean deep-sea trench (Figure 1). The sensors were installed during SO244 in 2015 and recovered during SO288 in 2022.

All stations were equipped with a high-resolution temperature sensor, a pressure sensor as well as a sound speed sensor and were deployed with average station distances of

less than 1 km (Figure 1). One sensor array was deployed on the oceanic plate and thus seaward of the deep-sea trench (Figure 1A). Two other arrays were placed on the lower (Figure 1B) and mid continental slope (Figure 1C). All arrays are located in the deep ocean with water depths ranging between 2600 m–5500 m.

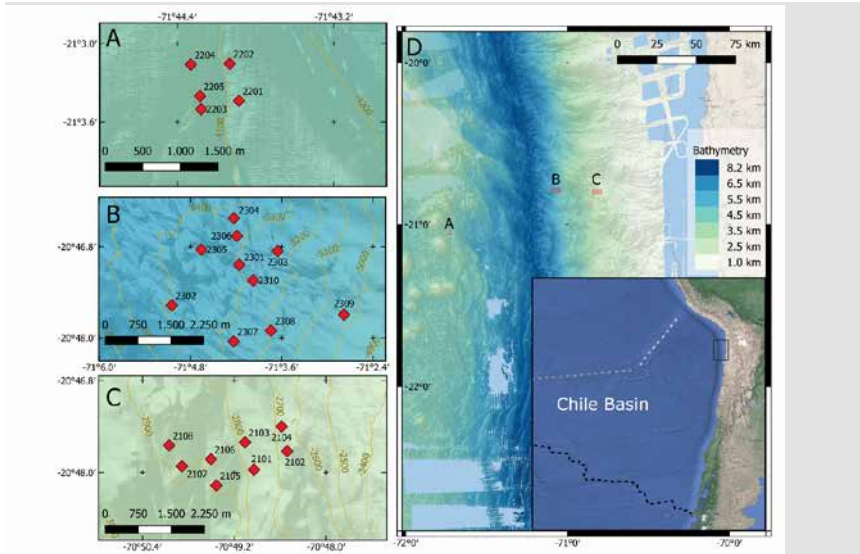


Figure 1: Location of the 23 seafloor stations measuring temperature, pressure and sound speed sensors. Panels A, B and C show the station locations on the oceanic plate, lower and mid continental slope arrays, respectively. Topography contour lines (100 m intervals) from autonomous underwater vehicle (AUV) bathymetry are shown in dark green in panels A-C. Red diamonds mark the locations of the stations. The overview map located within panel D shows the Chile Basin, bounded by the Chile Rise (dashed black line), the Sala y Gomez Ridge (dashed grey line) and the Nazca Ridge (dashed white line). The black rectangle indicates the location of the multi-array experiment.

The stations deployed on the lower continental slope are offset to those deployed on the oceanic plate by about 76 km and to those deployed on the mid continental slope by 26 km. The data, originally acquired for geodetic analyses, were used successfully to assess the spatial and temporal variability in the deep ocean offshore northern Chile. The data are calibrated with published oceanographic reference data from the GLODAPv2 climatology and analysed here in order to refine follow up geodetic analyses. After calibration with the GLODAPv2 reference data, the time series are understood as cold and warm anomalies that oscillate around the calibration value predicted by GLODAPv2.

The data reveal previously unknown de-coupled dynamical regimes seaward and landward of the deep-sea trench, periodic temperature anomalies as well as multi-year warming trends. Table 1 provides the observed variability and mean of the calibrated data.

	Oceanic plate	Lower continental slope	Mid continental slope
Water depth covered by array	4107 m to 4030 m	5028 m to 5374 m	2635 m to 2880 m
Potential temperature range (Mean)	1.373 °C to 1.443°C (1.42 °C)	1.311 °C to 1.37 °C (1.32 °C)	1.579°C to 1.741 °C (1.64 °C)
Mean Salinity	34.692 PSU	34.692 PSU	34.692 PSU
Mean potential density	1027.74 kg m ⁻³	1027.75 kgm ⁻³	1027.69 kgm ⁻³
Mean potential temperature trend	0.018 °Cyr ⁻¹	0.002 °Cyr ⁻¹	0.003 °Cyr ⁻¹

Table 1. Overview of potential temperature, determined multi-year trend, salinity and derived potential density range at each array after calibration.

TEMPORAL TEMPERATURE FLUCTUATIONS

The average potential temperatures recorded at the oceanic plate site, the mid and lower continental slope site (Figure 1) varies around 1.42 °C, 1.32 °C and 1.64 °C, and shows the expected decrease of temperature with increasing water depth (Tab. 1). Temporal temperature oscillations are pronounced and operate with a wide range of frequencies in the data of all three sensor arrays. However, a decrease in the amplitude range of the temperature oscillations with depth is observed both across arrays and within an array (Tab. 1), as would be expected based on the reduction of potential temperature with depth. This correlation is most pronounced along the continental slope, due to the greater depth range within the slope arrays (~350 m and ~250 m) compared to the array on the oceanic plate (~75 m).

We observe periodic temperature anomalies that propagate from north to south over the lower to mid continental slope. The events associated with the anomalies are cross-isopycnal and thus consistent with the prevailing tidal and topographic wave-induced short-term displacements that are evident in the spectral analysis of the time series. The presence of such spatial and temporal temperature heterogeneities is particularly severe for high-resolution or long-distance soundwave-based localisation systems (as used in seafloor geodesy studies), which usually assume a constant speed of sound. While the speed of sound in water is controlled by the ambient temperature, pressure and salinity, it is most sensitive to temperature changes.

The periodic potential temperature fluctuations are visible as warm or cool anomalies in the temperature/depth sections (T/z sections) that were calculated for each of the arrays. While the events stretch through the sensor field, the event's amplitude varies with depth as is particularly evident at the shallow mid continental slope, where the anomalies weaken with depth and show an absolute amplitude decay of ≤ 0.15 °C, over 245 m. The visible correlation of the lower continental slope's and the mid continental slope's periodic temperature fluctuations cannot be found at the oceanic plate site, where partly shorter time series (due to sensor problems) and a comparably small depth range of the array lead to less variability between sensors. The mid and lower continental slope temperature records show great intra-seasonal variability (fluctuations with periods of

about a week to a few months [or from ~7 to 90 days]), while the oceanic plate site records show much lower frequency variability. Making use of the sound speed observations, the salinity is estimated. A comparison of the sound speed-based salinity estimation and the potential temperature reveals that each sensor is affected by strong cross-diapycnal oscillations. Subsequently, the timing of warm anomalies was tracked through the individual arrays. Events associated with warm anomalies were used because they often displayed a more distinctive onset. The onset and amplitude modulation of individual anomalies was compared across arrays, which allowed us to derive information about the propagation of anomalies through the arrays and eventually mesoscale variability.

MULTI-YEAR WARMING TRENDS

Apart from the seasonal component, there is a linear warming trend observed in the temperature data from the lower continental slope. Linear regressions were calculated for the temperature data of all three arrays. Negative trends were determined for three of the five oceanic plate stations, with trends ranging between -0.0058 °C yr⁻¹ and 0.034 °C yr⁻¹ and an average trend of 0.010 °C yr⁻¹. In contrast, the majority of the linear regressions performed on the temperature series from the lower continental slope, suggest a positive trend, with determined gradients ranging between 0.000 °C yr⁻¹ and 0.002 °C yr⁻¹ with an average trend of 0.002 °C yr⁻¹. Comparable high-resolution temperature trends that range between 0.001 °C yr⁻¹ and 0.006 °C yr⁻¹ (average of 0.003 °C yr⁻¹) were determined for the mid continental slope temperature series. Even though the determined multi-year temperature trends are very small, we are confident that the determined temperature trends represent physical changes in ocean properties and not sensor drifts.

REFERENCES

De Lavergne C, Madec G, Roquet F, Holmes R M, McDougall T J, Abyssal ocean overturning shaped by seafloor distribution. *Nature* 2017, 551, 181–186.

Levin L A, Bett B J, Gates A R, Heimbach P, et al. Global Observing Needs in the Deep Ocean. *Frontiers in Marine Science* 2019, 6.

Petersen F, Kopp H, Lange D, Hannemann K, Urlaub M, Invited Review Article: Measuring tectonic seafloor deformation and strain-build up with acoustic direct-path ranging, *Journal of Geodynamics* 2019, 124, 14-24, doi:10.1016/j.jog.2019.01.002.

Sloyan B M, Wanninkhof R, Kramp M, Johnson G C, et al. The Global Ocean Ship-Based Hydrographic Investigations Program (GO-SHIP): A Platform for Integrated Multidisciplinary Ocean Science, *Frontiers in Marine Science* 2019, 6.

SCHRIFTENREIHE PROJEKTRÄGER JÜLICH

1. Technologie- und Erkenntnistransfer aus der Wissenschaft in die Industrie
Eine explorative Untersuchung in der deutschen Material- und Werkstoffforschung
hrsg. von A. Pechmann, F. Piller und G. Schumacher (2010), 230 Seiten
ISBN: 978-3-89336-624-8
2. STATUSTAGUNG SCHIFFFAHRT UND MEERESTECHNIK
Tagungsband der Statustagung 2010 (2010), 173 Seiten
ISBN: 978-3-89336-677-4
3. STATUSTAGUNG SCHIFFFAHRT UND MEERESTECHNIK
Tagungsband der Statustagung 2011 (2011), 227 Seiten
ISBN: 978-3-89336-745-0
4. STATUSTAGUNG SCHIFFFAHRT UND MEERESTECHNIK
Tagungsband der Statustagung 2012 (2012), 206 Seiten
ISBN: 978-3-89336-832-7
5. STATUSTAGUNG MARITIME TECHNOLOGIEN
Tagungsband der Statustagung 2013 (2013), 188 Seiten
ISBN: 978-3-89336-922-5
6. STATUSTAGUNG MARITIME TECHNOLOGIEN
Tagungsband der Statustagung 2014 (2014), 179 Seiten
ISBN: 978-3-95806-006-7
7. STATUSTAGUNG MARITIME TECHNOLOGIEN
Tagungsband der Statustagung 2015 (2015), 196 Seiten
ISBN: 978-3-95806-104-0
8. STATUSTAGUNG MARITIME TECHNOLOGIEN
Tagungsband der Statustagung 2016 (2016), 220 Seiten
ISBN: 978-3-95806-187-3
9. STATUSSEMINAR MEERESFORSCHUNG mit FS SONNE
14.–15. Februar 2017 in Oldenburg–Tagungsband (2017), 221 Seiten
ISBN: 978-3-95806-207-8
10. STATUSTAGUNG MARITIME TECHNOLOGIEN
Tagungsband der Statustagung 2017 (2017), 224 Seiten
ISBN: 978-3-95806-277-1
11. STATUSTAGUNG MARITIME TECHNOLOGIEN
Tagungsband der Statustagung 2018 (2018), 224 Seiten
ISBN: 978-3-95806-366-2

12. STATUSTAGUNG MARITIME TECHNOLOGIEN
Tagungsband der Statustagung 2019 (2018), 187 Seiten
ISBN: 978-3-95806-439-3

13. STATUS CONFERENCE RESEARCH VESSELS 2020
Conference transcript
Online-Publikation (2020), 411 Seiten
ISBN: 978-3-95806-479-9

14. STATUSTAGUNG MARITIME TECHNOLOGIEN
Tagungsband der Statustagung 2021 (2021), 300 Seiten
ISBN: 978-3-95806-594-9

15. STATUS CONFERENCE RESEARCH VESSELS 2022
Conference transcript
Online-Publikation (2022), 476 Seiten
ISBN: 978-3-95806-608-3

16. STATUSTAGUNG MARITIME TECHNOLOGIEN
Tagungsband der Statustagung 2022 (2022), 285 Seiten
ISBN: 978-3-95806-673-1

17. STATUSTAGUNG MARITIME TECHNOLOGIEN
Tagungsband der Statustagung 2023 (2023), 275 Seiten
ISBN: 978-3-95806-732-5

18. STATUS CONFERENCE RESEARCH VESSELS 2024
Conference transcript
Online-Publikation (2024), 574 Seiten
ISBN: 973-3-95806-747-9

